

**TRIAZOLE BASED PEPTIDOMIMETICS FOR MIMICKING  
PROTEIN-PROTEIN HOT SPOTS**

A Dissertation

by

YU LI ANGELL

Submitted to the Office of Graduate Studies of  
Texas A&M University  
in partial fulfillment of the requirements for the degree of

DOCTOR OF PHILOSOPHY

August 2007

Major Subject: Chemistry

**TRIAZOLE BASED PEPTIDOMIMETICS FOR MIMICKING  
PROTEIN-PROTEIN HOT SPOTS**

A Dissertation

by

YU LI ANGELL

Submitted to the Office of Graduate Studies of  
Texas A&M University  
in partial fulfillment of the requirements for the degree of

DOCTOR OF PHILOSOPHY

Approved as to Style and Content by:

Chair of Committee,  
Committee Members,

Kevin Burgess  
Daniel Singleton  
Coran Watanabe  
Jerry Tsai

Head of Department,

David Russell

August 2007

Major Subject: Chemistry

## ABSTRACT

Triazole Based Peptidomimetics for Mimicking Protein-Protein Hot Spots.

(August 2007)

Yu Li Angell, B.S., Wuhan University

Chair of Advisory Committee: Dr. Kevin Burgess

Copper-mediated alkyne-azide cycloadditions yield 1,4-disubstituted triazoles with high chemoselectivity that can be used in many ways. For instance, when alkyne or azido peptide units combine via this pathway the reaction is relatively insensitive to the amino acid side-chains. This serves as an excellent way to produce peptidomimetics, particularly because there is some stereoelectronic similarity between 1,2,3-triazoles and amide bonds.

Linear peptidomimetic substrates **60** were used to form the cyclic derivatives **61** via copper catalyzed azide alkyne cycloadditions. This reaction is fast, simple to perform and compatible with many solvents and functional groups. A library of eight cyclic peptidomimetics was prepared in solution and the low yield was mostly due to formation of dimers. Computational, NMR, and CD analyses of compounds **61a-c** indicate that their most favorable conformational states include type I and type II  $\beta$ -turn conformations.

Monovalent triazole mimics were prepared via cycloaddition reactions in solution. These triazole compounds contain two amino acid chain functionalities at 1- and 4-positions. One is derived from a natural amino acid and the other is a functional group that resembles the side chains of an amino acid. The 1,3-dipolar cycloaddition reactions allow quick and efficient generation of the desired peptidomimetics in good yields.

Two monovalent mimics were coupled to the linker scaffold sequentially in solution by simply manipulating the solvent systems. This method allows us to prepare large libraries of bivalent compounds quickly and efficiently. The two monomers were

combined with each other cleanly, to achieve one-compound-per-well in sufficient purity for biological testing.

Oxidative coupling to give 5,5'-bistriazoles is discussed. The bistriazole products predominate in the copper accelerated “click reaction” of alkynes and azides when carbonate bases are used as additives (ca 1 – 2 M). The reaction seems to be more efficient for propargylic ethers and less hindered substrates. Use of optically active azides could afford separable atropisomeric products, providing a convenient access into optically pure derivatives.

## **DEDICATION**

To my parents and my husband

## ACKNOWLEDGEMENTS

I would like to express my gratitude to my advisor, Dr. Kevin Burgess for his enthusiasm and guidance during my research in his group. I also would like to thank the members of my committee, Drs. Daniel Singleton, Coran Watanabe and Jerry Tsai.

I would like to acknowledge all my colleagues especially Jing Liu, David Chen, Sam Reyes, Eunhwa Ko, Amber Schaefer, Yu-chin Li and Liangxing Wu for their friendship and helpful discussions. I am also grateful to Eunhwa Ko for proofreading some of the chapters.

Finally, I would like to pay special thanks to my family for their love, support and patience.

## TABLE OF CONTENTS

	Page
ABSTRACT .....	iii
DEDICATION .....	v
ACKNOWLEDGEMENTS .....	vi
TABLE OF CONTENTS .....	vii
LIST OF FIGURES .....	x
LIST OF SCHEMES .....	xiv
LIST OF TABLES .....	xv
CHAPTER I INTRODUCTION .....	1
1.1 Copper-catalyzed Azide-alkyne Cycloadditions .....	1
1.2 Mechanism .....	4
1.3 1,2,3-Triazoles in Close Analogs of Peptides .....	6
1.3.1 Acyclic Compounds .....	6
1.3.2 Formation of Peptide-peptide Linkages .....	13
1.3.3 Cyclic Compounds .....	16
1.4 Compounds With Triazole Links to Other Functionalities .....	23
1.4.1 Carbohydrate- peptide .....	23
1.4.2 Organic- peptide .....	31
1.4.3 Polymer- and Dendrimer- peptide .....	33
1.4.3 Conjugates of Metal Complexes for Radiolabeling .....	36
1.5 1,2,3-Triazoles in Less Peptidic Compounds .....	37
1.5.1 Peptoids .....	37
1.5.2 Non-peptidic Mimics Where Triazoles Replace Amides .....	39
1.5.3 Other Non-peptidic Peptidomimetics .....	43
1.6 Conclusion .....	48

CHAPTER II RING CLOSURE TO BETA-TURN MIMICS VIA COPPER CATALYZED AZIDE ALKYNE CYCLOADDITIONS .....	49
2.1 Introduction .....	49
2.2 Solution Phase Synthesis of the Linear Peptidomimetics.....	54
2.3 Copper Catalyzed Azide Alkyne Cycloadditions.....	55
2.4 Conformational Analyses.....	57
2.5 Monomer/Dimer Selectivity Discussion.....	64
2.6 Biological Assays .....	67
2.7 Summary .....	69
CHAPTER III A COMBINATORIAL METHOD TO SOLUTION-PHASE SYNTHESIS OF LABELED BIVALENT BETA-TURN MIMICS.....	70
3.1 Introduction .....	70
3.2 Preparation of Monovalent Triazole Peptidomimetics .....	76
3.3 Adaptation of the Dimerization Method to Solution Phase .....	79
3.4 Application of the Solution-phase Procedure to Make a Library of Fluorescently Labeled Bivalent Mimics .....	81
3.5 Preparation of Biotin Labeled Bivalent Compounds.....	83
3.6 Direct Binding to Trk and p75 Transfected Cells .....	86
3.7 Summary .....	89
CHAPTER IV SOLUTION PHASE SYNTHESIS OF NON-PEPTIDIC MIMETICS USING ARYLALKYNE AS AMIDE BOND SURROGATES AND THEIR ASSEMBLY TO BIVALENT MOLECULES .....	90
4.1 Introduction .....	90
4.2 Preparation of Non-Peptidic Aryl-Alkyne Mimetics.....	93
4.3 Preparation of Bivalent Compounds 85.....	96
4.4 Biological Assays .....	99
4.5 Summary .....	102



	Page
CHAPTER V BASE DEPENDENCE IN COPPER CATALYZED HUISGEN REACTIONS: EFFICIENT FORMATION OF BISTRIAZOLS.....	103
5.1 Introduction .....	103
5.2 Base Screening for the Formation of the Bistriazole Compounds .....	105
5.3 Control Experiments .....	107
5.4 Syntheses of Compounds 88a-g .....	108
5.5 Synthesis of Compounds 88h-i via Convergent Desilylation .....	109
5.6 Physical Properties of Bistriazoles .....	111
5.7 Asymmetric Synthesis of Bistriazoles .....	112
5.8 Summary .....	114
CHAPTER VI CONCLUSIONS .....	115
REFERENCES.....	118
APPENDIX A .....	130
APPENDIX B .....	208
APPENDIX C .....	331
APPENDIX D .....	379
VITA .....	411

## LIST OF FIGURES

	Page
Figure 1.1. (a) Huisgen 1,3-dipolar cycloaddition reactions; (b) copper-catalyzed “click reactions”.....	1
Figure 1.2. Chemoselectivity of “click reactions”.....	4
Figure 1.3. Putative mechanism of the copper-mediated click reaction of alkynes and azides from DFT calculations. ....	5
Figure 1.4. Meldal’s split and mix construct, showing the: (a) photolabile linker; (b) Mis chain for enhanced MS detection; (c) generic structure of the azide components in the click reaction; (d) “Fmoc-arm”.....	7
Figure 1.5. Construction of a $\beta$ -sheet mimic. ....	9
Figure 1.6. Solid phase peptide synthesis by azo-transfer reactions.....	10
Figure 1.7. Triazole-based dipeptide surrogates in GCN4 mimics.....	11
Figure 1.8. Trimers of triazole-based amino acid surrogates: (a) must accommodate dipole moments of the triazole units; and, (b) appear to do this in zig-zag conformations that keep the dipoles <i>anti</i> (W = weak, S = strong).....	12
Figure 1.9. Triazoles serve as linkages between peptides. ....	14
Figure 1.10. Supported alkynes were joined to a cyclic peptide with <i>N</i> -terminal azide fragments. ....	15
Figure 1.11. Preparation of a 38-residue cyclic peptide from cyclodimerization reaction. ....	18
Figure 1.12. Syntheses of carbohydrate/amino acid hybrids. ....	19
Figure 1.13. Synthesis of <i>C</i> -linked glycopeptide analogs. ....	24

	Page
Figure 1.14. Synthesis of <i>N</i> -linked glycopeptide analogs. ....	25
Figure 1.15. (a) Tyrocidine; and (b) some of the analogs prepared. ....	27
Figure 1.16. Preparation of triazole derivative of dodecapetide. ....	31
Figure 1.17. Bovine serum albumin was attached to a polystyrene fragment. ....	33
Figure 1.18. Indole-based backbone amide linker. ....	36
Figure 1.19. Peptoids were derivatized with triazoles while supported on a resin. ....	38
Figure 1.20. Triazole derived inhibitors of cysteine protease cathepsin S. ....	47
Figure 2.1. Some $\beta$ -turn nomenclature, semi-peptidic mimics J and K usually prepared via solid phase reactions, and the identified lead compounds D3 and MPT18. ....	51
Figure 2.2. Substrate and product structures in this study. $R^{1'}$ and $R^{2'}$ denote protected side chains, $R^1$ and $R^2$ are deprotected ones. ....	53
Figure 2.3. General structure of compounds 61 and the overlaid structure with ideal type I $\beta$ -turn. ....	54
Figure 2.4. Correlations between ROE cross-peaks and distances from QMD. ....	58
Figure 2.5. Correlations between ROE cross-peaks of 61b and distances from QMD (PPA = propargyl amine residue) ....	60
Figure 2.6. Correlations between ROE cross-peaks of 61c and distances from QMD. ....	61
Figure 2.7. CD spectra of compounds 61a - c in 4:1 water/methanol at 0.1 mg/ml. ....	63
Figure 2.8. Formation of dimeric products in copper-mediated azide/alkyne cycloadditions may be associated with less populated “ <i>endo</i> -like” conformations relative to less well ordered, more populated, <i>exo</i> -like ones. ....	66

	Page
Figure 2.9. Cell Survival Data and Graphic Representation for Compounds 61.....	68
Figure 3.1. (a) The key distance of C <sup>b</sup> -separations of the $i + 1$ to $i + 2$ residues of a type 1 $\beta$ -turn and of the monovalent turn mimics 70 featured here; (b) an overlay of the mimics onto a type 1 $\beta$ -turn; and, (c) a comparison of their electrostatic charge separations for these two entities. ....	71
Figure 3.2. Weakly binding molecules could be jointed together to form bivalent molecules with higher binding affinity. ....	72
Figure 3.3. “Linker scaffold” strategy.....	73
Figure 3.4. Purities of the library of compounds 71 where the detection method was: (a) UV set at 254 nm; and, (b) SEDEX detection. The term “cap” is used for morpholine. ....	82
Figure 3.5. Purities of the library of compounds 72 where the detection method was: (a) UV set at 254 nm; and, (b) SEDEX detection. The term “cap” is used for morpholine. ....	85
Figure 3.6. Structures of compounds 71 that bind to TrkA from the preliminary FACS assay.....	87
Figure 3.7. Direct binding assay data and the graph presentation of the four “hits”. ....	88
Figure 4.1. Structures of the common peptide backbone replacements.....	91
Figure 4.2. Examples of non-peptidic scaffolds. ....	91
Figure 4.3. Generic structure of aryl-alkyne library.....	92
Figure 4.4. “Mix and match” linker design. ....	93
Figure 4.5. (a) General synthetic scheme and the short/long linkers; (b) Short/long linkers.....	94
Figure 4.6. HPLC purities of the bivalent turn mimics 85. ....	98

	Page
Figure 4.7. HPLC purities of 85 after resynthesis.....	99
Figure 4.8. Structures of 85gn, 85hn, 85jn and 85kn that bind TrkC from the preliminary FASC assay.....	100
Figure 5.1. Bistriazole formation in thermal conditions.....	105
Figure 5.2. Control experiments. ....	108
Figure 5.3 Bistriazole formation from TMS protected precursors <i>via</i> convergent desilylation.....	110
Figure 5.4. Representation of 88e from single crystal X-ray diffraction. ....	111
Figure 5.5. Synthesis of the optically active bistriazole from propargyl phenyl ether. .	112
Figure 5.6. Synthesis of the chiral bipyridyl product.....	113
Figure 5.7. The stereochemistry of the bistriazole atropisomeric chiral center in the minor diastereomer 88k.....	113

**LIST OF SCHEMES**

	Page
Scheme 2.1. Preparation of the linear substrates 60. $R^{1'}$ and $R^{2'}$ denote protected side chains, $R^1$ and $R^2$ are unprotected ones (see Table 2.1 for a – h definitions).....	55
Scheme 3.1. “Semi-solution phase” reactions illustrate the sequential addition of monomers and the surprising selective coupling of a piperidine over most nucleophilic amino acid side-chains.....	74
Scheme 3.2. Solution phase dimer assembly.....	75
Scheme 3.3. Two methods for preparing the monovalent mimics 70. Generally the least expensive and most direct route uses is: (a) featuring unprotected amino acid starting materials (except for Lys which was side-chain protected). Route (b) uses protected amino acids.....	77
Scheme 3.4. Solution phase method for the preparation of the library of compounds 71.....	80
Scheme 3.5. Preparation of biotin-labeled bivalent library 72.....	84
Scheme 4.1. Preparation of bivalent mimetics 85.....	97

**LIST OF TABLES**

	Page
Table 2.1. Copper catalyzed cyclization reactions of compounds 60. ....	56
Table 2.2. QMD results for the lowest energy conformer of compound 61a. ....	58
Table 2.3. QMD results for the lowest energy conformer of compound 61b. ....	59
Table 2.4. QMD results for the lowest energy conformer of compound 61c. ....	61
Table 2.5. Temperature coefficients and H/D exchange data of compounds 61a-c. ....	62
Table 3.1. Peptidomimetics 74 prepared via method A. ....	78
Table 4.1. Aryl-alkyne library 84. ....	95
Table 4.2. FACS Competition Assay ....	101
Table 4.3. Cell Survival Data for Compounds 85. ....	102
Table 5.1. Effects of bases on the oxidative dimerization process. ....	106
Table 5.2. Syntheses of bistriazole product 88. ....	109

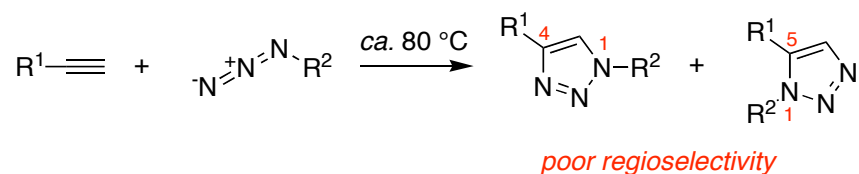
# CHAPTER I

## INTRODUCTION

### 1.1 Copper-catalyzed Azide-alkyne Cycloadditions

Huisgen 1,3-dipolar cycloaddition reactions of alkynes and organic azides are well known and have numerous applications in synthetic organic chemistry.<sup>1,2</sup> This transformation has the advantage of high chemoselectivity since few functional groups react with azides or alkynes in the absence of other reagents. However, it has the limitations associated with any process that requires heat, and, more importantly, that produces two regioisomers (1,4 and 1,5) as illustrated in Figure 1.1a.

a.



b.

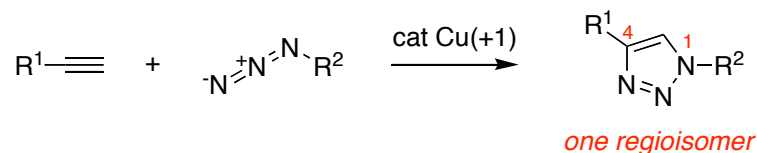


**Figure 1.1.** (a) Huisgen 1,3-dipolar cycloaddition reactions; (b) copper-catalyzed “click reactions”.

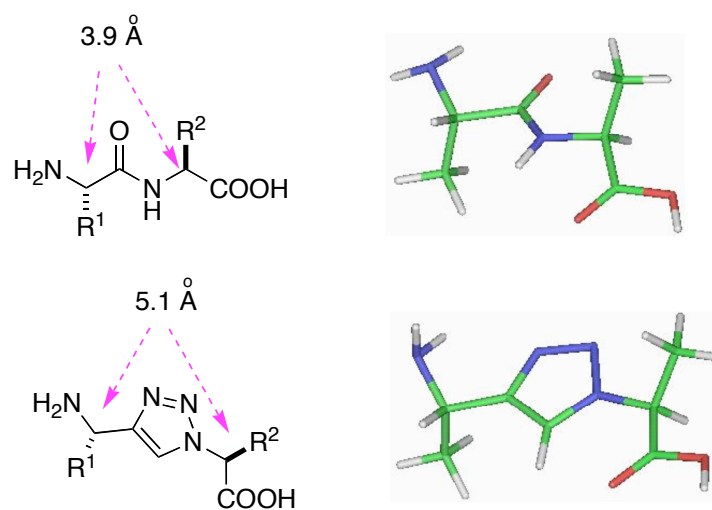


It is rare that contemporary science uncovers a very simple modification of a classical “named reaction” that dramatically improves its value, but in the case of the Huisgen cycloaddition, this happened. The groups of Meldal<sup>3</sup> then Sharpless,<sup>4</sup> independently, found copper (I) catalysts dramatically accelerate the reaction and make it totally regioselective for the 1,4-isomer (Figure 1.1b).

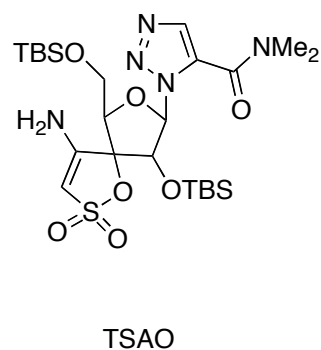
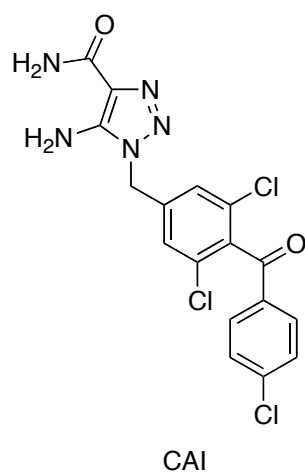
Sharpless and his co-workers have published many high quality papers to alert the scientific community to the value of copper-catalyzed cycloaddition reactions. They coined the term “click chemistry” to describe this and ones like it that proceed in very high yields and that almost invariably work. There are, in fact, too few transformations that fit these criteria in organic chemistry! Click reactions in general have been reviewed,<sup>5,6</sup> and there is one review specifically on copper-catalyzed azide-alkyne cycloadditions.<sup>7</sup>

Here, this introduction approaches the area with one focus: peptidomimetics. We are interested in combinatorial and/or high throughput syntheses of peptidomimetics of potential value in medicinal chemistry. Reaction in Figure 1.1b has several attributes that are highly attractive in this regard, specifically it:

- gives the 1,2,3-triazole nucleus that is a likely candidate for small molecule drugs;
- is compatible with the side chains of all the amino acids, at least in protected form;
- can potentially give high yields of products with few by-products; and,
- the molecular dimensions of the 1,4-disubstituted 1,2,3-triazoles are somewhat similar to amide bonds in terms of distance and planarity.



Potential pharmaceuticals based on 1,2,3-triazoles include the anti-cancer compound CAI<sup>8</sup> and the nucleoside derivative known as TSAO,<sup>9</sup> a non-nucleoside reverse transcriptase inhibitor. Both these compounds are (or have been) in clinical trials.



Meldal and co-workers were the first to begin to address the compatibility of protected amino acid side-chains with the featured copper-mediated click reaction. Figure 1.2 illustrates how various solid-supported tripeptides were reacted with an azide to give high product yields via HPLC analyses. These purities reflect the efficiencies of the cycloaddition and the base-mediated cleavage reaction together. To the best of our knowledge there has been no such systematic study featuring unprotected side chains, but research in our lab has indicated most amino acids side chains are compatible.

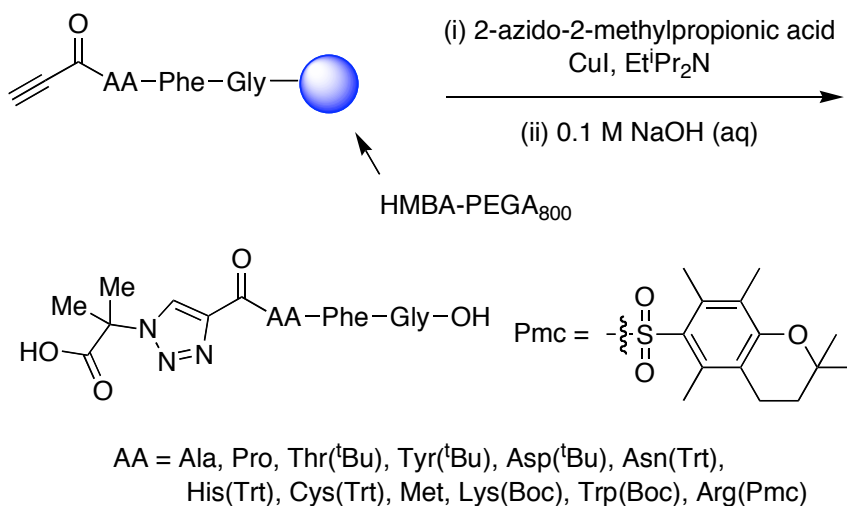


**Figure 1.2.** Chemoselectivity of “click reactions”.

## 1.2 Mechanism

The mechanistic interpretation shown in Figure 1.1 is supported by kinetic studies,<sup>10</sup> product distributions for specialized substrates,<sup>10</sup> and DFT calculations.<sup>11</sup>

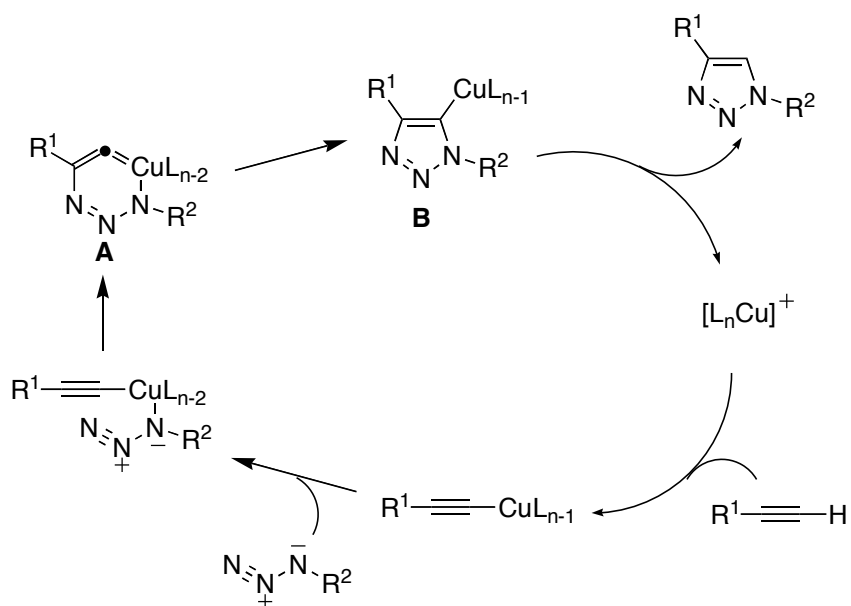


**Figure 1.3.** Putative mechanism of the copper-mediated click reaction of alkynes and azides from DFT calculations.

Kinetic studies indicate the reaction is second order in the Cu(1+) source when present at low concentrations; aggregates of the metal may form at higher concentrations. Under typical conditions, the reaction is not precisely first order in alkyne, but it is in the azide component. These observations lend support to the assertion that the reaction may involve rapidly equilibrating copper-alkyne complexes. Product inhibition does not tend to be prevalent in these reactions.

Experiments with constrained diazides show the reaction is difficult to stop even if only one equivalent of alkyne is used. This implies an intermediate involving only one triazole unit can be more reactive than the starting diazide. However, similar experiments with constrained alkynes do accumulate monotriazole intermediates. These observations should not be over-interpreted, but they do imply that monotriazole intermediates can react significantly faster if an azide is held proximal than in cases where an alkyne group is.

Postulated mechanisms have been tested using DFT calculations, and the theoretical data indicates the reaction pathway shown in Figure 1.3. It is important to note that other evidence points to the possible involvement of dicopper (and higher order) species; this was not tested in the DFT calculations because it is computationally difficult to do so. Nevertheless, these calculations provided several valuable insights into the reaction. They indicate that  $\pi$ -complexation of terminal alkynes greatly increases the acidity of the  $^{\text{sp}}\text{C-H}$  (“by up to 9.8 units”). Displacement of water ligands by alkynes is thermodynamically much more favorable than if an acetonitrile is liberated. Finally, theory supports the 6-membered metallocycle intermediate **A** and its contraction to the *C*-ligated triazole **B**.

### 1.3 1,2,3-Triazoles in Close Analogs of Peptides

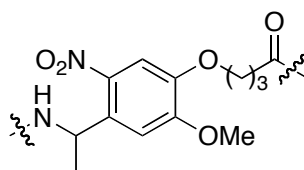
Some molecules have been made wherein a 1,2,3-triazole is a genuine surrogate for an amide bond, while others have an amide in cyclic structures where the analogy to a cyclic peptide maybe more tenuous. Both these types are covered in this section.

#### 1.3.1 Acyclic Compounds

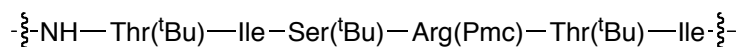
Meldal’s group prepared a huge library of compounds (over 400,000) via a split and mix approach, then screened them on resin.<sup>12</sup> Figure 1.4 shows the basic structure of the compounds that they produced. The resin was first masked with *two* different protecting groups (Aloc- and Fmoc-based). It was the Fmoc-protected arm that was subjected to most of the chemical changes. This was functionalized with a photolabile linker (Figure 1.4a), then with a peptide chain “Mis” (Figure 1.4b) designed to enhance the response of the photocleaved material to MALDI-MS analyses. Two randomized amino acids were coupled onto the *N*-terminus of this chain, the last one to be coupled being a propiolic acid amide. Copper-mediated cycloadditions were then performed using the Fmoc-protected, amino acid derived azides shown in Figure 1.4c. Finally, two more randomized amino acids were coupled. For each coupling step the Fmoc protected amino acids, and the azide in the click reaction, were doped with 10 % of the corresponding Boc-protected materials. These were, of course, not deprotected in the

piperidine-mediated steps, so a ladder of nested chain-terminated segments was produced as the synthesis evolved. Consequently, photocleavage and MS analysis of the chain revealed the sequence of monomers added via a series of mass differences. This so called “MS-laddering” technique<sup>13-15</sup> allows peptidomimetics on “active-beads” to be characterized. Thus the “Fmoc-arm” of the construct is shown in Figure 1.4d.

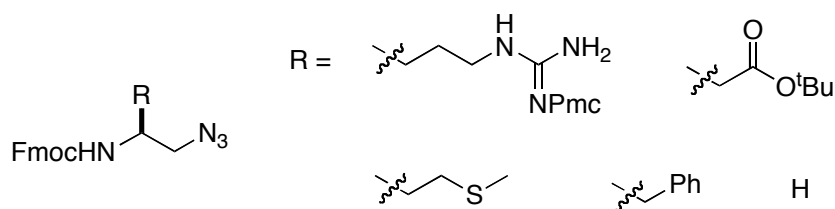
**a**



**b**



**c**



**d**

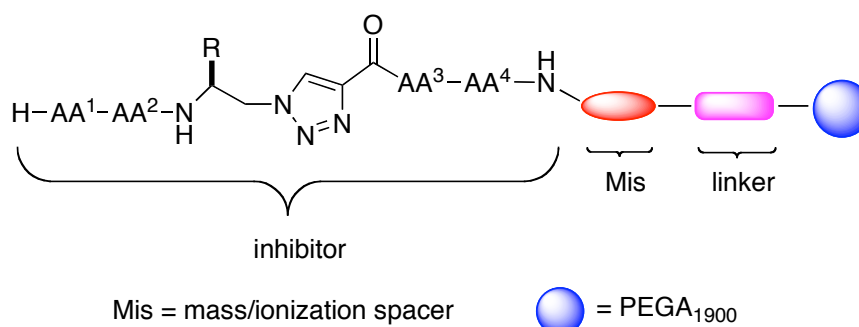


**Figure 1.4.** Meldal’s split and mix construct, showing the: (a) photolabile linker; (b) Mis chain for enhanced MS detection; (c) generic structure of the azide components in the click reaction; (d) “Fmoc-arm”.

The “Aloc-arm” of the construct was modified using orthogonal protecting group chemistry to give a peptide substrate for the target enzyme: a protease from the parasite *Leishmania mexicana*. This had an *N*-terminal 3-nitro-Tyr quencher and a *C*-terminal fluorescent group (2-aminobenzoic acid on a Lys side-chain) so that on cleavage by the protease the beads would fluoresce, *ie* when the quencher-containing *N*-terminal part was cleaved.

The beads in Meldal’s construct function as “microreactors”. When an inhibitor of the enzyme is produced in the split synthesis, the substrate is not cleaved, and the bead does not fluoresce. Most sequences in the split and mix procedure however give cleaved substrates and fluorescent beads. Screening gave a range of “hit” substances, which were characterized by MS. Statistical analysis of the structures of these then led to consensus sequences that were re-prepared and characterized in solution.

Data that emerged from the work shown in Figure 1.4 revealed that the target protease had an affinity for the Mis sequence; this is unfortunate because the only role of that sequence was to enhance MS binding. In retrospect this design weakness could be avoided, but to rectify the flaw the whole library would have to be prepared again. Overall this teaches an important lesson: simple encoding strategies tend to be best. If the complexity of the encoding molecules rivals that of the probe compound then this invites experimental difficulties.

One of the motivations for interest in compounds containing triazole and peptide segments is to prepare synthetic analogs of peptides with perturbed secondary structures. A straightforward illustration of this idea is shown in Figure 1.5.<sup>16</sup> In that work click chemistry was used to combine azido- and alkyne-functionalized peptides to give putative  $\beta$ -turn mimics. The secondary structures of these compounds were examined in chloroform, and showed NOE crosspeaks, temperature/concentration variations of  $\text{NH}$  chemical shifts, and FTIR data that are consistent with a small sheet-like structure. Of course, hydrogen-bonding effects are accentuated in non-protic media, so it remains to be established that these constructs are secondary structure mimics in aqueous solutions.

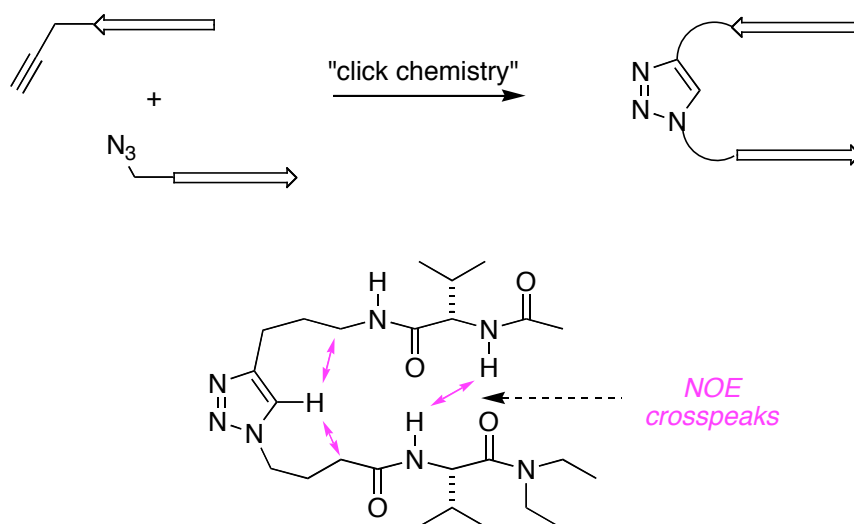
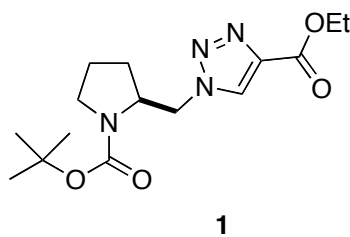


**Figure 1.5.** Construction of a  $\beta$ -sheet mimic.

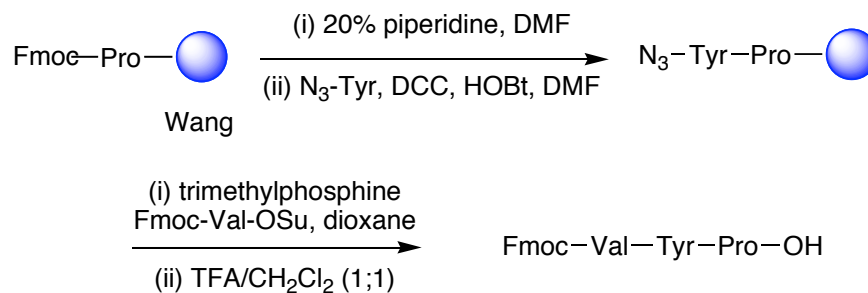
Proline-derived triazoles like **1** have been synthesized via click reactions. These molecules were of interest as surrogates for dipeptide segments to see how the triazole impacts *cis/trans* proline-amide bond ratios.<sup>17</sup>



Access to triazole-based peptidomimetics is greatly facilitated by a relatively convenient azo-transfer reaction<sup>18</sup> that generates 2-azido acids from  $\alpha$ -amino acids<sup>19</sup> or protected derivatives of these (Figure 1.6). This azo-transfer reaction tends to proceed without racemization of the amino acid chirality, even for peptide segments with one

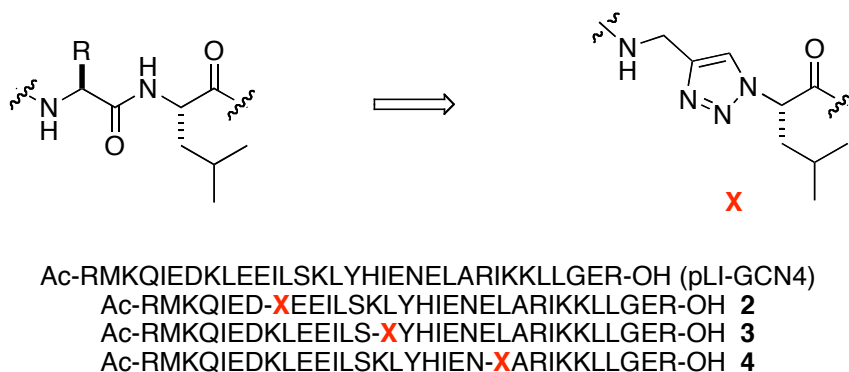


free amine group. Further azido acids can be activated and coupled to the *N*-terminus of a peptide without significant racemization.<sup>19</sup>



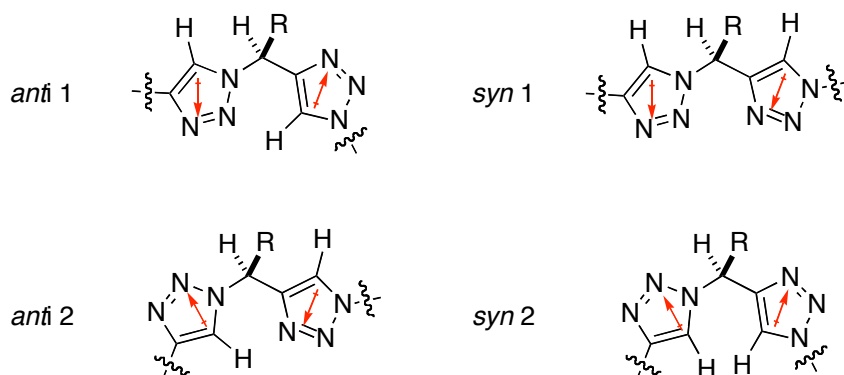
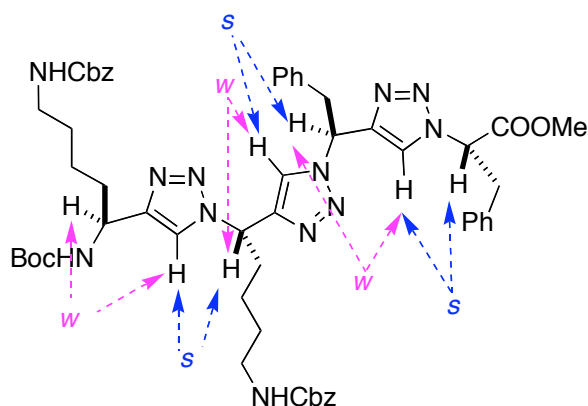
**Figure 1.6.** Solid phase peptide synthesis by azo-transfer reactions.

Using this azo-transfer reaction, Ghadiri and coworkers<sup>20</sup> explored click-combinations of *C*-terminal propargyl peptides with  $\alpha$ -azido-acids to give dipeptide surrogates (Figure 1.7). Thus the L-Leu-derived triazole  $\epsilon^2$ -amino acid was substituted to give sequences in the pLI-GCN4 sequence to test if the mimics retained the native  $\alpha$ -helical character. Mimic **2** in the solid state had a disordered structure about the triazole segment (X-ray), but **3** and **4** had helical structures in the peptide region. Like GCN4, peptide-mimics **2** and **4** formed tetramers in solution (as seen via gel permeation chromatography; presumably these are a four-helix-bundles), whereas **3** self-assembled into structures with two helices packed against each other.



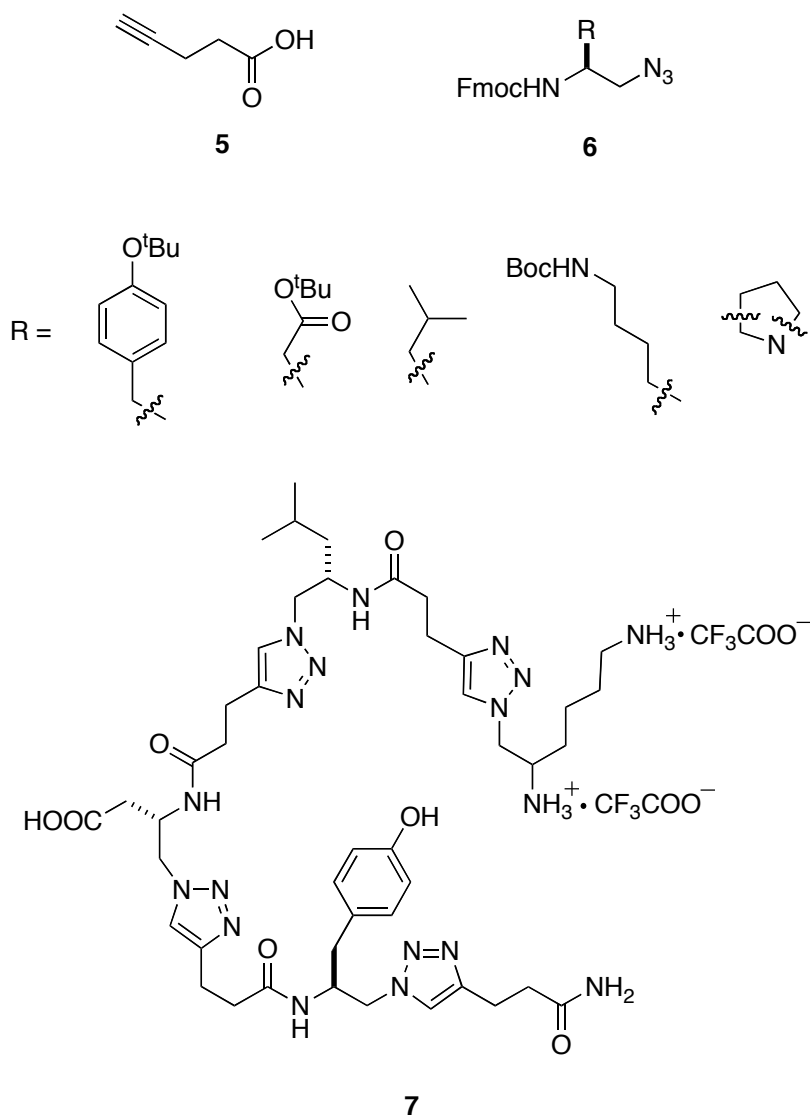
**Figure 1.7.** Triazole-based dipeptide surrogates in GCN4 mimics.

The research described above investigates the effect of placing single triazole-based amino acid surrogates in large peptides. At the other extreme is the use of several triazole-based residues in series. Trimeric molecules of this kind have been made wherein both the alkyne and azide fragments are derived from amino acids (Figure 1.8).<sup>21</sup> This is unlike the work above where the alkyne fragment was propargyl amine, *ie* did not have an amino acid side chain. It was recognized that the triazole units have distinct dipole moments, and conformers of oligomers containing them could be termed *syn* or *anti* based on the orientation of these dipoles. In fact the tripeptide derivatives prefer “zig-zag” conformations in the solid state (X-ray) and in DMSO solution (NMR) wherein the dipoles are opposite.

**a****b**

**Figure 1.8.** Trimers of triazole-based amino acid surrogates: (a) must accommodate dipole moments of the triazole units; and, (b) appear to do this in zig-zag conformations that keep the dipoles *anti* (W = weak, S = strong).

In between the two extremes of isolated triazole-based residues and several in series, are molecules with alternating triazole and amide linkages: these have also been investigated, to some degree.<sup>22</sup> Using solid phase syntheses to connect pentynoic acid **5** and the Fmoc protected amino-acid azides **6** it proved possible to prepare systems like **7**. Copper(1+) iodide and ascorbic acid combinations (DMF/piperidine) were found to be the most effective for formation of the triazole units.



### 1.3.2 Formation of Peptide-peptide Linkages

Orthogonal chemoselectivities for amino acid coupling reactions and the copper-catalyzed click-reaction can be useful for joining two peptide fragments.<sup>23</sup> Figure 1.9 shows a simple illustration where a supported alkyne was joined to a peptide with an *N*-terminal azide fragment. A more elaborate example of this ligation method is given in Figure 1.10. Here the cyclic protected peptide **8** has peripheral nitro, NHivDde, and

NHAloc groups. These were selectively converted to free amines under different conditions, coupled with alkyne-containing acid fragments, then “clicked” with *N*-terminal azidopeptides. Deprotection of the amino acid side chains and cleavage from the trityl-based resin gave the multimeric peptide **9**. The exact application of this particular product was not revealed.

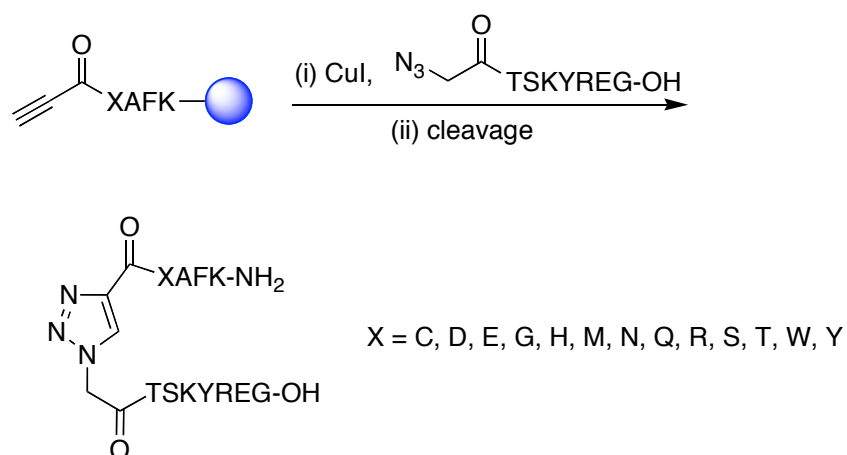


**Figure 1.9.** Triazoles serve as linkages between peptides.

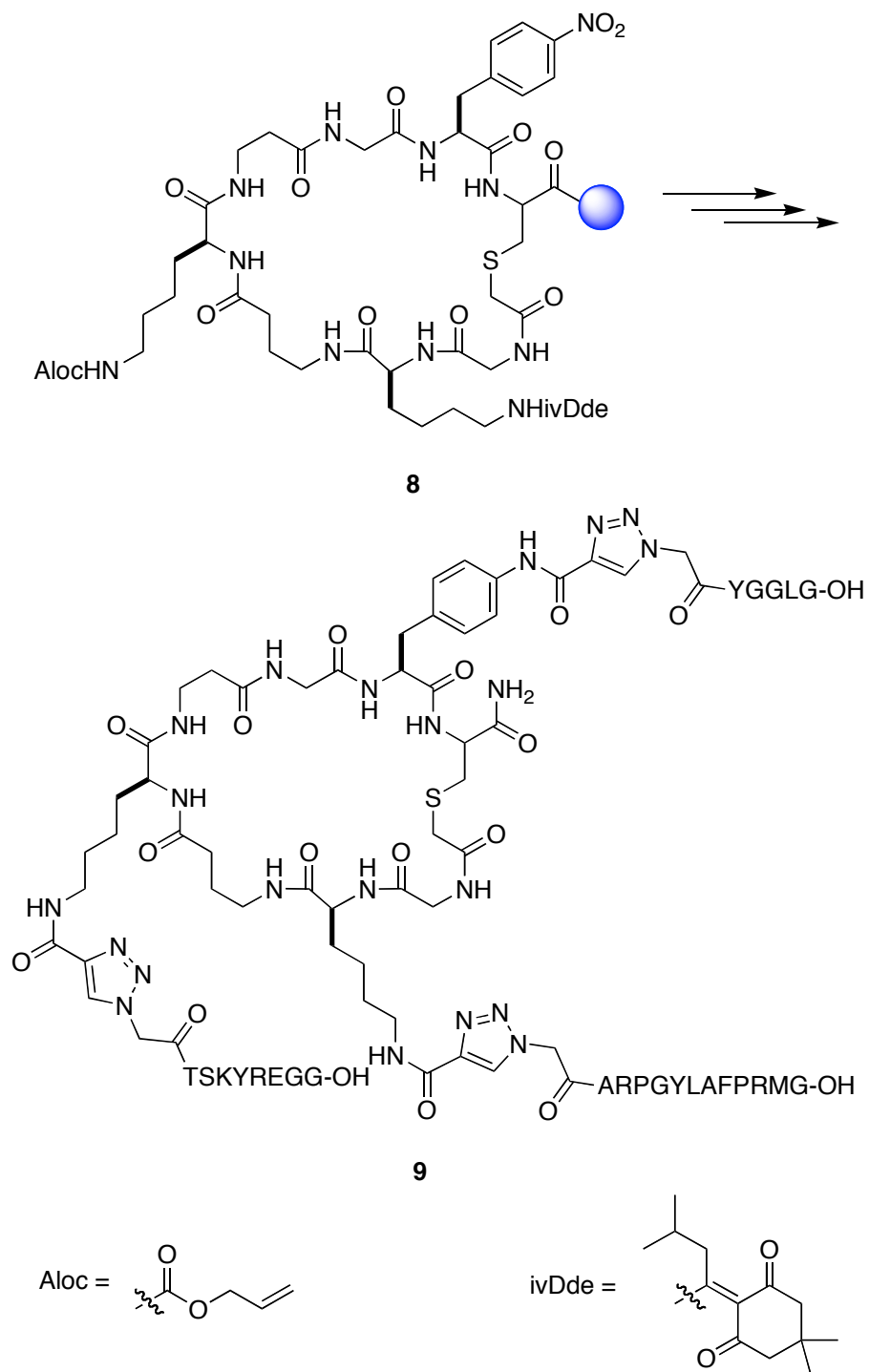
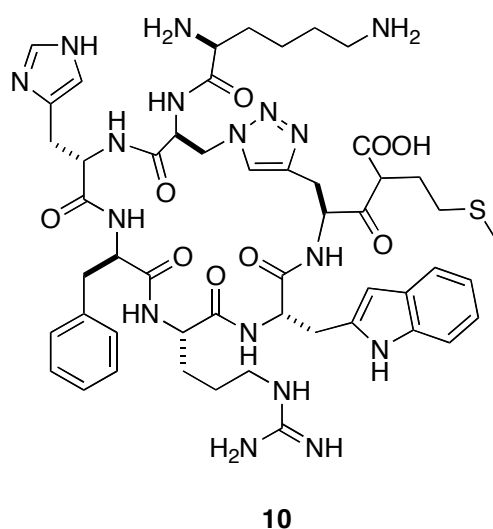


**Figure 1.10.** Supported alkynes were joined to a cyclic peptide with *N*-terminal azide fragments.

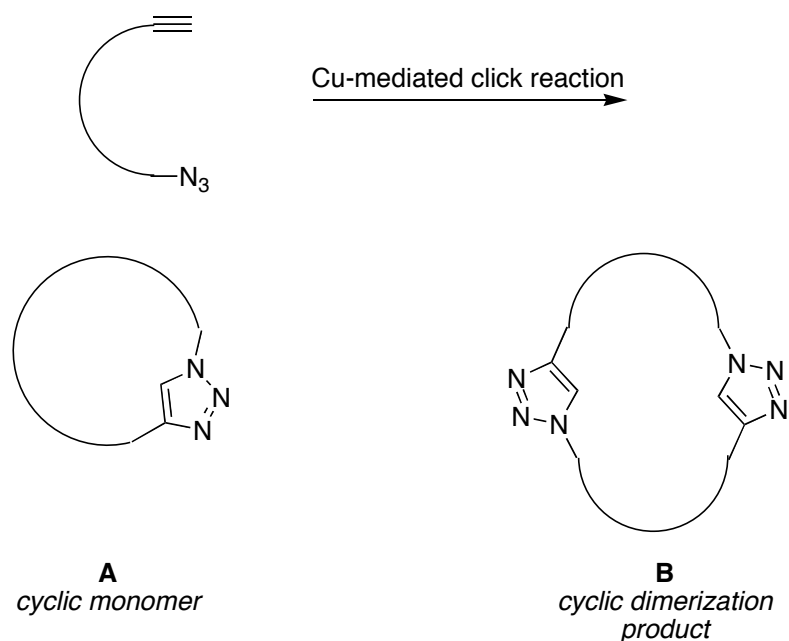
### 1.3.3 Cyclic Compounds

One compelling advantage of the orthogonal nature of the Cu-mediated alkyne/azide couplings is that they can be used to prepare cyclic peptides. Meldal and coworkers have done this to make an analog **10** of a disulfide-containing cyclic peptide. <sup>24</sup> They used their poly(ethylene glycol)-based amino polymer resins, which have excellent swelling characteristics in water. Cyclic product **10** was obtained with high purity and yield via two methods. In the first, the side-chains were deprotected and the supported peptide was cyclized via the Cu-mediated reaction, then cleaved from the resin. In the alternative procedure, the side-chain protection was removed *after* the cyclization. Both approaches gave over 70 % yield of HPLC-purified product. No mention of any dimerization products was made, even though such products can be prevalent, as described in the next section.



Compound **10** was the expected product (type **A**) from a click-mediated macrocyclization reaction. However, a surprising number of papers have reported macrocyclic dimers **B** as prevalent products in similar processes. This sub-section

discusses those examples and the possible origins of this anomaly.



A spectacular demonstration of this macrocyclodimerization effect featured two resin-bound 19-amino acid peptide molecules **11** combining into a 38-residue cyclic peptide **12** where 36 amino acid residues are in the ring.<sup>25</sup> (Figure 1.11) This cyclization required a certain density of molecules on the resin; if the supported concentration was too dilute then it failed. Attempts to form a similar ring system but via closure with amide bond formation also were largely unsuccessful, indicating the peptide sequence itself is not predisposed to cyclize. Yields of the cyclodimer were reduced when more than 0.5 equivalents of copper were used, and the process was completely interrupted if an excess of a simple alkyne (but not of an azide) were included. Thus the cyclodimerization seems to be favored by low catalyst concentrations, and bringing alkyne units into proximity was more important than it was for the azides. In **11** the azide and alkyne are on the *N*- and *C*-termini, respectively, but this did not seem to be critical because a model peptide with reversed orientation also cyclodimerized well



(though some more monomer was formed, data not shown). On the basis of these observations it was proposed that the reaction proceeds via two alkynes bound to a dicopper intermediate where the azide units interact with the Cu-atom that is not attached to the alkyne of the same substrate.

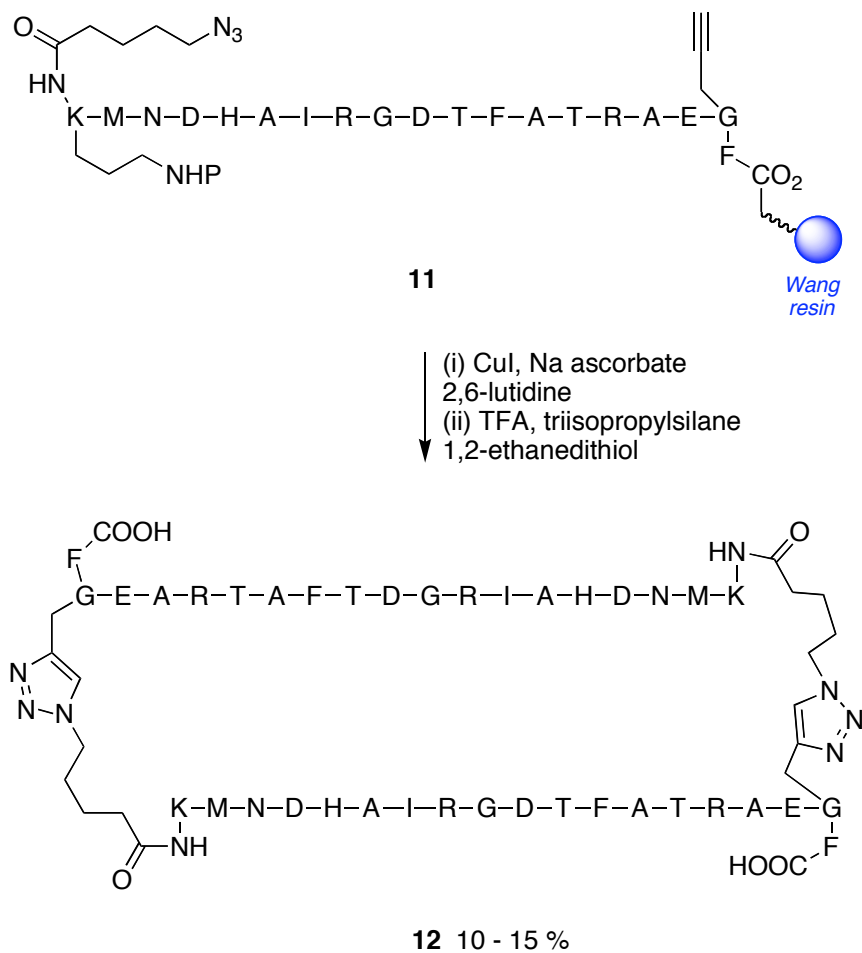


**Figure 1.11.** Preparation of a 38-residue cyclic peptide from cyclodimerization reaction.

Another surprisingly efficient macrocyclodimerization reaction occurred in syntheses of carbohydrate/amino acid hybrids as artificial receptors for small biomolecules. This time the click reactions were solution phase ones.<sup>26</sup> Various conditions were evaluated, and CuI combined with *N,N*-diisopropylethylamine in acetonitrile was best. Two similar substrates were investigated. These only differed by one amino acid residue, and both cyclized well (64 and 33 % before deprotection); Figure 1.12 shows the most efficient (the yield for the other was 33 %).

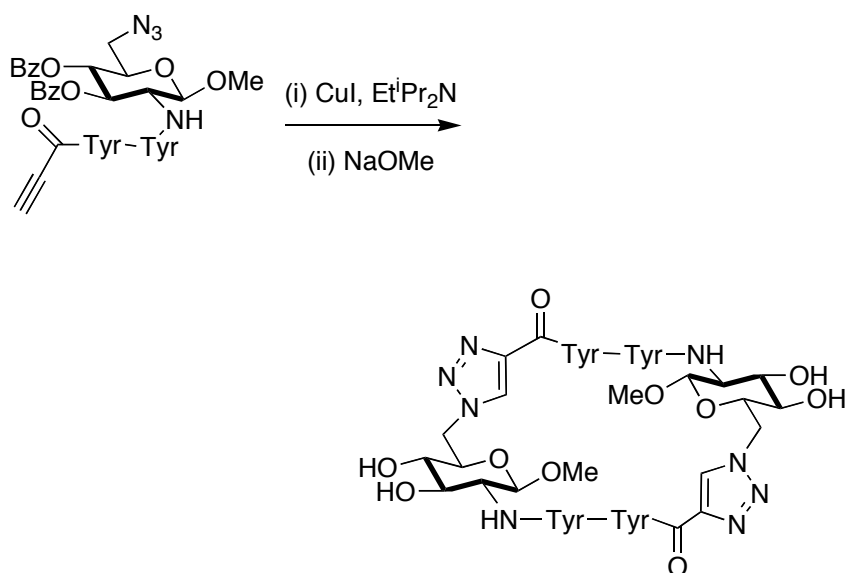
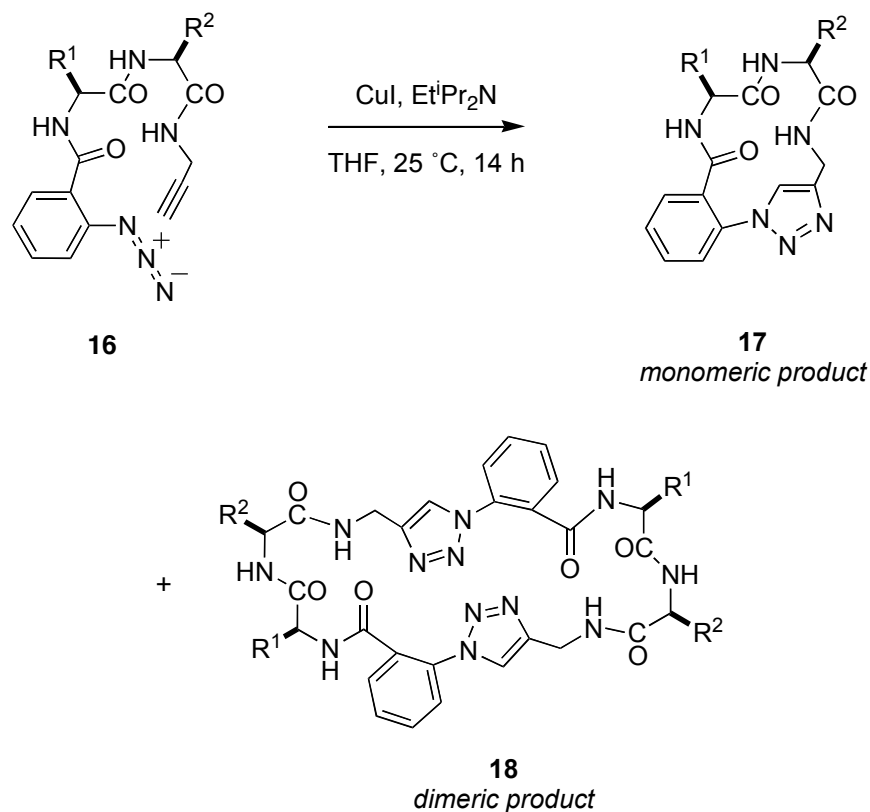


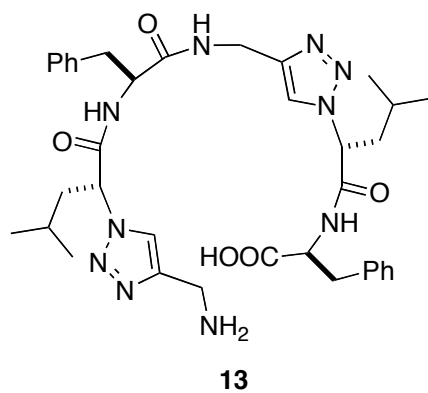
**Figure 1.12.** Syntheses of carbohydrate/amino acid hybrids.

Cyclic ditriazole **14** forms nicely organized nanotube structures in the solid state in which these doughnut-shaped molecules pack on top of each other via H-bonds. Originally monomers **14** were prepared via an amide bond forming reaction from linear peptidomimetic **13** (the yield for that step was 65 %).<sup>27</sup> Conversion of the alkyne/azide **15** into that same product was vulnerable to simple cyclization and to formation of

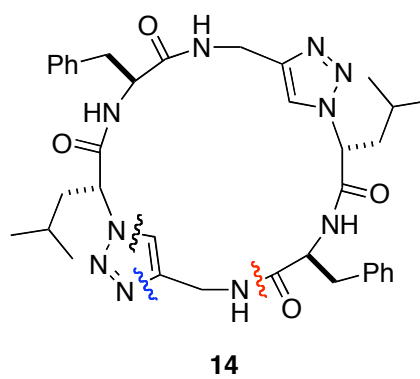
polymeric products. However, in the event, the macrocyclodimerization of the *N*-protected substrate **15** was shown to be quite efficient. A 94:6 mixture of the desired product **14** and the corresponding cyclotrimer was formed in this process, from which **14** was isolated in 80 % yield.<sup>28</sup>

Another solution-phase illustration of macrocyclodimerization in this area featured eight different azidoalkyne dipeptide substrates **16**, prepared via solution phase methods.<sup>29</sup> Mixtures of the monomeric and dimeric products **17** and **18** formed when these substrates were subjected to the copper-mediated bis-triazole formation reaction. The ratios of monomer-to-dimer ranged from 54:46 to 18:82, and the dimeric product was prevalent in all but one case.

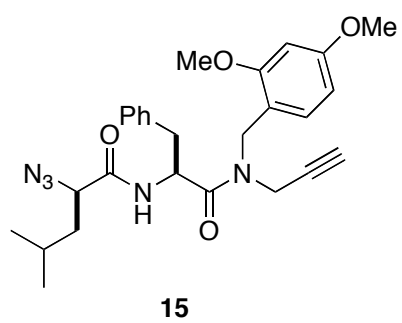
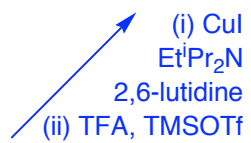




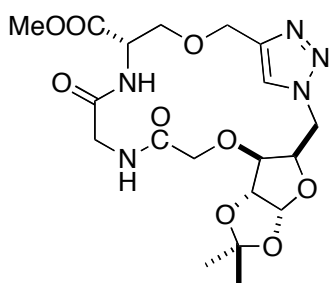
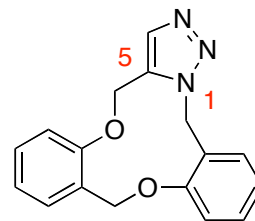
*cyclization via amide bond formation*



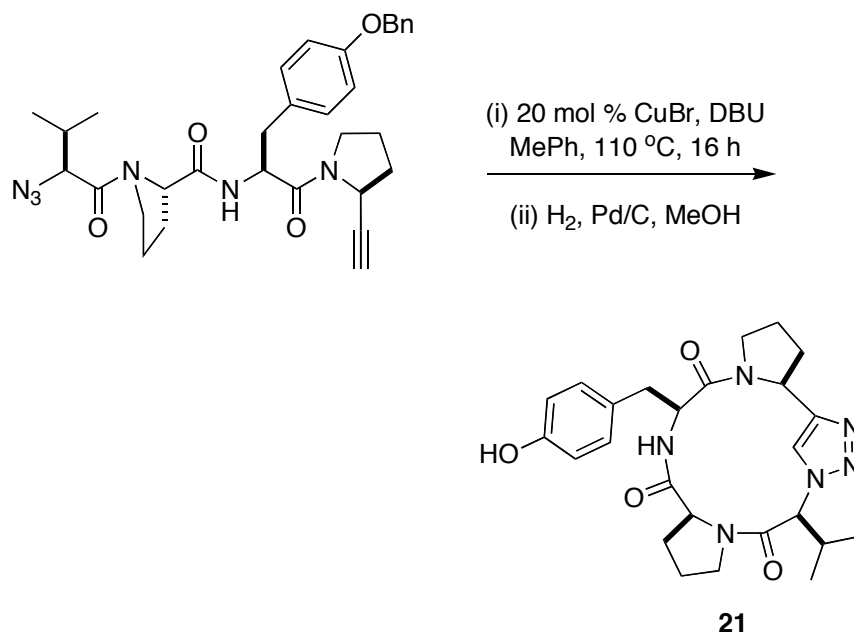
*cyclization via triazole formation*



Based on the examples given above, formation of macrocyclodimers can be expected, but it will not *always* occur. For example, compound **19** was one of four similar compounds prepared via Cu-mediated triazole formation to close 12- to 17-membered rings. No macrocyclodimers were observed in these cases, even though the researchers looked for them. Compound **20** is a 1,5-disubstituted triazole formed via the Cu-mediated process.<sup>30</sup> This is *highly* unusual for this type of reaction. It is tempting to assume that this product formed because of some particular constraint that prevented formation of the expected 11-membered ring. However, if that is the case, then a similar stereoelectronic constraint prevented formation of the macrocyclodimer from 1,4-triazoles. Clearly there are some unresolved issues surrounding this work.

**19****20**

Another anomaly is the synthesis of the cyclic triazole tetrapeptide **21** (a potential tyrosinase inhibitor).<sup>31</sup> Attempted cyclization by peptide bond formation at room temperature failed to provide the desired product: mixtures of dimers and higher oligomers were obtained. The copper (I) catalyzed azide-alkyne coupling was successful but only at 110 °C; the triazole tetrapeptide **21** was isolated in 70 % yield under these conditions. It is surprising to us that the reaction took such a high temperature (intermediate temperatures were also studied), and that no macrocyclodimer was observed.



At least one other example of a macrocyclization reactions that gives only cyclic monomers has been reported. This did not involve peptides or peptidomimetics.<sup>32</sup>

## 1.4 Compounds With Triazole Links to Other Functionalities

### 1.4.1 Carbohydrate- peptide

Glycopeptides are important compounds with a range of biological functions. Native *O*- and *N*-linked glycopeptides are relatively unstable to hydrolysis, but *C*-linked isosteres are far more robust to chemical and enzymatic degradation. They have potential as probes for glycopeptide biological activities and as drug candidates for diseases involving carbohydrate-based metabolic disorders.

*C*-Linked glycopeptide analogs like **23** can be formed very conveniently via Cu-mediated cycloadditions to carbohydrates with anomeric alkyne groups, *eg* **22**. This type of chemistry has been investigated by at least two groups using glucose- (Figure 1.13) and galactose-based starting materials.<sup>33-35</sup>

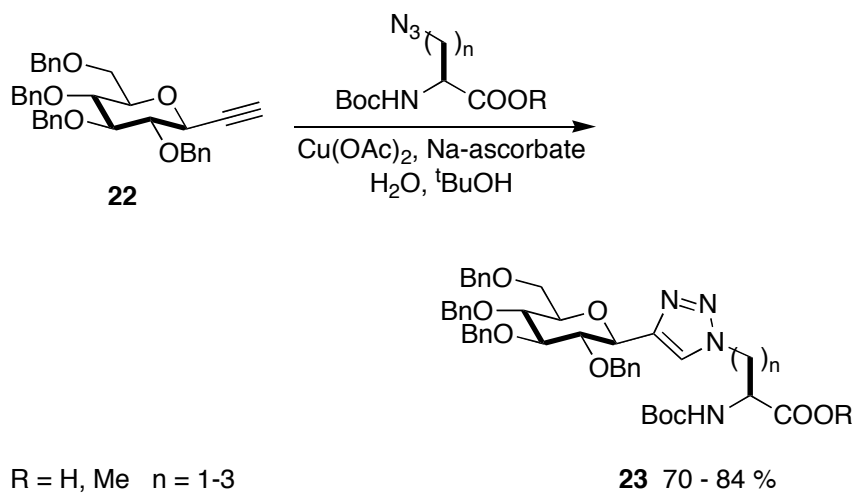


**Figure 1.13.** Synthesis of *C*-linked glycopeptide analogs.

*N*-Linked glycopeptides **25**, where the *N*-atom is part of the triazole, can be formed by reversing the orientation of the two functional groups in the Cu-mediated reaction. Thus, glycosidic azides, like **24**, can be coupled with alkyne-containing amino acids to give carbohydrates where the triazole is attached to the anomeric position (Figure 1.14).

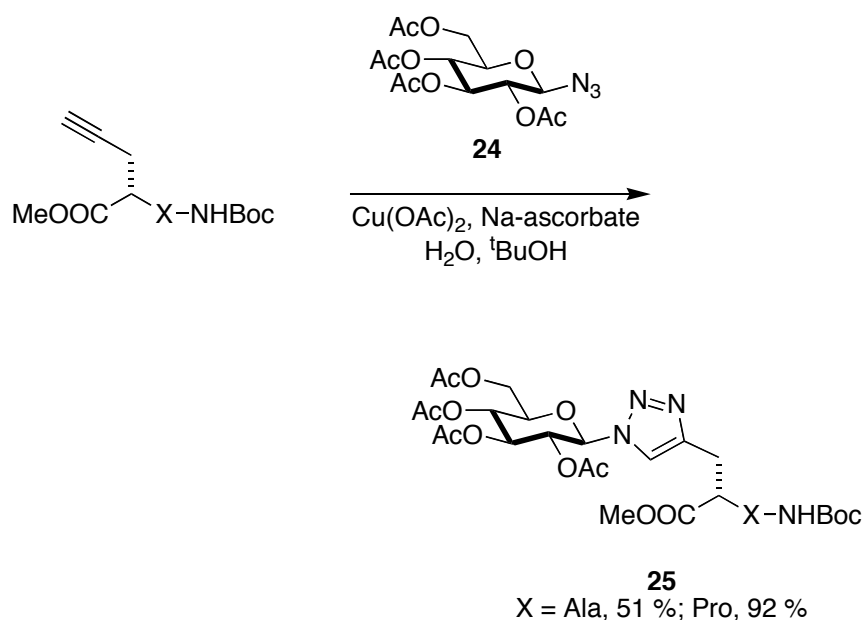
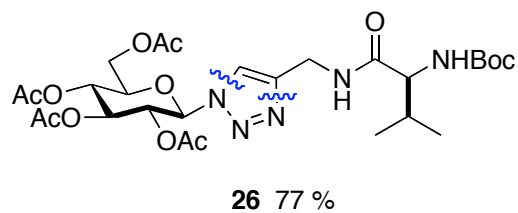


**Figure 1.14.** Synthesis of *N*-linked glycopeptide analogs.

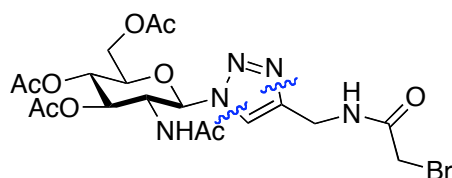
Anomeric azides<sup>36-40</sup> and unsaturated amino acid derivatives<sup>41</sup> are readily accessible so this chemistry has quite a wide scope. Indeed, one of the easiest ways to prepare unsaturated amino acids is to add an *N*-propargyl group; such substrates have also been investigated as click partners to make glycopeptide analogs like **26**.<sup>42</sup>



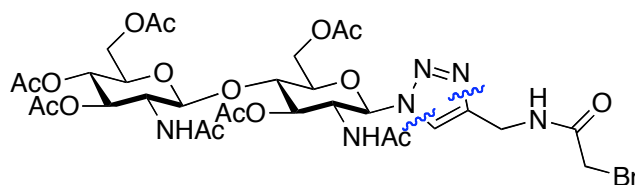
Mono- and disaccharide alkylating agents **27** and **28** have been prepared via the Cu-mediated click process, and used to couple with cysteine residues in a peptide.



Glycopeptide analogs produced in this way are compatible with native ligation methods involving *C*-terminal thioesters and *N*-terminal Cys-residues. Large peptides containing several unnatural *S*-linkages to carbohydrates have been prepared in this way.<sup>43</sup>

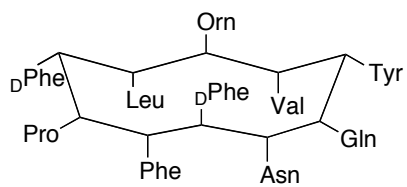
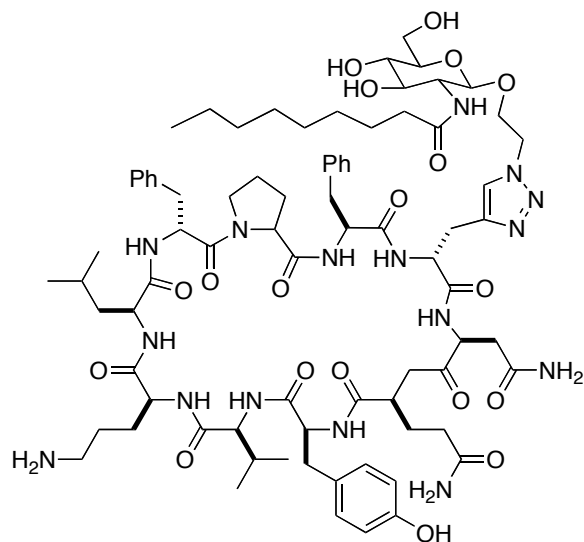
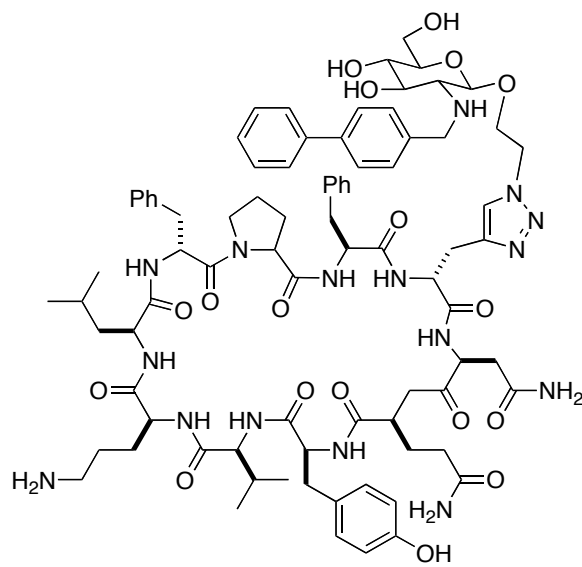


**27** 100 %

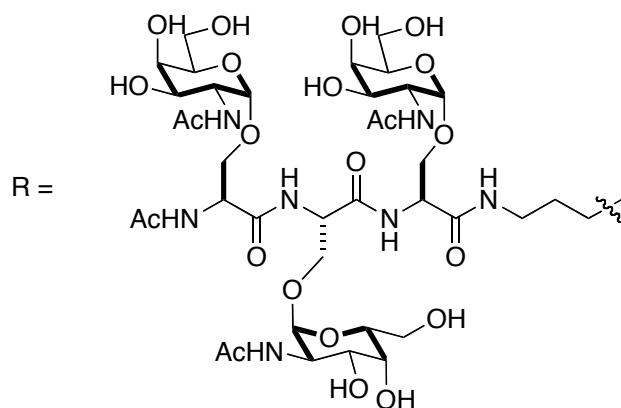


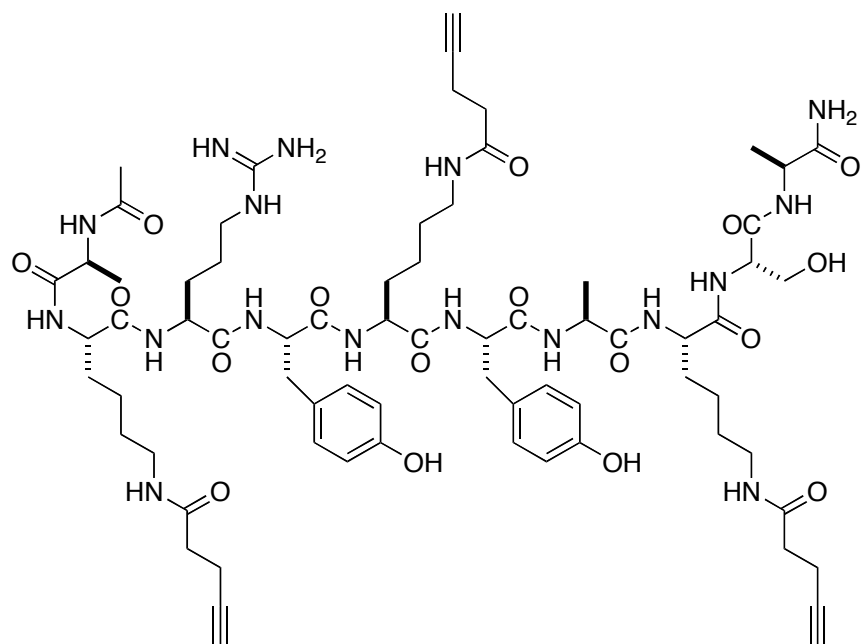
**28** 87 %

One of the most elaborate routes to glycopeptide analogs has been reported by Lin and Walsh.<sup>44</sup> They were motivated to prepare glycosylated forms of the cyclic peptide antibiotic known as tyrocidine or “Tyc”. To do this, about 17 linear decapeptides were prepared on a solid phase having the Tyc sequence except that one, two or three propargyl glycine residues had been substituted at select positions. These linear peptides were derivatized as *N*-acetyl cysteamine esters to facilitate chemoenzymatic cyclization using the excised thioesterase domain of tyrocidine synthetase. This afforded a small library of cyclic peptides containing one to three propargyl side chains. These were reacted with 21 different azidomonosaccharide derivatives to give a range of glycosidated Tyc analogs having triazole-based linkages to the sugar parts (Figure 1.15).

**a****tyrocidine (Tyc)****b****Tyc4PG-14****Tyc4PG-15****Figure 1.15.** (a) Tyrocidine; and (b) some of the analogs prepared.

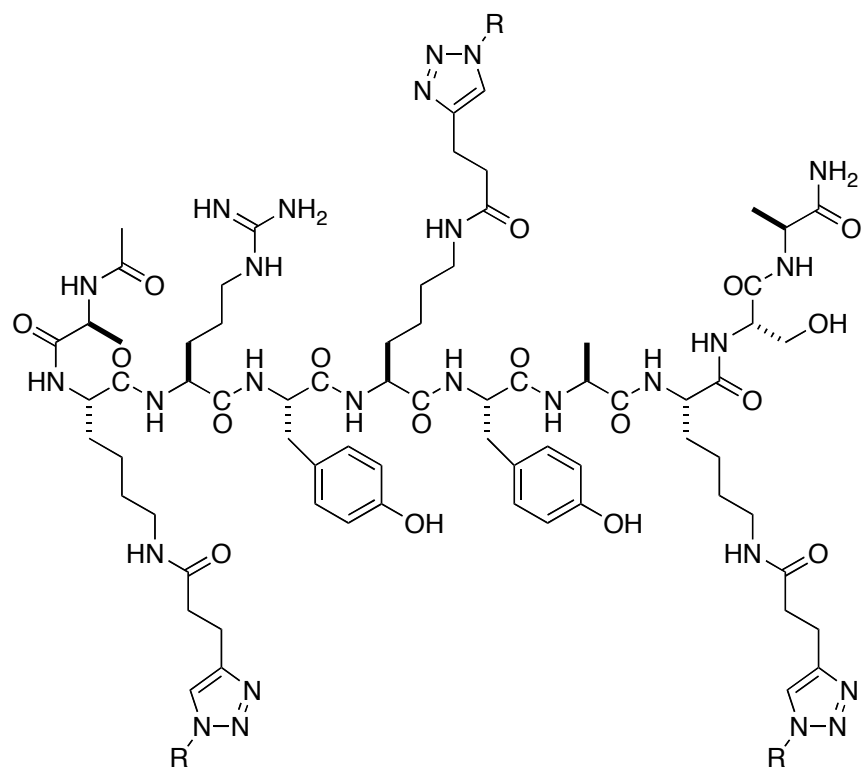
Another way to take advantage of the exquisite chemoselectivity of the copper-mediated cycloaddition reaction is to conjugate carbohydrate based antigens onto peptide substrates. The Danishefsky group has done this for a model peptide system, and infer that the same approach will work for proteins.<sup>45</sup> In this study, the model peptide system **29** was coupled with a trisaccharide antigen to provide the immunogenic conjugate **30**. If this approach is to be applied to proteins, it requires chemoselective introduction of alkyne or azide groups otherwise the labeling is non-uniform.





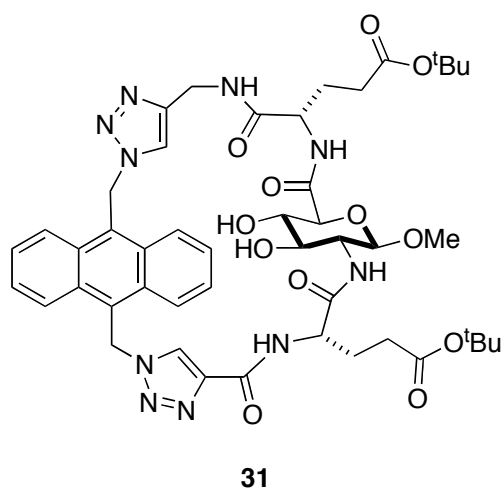
29

R-N<sub>3</sub>, Cu nano powder  
↓ phosphate buffer, pH = 7.2, 2 h

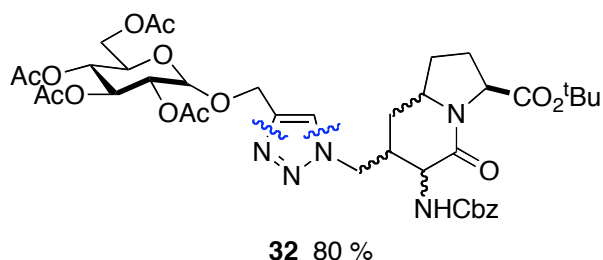


30

Carbohydrates can also form the basis of macrocyclic molecules for molecular recognition. Compound **31** is representative of a molecule prepared for this purpose.<sup>46</sup> It has a fluorescent reporter group (anthracene-based) which forms a hydrophilic face with the two triazole units. No specific target was suggested for this potential host molecule, though clearly the amino acid and sugar units might be varied to accommodate different hosts.



Finally, less peptidic peptidomimetics can also be fused to carbohydrate residues using the Cu-mediated reaction. An illustrative example is compound **32** wherein a conformationally restricted analog of the Ala-Pro dipeptide was joined with a glucose-based azide (and with fluorescein and biotin in other experiments, not shown).<sup>47</sup>



### 1.4.2 Organic- peptide

Alkyne- or azide-modified peptides can be transformed into a variety of structures beyond glycopeptide analogs. The last section briefly mentioned cases in which Cu-mediated cycloadditions were used to add biotin and fluorescein: these are clearly two very useful types of molecular probes for bioconjugation. The Cu-promoted process also provides convenient access to structural diversification for medicinal chemistry. For instance, *cis*-4-azidoproline was substituted for the Pro<sup>6</sup> residue in the dodecapeptide RINNIPWSEAMM to allow for preparation of a range of analogs via the Cu-promoted reactions with azides. Routine peptide synthesis methods were used to incorporate this azido-residue. The parent sequence was discovered via phage display; it binds to the gp120 protein of HIV-1 and prevents the HIV virus docking with CD4 cells. Preparation of over 20 derivatives via Cu-mediated click chemistry, and testing these for gp120 binding revealed addition of phenyl acetylene as shown in Figure 1.16 gave approximately a 500-fold increase in binding.<sup>48</sup>

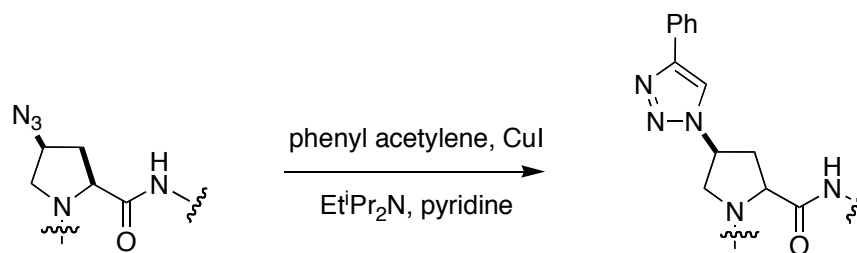
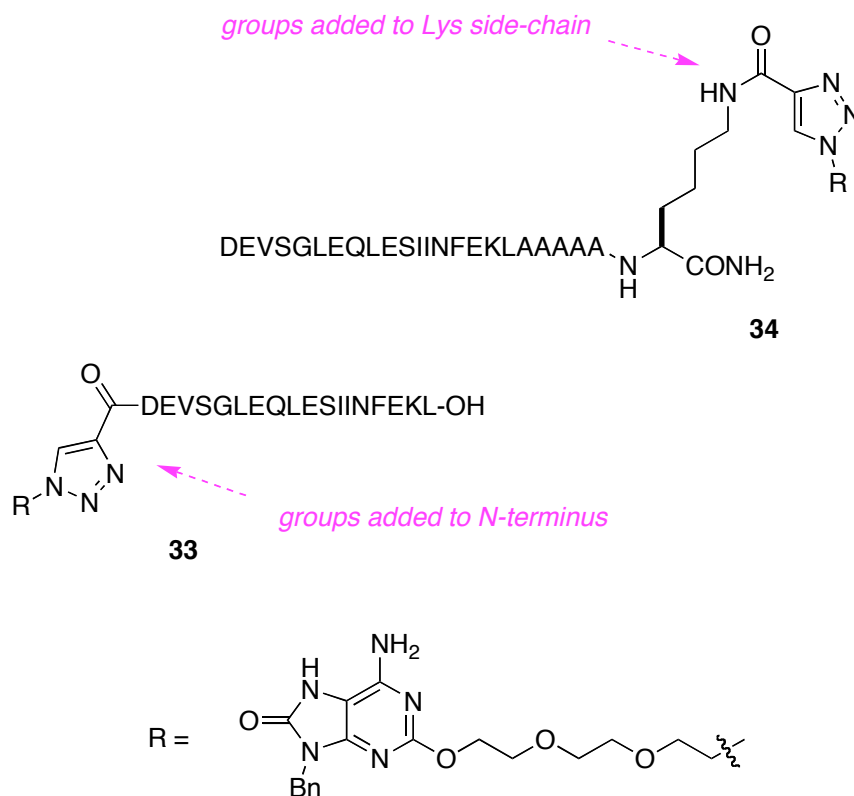


**Figure 1.16.** Preparation of triazole derivative of dodecapeptide.

Incorporation of azidoproline residues is quite a specialized modification; it is essentially only valuable for parent peptides containing proline and for modifications at that position. On the other hand, one of the simplest and most general approach to peptidomimetics of extended peptides is to couple propiolic acid to either the *N*-terminus or the to the side chains of Lys or Orn residues, then make modifications via the Cu-mediated cycloaddition process. This was done, for example, to peptide chains containing the SIINFEKL sequence (a major histocompatibility {MHC} class 1 epitope) to access derivatives **33** and **34** with conjugated 2-alkoxy-8-hydroxyadenine entities.<sup>49</sup>



### 1.4.3 Polymer- and Dendrimer- peptide

Most amphiphilic molecules are relatively small structures, like detergents. However, it is possible to make “amphiphilic-nanostructures” containing large, water-soluble, biomolecules attached to hydrophilic polymers of a comparable size. Copper-mediated cycloaddition reactions provide a convenient way to do this. In the example shown in Figure 1.17, bovine serum albumin was attached to a polystyrene fragment via this approach. Aggregates of the product molecules **35** were visualized via various microscopy techniques (SEM and TEM).<sup>50</sup>

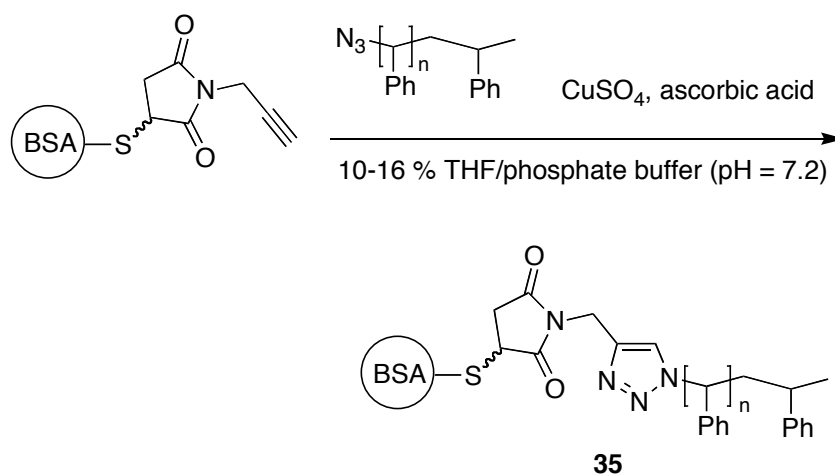
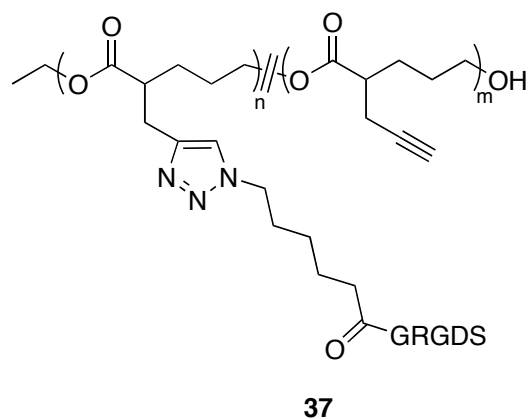
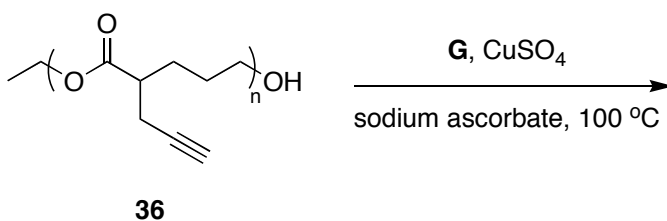
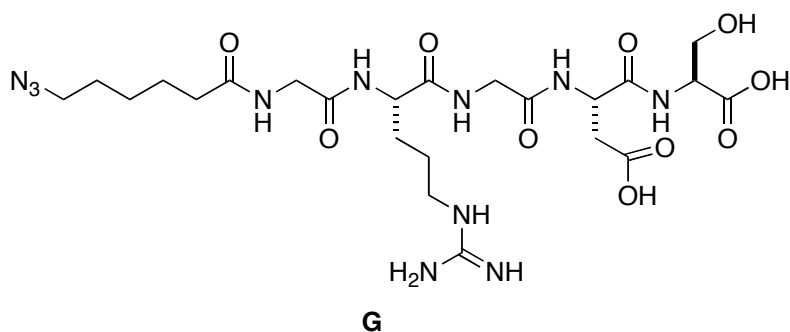


**Figure 1.17.** Bovine serum albumin was attached to a polystyrene fragment.

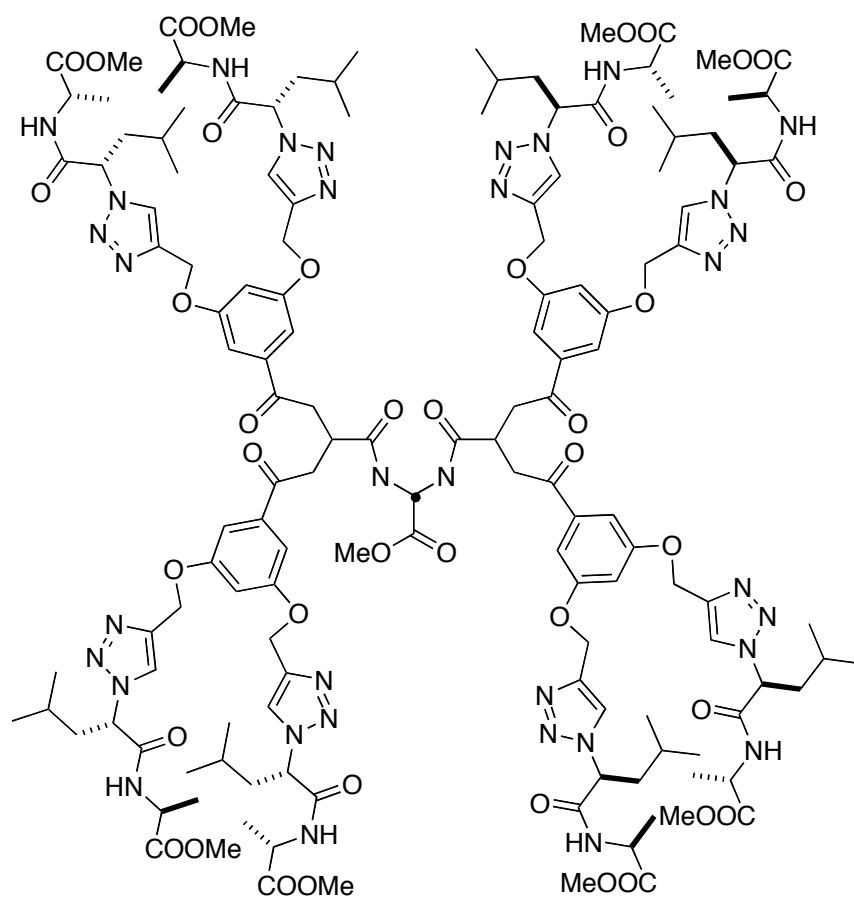
Polyesters are less chemically stable than polystyrene derivatives, but the conditions for Cu-mediated cycloadditions are sufficiently mild for their elaboration. Consequently, the polyester **36** from  $\epsilon$ -caprolactone was efficiently grafted with the RGD-containing azidopeptide **G** peptide to give the biomaterial **37** without a significant change in the polydispersity.<sup>51</sup>



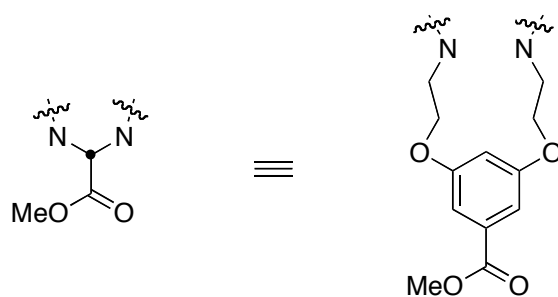


Click reactions can be used to elaborate dendrimers. Sharpless, Fréchet and co-workers used alternating Cu-mediated cycloadditions and  $S_N2$  substitutions to build up dendrimer cores.<sup>52</sup> So far, in the area of peptidomimetics, the Cu-mediated cycloadditions have only been used to add peptide residues to dendrimer surfaces. Thus, multivalent dendrimeric peptides like **38** were synthesized. The coupling reactions were slow and not high yielding under the regular conditions. However, microwave irradiation for 10 min to generate a temperature of 100 °C greatly accelerated the process and yields as high as 94 % for a fourth generation system elaborated with eight end

groups. Azide derived amino acids, linear- and cyclic peptides were coupled.<sup>53</sup>



38



Chloromethylpolystyrene and similar supports are easily transformed into the corresponding azides via simple nucleophilic displacement reactions. The azido resins so produced can be further functionalized by click reactions to add linkers. Figure 1.18 shows how this approach was used to prepare a indole-based backbone amide linker **39** (BAL).<sup>54,55</sup>

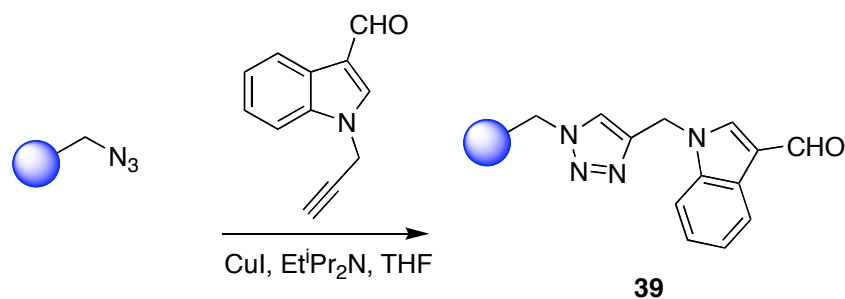
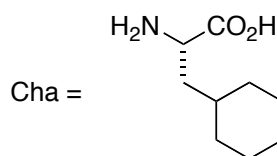
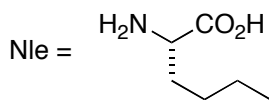
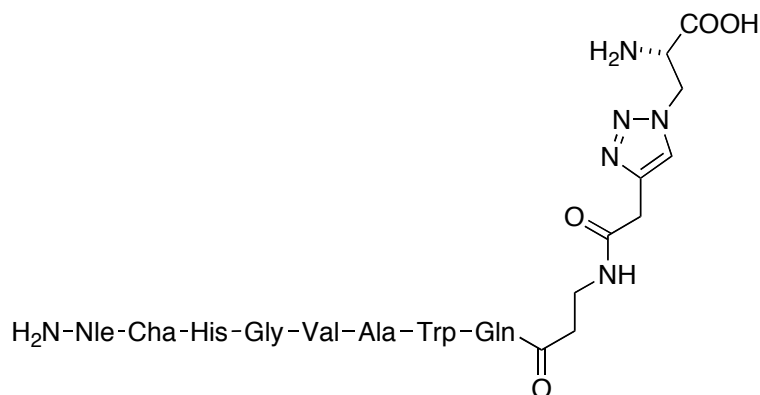
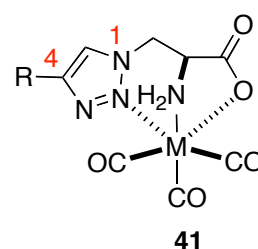
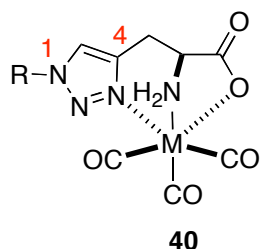


**Figure 1.18.** Indole-based backbone amide linker.

### 1.4.3 Conjugates of Metal Complexes for Radiolabeling

Triazoles are good ligands for transition metals. Peptides (or other biomolecules, in fact) can be *C*- or *N*-terminated with an amino acid derived alkyne or azide, then “clicked” with the complement in a copper catalyzed cycloaddition. This procedure fulfills two objectives simultaneously. First, it introduces a metal binding site onto the peptide. Second, the triazole linkage is itself part of the metal-ligand. The obvious application of this approach is in labeling bio-active peptides for imaging in cells or *in vivo*. Thus, complexes of the type **40** and **41** have been prepared, where the triazole units have different orientations but are still disposed to coordinate with metals. Technetium complexes of the derivatized peptide **42** have been prepared for this purpose.<sup>56</sup>



## 1.5 1,2,3-Triazoles in Less Peptidic Compounds

### 1.5.1 Peptoids

Peptoids (*N*-alkyl oligoglycines) are in some ways representative of molecules that bridge the gap between peptidic molecules and more organic based structures. The attractive feature of peptoids is that they are formed from primary amines, and a large selection of these is commercially available. If amines that are also functionalized with terminal alkynes are used, then Cu-promoted cycloadditions of azides can be used to increase the diversity even further. This elaboration could be done on each addition of an alkyne, or globally to every alkyne in the sequence prepared. The latter approach was

taken in the one paper that has appeared so far on combining peptoids and catalyzed azide/alkyne cycloadditions.<sup>57</sup> In fact, the peptoids were derivatized while supported on a resin, then cleaved. Fluorophores, nucleobases and other peptoids were conjugated and yields of up 96 % were obtained, *eg* Figure 1.19.

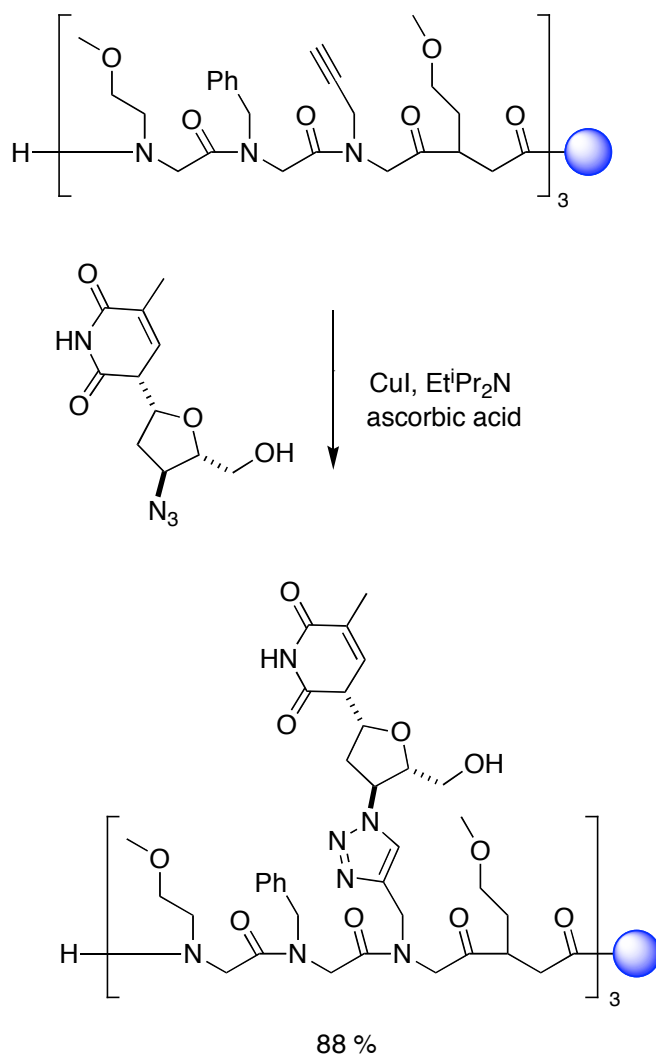
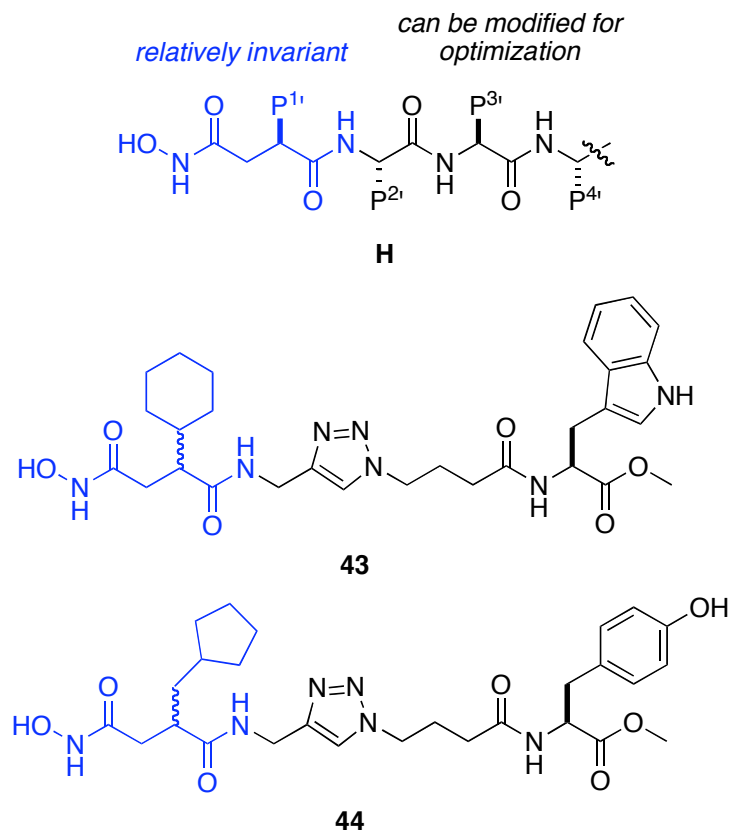


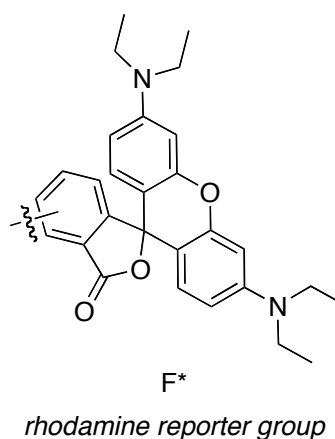
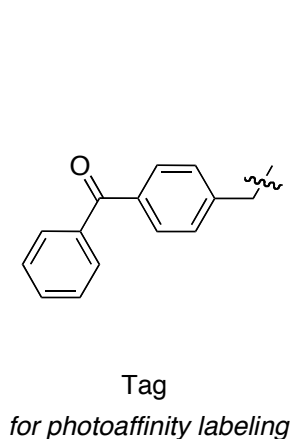
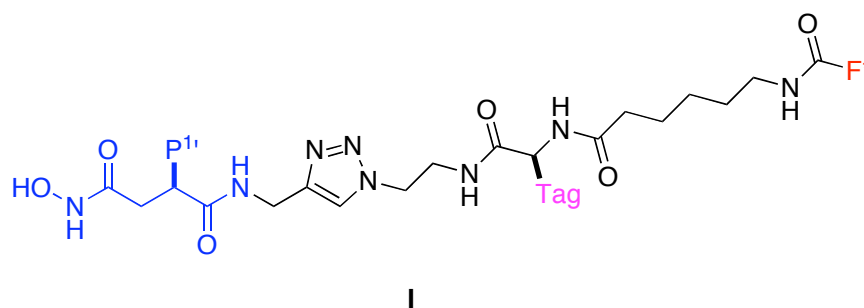
**Figure 1.19.** Peptoids were derivatized with triazoles while supported on a resin.

### 1.5.2 Non-peptidic Mimics Where Triazoles Replace Amides

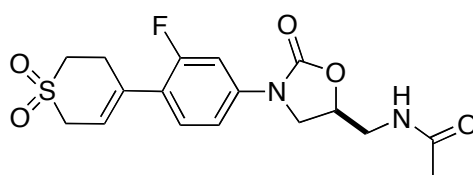
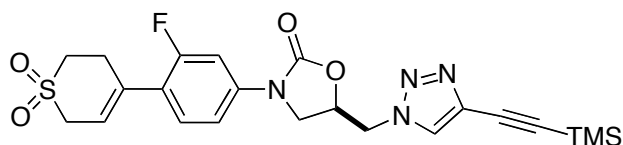
In medicinal chemistry, Cu-promoted cycloaddition reactions can be valuable in cases where a particular structural element is almost invariably required, but others are to be joined to it to promote high affinity, potency, and/or selectivity. A good example of this is in design of analogs of the matrix metalloprotease inhibitor type **H** where the hydroxamate dipeptide mimic (shown in blue) is essential for binding metals in these enzymes, and the other part can be varied. Thus a library of mimics including compounds **43** and **44** were conveniently produced and tested. These two molecules were selected from the library on the basis of selective binding to, and inhibition of, the MMP-7 enzyme relative to thermolysin and collagenase.<sup>58</sup>



In a sequel to the work above, 12 compounds **I** were prepared to test the effects of the P<sup>1'</sup> substituents on binding and selectivity.<sup>59</sup> To this the Eastern portion of the molecule was engineered to include a photoaffinity tag and a fluorescent label. Irradiation of the compounds with the enzymes anchored the photoaffinity tag, and the extent of the bound fluorescence was taken as a measure of the affinity. This approach assumes that all the enzymes have identical affinities for the Eastern segment, and that the extent of photobleaching is uniform for all the substrates. If these are valid assumptions, then the method facilitates rapid assay of binding and selectivity.



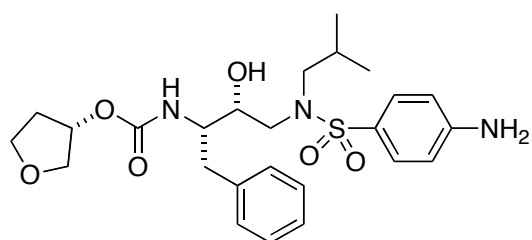
1,2,3-Triazoles with small 4-substituents can be useful as replacements for acetamide groups. A simple illustration of this is the lead structure **45** that was mimicked with triazole **46**. This was done to find analogs that would not display undesirable monoamine oxidase A side-effects but maintain the antibacterial properties. In the event, this was part of a much more extensive study and the compound formed by removal of TMS **46** emerged as an interesting lead.

**45****46**

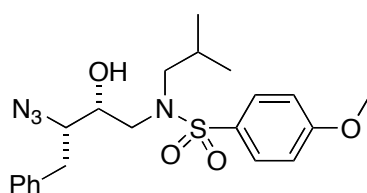
Amprenavir is one of the commercially available HIV-1 protease inhibitors. A library of 100 mimics of this structure was produced from the two starting azides **47** and **48** (accessible via diazo transfer chemistry to the amine, and via epoxide opening, respectively). These segments were joined with alkynes via Cu-mediated cycloadditions, and triazoles **49** and **50** emerged as potent inhibitors of both the wild type protease, and of three different mutants.<sup>60</sup> Intriguingly, when these compounds were cocrystallized with HIV-1 protease, the triazole unit revealed itself as an effective surrogate for the amide bond.<sup>61</sup> It has a large dipole moment (bisecting the ring plane near atoms N3 and C5) and the N2 and N3 electron lone pairs can function as hydrogen bond acceptors. In the specific case of **49**, the N2 atom serves as a H-bond acceptor



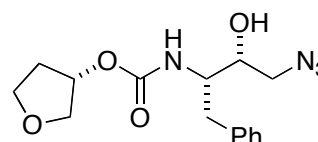
surrogate for the amide carbonyl of substrates in the protease. Further, the C5H serves as a hydrogen bond donor effectively mimicking the substrate amide NH.



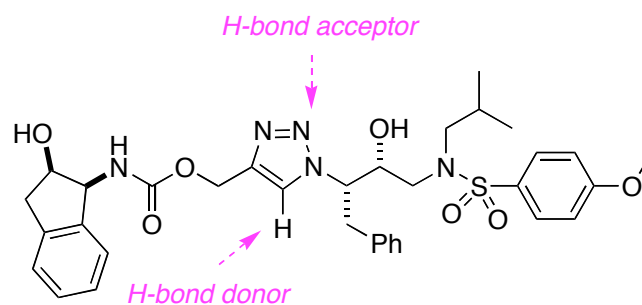
**amprenavir**



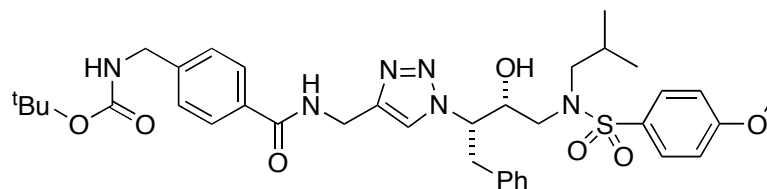
**47**



**48**

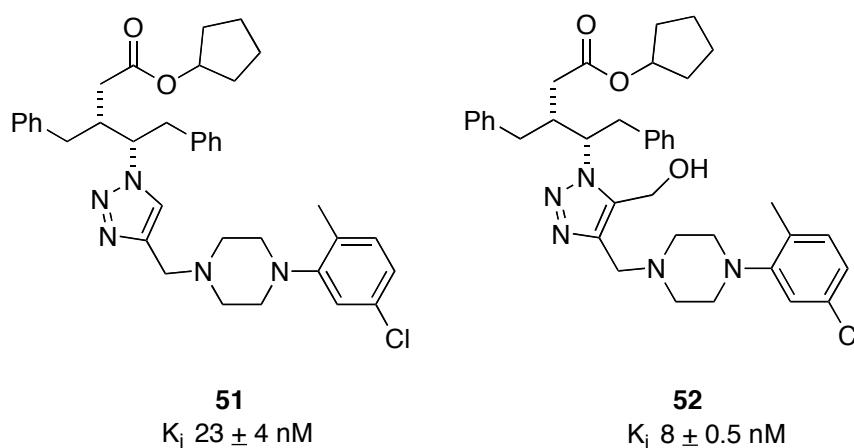


**49**



**50**

Sharpless and co-workers have prepared a series of compounds as potential HIV-1 protease inhibitors.<sup>62</sup> Molecular modeling indicated that triazole sub-units based on 1,2-amino azides, derived from amino acids, would be useful. Consequently, successive iterations of synthesis and testing led to the development of compounds **51** and **52**, which are nanomolar inhibitors. The latter compound was formed via a copper-mediated cycloaddition, followed by directed metalation and quenching with formaldehyde.

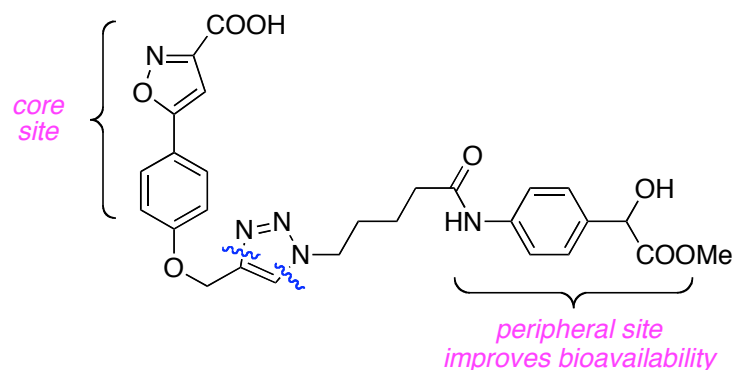


### 1.5.3 Other Non-peptidic Peptidomimetics

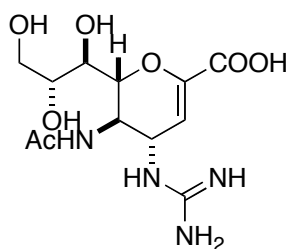
In many other branches of medicinal chemistry, triazoles from the click reaction have been used to extend molecules or replace similar functional groups.<sup>63</sup> This review focuses on peptidomimetics, so the discussion in this sub-section is restricted to compounds where the native substrate is a peptide, even if the synthetic analogs are not peptidic at all.

Inhibitors of tyrosine phosphatases may act via the active site or they may bind the enzyme peripherally. Moreover, some inhibitors have poor pharmacokinetic properties. Therefore, a logical approach to discovery of new inhibitors is to join two active segments into one molecule, and Cu-mediated cycloadditions are ideal for this.<sup>64</sup>

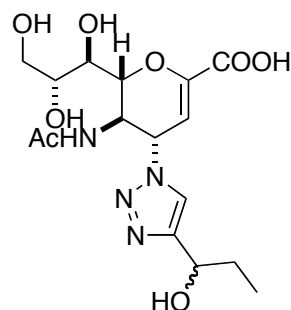
Compound **53** emerged from a library of 66 “bivalent” compounds prepared in this way; it inhibits protein tyrosine phosphatase 1B with an  $IC_{50}$  of 4.7  $\mu$ m.



Compound **54** is one of 16 triazole-based zanamivir analogues that were formed via Cu-mediated cycloadditions. Zanamivir is a licensed pharmaceutical that acts via inhibition of neuramidases. In the analog, the triazole is acting as a mimic of the guanidine functionality. Compound **54** showed moderate inhibition against avian influenza virus (subtype H5N1) in a cellular assay.<sup>65</sup>

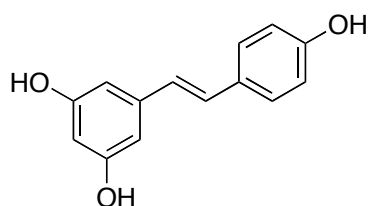
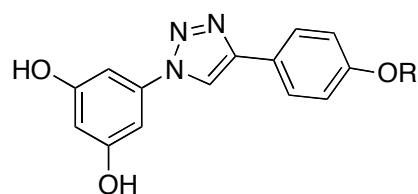


**zanamivir**

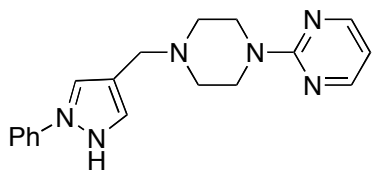


**54**

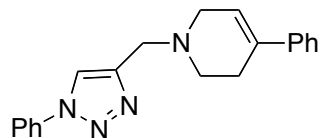
Resveratrol is a phytoalexin (antibiotic produced by plants under attack) displaying an array of biological activities. The problem with this compound is that it has a diverse array of activities at high concentrations. This has motivated research to find analogs by replacing the alkene with a triazole functionality, formed by the copper-mediated cycloaddition (and by other small heterocycles).<sup>66</sup> Compounds **55** were thus found to be more potent than the lead compound in cytotoxicity/antiproliferative assays.

**resveratrol****55**  
R = H , Me

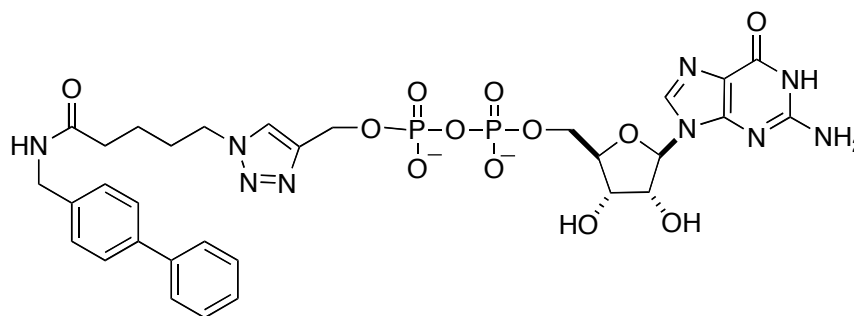
The lead compound NGD94-1 is a selective ligand for the D4 dopamine receptor. As part of a larger study, three compounds were prepared in which the triazole unit replaces the pyrazole part. The *N*-phenyl compound **56** had a  $K_i$  value of 3.2 nM for dopamine D4 receptor.<sup>67</sup>



NGD 94-1

**56**

A library of 85 GDP-triazole compounds has been synthesized and screened for inhibition of fucosyltransferase activity.<sup>68,69</sup> It is known that the most important binding determinant was in the GDP part of inhibitors, but the azide function was added to screen for increased binding. Compound **57** was identified as a promising hit ( $IC_{50}$  0.15 - 1.00 mM) depending on the enzyme used.

**57**

Ellman and coworkers have used a substrate-based screening method to identify key segments of inhibitors of the cysteine protease cathepsin S, which is implicated in autoimmune diseases.<sup>70</sup> In the first step, acylated amino coumarins were screened to find the most appropriate functionality at the *N*-terminus via the method indicated in Figure 1.20. The preferred acyl groups contained some triazoles derived from click products. It was later shown that simple replacement of the coumarin with a hydrogen gave potent inhibitors, including compounds **58** and **59**.

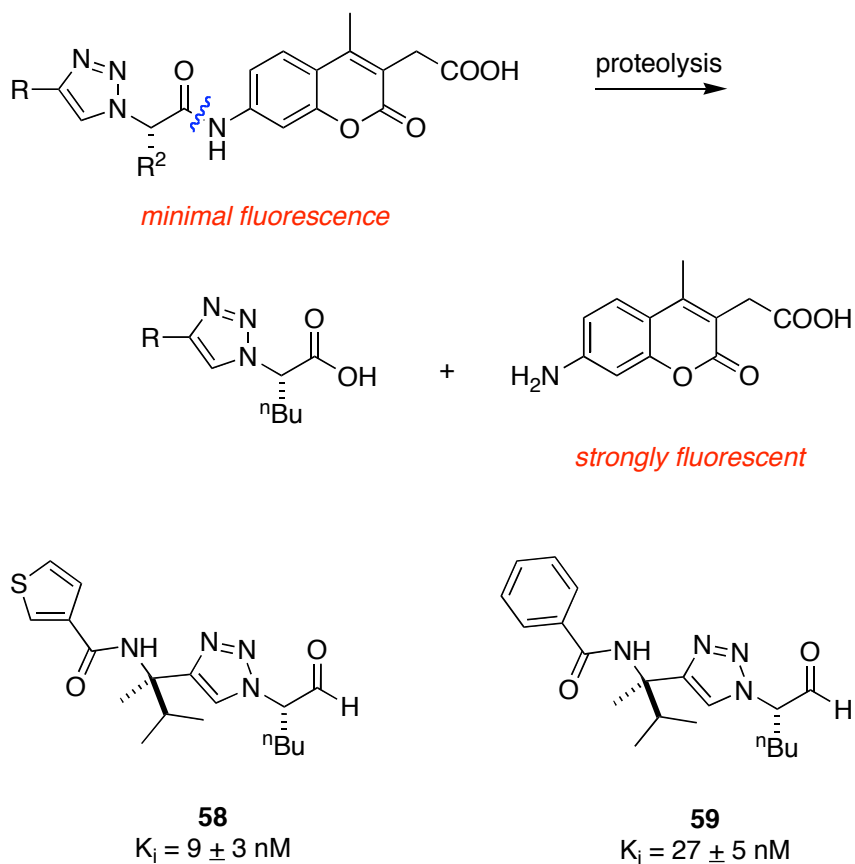


**Figure 1.20.** Triazole derived inhibitors of cysteine protease cathepsin S.

Copper-mediated cycloadditions can be used to elaborate selected parts of libraries that contain terminal alkyne or azide functionalities. For instance, split syntheses were recently used to produce a 10,000-membered library of which 78 compounds contained triazoles.<sup>71</sup> Such applications are beyond the focus of our research.

## 1.6 Conclusion

Copper-mediated cycloadditions proceed via pathways that feature activation of the alkyne part via coordination, then non-concerted cycloaddition of the azide component. This pathway is relatively unique, accounting for the superb chemoselectivity of the reaction. That chemoselectivity can be used in many ways. For instance, when alkyne or azido peptide units combine via this pathway the reaction is relatively insensitive to the amino acid side-chains. This serves as an excellent way to make peptidomimetics, particularly because there is some stereoelectronic similarity between 1,2,3-triazoles and amide bonds. Research on the three dimensional consequences of incorporating triazoles into peptides is at an early stage, and this is an exciting area for future studies. Further, Cu-mediated click processes can be used to conjugate peptides to carbohydrates, organic molecules, polymers, dendrimers, and labeling agents. Finally, 1,2,3-triazole cores may form the basis of small molecule pharmaceutical leads in which they fulfill some binding function of peptides, even though the molecular resemblance of these compounds to peptides is obscure.

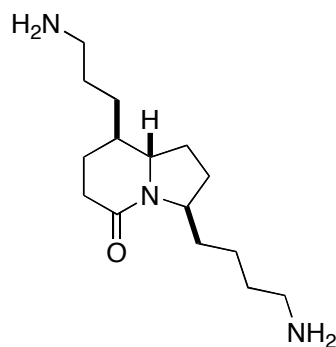
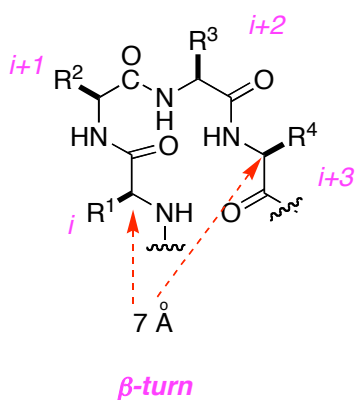
There are some disadvantages of copper-mediated click reactions. They use azides and copper, both of which pose safety- and environmental-hazards. Further, macrocyclization reactions can be complicated by somewhat mysterious macrodimerization events. Nevertheless, the fact that there are convenient routes to amino-acid-derived azides and alkynes, and the lack of practical obstacles to executing these Cu-mediated reactions, both point to a strong future for the peptidomimetics formed via this route.

## CHAPTER II

### RING CLOSURE TO BETA-TURN MIMICS VIA COPPER CATALYZED AZIDE ALKYNE CYCLOADDITIONS

#### 2.1 Introduction

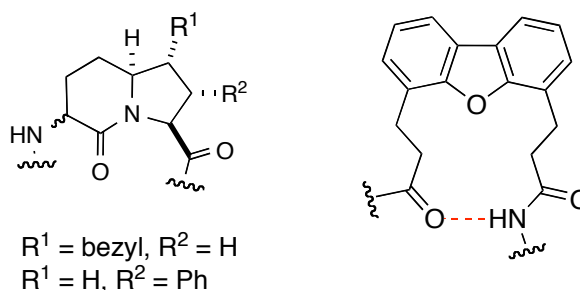
$\beta$ -Turn motifs are important targets for mimicry, both because they allow a protein chain to fold back upon itself to form a compact structure and because they are important recognition sites in peptides and proteins and often involved in protein-protein interactions. A wide variety of  $\beta$ -turn types are observed based on their topological features. Unlike  $\alpha$ -helices and  $\beta$ -sheets, the backbone conformation of  $\beta$ -turns is highly variable and any tetrapeptide sequence in which the  $\alpha C_i$ - $\alpha C_{i+3}$  distance is less than 7 Å is a  $\beta$ -turn.<sup>72</sup> The turn conformation can be stabilized by chelation of a cation, such as  $Ca^{2+}$ , or intramolecular hydrogen bonds. Kahn *et al* reported the very first  $\beta$ -turn mimic synthesis in 1986.<sup>73</sup> This indolizidinone mimic of the tuftsin tetrapeptide exhibited some bioactivity in a dose dependent manner.



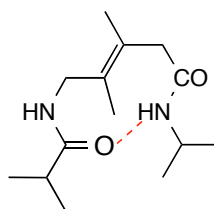


In the past two decades, many groups have been interested in syntheses of  $\beta$ -turn peptidomimetics that have potential applications in medicinal chemistry.<sup>74,75</sup> Cyclic structures were first synthesized as turn mimics in the mid-1980s and continue to be used for this purpose. Hruby et al<sup>76</sup> reported the synthesis of 6,5-bicyclic lactams that incorporate amino acid side chains in the appropriate position. Kelly et al<sup>77</sup> have used dibenzofuran units as turn mimics to align two peptide strands into a parallel  $\beta$ -sheet like structure. More recently, alkenes containing acyclic compounds have been developed and the alkene units in these compounds mimic the amide bonds that would be present in natural turns. Allylic strains and other acyclic conformational effects were explored in these turn mimics. Gardner et al<sup>78</sup> have reported the synthesis and conformational analyses for molecules containing trans-5-amino-3,4-dimethylpent-3-enoic acid residue (ADPA). A combination of NMR and IR data for the ADPA containing peptide analogues reveals that  $\beta$ -turn and  $\beta$ -hairpin-like folding is promoted in dichloromethane solution.

#### cyclic $\beta$ -turn mimics



#### acyclic $\beta$ -turn mimics



In our laboratory we have focused on constraining dipeptide fragments in appropriate conformations by using macrocyclizations, particularly to form 14-membered rings.<sup>79,80</sup> That ring size facilitates conformational arrangements of edge shared C<sup>10</sup> systems, one featuring the dipeptide and the other comprising of a non-peptidic fragment (Figure 2.1). Previous work from our laboratory has focused on  $\beta$ -turn mimics **J** and **K** via solid-phase, S<sub>N</sub>Ar macrocyclization reactions. It is evident that compounds **J** and **K** can disrupt some protein-protein interactions.<sup>81,82,83</sup> Small libraries of mimics **J** and **K** were prepared based on the  $i + 1$  and  $i + 2$  residues of the turn regions of the nerve growth factor (NGF). The turn regions of NGF are considered as the relevant hot spots for the interaction of this protein with its high affinity receptor TrkA. Several lead compounds such as **D3**<sup>84</sup> and **MPT18**<sup>85</sup> were identified based on pharmacological tests, implying that the combination of peptidic and nonpeptidic fragments in structures **J** and **K** might be especially favorable for mimicry of hot spots in protein-protein interactions that involve  $\beta$ -turn  $i + 1$  and  $i + 2$  regions.

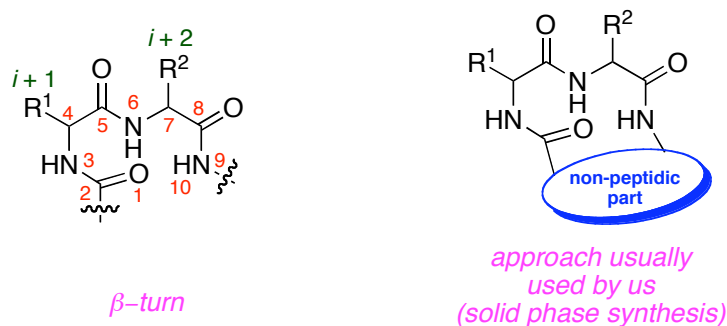


**Figure 2.1.** Some  $\beta$ -turn nomenclature, semi-peptidic mimics **J** and **K** usually prepared via solid phase reactions, and the identified lead compounds **D3** and **MPT18**.

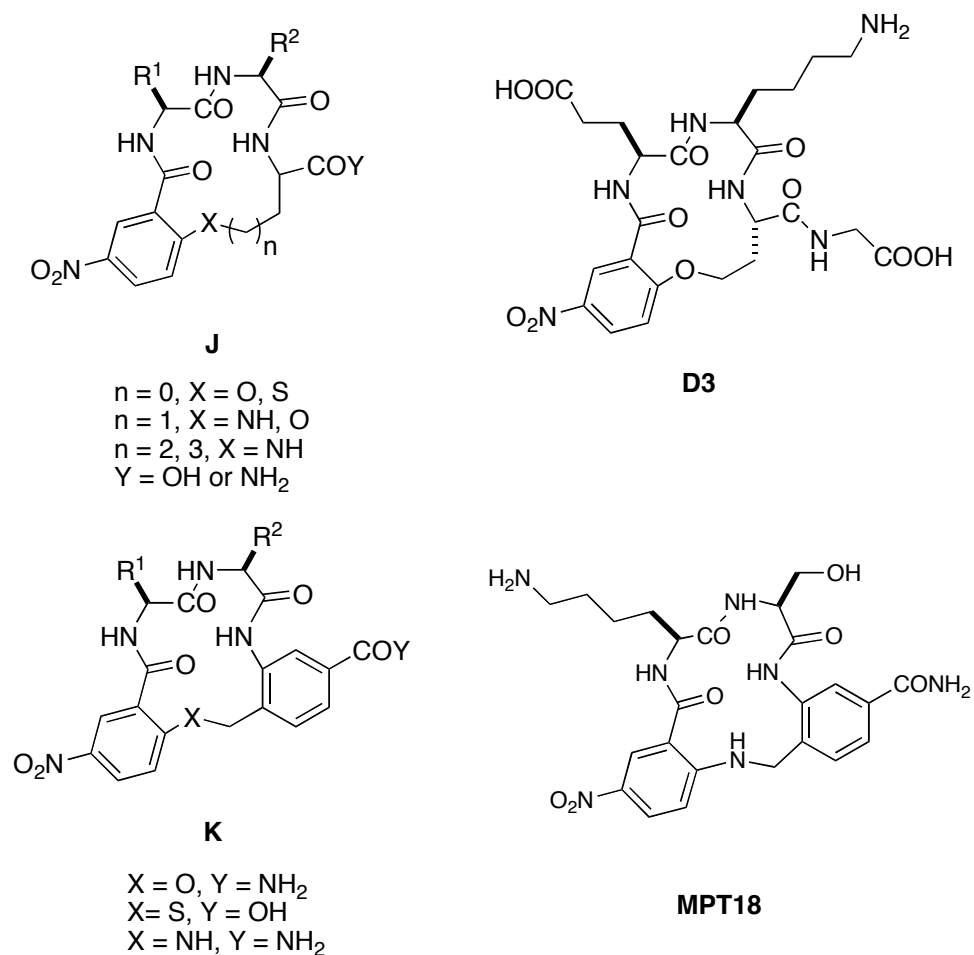


**Figure 2.1. Continued.**

Many non-peptidic fragments can be used in the peptidomimetics featured above. This is a means to incorporate diversity and to use different chemical reactions in the ring-closure step. Our bias is to avoid reactions that make the macrocycles more peptidic (*ie* amide bond formation) and to favor ones that give the small heterocyclic fragments found in pharmaceuticals. Moreover, we are currently interested in scalable solution phase methods to do this. Solid phase syntheses were used in all our previous syntheses of dipeptide containing peptidomimetics.<sup>86,83,82,87,88,89,90,91,92,80</sup> These have the advantage of *pseudo*-dilution caused by reactive site isolation on solid supports at

moderate to low loading. Solution phase methods, on the other hand, require ring closure via efficient reactions. Copper catalyzed azide alkyne cycloadditions, a “click reaction”,<sup>5</sup> were therefore an obvious choice. Consequently, this chapter features the concept depicted in Figure 2.2.

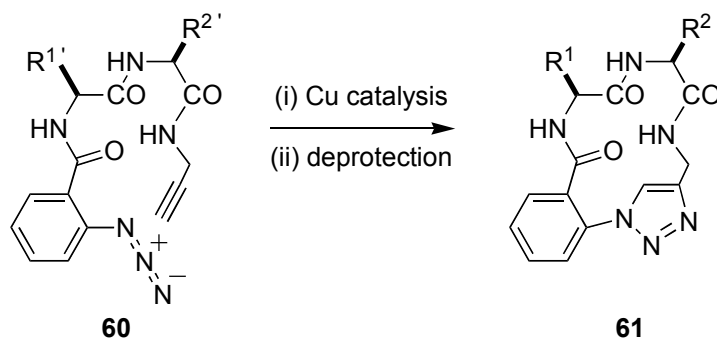


**Figure 2.2.** Substrate and product structures in this study. R<sup>1'</sup> and R<sup>2'</sup> denote protected side chains, R<sup>1</sup> and R<sup>2</sup> are deprotected ones.

A simple molecular modeling experiment was performed on compounds **61**, which was represented with a molecule containing Ala-Ala sequence. The dihedral angles around Ala-Ala residues were constrained and the energy was minimized. The resulting molecule was overlaid with the ideal type I  $\beta$ -turn as illustrated in Figure 2.3. The backbone of the cyclic mimic fit that of the  $\beta$ -turn fairly well and the side chains of the Ala-Ala residues were oriented in the appropriate region in space. This simple molecular modeling indicated that the triazole induced cyclic mimic could successfully sample  $\beta$ -turn conformation.

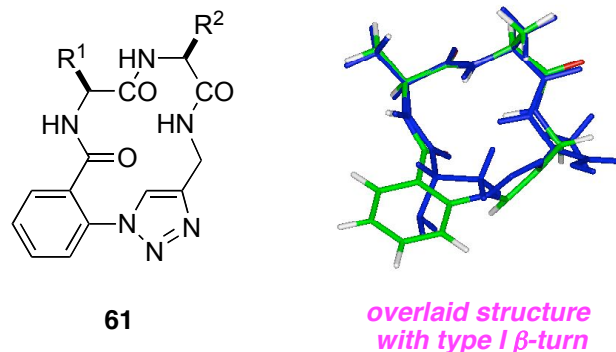
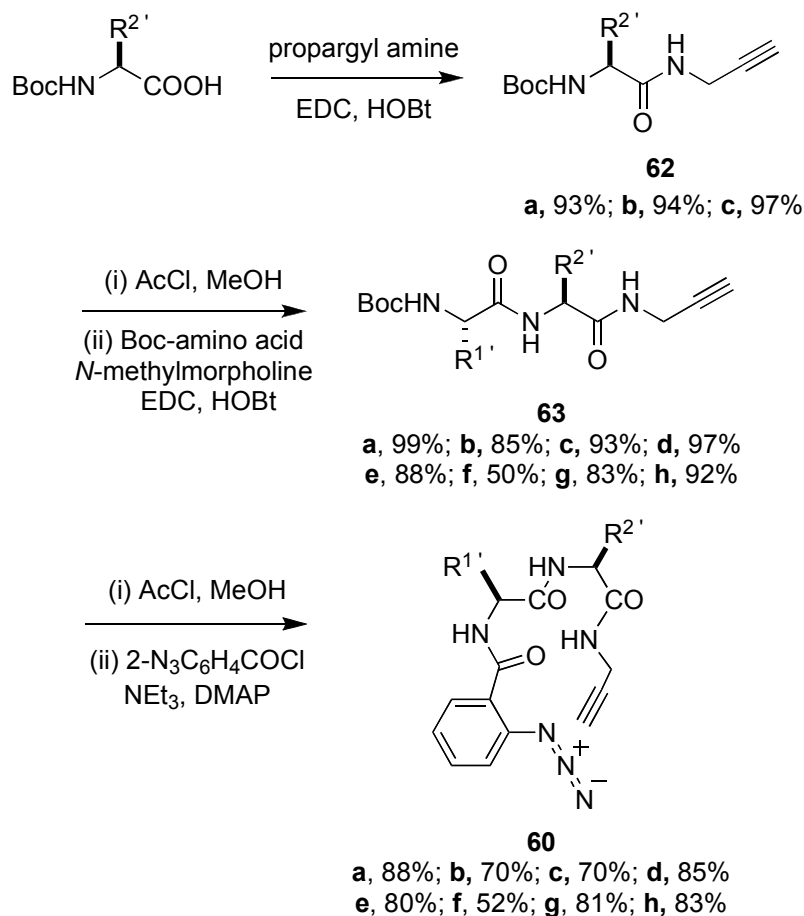


**Figure 2.3.** General structure of compounds **61** and the overlaid structure with ideal type I  $\beta$ -turn.

## 2.2 Solution Phase Synthesis of the Linear Peptidomimetics

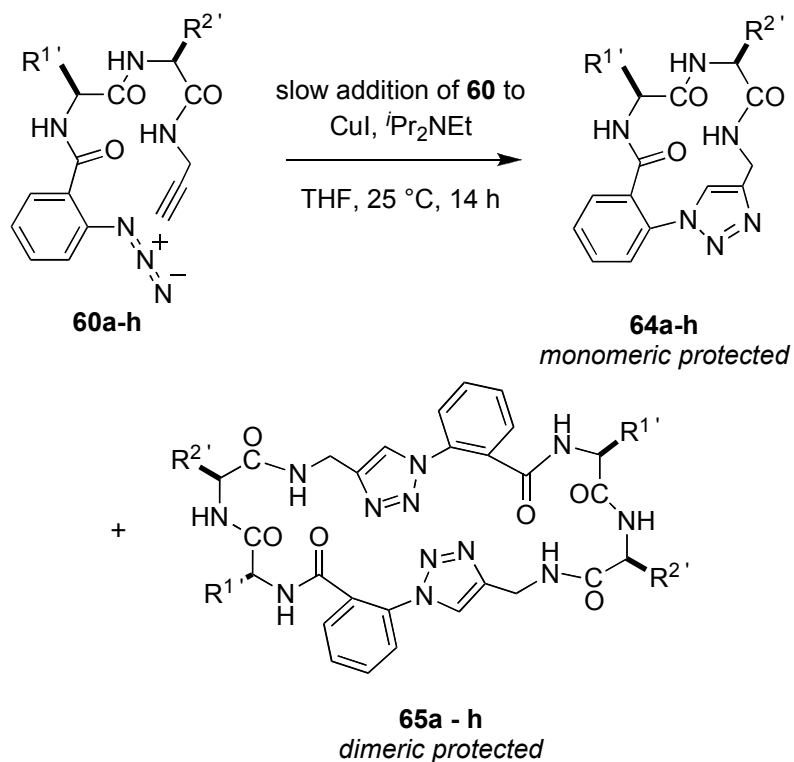
Scheme 2.1 outlines the preparation of the starting materials **60**. Side chain protection was necessary for the Lys (Cbz), Glu (Bn), Thr (Bn), Ser (Bn), Tyr (Bn) amino acids. These protecting groups render the intermediates relatively lypophilic, hence use of a water soluble diimide reagent in the coupling steps facilitated separation of the products via aqueous extractions. Finally, the linear precursors **60** were recrystallized and isolated in an overall average yield of 70 %. Thus the substrates **60** were conveniently accessible in gram amounts via syntheses that could be performed in parallel.<sup>93</sup>



**Scheme 2.1.** Preparation of the linear substrates **60**.  $R^{1'}$  and  $R^{2'}$  denote protected side chains,  $R^1$  and  $R^2$  are unprotected ones (see Table 2.1 for **a – h** definitions).

### 2.3 Copper Catalyzed Azide Alkyne Cycloadditions

Cyclization of the linear precursors gave the “monomeric” and “dimeric” products **64** and **65**. Two measures were taken to favor formation of the protected 14-membered ring products **64**: THF solutions of the azides **60** were added to the copper catalyst over 10 – 14 h via a syringe pump, and the final concentration was kept low (approximately 0.001 M). Nevertheless, dimeric products tend to predominate; data for the cyclization reactions are shown in Table 2.1.

**Table 2.1.** Copper catalyzed cyclization reactions of compounds **60**.

<b>64</b>	Amino Acids		<b>64:65</b> (monomer/dimer) <sup>a</sup>	Isolated Yield <b>64</b> (%) <sup>b</sup>
	<i>i</i> + 1	<i>i</i> + 2		
<b>a</b>	Ile	Lys	39 : 61	12
<b>b</b>	Glu	Lys	54 : 46	11
<b>c</b>	Thr	Gly	29 : 71	8
<b>d</b>	Gly	Lys	23 : 77	14
<b>e</b>	Lys	Gly	23 : 76	9
<b>f</b>	Gly	Ser	39 : 61	9
<b>g</b>	Ser	Gly	20 : 79	8
<b>h</b>	Tyr	Ser	18 : 82	12

<sup>a</sup> Monomer/dimer ratio was based on the UV peak area of HPLC traces at 254 nm.

<sup>b</sup> Calculated on the basis of the mass after preparative HPLC separation.

Even though the crude purities of the monomer/dimer mixtures are high after the cyclization described above, relatively low yields were isolated after purification via HPLC. This is mainly because of the limited solubility of the products in organic and in aqueous solvents. For example, the crude yield of compounds **64a** and **65a** together (39:61) was 92 %, but the isolated yield of **64a** was only 12 %.

Deprotection of the products **64** (Pd/C, H<sub>2</sub>, MeOH or EtOH) proceeded cleanly to give the unmasked products **61**; any losses of material at this stage probably were attributable to these relatively insoluble materials sticking to the catalyst. Lysine side chains of the peptidomimetics **64d** and **64e** were converted entirely to *N,N*-dimethyl and *N*-ethyl derivatives, respectively, under these conditions. Alkylation of amino groups during hydrogenolysis in methanol and ethanol is well-known.<sup>94,95</sup> However, it is curious that this was only observed for the two peptidomimetics containing Gly/Lys amino acids.

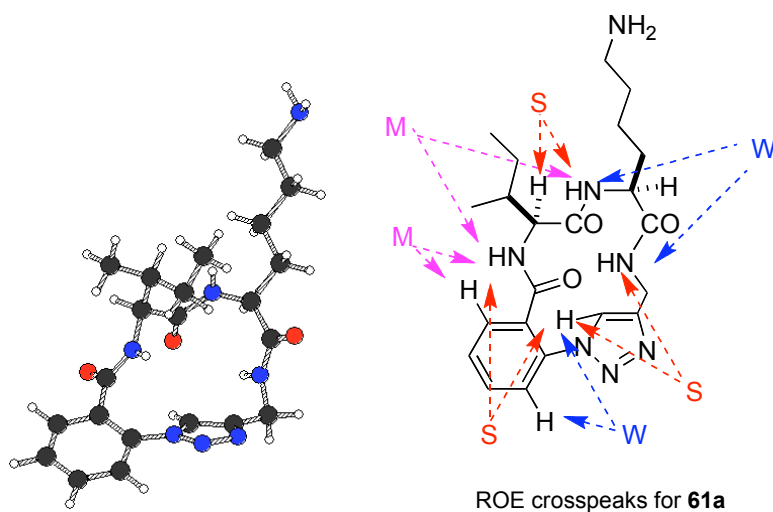
## 2.4 Conformational Analyses

Extensive conformational analyses were carried out for compounds **61a-c**. Full details of analyses data are given out in Appendix A. Sequential assignments for all compounds were made from analyses of one-dimensional <sup>1</sup>H NMR, gCOSY, TOSCY, and ROESY spectra of samples in DMSO-*d*<sub>6</sub> at 275 K.<sup>96</sup> DMSO was used as the solvent for the solubility problems and also because it has a dipole moment ( $\epsilon=45$ ) in between water and a lipophilic binding pocket which resembles biologically relevant media. Proton close contacts were obtained from ROESY spectra. Hydrogen bonding information was accessed from the measurements of the temperature coefficients<sup>97,98</sup> and deuterium exchange rates<sup>99</sup> of backbone amide protons. Molecular simulations were made via the quenched molecular dynamics technique (QMD)<sup>100,101</sup> without any constrain from the spectra measurements. Data obtained from 1D and 2D NMR experiments were then compared with the families of low energy conformations derived from QMD calculation. Good agreements of the parameters provided by the simulated physical model and the experimentally observed data are indicative of a realistic model.



**Table 2.2.** QMD results for the lowest energy conformer of compound **61a**.

Amino acid residue	Dihedral angle (°)	Lowest energy conformer of <b>61a</b>
Ile (R <sup>1</sup> )	$\phi$	-84.44
	$\psi$	-121,20
Lys (R <sup>2</sup> )	$\phi$	-77.74
	$\psi$	-92.39
Distance (Å)CO <sub>i</sub> – NH <sub>i+3</sub>		5.114
Type of beta-turn		Type I



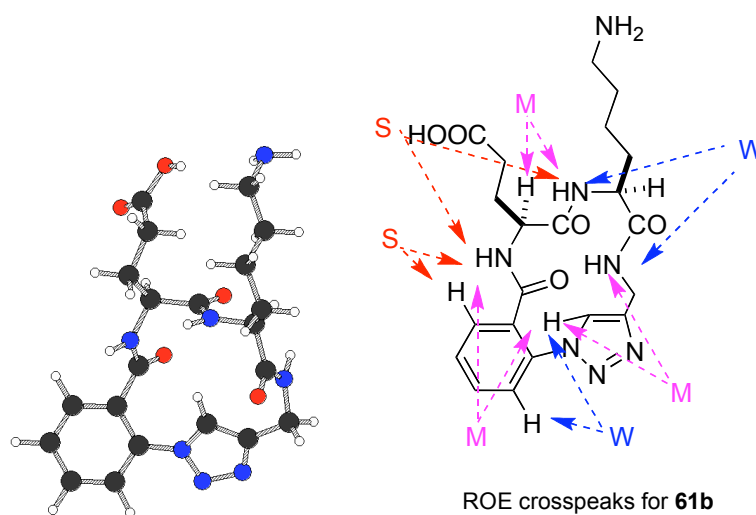
<u>Hydrogen</u>	<u>ROE</u>	<u>QMD distance (Å)</u>
Ile <sub>NH</sub> - Lys <sub>NH</sub>	medium	3.822
Ile <sub>C<math>\alpha</math>H</sub> - Lys <sub>NH</sub>	medium	3.313
Lys <sub>NH</sub> - PPA <sub>NH</sub>	weak	4.108
triazole <sub>CH</sub> - PPA <sub>NH</sub>	strong	2.943

**Figure 2.4.** Correlations between ROE cross-peaks and distances from QMD (PPA = propargyl amine residue).

To access if compounds **61** adopt  $\beta$ -turn conformation, QMD, NMR and CD experiments were performed on **61a-c**. Table 2.2 shows the QMD analysis of compound **61a**. The lowest energy conformers from four different families were generated. The lowest energy conformer that best fit the physical data was chosen as the most representative structure of compound **61a**. (Figure 2.4) The dihedral angles around the Ile and Lys residues have some correlation with the type I  $\beta$ -turn ( $-60^\circ$ ,  $-30^\circ$ ,  $-90^\circ$  and  $0^\circ$ ).<sup>72</sup> However the distance between the oxygen of the carbonyl (C=O) of the  $i$  residue and the NH hydrogen of the  $i + 3$  residue is not very indicative of hydrogen bond formation.

**Table 2.3** QMD results for the lowest energy conformer of compound **61b**.

Amino acid residue	Dihedral angle ( $^\circ$ )	Lowest energy conformer of <b>61b</b>
Glu ( $R^1$ )	$\phi$	-65.35
	$\psi$	-74.63
Lys ( $R^2$ )	$\phi$	-96.95
	$\psi$	94.64
Distance ( $\text{\AA}$ )CO $_i$ – NH $_{i+3}$		4.441
Type of beta-turn		Type I



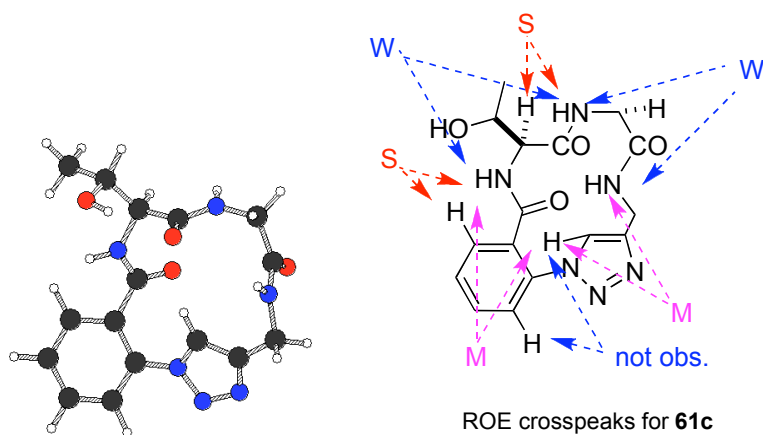
<u>Hydrogen</u>	<u>ROE</u>	<u>QMD distance (Å)</u>
Glu <sub>NH</sub> - Lys <sub>NH</sub>	strong	3.026
Glu <sub>C<math>\alpha</math>H</sub> - Lys <sub>NH</sub>	medium	3.583
Lys <sub>NH</sub> - PPA <sub>NH</sub>	weak	4.101
triazole <sub>CH</sub> - PPA <sub>NH</sub>	medium	3.274

**Figure 2.5.** Correlations between ROE cross-peaks of **61b** and distances from QMD (PPA = propargyl amine residue)

For compound **61b**, four families were also generated and the physical data of lowest energy conformers were compared with the experimental data. (Figure 2.5) The dihedral angles around Glu and Lys residues indicated that compound **61b** was a type I  $\beta$ -turn analogue. (Table 2.3) Again, the distance between the oxygen of the carbonyl (C=O) of the *i* residue and the NH hydrogen of the *i* + 3 residue is not very indicative for the hydrogen bond formation.

**Table 2.4.** QMD results for the lowest energy conformer of compound **61c**.

Amino acid residue	Dihedral angle (°)	Lowest energy conformer of <b>61c</b>
Thr (R <sup>1</sup> )	$\phi$	-71.12
	$\psi$	117.60
Gly (R <sup>2</sup> )	$\phi$	-87.73
	$\psi$	-106.60
Distance (Å)CO <sub>i</sub> – NH <sub>i+3</sub>		4.979
Type of beta-turn		Type II



<u>Hydrogen</u>	<u>ROE</u>	<u>QMD distance (Å)</u>
Thr <sub>NH</sub> - Gly <sub>NH</sub>	weak	4.462
Thr <sub>C<math>\alpha</math>H</sub> - Gly <sub>NH</sub>	strong	2.104
Gly <sub>NH</sub> - PPA <sub>NH</sub>	weak	4.299
triazole <sub>CH</sub> - PPA <sub>NH</sub>	medium	2.999

**Figure 2.6.** Correlations between ROE cross-peaks of **61c** and distances from QMD (PPA = propargyl amine residue).

As for compound **61c**, only three families were generated and the physical data of lowest energy conformers were compared with the experimental data. (Figure 2.6) The dihedral angles around Thr and Gly residues indicated that compound **61c** was a type II  $\beta$ -turn analogue. (Table 2.4) The distance between the oxygen of the carbonyl (C=O) of the  $i$  residue and the NH hydrogen of the  $i + 3$  residue is not very indicative for the hydrogen bond formation.

**Table 2.5.** Temperature coefficients and H/D exchange data of compounds **61a-c**.

Comp'd	- $\Delta\delta$ /K[ppb/K]/H-D		
	AA <sup><i>i</i>+1</sup>	AA <sup><i>i</i>+2</sup>	AA <sup><i>i</i>+3</sup>
<b>61a</b>	3.8/M	4.6/F	5.3/F
<b>61b</b>	1.5/S	3.8/F	6.6/F
<b>61c</b>	7.0/M	6.0/M	6.4/M

The temperature dependence and the H/D exchange rate of the  $i + 3$  residue are indicative of the presence of 10-membered ring intramolecular hydrogen bonding. From the data showed in Table 2.5, the relatively high temperature dependence and fast to medium H/D exchange rates indicated that the intramolecular hydrogen bonding were not present, which correlated well with the data obtained from the best fit lowest energy conformers.

Circular dichroism (CD) spectra<sup>102,103</sup> were also recorded. Compounds **61a-c** were dissolved in 20% MeOH/H<sub>2</sub>O, the ratio of which approximates the dielectric constant of DMSO used in the NMR studies. Overlaid CD spectra of the three compounds are shown in Figure 2.7. While there is a maxima around 190 nm for compound **61a** and **61b**, the negative minima band at 205 nm is absent. Typical type I and type II turns have minima around 205 nm and 225 nm, respectively; and maxima

around 190 and 205 nm, respectively. Clearly, the CD data do not closely fit the shape spectra commonly associated with type I and II turn conformations,<sup>104,105,106</sup> indicating non-ideal matches and/or other important contributions to the conformational ensemble.

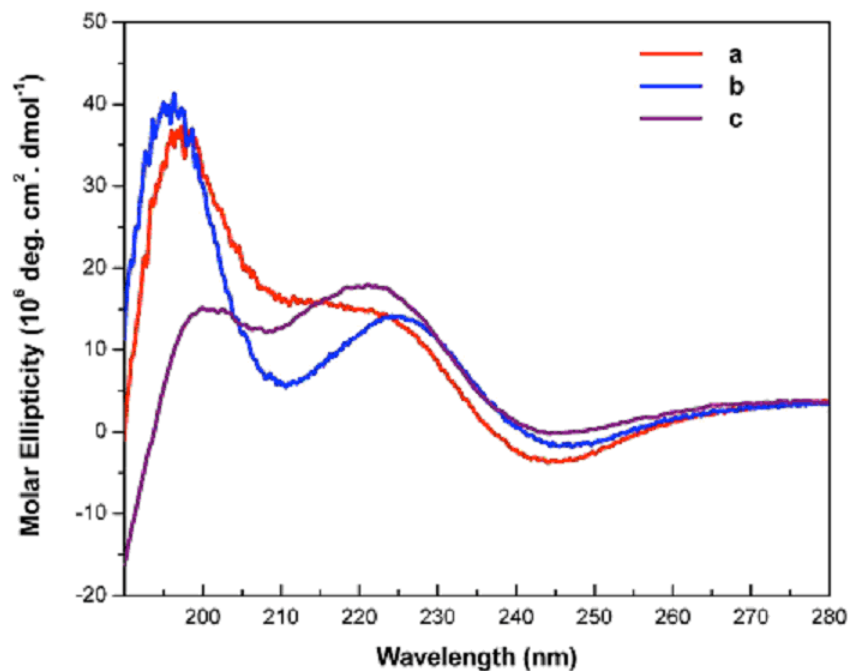
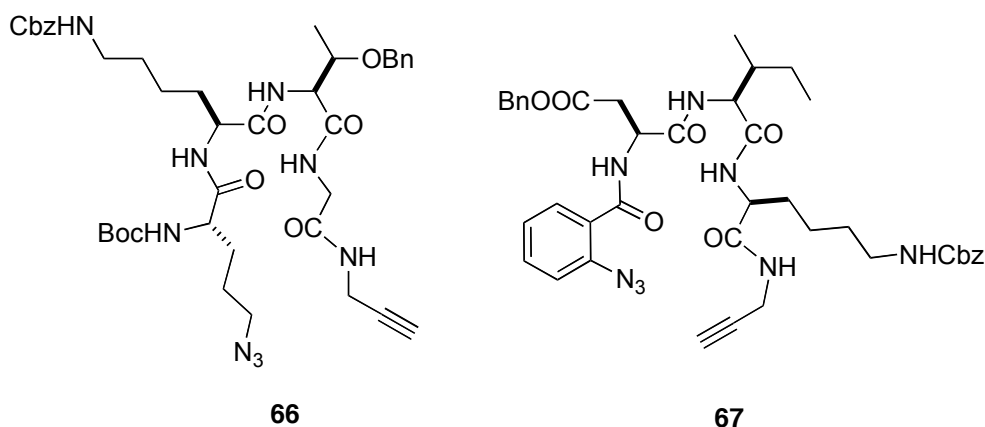


**Figure 2.7.** CD spectra of compounds **61a** - **c** in 4:1 water/methanol at 0.1 mg/ml.

## 2.5 Monomer/Dimer Selectivity Discussion

The studies described above successfully generated monomeric  $\beta$ -turn mimics: the original goal of this work. However, it was surprisingly difficult to do this. Dimers **65** were preferred for seven of the eight cases cited in Table 2.1. Further, azidoalkynes similar to the linear substrates **60** were also tested as cyclization precursors, but without success. For instance, when substrates **66** and **67** were subjected to the copper-catalyzed conditions described above there was no evidence of the monomeric cyclized product in the ESI-MS of the crude reaction material; instead, complex mixtures of compounds formed.

The literature reveals that at least three groups have attempted to use copper-mediated azide/alkyne cycloaddition reactions to form macrocyclic rings, but “dimers” were formed in each case.<sup>25-28</sup> Finn *et al.*<sup>25</sup> described dramatic examples in which 76- and 124-membered rings were formed in preference to the corresponding monomeric ones. This result was unexpected particularly since solid phase syntheses were used, *ie* conditions in which there is an inherent dilution effect.



Finn and co-workers hypothesized that preferential formation of dimeric products could be due to coordination of two alkynes prior to the cycloaddition, and/or to coordination of the catalyst to the peptidic part of the molecule. The immediate precursor to cycloaddition in the copper-mediated transformations is not known, but the kinetic studies<sup>10</sup> suggest it contains two copper atoms and possibly two alkynes. Intermediates **L** and **M**, are possible candidates (Figure 2.8). For the following discussion, intermediates **M** is assumed to be the important ones (though this is not critical).

In a simple elaboration of the hypothesis presented by Finn *et al*, we suggest that selectivity for dimers in these copper mediated cyclizations may be explained as follows. The perfect regioselectivity of the copper mediated cycloaddition processes for 1,4-disubstituted triazoles would require that the azido alkyne coils in an *endo*-like conformation to form a monomeric cyclization product. In the absence of extenuating circumstances, this conformational state would be less populated than *exo*-like ones that are intrinsically less ordered. The effects in question are small, but so are the rate differences leading to mixtures of monomeric and dimeric products. We suggest the preference for the *exo*-like orientation **M** prevails over the conformational biases of the peptide part, or secondary copper coordination effects, that might sometimes favor reactions via *endo*-like conformations.



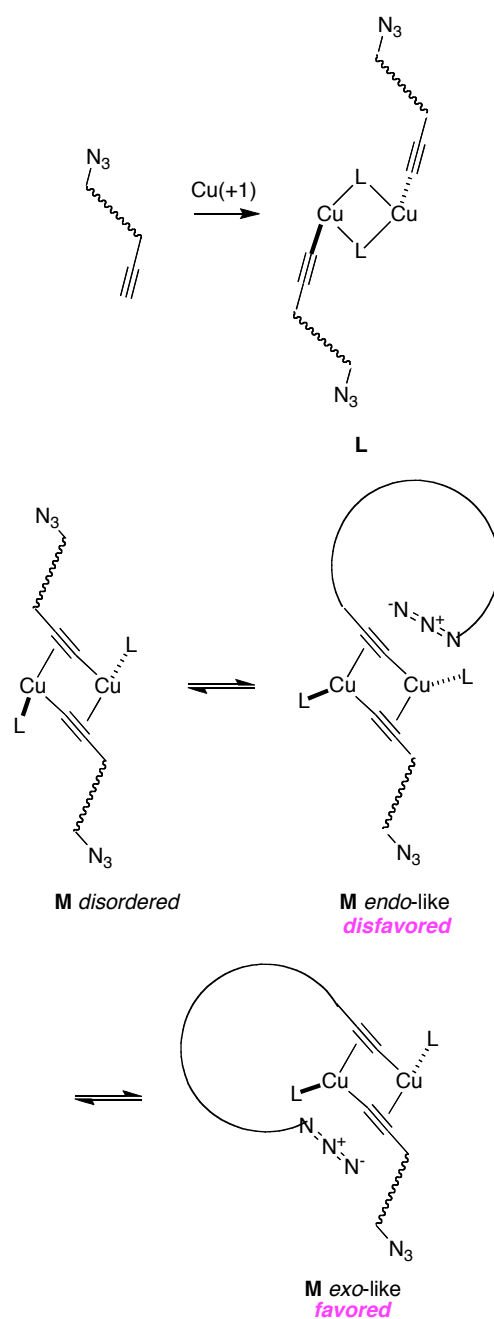


**Figure 2.8.** Formation of dimeric products in copper-mediated azide/alkyne cycloadditions may be associated with less populated “*endo-like*” conformations relative to less well ordered, more populated, *exo-like* ones.

## 2.6 Biological Assays

Biological assays for compounds **61** were conducted by Dr. Uri Saragovi and his coworkers at McGill University in Canada. Cell survival assays were performed to access the compounds' activities as neurotrophin mimics. One of the functions of NGF is to control cell survival. Untreated E25 cells (NIH cells that express TrkA receptor) in serum-free media (SFM) generally die without addition of NGF (0 % survival). Cells can be rescued by adding NGF or functional mimic ligands. Untreated E25 cells were cultured with SFM supplemented with NGF control (low and high) and peptidomimetics (1 or 10  $\mu$ m) with and without addition of low NGF. The effect of peptides **61a**, **b**, **d**, **e**, **g**, **h** on the survival rate of E25 cells were evaluated through MTT assays. In this test, the MTT is captured and metabolized only by living cells, producing a change in the color of media that can be measured with a spectrophotometer. Different concentrations of DMSO were used as negative controls.

Data from the cell survival assay is given in Figure 2.9. Peptides **61a**, **61b** and **61d** displayed only a marginal increase in survival with or without NGF. On the other hand, peptides **61e** and **61h** showed an increase of approximately a 5 % in the rate of survival of E25 cells in SFM and 13 % with NGF. The only exception was **61g** (10  $\mu$ m) that brought a relative survival of more than 20 % in the presence of NGF. However, it is important to consider that the negative controls (DMSO) also increase the survival of E25 cells. So probably this value is not very significant.

a.

Comp'd <b>61</b>	% survival of E25 cells		Comp'd <b>61</b>	% survival of E25 cells	
	SFM	low NGF		SFM	low NGF
untreated	0.00	0.00	untreated	0.00	0.00
a (10 uM)	10.26	6.41	e (10 uM)	6.45	13.36
b (10 uM)	3.85	4.27	g (10 uM)	8.29	21.66
d (10 uM)	2.99	3.85	h (10 uM)	5.99	14.75
a (1 uM)	1.28	1.28	e (1 uM)	5.99	11.06
b (1 uM)	1.28	0.00	g (1 uM)	4.15	6.91
d (1 uM)	0.00	0.00	h (1 uM)	3.23	13.36
50% DMSO	-1.71	2.14	40% DMSO	1.84	13.36
10% DMSO	2.56	5.56	30% DMSO	1.38	5.99

b.

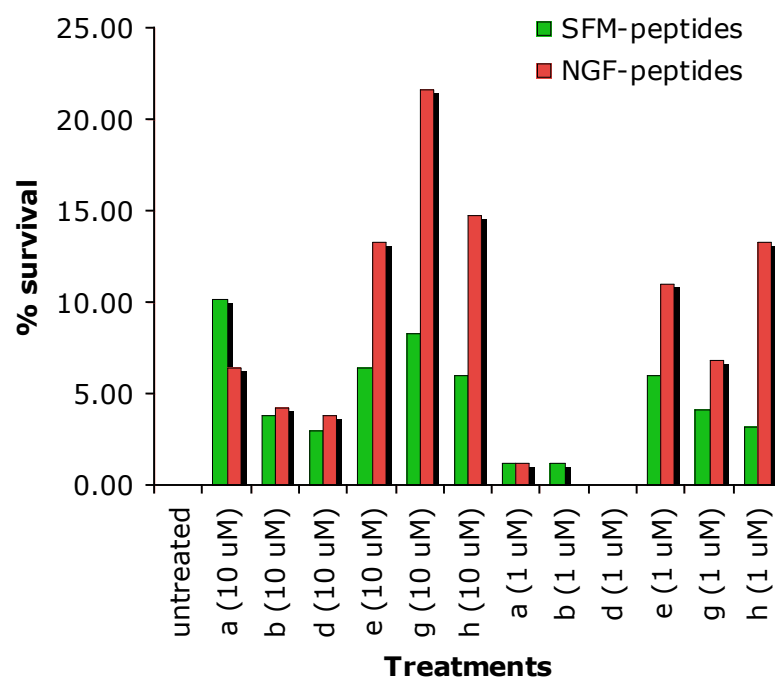


**Figure 2.9.** Cell Survival Data and Graphic Representation for Compounds **61**.

## 2.7 Summary

Copper catalyzed azide alkyne cycloadditions of the linear substrates **60** were used to form the cyclic derivatives **61**. This 1,3-dipolar cycloaddition reaction is fast, simple to perform and compatible with many solvents and functional groups. A library of eight cyclic peptidomimetics was prepared in solution and the low yield was mostly due to formation of dimers.

Computational, NMR, and CD analyses of compounds **61a-c** indicate that their most favorable conformational states include type I and type II  $\beta$ -turn conformations. The low energy conformers that best fit with the observed physical data were identified for compounds **61a – c**. These conformations of compounds **61a** and **61b** resemble type I  $\beta$ -turns, and for **61c** a type II  $\beta$ -turn is most relevant. These data indicate the compounds can sample turn conformations. However, the CD data do not closely fit the shape spectra commonly associated with type I and II turn conformations, indicating non-ideal matches and/or other important contributions to the conformational ensemble.

Selectivity for the dimeric products **65** in these cyclisation reactions is discussed. We suggest that the perfect regioselectivity of the copper mediated cycloaddition processes for 1,4-disubstituted triazoles would require that the azido alkyne coils in an *endo*-like conformation to form a monomeric cyclization product.

## CHAPTER III

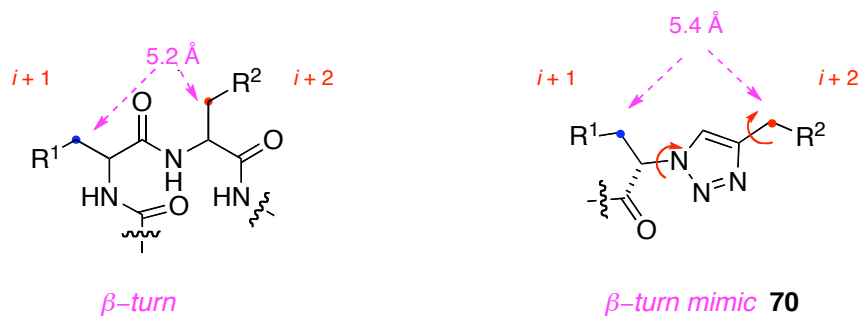
### A COMBINATORIAL METHOD TO SOLUTION-PHASE SYNTHESIS OF LABELED BIVALENT BETA-TURN MIMICS

#### 3.1 Introduction

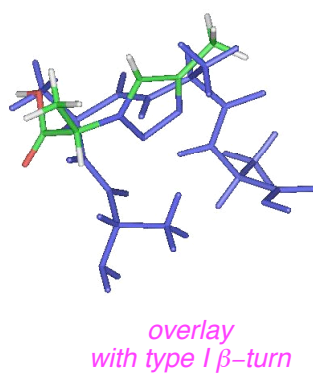
Peptides and proteins play a crucial role in many biological systems. However, their intrinsic instability limits their potential as reagents in drug discovery. Replacement of the amide bond with surrogates in potential drug candidates has been a continual strategy in medicinal chemistry. Successful replacements provide improved oral bioavailability via increased lipophilicity and stability. Many amide bond surrogates have been used,<sup>107-112</sup> but some of these compounds are not very easily accessible from amino acid derivatives.<sup>109,112</sup> Therefore, discovery of new peptide surrogates more compatible with amino acid side-chains is highly desirable. Meanwhile, such innovations have to allow the rapid synthesis of peptidomimetics in large numbers for high throughput screening.

Meldal and Sharpless reported independently the efficient synthesis of 1,2,3-triazoles by Cu(I)-catalyzed azide-alkyne cycloaddition reactions in 2002.<sup>3,4</sup> This 1,3-dipolar cycloaddition reaction is fast, simple to perform, and compatible with many solvents and functional groups. In our search of convergent syntheses of  $\beta$ -turn mimics, this regioselective formation of triazole motifs attracted our attention.<sup>16</sup> As shown in Figure 3.1, the molecular modeling indicated that the triazole moiety has topological similarities with the amide bond and pharmacophores could be placed around the triazole core with limited degrees of freedom,<sup>25,24</sup> but enough to find the appropriate region of space for docking to occur.<sup>113</sup> (Figure 3.1)

a.



b.



c.

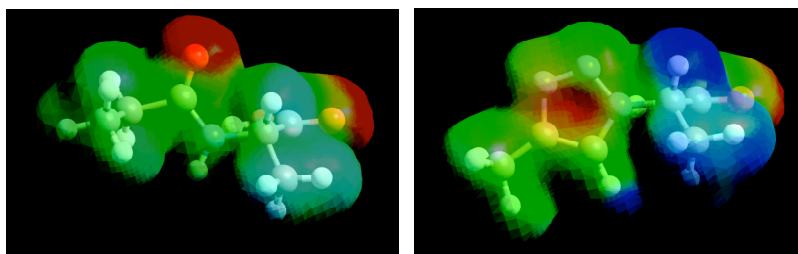


**Figure 3.1.** (a) The key distance of  $C^b$ -separations of the  $i + 1$  to  $i + 2$  residues of a type 1  $\beta$ -turn and of the monovalent turn mimics **70** featured here; (b) an overlay of the mimics onto a type 1  $\beta$ -turn; and, (c) a comparison of their electrostatic charge separations for these two entities.

In screening random libraries of small molecules against targets involving protein-protein interactions<sup>114,115</sup>, hit rates for screening are usually low for the following two reasons: (i) small molecules may bind at one hot-spot, but rarely bind two or more simultaneously; and (ii) weakly binding molecules are difficult to identify when screened against natural ligands which usually have extremely high affinities.<sup>116,117</sup> Thus, it is possible to join two small molecules together to impact two hot-spots simultaneously, *ie* to combine monovalent ones to form bivalent ligands that bind protein surfaces more strongly.<sup>118,119</sup> Fesik and co-workers proposed that two small molecules that each weakly binds a protein, can be linked to form higher affinity bifunctional ligands.<sup>120,118</sup> Thus weakly binding ligands could be identified *via* an NMR-based screen of a combinatorial library.<sup>121,119</sup> “Bivalent analogs”, which are two of these ligands linked together, should have much higher affinity than their monovalent components.<sup>122,123</sup> We propose that two mimics that bind a single receptor molecule should be more potent antagonists than their monovalent constituents. They can be called “superantagonists”. Moreover, coupling of two mimics that bind two different receptor molecules simultaneously could provide optimal agonists with much higher affinity. (Figure 3.2)

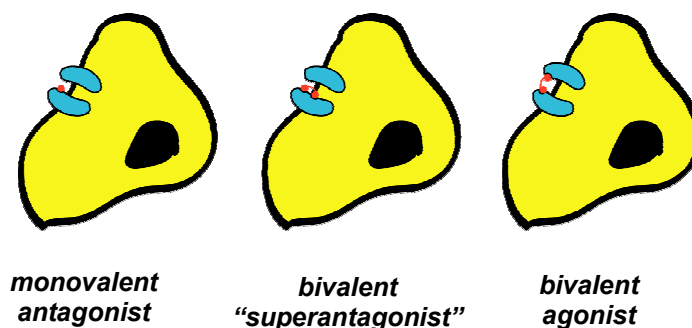


**Figure 3.2.** Weakly binding molecules could be jointed together to form bivalent molecules with higher binding affinity.

Our “linker scaffold” strategy<sup>124,125</sup> to form bivalent compounds is shown in Figure 3.3. If  $n$  monovalent compounds are combined with themselves in all possible ways, then  $n(n + 1)/2$  bivalent compounds could be formed. Bivalent molecules are ideal targets for combinatorial libraries directed at protein-protein interactions for two reasons. First, combining two monovalent ligands into a bivalent system can increase the affinity of the molecule. Secondly, small additions to the monomer pool lead to dramatic increases in the number of permutations available.<sup>126</sup>

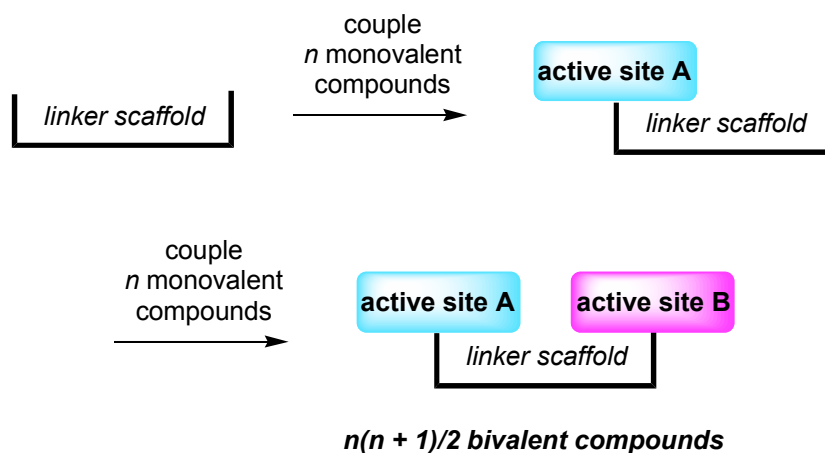
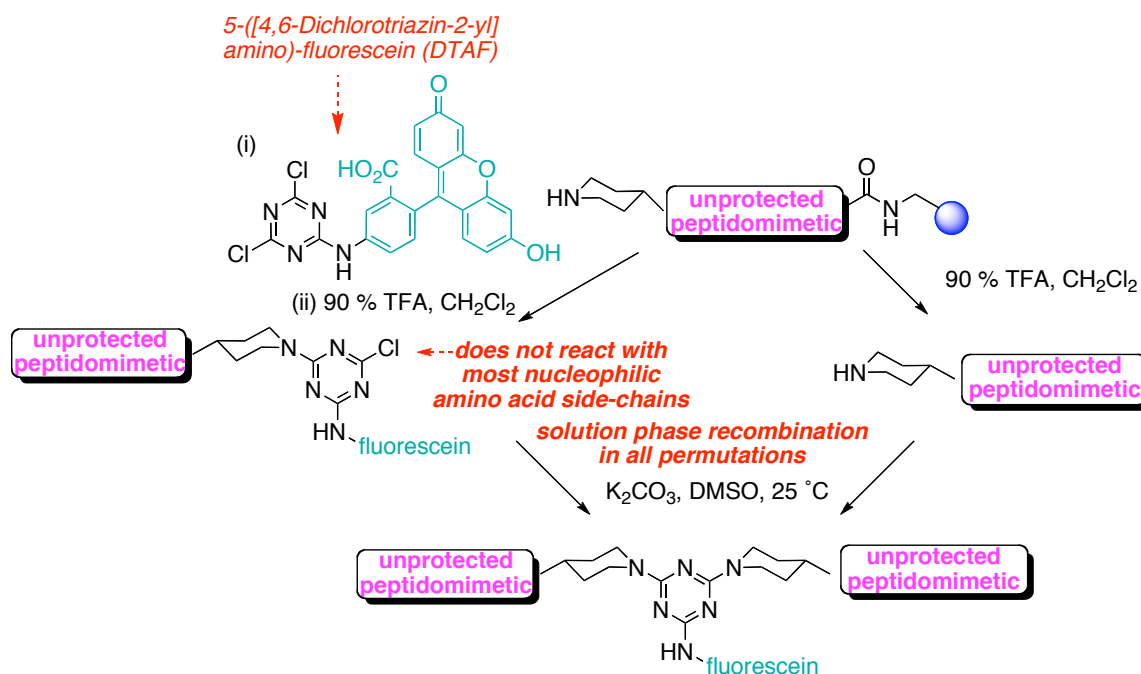


**Figure 3.3.** “Linker scaffold” strategy.

Cyanuric chloride is more reactive to nucleophiles than 2-amino-4,6-dichlorotriazines, and both of them are more reactive than 2,4-diamino-6-chlorotriazines.<sup>127,128</sup> In the search of linker scaffolds for dimerization, the aminofluorescein labeled triazine derivative (DTAF) has proven an excellent scaffold in our research group based on this type of selectivity.<sup>129</sup> Scheme 3.1 shows our initial

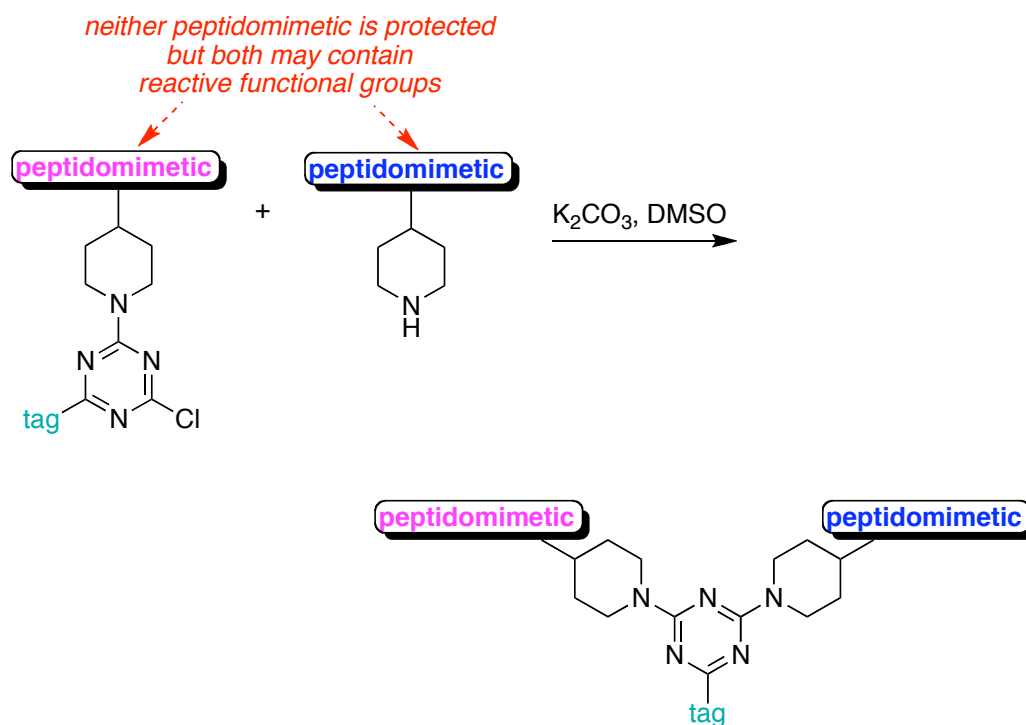


“semi-solution phase” strategy to dimers. In the reactions shown, one monomer was coupled to the DTAF linker on solid phase and the other was later combined to give heterodimers selectively in solution. Only potassium carbonate was required to affect the coupling, and no protecting groups were involved. The final product does not have to be purified from protecting group residues and scavenger material, and the bivalent materials were obtained in high purities.



**Scheme 3.1.** “Semi-solution phase” reactions illustrate the sequential addition of monomers and the surprising selective coupling of a piperidine over most nucleophilic amino acid side-chains.

The observations in Scheme 3.1 were exploited to make 78 dimeric, unprotected peptidomimetics.<sup>129</sup> The triazine scaffold can therefore be used as a scaffold to transform unprotected peptidomimetic monomers into dimers. However, several issues have to be overcome before this method could be suitable for preparing much bigger libraries. First, the monomers had to be made in solution to get the quantities required since solid phase methods are intended for small amounts and HPLC purification is sometimes necessary. Second, dimerization conditions have to be devised so that both components could be reacted in solution, and meanwhile the monovalent components have to be accessible and usable without protecting groups. Finally, monomers have to combine with each other cleanly, to give one-compound-per-well with sufficient purity for testing. (Scheme 3.2) This chapter focuses on the rapid synthesis of small molecule mimics in large scale and their efficient assembly to dimers in solution.



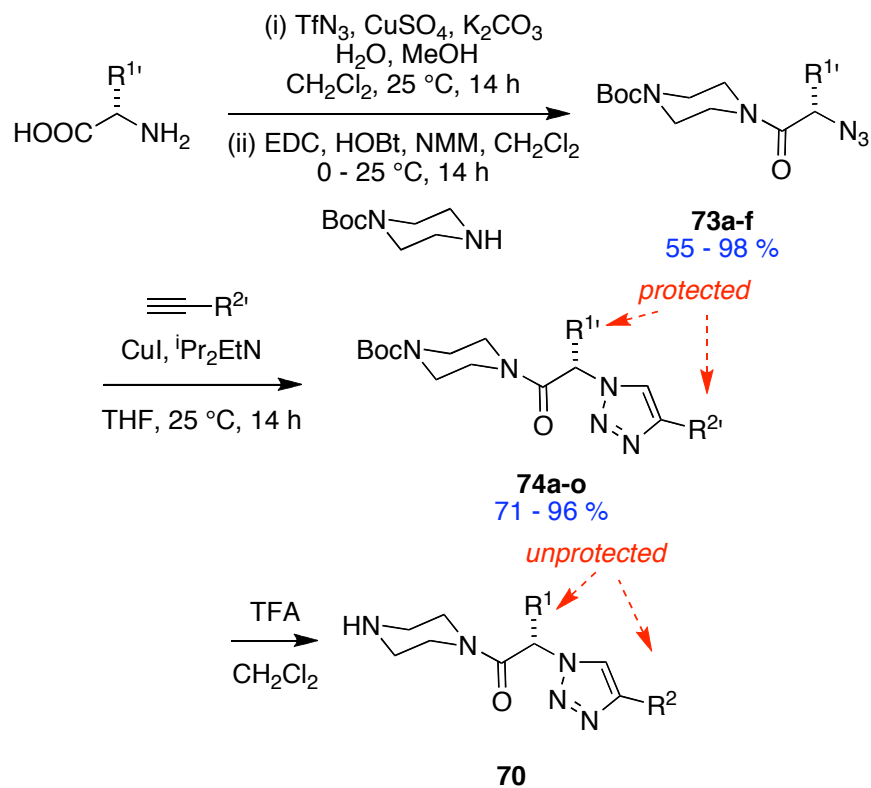
**Scheme 3.2.** Solution phase dimer assembly.

### 3.2 Preparation of Monovalent Triazole Peptidomimetics

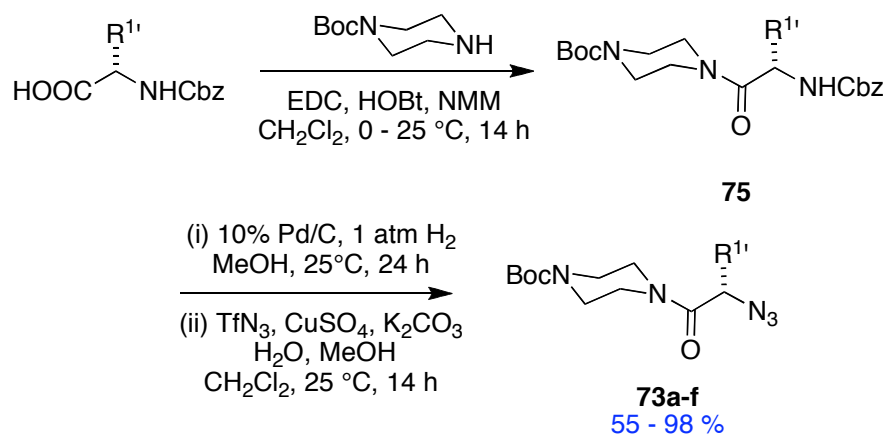
Two methods were used to prepare the monovalent building blocks **70**. The most economical and direct route (Scheme 3.3a) begins with amino acids that were converted to the corresponding azides via known azo-transfer reactions, coupled with Boc-piperazine, and combined with appropriately substituted alkynes via copper-mediated cycloaddition processes. Only the final products **74** were purified via flash chromatography; the intermediates were isolated via aqueous work-up (crude yields of **73** are shown) and used in the next step without further purification. This route was successful for all the amino acid/alkyne combinations tested, *ie* those shown in Table 3.1. Scheme 3.3a uses R<sup>1'</sup> and R<sup>2'</sup> to denote protected side chains (and R<sup>1</sup> and R<sup>2</sup> to indicate deprotected ones). In fact, the only side-chain of the amino acid starting materials (R<sup>1</sup> shown in Table 3.1) that had to be protected was the amino group of Lys (Boc-protected to mask it during the azo-transfer step).

Method B in Scheme 3.3b is a more conservative approach that begins with Cbz-protected amino acids, and requires an additional deprotection step. This was our original approach, but as the work evolved it was found that this route had no advantages over Method A for the amino acids shown in Table 3.1. However, Method B is shown here just in case the work is later expanded to other amino acids for which it might have some merit.

a



b



**Scheme 3.3.** Two methods for preparing the monovalent mimics **70**. Generally the least expensive and most direct route uses is: (a) featuring unprotected amino acid starting materials (except for Lys which was side-chain protected). Route (b) uses protected amino acids.

**Table 3.1.** Peptidomimetics **74** prepared via method A.

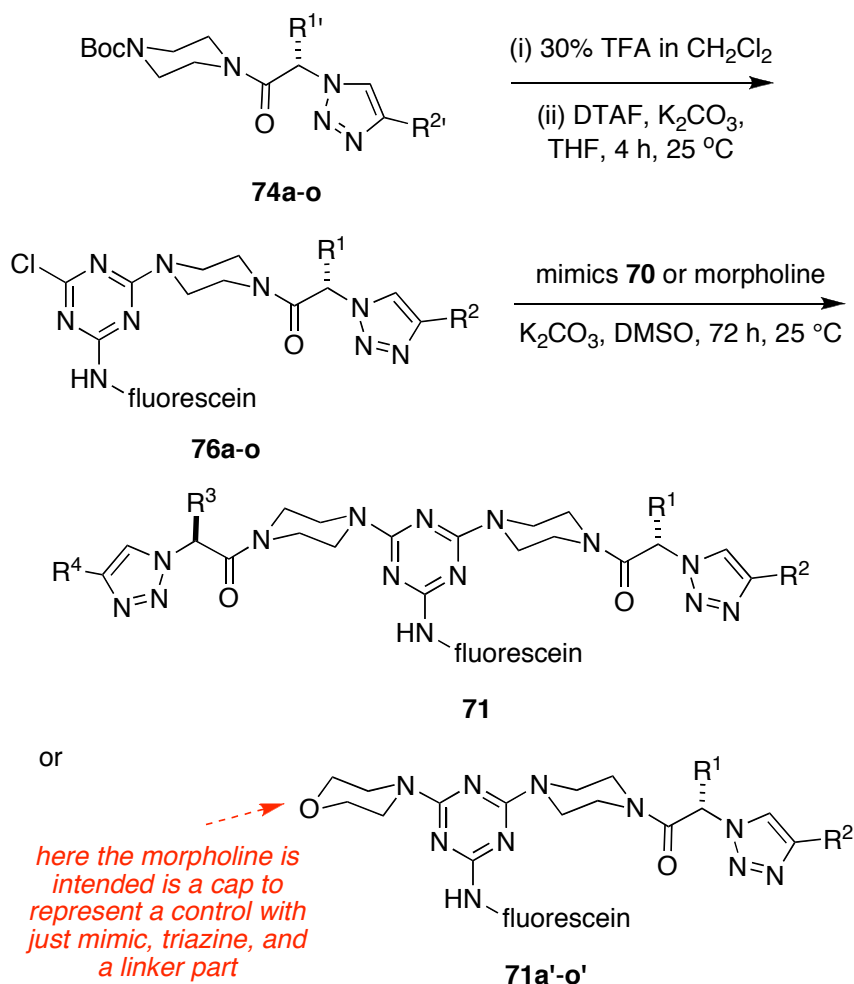
compound <b>74</b>	R <sup>1</sup> ,	R <sup>2</sup> ,	yield (%) <sup>a</sup>
<b>a</b>			78
<b>b</b>	H		79
<b>c</b>			80
<b>d</b>	H		94
<b>e</b>	H		96
<b>f</b>			80
<b>g</b>			71
<b>h</b>			92
<b>i</b>	Me		77
<b>j</b>			94
<b>k</b>			87
<b>l</b>	Me		87
<b>m</b>	H		86
<b>n</b>			89
<b>o</b>			96

<sup>a</sup> From intermediate **5** after flash chromatography.

### 3.3 Adaptation of the Dimerization Method to Solution Phase

After considerable optimization studies, the solution-phase method for assembly of the bivalent compounds shown in Scheme 3.4 was developed. The protected compounds **74** were unmasked to give mimics **70** then reacted with a dichlorotriazine derivative of aminofluorescein (*ie* DTAF) to give the electrophiles **76**. These were then reacted with second aliquots of the mimics **70**, in all permutations, to give the library of bivalent mimics **71**. Morpholine was also used in the second couplings. This resulted in syntheses of the specific mimics **71a'-o'** that represent controls for testing which contain only one mimic, triazine with the fluorescein label, and the morpholine part which represents the linker.

Some attributes of the method in Scheme 3.4 are follows. Our goal was to prepare compounds **71** in over 85 % purity, so the threshold of acceptable purity applied to the intermediates **76** had to be above this. The crude intermediates (chlorotriazines **76**) were assayed by reverse phase HPLC (UV and SEDEX detection) and found to be above 85 % purity, so no chromatographic isolation was necessary. In the first coupling, THF facilitated addition of just one monomer, giving monochloro-intermediates **76** in satisfactory purities for use in the next stage without further purification. Removal of THF after the synthesis of the intermediates **76** is convenient because it is volatile relative to some other solvents. It seems that DMSO facilitates faster coupling of nucleophiles to triazines than THF. Indeed, we found that DMSO as solvent for coupling the second monovalent compounds was critical; other solvents tested gave unsatisfactory results. The bivalent molecules formed in good overall purities, even though the monovalent building blocks used to assemble them were completely unprotected. The reactions were typically performed on a small scale to form a few milligrams of product. However, no problems were encountered scaling-up syntheses of some selected bivalent compounds to give 100 mg of product.



**Scheme 3.4.** Solution phase method for the preparation of the library of compounds **71**.

Briefly, the exploratory work that led to the method shown above illustrated several valuable conclusions. The solvents tested for the coupling reactions were THF, MeCN, MeOH, DMF, and DMSO); THF proved to be best for the first addition and DMSO for the second (see above). When DMF or DMSO was used for the first coupling reaction, the major products tended to be homobivalent molecules. Methanol was unsuitable for the first coupling because it tends to react with the DTAF. Acetonitrile gave similar results to THF in the first coupling, but it is more toxic and slightly harder to remove. For the second addition, the reaction went very slow in THF,

MeCN and MeOH at 25 °C and could not be completed in a reasonable time period. It was harder to remove DMF than DMSO, but it seems to be an equally good solvent for the second coupling in all other respects. Use of  $(\text{NH}_4)_2\text{CO}_3$  as a base was investigated but it gave incomplete complete coupling reactions. This is particularly unfortunate because ammonium salt residues are volatile, whereas sodium chloride residues are not and have to be removed via using differential solubilities.

### 3.4 Application of the Solution-phase Procedure to Make a Library of Fluorescently Labeled Bivalent Mimics

The method outlined in Scheme 3.4 was applied to synthesis of a library of 135 fluorescently-labeled bivalent mimics. Thus the monovalent compounds **74** were deprotected with TFA; no scavenger was required. The resulting unmasked intermediates **70** dissolved in THF were reacted with equimolar amounts of DTAF and excess  $\text{K}_2\text{CO}_3$  for 4 h to give the intermediates **76**. The THF was removed, then these intermediates were dissolved in DMSO, split into small portions, then coupled with another equivalent of the deprotected monomers **70** to give the bivalent compounds **71**. Alternatively, to generate a set of control compounds, morpholine was used instead of the deprotected monomers as a capping group giving compounds **71a' – o'**.

The purities of intermediates **76** were monitored by analytical HPLC, and they were judged to be high enough to use in the next step without purification. After the second coupling, a major practical issue was removal of inorganic salts; two procedures were developed for this. Most of the bivalent products were not very water soluble so they could be precipitated from the basic solutions by adding 5 % HCl; presumably the acid protonates the fluorescein labels transforming them into their less soluble, ring-closed forms. However, some of the bivalent molecules have side chains that promote solubilities in slightly acidic aqueous media (*eg* those in the **g**, **h**, and **k** series). Bivalent molecules in this second category were separated from most of the inorganic salts by removing the solvent and extracting them into methanol. After these procedures, more than 80% of the bivalent compounds **71** were produced with a minimum of 85% purity. It appears that the other 20 % were not as pure due to pipetting errors because all gave



purities above 85 % when they were re-prepared. HPLC and MALDI analyses were performed on all the compounds. Both UV and SEDEX detectors were used to determine the purities shown in Figure 3.4, which includes the ones that were re-prepared. Purity data before and after the re-preparation procedures is given in the supporting material. In summary, this new methodology allows the monovalent compounds to combine with each other cleanly in a one-compound-per-well format.

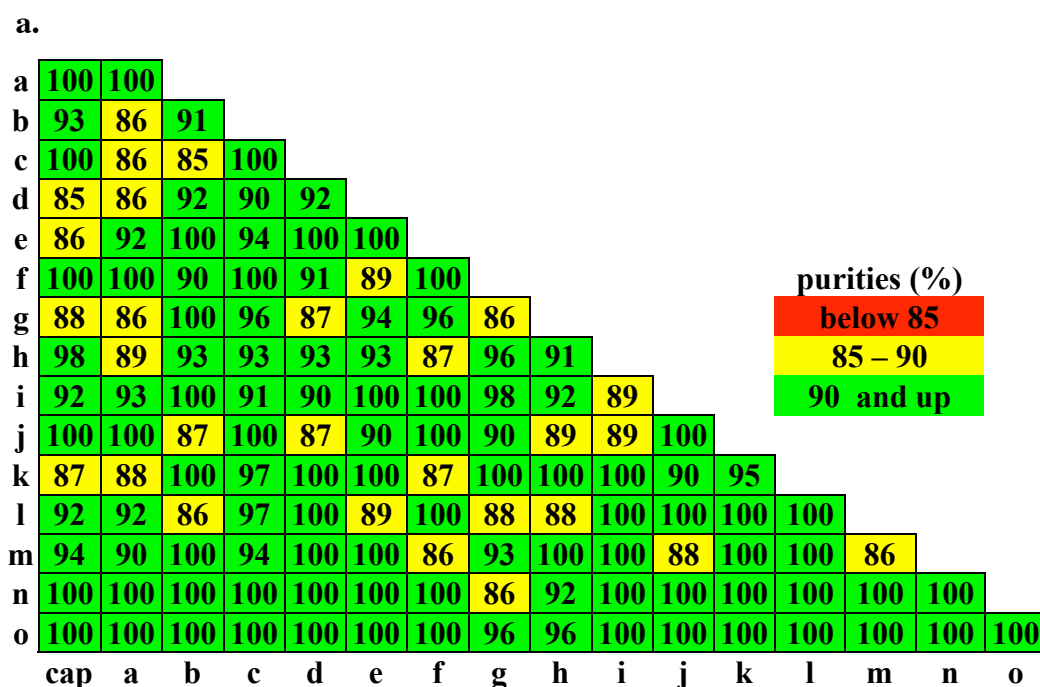


**Figure 3.4.** Purities of the library of compounds **71** where the detection method was: (a) UV set at 254 nm; and, (b) SEDEX detection. The term “cap” is used for morpholine.

b.

a	100	100																
b	100	100	100															
c	100	92	92	100														
d	92	100	100	100	100													
e	90	94	100	100	100	100												
f	100	100	100	100	100	100	94											
g	98	92	100	98	100	100	100	100										
h	100	93	100	100	100	100	94	98	100									
i	87	91	100	100	100	100	100	97	100	96								
j	100	93	93	100	86	92	100	94	93	95	91							
k	100	94	100	100	100	100	100	100	100	100	90	100						
l	97	100	92	100	100	100	100	96	87	100	100	100	100					
m	99	95	100	100	100	100	93	90	100	100	93	100	100	100				
n	100	96	100	100	100	100	98	100	100	100	100	100	100	100	100			
o	100	100	100	100	100	100	100	100	100	100	98	100	100	100	100	100	100	100
	cap	a	b	c	d	e	f	g	h	i	j	k	l	m	n	o		

purities (%)

below 85
85 – 90
90 and up

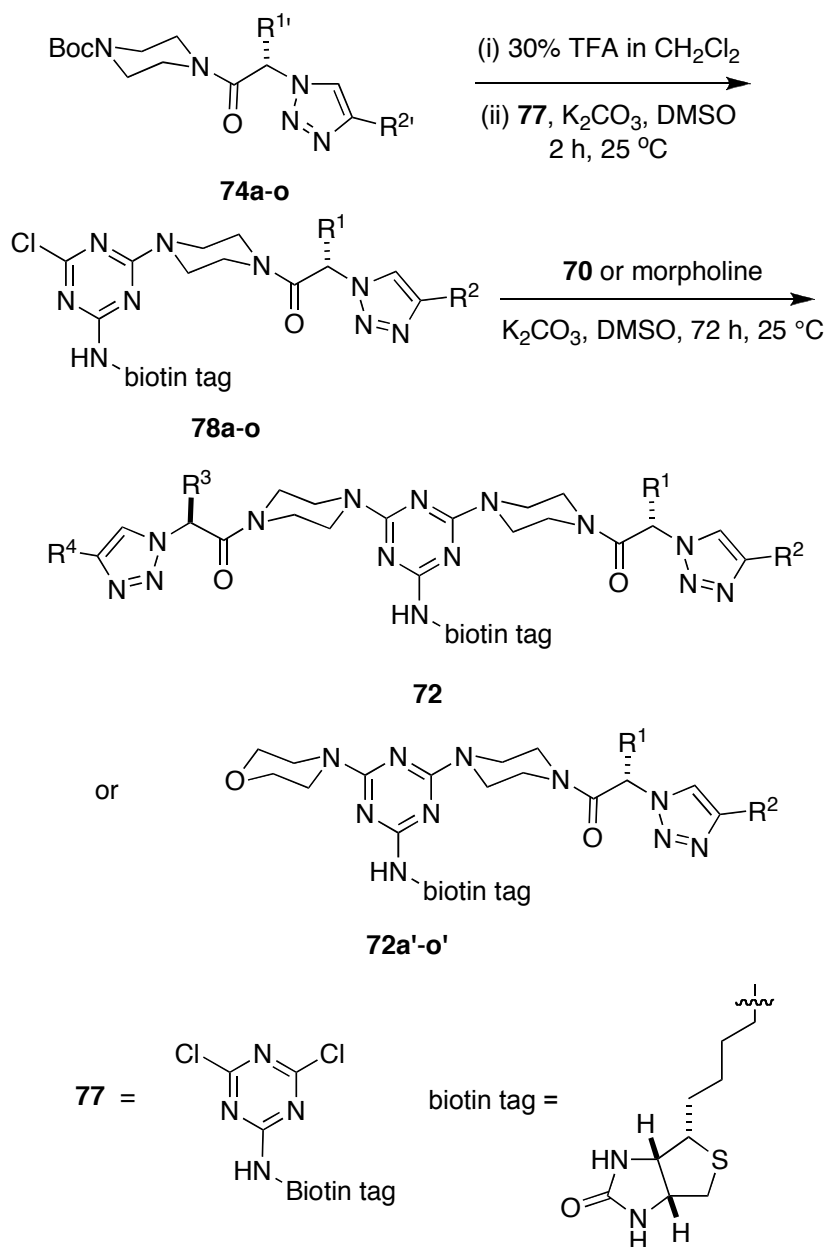
Figure 3.4. Continued.

### 3.5 Preparation of Biotin Labeled Bivalent Compounds

A library of 135 compounds **72** labeled with biotin was also prepared from monovalent compounds **74a-o**. The preparation procedure is similar to that used to prepare fluorescent labeled compounds **71**. As shown in Scheme 3.5, the difference is that DMSO was used as the solvent in the first monomer addition and the lower concentration was necessary due to reduced solubility of the Biotin-containing linker **77**. Purities of the crude materials of compounds **72** were evaluated by analytical HPLC, monitored by UV and SEDEX detectors. Figure 3.5 shows the final purities of bivalent compounds **72**. Initially, about 10 bivalent compounds gave unsatisfactory purity by UV and/or SEDEX but this was remedied upon resynthesis.

Twenty percent of bivalent compounds were characterized by one-dimensional and two-dimensional NMR experiments. (See Appendix B) All the compounds gave

satisfactory molecular ions in MALDI-MS analyses. The product yields were not determined either due to the small scale of the synthesis.



**Scheme 3.5.** Preparation of biotin-labeled bivalent library **72**.

a.

h	89	87																
g	100	100	89															
j	100	88	85	90														
k	96	87	86	94	91													
c	100	88	89	90	88	100												
a	100	89	87	92	99	91	93											
d	100	92	89	100	86	97	100	100										
e	100	89	85	85	86	86	100	87	100									
f	100	100	100	87	86	87	90	89	89	100								
l	100	89	90	87	92	86	86	87	96	86	91							
b	100	90	91	86	90	86	90	87	89	98	100	97						
i	100	93	100	95	89	97	95	91	92	96	100	98	91					
m	100	94	100	94	87	96	95	92	97	90	94	100	87	98				
n	100	97	85	91	87	93	89	92	90	100	86	85	87	85	96			
o	100	95	100	100	88	93	100	87	87	100	89	95	90	91	87	96		
	cap	h	g	j	k	c	a	d	e	f	l	b	i	m	n	o		

UV  
Purities(%)

below 85
85 – 90
90 and up

b.

h	87	89																
g	100	100	97															
j	98	93	92	92														
k	100	87	86	100	96													
c	100	91	94	85	86	87												
a	98	91	90	87	100	91	100											
d	100	89	100	100	85	100	100	100										
e	100	90	89	100	89	92	100	100	100									
f	100	100	100	100	98	91	85	94	93	99								
l	100	88	90	97	92	100	86	94	100	85	89							
b	100	87	92	100	88	91	100	100	100	100	100	100						
i	100	91	92	100	86	96	100	90	100	92	100	100	95					
m	100	93	92	100	88	95	100	90	94	92	100	100	90	97				
n	100	88	90	85	86	90	100	100	95	92	100	100	94	87	96			
o	97	100	100	100	85	100	88	91	88	94	95	100	91	92	92	100		
	cap	h	g	j	k	c	a	d	e	f	l	b	i	m	n	o		

Sedex  
purities (%)

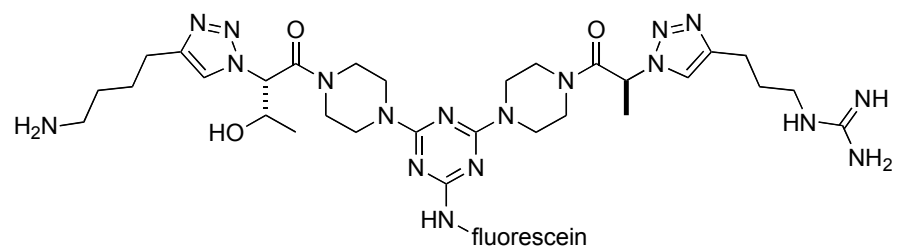
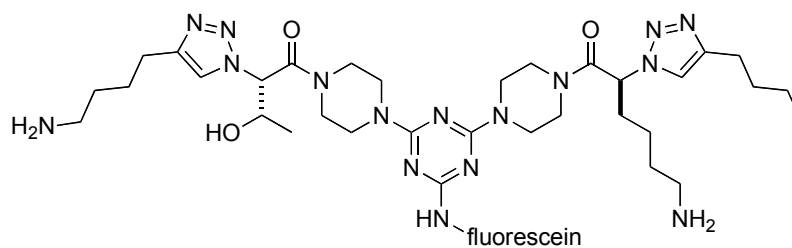
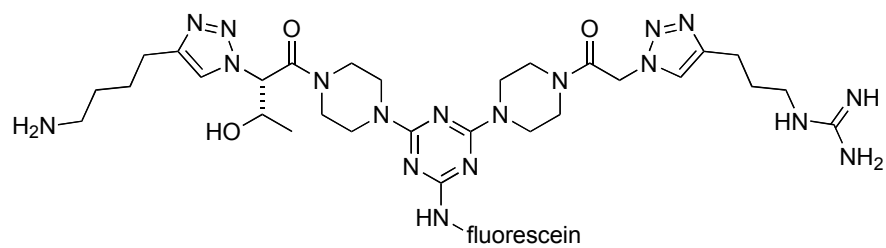
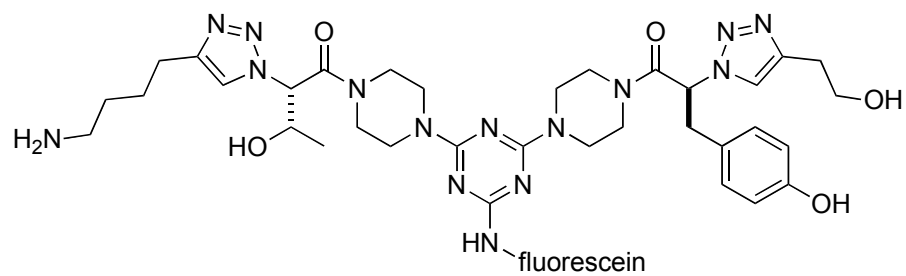
below 85
85 – 90
90 and up

**Figure 3.5.** Purities of the library of compounds **72** where the detection method was: (a) UV set at 254 nm; and, (b) SEDEX detection. The term “cap” is used for morpholine.

### 3.6 Direct Binding to Trk and p75 Transfected Cells

Direct binding assays were performed to assess the ability of peptidomimetics **71** to bind Trk and p75 receptors.<sup>130,129,85,131</sup> The library of 135 bivalent compounds was tested for binding to transfected TrkC-expressing, TrkA-expressing or p75-expressing cells in a fluorescence activated cell sorting (FACScan) assay. Live cells expressing the indicated receptors were incubated with ligands (20  $\mu$ M), washed, and immediately studied by FACScan. Data was acquired and analyzed CellQuest software. Mean channel fluorescence (MCF)  $\pm$  sem, n =5 independent experiments, in each 3,000 to 6,000 cells were acquired. In all cases cellular controls and antibody controls were used (not shown). The NIH-IGFR-1 cells which do not express any neurotrophin receptor served as a negative control. Each compound was tested three times and the mean channel fluorescence was determined.

From the preliminary screening data, four bivalent compounds exhibited relatively high binding affinity and better selectivity against TrkA-expressing cells. These compounds were purified by preparative HPLC and their direct binding data has been confirmed. The structures of the four compounds are illustrated in Figure 3.6. As shown in Figure 3.7, compounds **71gj**, **71gm**, **71gn** bind to TrkA, and to a lower degree they also bind to TrkC and p75, and **71gi** binds to TrkA, but it does not bind significantly to TrkC or p75. Interestingly, four “hits” all contain Thr-Lys sequences.

**71gi****71gj****71gm****71gn**

**Figure 3.6.** Structures of compounds **71** that bind to TrkA from the preliminary FACS assay.

a.

Comp'd 71	NIHTrkA			NIHTrkC			p75		
	Mean	Stdev	Sem	Mean	Stdev	Sem	Mean	Stdev	Sem
<b>gj</b>	805.26	318.52	142.45	319.57	145.71	65.16	560.89	459.18	205.35
<b>gm</b>	1152.98	3378.26	150.83	586.24	195.28	87.33	628.95	198.75	88.88
<b>gn</b>	880.04	256.37	114.65	349.78	159.02	71.12	585.71	414.53	185.39
<b>gi</b>	482.23	228.37	102.13	101.33	99.83	44.64	295.81	369.1	165.07

b.

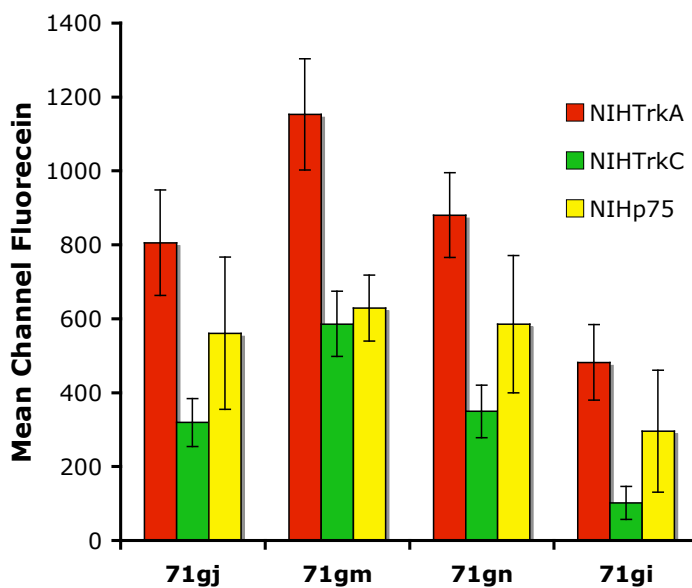


**Figure 3.7.** Direct binding assay data and the graph presentation of the four “hits”.

### 3.7 Summary

Copper(I)-catalyzed azide/alkyne cycloaddition reactions can be used to make 1,2,3-triazoles that serve as amide bond surrogates. These reactions are mild, easy to work-up and compatible with many functional groups and solvent systems. A library of 15 monovalent triazole mimics is prepared via “click” reactions in solution. These triazoles compounds contain two amino acid chain functionalities at 1- and 4- positions. One is derived from a natural amino acid and the other is functional group that assembles the side chains of an amino acid. “Click” reactions allow quick and efficient generation of the desired peptidomimetics in good yields.

Initially, our dimers syntheses are achieved via addition of one monomer on solid phase and the other in solution. This “semi-solution phase” methodology requires expensive resins and HPLC purification, and tends to give small amount of materials. In our new strategy, both monomers are coupled to the linker scaffold sequentially in solution by simply manipulating the solvent systems. This method allowed us to prepare large libraries of bivalent compounds quickly and efficiently. The two monomers are combined with each other cleanly, to achieve one-compound-per-well in sufficient purity for biological testing.

The fluorescence activated cell sorting (FACScan) assay has performed on the fluorescently labeled compounds for binding to transfected TrkC-expressing, TrkA-expressing or p75-expressing cells. Four bivalent compounds **71gi**, **71gj**, **71gm** and **71gn** have exhibited relatively high binding affinity and better selectivity against TrkA-expressing cells. All of these molecules contain Thr-Lys sequence. The assay has been repeated on the purified compounds and the binding data is confirmed.



## CHAPTER IV

### SOLUTION PHASE SYNTHESIS OF NON-PEPTIDIC MIMETICS USING ARYLALKYNE AS AMIDE BOND SURROGATES AND THEIR ASSEMBLY TO BIVALENT MOLECULES

#### 4.1 Introduction

Peptidomimetic synthesis has benefited greatly from the rapid development of combinatorial chemistry. Fast generation of molecular diversity libraries, followed by their evaluation using highthroughput screening, has produced many potential drug candidates.<sup>132,133,134</sup> About a decade ago, many new approaches were discovered and applied to the generation of non-peptidic, “drug-like” small molecule libraries.<sup>135,136</sup>

Peptides and proteins play a crucial role in many biological systems. However, their utility as therapeutic agents is limited due to their low metabolic stability and poor absorption after oral ingestion.<sup>137,138</sup> Efforts to alleviate these problems have fueled the rapid growth of non-peptidic small molecule peptidomimetics. In general there are two ways to generate this type of mimics. One is to install a unit that can replace the amide bond<sup>139</sup>; the other is to use scaffolds that contain sites for attachment<sup>140</sup>. The purpose of these modifications is to increase the selectivity and potency of drug candidates at the target binding sites and decrease their possibility of degradation. Further, the lipophilicity can be increased and the compounds will be more easily absorbed into the biological systems.

Backbond modifications generally involve the isosteric or isoelectronic replacement of the amide moiety in the peptide chain and /or introduction of additional groups.<sup>141</sup> Although a number of amide bond replacements have been reported in the literature<sup>142-145</sup>, the most widely used surrogates are illustrated in Figure 4.1. Incorporation of peptide side chains may be varied due to the unique physicochemical properties of each surrogate.

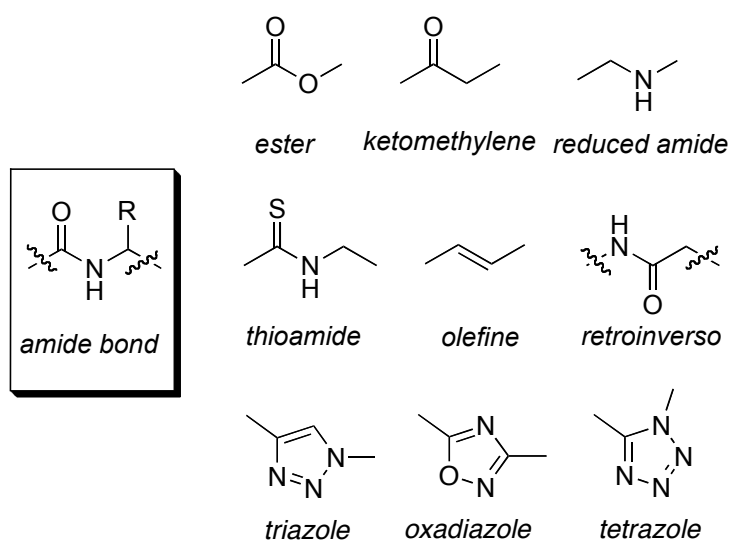


**Figure 4.1.** Structures of the common peptide backbone replacements.

Rigid scaffolds have been utilized to attach amino acid side chain moieties and display them in the appropriate region of space.<sup>146-148</sup> As shown in Figure 4.2, some of these mimics hardly resemble peptides, with the exception that side chain-like motifs are attached to the rigid core structure.<sup>149,150</sup> The conformation of the peptide pharmacophore can be locked or strongly influenced by the rigidity of the core structure. Combinatorial libraries were prepared on solid support since some scaffolds are suitable for solid phase synthesis.<sup>151,152</sup>

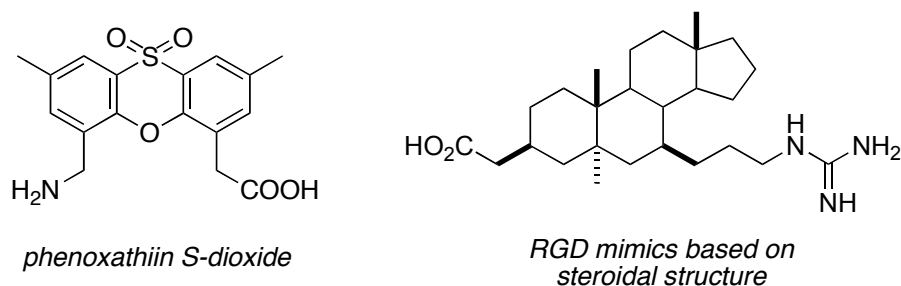


**Figure 4.2.** Examples of non-peptidic scaffolds.

Our efforts to development small molecules with less peptide character include using a simple substituted iodobenzene<sup>153</sup> that will serve as a scaffold to attach functional groups that analogue side chains found in the amino acids in the loop region of the neurotrophins. As shown in Figure 4.3, the big advantage of this design is that the monovalent compounds are easy to make on a large scale, and the molecular fragments that correspond to protein amino acids are highly accessible. Also, turn analogs of this type are “non-directional” so that the side-chains can mimic  $i+1$  and  $i+2$  or  $i+2$  and  $i+1$ .

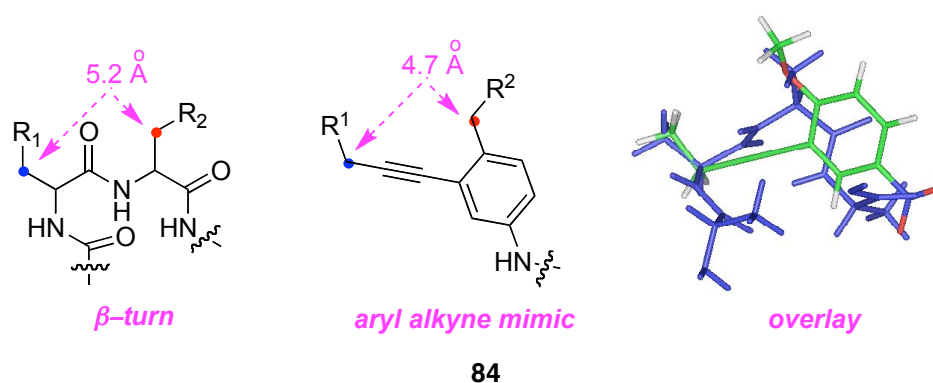


**Figure 4.3.** Generic structure of aryl-alkyne library.

In the attempt to mimic neurotrophins function, one of our goals is to develop simple methodologies to assemble bivalent libraries. Neurotrophins exist and function as dimers, and the distances of the relevant loop region are varied.<sup>154,155,156</sup> It is expected that bivalent turn mimics with optimal-length linkage should be more selective and bind to neurotrophin receptors with higher affinity. We call this simple idea as “*mix and match*” linker design presented in Figure 4.4. It involves matching short and long linkers in all three possible ways and the diversity of the molecules will be greatly increased. The approach is a general one for all dimeric ligands docking with dimeric receptors, even when the ideal linker dimensions are unknown. Thus, if 50 monovalent peptidomimetics were to be transformed into dimers, then they could each be coupled

with the linker molecules to give a library of 100 monovalent species. If 50 compounds are combined with themselves then the total maximum library size would be 1275, but for 100 it is 5050, and the latter library would be far more interesting because it would cover a range of linker geometries.

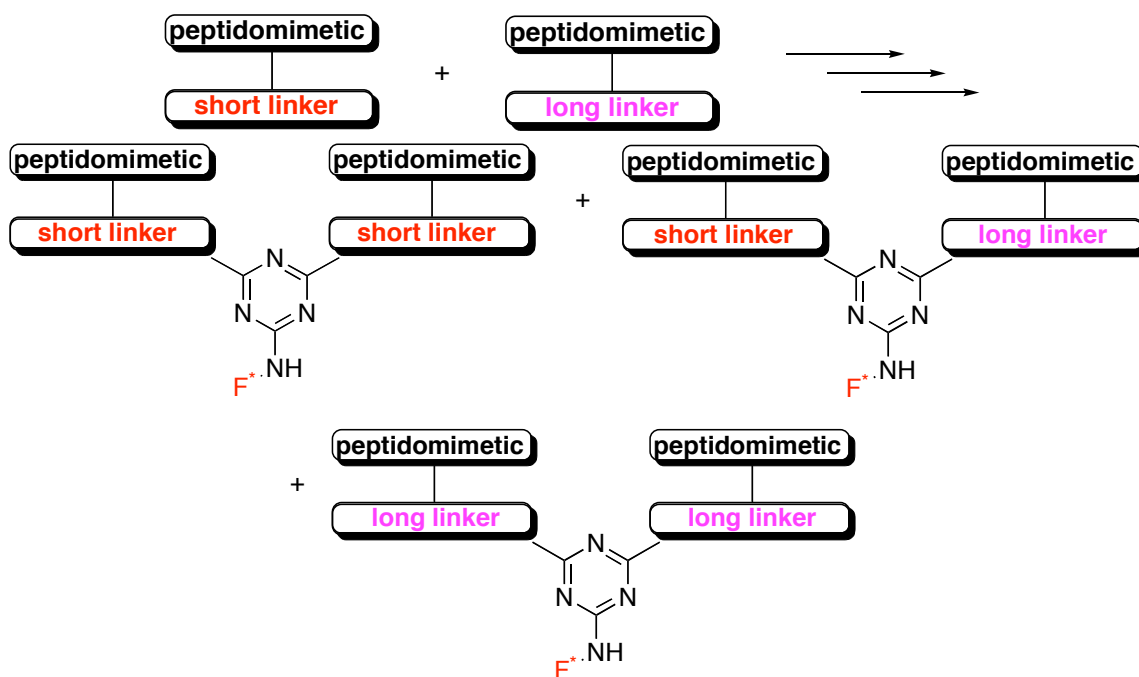
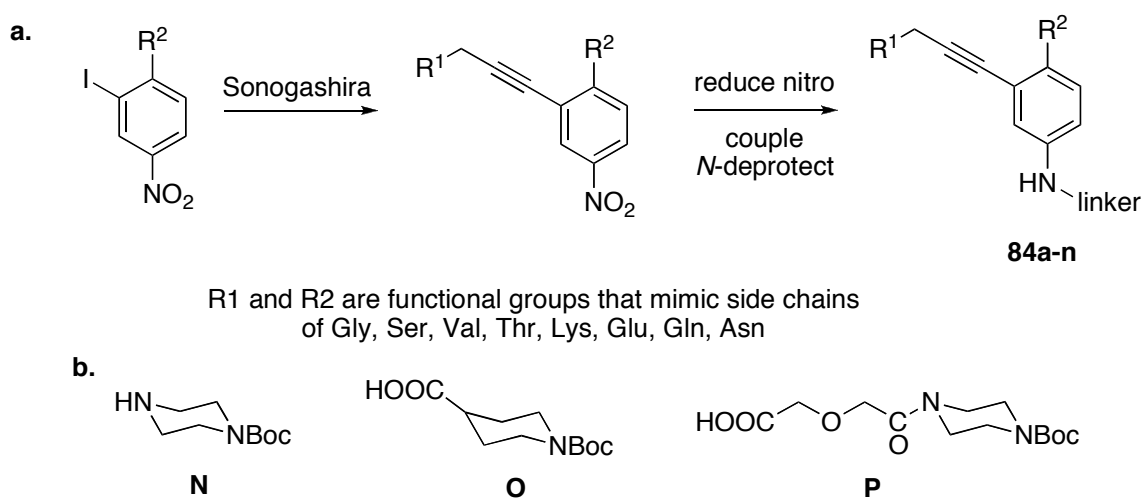


**Figure 4.4.** “Mix and match” linker design.

## 4.2 Preparation of Non-Peptidic Aryl-Alkyne Mimetics

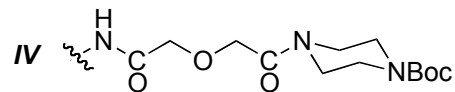
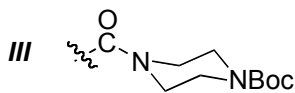
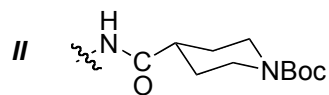
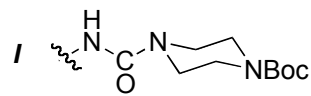
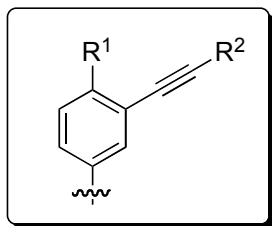
In our laboratory, a library of 14 non-peptidic aryl-alkyne mimetics was prepared in solution. Substituted iodobenzene served as a scaffold and a simple Sonogashira coupling<sup>157</sup> reaction afforded the aryl-alkyne core structure. The solution phase approach featured in Figure 4.5-a is my part of a group effort. Other people in our group prepared the alternative similar monomers. The general synthesis route begins with a

Sonogashira coupling followed by an  $S_NAr$  step to give another side-chain variety. In my part of work, the compounds that mimic glycine, serine and/or valine side chains simply start from a iodonitrobenzene to prepare mimics only with Sonogashira coupling reactions. A set of three linkers was used in this work. Both **N** and **O** are short linkers. They were picked from different synthetic strategies. Linker **P** is a long linker that was prepared from **N** and diglycolic anhydride.



**Figure 4.5.** (a) General synthetic scheme and the short/long linkers; (b) Short/long linkers.

The library of 14 monovalent peptidomimetics is listed below (Table 4.1). Compounds **84a-g** were functionalized with short linkers **N** or **O** and the long linker **P** was attached to the compounds **84h-n**. Most compounds were prepared following the route shown in Figure 4.5-**a** except that **84a**, **84b**, **84f** and **84g** were prepared from substituted benzoic acids. Urea (**84a**, **84b**, **84f**) or amide (**84g**) formation led to the desired molecules for the synthetic convenience.

**Table 4.1.** Aryl-alkyne library **84**.

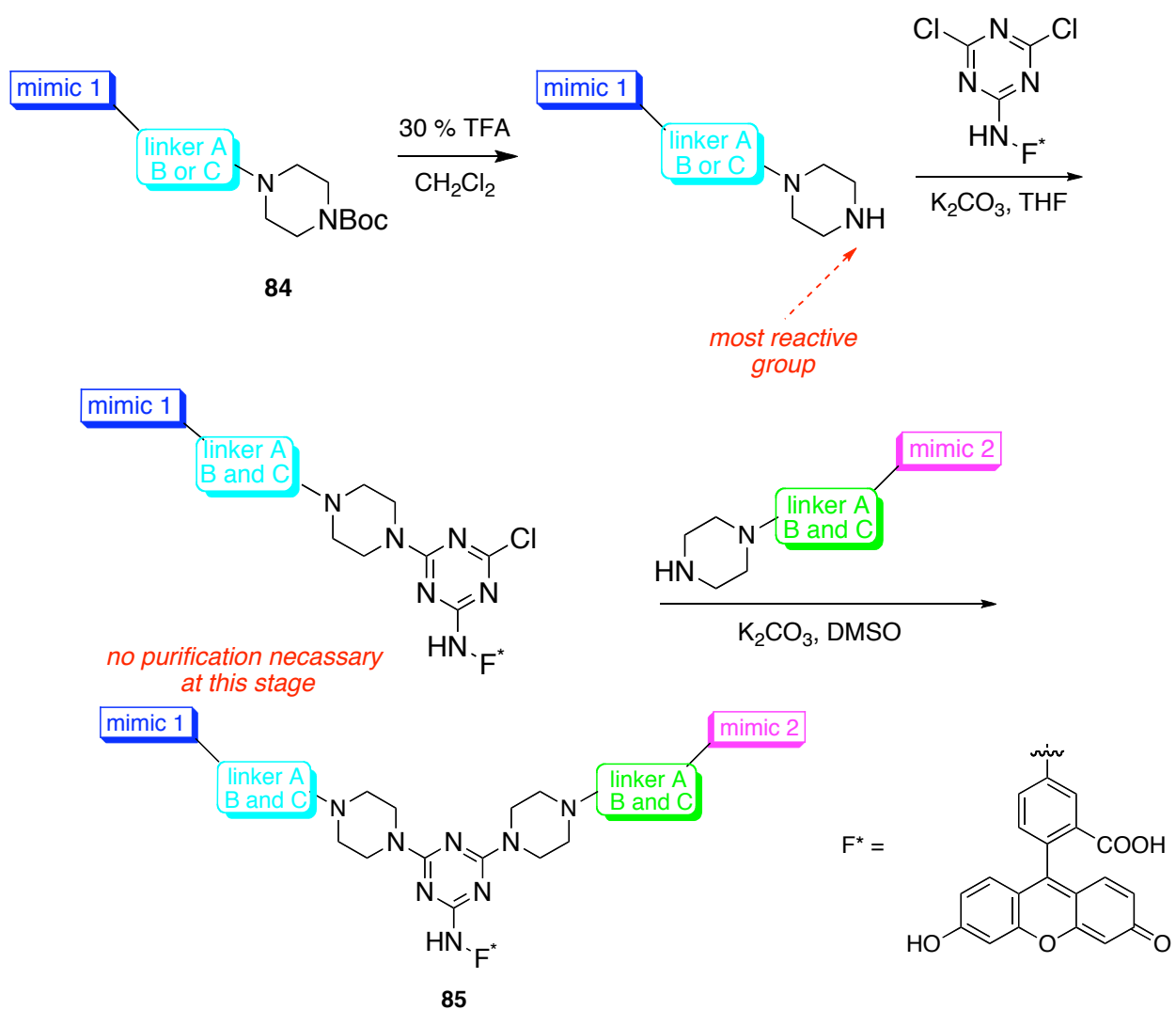
Comp'd <b>84</b>	Scaffold	R <sup>1</sup>	R <sup>2</sup>	Overall Yield (%)
<b>a</b>	I	H		61
<b>b</b>	I	H		56
<b>c</b>	II		H	92
<b>d</b>	II	CH <sub>3</sub>		49
<b>e</b>	II	CH <sub>3</sub>		45
<b>f</b>	I	H		48
<b>g</b>	III	CH <sub>3</sub>		72
<b>h</b>	IV	H		56
<b>i</b>	IV	H		52
<b>j</b>	IV		H	65
<b>k</b>	IV	CH <sub>3</sub>		42
<b>l</b>	IV	CH <sub>3</sub>		37
<b>m</b>	IV	H		42
<b>n</b>	IV	CH <sub>3</sub>		32

### 4.3 Preparation of Bivalent Compounds **85**

The preparation of the bivalent library of compounds **85** is similar to that discussed in Chapter III. As shown in Scheme 4.1, the Boc protecting groups of the monovalent compounds from Table 4.1 were removed by TFA and treated with DTAF and  $K_2CO_3$  in THF for 4 h at 25 °C. The resulting intermediate was concentrated and redissolved in DMSO and split into small portions. An equimolar of the deprotected monomer was added to each portion followed with the addition of excess of  $K_2CO_3$ . The resulting mixture was placed on a shaker and reacted for 72 h to afford compounds **85**.

Purities of the crude materials of compounds **85** were evaluated by analytical HPLC, monitored at 254 nm by a UV detector. Figure 4.6 shows the crude purities of bivalent compounds **85**. Among the 105 compounds, 81% were obtained with the purity above 85%. The compounds with less than 85% purity were resynthesized by the same method shown in Scheme 4.8 and the purities were shown in Figure 4.7. Most of the compounds gave satisfactory purities after they were prepared again. The only exception was that the purities of compounds **85ml** and **85mh** were still below 85% but they were significantly improved. This reveals that the impurities were mainly caused by the pipetting errors and the dimerization method is fairly efficient.

One-dimensional and two-dimensional NMR experiments were conducted on 20% compounds that were randomly picked (See Appendix C). All the compounds gave satisfactory molecular ions in MALDI-MS analyses. The product yields were not determined because of the small scale of the synthesis.



**Scheme 4.1.** Preparation of bivalent mimetics **85**.



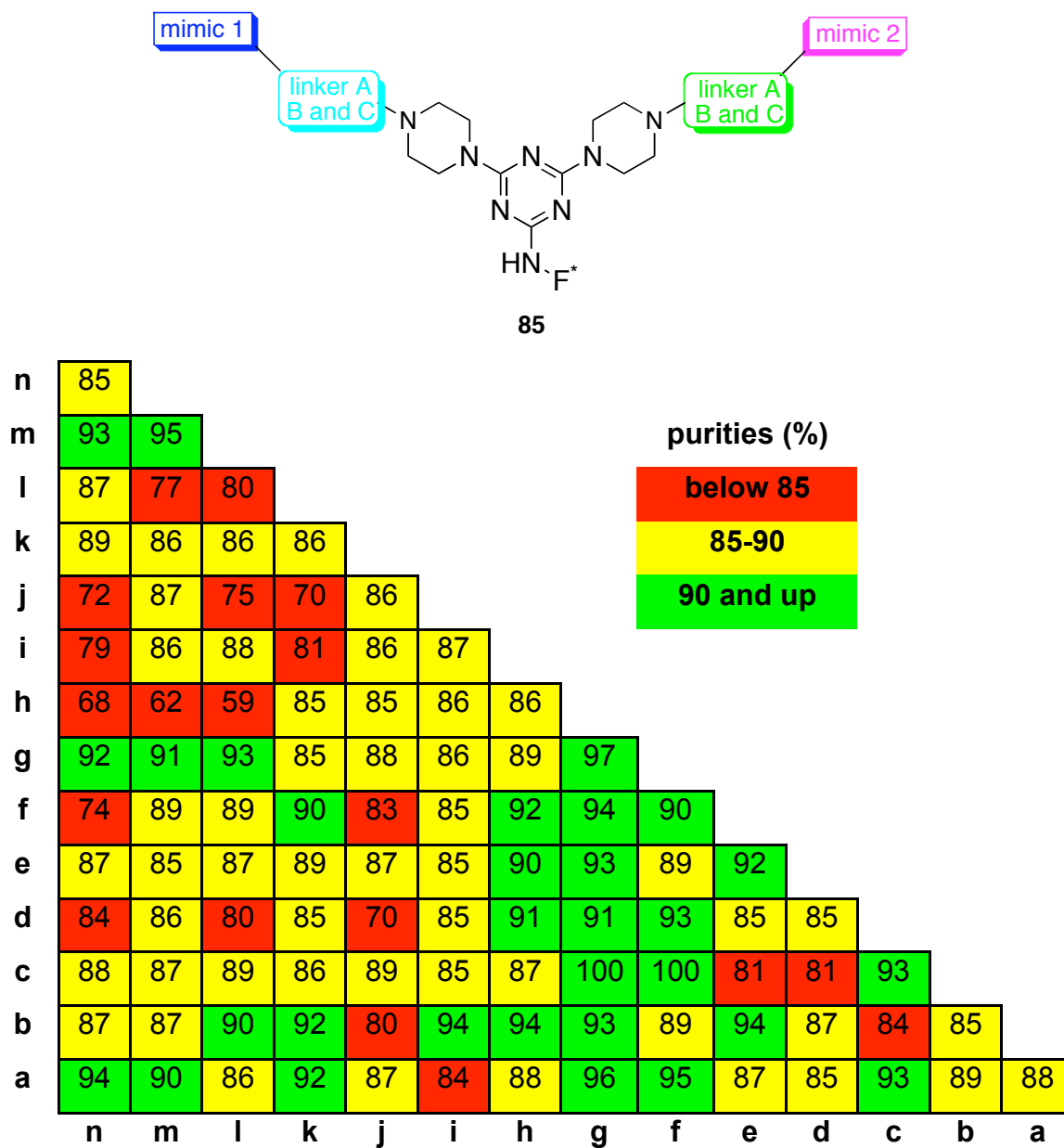


**Figure 4.6.** HPLC purities of the bivalent turn mimics **85**.

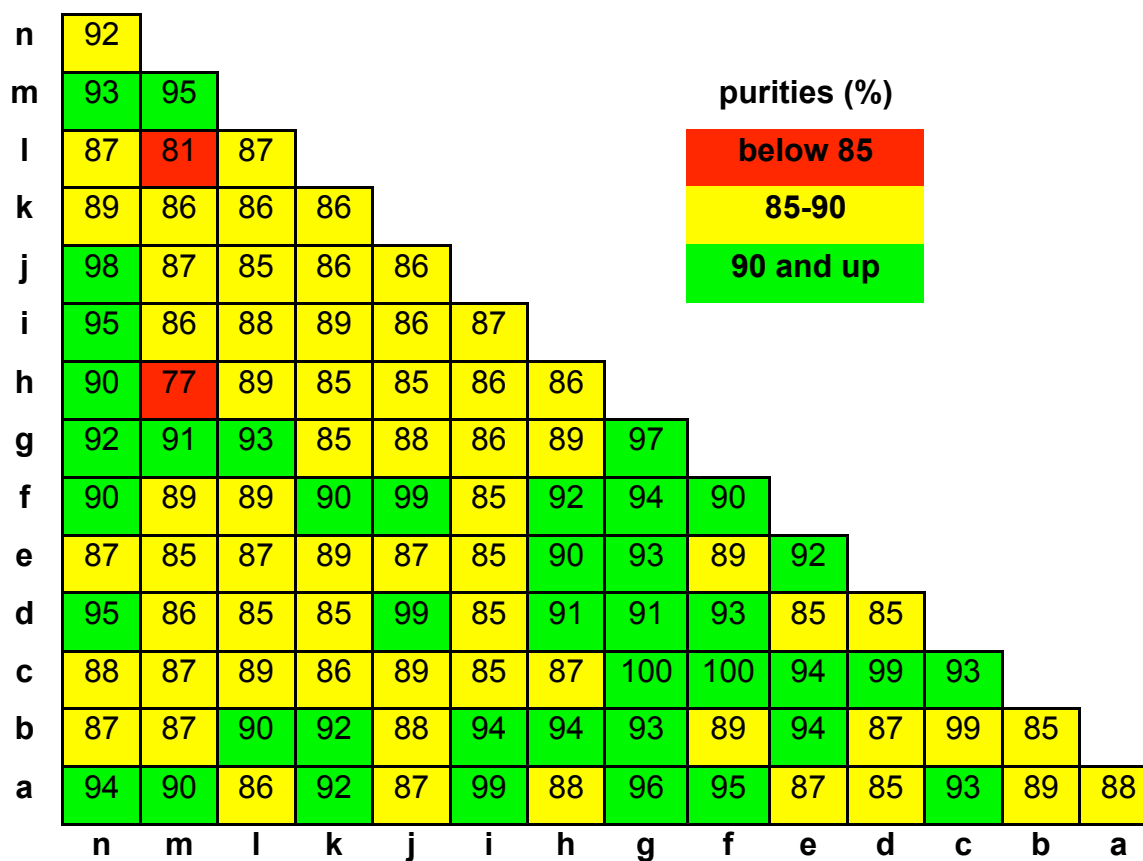


**Figure 4.7.** HPLC purities of **85** after resynthesis.

#### 4.4 Biological Assays

Direct binding assays were performed in a fluorescence activated cell sorting (FACScan) as previously discussed in Chapter III. The library of 105 bivalent molecules was screened for binding to Jurkat and NIH cells. The histograms were analyzed on the compounds that exhibited high mean channel fluorescence (MCF) on the assays performed with Jurkat or NIH cells.

The histograms are curves that show the relation between the amount of cells (events) and their fluorescence level. If there is binding of the peptide to the cells it is

expected a shift in the curve to the right (i.e. more event with higher fluorescence). Cells IGF1-R do not express any neurotrophin receptor served as negative control. The majority of the evaluated peptides displayed a higher tropism toward NIH-Trk-C and NIH-p75 cells. The most promising peptides were **85gn**, **85hn**, **85jn** and **85kn** (Figure 4.7), which binded preferentially to Trk-C, with a lower binding to Trk-A expressing cells. However, we did not find any peptide with higher tropism by TNF receptor, which is over-expressed in Jurkat cells cultivated in SFM.

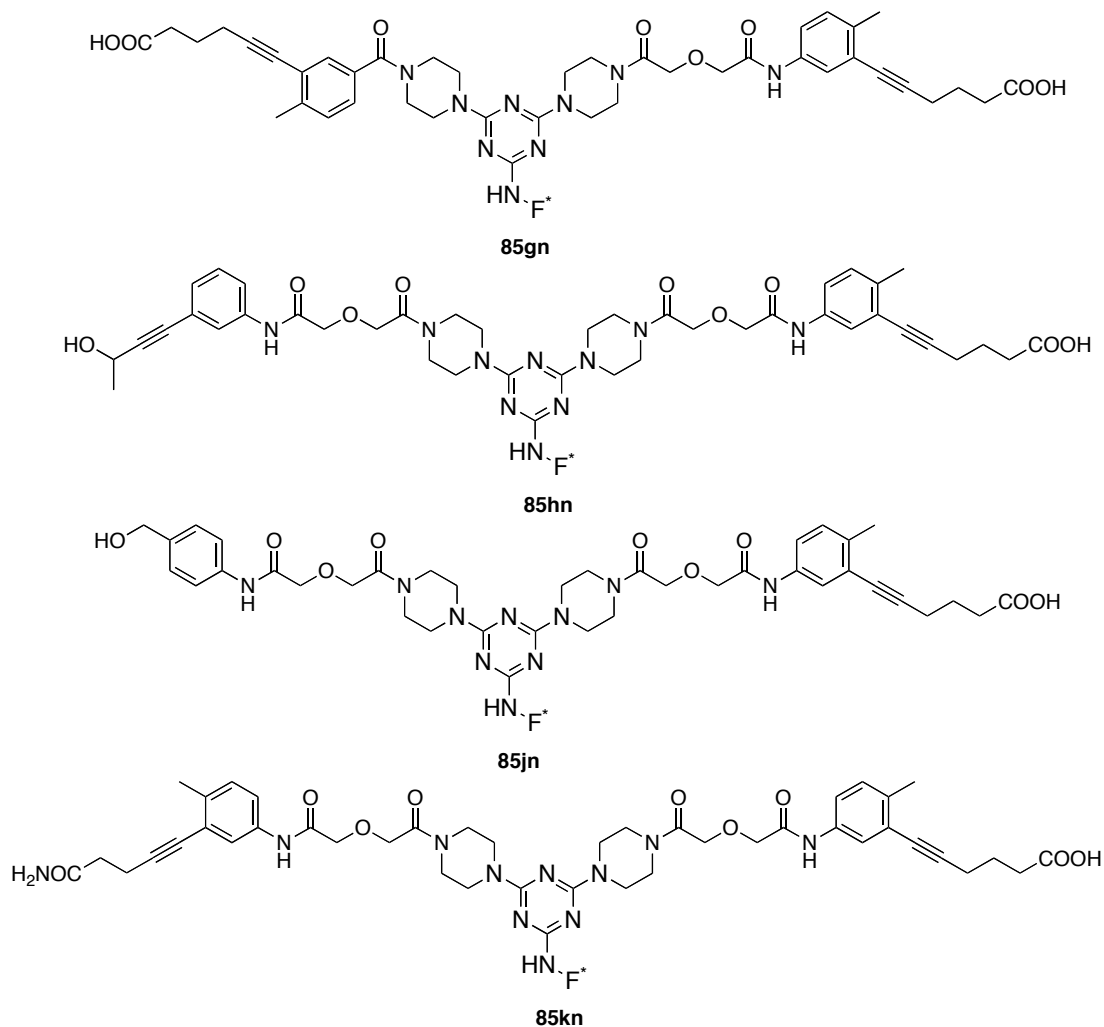


**Figure 4.8.** Structures of **85gn**, **85hn**, **85jn** and **85kn** that bind TrkC from the preliminary FASC assay.

A FACS competition test was performed with peptide mimics **85gn**, **85hn**, **85jn** and **85kn**, using 2B7 (anti-Trk C monoclonal antibody) or NT-3 at saturating concentrations as competitors. The mIgG was used as an irrelevant competitor, so these values reflect the standard binding of the peptides to the cells. The presence of competitors, especially 2B7, reduces the MCF of the peptide mimics **85gn** to **85kn**, without reaching the background level. Thus, it seems (Table 4.2) that unspecific union exists while the peptide mimics join to TrkC receptor near to the antibody binding site, as well as other places all over the cell surface.

**Table 4.2.** FACS Competition Assay.

Comp'd	NIH TrkC cells		
	mIgG	NT-3	2B7
<b>85gn</b>	207.34	189.49	165.67
<b>85hn</b>	274.88	255.35	233.38
<b>85jn</b>	248.77	241.48	213.43
<b>85kn</b>	306.83	314.52	282

To determine if these four compounds were bioactive, a MTT assay was performed using a concentration of 10  $\mu$ M (see Chapter II for the details of MTT assay). None of the compounds induces survival on NIH-Trk C cells (Table 4.3); this seems to confirm lack of specific binding to TrkC receptors.

**Table 4.3.** Cell Survival Data for Compounds **85**.

Comp'd	NIH-TrkA cells		NIH-TrkC-C1 cells		NIH-IGF1-R cells	
	SFM	NGF low	SFM	NT-3 low	SFM	IGF low
untreated	0	0	0	0	0	0
<b>85gn</b>	0.88	6.11	-0.07	-3.84	-0.75	3.3
<b>85hn</b>	-1.19	5.44	-0.91	-0.06	-0.75	2.98
<b>85jn</b>	0.31	8.21	-0.78	2.61	-4.05	-2.24
<b>85kn</b>	0.17	4.32	-1.8	-2.8	-4.58	-7.35

#### 4.5 Summary

Syntheses of rationally designed non-peptidic mimics normally involve peptide bond surrogates or scaffolds wherein the critical side-chains are retained and presented in the proper region of space to maintain the desired biological properties. Our efforts toward the synthesis of non-peptide mimetics have utilized an aryl-alkyne scaffold that retains some properties of the amide bond. Also, the functionalized amide acid side chains can be sequentially introduced via Sonogashira coupling reactions.

This method produced a library of non-peptide mimics **84**. These compounds contain variable side-chain analogs, *ca.* norleucine, isoleucine, arginine and lysine. Short or long linkers were attached to the mimetics by amide or urea formation reactions. After removal of the Boc protecting groups, the monovalent compounds were introduced onto the fluorescent-labeled triazine scaffold sequentially. The bivalent library of 105 compounds **85** was obtained in satisfactory analytical HPLC purity.

## CHAPTER V

### BASE DEPENDENCE IN COPPER CATALYZED HUISGEN REACTIONS: EFFICIENT FORMATION OF BISTRIAZOLS\*

#### 5.1 Introduction

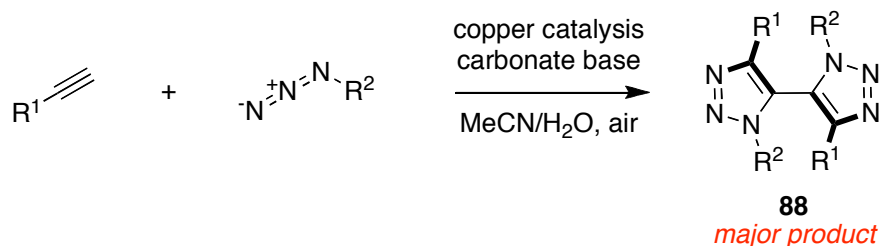
“Click chemistry” has offered a pool of potential active compounds of lead optimization and drug discovery.<sup>158</sup> Reactions defined as “click” reactions take place with high yields, mild conditions, and using reagents that have no impact on most other functional groups. Sharpless and coworkers have identified a number of reactions that meet these criteria,<sup>5,6</sup> the most powerful of which is the copper-accelerated<sup>3,4</sup> Huisgen additions<sup>1,159</sup> of azides to alkynes. They are undeniably useful in contemporary organic chemistry for two reasons. The first is that they are highly chemoselective; the conditions of the reaction tend not to influence functional groups other than azides and alkynes. The second is that this type of click reaction is very robust. They are experimentally simple to run, and the conditions seem tolerant of many minor changes. It has often been claimed that the copper mediated alkyne/azide cycloaddition reaction is not sensitive to pH<sup>11,10</sup>. However, we find that the course of the reaction can be altered dramatically by adding carbonate bases, and that discovery is the basis of this chapter.

In our laboratory, a minor impurity was often observed via analytical HPLC when preparing libraries of triazoles via these copper-mediated reactions. LC-MS analyses indicated these were oxidative dimers of the desired product (*ie* twice the desired M<sup>+</sup>, less 2H). Sharpless *et al* have previously noticed such minor by-products, without reporting their characterization, and attributed them to direct use of Cu<sup>I</sup> species.<sup>4</sup>

---

\* Reproduced in part with permission from “Base Dependence of Copper Catalyzed Huisgen Reactions: Efficient Formation of Bistriazoles” by Angell Y. and Burgess K. *Angew. Chem. Int. Ed.*, **2007**, *46*, 3649-3651. Copyright © 2007 WILEY-VCH Verlag GmbH & Co. KGaA, Weinheim

However, we observed significant amounts of these products when attempting azide-alkyne couplings of crude substrates, even with a  $\text{CuSO}_4/\text{Cu}$  powder system. Here we report that these oxidative dimers have the structure **88** and that, under basic conditions, they can be the major products.



Several groups have attempted to prepare bistriazoles by the 1,3-dipolar cycloaddition reactions. All of them were conducted under thermal conditions and elevated temperatures were required. These cycloaddition reactions are not regioselective and the isomers have to be isolated with column chromatography. Meanwhile, the scaffolds were rarely functionalized. Huisgen 1,3-dipolar cycloaddition reactions have been utilized to the syntheses of bistriazoles from diacetylene derivatives with azides.<sup>160,161</sup> The cycloaddition between azides and alkynes is typically carried out refluxing xylene, benzene or toluene. Figure 5.1 shows the sequential cycloaddition of diacetylene derivatives with azides.<sup>160</sup> Bistriazoles **Q**, **R**, **S** and **T** were generated when azides refluxed with triazole derivatives **A** and **B** in xylene.

In this chapter, oxidative “click” coupling to give 5,5'-bistriazoles is discussed. The bistriazole products predominate in the copper accelerated “click reaction” of alkynes and azides when carbonate bases are used as additives (ca 1 – 2 M). The reaction seems to be more facile for propargylic ethers and less hindered substrates. Use of an optically active azide gave separable atropisomeric products, providing a convenient access into optically pure derivatives.

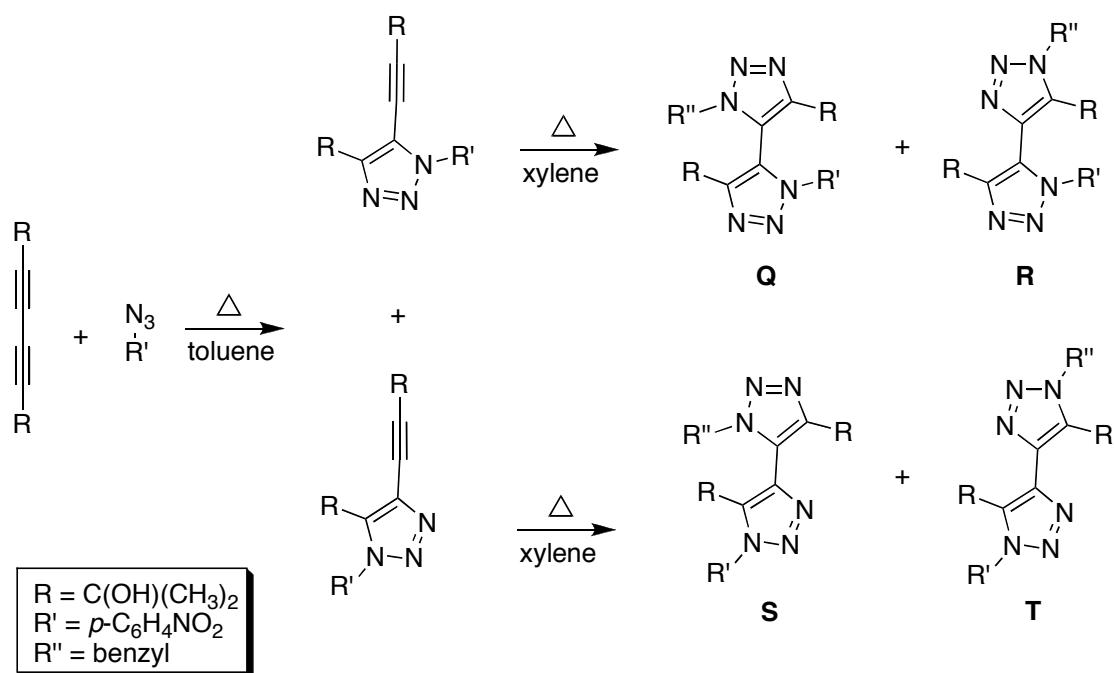


**Figure 5.1.** Bistriazole formation in thermal conditions.

## 5.2 Base Screening for the Formation of the Bistriazole Compounds

Variation of the reaction conditions was attempted to optimize the yield of compound **88a** in this Cu-mediated process; most of the data collected were negative (see Appendix D). For instance, triazole **89** was the main product when the reaction was performed under nitrogen with Cu/CuSO<sub>4</sub> as catalyst, but the catalyst was rapidly deactivated and the starting materials remained when that reaction was performed under pure oxygen. Attempts were made to increase the amounts of oxidative dimer by adding palladium catalysts, but these had little effect. Finally, pH was identified as the key variable. The model transformation in Table 5.1 was chosen because the oxidative dimerization product **88a** was fully characterized at an early stage in the work. Compound **88a** was a by-product in the presence of 1.5 M NaHCO<sub>3</sub>, and it was the major one when K<sub>2</sub>CO<sub>3</sub> was used. The optimal base strength was 1 – 2 M; at higher



concentrations the alkyne **90** became more prevalent. Ammonium carbonate (entry 6) gave only the normal click product **90** implying that Cu-NH<sub>3</sub> coordination prevents oxidative dimerization. Entries 7 – 9 show that hydroxide or phosphate bases give mixed results; this could mean that ligation of the carbonate to the copper assists formation of oxidative dimer. Other experiments with K<sub>2</sub>CO<sub>3</sub> additive indicate that oxidative dimerization is more prevalent in 1:1 MeCN/H<sub>2</sub>O than THF/H<sub>2</sub>O or MeOH/H<sub>2</sub>O, but the differences were relatively small. The extent of oxidative dimerization was less when an inert atmosphere was used, but under pure oxygen the reaction gave mostly starting materials.

**Table 5.1.** Effects of bases on the oxidative dimerization process.

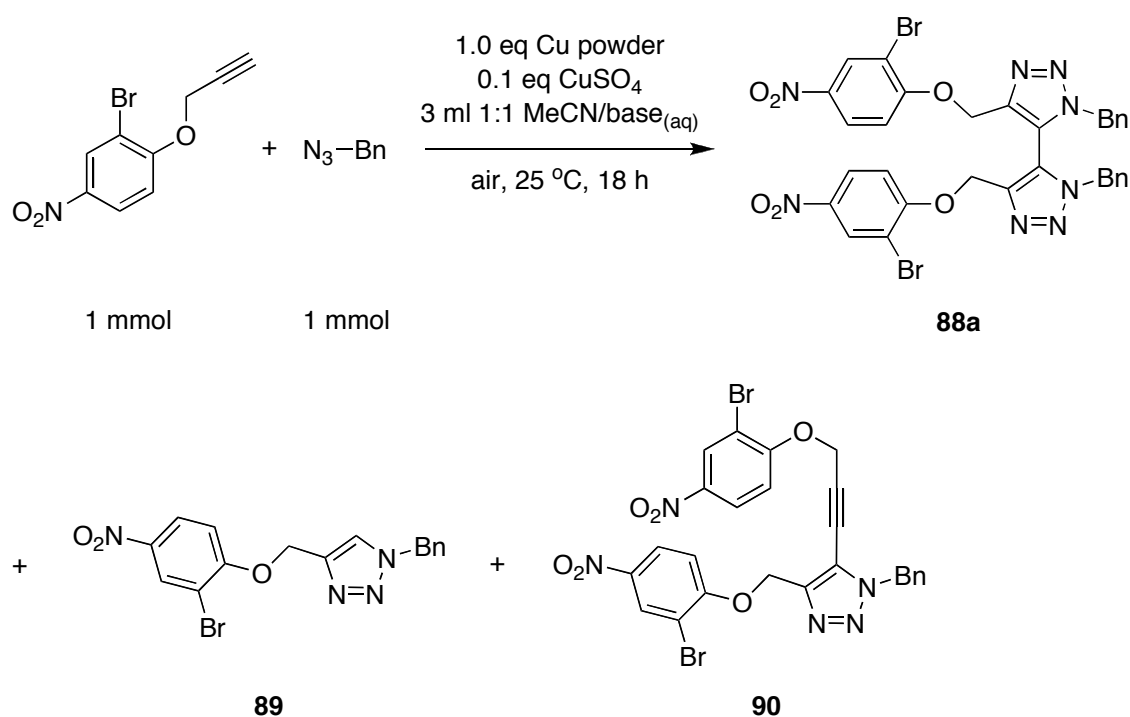


**Table 5.1. Continued.**

entry	base	base <sub>(aq)</sub> (M)	product		
			distribution (%) <sup>a</sup>		
			<b>88a</b>	<b>89</b>	<b>90</b>
1	NaHCO <sub>3</sub>	1.5	12	88	0
2	K <sub>2</sub> CO <sub>3</sub>	1.5	95	2	3
3	K <sub>2</sub> CO <sub>3</sub>	2.0	93	3	4
4	K <sub>2</sub> CO <sub>3</sub>	4.0	84	2	13
5	Na <sub>2</sub> CO <sub>3</sub>	2.0	95	3	2
6	(NH <sub>4</sub> ) <sub>2</sub> CO <sub>3</sub>	2.0	0	100	0
7	LiOH	1.5	33	57	10
8	KOH	5.0	50	0	50
9	K <sub>3</sub> PO <sub>4</sub>	4.0	56	38	6

<sup>a</sup> Determined via analytical HPLC on a C18 column (MeCN, H<sub>2</sub>O).

### 5.3 Control Experiments

Figure 5.2 illustrates some control experiments performed to elucidate the origin of the oxidative dimer **88a**. None of this material formed when the triazole **89** was isolated then exposed to the conditions in Table 5.1, entry 2. Similarly, isolated compound **90** did not give any detectable amount of the oxidative dimer **88a** when it was mixed with benzyl azide then subjected to those reaction conditions. Compounds **89** and **90** are therefore not intermediates in the formation of the oxidative dimer **88a**.

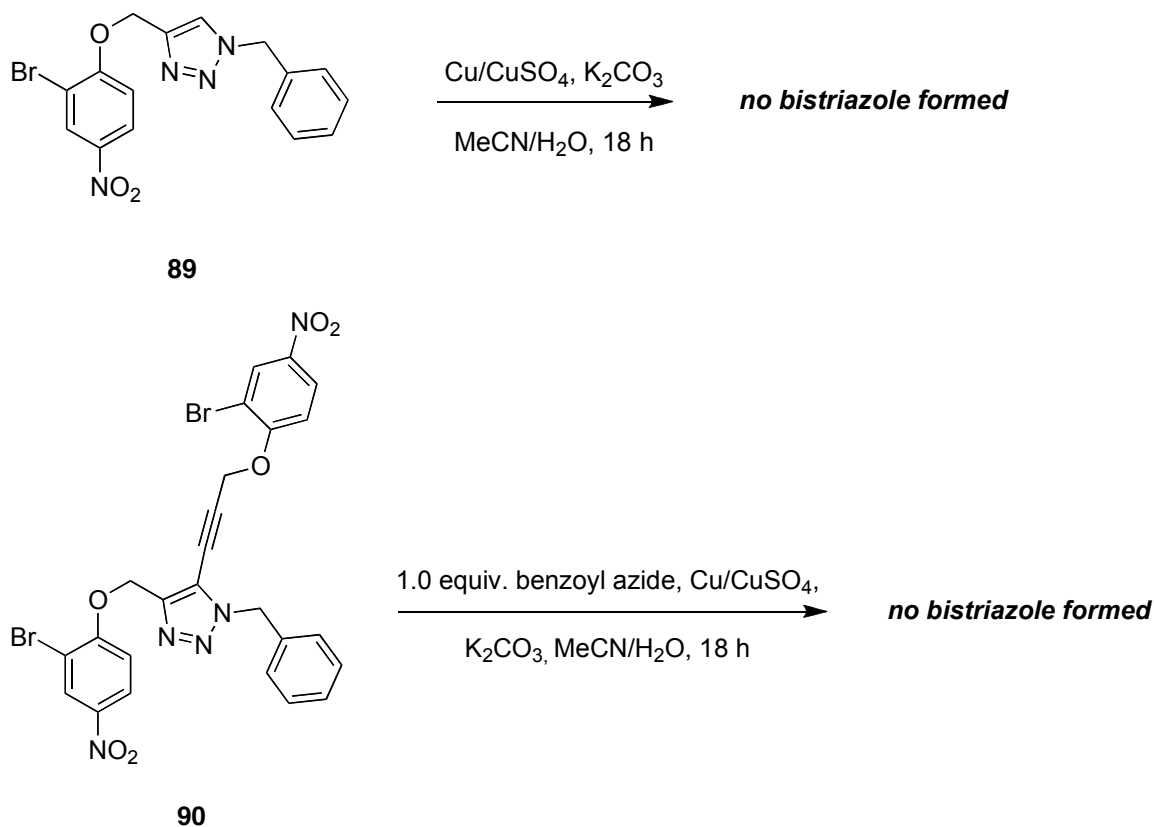


**Figure 5.2.** Control experiments.

#### 5.4 Syntheses of Compounds **88a-g**

Table 5.2 shows examples where the oxidative dimerization methodology was extrapolated to other substrates. In all cases the oxidative dimerization products **88** were conveniently separated from the other materials via a simple flash chromatography. Compounds **88a – d** all gave propargylic *O*-atoms: this seems to enhance the yields relative to compounds **88e – g**. The reaction did *not* work when the reactants were hindered and, in such cases, the triazole forms but this requires more reaction time than under neutral conditions (data not shown).

**Table 5.2.** Syntheses of bistriazole product **88**.

$$\text{R}^1\text{-}\equiv\text{C} + \text{N}_3\text{-R}^2 \xrightarrow[\text{air, 25 }^\circ\text{C, 18 h}]{\text{1.0 Cu powder/0.1 CuSO}_4, \text{1:1 MeCN/2M Na}_2\text{CO}_3 \text{ (aq)}} \text{88}$$

comp'd	R <sup>1</sup>	R <sup>2</sup>	isol'd yield (%)
<b>88a</b>			87
<b>88b</b>			72
<b>88c</b>			47
<b>88d</b>			69
<b>88e</b>			37
<b>88f</b>			23
<b>88g</b>			34

### 5.5 Synthesis of Compounds 88h-i via Convergent Desilylation

Many researchers using the Cu-mediated cycloaddition reactions access their alkyne starting materials via Sonogashira<sup>157</sup> reactions of trimethylsilylethyne, then desilylation. Trimethylsilyl protecting groups could also be deprotected with Ag(I) and

“click” in one pot.<sup>162</sup> In our research, the oxidative dimerization products **88** are the desired end-point and we thought the basic conditions of the reaction might facilitate deprotection of 1-trimethylsilyl alkynes *in situ*, saving a step. Reactions in Figure 5.3 show how this idea was validated.

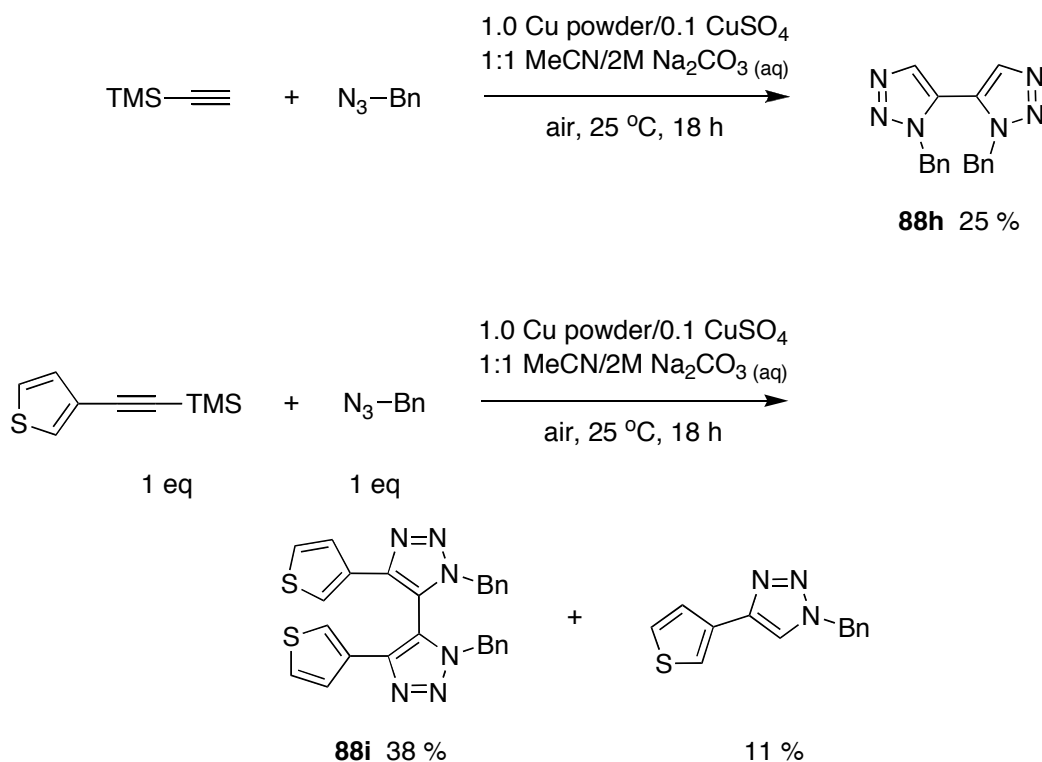


**Figure 5.3.** Bistriazole formation from TMS protected precursors *via* convergent desilylation.

## 5.6 Physical Properties of Bistriazoles

The bistriazole core of molecules **88** has not previously been reported with this substitution pattern (though regioisomeric materials have been made).<sup>160</sup> Figure 5.4 shows a molecular representation from a single crystal X-ray diffraction analysis of compound **88e**. Rotation around the C-C bond that connects the two rings is highly hindered, hence the molecules are chiral and the enantiomeric forms do not interconvert under ambient conditions. Consistent with this, the AB quartet pattern observed for the benzylic protons of compound **88e** at ambient temperature did not coalesce into a singlet when the sample was heated to 115 °C in DMSO.

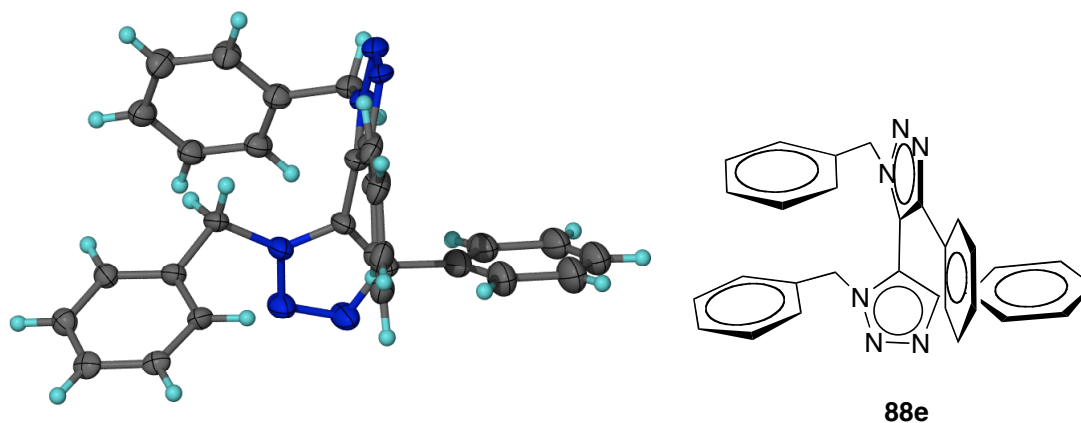


**Figure 5.4.** Representation of **88e** from single crystal X-ray diffraction.

## 5.7 Asymmetric Synthesis of Bistriazoles

Production of optically active 5,5'-bistriazoles is likely to be of most interest for syntheses of new chiral ligands and auxiliaries. In such compounds the heterocyclic core is a stereoelectronic variation, and a patentable modification, of chiral biaryl cores, very frequently encountered in ligands.<sup>163</sup> Two reactions were performed to explore this concept. Reactions shown in Figure 5.5 and Figure 5.6 gave unexceptional diastereoselections, but the products were easily separated via flash chromatography, so the approach is extremely practical. In the case of the chiral bipyridyl product, the stereochemistry of the atropisomeric chiral center of the minor product was proven via single crystal X-ray crystallographic analysis. (Figure 5.7)

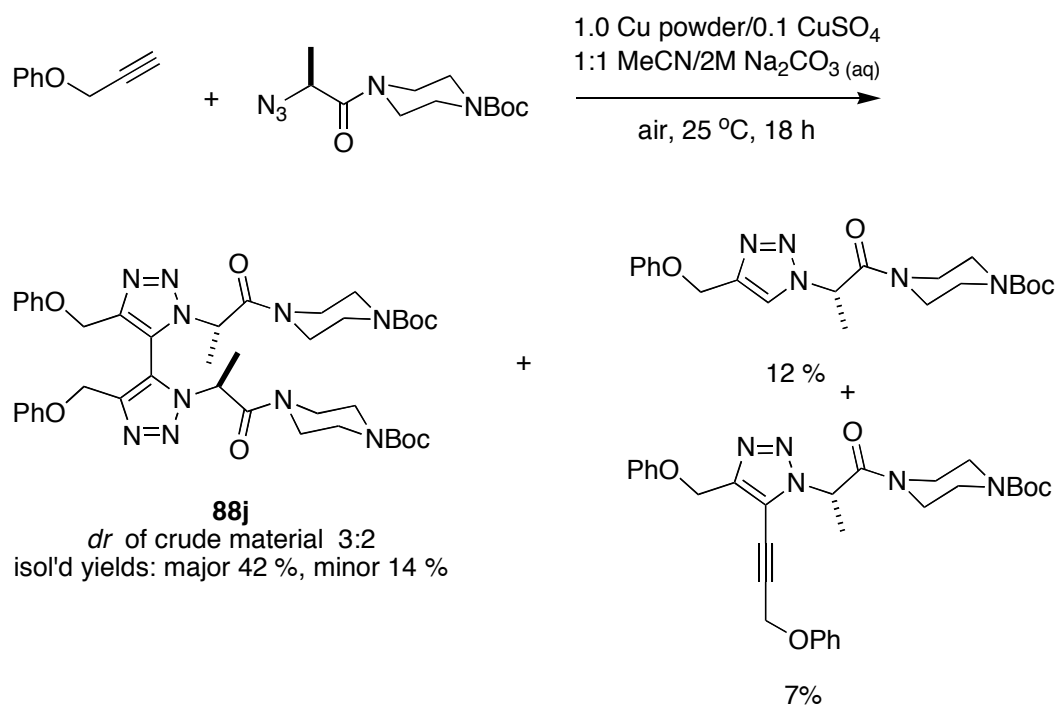


**Figure 5.5.** Synthesis of the optically active bistriazole from propargyl phenyl ether.

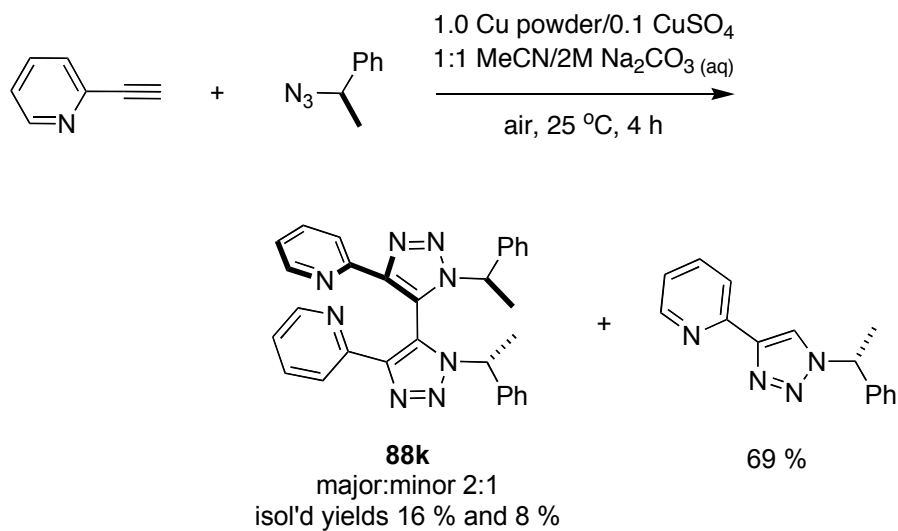


**Figure 5.6.** Synthesis of the chiral bipyridyl product.

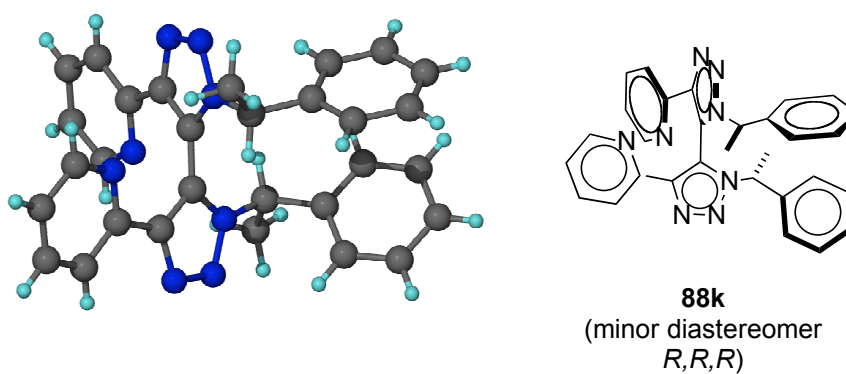


**Figure 5.7.** The stereochemistry of the bistriazole atropisomeric chiral center in the minor diastereomer **88k**.



The fact that compounds **89** and **90** (Table 5.1) do not react to form the 5,5'-bistriazole **88a** rules out these as intermediates for the reaction, and the possible involvement of diynes. It seems highly likely that the reaction therefore proceeds via coupling of two organocopper species. Sodium or potassium carbonate is favorable for the dimerization process. It could be that carbonate bridged copper dimers are particularly well suited to the process, and these do not form efficiently from sodium bicarbonate (entry 1). Ammonia from ammonium bicarbonate may inhibit formation of this carbonate complex or its mode of action (entry 6). Dicopper species have been implicated in copper-mediated additions of azide to alkyne,<sup>4,10</sup> and carbonate bridged dicopper complexes are known.<sup>164-166</sup> A plausible mechanism for the reaction therefore features two  $\sigma$ -bonded triazole units coming together in oxidative coupling reaction, for which carbonate is a particularly favorable bridging ligand. However, we have no direct evidence to implicate dicopper species or the bridging carbonate ligand at this time.

## 5.8 Summary

In summary, oxidative coupling can be the prevalent pathway in copper-mediated Huisgen reactions of azides and terminal alkynes. This is surprising because it has been stated several times in the literature that pH is relatively unimportant for copper-mediated cycloadditions to give triazoles.<sup>4,10</sup> 5,5'-Bistriazoles are an under-explored heterocyclic backbone. However, the reactions described here allow ready access to these compounds and should provide a foundation for further studies. In particular, use of optically active constituents provides a way to make and isolate diastereomerically pure derivatives representing different atropisomeric forms. Overall, these findings may impact ligand syntheses and development of libraries to screen for pharmaceutical lead compounds; it should influence the strategies used by researchers to design conditions for formation of triazole or bistriazole products.

## CHAPTER VI

### CONCLUSIONS

Strategies in design and synthesis of triazole based  $\beta$ -turn peptidomimetics have been discussed. The approaches involve preparation of new type of triazole mimics and bivalent turn analogs to enhance the probability of finding bioactive molecules. Copper-mediated Huisgen 1,3-dipolar cycloaddition reaction has been used to synthesis small molecule peptidomimetics in solution phase. The cycloaddition reaction is fast, simple to perform, and compatible with many solvents and functional groups. This serves as an excellent way to make peptidomimetics, particularly because there is some stereoelectronic and topological similarity between 1,2,3-triazoles and amide bonds. It is expected that 1,2,3-triazole cores could form the basis of small molecule pharmaceutical leads in which they fulfill some binding function of peptides, even though the molecular resemblance of these compounds to peptides is obscure.

Chapter II has illustrated the approach to  $\beta$ -turn conformations using copper-mediated cycloaddition reaction as macrocyclization method. In solution, linear peptidomimetic substrates were used to form the cyclic derivatives. A library of eight cyclic peptidomimetics was prepared and the low yield was mostly due to formation of dimers. Computational and NMR analyses of the cyclic compounds **61a-c** indicate that their most favorable conformational states include type I and type II  $\beta$ -turn conformations. However, the CD data do not closely fit the spectra commonly associated with type I and II turn conformations, indicating non-ideal matches and/or other important contributions to the conformational ensemble. Selectivity for the dimeric products **65** in these cyclisation reactions is discussed. We suggest that the perfect regioselectivity of the copper mediated cycloaddition processes for 1,4-disubstituted triazoles would require that the azido alkyne coils in an *endo*-like conformation to form a monomeric cyclization product.

In our search of more reliable models that can be used to prepare later generation of therapeutic candidates, second generation peptidomimetics with less peptidic structure and more convergent synthesis were developed. Our molecular modeling indicated that the triazole moiety shares very close topological similarities with the amide bond. The pharmacophores placed around the triazole core are allowed to rotate freely to find the appropriate region of space for docking to occur. As described in Chapter III, a library of small-molecule triazole mimics was prepared via “click” reactions in solution. Compared to the traditional solid phase synthesis, the new design is far more convergent and low cost. The “click” reactions allow quick and efficient generation of the desired peptidomimetics in good yields. One major drawback in this design is that one of the functionalities placed around the triazole core is not derived from a nature amino acid. This might lower the similarity of the designed molecule to the natural  $\beta$ -turn. Another group member has prepared a library of triazole mimics with both side-chains derived from natural amino acids. The biological assay of the new library is in progress.

The more challenging approach in our turn analog synthesis involves the development of the methodology for the formation of bivalent mimics in solution. Both Chapter III and IV have described the approach that monovalent mimics are coupled to the linker scaffold sequentially in solution by simply manipulating the solvent systems. Libraries of simple bivalent systems containing guanidine, primary amine, alcohol and carboxylic acid functionalities have been prepared to demonstrate this principle. In the attempt to mimic neurotrophins function, the “mix and match” linker design was developed in Chapter IV. Bivalent turn mimics with optimal-length linkage have been prepared. The new solution-phase combinatorial method allows us to prepare large libraries of bivalent compounds quickly and efficiently. The two monovalent components were combined with each other to achieve one-compound-per-well in sufficient purity for biological testing.

As shown in Chapter V, Oxidative coupling to give 5,5'-bistriazoles has been discussed. The bistriazoles become the predominant products in the copper accelerated “click reaction” of alkynes and azides when manipulating the bases in the reaction.

Conditions with carbonate bases as additives (ca 1 – 2 M) have been found to be the most effective. Starting materials like propargylic ethers and less hindered substrates could give higher yields. Use of optically active azides has afforded separable atropisomeric products, providing a convenient access to optically pure derivatives.

Copper-catalyzed 1,3-dipolar cycloaddition reactions are undeniably useful in contemporary organic chemistry, but disadvantages still exist in these reactions. Azides and copper used in the reactions are both possible safety- and environmental-hazards. Further, macrocyclization reactions can be complicated by somewhat mysterious macrodimerization events. Nevertheless, the fact that there are convenient routes to amino-acid-derived azides and alkynes, and the lack of practical obstacles to executing these Cu-mediated reactions, both exhibit a promising future for the peptidomimetics formed via this route.

## REFERENCES

- (1) Huisgen, R. In *1,3-Dipolar Cycloaddit. Chem.*; Padwa, A., Ed.; Wiley: New York, 1984; Vol. 1, p 1-176.
- (2) Huisgen, R.; Szeimies, G.; Moebius, L. *Chem. Ber.* **1967**, *100*, 2494-2507.
- (3) Tornøe, C. W.; Christensen, C.; Meldal, M. *J. Org. Chem.* **2002**, *67*, 3057-3064.
- (4) Rostovtsev, V. V.; Green, L. G.; Fokin, V. V.; Sharpless, K. B. *Angew. Chem. Int. Ed.* **2002**, *41*, 2596-2599.
- (5) Kolb, H. C.; Finn, M. G.; Sharpless, K. B. *Angew. Chem. Int. Ed.* **2001**, *40*, 2004-21.
- (6) Kolb, H. C.; Sharpless, K. B. *Drug Discovery Today* **2003**, *8*, 1128-1137.
- (7) Bock, V. D.; Hiemstra, H.; van Maarseveen, J. H. *Eur. J. Org. Chem.* **2006**, 51-68.
- (8) Soltis, M. J.; Yeh, H. J.; Cole, K. A.; Whittaker, N.; Wersto, R. P.; Kohn, E. C. *Drug Metabolism and Disposition* **1996**, *24*, 799-806.
- (9) Alvarez, R.; Velazquez, S.; San-Felix, A.; Aquaro, S.; De Clercq, E.; Perno, C.-F.; Karlsson, A.; Balzarini, J.; Camarasa, M. J. *J. Med. Chem.* **1994**, *37*, 4185-94.
- (10) Rodionov, V. O.; Fokin, V. V.; Finn, M. G. *Angew. Chem. Int. Ed.* **2005**, *44*, 2210-2215.
- (11) Himo, F.; Lovell, T.; Hilgraf, R.; Rostovtsev, V. V.; Noodleman, L.; Sharpless, K. B.; Fokin, V. V. *J. Am. Chem. Soc.* **2004**, *127*, 210-216.
- (12) Tornøe, C. W.; Sanderson, S. J.; Mottram, J. C.; Coombs, G. H.; Meldal, M. *J. Comb. Chem.* **2004**, *6*, 312-324.

- (13) Youngquist, R. S.; Fuentes, G. R.; Lacey, M. P.; Keough, T. *Rapid Commun. Mass Spec.* **1994**, *8*, 77-81.
- (14) Youngquist, R. S.; Fuentes, G. R.; Lacey, M. P.; Keough, T. *J. Am. Chem. Soc.* **1995**, *117*, 3900-6.
- (15) St. Hilaire, P. M.; Lowary, T. L.; Meldal, M.; Bock, K. *J. Am. Chem. Soc.* **1998**, *120*, 13312-13320.
- (16) Oh, K.; Guan, Z. *Chem. Commun.* **2006**, 3069-3071.
- (17) Paul, A.; Bittermann, H.; Gmeiner, P. *Tetrahedron* **2006**, *62*, 8919-8927.
- (18) Alper, P. B.; Hung, S.-C.; Wong, C.-H. *Tetrahedron Lett.* **1996**, *37*, 6029-32.
- (19) Lundquist, I., J. T.; Pelletier, J. C. *Org. Lett.* **2001**, *3*, 781-3.
- (20) Horne, W. S.; Yadav, M. K.; Stout, C. D.; Ghadiri, M. R. *J. Am. Chem. Soc.* **2004**, *126*, 15366-15367.
- (21) Angelo, N. G.; Arora, P. S. *J. Am. Chem. Soc.* **2005**, *127*, 17134-17135.
- (22) Zhang, Z.; Fan, E. *Tetrahedron Lett.* **2006**, *47*, 665-669.
- (23) Franke, R.; Doll, C.; Eichler, J. *Tetrahedron Lett.* **2005**, *46*, 4479-4482.
- (24) Roice, M.; Johannsen, I.; Meldal, M. *QSAR Comb. Sci.* **2004**, *23*, 662-673.
- (25) Punna, S.; Kuzelka, J.; Wang, Q.; Finn, M. G. *Angew. Chem. Int. Ed.* **2005**, *44*, 2215-2220.
- (26) Billing, J. F.; Nilsson, U. J. *J. Org. Chem.* **2005**, *70*, 4847-4850.
- (27) Horne, W. S.; Stout, C. D.; Ghadiri, M. R. *J. Am. Chem. Soc.* **2003**, *125*, 9372-9376.
- (28) van Maarseveen, J. H.; Horne, W. S.; Ghadiri, M. R. *Org. Lett.* **2005**, *7*, 4503-4506.
- (29) Angell, Y.; Burgess, K. *J. Org. Chem.* **2005**, *70*, 9595-9598.

- (30) Ray, A.; Manoj, K.; Bhadbhade, M. M.; Mukhopadhyay, R.; Bhattacharjya, A. *Tetrahedron Lett.* **2006**, *47*, 2775-2778.
- (31) Bock, V. D.; Perciaccante, R.; Jansen, T. P.; Hiemstra, H.; Maarseveen, J. H. V. *Org. Lett.* **2006**, *8*, 919-922.
- (32) Looper, R. E.; Pizzirani, D.; Schreiber, S. L. *Org. Lett.* **2006**, *8*, 2063-2066.
- (33) Dondoni, A.; Giovannini, P. P.; Massi, A. *Org. Lett.* **2004**, *6*, 2929-2932.
- (34) Kuijpers, B. H. M.; Groothuys, S.; Keereweer, A. R.; Quaedflieg, P. J. L. M.; Blaauw, R. H.; van Delft, F. L.; Rutjes, F. P. J. T. *Org. Lett.* **2004**, *6*, 3123-3126.
- (35) Groothuys, S.; Kuijpers, B. H. M.; Quaedflieg, P. J. L. M.; Roelen, H. C. P. F.; Wiertz, R. W.; Blaauw, R. H.; Delft, F. L. v.; Rutjes, F. P. J. T. *Synthesis* **2006**, *18*, 3146-3152.
- (36) Suzuki, T.; Suzuki, S. T.; Yamada, I.; Koashi, Y.; Yamada, K.; Chida, N. *J. Org. Chem.* **2002**, *67*, 2874-2880.
- (37) Boullanger, P.; Maunier, V.; Lafont, D. *Carbohydr. Res.* **2000**, *324*, 97-106.
- (38) Inazu, T.; Kobayashi, K. *Synlett* **1993**, 869-70.
- (39) Maunier, V.; Boullanger, P.; Lafont, D. *J. Carbohydr. Chem.* **1997**, *16*, 231-235.
- (40) Cohen-Anisfeld, S. T.; Lansbury, P. T., Jr. *J. Am. Chem. Soc.* **1993**, *115*, 10531-7.
- (41) Kaiser, J.; Kinderman, S. S.; van Esseveldt, B. C. J.; van Delft, F. L.; Schoemaker, H. E.; Blaauw, R. H.; Rutjes, F. P. J. T. *Org. Biomol. Chem.* **2005**, *3*, 3435-3467.
- (42) Wilkinson, B. L.; Bornaghi, L. F.; Poulsen, S.-A.; Houston, T. A. *Tetrahedron* **2006**, *62*, 8115-8125.
- (43) Macmillan, D.; Blanc, J. *Org. Biomol. Chem.* **2006**, *4*, 2847-2850.
- (44) Lin, H.; Walsh, C. T. *J. Am. Chem. Soc.* **2004**, *126*, 13998-14003.

- (45) Wan, Q.; Chen, J.; Chen, G.; Danishefsky, S. J. *J. Org. Chem.* **2006**, *71*, 8244-8249.
- (46) Aagren, J. K. M.; Billing, J. F.; Grundberg, H. E.; Nilsson, U. J. *Synthesis* **2006**, 3141-3145.
- (47) Arosio, D.; Bertoli, M.; Manzoni, L.; Scolastico, C. *Tetrahedron Lett.* **2006**, *47*, 3697-3700.
- (48) Gopi, H. N.; Tirupula, K. C.; Baxter, S.; Ajith, S.; Chaiken, I. M. *ChemMedChem* **2006**, *1*, 54-57.
- (49) Weterings, J. J.; Khan, S.; Van der Heden, G. J.; Drijfhout, J. W.; Melief, C. J. M.; Overkleeft, H. S.; Van der Burg, S. H.; Ossendorp, F.; Van der Marel, G. A.; Filippov, D. V. *Bioorg. Med. Chem. Lett.* **2006**, *16*, 3258-3261.
- (50) Dirks, A. J. T.; van Berkel, S. S.; Hatzakis, N. S.; Opsteen, J. A.; van Delft, F. L.; Cornelissen, J. J. L. M.; Rowan, A. E.; van Hest, J. C. M.; Rutjes, F. P. J. T.; Nolte, R. J. M. *Chem. Commun.* **2005**, 4172-4174.
- (51) Parrish, B.; Breitenkamp, R. B.; Emrick, T. *J. Am. Chem. Soc.* **2005**, *127*, 7404-7410.
- (52) Wu, P.; Feldman, A. K.; Nugent, A. K.; Hawker, C. J.; Scheel, A.; Voit, B.; Pyun, J.; Frechet, J. M. J.; Sharpless, K. B.; Fokin, V. V. *Angew. Chem. Int. Ed.* **2004**, *43*, 3928-32.
- (53) Rijkers, D. T. S.; van Esse, G. W.; Merkx, R.; Brouwer, A. J.; Jacobs, H. J. F.; Pieters, R. J.; Liskamp, R. M. J. *Chem. Commun.* **2005**, 4581-4583.
- (54) Lober, S.; Rodriguez-Loaiza, P.; Gmeiner, P. *Org. Lett.* **2003**, *5*, 1753-1755.
- (55) Bettinetti, L.; Lober, S.; Hubner, H.; Gmeiner, P. *J. Comb. Chem.* **2005**, *7*, 309-316.
- (56) Mindt, T. L.; Struthers, H.; Brans, L.; Anguelov, T.; Schweinsberg, C.; Maes, V.; Tourwé, D.; Schibli, R. *J. Am. Chem. Soc.* **2006**, *128*, 15096-15097.



- (57) Jang, H.; Fafarman, A.; Holub, J. M.; Kirshenbaum, K. *Org. Lett.* **2005**, *7*, 1951-1954.
- (58) Wang, J.; Uttamchandani, M.; Li, J.; Hu, M.; Yao, S. Q. *Org. Lett.* **2006**, *8*, 3821-3824.
- (59) Wang, J.; Uttamchandani, M.; Li, J.; Hu, M.; Yao, S. Q. *Chem. Commun.* **2006**, 3783-3785.
- (60) Brik, A.; Muldoon, J.; Lin, Y.-C.; Elder, J. H.; Goodsell, D. S.; Olson, A. J.; Fokin, V. V.; Sharpless, K. B.; Wong, C.-H. *ChemBioChem* **2003**, *4*, 1246-1248.
- (61) Brik, A.; Alexandratos, J.; Lin, Y.-C.; Elder, J. H.; Olson, A. J.; Wlodawer, A.; Goodsell, D. S.; Wong, C.-H. *ChemBioChem* **2005**, *6*, 1167-1169.
- (62) Whiting, M.; Tripp, J. C.; Lin, Y.-C.; Lindstrom, W.; Olson, A. J.; Elder, J. H.; Sharpless, K. B.; Fokin, V. V. *J. Med. Chem.* **2006**, *49*, 7697-7710.
- (63) Chang, K.-H.; Lee, L.; Chen, J.; Li, W.-S. *Chem. Commun.* **2006**, 629-631.
- (64) Srinivasan, R.; Uttamchandani, M.; Yao, S. Q. *Org. Lett.* **2006**, *8*, 713-716.
- (65) Li, J.; Zheng, M.; Tang, W.; He, P.-L.; Zhu, W.; Li, T.; Zuo, J.-P.; Liu, H.; Jiang, H. *Bioorg. Med. Chem. Lett.* **2006**, *16*, 5009-5013.
- (66) Pagliai, F.; Pirali, T.; Del Grosso, E.; Di Brisco, R.; Tron, G. C.; Sorba, G.; Genazzani, A. A. *J. Med. Chem.* **2006**, *49*, 467-470.
- (67) Lober, S.; Hubner, H.; Gmeiner, P. *Bioorg. Med. Chem. Lett.* **2006**, *16*, 2955-9.
- (68) Lee, L. V.; Mitchell, M. L.; Huang, S.-J.; Fokin, V. V.; Sharpless, K. B.; Wong, C.-H. *J. Am. Chem. Soc.* **2003**, *125*, 9588-9.
- (69) Bryan, M. C.; Lee, L. V.; Wong, C.-H. *Bioorg. Med. Chem. Lett.* **2004**, *14*, 3185-3188.
- (70) Wood, W. J. L.; Patterson, A. W.; Tsuruoka, H.; Jain, R. K.; Ellman, J. A. *J. Am. Chem. Soc.* **2005**, *127*, 15521-15527.

- (71) Goess, B. C.; Hannoush, R. N.; Chan, L. K.; Kirchhausen, T.; Shair, M. D. *J. Am. Chem. Soc.* **2006**, *128*, 5391-5403.
- (72) Ball, J. B.; Hughes, R. A.; Alewood, P. F.; Andrews, P. R. *Tetrahedron* **1993**, *49*, 3467-78.
- (73) Kahn, M.; Devens, B. *Tetrahedron Lett.* **1986**, *27*, 4841-4844.
- (74) Blomberg, D.; Hedenstrom, M.; Kreye, P.; Sethson, I.; Brickmann, K.; Kihlberg, J. *J. Org. Chem.* **2004**, *69*, 3055-3508.
- (75) Nagula, G.; Urban, J.; Kim, H.-O.; Lum, C.; Nakanishi, H. In *international Bureau United States*, 2003, p WO 03/030907 AI.
- (76) Wang, W.; Yang, J.; Ying, J.; Xiong, C.; Zhang, J.; Cai, C.; Hraby, V. *J. Org. Chem.* **2002**, *67*, 6353-60.
- (77) Chitnumsub, P.; Fiori, W. R.; Lashuel, H. A.; Diaz, H.; Kelly, J. W. *Bioorg. Med. Chem.* **1999**, 39-59.
- (78) Gardner, R. R.; Liang, G.-B.; Gellman, S. H. *J. Am. Chem. Soc.* **1999**, *121*, 1806-1816.
- (79) Reyes, S. J.; Burgess, K. *Tetrahedron: Asymm.* **2005**, *16*, 1061-1069.
- (80) Burgess, K. *Acc. Chem. Res.* **2001**, *34*, 826-35.
- (81) Feng, Y.; Wang, Z.; Jin, S.; Burgess, K. *J. Am. Chem. Soc.* **1998**, *120*, 10768-9.
- (82) Feng, Y.; Burgess, K. *Chem. Eur. J.* **1999**, *5*, 3261-72.
- (83) Feng, Y.; Burgess, K. *Biotech. Bioeng. Comb. Chem.* **2000**, *71*, 3-8.
- (84) Maliartchouk, S.; Feng, Y.; Ivanisevic, L.; Debeir, T.; Cuello, A. C.; Burgess, K.; Saragovi, H. U. *Molec. Pharmacol.* **2000**, *57*, 385-91.
- (85) Pattarawarapan, M.; Zaccaro, M. C.; Saragovi, U.; Burgess, K. *J. Med. Chem.* **2002**, *45*, 4387-90.
- (86) Feng, Y.; Wang, Z.; Jin, S.; Burgess, K. *Chem. Eur. J.* **1999**, *5*, 3273-8.

- (87) Feng, Y.; Pattarawarapan, M.; Wang, Z.; Burgess, K. *Org. Lett.* **1999**, *1*, 121-4.
- (88) Burgess, K. *Solid-Phase Organic Synthesis*; Wiley Interscience: New York, 2000.
- (89) Burgess, K. In *Solid-Phase Organic Synthesis*; Burgess, K., Ed.; Wiley Interscience: New York, 2000, p 1-23.
- (90) Reyes, S.; Pattarawarapan, M.; Roy, S.; Burgess, K. *Tetrahedron* **2000**, *56*, 9809-18.
- (91) Pattarawarapan, M.; Burgess, K. *Angew. Chem., Int. Ed.* **2000**, *39*, 4299-301.
- (92) Pattarawarapan, M.; Chen, J.; Steffensen, M.; Burgess, K. *J. Comb. Chem.* **2001**, *3*, 102-16.
- (93) Cheng, S.; Comer, D. D.; Williams, J. P.; Meyers, P. L.; Boger, D. L. *J. Am. Chem. Soc.* **1996**, *118*, 2567-73.
- (94) Mazaleyrat, J.-P.; Xie, J.; Wakselman, M. *Tetrahedron Lett.* **1992**, *33*, 4301-4302.
- (95) Filira, F.; Biondi, L.; Gobbo, M.; Rocchi, R. *Tetrahedron Lett.* **1991**, *32*, 7463-7464.
- (96) Wüthrich, K. *NMR of Proteins and Nucleic Acids*; Wiley: New York, 1986.
- (97) Ohnishi, M.; Urry, D. W. *Biochem. Biophys. Res. Commun.* **1969**, *36*, 194-202.
- (98) Kopple, K. D.; Ohnishi, M.; Go, A. *J. Am. Chem. Soc.* **1969**, *91*, 4264-72.
- (99) Englander, S. W.; Downer, N. W.; Teitelbaum, H. *Annu. Rev. Biochem* **1972**, *41*, 903-24.
- (100) Pettitt, B. M.; Matsunaga, T.; Al-Obeidi, F.; Gehrig, C.; Hruby, V. J.; Karplus, M. *Biophys. J. Biophys. Soc.* **1991**, *60*, 1540-4.
- (101) O'Connor, S. D.; Smith, P. E.; Al-Obeidi, F.; Pettitt, B. M. *J. Med. Chem.* **1992**, *35*, 2870-81.

- (102) Perczel, A.; Hollosi, M. In *Circular Dichroism and the Conformational Analysis of Biomolecules*; Fasman, G. D., Ed.; Plenum Press: New York, 1996, p 362-364.
- (103) Greenfield, N.; Fasman, G. D. *Biochemistry* **1969**, *8*, 4108-16.
- (104) Bush, C. A.; Sarkar, S. K.; Kopple, K. D. *Biochemistry* **1978**, *17*, 4951-4.
- (105) Johnson, W. C. *Ann. Rev. Biophys. Biophys. Chem.* **1988**, *17*, 145-66.
- (106) Johnson, W. C. *PROTEINS: Structure, Function, and Genetics* **1990**, *7*, 205-14.
- (107) Spatola, A. F.; Anwer, M. K.; Rockwell, A. L.; Gierasch, L. M. *J. Am. Chem. Soc.* **1986**, *108*, 825-31.
- (108) Harrison, B. A.; Verdine, G. L. *Org. Lett.* **2001**, *3*, 2157-9.
- (109) Sommerfeld, T.; Seebach, D. *Angew. Chem. Int. Ed.* **1995**, *34*, 553-4.
- (110) Borg, S.; Estenne-Bouhtou, G.; Luthman, K.; Csoregh, I.; Hesselink, W.; Hacksell, U. *J. Org. Chem.* **1995**, *60*, 3112-20.
- (111) Boeglin, D.; Cantel, S.; Heitz, A.; Martinez, J.; Fehrentz, J.-A. *Org. Lett.* **2003**, *5*, 4465-8.
- (112) Rotella, D. P. *J. Am. Chem. Soc.* **1996**, *118*, 12246-7.
- (113) Veber, D. F.; Johnson, S. R.; Cheng, H.-Y.; Smith, B. R.; Ward, K. W.; Kopple, K. D. *J. Med. Chem.* **2002**, *45*, 2615-23.
- (114) Tsai, C.-J.; Lin, S. L.; Wolfson, H. J.; Nussinov, R. *Crit. Rev. Biochem. Mol. Biol.* **1996**, *31*, 127-52.
- (115) Salmon, S. E.; Lam, K. S.; Lebl, M.; Kandola, A.; Khattri, P. S.; Wade, S.; Pátek, M.; Kocis, P.; Krchnák, V.; Thorpe, D.; Felder, S. *PNAS* **1993**, *90*, 11708-12.
- (116) Cochran, A. G. *Chemistry & Biology* **2000**, *7*, R85-R94.
- (117) Cochran, A. G.; Skelton, N. J.; Starovasnik, M. A. *PNAS* **2001**, *98*, 5578-83.
- (118) Shuker, S. B.; Hajduk, P. J.; Meadows, R. P.; Fesik, S. W. *Science* **1996**, *274*, 1531-4.

- (119) Hajduk, P. J.; Dinges, J.; Miknis, G. F.; Merlock, M.; Middleton, T.; Kempf, D. J.; Egan, D. A.; Walter, K. A.; Robins, T. S.; Shuker, S. B.; Holzman, T. F.; Fesik, S. W. *J. Med. Chem* **1997**, *40*, 3144-50.
- (120) Kessler, H. *Angew. Chem. Int. Ed.* **1997**, *36*, 829-31.
- (121) Hajduk, P. J.; Olejniczak, E. T.; Fesik, S. W. *J. Am. Chem. Soc.* **1997**, *119*, 12257-61.
- (122) Rao, J.; Whitesides, G. M. *J. Am. Chem. Soc.* **1997**, *119*, 10286-90.
- (123) Trent, J. O.; Clark, G. R.; Kumar, A.; Wilson, W. D.; Boykin, D. W.; Hall, J. E.; Tidwell, R. R.; Blagburn, B. L.; Neidle, S. *J. Med. Chem.* **1996**, *39*, 4554-62.
- (124) Boger, D. L.; Chai, W. *Tetrahedron* **1998**, *54*, 3955-70.
- (125) Royo, M.; del Fresno, M.; Frieden, A.; Nest, W. V. D.; Sanseverino, M.; Alsina, J.; Kates, S. A.; Barany, G.; Albericio, F. *React. Funct. Polym.* **1999**, *41*, 103-10.
- (126) Reyes, S. J.; Burgess, K. *Chem. Soc. Rev.* **2006**, *35*, 416-23.
- (127) Gustafson, G. R.; Baldino, C. M.; O'Donnell, M. M. E.; Sheldon, A.; Tarsa, R. J.; Verni, C. J.; Coffen, D. L. *Tetrahedron* **1998**, *54*, 4051-65.
- (128) Johnson, C. R.; Zhang, B.; Fantauzzi, P.; Hocker, M.; Yager, K. M. *Tetrahedron* **1998**, *54*, 4097-4106.
- (129) Pattarawarapan, M.; Reyes, S.; Xia, Z.; Zaccaro, M. C.; Saragovi, H. U.; Burgess, K. *J. Med. Chem.* **2003**, *46*, 3565-7.
- (130) Zaccaro, M. C.; B.Lee, H.; Pattarawarapan, M.; Xia, Z.; Caron, A.; L'Heureux, P.-J.; Bengio, Y.; Burgess, K.; Saragovi, H. U. *Chemistry & Biol.* **2005**, *12*, 1015-28.
- (131) Lee, H. B.; Zaccaro, M. C.; Pattarawarapan, M.; Roy, S.; Saragovi, H. U.; Burgess, K. *J. Org. Chem.* **2004**, *69*, 701-13.
- (132) Pavia, M. R.; Sawyer, T. K.; Moos, W. H. *Bioorg. Med. Chem. Lett.* **1993**, *3*, 387-96.

- (133) Gallop, M. A.; Barrett, R. W.; Dower, W. J.; Fodor, S. P. A.; Gordon, E. M. *J. Med. Chem.* **1994**, *37*, 1233-51.
- (134) Gordon, E. M.; Barrett, R. W.; Dower, W. J.; Fodor, S. P. A.; Gallop, M. A. *J. Med. Chem.* **1994**, *37*, 1385-401.
- (135) Bunin, B. A.; Plunkett, M. J.; Ellman, J. A. *Proc. Natl. Acad. Sci. USA* **1994**, *91*, 4708-12.
- (136) DeWitt, S. H.; Kiely, J. S.; Stankovic, C. J.; Schroeder, M. C.; Cody, D. M. R.; Pavia, M. R. *Proc. Natl. Acad. Sci.* **1993**, *90*, 6909-13.
- (137) Kenner, G. W.; Laird, A. H. *Chem. Commun.* **1965**, 305-6.
- (138) Rozek, A.; Powers Jon-Paul, S.; Friedrich Carol, L.; Hancock Robert, E. W. *Biochemistry (Mosc)*. **2003**, *42*, 14130-8.
- (139) Hanessian, S.; McNaughton-Smith, G.; Lombart, H.-G.; Lubell, W. D. *Tetrahedron* **1997**, *53*, 12789-854.
- (140) Pavia, M. R.; Cohen, M. P.; Dilley, G. J.; Dubuc, G. R.; Durgin, T. L.; Forman, F. W.; Hediger, M. E.; Milot, G.; Powers, T. S.; Sucholeiki, I.; Zhou, S.; Hangauer, D. *G. Bioorg. Med. Chem.* **1996**, *4*, 659-66.
- (141) Venkatesan, N.; Kim, B. H. *Curr. Med. Chem.* **2002**, *9*, 2243-2270.
- (142) Hirschmann, R.; Sprengeler, P. A.; Kawasaki, T.; Leahy, J. W.; Shakespeare, W. C.; Amos B. Smith, I. *JACS* **1992**, *114*, 9699-701.
- (143) Bursavich, M. G.; West, C. W.; Rich, D. H. *Org. Lett.* **2001**, *3*, 2317-2320.
- (144) Kawato, H. C.; Nakayama, K.; Inagaki, H.; Ohta, T. *Org. Lett.* **2001**, *3*, 3451-4.
- (145) Gottschling, D.; Boer, J.; Schuster, A.; Holzmann, B.; Kessler, H. *Angew. Chem-Int. Ed. Engl.* **2002**, *41*, 3007-3011.
- (146) Ellman, J. A. *Acc. Chem. Res.* **1996**, *29*, 132-43.
- (147) Abell, A. D. *Letters in Peptide Science* **2002**, *8*, 267-272.

- (148) Maltais, R.; Tremblay, M. R.; Ciobanu, L. C.; Poirier, D. *J. Comb. Chem.* **2004**, *6*, 443-456.
- (149) Feigel, M. *J. Am. Chem. Soc.* **1986**, *108*, 181-182.
- (150) Hirschmann, R.; Sprengeler, P. A.; Kawasaki, T.; Leahy, J. W.; Shakespeare, W. C.; Amos B. Smith, I. *J. Am. Chem. Soc.* **1992**, *114*, 9699-701.
- (151) Lam, K. S.; Lebl, M.; Krchnak, V. *Chem. Rev.* **1997**, *97*, 411-48.
- (152) Pátek, M.; Drake, B.; Lebl, M. *TL* **1994**, *35*, 9169-72.
- (153) Olah, G. A.; Wang, Q.; Sandford, G.; Prakash, G. K. S. *J. Org. Chem.* **1993**, *58*, 3194-3195.
- (154) Snider, W. D. *Cell* **1994**, *77*, 627-638.
- (155) Wiesmann, C.; Ultsch, M. H.; Bass, S. H.; de Vos, A. M. *Nature* **1999**, *401*, 184-8.
- (156) Robertson, A. G. S.; Banfield, M. J.; Allen, S. J.; Dando, J. A.; Mason, G. G. F.; Tyler, S. J.; Bennett, G. S.; Brain, S. D.; Clarke, A. R.; Naylor, R. L.; Wilcock, G. K.; Brady, R. L.; Dawbarn, D. *Biochem. Biophys. Res. Commun.* **2001**, *282*, 131-41.
- (157) Sonogashira, K.; Tohda, Y.; Hagihara, N. *Tetrahedron Lett.* **1975**, *16*, 4467-70.
- (158) Angell, Y.; Burgess K. *Angew. Chem. Int. Ed.*, **2007**, *46*, 3649-3651.
- (159) Padwa, A. In *Comprehensive Organic Synthesis*; Trost, B. M., Ed.; Pergamon: Oxford, 1991; Vol. 4, p 1069-1109.
- (160) Dornow, A.; Rombusch, K. *Chem. Ber.* **1958**, *91*, 1841-1851.
- (161) Sokolyanskaya, L. V.; Volkov, A. N.; Trofimov, B. A. *Khim. Geterotsykl. Soedin.* **1979**, 849.
- (162) Aucagne, V.; Leigh, D. A. *Org. Lett.* **2006**, *8*, 4505-4507.
- (163) Berthod, M.; Mignani, G.; Woodward, G.; Lemaire, M. *Chem. Rev.* **2005**, *105*, 1801-36.

- (164) Sorrell, T. N.; Allen, W. E.; White, P. S. *Inorg. Chem.* **1995**, *34*, 952-60.
- (165) Davis, A. R.; Einstein, F. W. B. *Inorg. Chem.* **1980**, *19*, 1203-7.
- (166) Davis, A. R.; Einstein, F. W. B.; Curtis, N. F.; Martin, J. W. L. *J. Am. Chem. Soc.* **1978**, *100*, 6258-60.

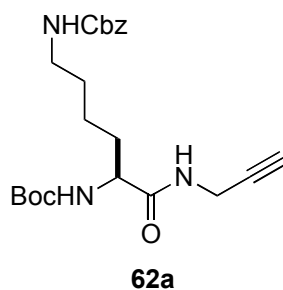


## APPENDIX A

### EXPERIMENTAL FOR CHAPTER II

**General Methods.** All the amino acids used had the L-configuration and they were purchased from NovaBiochem, Advance BioTech or Chem-Impex. All chemicals were obtained from commercial suppliers and used without further purification. *N*-Hydroxybenzotriazole (HOBt), *N*-methylmorpholine, *N,N*-diisopropylethylamine, acetyl chloride (AcCl) were purchased from Aldrich. Ethyl-(*N,N'*-dimethylamino)propylcarbodiimide (EDC) was obtained from Advanced ChemTech. Dichloromethane was obtained anhydrous by distillation over calcium hydride and THF was distilled over sodium metal and benzophenone. Reverse phase high performance liquid chromatography (RP-HPLC) was carried out on Vydac C-18 column with the dimension of 25 x 0.46 cm for analytical studies, and on XTerra C – 18 column with the dimension of 10 x 1.9 cm for preparative work. All HPLC experiments were performed using gradient conditions. The eluents used were: solvent A (H<sub>2</sub>O with 0.1% TFA) and solvent B (CH<sub>3</sub>CN with 0.1% TFA). The flow rate used was 1.0 mL/min for analytical, and 10 ml/min for preparative HPLC. NMR spectra of compounds **62a-c**, **63a-h**, **61a-h**, **66** and **67** were recorded on Inova instruments at 300 MHz and at 500 MHz for compounds **64a-h** and **61a-h**. NMR chemical shifts were expressed in ppm relative to internal solvent peaks, and coupling constants were measured in Hz.

**General Procedure for Preparation of 62a-c.** Propargyl amine (1.0 equiv) was added to a suspension of Boc protected amino acid (1.1 equiv) (0.2 M) in dry CH<sub>2</sub>Cl<sub>2</sub>. *N*-methylmorpholine (1.1 equiv) was added to the above suspension followed with HOBt (1.1 equiv) and EDC (1.1 equiv). The resulting solution was stirred at room temperature for 4h. Ethyl acetate (40 ml) was added to the reaction mixture, and the resulting suspension was washed with 5% HCl (30 ml), H<sub>2</sub>O (30 ml), 5% Na<sub>2</sub>CO<sub>3</sub> (30 ml) and brine (30 ml). The organic layer was separated and dried with Na<sub>2</sub>SO<sub>4</sub> and concentrated to dryness. Recrystallization with EtOAc and hexanes afforded **62a-c**.

Lysine Derivative **62a**

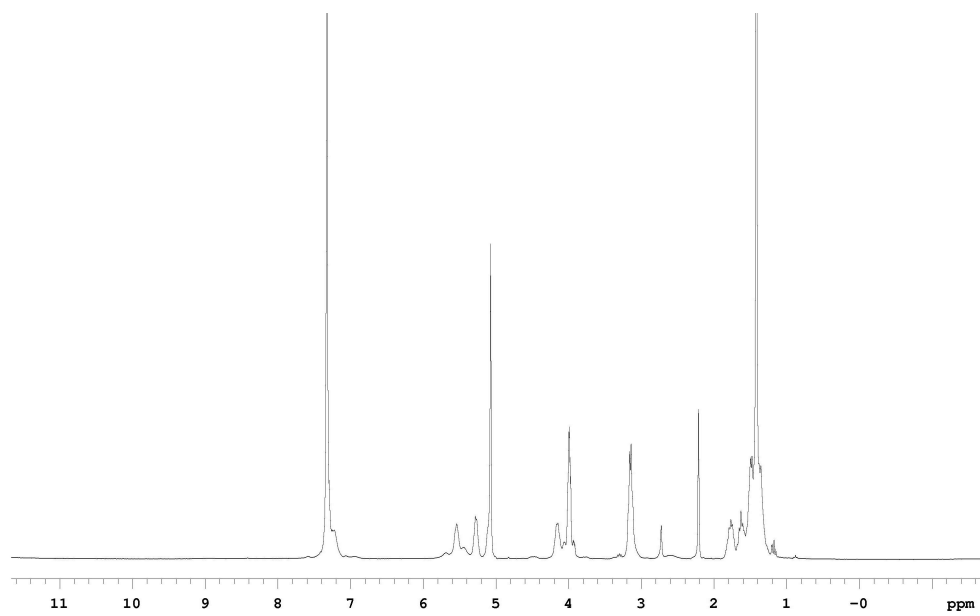
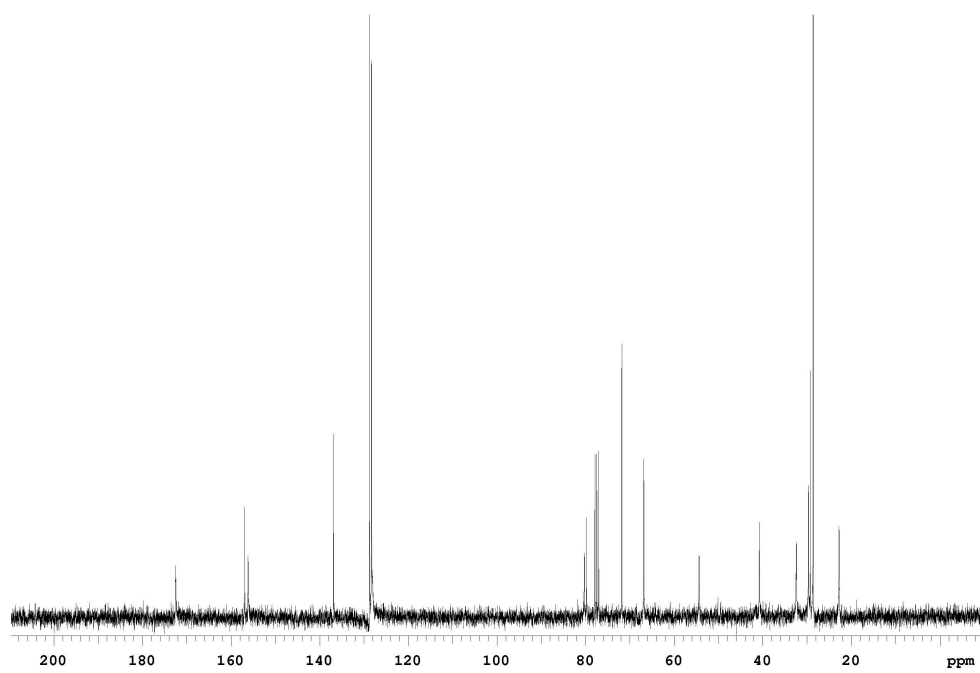
Compound **62a** was prepared from Boc-Lys(Cbz)-OH (5.50 mmol, 2.09 g).

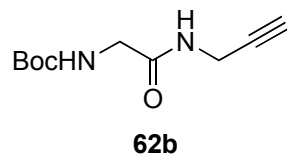
Recrystallization afforded **62a** (1.94 g, 93%) as a white solid.

**<sup>1</sup>H NMR (CDCl<sub>3</sub>)** 7.32 (m, 5H), 5.54 (s, 1H), 5.28 (d, 1H, J = 4.8 Hz), 5.07 (s, 2H), 4.16 (d, 1H, J = 5.4 Hz), 3.98 (dd, 2H, J = 5.4 Hz, 2.7 Hz), 3.15 (m, 2H), 2.21 (t, 1H, J = 2.1 Hz), 1.77 (m, 1H), 1.63 (m, 1H), 1.48 (m, 2H), 1.42 (s, 9H), 1.36 (m, 2H)

**<sup>13</sup>C NMR (CDCl<sub>3</sub>)** 172.5, 156.9, 156.1, 136.9, 128.7, 128.3, 128.1, 80.2, 79.8, 71.8, 66.8, 54.4, 40.8, 32.4, 29.7, 29.2, 28.6, 22.8

**MS (ESI, m/z)** 440 (M+Na)<sup>+</sup>

 **$^1\text{H}$  NMR of 62a** **$^{13}\text{C}$  NMR of 62a**

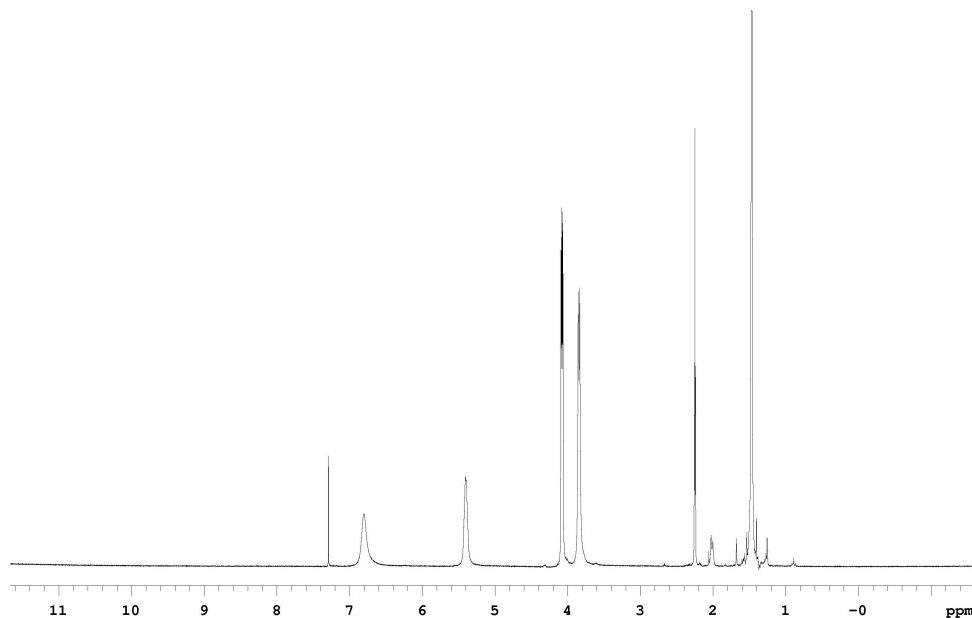
Glycine Derivative **62b**

Compound **62b** was prepared from Boc-Gly-OH (5.50 mmol, 0.88 g). Recrystallization afforded **62b** (1.0 g, 94%) as a white solid.

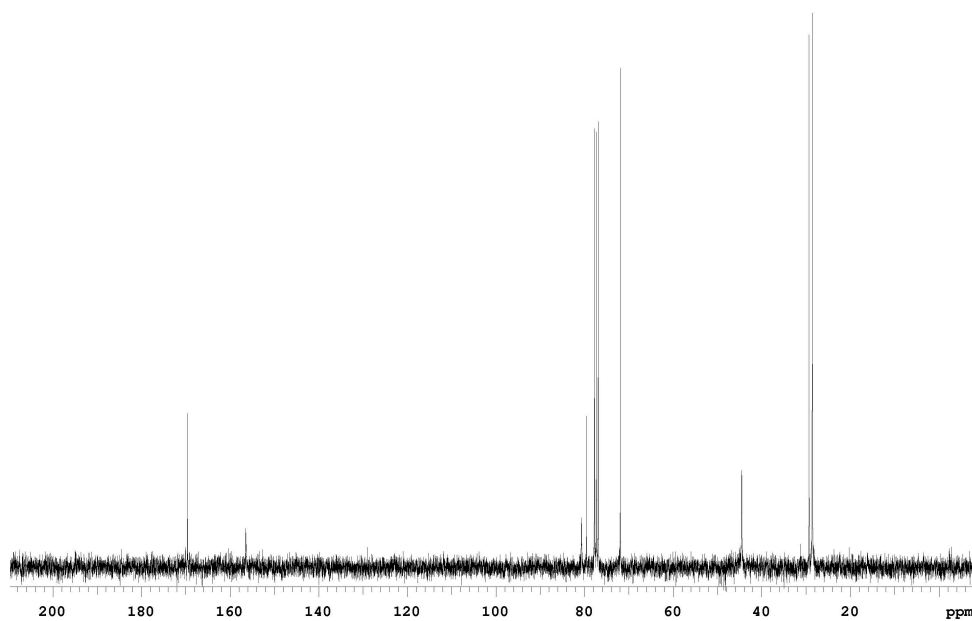
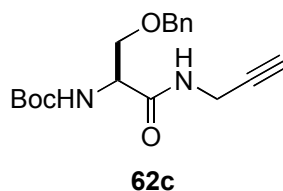
<sup>1</sup>H NMR (CDCl<sub>3</sub>) 7.29 (s, 1H), 5.41 (s, 1H), 4.08 (dd, 2H, J = 5.4 Hz, 2.7 Hz), 3.84 (d, 2H, J = 5.7 Hz), 2.25 (t, 1H, J = 2.7 Hz), 1.47 (s, 9H)

<sup>13</sup>C NMR (CDCl<sub>3</sub>) 169.6, 156.4, 80.7, 79.5, 71.9, 44.5, 29.3, 28.6

MS (ESI, m/z) 213 (M+H)<sup>+</sup>



<sup>1</sup>H NMR of **62b**

 $^{13}\text{C}$  NMR of **62b**Serine Derivative **62c**

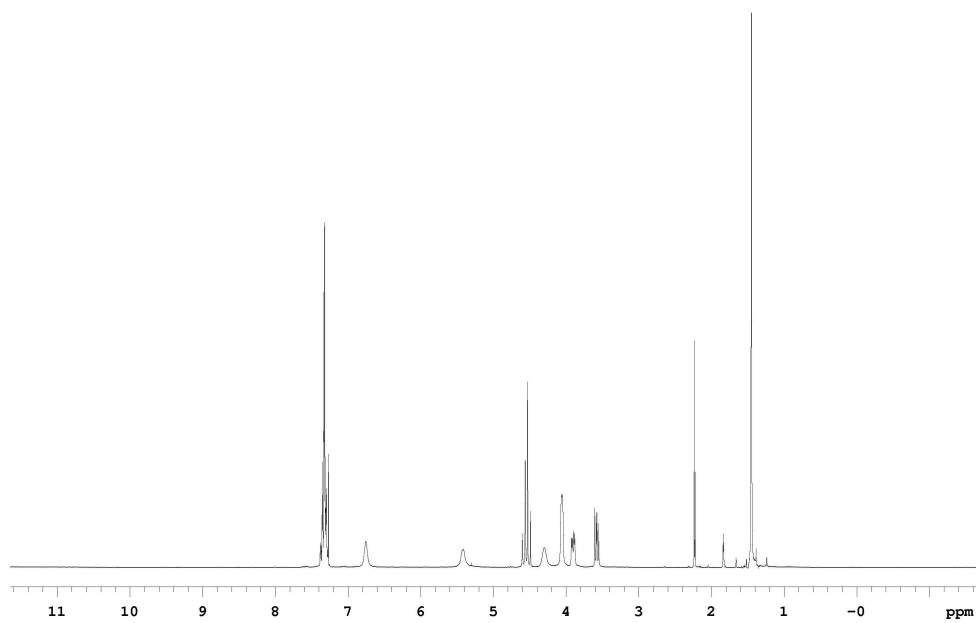
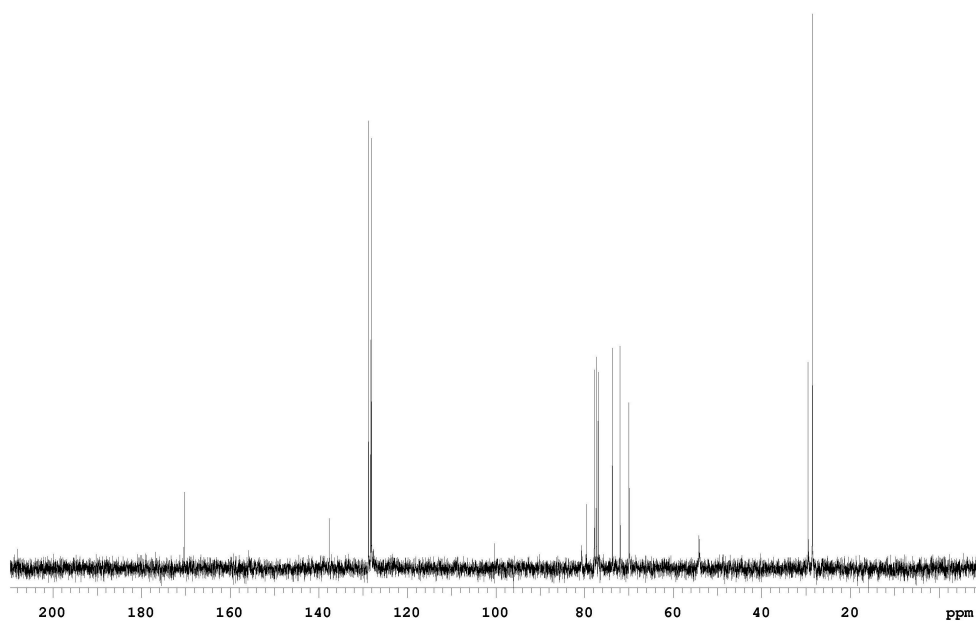
Compound **62c** was prepared from Boc-Ser(Bn)-OH (5.5 mmol, 1.48 g).

Recrystallization afforded **62c** (1.61 g, 97%) as a white solid.

$^1\text{H}$  NMR ( $\text{CDCl}_3$ ) 7.38-7.27 (m, 5H), 6.76 (s, 1H), 5.41 (s, 1H), 4.55 (dd, 2H,  $J = 21.3$  Hz, 9.3 Hz), 4.30 (s, 1H), 4.06 (d, 2H,  $J = 2.4$  Hz), 3.90 (dd, 1H,  $J = 9.0$  Hz, 5.4 Hz), 3.58 (dd, 1H,  $J = 9.3$  Hz, 6.3 Hz), 2.23 (t, 1H,  $J = 2.6$  Hz), 1.45 (s, 9H)

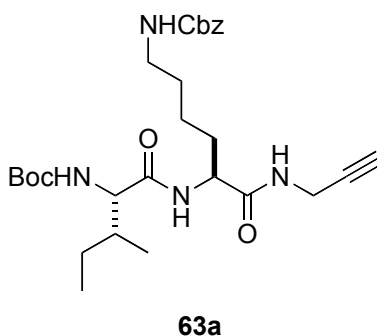
$^{13}\text{C}$  NMR ( $\text{CDCl}_3$ ) 170.4, 156.4, 137.6, 128.8, 128.2, 128.1, 80.7, 79.5, 73.7, 72.0, 70.0, 54.1, 29.5, 28.6

MS (ESI,  $m/z$ ) 339 ( $\text{M}+\text{Li}$ ) $^+$

 $^1\text{H}$  NMR of 62c $^{13}\text{C}$  NMR of 62c

**General Procedure for Preparation of 63a-h.** To a solution of **62a-c** in 20:1 EtOAc/MeOH (0.15 M) was added AcCl (5 equiv) dropwise and the resulting mixture was stirred at 0 °C for 2 h in a sealed flask, then warmed to room temperature for another 2h. Solvent was removed and the residue was used without further purification. To a suspension of the above residue (1 equiv) in dry CH<sub>2</sub>Cl<sub>2</sub> was added Boc protected amino acid (1.1 equiv) followed by addition of NEt<sub>3</sub> (2.5 equiv), HOBt (1.1 equiv) and EDC (1.1 equiv). The resulting suspension (0.075 M) was stirred at room temperature for 4 h. EtOAc was added to the reaction and extracted with 5% HCl, H<sub>2</sub>O, 5% Na<sub>2</sub>CO<sub>3</sub> and brine. The organic layer was dried with Na<sub>2</sub>SO<sub>4</sub> and concentrated to dryness. Recrystallization with EtOAc and hexanes provided **63a-h**.

Isoleucine – Lysine Derivative **63a**

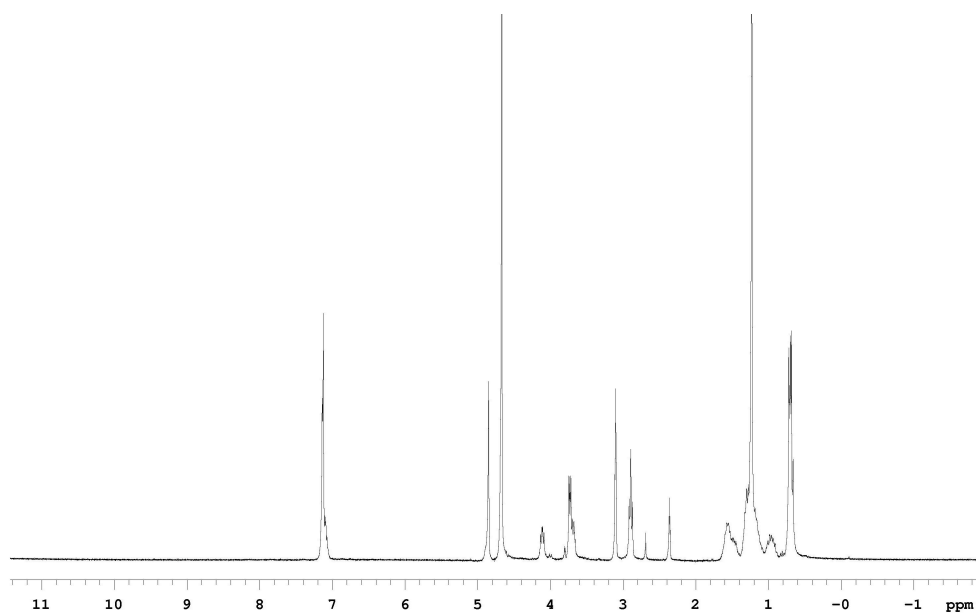
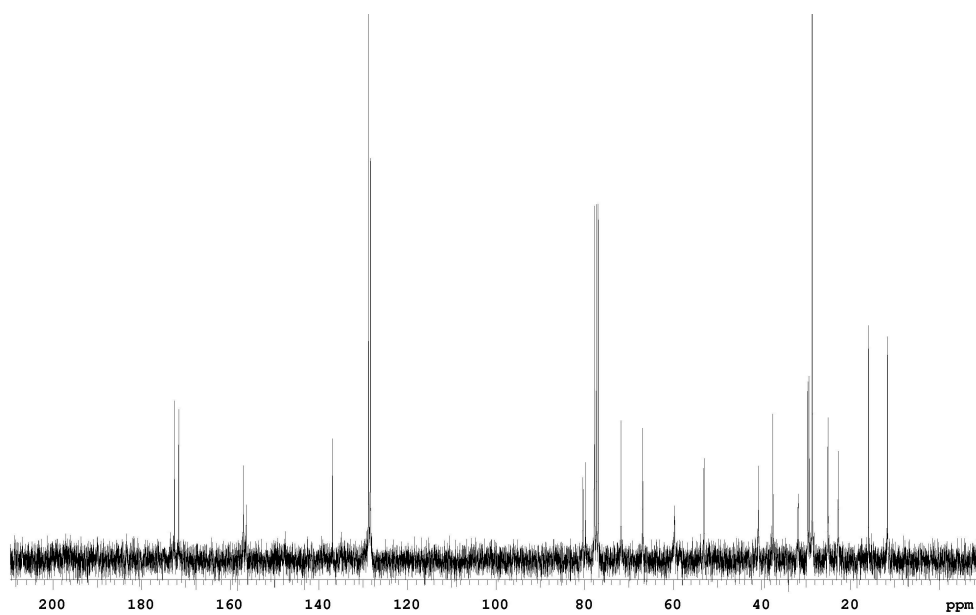


Compound **63a** was prepared from **62a** (3.0 mmol, 1.25 g) and Boc-Ile-OH·0.5 H<sub>2</sub>O (3.3 mmol, 0.79 g). Recrystallization afforded 1.60 g (99%) **63a** as a white solid

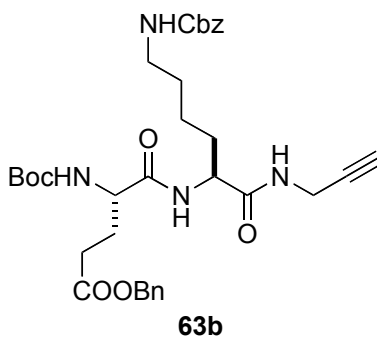
<sup>1</sup>H NMR (CD<sub>3</sub>OD) 7.19-7.07 (m, 5H), 4.85 (s, 2H), 4.11 (dd, 1H, J = 8.4 Hz, 2.7 Hz), 3.73 (dd, 2H, J = 7.5 Hz, 2.4 Hz), 3.68 (t, 1H, J = 6.3 Hz), 2.89 (t, 2H, J = 6.6 Hz), 2.36 (t, 1H, J = 2.1 Hz), 1.57 (m, 2H), 1.48 (m, 1H), 1.28 (m, 3H), 1.23 (s, 9H), 1.18 (m, 2H), 0.96 (m, 1H), 0.72-0.66 (m, 6H)

<sup>13</sup>C NMR (CDCl<sub>3</sub>) 172.5, 171.6, 156.9, 156.3, 136.9, 128.7, 128.3, 128.1, 80.3, 79.7, 71.8, 66.8, 59.7, 53.0, 40.7, 37.5, 31.8, 29.6, 29.3, 28.6, 25.0, 22.7, 15.9, 11.6

MS (ESI, m/z) 553 (M+Na)<sup>+</sup>

 **$^1\text{H}$  NMR of 63a** **$^{13}\text{C}$  NMR of 63a**

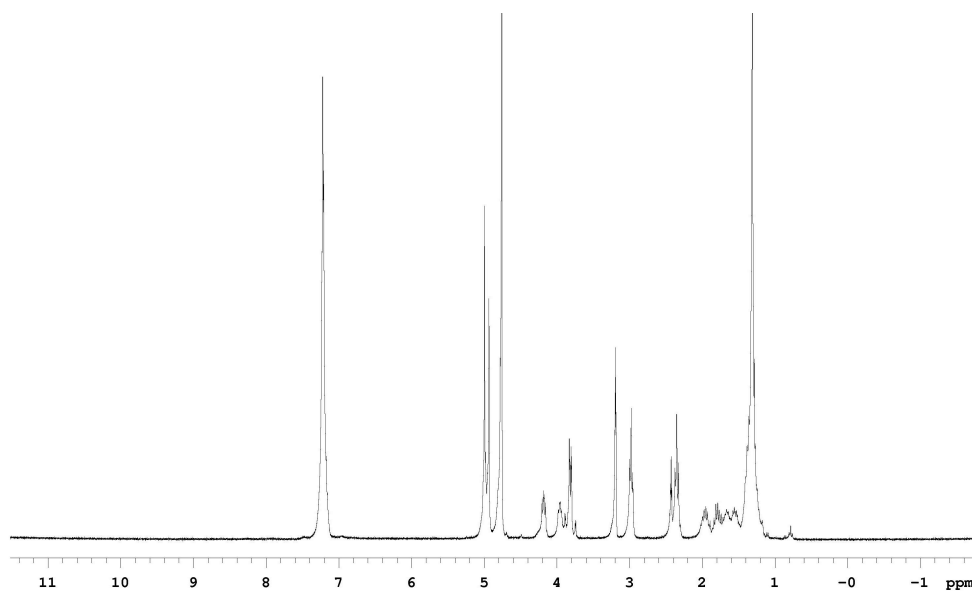


Glumatic Acid – Lysine Derivative **63b**

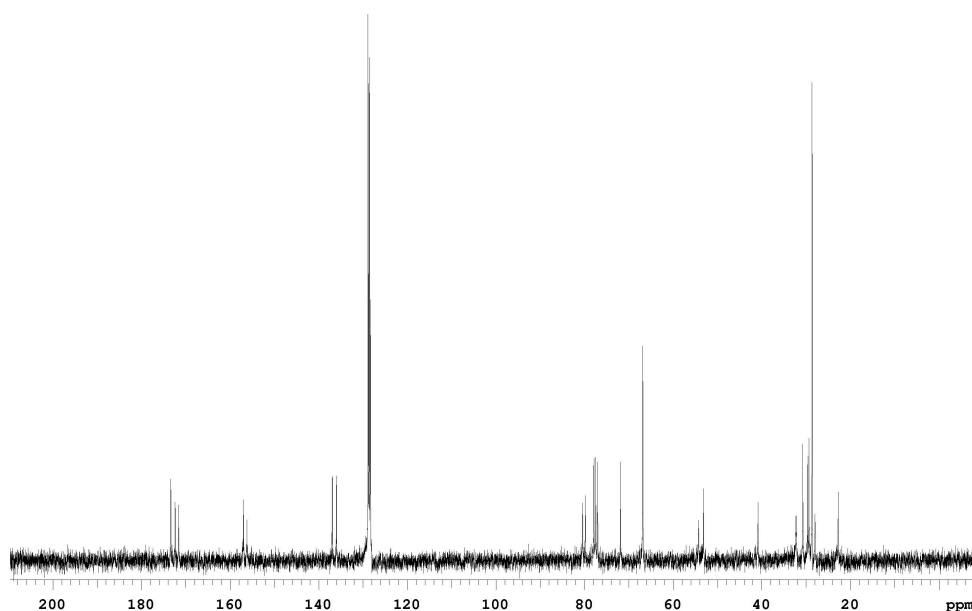
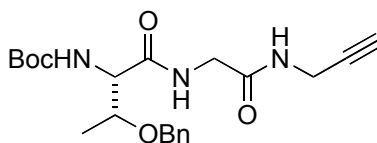
Compound **63b** was prepared from **62a** (3.0 mmol, 1.25 g) and Boc-Glu(Bn)-OH (3.3 mmol, 1.10 g). Recrystallization with EtOAc and hexanes afforded 1.45 g (85%) **63b** as a white solid.

**<sup>1</sup>H NMR (CD<sub>3</sub>OD)** 7.22-7.17 (m, 10H), 5.00 (s, 2H), 4.98 (s, 2H), 4.18 (dd, 1H, J = 8.4 Hz, 3.0 Hz); 3.95 (m, 2H), 2.98 (t, 2H, J = 6.6 Hz), 2.43 (t, 1H, J = 2.4 Hz), 2.35 (t, 2H, J = 7.5 Hz), 1.95 (m, 1H), 1.79(m, 1H), 1.71 (m, 1H), 1.67 (m, 1H), 1.53-1.18 (m, 13H)  
**<sup>13</sup>C NMR (CDCl<sub>3</sub>)** 173.4, 172.4, 171.6, 157.0, 156.2, 136.9, 136.0, 128.8, 128.7, 128.5, 128.4, 128.3, 128.1, 80.4, 79.8, 71.9, 66.8, 54.2, 53.1, 40.8, 32.2, 30.7, 29.6, 29.3, 28.6, 28.0, 22.7

**MS (ESI, m/z)** 659 (M+K)<sup>+</sup>



**<sup>1</sup>H NMR of 63b**

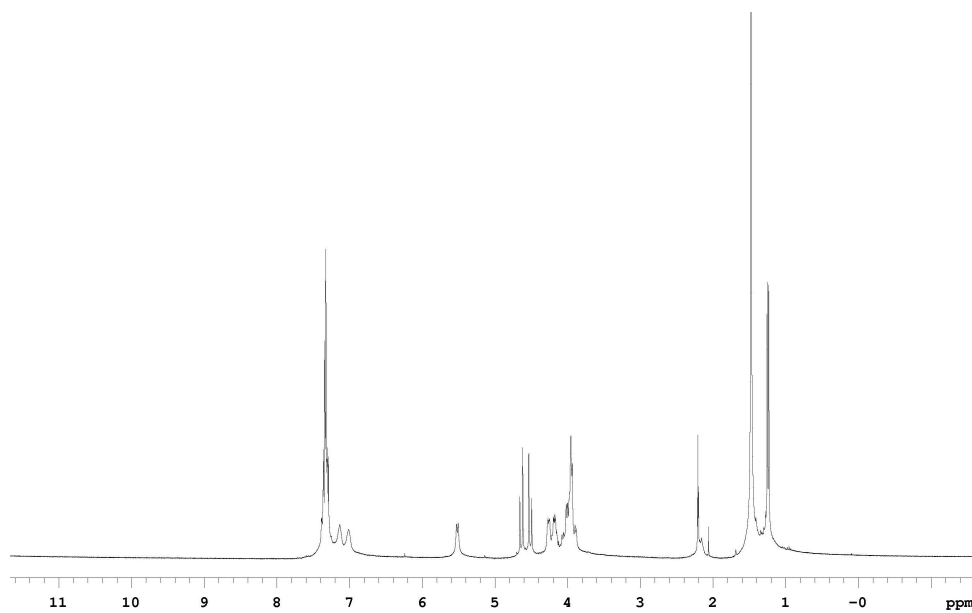
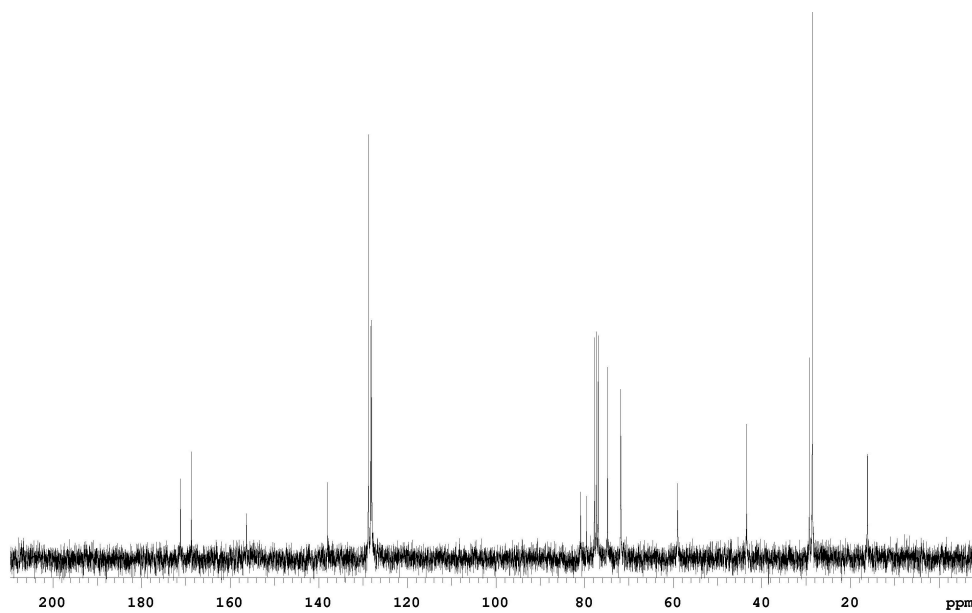
 $^{13}\text{C}$  NMR of **63b**Threonine – Glycine Derivative **63c****63c**

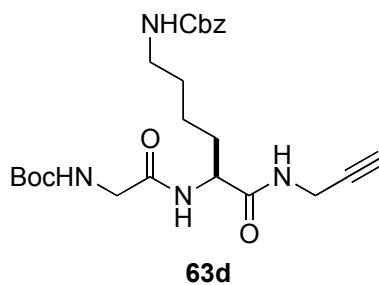
Compound **63c** was prepared from **62b** (2.7 mmol, 0.57 g) and Boc-Thr(BnI)-OH (3.0 mmol, 0.93 g). Recrystallization afforded 1.01 g (93%) **63c** as a white solid.

$^1\text{H}$  NMR ( $\text{CDCl}_3$ ) 7.39-7.23 (m, 5H), 7.13 (s, 1H), 7.01 (s, 1H), 5.52 (d, 1H,  $J = 6.6$  Hz), 5.23 (d, 1H), 4.58 (q, 2H,  $J = 36$  Hz, 11.4 Hz), 4.26 (dd, 1H,  $J = 6.6$  Hz, 3.0 Hz), 4.17 (dd, 1H,  $J = 6.3$  Hz, 3.0 Hz), 3.95 (m, 2H), 2.21 (t, 1H,  $J = 2.4$  Hz), 1.48 (s, 9H), 1.25 (d, 3H,  $J = 6.3$  Hz)

$^{13}\text{C}$  NMR ( $\text{CDCl}_3$ ) 171.2, 168.7, 156.3, 137.9, 128.8, 128.2, 128.0, 80.9, 79.6, 74.8, 71.8, 66.8, 59.0, 43.4, 29.3, 28.6, 16.1

MS (ESI,  $m/z$ ) 410 ( $\text{M}+\text{Li}$ ) $^+$

 $^1\text{H}$  NMR of 63c $^{13}\text{C}$  NMR of 63c

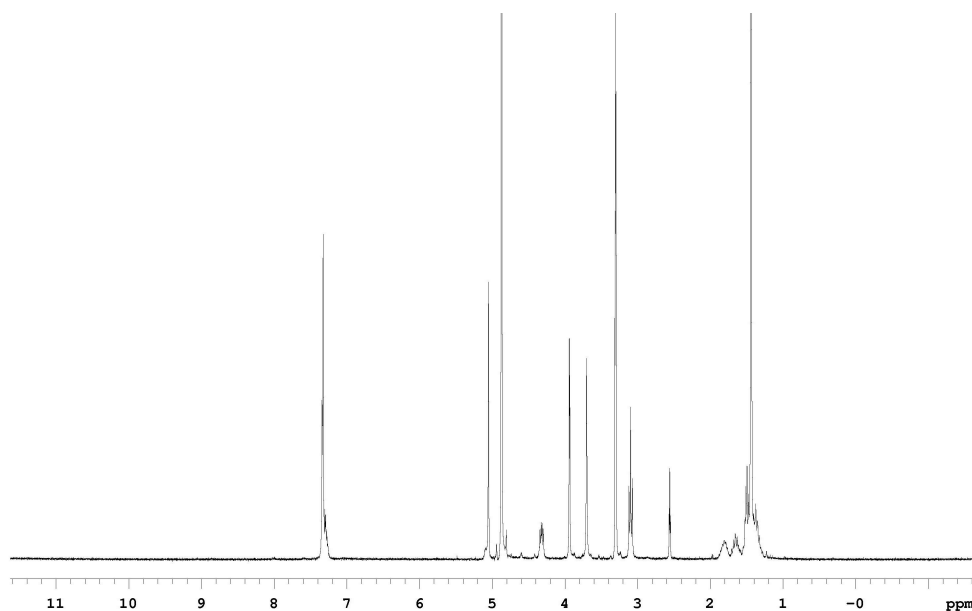
Glycine – Lysine Derivative **63d**

Compound **63d** was prepared from **62a** (3.0 mmol, 1.25 g) and Boc-Gly-OH (3.3 mmol, 0.58 g). Recrystallization afforded 1.38 g (97%) **63d** as a white solid.

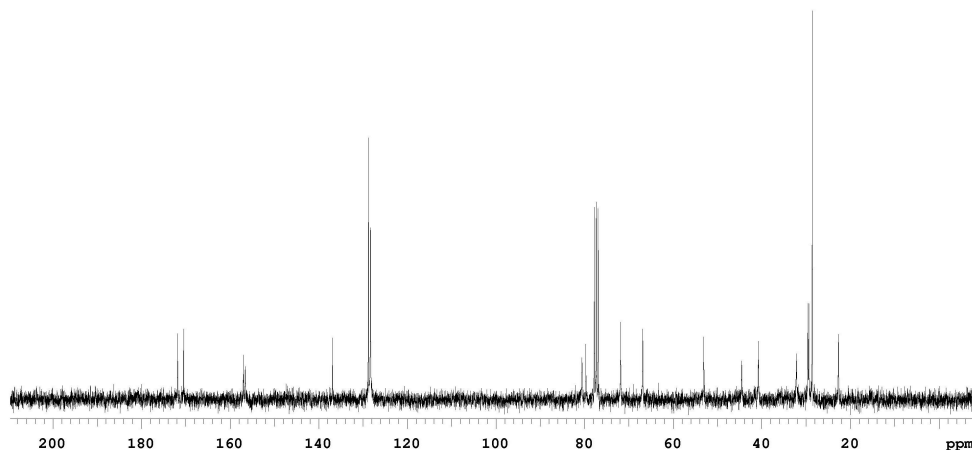
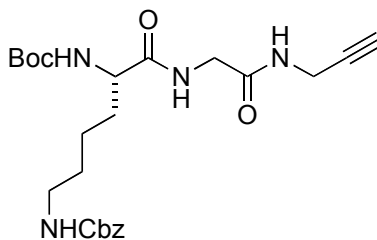
**<sup>1</sup>H NMR (CD<sub>3</sub>OD)** 7.34-7.27 (m, 5H), 5.05 (s, 2H), 4.32 (dd, 1H, J = 7.5 Hz, 3.3 Hz), 3.94 (d, 2H, J = 2.4 Hz), 3.70 (s, 2H), 3.10 (t, 2H, J = 6.9 Hz), 2.56 (t, 1H, J = 2.4 Hz), 1.67 (m, 1H), 1.61 (m, 1H), 1.49 (m, 2H), 1.44 (s, 9H), 1.35(m, 2H)

**<sup>13</sup>C NMR (CDCl<sub>3</sub>)** 171.8, 170.4, 157.0, 156.6, 136.9, 128.8, 128.3, 128.1, 80.6, 79.7, 71.8, 66.8, 53.1, 44.5, 40.7, 32.1, 29.6, 29.3, 28.6, 22.7

**MS (ESI, m/z)** 475 (M+H)<sup>+</sup>



**<sup>1</sup>H NMR of 63d**

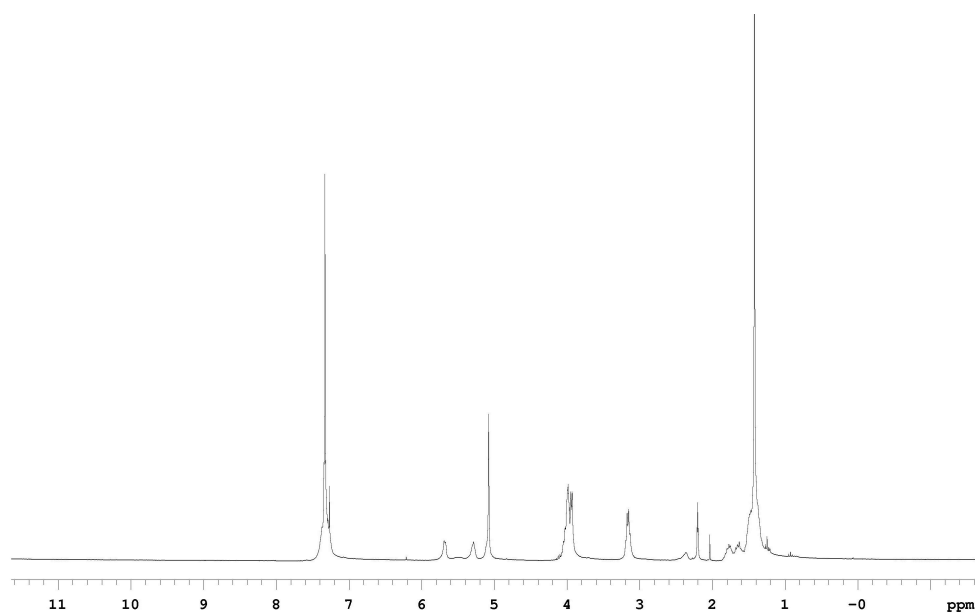
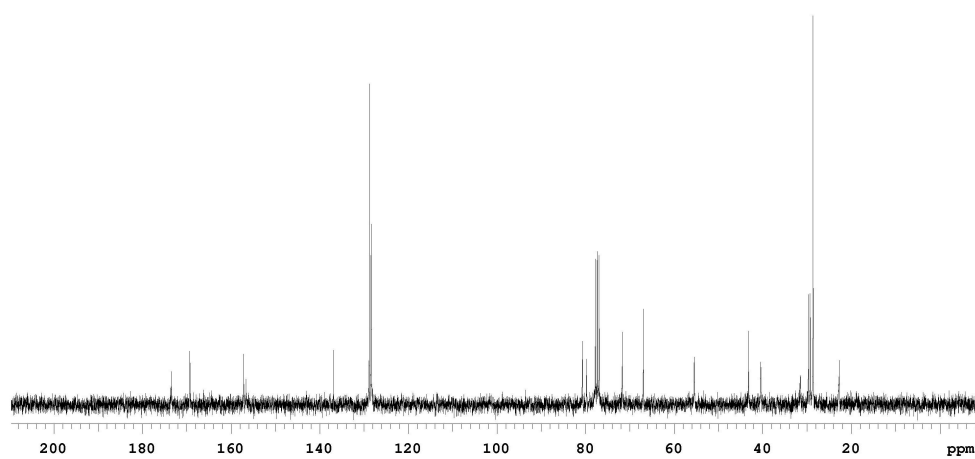
 $^{13}\text{C}$  NMR of **63d**Lysine – Glycine Derivative **63e****63e**

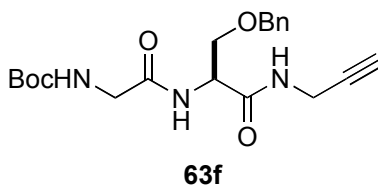
Compound **63e** was prepared from **62b** (3.0 mmol, 0.63 g) and Boc-Lys(Cbz)-OH (3.3 mmol, 1.26 g). Recrystallization afforded 1.25 g (88%) **63e** as a white solid.

$^1\text{H}$  NMR ( $\text{CDCl}_3$ ) 7.37-7.29 (m, 5H), 5.68 (d, 1H,  $J = 5.4$  Hz), 5.29 (s, 1H), 5.08 (s, 2H), 4.02 (m, 3H), 3.94 (d, 2H,  $J = 5.4$  Hz), 3.15 (t, 2H,  $J = 6.3$  Hz), 2.20 (t, 1H,  $J = 2.4$  Hz), 1.80 (m, 1H), 1.65 (m, 1H), 1.50 (m, 2H), 1.42 (s, 9H), 1.36 (m, 2H)

$^{13}\text{C}$  NMR ( $\text{CDCl}_3$ ) 173.5, 169.3, 157.1, 156.6, 136.8, 128.8, 128.4, 128.1, 80.7, 79.7, 71.7, 66.9, 55.5, 43.2, 40.4, 31.5, 29.7, 29.3, 28.6, 22.7

MS (ESI,  $m/z$ ) 475 ( $\text{M}+\text{H}$ ) $^+$

 $^1\text{H}$  NMR of 63e $^{13}\text{C}$  NMR of 63e

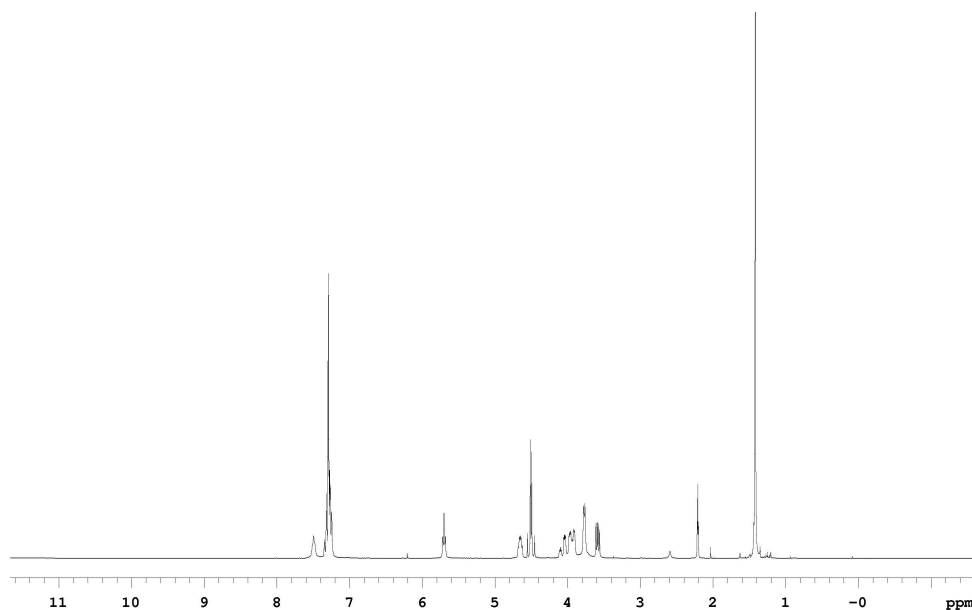
Glycine – Serine Derivative **63f**

Compound **63f** was prepared from **62c** (1.5 mmol, 0.50 g) and Boc-Gly-OH (1.64 mmol, 0.29 g). Recrystallization with EtOAc and hexanes afforded 0.23 g (50%) **63f** as a white solid.

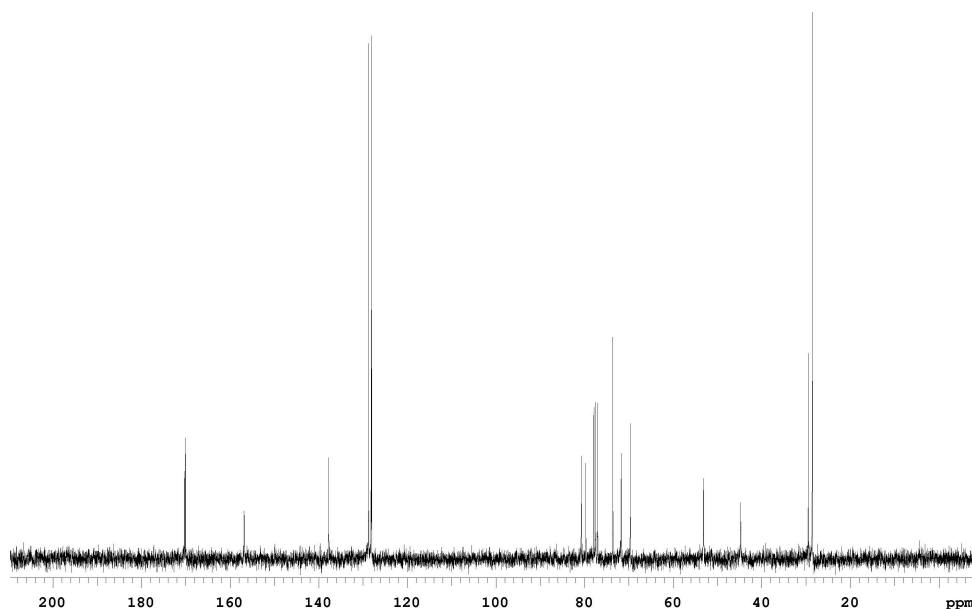
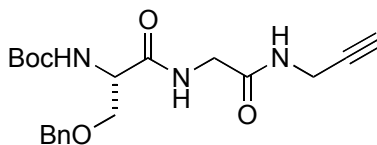
**<sup>1</sup>H NMR (CDCl<sub>3</sub>)** 7.49 (s, 1H), 7.37-7.25 (m, 5H), 5.70 (t, 1H, J = 5.4 Hz), 4.65 (t, 1H, J = 3.6 Hz), 4.50 (dd, 2H, J = 14.4 Hz, 12.0 Hz), 4.05-3.91 (m, 3H), 3.77 (d, 1H, J = 5.1 Hz), 3.59 (dd, 1H, J = 9.6 Hz, 5.4 Hz), 2.21 (t, 1H, J = 2.4 Hz), 1.44 (s, 9H)

**<sup>13</sup>C NMR (CDCl<sub>3</sub>)** 170.2, 170.0, 156.8, 137.7, 128.7, 128.1, 128.0, 80.7, 79.7, 73.6, 71.7, 69.7, 53.1, 44.7, 29.5, 28.6

**MS (ESI, m/z)** 390 (M+H)<sup>+</sup>



**<sup>1</sup>H NMR of 63f**

**<sup>13</sup>C NMR of 63f**Serine – Glycine Derivative **63g****63g**

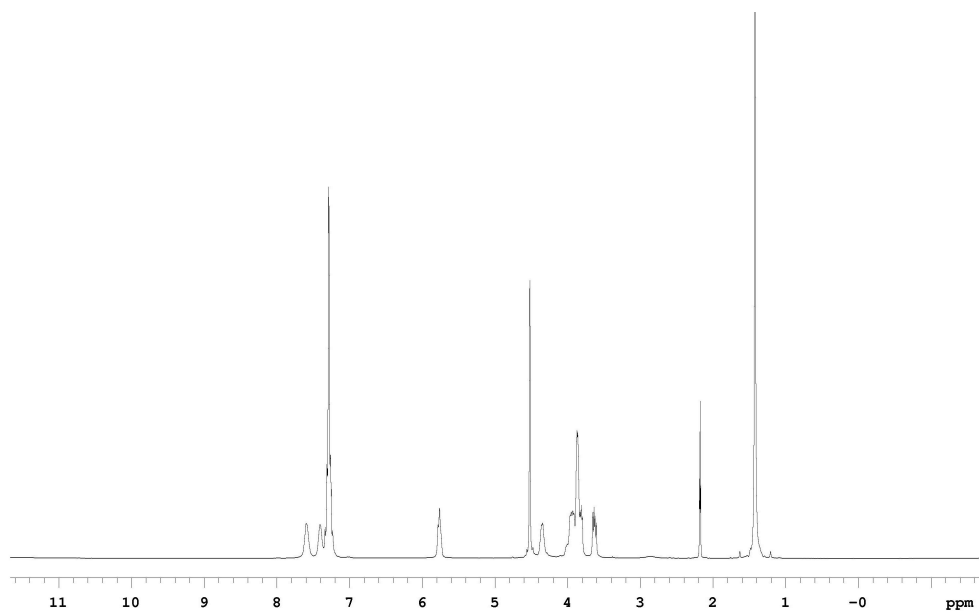
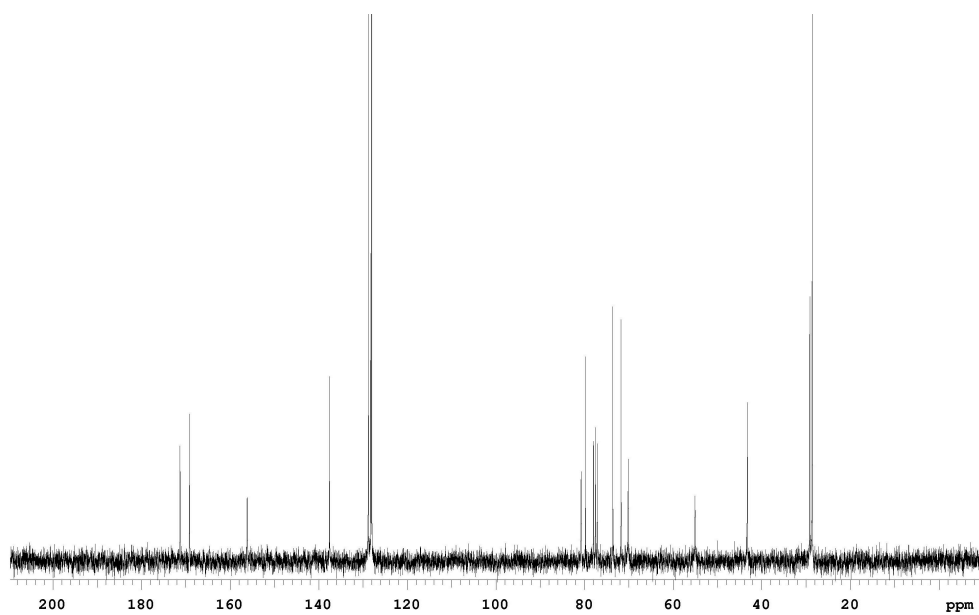
Compound **63g** was prepared from **62a** (3.0 mmol, 1.25 g) and Boc-Ser(Bn)-OH (3.3 mmol, 0.97 g). Recrystallization afforded 0.97 g (83%) **63g** as a white solid.

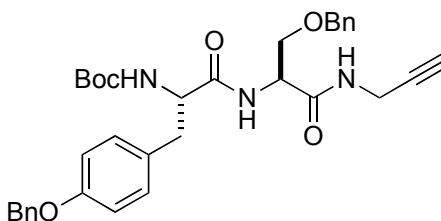
**<sup>1</sup>H NMR (CDCl<sub>3</sub>)** 7.60 (s, 1H), 7.41 (s, 1H), 7.31-7.25 (m, 5H), 5.76 (t, 1H, J = 6.3 Hz), 4.52 (s, 2H), 4.35 (t, 1H, J = 3.6 Hz), 4.96-3.81 (m, 5H), 3.63 (dd, 1H, J = 15.3 Hz, 5.4 Hz), 2.18 (t, 1H, J = 2.4 Hz), 1.42 (s, 9H)

**<sup>13</sup>C NMR (CDCl<sub>3</sub>)** 171.3, 169.1, 156.1, 137.5, 128.8, 128.2, 128.0, 80.7, 79.8, 73.6, 71.7, 70.1, 55.1, 43.2, 29.1, 28.6

**MS (ESI, m/z)** 412 (M+Na)<sup>+</sup>



 $^1\text{H}$  NMR of 63g $^{13}\text{C}$  NMR of 63g

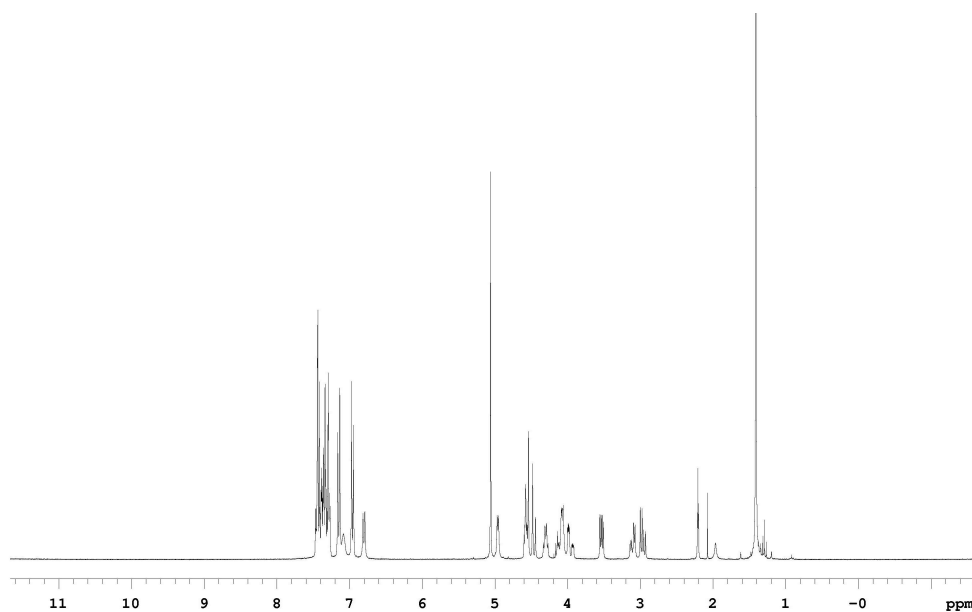
Tyrosine – Serine Derivative **63h****63h**

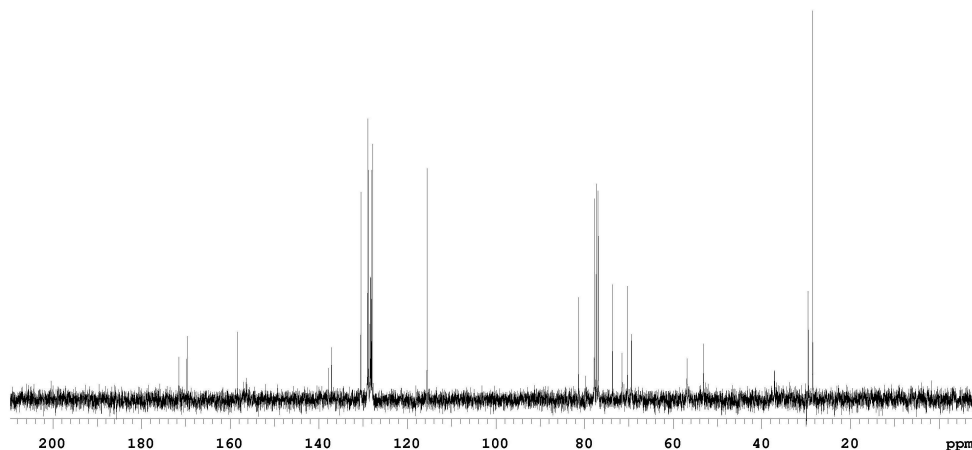
Compound **63h** was prepared from **63c** (1.5 mmol, 0.50 g) and Boc-Tyr(Bn)-OH (1.64 mmol, 0.61 g). Recrystallization with EtOAc and hexanes afforded 0.80 g (92%) **63h** as a white solid.

$^1\text{H NMR}$  ( $\text{CDCl}_3$ ) 7.47-7.27 (m, 10H), 7.15 (d, 2H,  $J = 8.4$  Hz), 7.08 (s, 1H), 6.96 (d, 2H,  $J = 8.4$  Hz), 6.80 (d, 1H,  $J = 7.8$  Hz), 5.06 (s, 1H), 4.96 (d, 1H,  $J = 5.1$  Hz), 4.60-4.44 (m, 3H), 4.31 (dd, 1H,  $J = 7.2$  Hz, 5.7 Hz), 4.14-3.97 (m, 3H), 3.54 (dd, 1H,  $J = 9.3$  Hz, 5.1 Hz), 3.12 (dd, 1H,  $J = 14.3$  Hz, 8.7 Hz), 2.96 (dd, 1H,  $J = 14.1$  Hz, 7.8 Hz), 2.21 (t, 1H,  $J = 2.4$  Hz), 1.41 (s, 9H)

$^{13}\text{C NMR}$  ( $\text{CDCl}_3$ ) 171.5, 169.7, 158.3, 137.8, 137.1, 130.5, 128.9, 128.7, 128.4, 128.3, 128.2, 128.0, 127.8, 115.5, 81.3, 79.9, 73.6, 71.5, 70.3, 69.4, 56.8, 53.1, 37.1, 29.5, 28.5

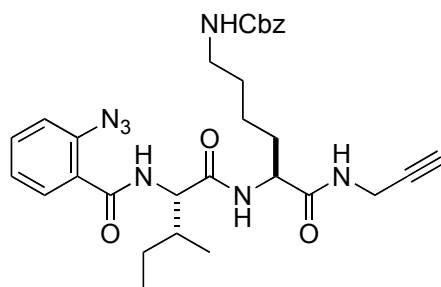
$\text{MS (ESI, } m/z)$  586 ( $\text{M}+\text{H}$ ) $^+$

 $^1\text{H NMR}$  of **63h**



<sup>13</sup>C NMR of **63h**

**General Procedure for preparation of 60a-h.** To a solution of **63a-h** in 20:1 EtOAc/MeOH (0.15 M) was added AcCl (5 equiv) dropwise and the resulting mixture was stirred at 0 °C for 2 h in a sealed flask and warmed to room temperature for another 2h. Solvent was removed and the residue was used without further purification. Triethylamine (2.5 equiv) was added to a solution of the above residue (1 equiv) in dry THF (0.1-0.2 M). The resulting mixture was stirred for 10 min and treated with DMAP (0.7 equiv). Freshly prepared 2-azido-benzoyl chloride (from 1 equiv. of 2-azidobenzoic acid, See Takeuchi, H.; Hagiwara, Eguchi, S. *Tetrahedron* **1989**, *45*, 6375-6386) in dry THF (0.5 M) was added dropwise to the solution and the resulting mixture was stirred for 2h at room temperature. The reaction mixture was poured into ice water and the white precipitate was filtered with a fine frit funnel and rinsed with small portions of water three times. The precipitate was dried under vacuum and recrystallized with EtOAc and hexanes afforded **60a-h** as white or slightly yellow solid.

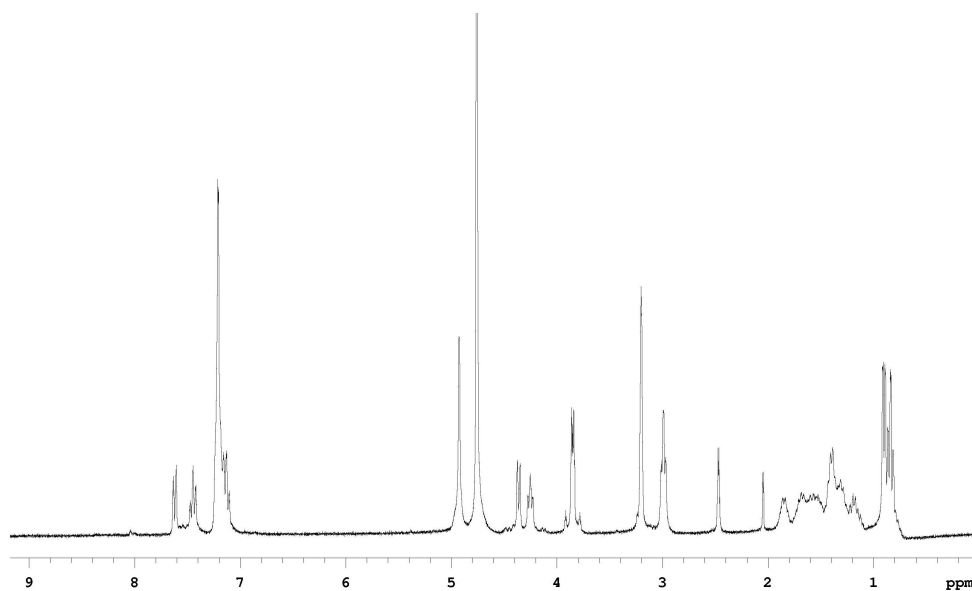
Linear Isoleucine – Lysine Derivative **60a****60a**

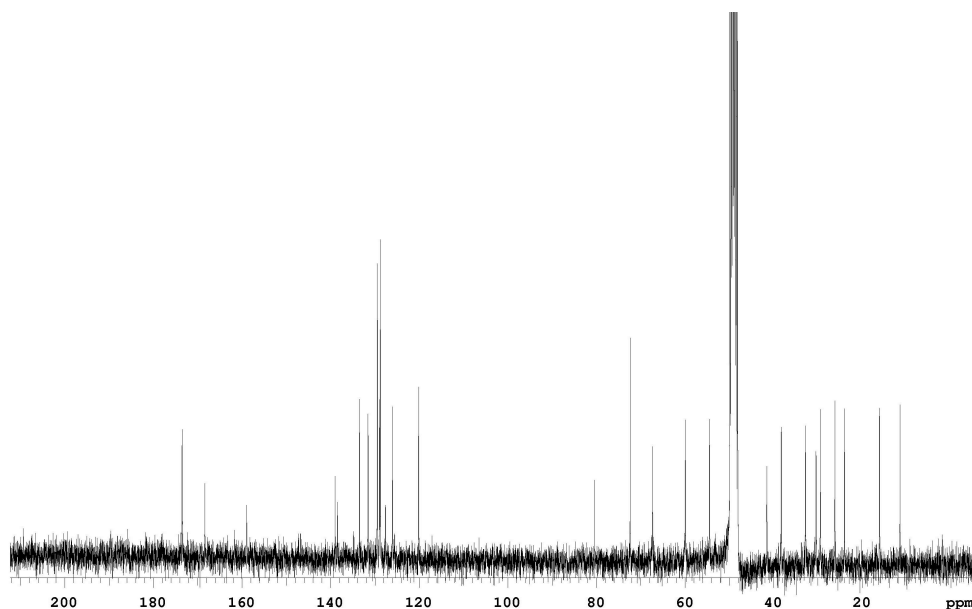
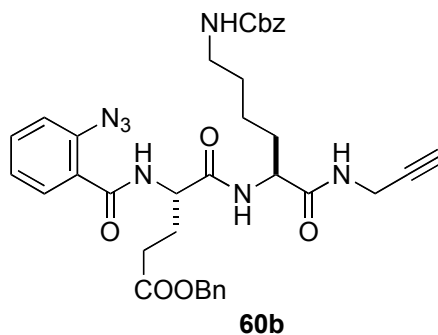
Compound **60a** was prepared from (1.9 mmol, 0.98 g) of **63a**. Crystallization afforded 0.76 g (88%) **60a** as a white solid.

**<sup>1</sup>H NMR (CD<sub>3</sub>OD)** 7.62 (d, 1H, J = 7.8 Hz), 7.47 (t, 1H, 7.8 Hz), 7.21-7.10 (m, 7H), 4.93 (s, 2H), 4.36 (d, 1H, J = 7.5 Hz), 4.25 (t, 1H, J = 6.6 Hz), 3.85 (m, 2H), 2.99 (t, 2H, J = 5.6 Hz), 2.47 (t, 1H, J = 2.6 Hz), 1.86-1.23 (m, 9H), 0.90 (d, 3H, J = 4.8 Hz), 0.83 (t, 3H, J = 7.2 Hz)

**<sup>13</sup>C NMR (CD<sub>3</sub>OD)** 173.6, 173.5, 168.4, 158.9, 139.0, 138.4, 133.5, 131.5, 129.5, 128.9, 128.8, 127.6, 126.1, 120.1, 80.4, 72.4, 67.3, 59.9, 54.5, 41.5, 38.3, 32.8, 30.4, 29.5, 26.2, 24.0, 16.1, 11.5

**MS (ESI, m/z)** 576 (M+H)<sup>+</sup>

**<sup>1</sup>H NMR of 60a**

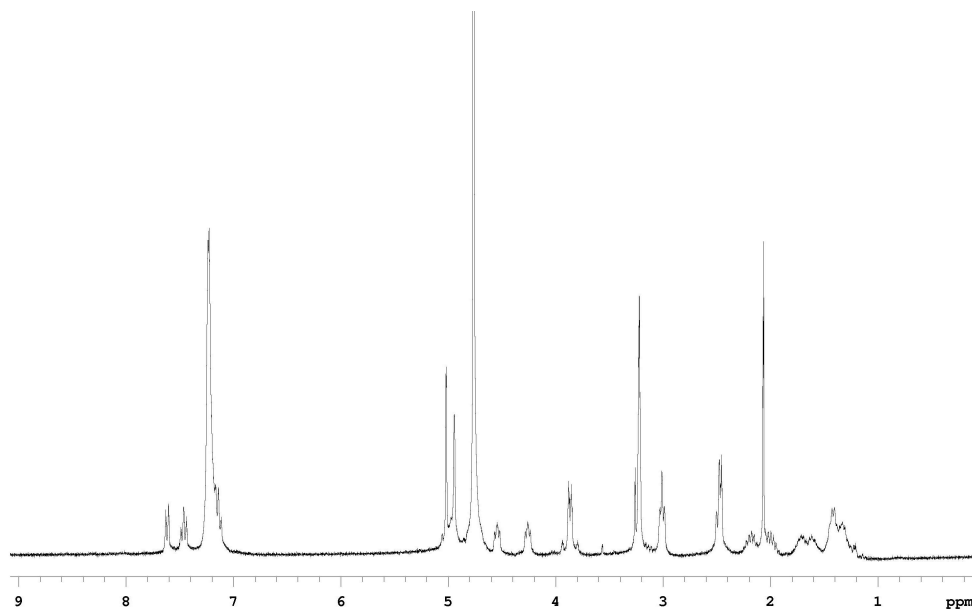
 $^{13}\text{C}$  NMR of **60a**Linear Glutamic Acid – Lysine Derivative **60b**

Compound **60b** was prepared from (1.0 mmol, 0.64 g) of **63b**. Crystallization afforded 0.52 g (70%) **60b** as a white solid.

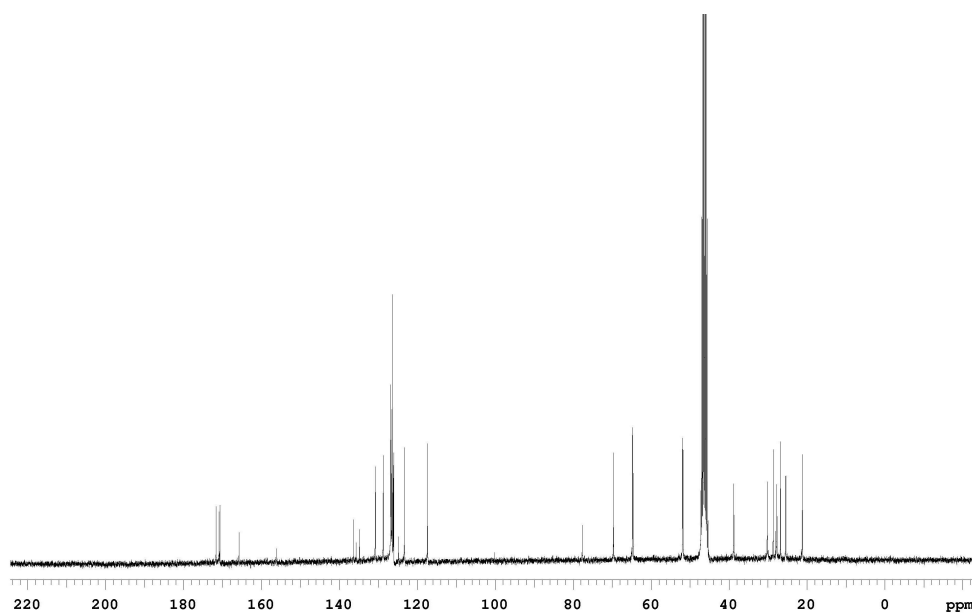
$^1\text{H}$  NMR ( $\text{CD}_3\text{OD}$ ) 7.62 (d, 1H,  $J = 8.1$  Hz), 7.46 (t, 1H, 7.8 Hz), 7.24-7.11 (m, 7H), 5.06 (s, 2H), 5.02 (s, 2H), 4.55 (t, 1H,  $J = 6.8$  Hz), 4.26 (t, 1H,  $J = 6.8$  Hz), 3.85 (dd, 2H,  $J = 17.4, 25.2$ ), 3.01 (t, 2H,  $J = 7.8$  Hz), 2.48 (m, 3H), 2.20 (m, 1H), 2.00 (m, 1H), 1.72, (m, 1H), 1.62 (m, 1H), 1.43-1.33 (m, 4H)

**$^{13}\text{C}$  NMR ( $\text{CD}_3\text{OD}$ )** 171.6, 170.9, 170.6, 165.7, 158.9, 136.3, 125.9, 134.8, 130.8, 128.7, 126.8, 126.7, 126.5, 126.2, 126.0, 124.8, 123.3, 117.3, 77.7, 69.6, 64.7, 64.6, 51.9, 51.8, 38.7, 30.2, 28.6, 27.7, 26.8, 25.4, 21.2

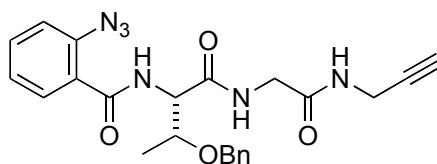
**MS (ESI,  $m/z$ )** 704 ( $\text{M}+\text{Na}$ )<sup>+</sup>



**$^1\text{H}$  NMR of 60b**



**$^{13}\text{C}$  NMR of 60b**

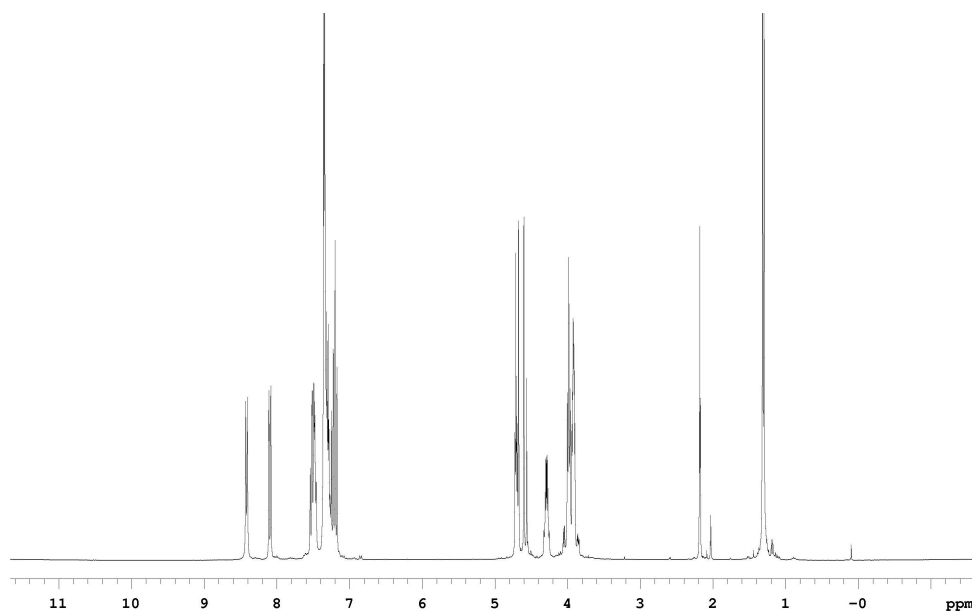
Linear Threonine – Glycine Derivative **60c****60c**

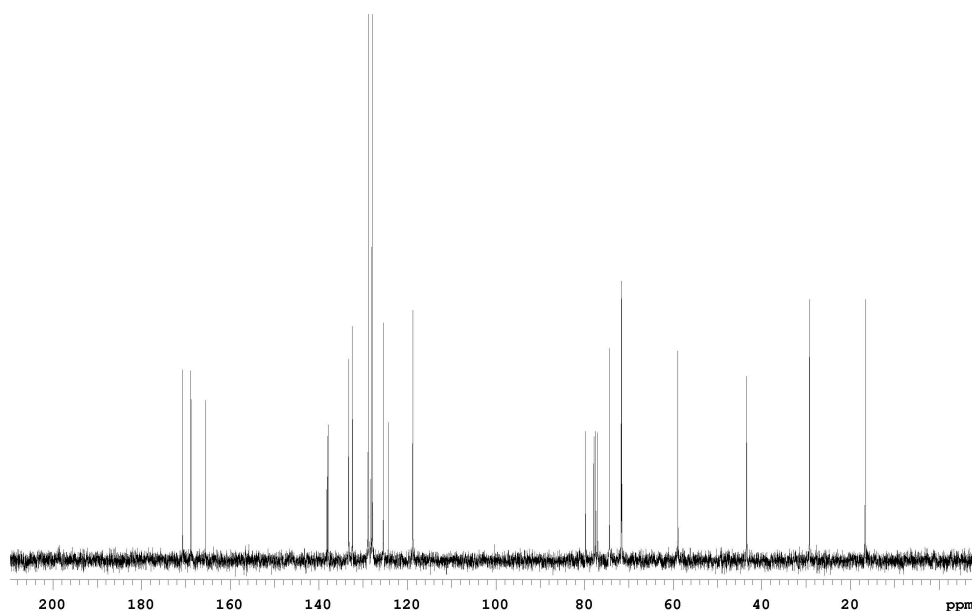
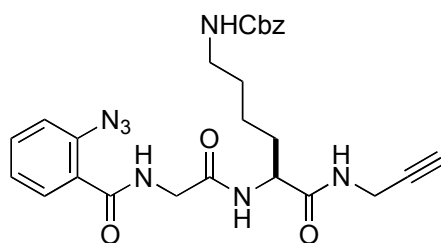
Compound **60c** was prepared from (1.0 mmol, 0.40 g) of **63c**. Crystallization afforded 0.35 g (70%) **60c** as a slightly yellowish solid.

**<sup>1</sup>H NMR (CDCl<sub>3</sub>)** 8.41 (d, 1H, J = 6.6 Hz), 8.10 (dd, 1H, 7.8 Hz, 1.5 Hz), 7.50 (m, 2H), 7.36-7.27 (m, 5H), 7.20 (m, 2H), 4.72-4.56 (m, 3H), 4.29 (dd, 1H, J = 6.3 Hz, 3.0 Hz), 3.98 (t, 2H, J = 5.9 Hz), 2.18 (t, 1H, 2.4 Hz), 1.31 (d, 6.3 Hz)

**<sup>13</sup>C NMR (CDCl<sub>3</sub>)** 170.71, 168.8, 165.6, 138.1, 137.9, 133.2, 132.4, 128.8, 128.2, 127.8, 125.4, 124.3, 118.7, 79.7, 74.4, 71.7, 71.6, 58.9, 43.4, 29.2, 16.6

**MS (ESI, m/z)** 471 (M+Na)<sup>+</sup>

**<sup>1</sup>H NMR of 60c**

 $^{13}\text{C}$  NMR of **60c**Linear Glycine – Lysine Derivative **60d****60d**

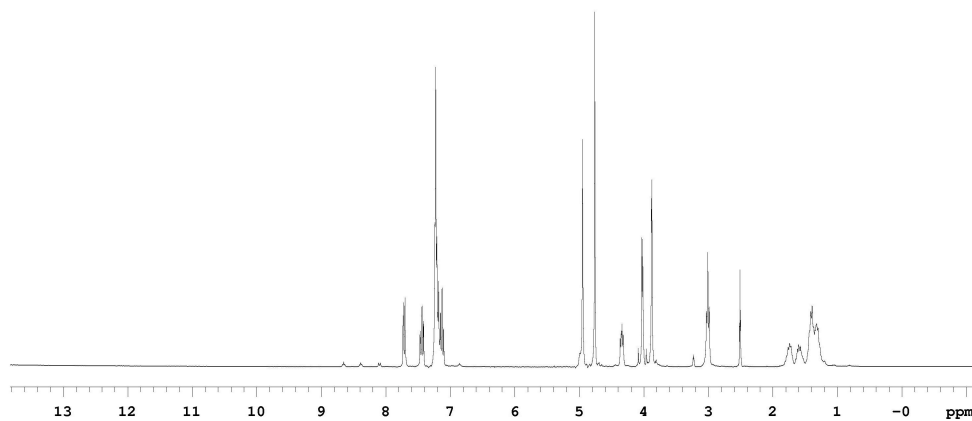
Compound **60d** was prepared from (1.1 mmol, 0.52 g) of **63d**. Crystallization afforded 0.49 g (85%) **60d** as a white solid.

$^1\text{H}$  NMR ( $\text{CD}_3\text{OD}$ ) 7.67 (d, 1H,  $J = 7.8$  Hz), 7.44 (t, 1H,  $J = 8.1$  Hz), 7.24-7.10 (m, 7H), 4.95 (s, 2H), 4.34 (q, 5.4 Hz, 8.7 Hz, 3.3 Hz), 4.02 (dd, 2H, 21.0 Hz, 5.2H), 3.88 (d, 2H, 2.1 Hz), 3.01 (t, 1H,  $J = 6.6$  Hz), 2.51 (t, 1H, 2.6 Hz), 1.74 (m, 1H), 1.60 (m, 1H), 1.43-1.30 (m, 4H)

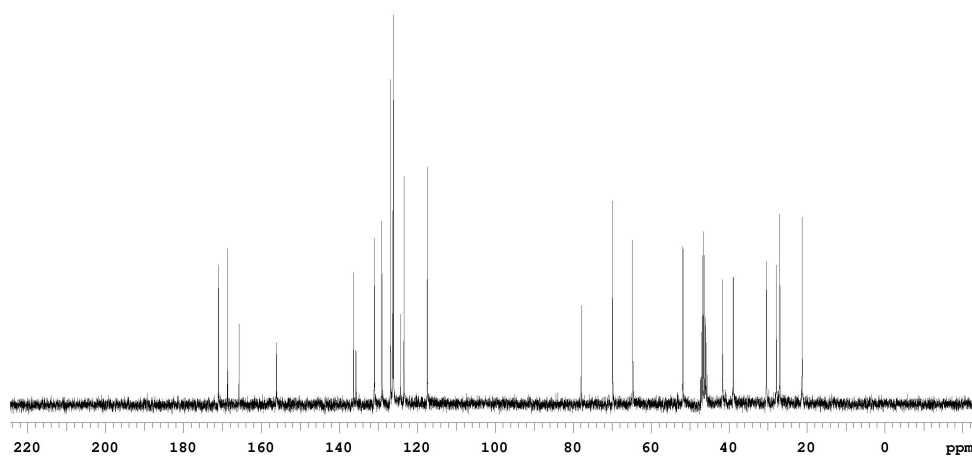


**$^{13}\text{C}$  NMR ( $\text{CD}_3\text{OD}$ )** 171.0, 168.7, 165.7, 156.2, 136.3, 135.8, 131.0, 129.1, 126.9, 126.3, 126.1, 124.3, 123.4, 117.4, 77.9, 69.9, 64.7, 51.8, 41.6, 38.9, 30.4, 27.8, 26.9, 21.2

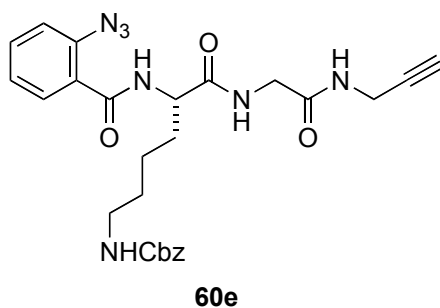
**MS (ESI,  $m/z$ )** 526 ( $\text{M}+\text{Li}^+$ )



**$^1\text{H}$  NMR of 60d**



**$^{13}\text{C}$  NMR of 60d**

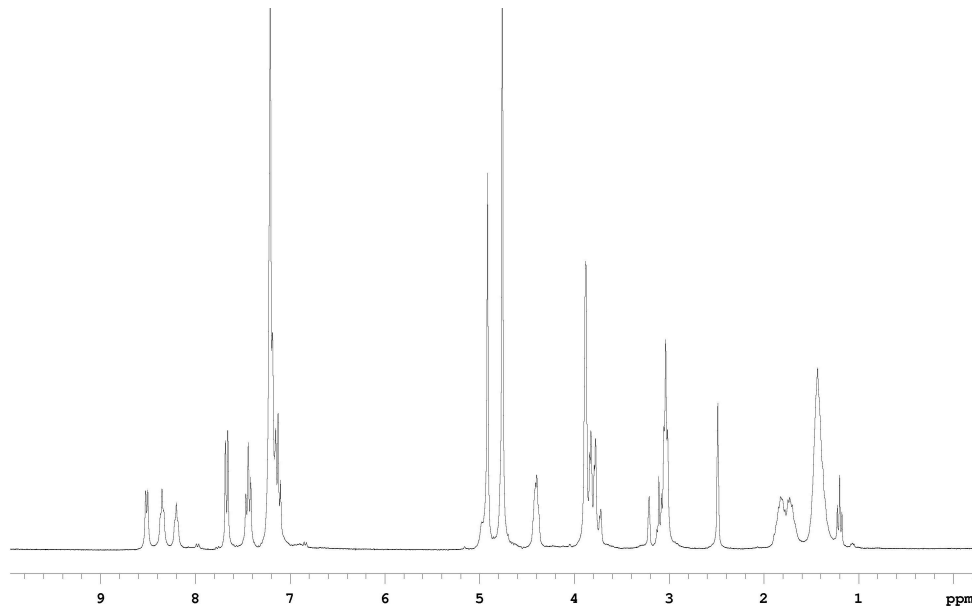
Linear Lysine – Glycine Derivative **60e**

Compound **60e** was prepared from (1.0 mmol, 0.47 g) of **63e**. Crystallization afforded 0.42 g (80%) **60e** as a white solid.

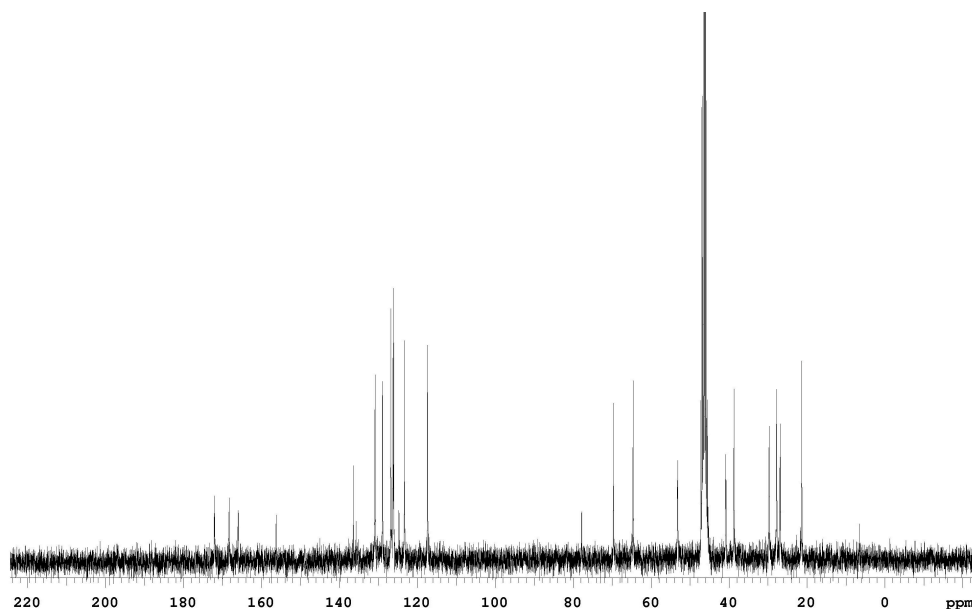
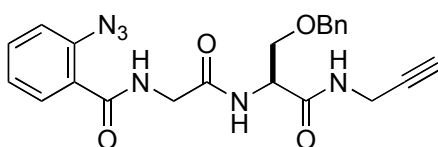
**<sup>1</sup>H NMR (CD<sub>3</sub>OD)** 7.67 (d, 1H, J = 7.5 Hz), 7.44 (t, 1H, J = 7.5 Hz), 7.21-7.10 (m, 7H), 4.92 (s, 2H), 4.40 (dd, 1H, 5.4 Hz, 3 Hz), 3.80 (m, 4H), 3.04 (t, 2H, 6.2 Hz), 2.49 (t, 1H, J = 2.4 Hz), 1.83 (m, 1H), 1.73 (m, 1H), 1.43 (m, 4H)

**<sup>13</sup>C NMR (CD<sub>3</sub>OD)** 172.1, 168.3, 166.0, 156.2, 136.4, 130.8, 128.9, 126.8, 126.2, 126.1, 124.7, 123.3, 117.3, 77.8, 69.6, 64.6, 53.1, 40.9, 38.7, 29.7, 27.7, 26.9, 26.8, 21.3

**MS (ESI, m/z)** 520 (M+H)<sup>+</sup>



**<sup>1</sup>H NMR of 60e**

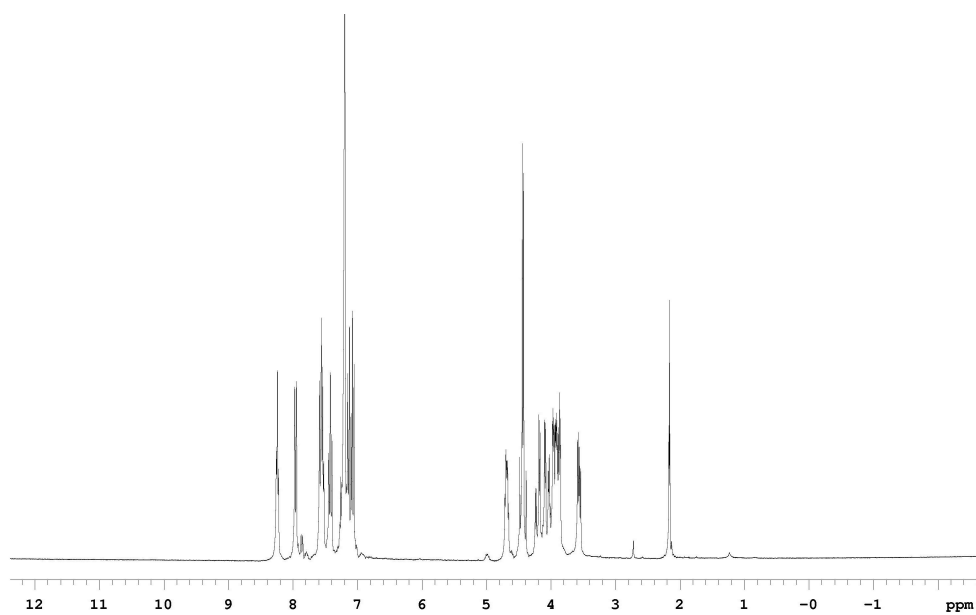
**<sup>13</sup>C NMR of 60e****Linear Glycine – Serine Derivative 60f****60f**

Compound **60f** was prepared from (0.7 mmol, 0.27 g) of **63f**. Crystallization afforded 0.17 g (52%) **60f** as a slightly yellowish solid.

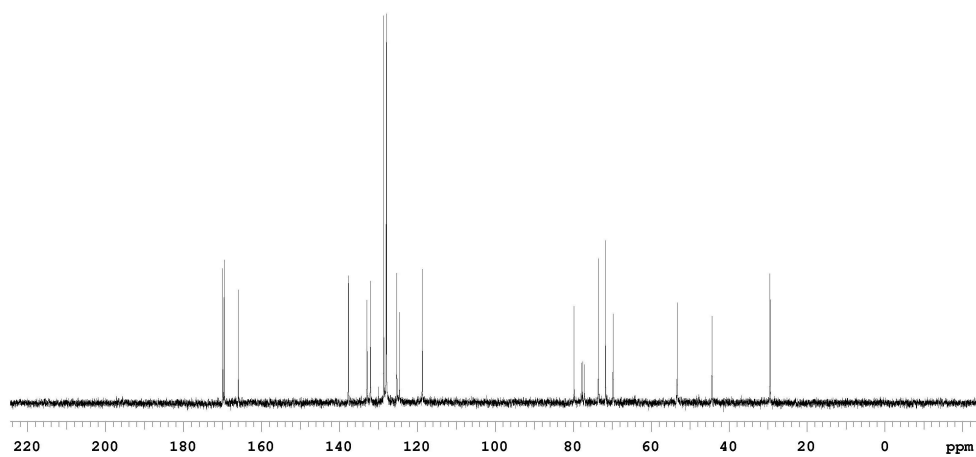
**<sup>1</sup>H NMR (CDCl<sub>3</sub>)** 8.24 (t, 1H, J = 5.1 Hz), 7.96 (q, 1H, 7.8 Hz, 1.2 Hz), 7.55 (m, 2H), 7.42 (m, 1H), 7.20 (m, 5H), 7.16 (d, 1H, J = 7.5 Hz), 7.08 (m, 1H), 4.69 (dd, 1H, J = 8.4 Hz, 4.8 Hz), 4.43 (dd, 1H, 18 Hz, 6 Hz), 4.20 (dd, 1H, 11.4 Hz, 5.7 Hz), 4.06 (dd, 1H, 11.4 Hz, 5.7 Hz), 4.03 (dd, 1H, J = 5.4 Hz, 2.7 Hz), 3.96 (dd, 1H, 5.4 Hz, 2.7 Hz), 3.92 (dd, 1H, J = 4.8 Hz, 2.4 Hz), 3.87 (dd, 1H, 9.6Hz, 5.4Hz), 3.56 (dd, 1H, 9.3 Hz, 5.4 Hz), 2.16 (t, 1H, J = 2.1 Hz)

**<sup>13</sup>C NMR (CDCl<sub>3</sub>)** 169.9, 169.6, 165.9, 137.7, 137.7, 132.9, 132.0, 128.6, 128.0, 127.9, 125.2, 124.6, 118.7, 79.8, 73.5, 71.7, 69.7, 53.3, 44.3, 29.5

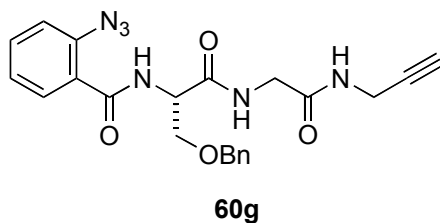
**MS (ESI, m/z)** 441 (M+Li)<sup>+</sup>



$^1\text{H}$  NMR of 60f



$^{13}\text{C}$  NMR of 60f

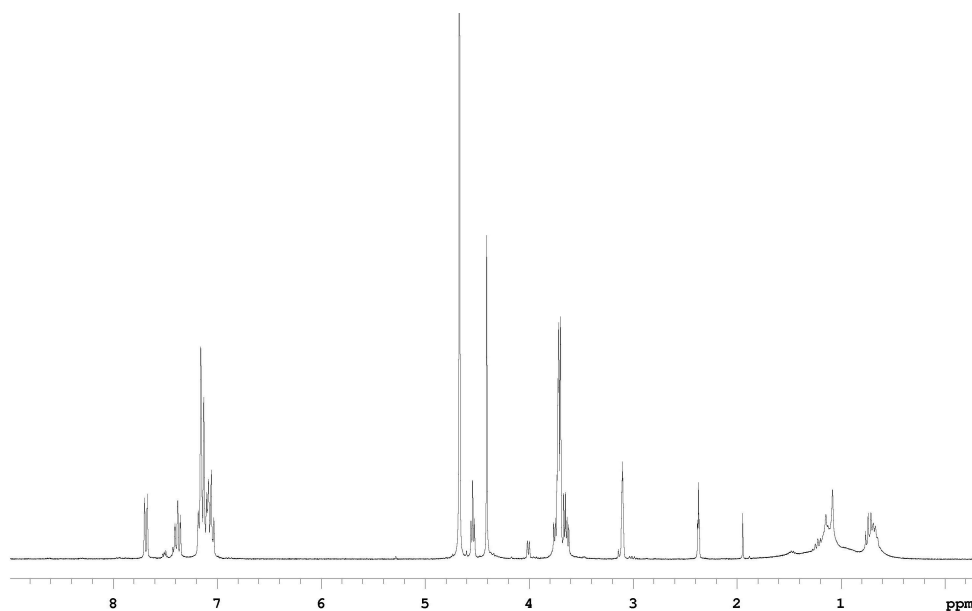
Linear Serine – Glycine Derivative **60g**

Compound **60g** was prepared from (1.0 mmol, 0.39 g) of **63g**. Crystallization afforded 0.35 g (81%) **60g** as a yellowish solid.

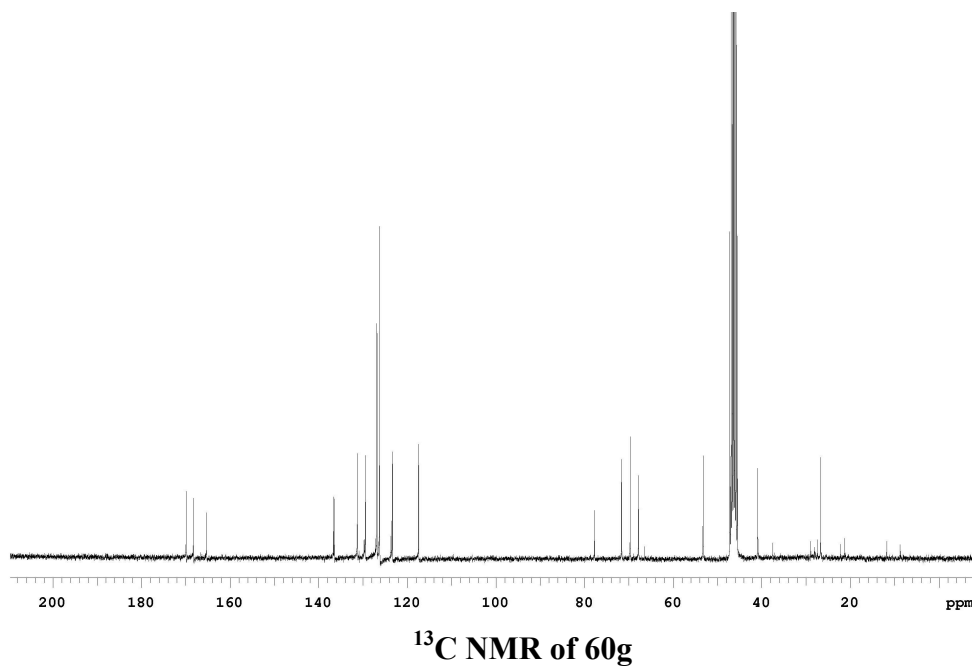
$^1\text{H NMR}$  ( $\text{CD}_3\text{OD}$ ) 7.55 (d, 1H,  $J = 7.8$  Hz), 7.42 (d, 1H,  $J = 7.8$  Hz), 7.18-7.03 (m, 7H), 4.54 (t, 1H,  $J = 4.8$  Hz), 4.41 (s, 2H), 3.76-3.62 (m, 6H), 2.37 (t, 1H,  $J = 2.4$  Hz)

$^{13}\text{C NMR}$  ( $\text{CD}_3\text{OD}$ ) 169.9, 168.3, 165.3, 136.6, 136.4, 131.3, 129.4, 126.8, 126.2, 125.2, 123.6, 123.3, 117.4, 77.7, 71.6, 69.7, 67.8, 53.2, 40.9, 26.7

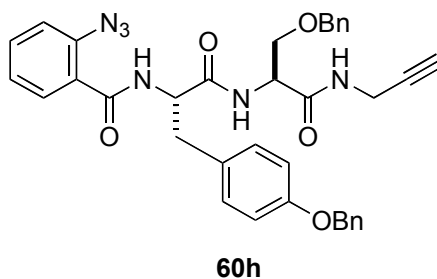
$\text{MS (ESI, m/z)}$  457 ( $\text{M}+\text{Na}$ ) $^+$



$^1\text{H NMR}$  of **60g**



### Linear Tyrosine – Serine Derivative **60h**

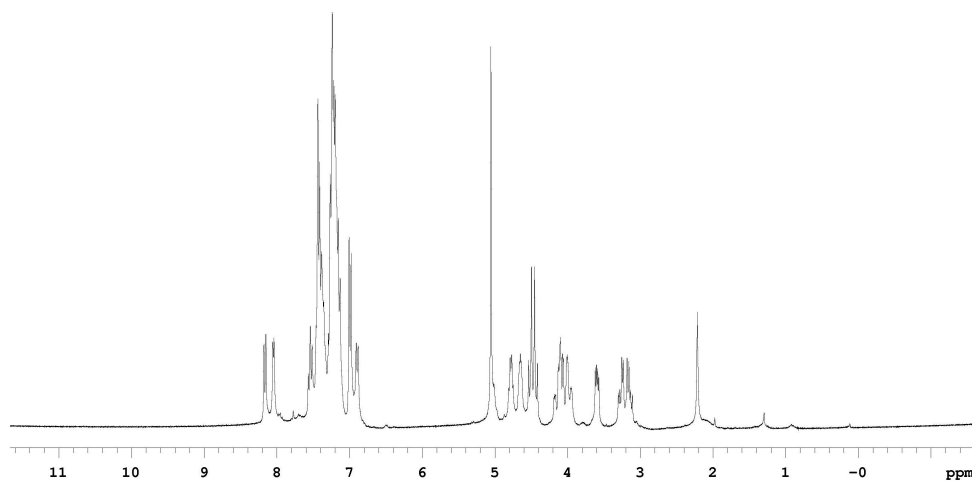


Compound **60h** was prepared from (1.0 mmol, 0.59 g) of **63h**. Crystallization afforded 0.52 g (83%) **60h** as a yellowish solid.

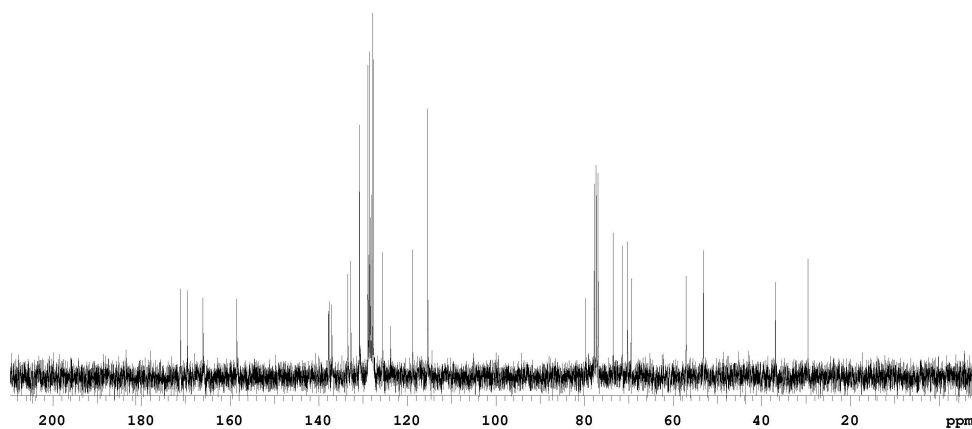
$^1\text{H}$  NMR ( $\text{CDCl}_3$ ) 8.16 (d, 1H,  $J = 7.8$  Hz), 8.04 (t, 1H,  $J = 4.5$  Hz), 7.54 (t, 1H,  $J = 7.8$  Hz), 7.46-7.35 (m, 6H), 7.29-7.10 (m, 13H), 6.99 (d, 2H,  $J = 8.4$  Hz), 6.89 (d, 1H,  $J = 4.8$  Hz), 5.05 (s, 2H), 4.78 (dd, 1H,  $J = 12$  Hz, 6 Hz), 4.66 (dd, 1H,  $J = 8.4$  Hz, 4.2 Hz), 4.48 (dd, 2H,  $J = 24.6$  Hz, 12.6 Hz), 4.18-3.95 (m, 3H), 3.59 (dd, 1H,  $J = 9.6$  Hz, 4.2 Hz), 3.27 (dd, 1H,  $J = 13.8$  Hz, 7.8 Hz), 3.15 (dd, 1H,  $J = 14.1$  Hz, 6.6 Hz), 2.21 (t, 1H,  $J = 2.4$  Hz)

**$^{13}\text{C}$  NMR ( $\text{CDCl}_3$ )** 171.1, 169.7, 166.1, 158.5, 137.7, 137.7, 137.0, 133.4, 132.7, 130.8, 128.9, 128.6, 128.4, 128.3, 128.0, 127.8, 127.7, 125.5, 123.8, 118.8, 115.4, 79.8, 73.5, 71.5, 70.3, 69.5, 57.1, 53.2, 36.9, 29.5

**MS (ESI,  $m/z$ )** 653 ( $\text{M}+\text{Na}$ )<sup>+</sup>



**$^1\text{H}$  NMR of 60h**

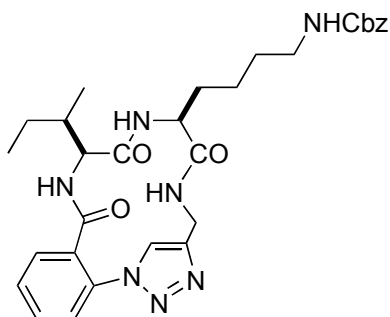


**$^{13}\text{C}$  NMR of 60h**

### General Procedure for Cyclization

*N,N*-diisopropylethylamine (4.0 mmol, 0.70 ml, 20 equiv) was added to a suspension of CuI (0.4 mmol, 76 mg, 2 equiv) in 200 ml dry THF. A solution of **60a-h** (0.2 mmol, 1.0 equiv) in 20 ml dry THF was added to the suspension slowly at for 10 h and stirred for another 4 h under nitrogen. The suspension was filtered with a pad of celite and concentrated. Flash chromatography on silica gel (3% MeOH in CH<sub>2</sub>Cl<sub>2</sub>) gave a mixture of monomeric and dimeric compounds. Preparative HPLC (20-90% B in 30 min) was carried out to provide **64a-h** as white powder.

### Cyclic Isoleucine – Lysine Mimic **64a**

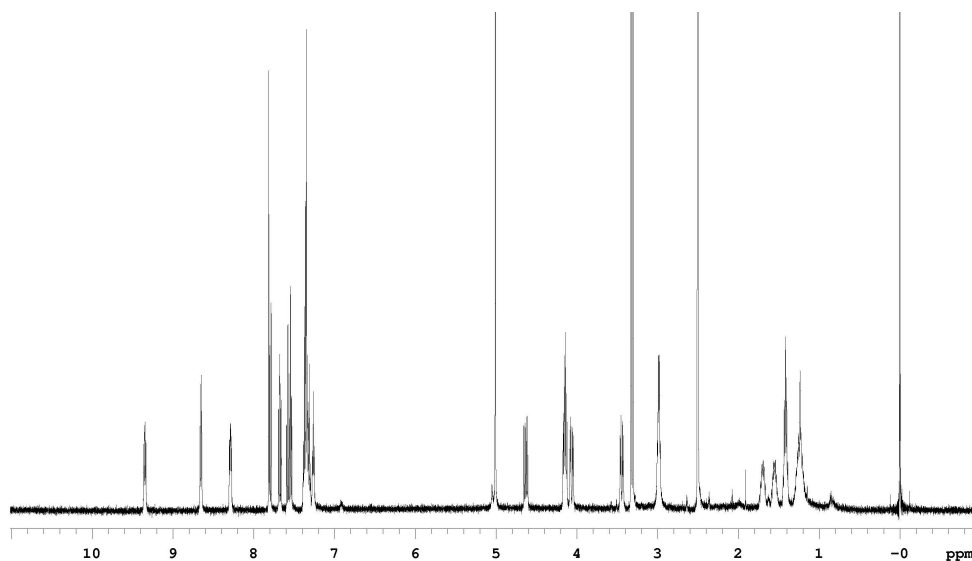
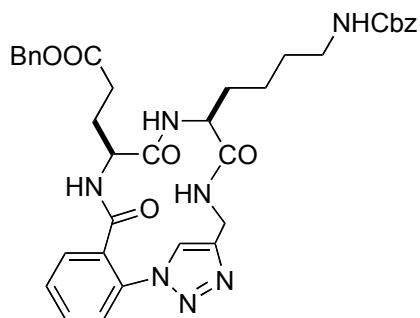


**64a**

**<sup>1</sup>H NMR (DMSO-*d*<sub>6</sub>)** 8.62 (d, 1H, *J* = 8.5 Hz), 8.32 (s, 1H), 8.01 (d, 1H, *J* = 8.5 Hz), 7.85 (s, 1H), 7.79 (d, 1H, *J* = 7.5 Hz), 7.69 (m, 1H), 7.61 (t, 1H, *J* = 7.5 Hz), 7.53 (d, 1H, *J* = 6.0 Hz), 7.38-7.31 (m, 5H), 7.24 (t, 1H, *J* = 6.0 Hz), 5.00 (s, 2H), 4.67 (dd, 1H, *J* = 15.5 Hz, 8.0 Hz), 4.06 (m, 3H), 2.97 (dd, 2H, *J* = 12.5 Hz, 6.0 Hz), 1.77 (m, 1H), 1.59 (m, 1H), 1.40 (m, 2H), 1.24 (m, 5H), 0.87 (m, 6H)

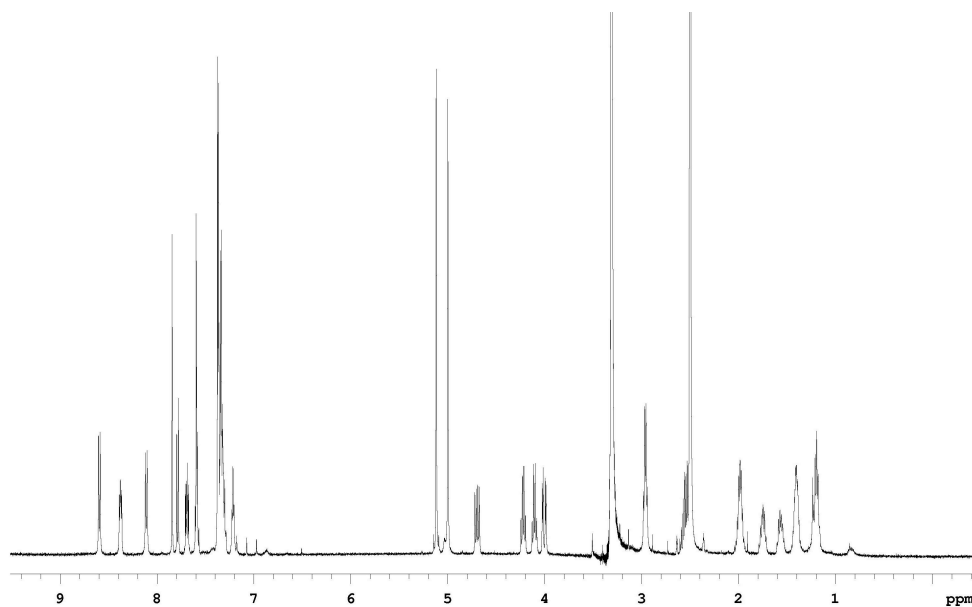
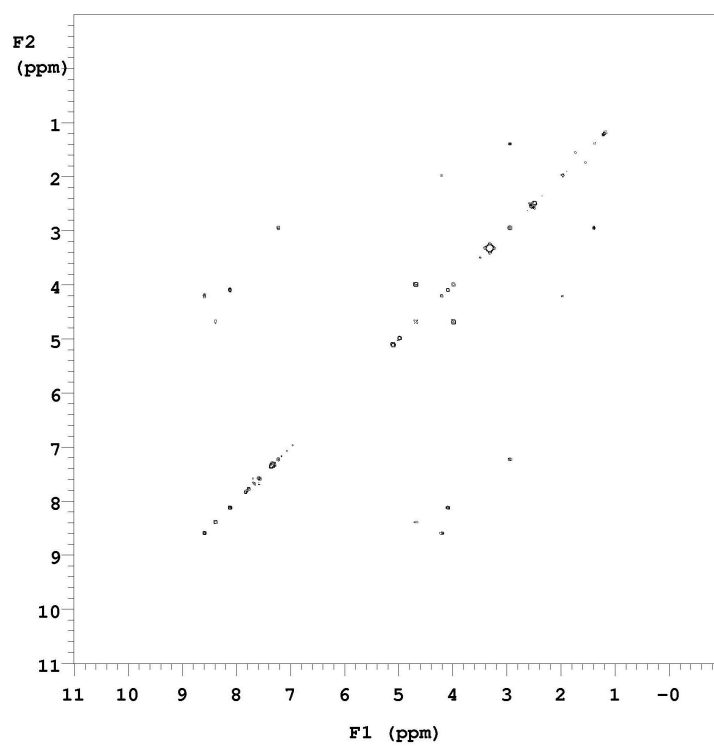
**MS (ESI, *m/z*)** 576 (M+H)<sup>+</sup>

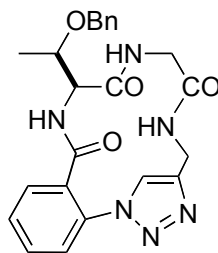


**<sup>1</sup>H NMR of 64a****Cyclic Glutamic Acid – Lysine Mimic 64b****64b**

**<sup>1</sup>H NMR (DMSO-*d*<sub>6</sub>)** 8.59 (d, 1H, *J* = 8.0 Hz), 8.38 (dd, 1H, *J* = 7.5 Hz, 4.5 Hz), 8.11 (d, 1H, *J* = 8.5 Hz), 7.85 (s, 1H), 7.84 (d, 1H, *J* = 8.0 Hz), 7.69 (m, 1H), 7.59 (m, 2H), 7.38-7.30 (m, 5H), 7.22 (t, 1H, *J* = 5.5 Hz), 5.12 (s, 2H), 5.00 (s, 2H), 4.70 (dd, 1H, *J* = 15.5 Hz, 8.0 Hz), 4.21 (dd, 1H, *J* = 15.0 Hz, 7.0 Hz), 4.11 (dd, 1H, *J* = 16.0 Hz, 8.0 Hz), 4.00 (dd, 1H, *J* = 10.0 Hz, 4.0 Hz), 2.96 (dd, 2H, *J* = 13.0 Hz, 6.5 Hz), 2.55 (m, 2H), 1.99 (m, 2H), 1.75 (m, 1H), 1.57 (m, 1H), 1.41 (m, 2H), 1.21 (m, 2H)

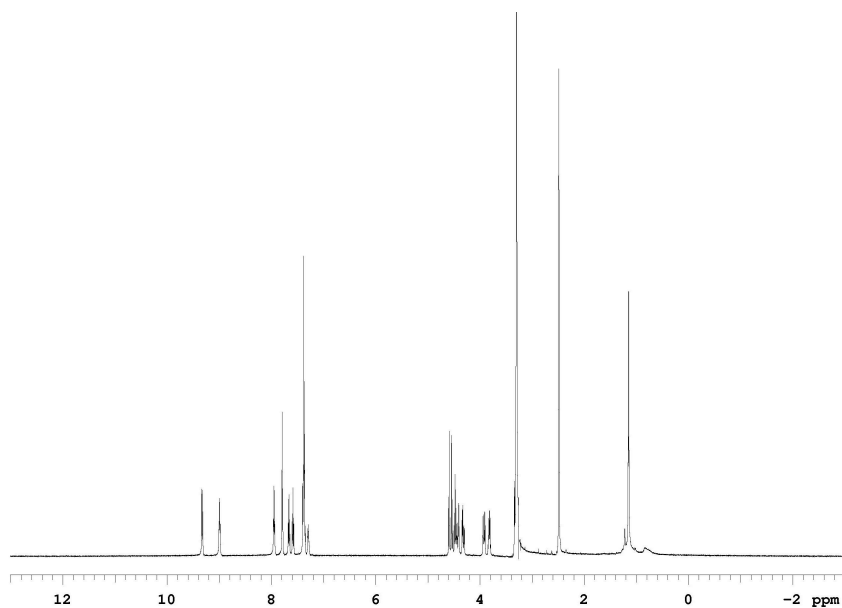
**MS (ESI, *m/z*)** 682 (M+H)<sup>+</sup>

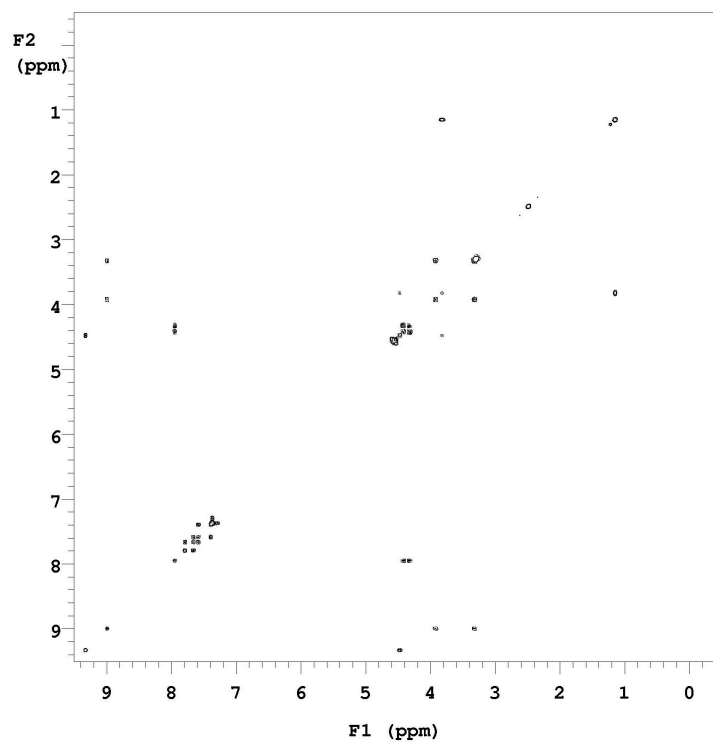
 **$^1\text{H}$  NMR of 64b****COSY of 64b**

Cyclic Threonine – Glycine Mimic **64c****64c**

**$^1\text{H NMR}$  (DMSO- $d_6$ )** 9.32 (d, 1H,  $J = 8.5$  Hz), 8.99 (t, 1H,  $J = 6.0$ ), 7.95 (d, 1H,  $J = 7.0$  Hz), 7.79 (s, 1H), 7.78 (d, 1H,  $J = 7.5$  Hz), 7.66 (t, 1H,  $J = 7.5$  Hz), 7.59 (t, 1H,  $J = 7.5$  Hz), 7.40-7.29 (m, 6H), 4.56 (dd, 1H,  $J = 28.0$  Hz, 12.0 Hz), 4.47 (t, 1H,  $J = 8.5$  Hz), 4.42 (dd, 1H,  $J = 15.0$  Hz, 7.0 Hz), 4.32 (dd, 1H,  $J = 15.0$  Hz, 7.0 Hz), 3.92 (dd, 1H,  $J = 13.0$  Hz, 6.5 Hz), 4.82 (m, 1H), 1.15 (d, 3H,  $J = 5.5$  Hz)

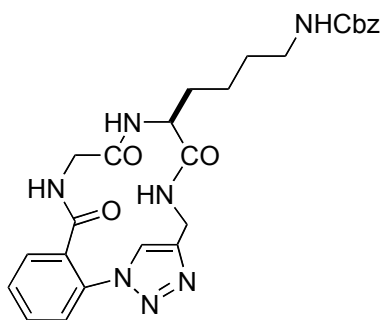
**MS (ESI,  $m/z$ )** 449 (M+H) $^+$

 **$^1\text{H NMR}$  of **64c****



**COSY of 64c**

**Cyclic Glycine – Lysine Mimic 64d**

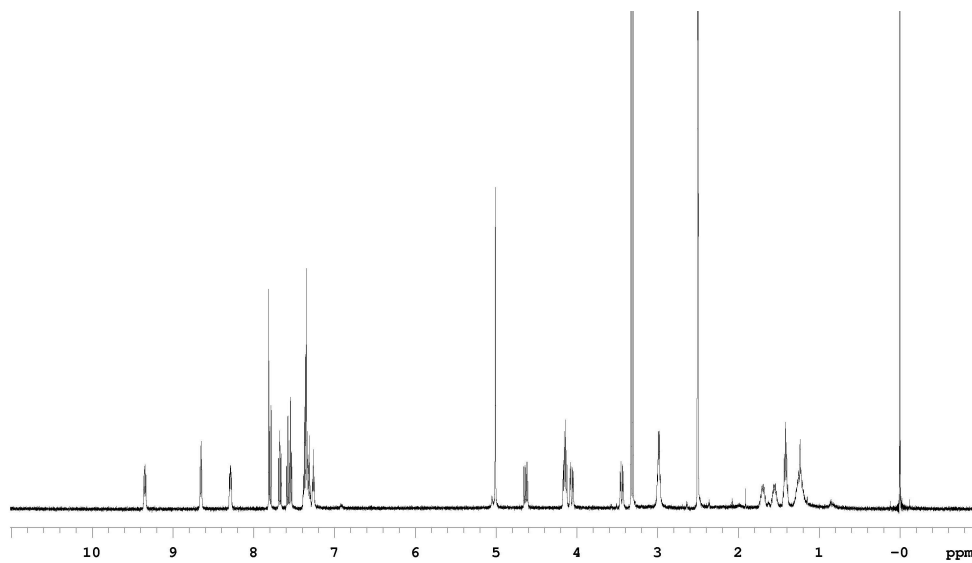


**64d**

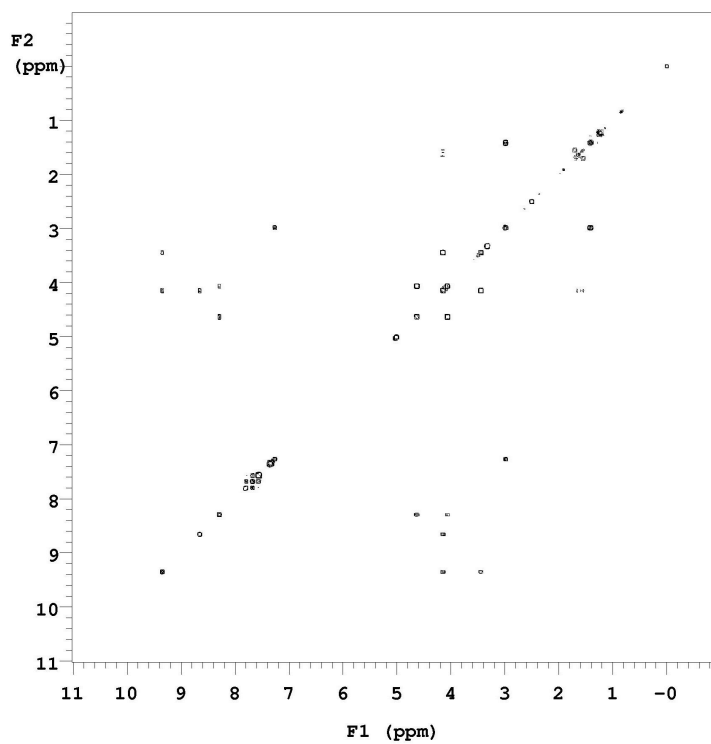
**<sup>1</sup>H NMR (DMSO-*d*<sub>6</sub>)** 9.32 (t, 1H, *J* = 7.5 Hz), 8.65 (d, 1H, *J* = 8.0), 7.95 (dd, 1H, *J* = 8.0 Hz, 5.0 Hz), 7.81 (s, 1H), 7.78 (dd, 1H, *J* = 8.0 Hz, 1.0 Hz), 7.67 (m, 1H), 7.56 (m, 2H), 7.37-7.26 (m, 5H), 7.26 (t, 1H, *J* = 6.0 Hz), 5.01 (s, 2H), 4.63 (dd, 1H, *J* = 15.5 Hz, 8.0 Hz), 4.15 (m, 2H), 4.06 (dd, 1H, *J* = 15.5 Hz, 4.0 Hz), 3.44 (dd, 1H, *J* = 14.5 Hz, 5.0

Hz), 2.98 (q, 2H,  $J = 13.5$  Hz, 7.0 Hz), 1.69 (m, 1H), 1.54 (m, 1H), 1.41 (m, 2H), 1.23 (m, 2H)

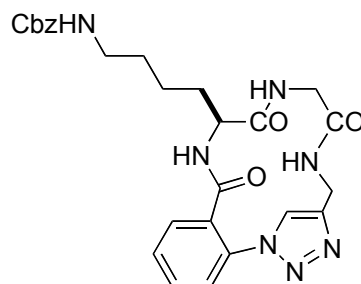
**MS (ESI,  $m/z$ ) 520 ( $M+H$ )<sup>+</sup>**



**<sup>1</sup>H NMR of 64d**

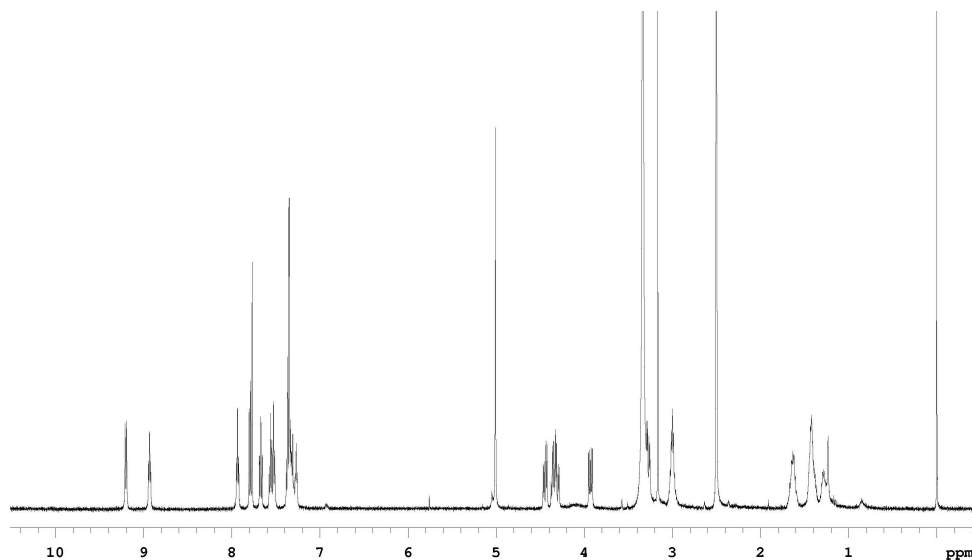


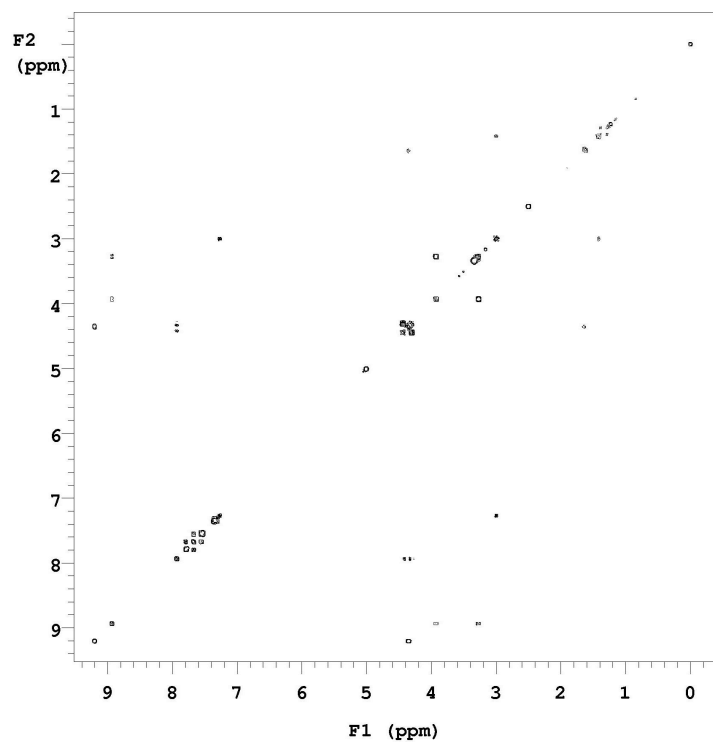
**COSY of 64d**

Cyclic Lysine – Glycine Mimic **64e****64e**

**<sup>1</sup>H NMR (DMSO-*d*<sub>6</sub>)** 9.20 (d, 1H, *J* = 8.0 Hz), 8.93 (t, 1H, *J* = 6.0), 7.93 (t, 1H, *J* = 6.0), 7.79 (d, 1H, *J* = 8.0 Hz), 7.77 (s, 1H), 7.67 (m, 1H), 7.56 (t, 1H, *J* = 8.0 Hz), 7.52 (d, 1H, *J* = 6.5 Hz), 7.38-7.27 (m, 5H), 7.27 (t, 1H, *J* = 6.0 Hz), 5.01 (s, 2H), 4.43 (dd, 1H, *J* = 15.5 Hz, 6.5 Hz), 4.35 (dd, 1H, *J* = 15.5 Hz, 9.0 Hz), 4.30 (dd, 1H, *J* = 15.5 Hz, 5.5 Hz), 3.93 (dd, 1H, *J* = 13.5 Hz, 7.0 Hz), 3.27 (dd, 1H, *J* = 13.5 Hz, 5.0 Hz), 3.01 (m, 2H), 1.63 (m, 2H), 1.42 (m, 2H), 1.28 (m, 2H);

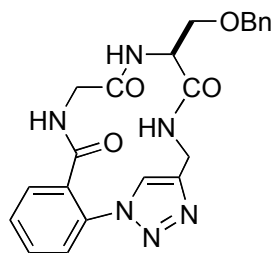
**MS (ESI, *m/z*)** 520 (M+H)<sup>+</sup>

**<sup>1</sup>H NMR of 64e**



COSY of 64e

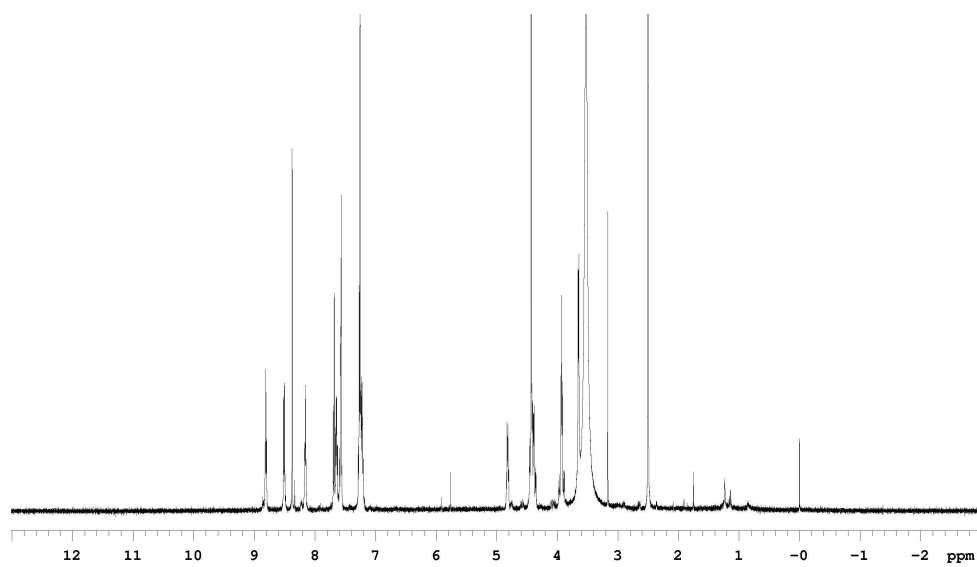
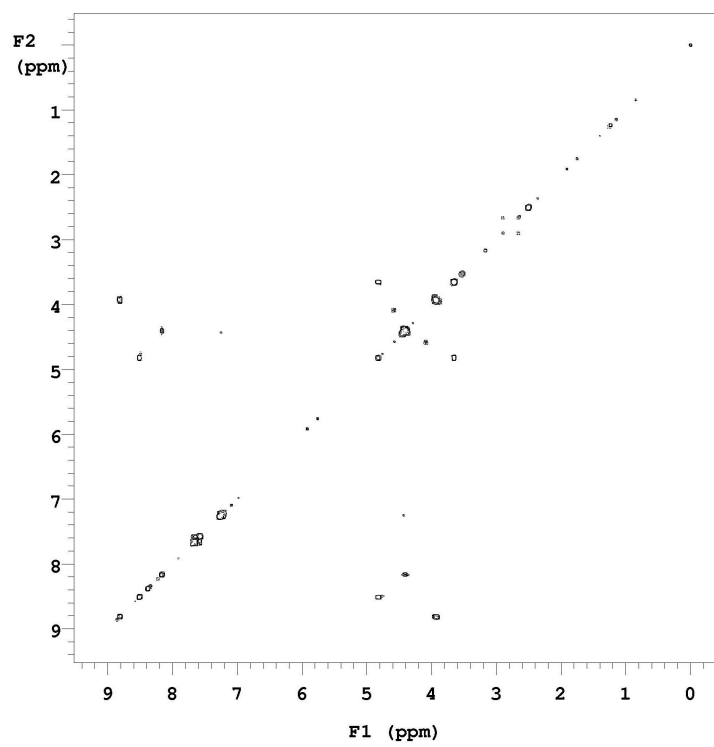
Cyclic Glycine – Serine Mimic **64f**



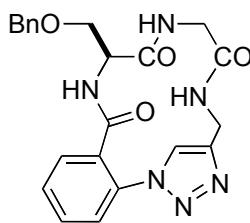
**64f**

$^1\text{H NMR}$  ( $\text{DMSO-}d_6$ ) 8.81 (t, 1H,  $J = 6.0$  Hz), 8.51 (d, 1H,  $J = 8.5$ ), 8.38 (s, 1H), 8.16 (t, 1H,  $J = 5.5$ ), 7.68 (d, 1H,  $J = 8.0$  Hz), 7.65 (m, 1H), 7.57 (m, 1H), 7.28-7.20 (m, 6H), 4.81 (dd, 1H,  $J = 12.0$  Hz, 6.0 Hz), 4.41 (m, 4H), 3.93 (m, 2H), 3.65 (d, 2H,  $J = 6.0$  Hz)

$\text{MS}$  ( $\text{ESI}$ ,  $m/z$ ) 457 ( $\text{M}+\text{H}$ ) $^+$

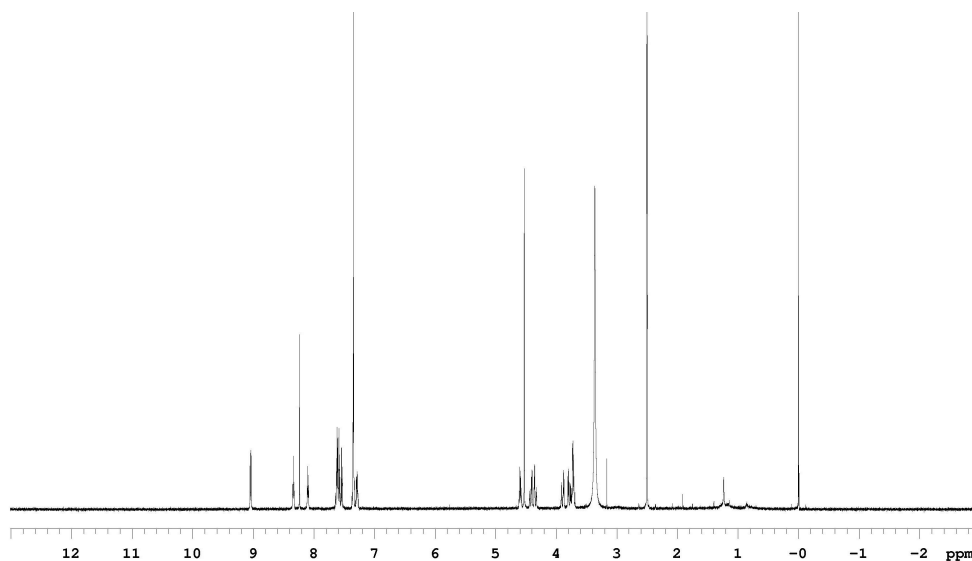
 **$^1\text{H}$  NMR of 64f****COSY of 64f**



Cyclic Serine – Glycine Mimic **64g****64g**

**<sup>1</sup>H NMR (DMSO-*d*<sub>6</sub>)** 9.04 (t, 1H, J = 7.5 Hz), 8.34 (t, 1H, J = 6.0 Hz), 8.24 (s, 1H), 8.10 (t, 1H, J = 6.0), 7.63 (m, 1H), 7.61 (m, 1H), 7.56 (m, 1H), 7.51 (m, 1H), 7.37-7.34 (m, 5H), 7.29 (m, 1H), 4.59 (dd, 1H, J = 12.5 Hz, 7.0 Hz), 4.53 (s, 2H), 4.41 (dd, 1H, J = 14.5 Hz, 5.0 Hz), 4.34 (dd, 1H, J = 16.0 Hz, 5.0 Hz), 3.89 (dd, 1H, J = 16.5, 6.0 Hz), 3.78 (dd, 1H, J = 16.5 Hz, 6.0 Hz), 3.72 (m, 2H)

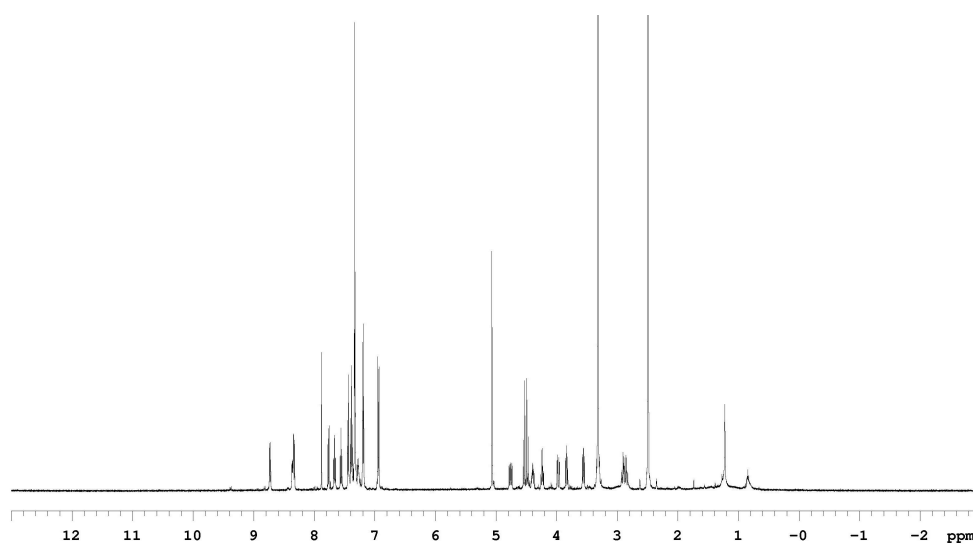
**MS (ESI, m/z)** 457 (M+Na)<sup>+</sup>

**<sup>1</sup>H NMR of 64g**

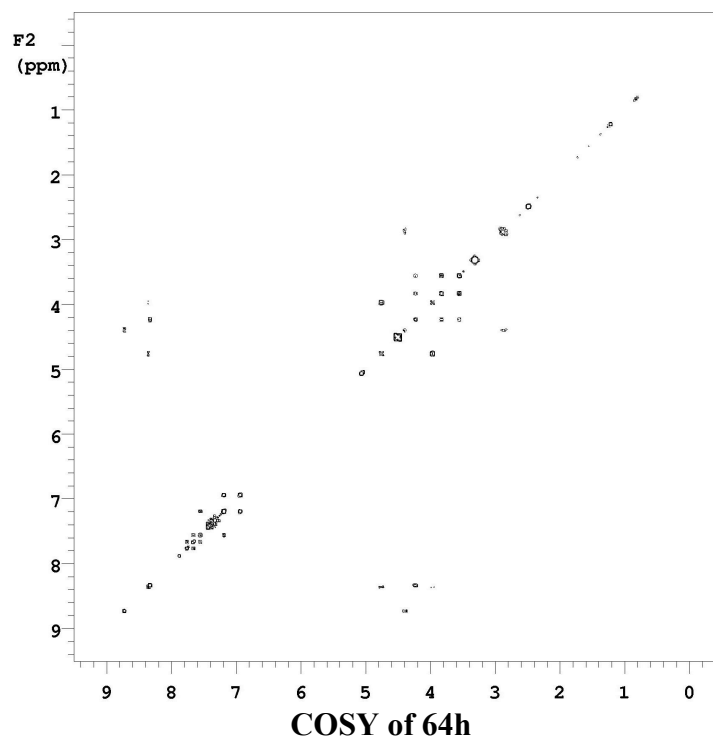


24.0 Hz, 7.0 Hz), 4.38 (m, 1H), 4.23 (dd, 1H,  $J = 15.5$  Hz, 7.5 Hz), 3.97 (dd, 1H,  $J = 15.5, 4.0$  Hz), 3.83 (dd, 1H,  $J = 9.5$  Hz, 8.0 Hz), 3.56 (dd, 1H,  $J = 9.5$  Hz, 7.5 Hz), 2.89 (m, 2H)

**MS (ESI, m/z) 631(M+H)<sup>+</sup>**



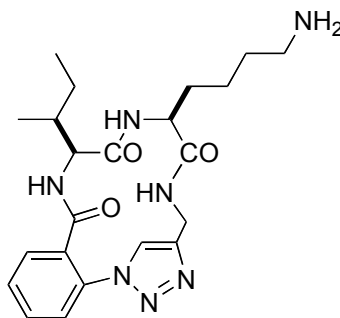
**<sup>1</sup>H NMR of 64h**



### General Procedure for Side Chain Deprotection

One molar equivalent of 10% Pd/C was added to a 10 ml methanol or ethanol solution of 5-10 mg cyclic compounds **64a-h**. The resulting suspension was stirred under 1 atm H<sub>2</sub> for 24 h and filtered with a pad of Celite. The solution was concentrated and dried under vacuum overnight to give **61a-h** as a white solid.

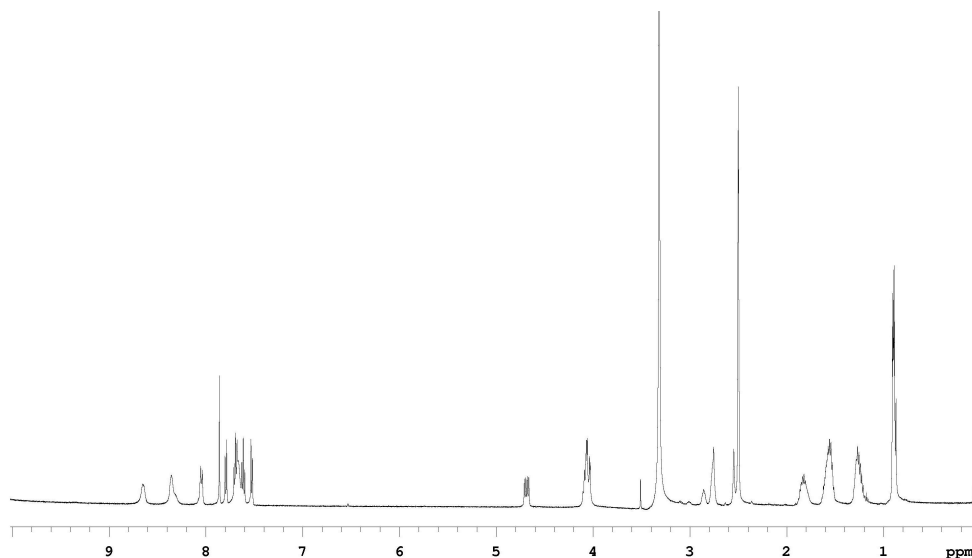
Deprotected Cyclic Isoleucine – Lysine Mimic **61a**.



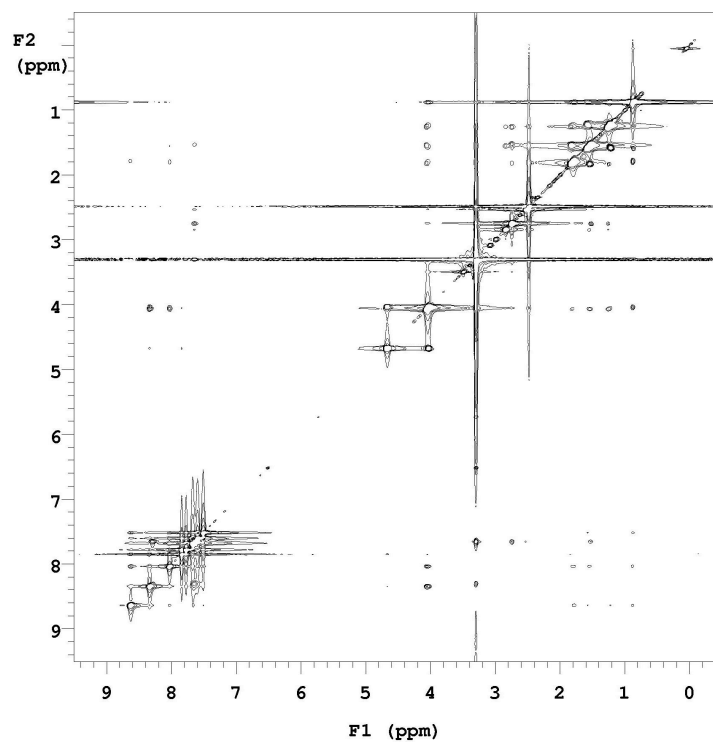
**61a**

<sup>1</sup>H NMR (DMSO-d<sub>6</sub>) 8.65 (d, 1H, J = 8.5 Hz), 8.35 (t, 1H, J = 7.0 Hz), 8.04 (d, 1H, J = 8.5 Hz), 7.85 (s, 1H), 7.78 (d, 1H, J = 7.5 Hz), 7.70 (b, 2H), 7.69 (m, 1H), 7.61 (m, 1H), 7.52 (dd, 1H, J = 7.5 Hz, 1.5 Hz), 4.67 (dd, 1H, J = 15.0 Hz, 7.5 Hz), 4.06 (m, 3H), 2.75 (m, 2H), 1.82 (m, 2H), 1.56 (m, 4H), 1.27 (m, 3H), 0.89 (m, 6H)

MS (ESI, m/z) 442 (M+H)<sup>+</sup>

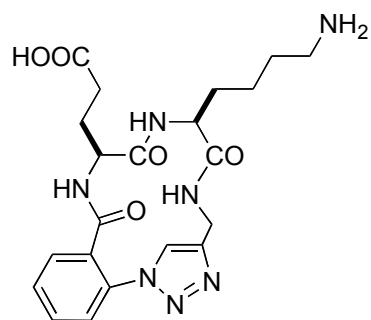


<sup>1</sup>H NMR of **61a**



**ROESY of 61a**

Deprotected Cyclic Glutamic Acid – Lysine Mimic **61b**

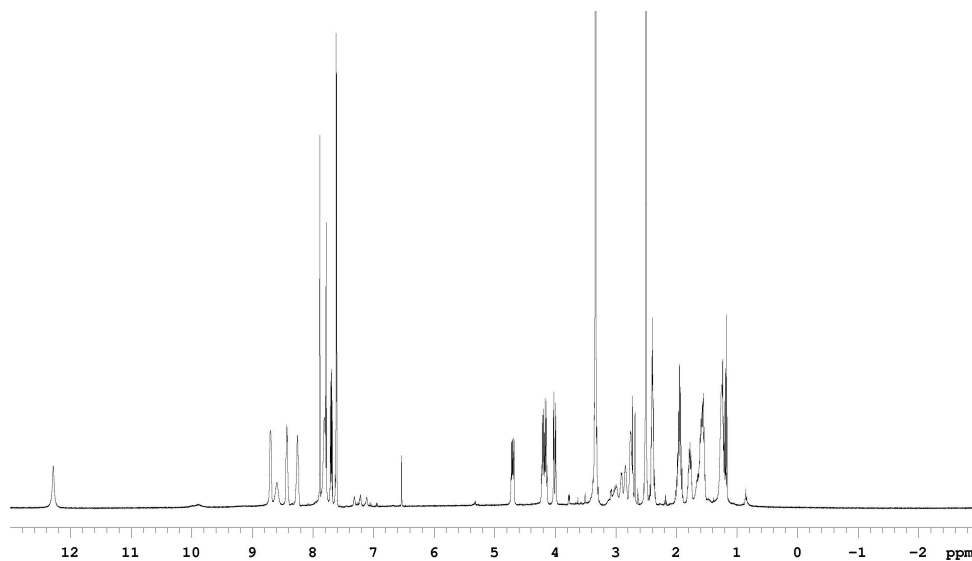


**61b**

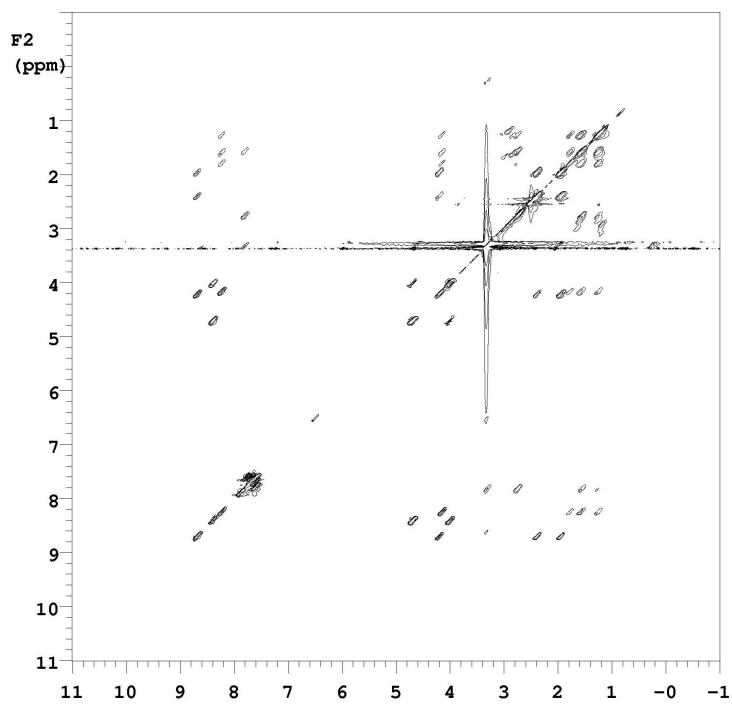
**<sup>1</sup>H NMR (DMSO-d<sub>6</sub>)** 12.28 (s, 1H), 8.69 (d, 1H, J = 8.0 Hz), 8.60 (b, 1H), 8.41 (q, 1H, J = 8.0 Hz, 4.5 Hz), 8.24 (d, 1H, J = 8.5 Hz), 7.89 (s, 1H), 7.81 (b, 1H), 7.78 (d, 1H, J = 8.0 Hz), 7.69 (m, 1H), 7.61 (d, 2H, J = 4.0 Hz), 4.70 (dd, 1H, J = 15.0 Hz, 8.0 Hz), 4.21 (dd, 1H, J = 15.0 Hz, 8.0 Hz), 4.16 (dd, 1H, J = 15.0 Hz, 8.5 Hz), 4.02 (dd, 1H, J = 15.5

Hz, 4.5 Hz), 2.73 (m, 2H), 2.41 (m, 2H), 1.96 (m, 2H), 1.78 (m, 1H), 1.61(m, 3H), 1.25 (m, 2H)

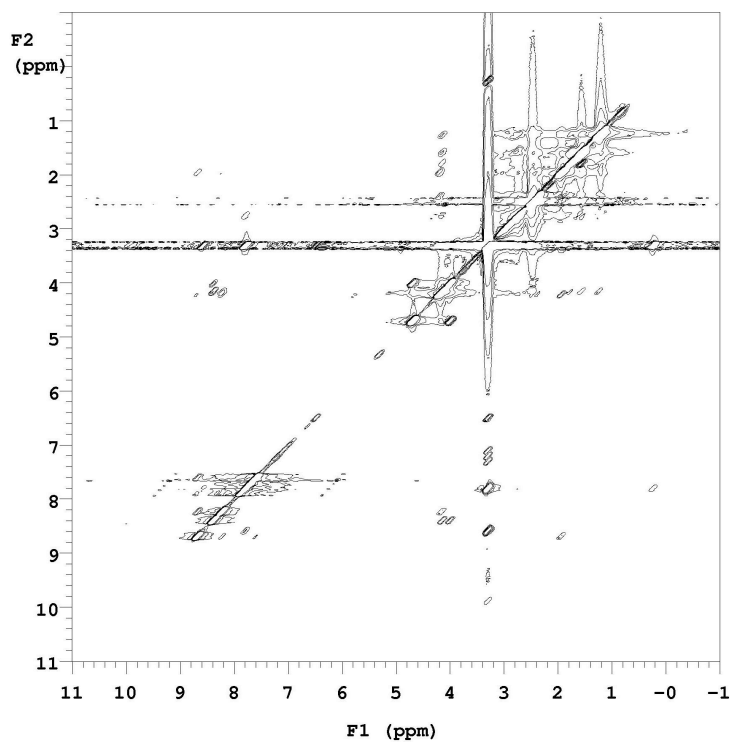
**MS (ESI, m/z) 458 (M+H)<sup>+</sup>**



**<sup>1</sup>H NMR of 61b**

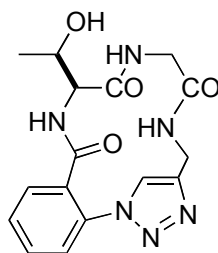


**TOCSY of 61b**



**ROESY of 61b**

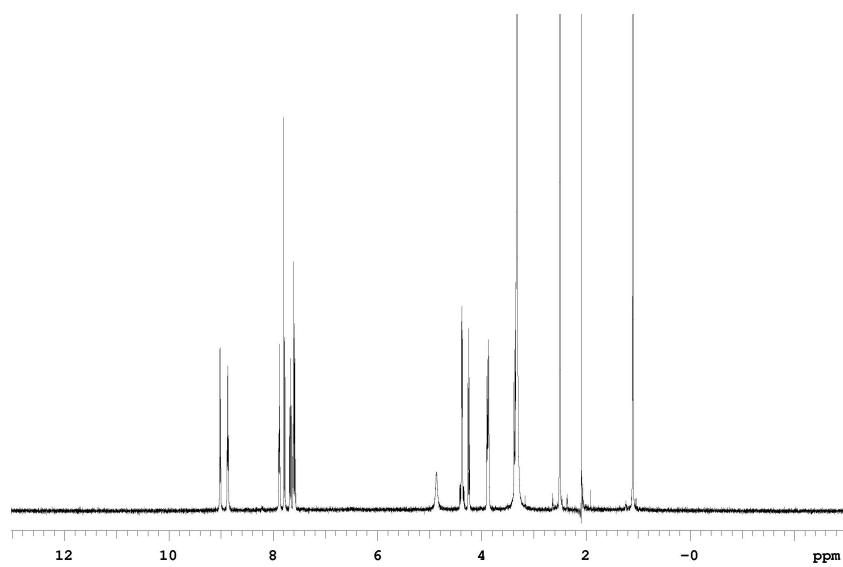
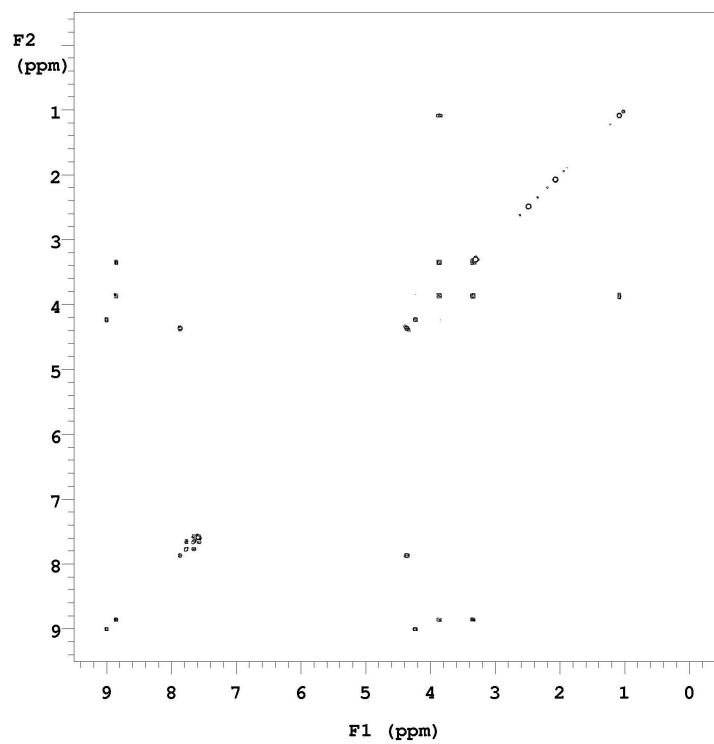
Deprotected Cyclic Threonine – Glycine Mimic **61c**



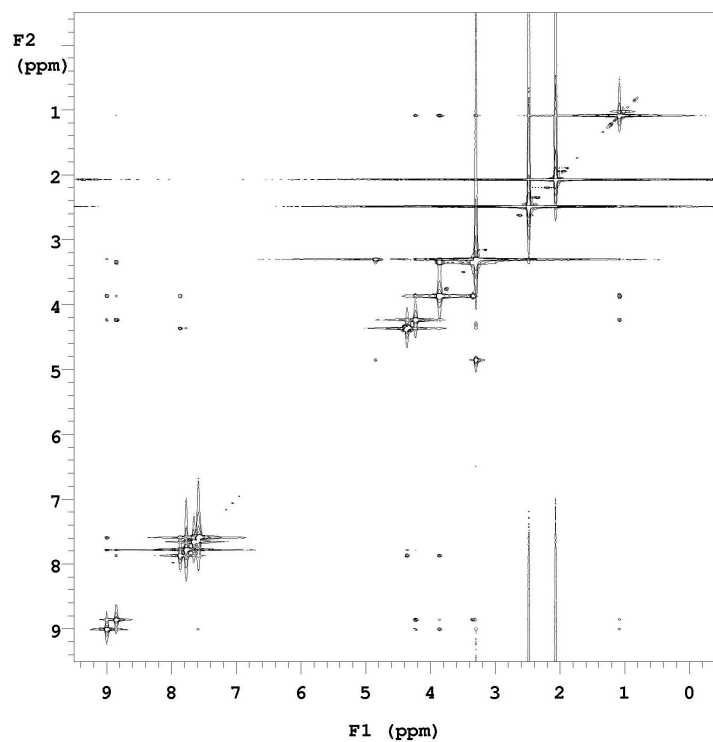
**61c**

$^1\text{H NMR}(\text{DMSO-}d_6)$  9.64 (d, 1H,  $J = 7.5$  Hz), 9.20 (t, 1H,  $J = 6.0$ ), 8.05 (t, 1H,  $J = 6.0$  Hz), 7.84 (s, 1H), 7.75 (d, 1H,  $J = 7.5$  Hz), 7.66 (m, 1H), 7.56 (m, 2H), 4.36 (m, 2H), 4.19 (t, 1H,  $J = 7.5$  Hz), 3.88 (dd, 1H,  $J = 14.0$  Hz, 6.5 Hz), 3.35 (dd, 1H,  $J = 14.0$  Hz, 6.5 Hz), 1.07 (d, 3H,  $J = 6.5$  Hz)

**MS (ESI,  $m/z$ )** 381 ( $M+\text{Na}$ ) $^+$

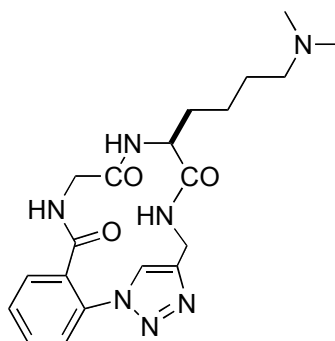
 **$^1\text{H}$  NMR of 61c****TOCSY of 61c**





ROESY of 61c

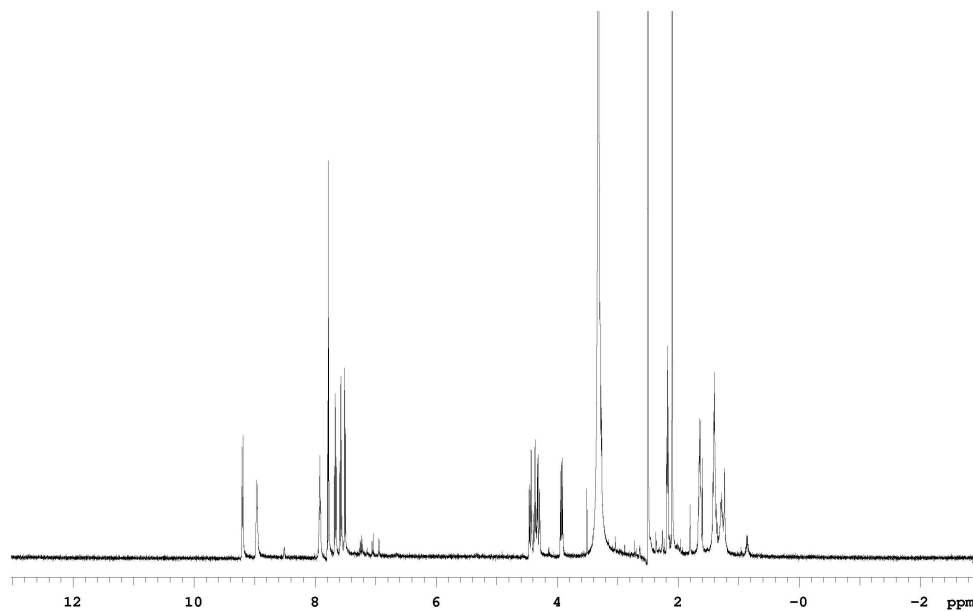
Deprotected Cyclic Glycine – Lysine Mimic **61d**

**61d**

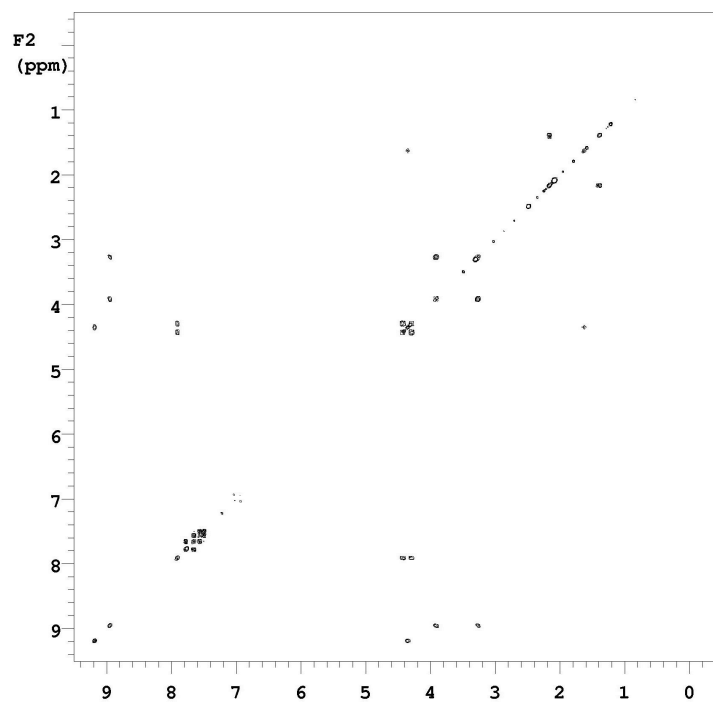
$^1\text{H NMR}$  (DMSO- $d_6$ ) 9.20 (d, 1H,  $J = 9.0$  Hz), 8.96 (t, 1H,  $J = 6.0$ ), 7.92 (t, 1H,  $J = 6.0$  Hz), 7.79 (d, 1H,  $J = 8.0$  Hz), 7.77 (s, 1H), 7.67 (m, 1H), 7.57 (m, 1H), 7.51 (dd, 1H,  $J = 7.5$  Hz, 1.5 Hz), 4.44 (dd, 1H,  $J = 15.5$  Hz, 6.5 Hz), 4.36 (dd, 1H,  $J = 16.0$  Hz, 8.0 Hz), 4.30 (dd, 1H,  $J = 15.5$  Hz, 6.0 Hz), 3.93 (dd, 1H,  $J = 13.5$  Hz, 7.0 Hz), 3.28 (dd, 1H,  $J =$

13.5 Hz, 4.5 Hz), 2.18 (t, 2H,  $J = 7.0$  Hz), 2.10 (s, 6H), 1.64 (m, 2H), 1.41 (m, 2H), 1.26 (m, 2H)

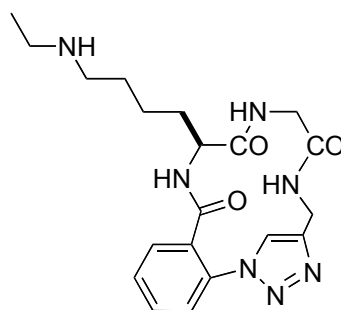
**MS (ESI,  $m/z$ ) 414 ( $M+H$ )<sup>+</sup>**



**<sup>1</sup>H NMR of 61d**



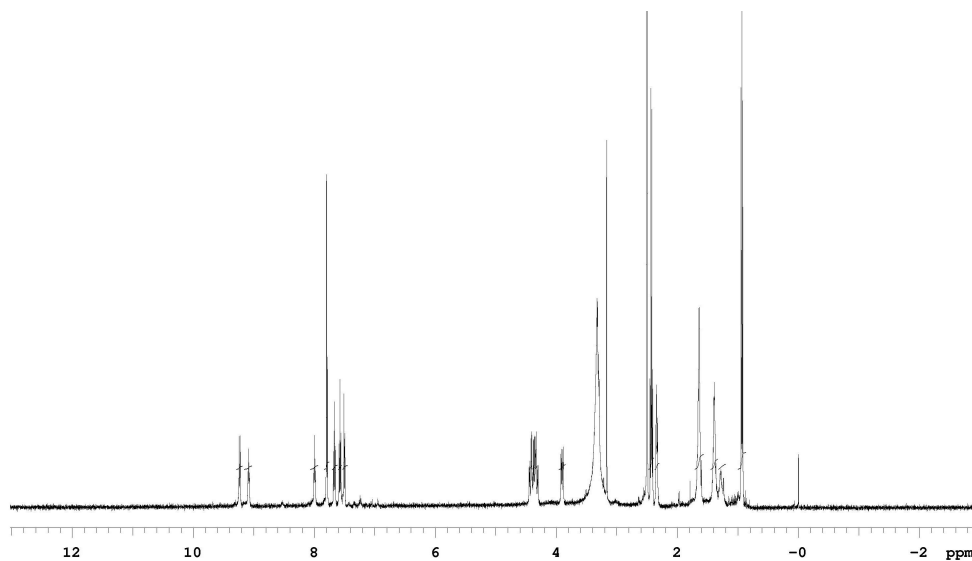
**COSY of 61d**

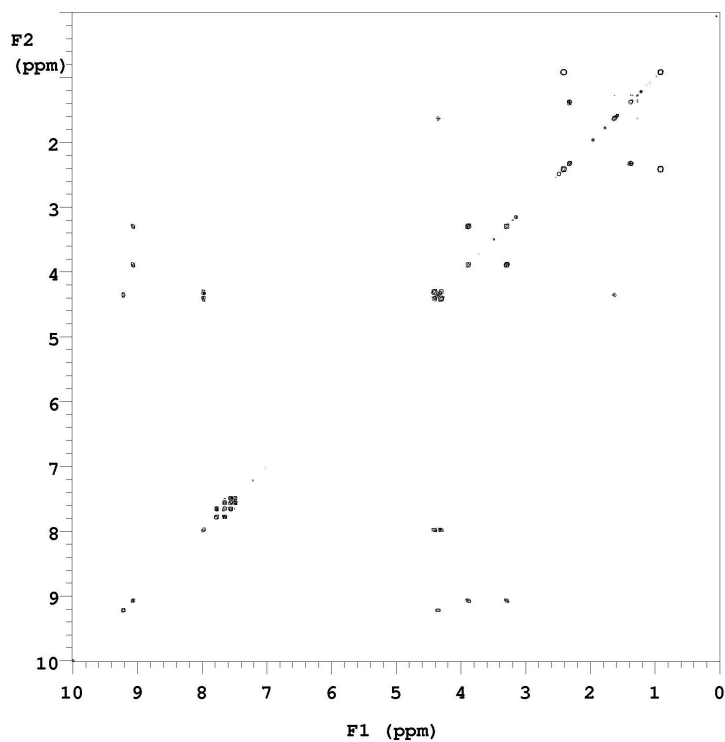
Deprotected Cyclic Lysine – Glycine Mimic **61e****61e**

Compound **64e** was deprotected from an ethanol solution.

**<sup>1</sup>H NMR (DMSO-*d*<sub>6</sub>)** 9.23 (t, 1H, *J* = 9.0 Hz), 9.10 (t, 1H, *J* = 6.0 Hz), 8.01 (t, 1H, *J* = 6.0 Hz), 7.79 (s, 1H), 7.77 (d, 1H, *J* = 8.5 Hz), 7.65 (t, 1H, *J* = 8.5 Hz), 7.56 (m, 1H), 7.56 (m, 1H), 7.48 (d, 1H, *J* = 6.0 Hz), 4.42 (dd, 1H, *J* = 15.5 Hz, 6.0 Hz), 4.36 (m, 1H), 4.30 (dd, 1H, *J* = 15.5 Hz, 6.0 Hz), 3.89 (m, 1H), 3.28 (m, 1H), 2.41 (q, 2H, *J* = 7.0 Hz), 2.32 (t, 2H, *J* = 7.0 Hz), 1.62 (m, 2H), 1.37 (m, 2H), 1.26 (m, 2H), 0.92 (t, 3H, *J* = 7.0 Hz)

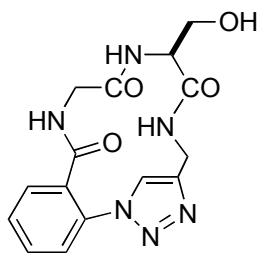
**MS (ESI, *m/z*)** 414 (M+H)<sup>+</sup>

**<sup>1</sup>H NMR of 61e**



**COSY of 61e**

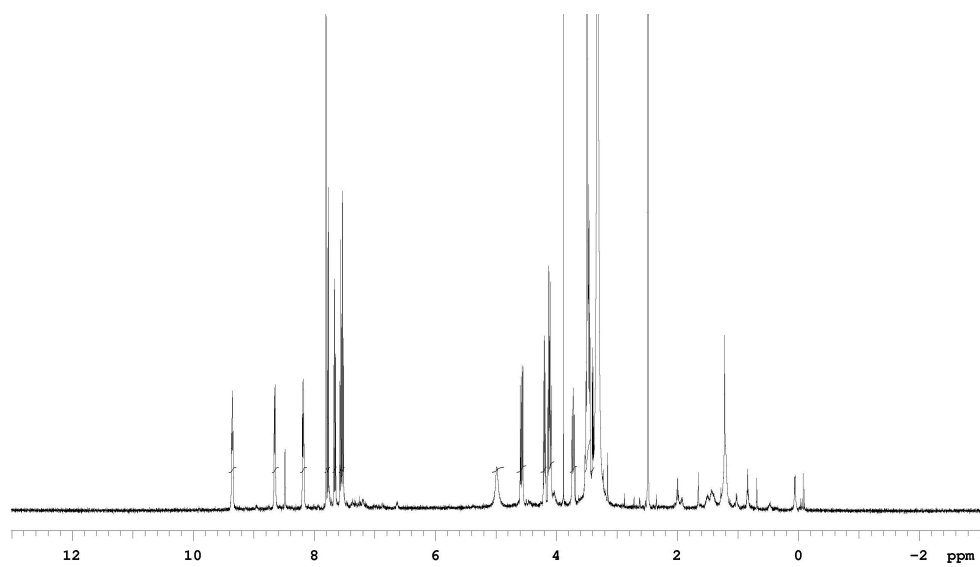
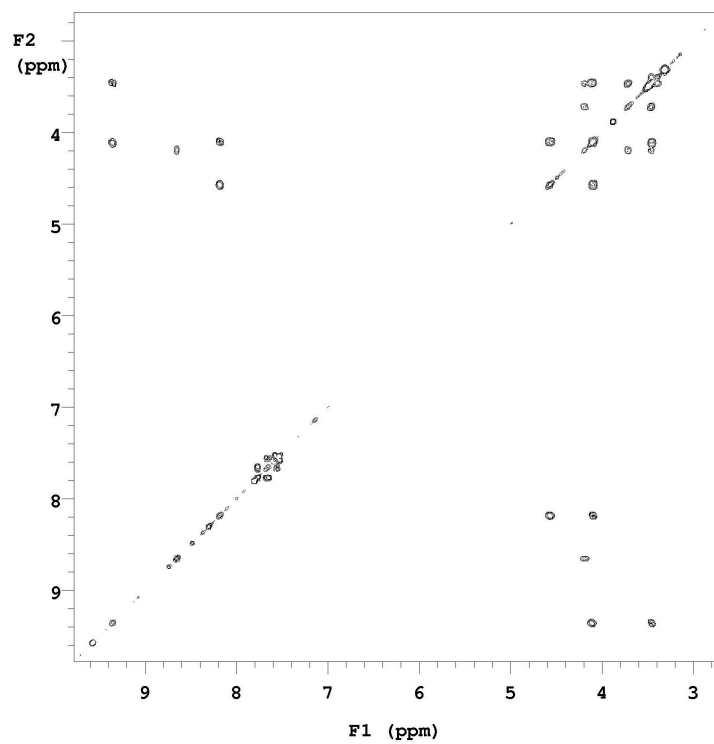
Deprotected Cyclic Glycine – Serine Mimic **61f**

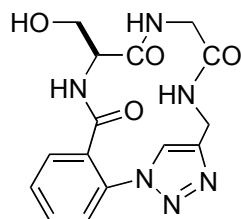


**61f**

**<sup>1</sup>H NMR (DMSO-*d*<sub>6</sub>)** 9.35 (t, 1H, *J* = 6.0 Hz), 8.65 (d, 1H, *J* = 7.5), 8.18 (dd, 1H, *J* = 7.5 Hz, 5.5 Hz), 7.81 (s, 1H), 7.77 (d, 1H, *J* = 7.5 Hz), 7.57 (dd, 1H, *J* = 7.5 Hz, 1.0 Hz), 7.53 (m, 1H), 4.98 (b, 1H), 4.57 (dd, 1H, *J* = 15.5 Hz, 7.0 Hz), 4.20 (dd, 1H, 14.0 Hz, 7.5 Hz), 4.11 (m, 2H), 3.71 (m, 1H)

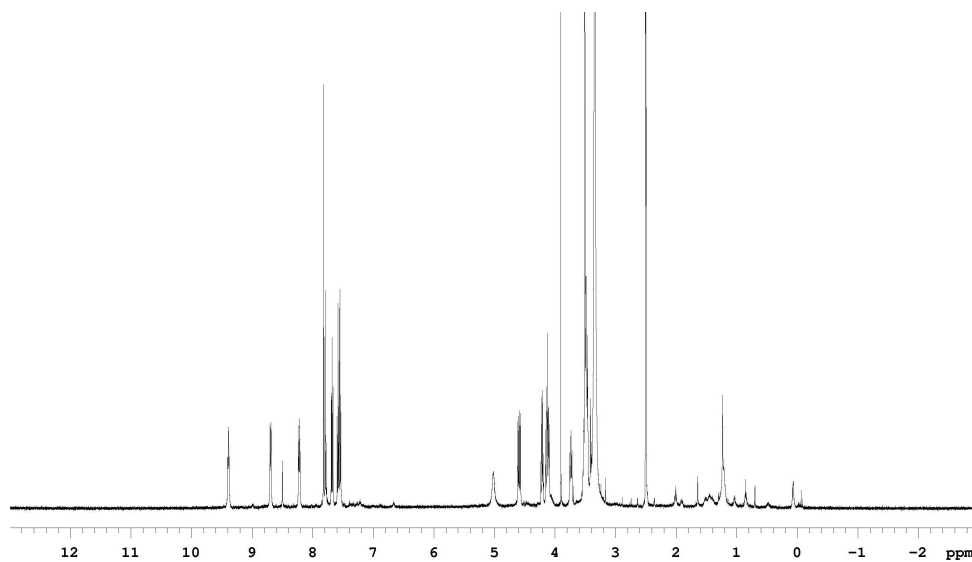
**MS (ESI, *m/z*)** 345 (M+H)<sup>+</sup>

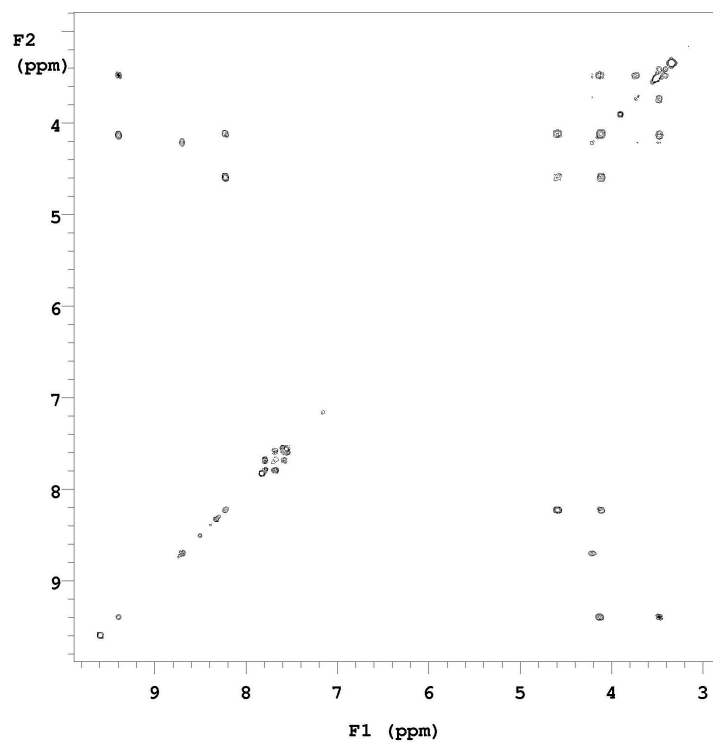
**<sup>1</sup>H NMR of 61f****COSY of 61f**

Deprotected Cyclic Serine – Glycine Mimic **61g****61g**

**<sup>1</sup>H NMR (DMSO-d<sub>6</sub>)** 9.39 (t, 1H, J = 6.0 Hz), 8.69 (d, 1H, J = 7.5), 8.22 (dd, 1H, J = 7.0 Hz, 5.0 Hz), 7.82 (s, 1H), 7.82 (dd, 1H, J = 7.5 Hz, 1.0 Hz), 7.67 (m, 1H), 7.58 (m, 1H), 7.54 (dd, 1H, J = 7.5, 1.5 Hz), 5.02 (b, 1H), 4.58 (dd, 1H, J = 15.5 Hz, 7.0 Hz), 4.21 (dd, 1H, 14.0 Hz, 7.5 Hz), 4.11 (m, 2H), 3.73 (m, 1H)

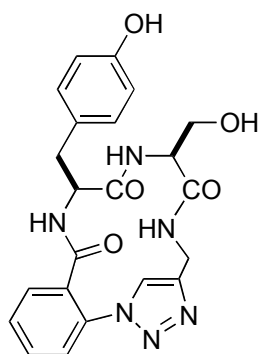
**MS (ESI, m/z)** 367 (M+Na)<sup>+</sup>

**<sup>1</sup>H NMR of 61g**



**COSY of 61g**

**Deprotected Cyclic Tyrosine – Serine Mimic 61h**

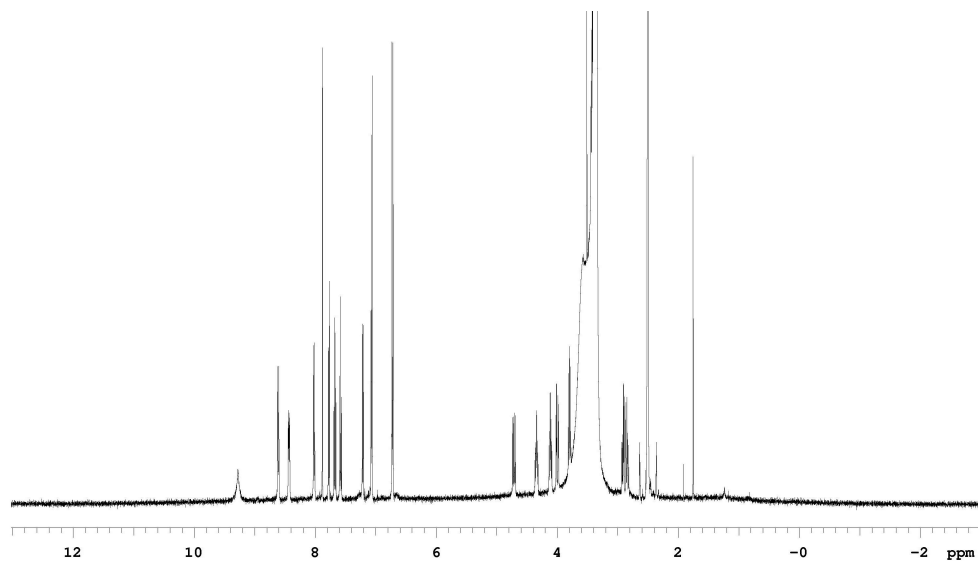


**61h**

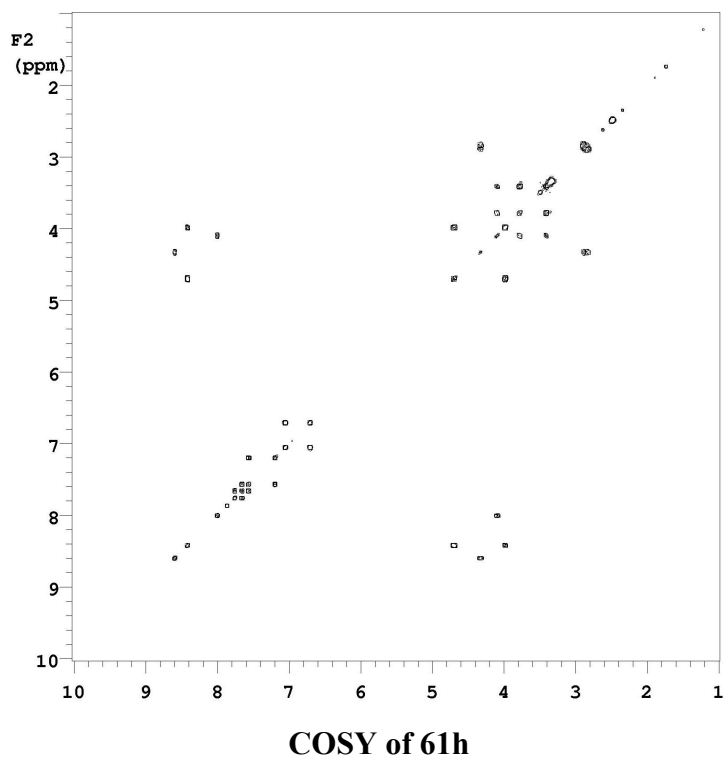
**$^1\text{H}$  NMR (DMSO- $d_6$ )** 9.28 (b, 1H), 8.61 (d, 1H,  $J = 8.5$  Hz), 8.43 (dd, 1H,  $J = 8.0$  Hz, 4.0 Hz), 8.01 (d, 1H,  $J = 9.0$  Hz), 7.88 (s, 1H), 7.77 (m, 1H), 7.67 (m, 1H), 7.57 (m, 1H), 7.21 (dd, 1H,  $J = 7.5$  Hz, 1.5 Hz), 7.06 (d, 2H,  $J = 7.5$  Hz), 6.73 (d, 2H,  $J = 7.5$  Hz), 7.71 (dd, 1H,  $J = 15.5$  Hz, 8.0 Hz), 4.34 (m, 1H), 4.10 (m, 1H), 4.00 (dd, 1H,  $J = 15.5$  Hz, 9.5

Hz), 3.79 (dd, 1H,  $J = 10.5$  Hz,  $8.5$  Hz), 2.91 (dd, 1H,  $J = 14.0$  Hz,  $6.0$  Hz), 2.84 (dd, 1H,  $J = 14.0$  Hz,  $9.5$  Hz)

**MS (ESI,  $m/z$ ) 473 ( $M+Na$ )<sup>+</sup>**

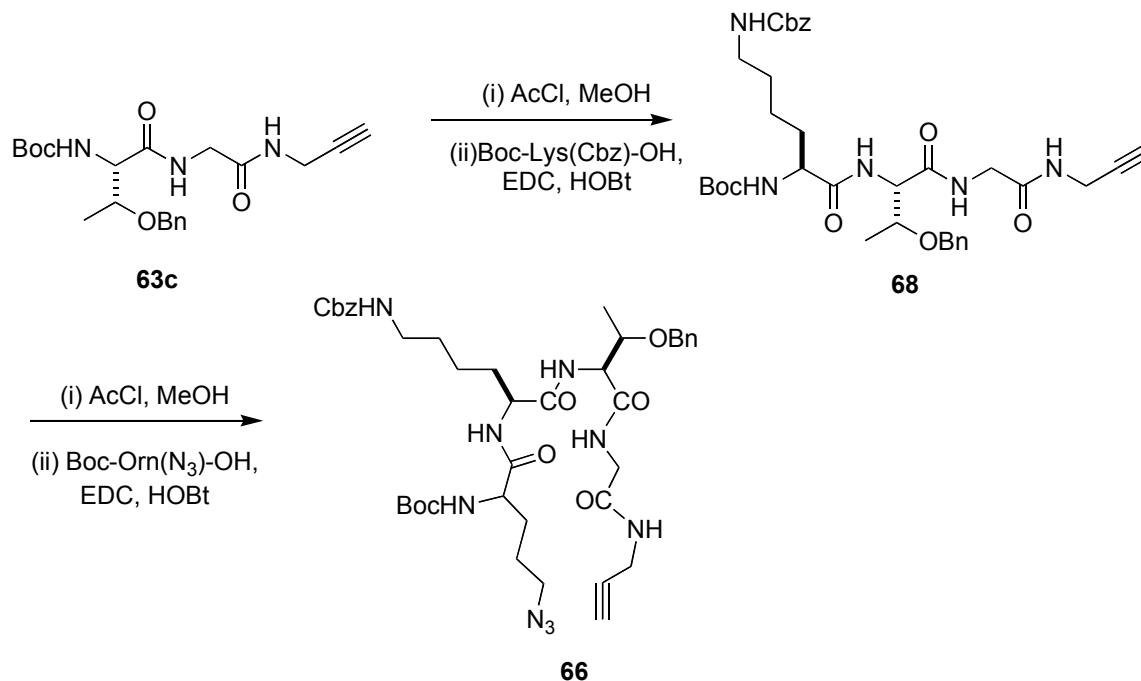


**<sup>1</sup>H NMR of 61h**





## Preparation of Compounds **66** and **67**

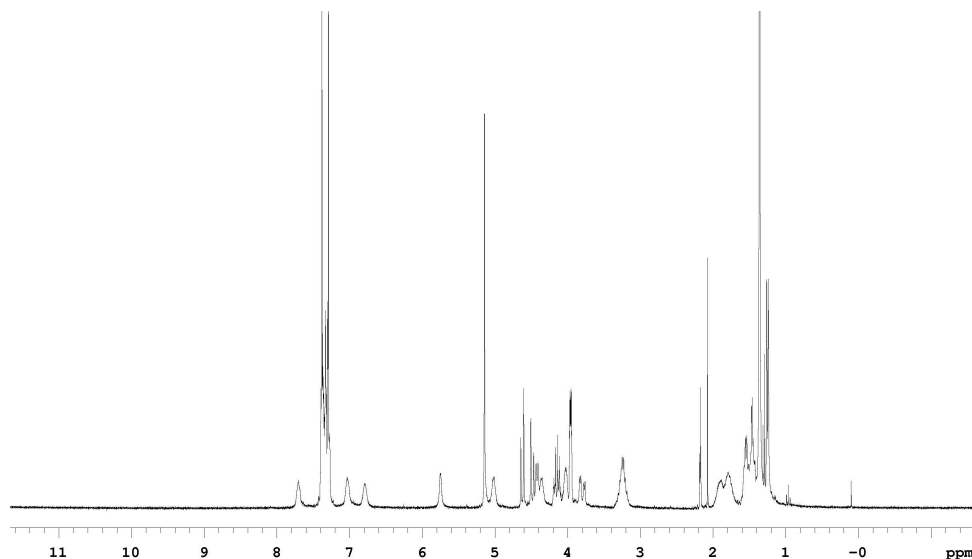


**Scheme A1.** Synthesis of Linear Lys-Thr-Gly Mimic.

Preparation of Lysine – Threonine – Glycine Derivative **68**. (Scheme A1) To a 5 ml solution of **63c** (0.5 mmol, 0.20 g) in 20:1 EtOAc/MeOH was added AcCl (2.5 mmol, 0.17 ml, 5 equiv) dropwise and the resulting mixture was stirred at 0 °C for 2 h in a sealed flask, then warmed to room temperature for another 2h. Solvent was removed and the residue was used without further purification. To a suspension of the above residue (1 equiv) in 10 ml dry CH<sub>2</sub>Cl<sub>2</sub> was added Boc-Lys(Cbz)-OH (0.55 mmol, 0.21 g, 1.1 equiv.) followed by addition of NEt<sub>3</sub> (1.25 mmol, 0.14 ml, 2.5 equiv), HOBT (0.55 mmol, 0.07 g, 1.1 equiv) and EDC (0.55 mmol, 0.11 g, 1.1 equiv). The resulting suspension was stirred at room temperature for 4 h. EtOAc (20 ml) was added to the reaction and extracted with 5% HCl, H<sub>2</sub>O, 5% Na<sub>2</sub>CO<sub>3</sub> and brine. The organic layer was dried with Na<sub>2</sub>SO<sub>4</sub> and concentrated to dryness. Recrystallization with EtOAc and hexanes provided 0.15 g (45%) **68** as a white solid.

<sup>1</sup>H NMR (CDCl<sub>3</sub>) 7.70 (s, 1H), 7.39-7.28 (m, 10H), 7.03 (s, 1H), 6.79 (s, 1H), 5.75 (s, 1H), 5.14 (s, 2H), 5.01 (s, 1H), 4.56 (dd, 2H, J = 41.1 Hz, 11.7 Hz), 4.42 (d, 1H, J = 7.5

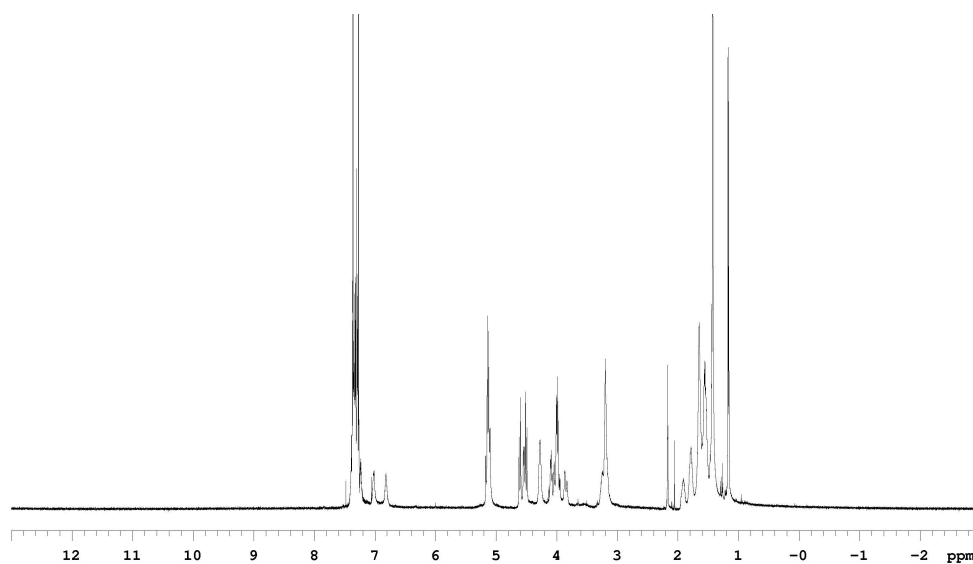
Hz), 4.35 (m, 1H), 4.14 (t, 1H,  $J = 7.2$  Hz), 4.03 (m, 1H), 3.96 (m, 2H), 3.80 (m, 1H), 3.23 (m, 2H), 2.18 (t, 1H,  $J = 2.6$  Hz), 1.93-1.43 (m, 6H), 1.36 (s, 9H), 1.25 (d, 3H,  $J = 6.6$  Hz)



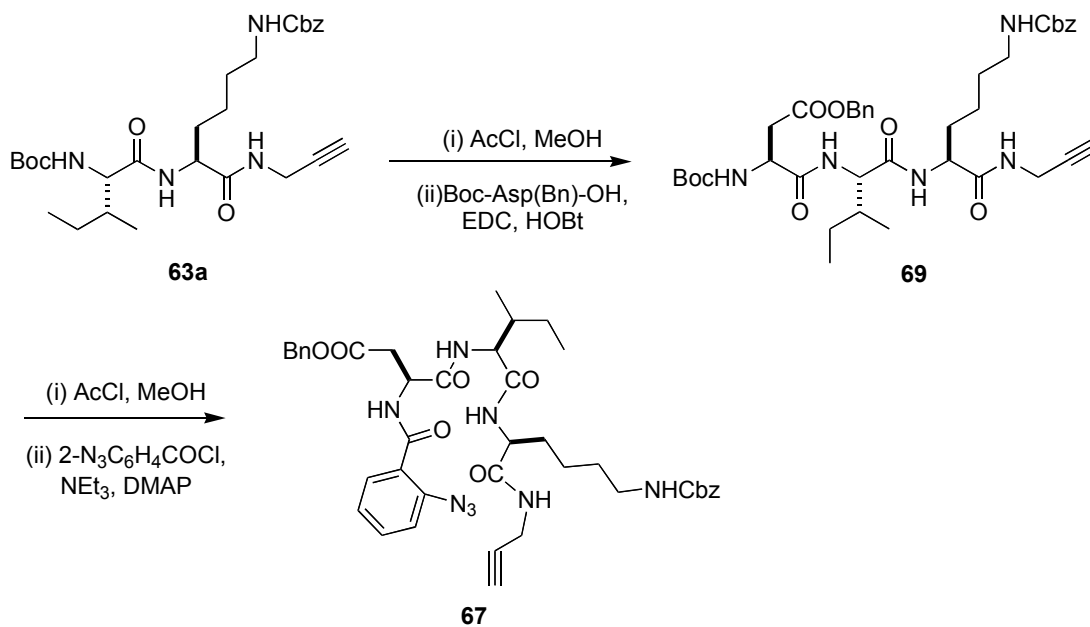
### <sup>1</sup>H NMR of **68**

Preparation of Linear Lysine – Threonine – Glycine Mimic **66**. To a 3 ml solution of **68** (0.23 mmol, 0.15 g) in 20:1 EtOAc/MeOH was added AcCl (1.1 mmol, 0.08 ml, 5 equiv) dropwise and the resulting mixture was stirred at 0 °C for 2 h in a sealed flask, then warmed to room temperature for another 2h. Solvent was removed and the residue was used without further purification. To a suspension of the above residue (1 equiv) in 10 ml dry CH<sub>2</sub>Cl<sub>2</sub> was added (0.39 mmol, 0.10 g, 1.1 equiv.) of N-  -Boc protected ornithine azide (prepared from required amine via azido transfer using TfN<sub>3</sub>, see Lundquist, J. T.; Pelletier, J. C. *Org. Lett.* **2001**, 3, 781-783) followed by addition of NEt<sub>3</sub> (0.68 mmol, 0.1 ml, 2.5 equiv), HOBt (0.39 mmol, 0.05 g, 1.1 equiv) and EDC (0.39 mmol, 0.07 g, 1.1 equiv). The resulting suspension (0.075 M) was stirred at room temperature for 4 h. EtOAc was added to the reaction and extracted with 5% HCl, H<sub>2</sub>O, 5% Na<sub>2</sub>CO<sub>3</sub> and brine. The organic layer was dried with Na<sub>2</sub>SO<sub>4</sub> and concentrated to dryness. Recrystallization with EtOAc and hexanes provided 0.15 g (83%) **66** as a slightly yellow solid.

**$^1\text{H NMR}$  ( $\text{CDCl}_3$ )** 7.39-7.22 (m, 10H), 7.21 (s, 1H), 7.01 (s, 1H), 6.82 (s, 1H), 5.13 (dd, 2H,  $J = 14.1$  Hz, 7.5 Hz), 4.56 (dd, 2H,  $J = 31.8$  Hz, 7.2 Hz), 4.52 (m, 1H), 4.27 (m, 2H), 4.07 (m, 2H), 3.99 (m, 2H), 3.85 (m, 1H), 3.24 (m, 4H), 2.17 (t, 1H,  $J = 1.5$  Hz), 1.91-1.54 (m, 10 H), 1.44 (s, 9H), 1.16 (d, 3H,  $J = 3.9$  Hz)  
**MS (ESI,  $m/z$ )** 806 ( $\text{M}+\text{H}$ )<sup>+</sup>



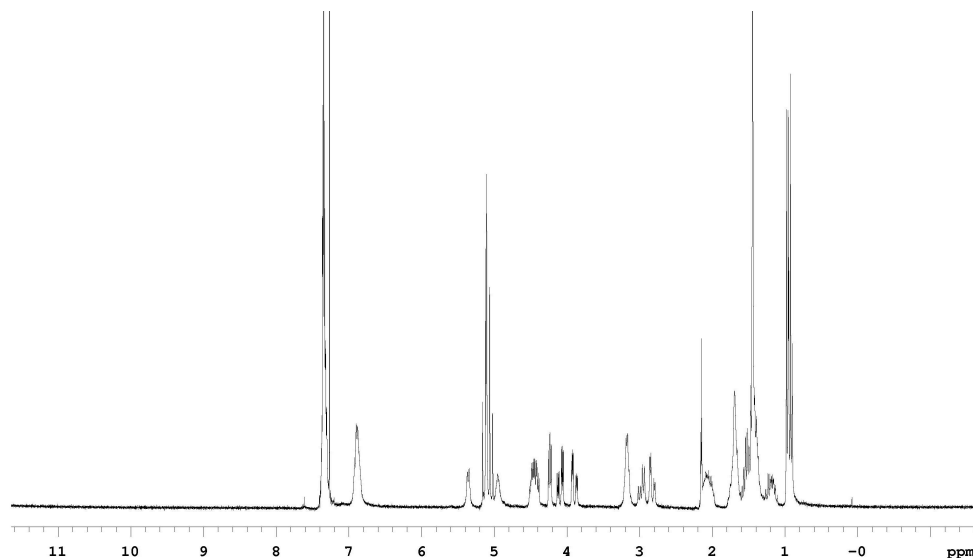
**$^1\text{H NMR}$  of 66**



**Scheme A2.** Synthesis of Linear Asp-Ile-Lys Mimic.

Preparation of Aspartic acid – Isoleucine – Lysine Derivative **69**. (Scheme A2) To a 5 ml solution of **63a** (1.0 mmol, 0.48 g) in 20:1 EtOAc/MeOH was added AcCl (5.0mmol, 0.34 ml, 5 equiv) dropwise and the resulting mixture was stirred at 0 °C for 2 h in a sealed flask, then warmed to room temperature for another 2h. Solvent was removed and the residue was used without further purification. To a suspension of the above residue (1 equiv) in 20 ml dry CH<sub>2</sub>Cl<sub>2</sub> was added Boc-Asp(Bn)-OH (1.1 mmol, 0.36 g, 1.1 equiv.) followed by addition of NEt<sub>3</sub> (2.5 mmol, 0.27 ml, 2.5 equiv), HOBt (1.1 mmol, 0.15 g, 1.1 equiv) and EDC (1.1 mmol, 0.21 g, 1.1 equiv). The resulting suspension was stirred at room temperature for 4 h. EtOAc (40 ml) was added to the reaction and extracted with 5% HCl, H<sub>2</sub>O, 5% Na<sub>2</sub>CO<sub>3</sub> and brine. The organic layer was dried with Na<sub>2</sub>SO<sub>4</sub> and concentrated to dryness. Recrystallization with EtOAc and hexanes provided 0.68 g (97%) **69** as a white solid.

<sup>1</sup>H NMR (CDCl<sub>3</sub>) 7.39-7.31 (m, 10H), 6.90 (m, 3H), 5.35 (d, 1H, J = 7.2 Hz), 5.12 (s, 2H), 5.09 (dd, 2H, J = 23.4 Hz, 6.0 Hz), 4.95 (m, 1H), 4.43 (m, 2H), 4.23 (dd, 1H, J = 6.5 Hz, 5.0 Hz), 4.10 (m, 1H), 3.90 (m, 1H), 3.18 (m, 2H), 2.86 (m, 2H), 2.15 (t, 1H, J = 2.6 Hz), 2.05 (m, 2H), 1.69 (m, 4H), 1.56 (m, 2H), 1.45 (s, 9H), 1.17 (m, 1H), 0.95 (m, 6H)



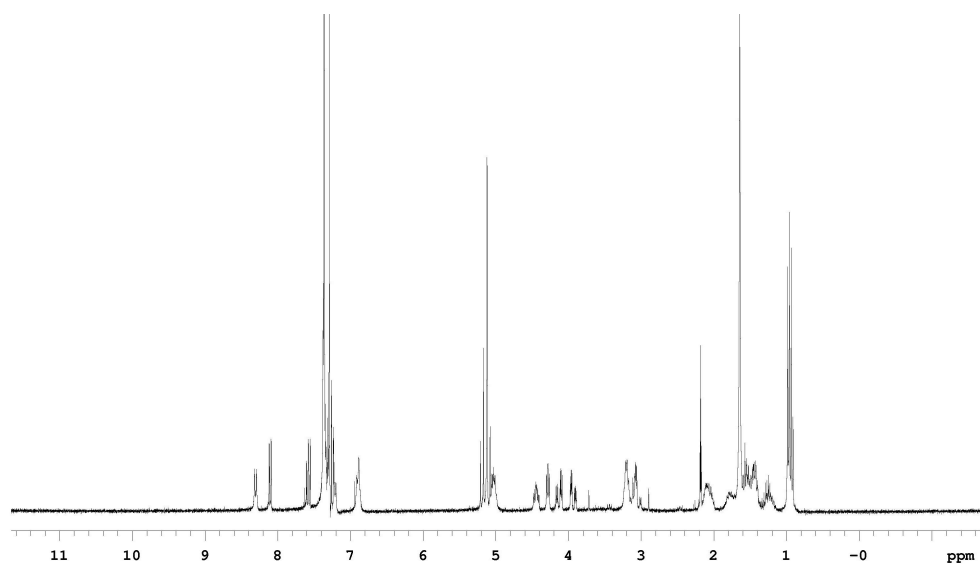
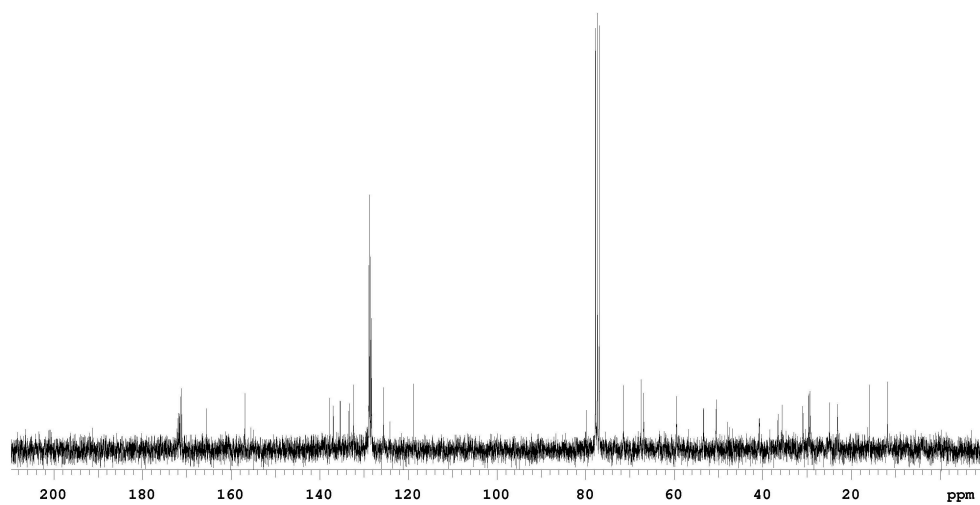
<sup>1</sup>H NMR of **69**

Preparation of Linear Aspartic Acid – Isoleucine – Lysine Mimic **67**. To a 5 ml solution of **69** (0.5 mmol, 0.34g) in 20:1 EtOAc/MeOH was added AcCl (2.5 mmol, 0.18 ml, 5 equiv) dropwise and the resulting mixture was stirred at 0 °C for 2 h in a sealed flask, then warmed to room temperature for another 2h. Solvent was removed and the residue was used without further purification. Triethylamine (1.3 mmol, 0.17 ml, 2.5 equiv) was added to a solution of deprotected **69** (1 equiv) in 5 ml dry THF. The resulting mixture was stirred for 10 min and treated with DMAP (0.35 mmol, 0.04 g, 0.7 equiv). Freshly prepared 2-azido-benzoyl chloride (from 1 equiv.of 2-azidobenzoic acid) in 1 ml dry THF was added dropwise to the solution and the resulting mixture was stirred for 2h at room temperature. The reaction mixture was poured into ice water and the white precipitate was filtered with a fine frit funnel and rinsed with small portions of water three times. The precipitate was dried under vacuum and recrystallized with EtOAc and hexanes afforded 0.32 g (86%) **67** as a slightly yellow solid.

**<sup>1</sup>H NMR (CDCl<sub>3</sub>)** 8.30 (d, 1H, J = 7.8 Hz), 8.10 (dd, 1H, J = 7.8 Hz, 1.5 Hz), 7.58 (m, 1H), 7.40-7.31 (m, 10H), 7.22 (m, 2H), 6.91 (m, 2H), 5.17 (m, 4H), 5.01 (m, 1H), 4.46 (m, 1H), 4.28 (dd, 1H, J = 6.3 Hz, 4.8 Hz), 4.13 (m, 1H), 3.92 (m, 1H), 3.19 (m, 2H), 3.01 (m, 2H), 2.18 (t, 1H, J = 2.7 Hz), 2.07 (m, 2H), 1.76 (m, 2H), 1.53 (m, 2H), 1.43 (m, 2H), 1.27 (m, 1H), 0.96 (m, 6H)

**<sup>13</sup>C NMR (CDCl<sub>3</sub>)** 172.0, 171.9, 171.5, 171.1, 165.5, 156.9, 137.7, 136.9, 135.4, 133.3, 132.3, 128.9, 128.7, 128.5, 128.3, 128.1, 125.6, 123.3, 118.8, 79.8, 71.5, 67.5, 66.8, 59.4, 53.3, 50.5, 40.7, 36.5, 35.6, 30.9, 29.6, 29.3, 24.9, 23.1, 15.9, 11.9

**MS (ESI, m/z)** 781 (M+H)<sup>+</sup>

 $^1\text{H}$  NMR of 67 $^{13}\text{C}$  NMR of 67

## Conformational Analyses of Compounds 61a, 61b and 61c

**NMR studies.** NMR spectra recorded for conformation analyses of compounds **61a**, **61b** and **61c** were conducted on an Inova500 spectrometer. Proton NMR assignments were made via COSY, TOCSY and ROESY experiments. The concentration of each sample was approximately 4mM in DMSO- $d_6$  throughout. Temperature coefficients of amide protons were measured via several 1D experiments in the range of 25-55 °C adjusted in 5 °C increments with an equilibration time of approximately 30 min after successive temperature steps. H/D exchange data was measured via addition of 10  $\mu$ l of CD<sub>3</sub>OD to the DMSO solution. H/D exchange data was recorded at 25 °C.

Through-bond connectivities were elucidated by COSY and TOCSY, and through-space interactions were identified by ROESY spectra. ROESY experiments were performed using mixing times of 100, 200 and 300 ms; normally a mixing time of 300 ms was superior. The intensities of ROESY cross peaks were assigned as strong, medium, weak and/or not obs. (not observed) from the magnitude of their volume integrals.

**CD studies.** CD measurements were obtained on an Aviv (Model 202 DS) spectrometer. For these experiments the cyclic peptidomimetics were dissolved in 80:20 water/methanol (v:v) ( $c = 0.1$  mg/ml, 0.1 cm path length). The CD spectra were recorded at 25 °C.

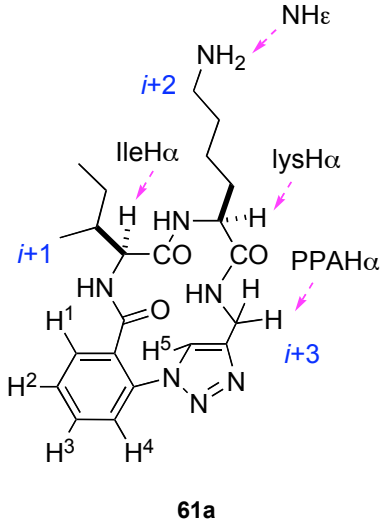
**Molecular simulations.** QUANTA2000 (Molecular Simulations Inc.) was used to build the residue topologies files (RTF) for all the peptidomimetics. Quenched molecular Dynamics simulations were performed using CHARMM standard parameters. All three molecules were modeled in a dielectric continuum of 45 (simulating DMSO). The starting conformers were minimized using 1000 steps of steepest descent and 3000 steps of the Adopted Basis Newton-Pophson method. The minimized structures were subjected to heating, equilibration and dynamic simulation. Throughout, SHAKE was used to constrain all bond lengths containing polar hydrogens. Each molecule was heated to 1000 K over 10 ps and equilibrated at 1000 K for another 10 ps, and then molecular dynamics were performed for a total time of 600 ps with trajectories saved per ps. The resulting 600 structures were minimized and about 100 structures were selected for further analysis.

QUANTA2000 was used again to classify the selected structures in conformational groups. The grouping method was based on calculation of RMS deviation of a subset of ring backbone atoms. The lowest energy conformer from each family was considered as the typical representative. Inter-proton distance and dihedral angles of the lowest energy conformer from each family were calculated for comparison with the ROE data.



### Conformational Studies of Compound 61a

**Table A1.** Important Chemical Shifts and Coupling Constants of Compound **61a**.

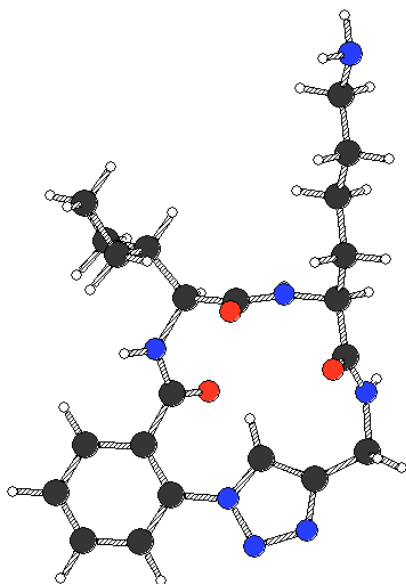
	sequence	proton	$\delta$ (ppm)	J (Hz)
 <p style="text-align: center;"><b>61a</b></p>	<b>Ile</b>	<u>NH</u>	8.65(d)	8.5
		<u>CaH</u>	4.06(m)	
<b>Lys</b>	<u>NH</u>	8.04(d)	8.5	
	<u>CaH</u>	4.06(m)		
<b>PPA</b>	<u>NH</u>	7.70(b)		
	NH	8.35(t)	7.0	
	CH	4.67(dd)	15.0, 7.0	
<b>Ar</b>	CH	4.06(m)		
	H <sup>1</sup>	7.52(dd)	7.5, 1.5	
	H <sup>2</sup>	7.61(m)		
	H <sup>3</sup>	7.69(m)		
	H <sup>4</sup>	7.78(d)	7.5	
		H <sup>5</sup>	7.85(s)	

\* PPA: propargyl amine derived fragment

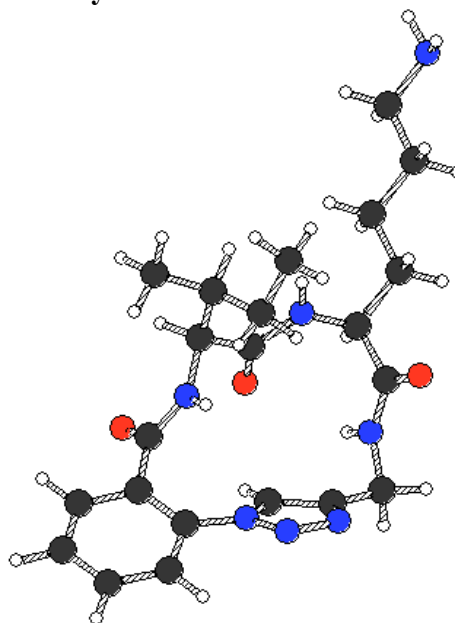
**Table A2.** Data From Conformational Analysis of Peptidomimetics **61a**.

<b>QMD Data</b>					
Residue		dihedral angles for lowest energy conformers (degrees)			
		family 1	family 2	family 3	family 4
<b>Ile</b>	$\Phi$	-81.09	-84.44	67.18	69.75
	$\Psi$	121	-121.2	-99.91	114.6
<b>Lys</b>	$\Phi$	62.1	-77.74	-101.5	62.58
	$\Psi$	84.57	92.39	105.1	63.13
number in family		17	28	61	3
Lowest energy conformer (kcal·mol <sup>-1</sup> )		30.1002	30.5227	30.5442	31.9028
CO <sub>i</sub> – NH <sub>i+3</sub> distance (Å)		4.252	5.114	4.912	5.984
<b>Fit of Lowest Conformers with NMR Data</b>					
contracts/characteristic	ROE intensity	calc. dist. from QMD (Å)			
		family 1	family 2	family 3	family 4
(Ile)NH – (Aryl)H <sup>1</sup>	medium	2.318	4.052	2.338	4.012
(Ile)NH – (Lys)NH	medium	4.436	3.822	4.293	3.700
(Ile)C <sub>α</sub> H – (Lys)NH	strong	2.069	3.313	3.501	2.066
(Lys)NH – (PPA)NH	weak	3.212	4.108	4.205	2.755
(Aryl)H <sup>5</sup> – (PPA)NH	strong	3.458	2.943	3.009	3.800
(Aryl)H <sup>5</sup> – (Aryl)H <sup>4</sup>	weak	4.556	4.558	4.564	4.605
(Aryl)H <sup>5</sup> – (Ile)NH	strong	3.446	3.158	3.405	3.107
		<sup>3</sup> J <sub>obs</sub> (Hz)	<sup>3</sup> J <sub>calc</sub> (Hz)		
(Ile) C <sub>α</sub> H – NH	8.5	6.9	7.3	6.9	6.7
(Lys) C <sub>α</sub> H – NH	8.5	6.9	6.4	9.0	6.9
(PPA) C <sub>α</sub> H – NH	7.0	5.8	6.1	6.9	4.3

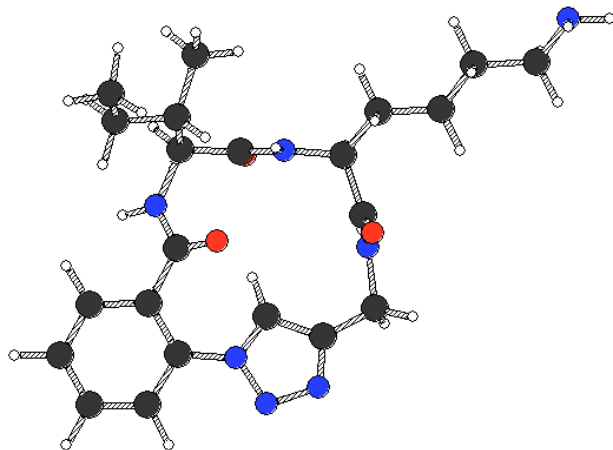
family 1



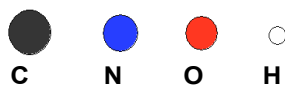
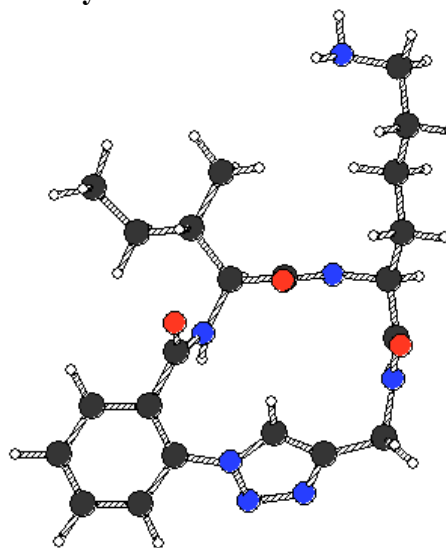
family 2



family 3



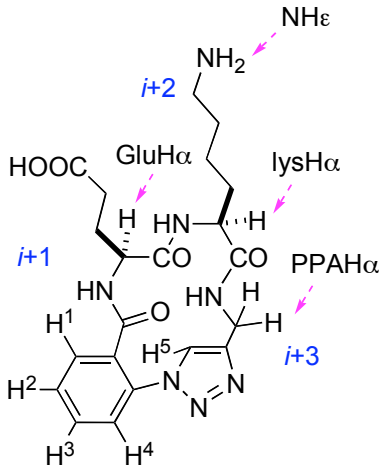
family 4



**Figure A1.** Backbone Conformation of the Lowest Energy Structures for Compound 61a.

### Conformational Studies of Compound 61b

**Table A3.** Important Chemical Shifts and Coupling Constants of Compound **61b**.

	sequence	proton	$\delta$ (ppm)	J (Hz)
 <p style="text-align: center;"><b>61b</b></p>	<b>Glu</b>	NH	8.69(d)	8.0
		CaH	4.21(dd)	15.0, 8.0
		COOH	12.28(b)	
<b>Lys</b>		NH	8.24(d)	8.5
		CaH	4.16(dd)	15.5, 8.5
		NH	8.60(b), 7.81(b)	
<b>PPA</b>		NH	8.41(dd)	8.0, 4.5
		CH	4.70(dd)	15.0, 8.0
		CH	4.02(dd)	15.0, 4.5
<b>Ar</b>		H <sup>1</sup>	7.61(d)	4.0
		H <sup>2</sup>	7.61(d)	4.0
		H <sup>3</sup>	7.69(m)	
		H <sup>4</sup>	7.78(d)	8.0
		H <sup>5</sup>	7.89(s)	

\* PPA: propargyl amine derived fragment

**Table A4.** Data From Conformational Analysis of Peptidomimetics **61b**.

<b>QMD Data</b>					
Residue		dihedral angles for lowest energy conformers (degrees)			
		family 1	family 2	family 3	family 4
<b>Glu</b>	$\Phi$	-140.3	-96.25	-65.35	70.45
	$\Psi$	123.8	106.8	-74.63	114.3
<b>Lys</b>	$\Phi$	59.79	71.97	-96.95	61.09
	$\Psi$	58.88	-83.17	94.64	64.91
number in family		61	25	21	3
Lowest energy conformer (kcal·mol <sup>-1</sup> )		27.9018	28.0635	28.1124	29.3325
CO <sub>i</sub> – NH <sub>i+3</sub> distance (Å)		5.175	5.669	4.441	6.024
<b>Fit of Lowest Conformers with NMR Data</b>					
contracts/characteristic	ROE intensity	calc. dist. from QMD (Å)			
		family 1	family 2	family 3	family 4
(Glu)NH – (Aryl)H <sup>1</sup>	strong	4.081	3.899	2.530	3.999
(Glu)NH – (Lys)NH	strong	4.159	4.225	3.026	3.687
(Glu)C <sub>α</sub> H – (Lys)NH	medium	2.071	2.088	3.583	2.079
(Lys)NH – (PPA)NH	weak	2.764	4.063	4.101	2.813
(Aryl)H <sup>5</sup> – (PPA)NH	medium	2.907	3.672	3.274	3.832
(Aryl)H <sup>5</sup> – (Aryl)H <sup>4</sup>	weak	4.579	4.612	4.548	4.067
(Aryl)H <sup>5</sup> – (Glu)NH	medium	3.065	3.229	3.166	3.129
		<sup>3</sup> J <sub>obs</sub> (Hz)	<sup>3</sup> J <sub>calc</sub> (Hz)		
(Glu) C <sub>α</sub> H – NH	8.0	8.9	8.5	4.8	7.0
(Lys) C <sub>α</sub> H – NH	8.5	5.9	6.7	8.6	5.9
(PPA) C <sub>α</sub> H – NH	7.5	6.0	7.7	6.2	4.3

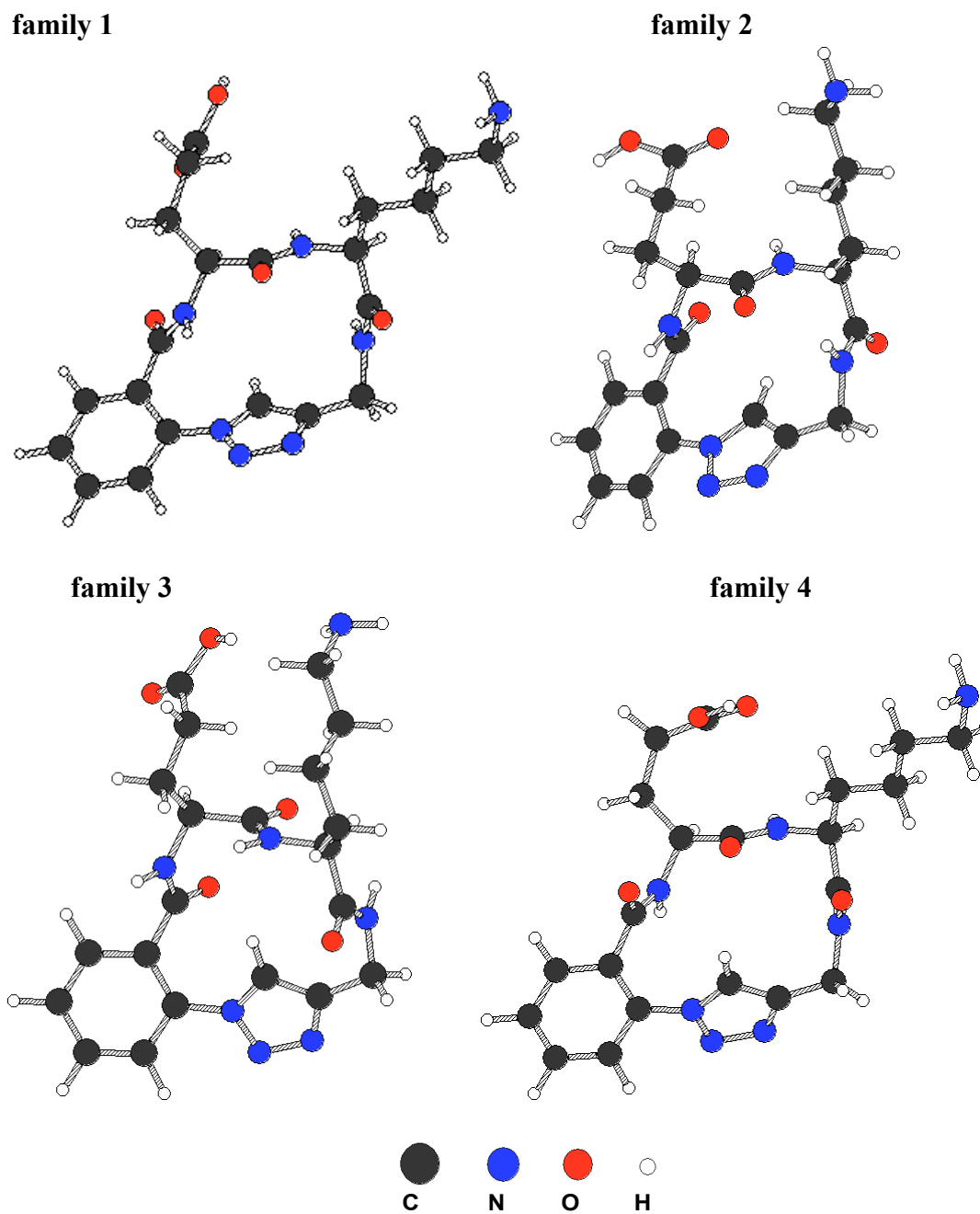


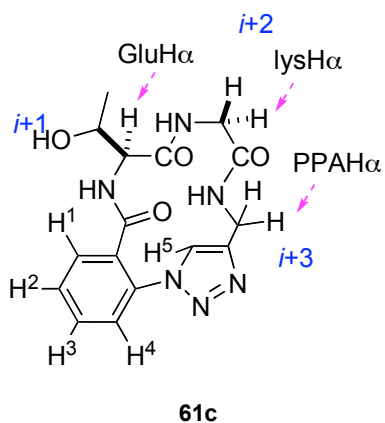
**Figure A2.** Backbone Conformation of the Lowest Energy Structures for Compound 61b.

### Conformational Studies of Compound 61c

**Table A5.** Important Chemical Shifts and Coupling Constants of Compound **61c**.

	sequence	proton	$\delta$ (ppm)	J (Hz)
	<b>Thr</b>	NH	9.64(d)	7.5
		CaH	4.19(t)	7.5
	<b>Gly</b>	NH	8.05(t)	6.5
		CaH <sup>1</sup>	3.88(dd)	14.0, 6.5
		CaH <sup>2</sup>	3.35(dd)	14.0, 6.5
	<b>PPA</b>	NH	9.20(t)	6.0
		CaH <sup>1</sup>	4.36(m)	
		CaH <sup>2</sup>	4.36(m)	
	<b>Ar</b>	H <sup>1</sup>	7.56(m)	
		H <sup>2</sup>	7.56(m)	
		H <sup>3</sup>	7.66(m)	
		H <sup>4</sup>	7.75(d)	7.5
		H <sup>5</sup>	7.84(s)	

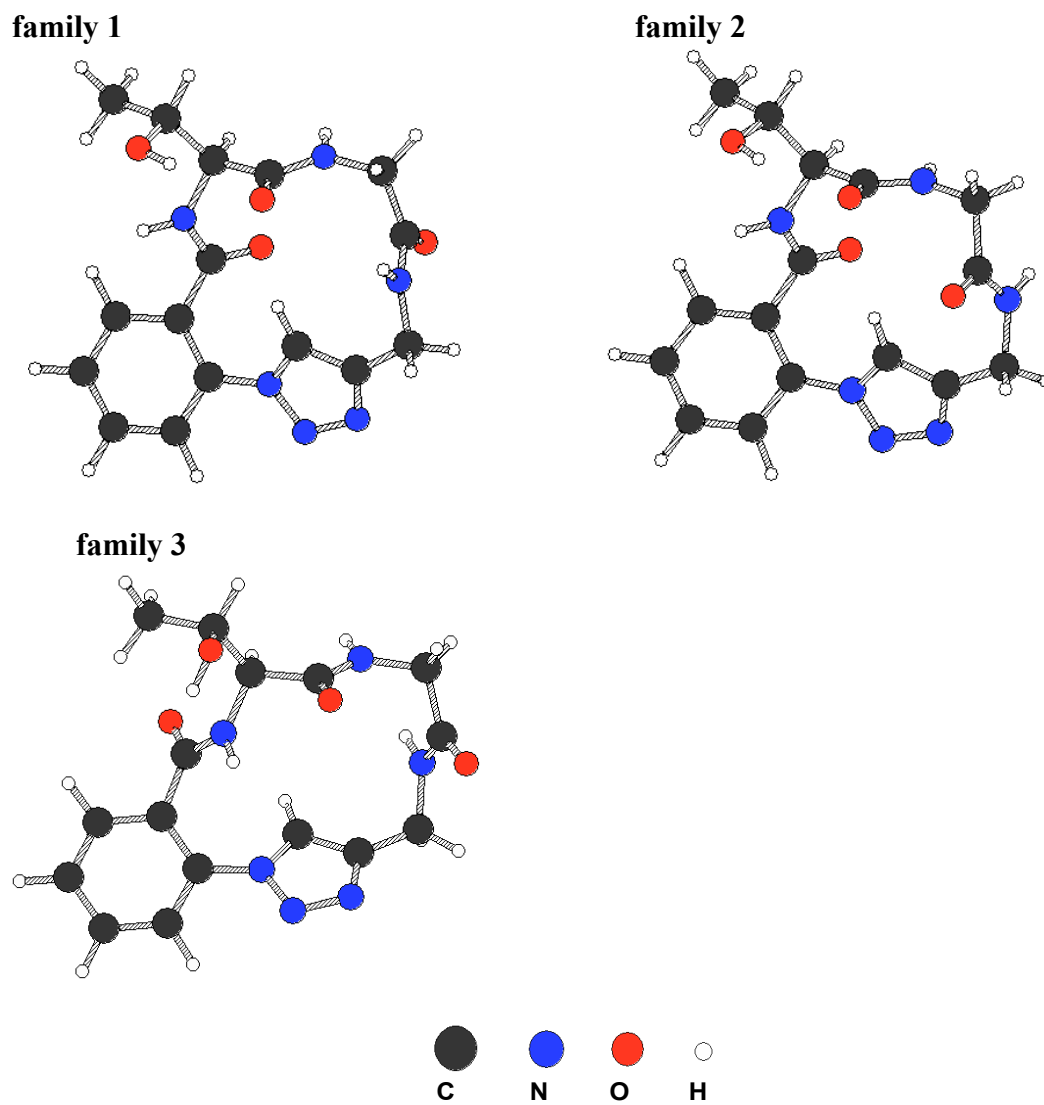
\* PPA: propargyl amine derived fragment



**Table A6.** Data From Conformational Analysis of Peptidomimetics **61c**.

<b>QMD Data</b>				
Residue		dihedral angles for lowest energy conformers (degrees)		
		family 1	family 2	family 3
<b>Thr</b>	$\Phi$	-71.12	-82.16	-140.3
	$\Psi$	117.60	108.0	120.7
<b>Gly</b>	$\Phi$	87.73	74.73	68.21
	$\Psi$	-106.6	85.20	53.58
number in family		33	55	11
Lowest energy conformer (kcal·mol <sup>-1</sup> )		31.8227	32.2123	32.4951
CO <sub>i</sub> – NH <sub>i+3</sub> distance (Å)		4.979	4.274	5.107
<b>Fit of Lowest Conformers with NMR Data</b>				
contracts/characteristic	ROE intensity	calc. dist. from QMD (Å)		
		family 1	family 2	family 3
(Thr)NH – (Aryl)H1	strong	2.373	2.316	4.040
(Thr)NH – (Gly)NH	weak	4.462	4.317	4.413
(Thr)CaH – (Gly)NH	strong	2.104	2.119	2.090
(Gly)NH – (PPA)NH	weak	4.299	3.107	2.595
(Aryl)H5 – (PPA)NH	medium	2.999	3.486	2.959
(Aryl)H5 – (Aryl)H4	not obs.	4.551	4.557	5.597
(Aryl)H5 – (Thr)NH	medium	3.379	3.445	3.096
		3Jobs (Hz)	3Jcalc (Hz)	
(Thr) C <sub>α</sub> H – NH	7.5	6.5	7.1	6.0
(Gly) C <sub>α</sub> H – NH	6.0	5.7	5.7	5.6
(PPA) C <sub>α</sub> H – NH	6.5	6.8	8.9	6.9



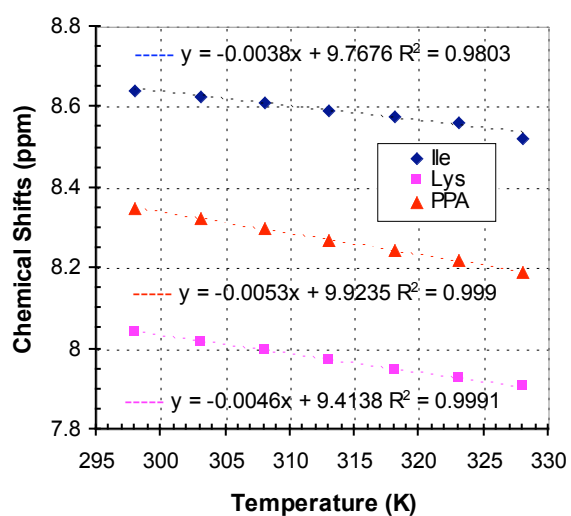
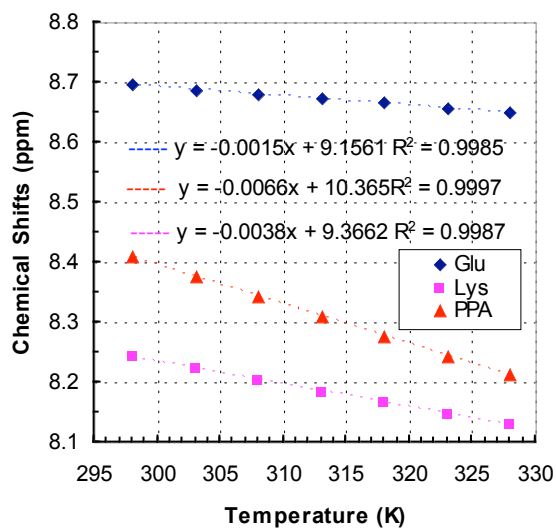


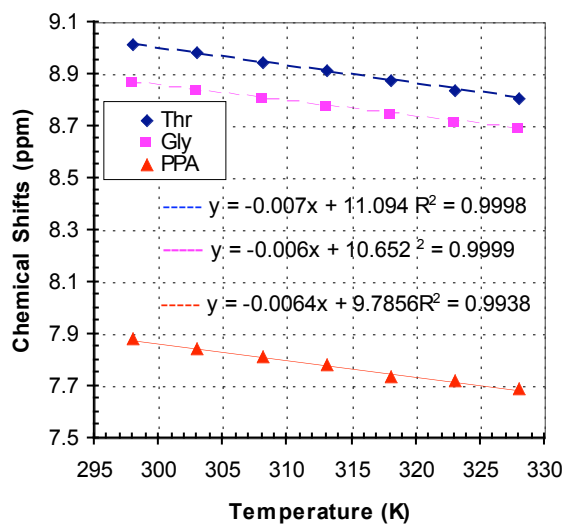
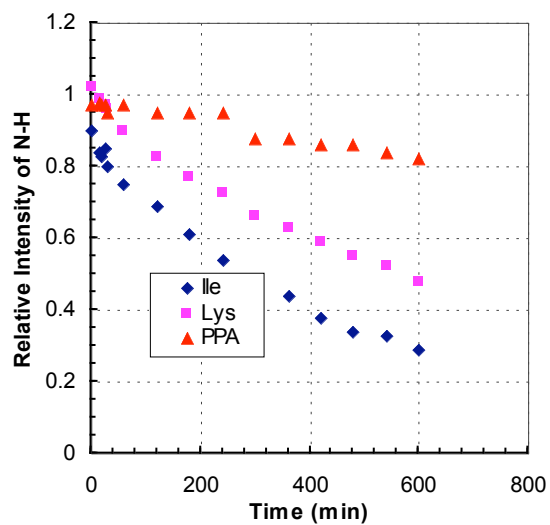
**Figure A3.** Backbone Conformation of the Lowest Energy Structures for Compound 61c.

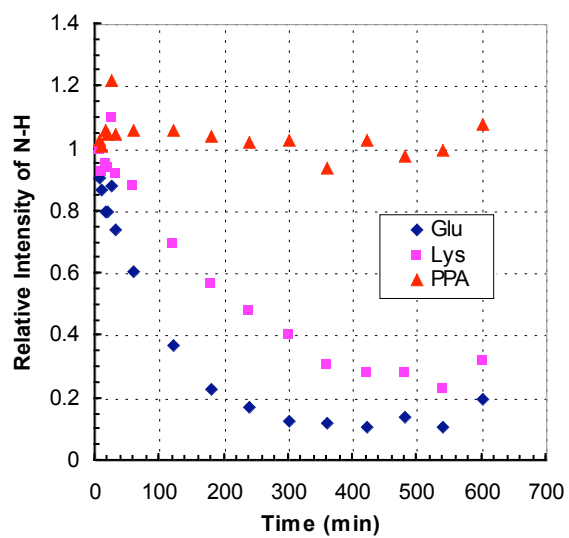
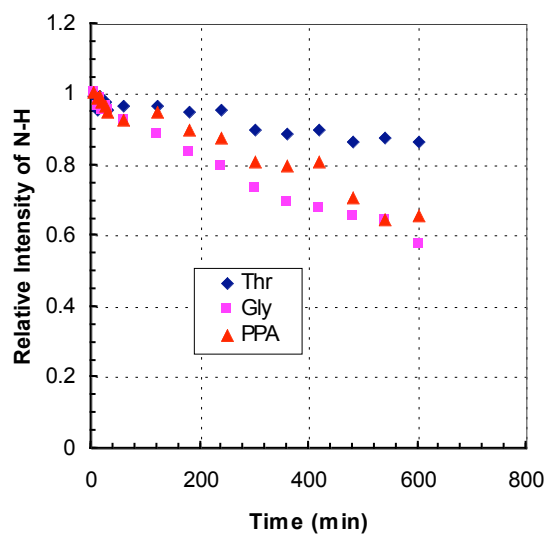
**Table A7.** Temperature Coefficients ( $-\Delta\delta K[\text{ppb/K}]$ ), H-D Exchange Data for **61a-c**.

compound	$-\Delta\delta K[\text{ppb/K}]/\text{H-D}$		
	AA $i+1$	AA $i+2$	AA $i+3$
<b>a</b>	3.8/ M	4.6/ F	5.3/F
<b>b</b>	1.5/S	3.8/F	6.6/F
<b>c</b>	7.0/M	6.0/M	6.4/M

\* For H-D exchange, F: Fast, M: medium, S: slow

Temperature Coefficients for Compound **61a** in DMSO- $d_6$ Temperature Coefficients for Compound **61b** in DMSO- $d_6$ 

Temperature Coefficients for Compound **61c** in DMSO-d<sub>6</sub>H-D Exchange Data for **61a** in 10% CD<sub>3</sub>OD/DMSO-d<sub>6</sub>

H-D Exchange Data for **61b** in 10% CD<sub>3</sub>OD/DMSO-d<sub>6</sub>H-D Exchange Data for **61c** in 10% CD<sub>3</sub>OD/DMSO-d<sub>6</sub>

**Table A 8.** OD values of Compounds **61a, b, d**.

Treatments		OD Value	
		Mean	SD
SFM		0.083	0.004
5% Serum		0.477	0.013
Low NGF		0.166	0.001
High NGF		0.317	0.015
<b>SFM</b>	a (10 uM)	0.107	0.009
	b (10 uM)	0.092	0.006
	d (10 uM)	0.090	0.006
	a (1 uM)	0.086	0.004
	b (1 uM)	0.086	0.004
	d (1 uM)	0.083	0.007
	50% DMSO	0.079	0.002
	10% DMSO	0.089	0.004
	<b>Low NGF</b>	a (10 uM)	0.181
b (10 uM)		0.176	0.003
d (10 uM)		0.175	0.010
a (1 uM)		0.169	0.007
b (1 uM)		0.166	0.002
d (1 uM)		0.166	0.009
50% DMSO		0.171	0.004
10% DMSO		0.179	0.004

**Table A 9.** OD values of Compounds **61e, g, h**.

Treatments		OD Value	
		Mean	SD
SFM		0.079	0.004
5% Serum		0.492	0.015
Low NGF		0.145	0.003
High NGF		0.296	0.004
<b>SFM</b>	e (10 uM)	0.093	0.013
	g (10 uM)	0.097	0.004
	h (10 uM)	0.092	0.001
	e (1 uM)	0.092	0.004
	g (1 uM)	0.088	0.009
	h (1 uM)	0.086	0.01
	40% DMSO	0.083	0.005
	30% DMSO	0.082	0.007
<b>Low NGF</b>	e (10 uM)	0.174	0.003
	g (10 uM)	0.192	0.006
	h (10 uM)	0.177	0.018
	e (1 uM)	0.169	0.008
	g (1 uM)	0.160	0.012
	h (1 uM)	0.174	0.006
	40% DMSO	0.174	0.002
	30% DMSO	0.158	0.002

## APPENDIX B

### EXPERIMENTAL ON CHAPTER III

**General Methods.** All chemicals were obtained from commercial suppliers and used without further purification. Dichloromethane was obtained anhydrous by distillation over calcium hydride and THF was distilled over sodium metal and benzophenone. Analytical HPLC analyses were carried out on 25 x 0.46 cm C-18 column using gradient conditions (5 – 95% B). The eluents used were: solvent A (H<sub>2</sub>O with 0.1% TFA) and solvent B (CH<sub>3</sub>CN with 0.1% TFA). The flow rate used was 1.0 mL/min. NMR spectra were recorded at 300 MHz if otherwise indicated. NMR chemical shifts were expressed in ppm relative to internal solvent peaks, and coupling constants were measured in Hz. All calculations were performed at the semi-empirical level of theory with the AM1 (Austin model 1) method as implemented in the MOPAC module in Cerius<sup>2</sup> (4.10). The standard type I  $\beta$ -turn was used without optimization of the geometry and the triazole molecule was optimized and modified to match the conformation of the type I  $\beta$ -turn by twisting the torsion angles of the carboxylic acid group. The overlay of the fully optimized structure and the modified one is shown in Figure B1. The single point energy of both molecules was calculated with high convergence criteria. The electrostatic potential was mapped on the density with an isodensity value of 0.1.

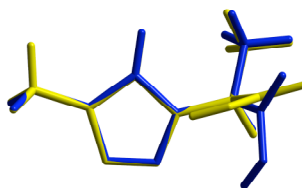
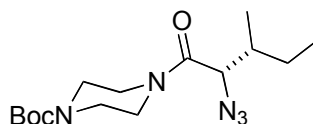


**Figure B1.** Overlay of the fully optimized triazole molecule (blue) and the modified one (yellow).

### Preparation of Compound 73a-f

Method A. The free amino acids were transformed into azides **73a-f** with copper(I)-catalyzed diazo transfer method followed by a linker coupling reaction. A representative synthesis of the amino acid azide derivative **73a** is described below.



**73a**

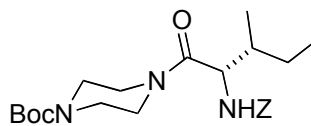
A solution of sodium azide (549.0 mmol, 35.6 g) was dissolved in a 1:1 mixture of H<sub>2</sub>O (80 ml) and CH<sub>2</sub>Cl<sub>2</sub> (80 ml) and cooled using an ice bath. Triflic anhydride (111.0 mmol, 18.6 ml) was added over 5 min and the solution was then stirred at 0 °C for a further 2 h. The CH<sub>2</sub>Cl<sub>2</sub> phase was separated, and the aqueous portion was extracted with CH<sub>2</sub>Cl<sub>2</sub> (2 x 80 mL). The organic fractions were combined, washed once with saturated Na<sub>2</sub>CO<sub>3</sub>, and the solution used without further purification (this is to avoid risks with the triflic azide in the solution). Isoleucine (55.8 mmol, 7.3 g) was combined with K<sub>2</sub>CO<sub>3</sub> (83.6 mmol, 11.6 g), CuSO<sub>4</sub> · 5H<sub>2</sub>O (0.56 mmol, 0.14 g), H<sub>2</sub>O (180 ml) and CH<sub>3</sub>OH (360 ml). The CH<sub>2</sub>Cl<sub>2</sub> solution of triflyl azide prepared above was added in one portion, and the mixture was stirred at 25 °C for 14 h. The organic solvents were then removed under reduced pressure, giving an aqueous slurry that was diluted with H<sub>2</sub>O (500 ml) and the pH was adjusted to 6 with concentrated HCl. The solution was extracted with EtOAc (4 x 200 ml) and the organic layers were separated. The pH of the aqueous phase was adjusted to 2 and extracted with EtOAc (3 X 300 ml). The organic extracts were combined, dried (NaSO<sub>4</sub>), and evaporated to dryness giving the Isoleucine azide, which was used without further purification.

Boc-piperazine (1.0 mmol, 0.19 g) was added to a suspension of the above Isoleucine azide (1.0 mmol, 0.19 g) in CH<sub>2</sub>Cl<sub>2</sub> (to give a 0.2 M solution) at 0 °C. *N*-Methylmorpholine (2.0 mmol, 0.22 ml) was added to the above suspension followed by HOBt (1.1 mmol, 0.15 g) and EDC (1.1 mmol, 0.22 g). The resulting solution was stirred at 0 °C for 1 h and warmed to 25 °C and stirred for another 3 h. Ethyl acetate (*ca*



20 ml) was added to the reaction mixture, and the resulting suspension was washed with 5% HCl, H<sub>2</sub>O, 5% Na<sub>2</sub>CO<sub>3</sub> and brine. The organic layer was separated, dried with Na<sub>2</sub>SO<sub>4</sub>, and concentrated to afford **73a** as clear oil (0.3 g, 95 %). This sample (and others in the series **73**) was used without further purification.

Method B. Boc-piperazine (3.0 mmol, 0.56 g) was added to a suspension of Cbz protected Isoleucine (3.3 mmol, 0.88 g) in dry CH<sub>2</sub>Cl<sub>2</sub> (0.2 M) at 0 °C. *N*-Methylmorpholine (3.3 mmol, 0.36 ml) was added to the above suspension followed by HOBt (3.3 mmol, 0.45 g) and EDC (3.3 mmol, 0.63 g). The resulting solution was stirred at 0 °C for 1 h and warmed to 25 °C and stirred for another 3 h. Ethyl acetate (ca. 40 ml) was added to the reaction mixture, and the resulting suspension was washed with 5% HCl, H<sub>2</sub>O, 5% Na<sub>2</sub>CO<sub>3</sub> and brine. The organic layer was separated, dried with Na<sub>2</sub>SO<sub>4</sub>, and concentrated to afford **75a** as clear oil (1.10 g, 85%).



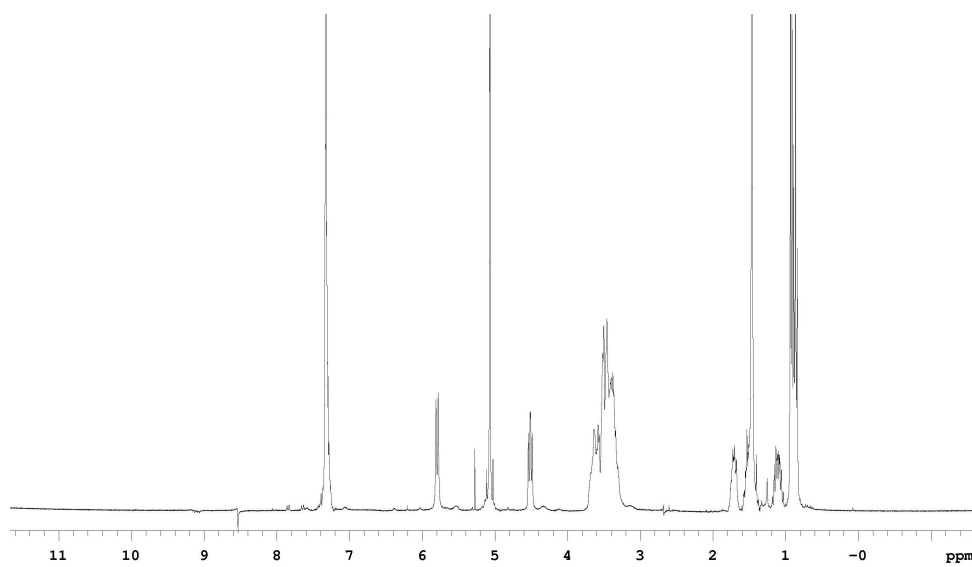
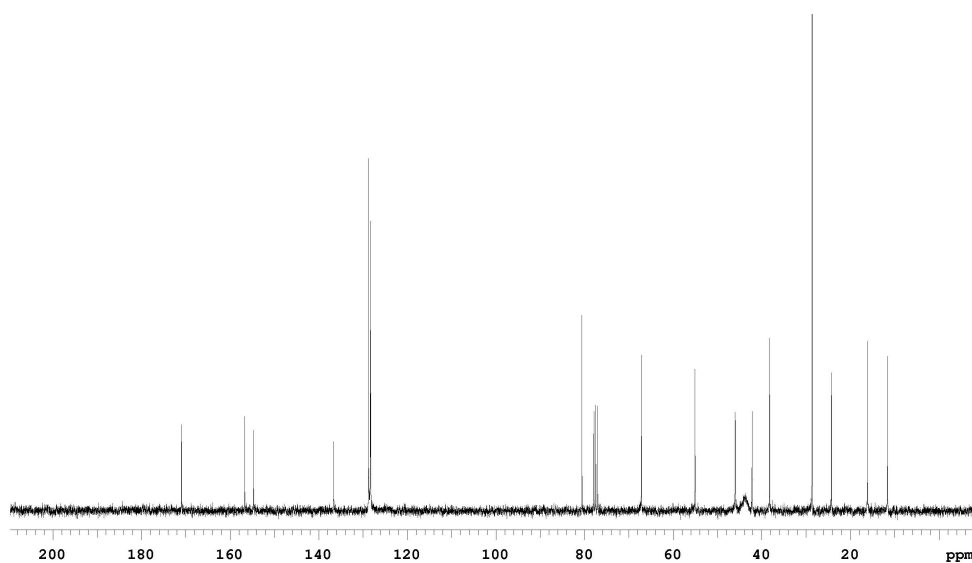
**75a**

#### Data for Compound **75a**

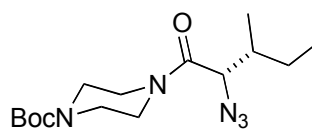
<sup>1</sup>H NMR (CDCl<sub>3</sub>) δ 7.32 (m, 5H), 5.80 (d, 1H, J = 9 Hz), 5.07 (dd, 2H, J = 9Hz, 7.2 Hz), 4.51 (m, 1H), 3.64-3.01 (m, 8H), 1.71 (m, 1H), 1.47 (s, 9H), 1.11 (m, 1H), 0.93-0.84 (m, 6H)

<sup>13</sup>C NMR (CDCl<sub>3</sub>) δ 171.0, 156.7, 154.7, 136.6, 128.7, 128.3, 128.34, 128.30, 80.6, 67.1, 55.0, 46.0, 44.0, 42.2, 38.2, 28.6, 24.2, 16.1, 11.6

MS (ESI, m/z) 434 (M+H)<sup>+</sup>

**<sup>1</sup>H NMR of 75a****<sup>13</sup>C NMR of 75a**

The above residue of compound **75a** was dissolved in MeOH (0.2 M) and 10 % Pd/C (0.4 g) was added. The suspension was stirred at room temperature with 1 atm H<sub>2</sub> overnight and filtered with a pad of Celite and concentrated to dryness. The amines were transformed into azide **73a** with 82 % yield *via* copper(I)-catalyzed diazo transfer method as described in method A.

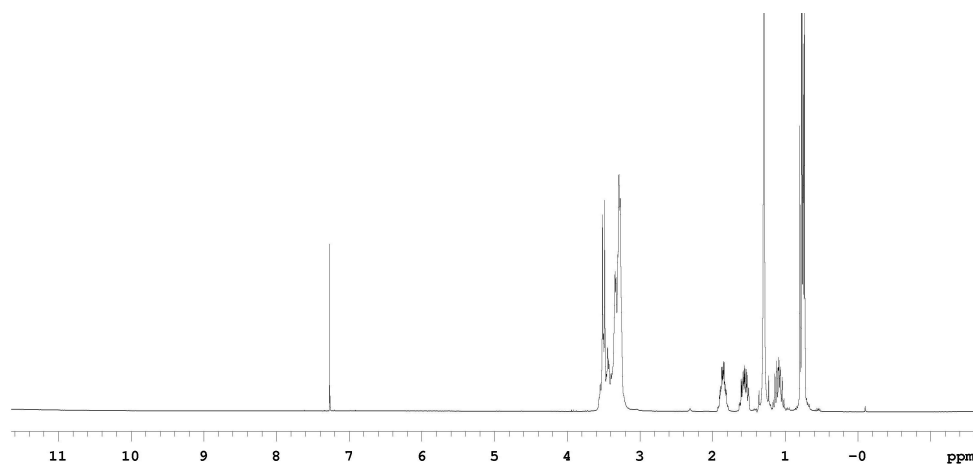
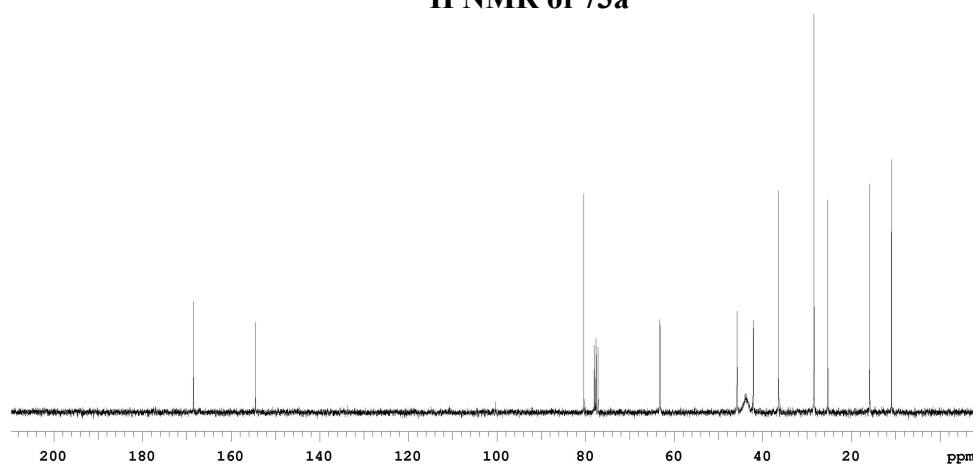
**73a**

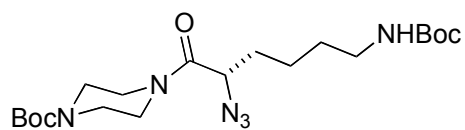
**Data for Compound 73a.** Compound **73a** was prepared from NH<sub>2</sub>-Ile-OH as a slightly yellow oil: (0.9 g, 98%)

<sup>1</sup>H NMR (CDCl<sub>3</sub>) δ 3.55 (d, 1H, J = 12.0 Hz), 3.50-3.27 (m, 8H), 1.86 (m, 1H), 1.57 (m, 1H), 1.30 (s, 9H), 1.08 (m, 1H), 1.04-0.74 (m, 6H)

<sup>13</sup>C NMR (CDCl<sub>3</sub>) δ 168.5, 154.5, 80.3, 63.2, 45.8, 43.8, 42.1, 36.4, 28.4, 25.3, 15.8, 10.9

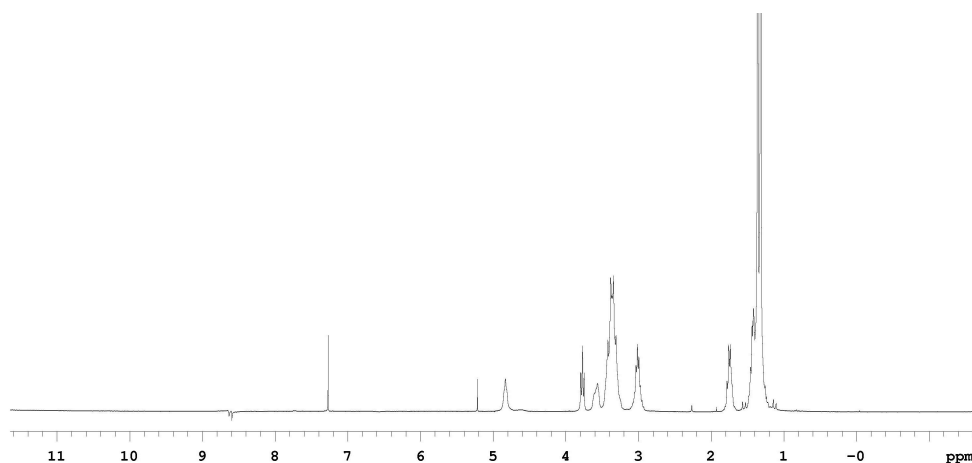
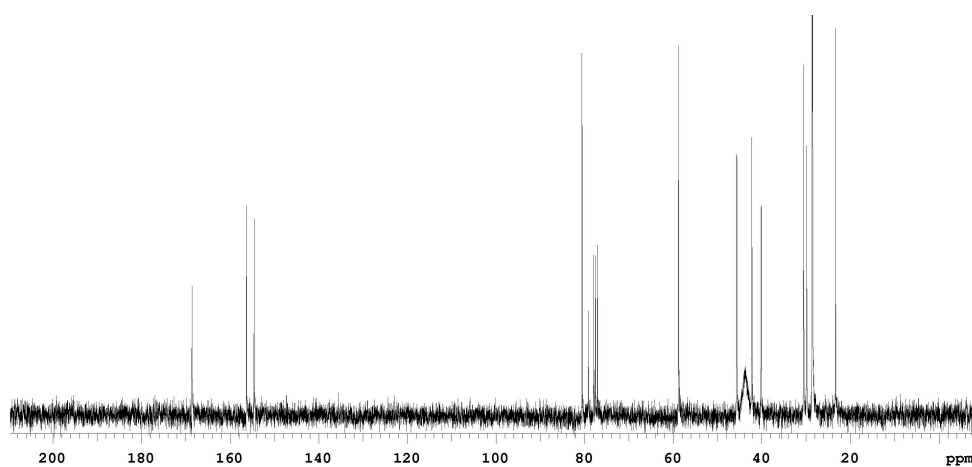
MS (ESI, m/z) 332 (M+Li)<sup>+</sup>

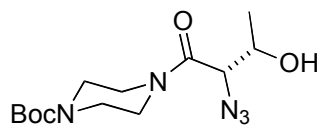
**<sup>1</sup>H NMR of 73a****<sup>13</sup>C NMR of 73a**

**73b****Data for Compound 73b**

$^1\text{H NMR}$  ( $\text{CDCl}_3$ )  $\delta$  4.74 (b, 1H), 3.79 (t, 1H,  $J = 7.2$  Hz), 3.64-3.29 (m, 8H), 3.01 (m, 2H), 1.77 (m, 2H), 1.44 (m, 2H), 1.36 (m, 2H), 1.30 (s, 9H), 1.28 (s, 9H)

$^{13}\text{C NMR}$  ( $\text{CDCl}_3$ )  $\delta$  168.5, 156.3, 154.6, 80.6, 78.3, 58.8, 45.6, 43.8, 42.2, 40.3, 30.5, 29.9, 28.6, 28.5, 23.3

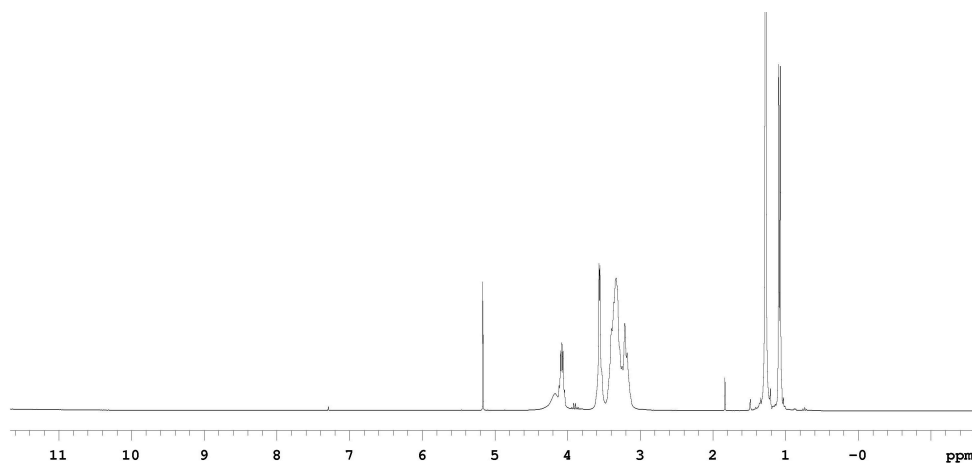
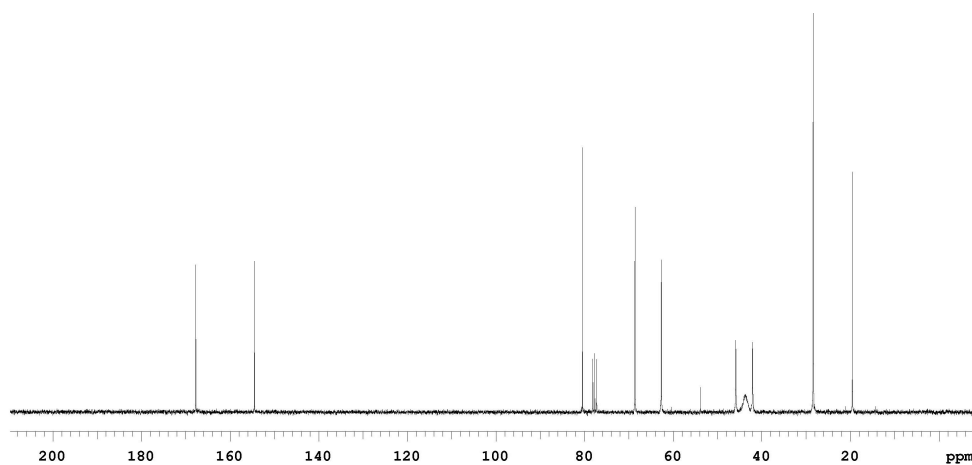
 **$^1\text{H NMR}$  of 73b** **$^{13}\text{C NMR}$  of 73b**

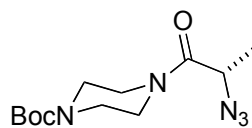
**73c****Data for Compound 73c**

**<sup>1</sup>H NMR (CDCl<sub>3</sub>)** δ 4.10 (b, 1H), 4.08 (m, 1H), 3.40-3.18 (m, 8H), 1.28(s, 9H), 1.08 (d, 3H, J = 6.6 Hz)

**<sup>13</sup>C NMR (CDCl<sub>3</sub>)** δ 167.7, 154.5, 80.5, 68.6, 62.7, 45.8, 43.6, 42.0, 28.4, 19.5

**MS (ESI, m/z)** 314 (M+H)<sup>+</sup>

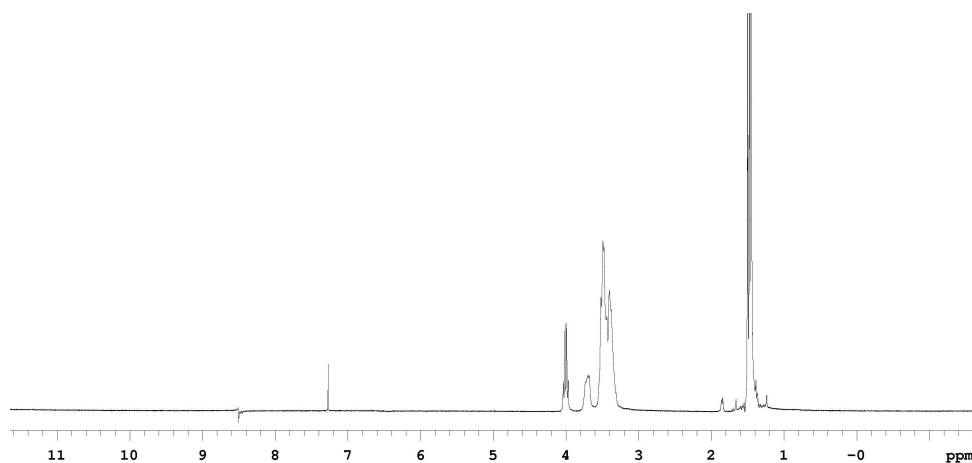
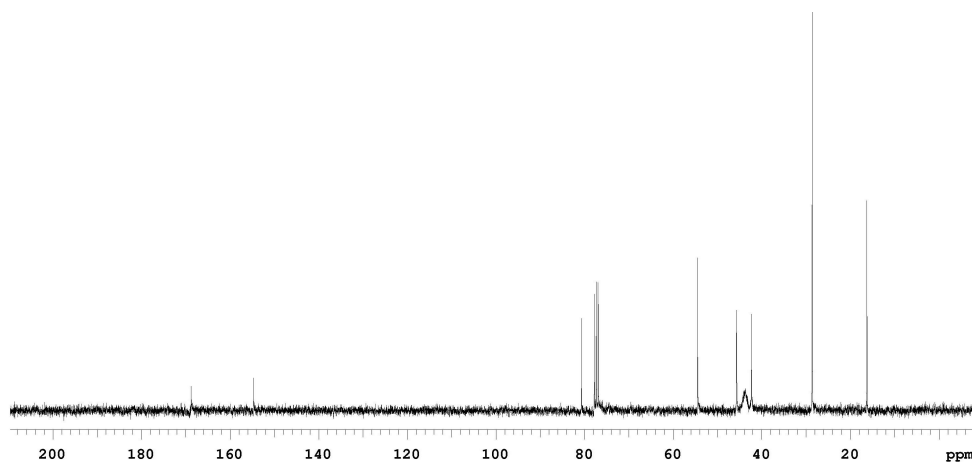
**<sup>1</sup>H NMR of 73c****<sup>13</sup>C NMR of 73c**

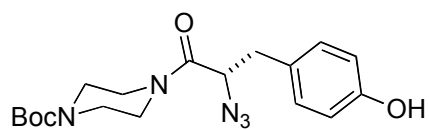
**73d****Data for Compound 73d**

$^1\text{H NMR}$  ( $\text{CDCl}_3$ )  $\delta$  4.00 (q, 1H,  $J = 6.6$  Hz), 3.70-3.40 (m, 8H), 1.50 (d, 3H,  $J = 6.6$  Hz), 1.45 (s, 9H)

$^{13}\text{C NMR}$  ( $\text{CDCl}_3$ )  $\delta$  168.8, 154.7, 80.7, 54.5, 45.7, 43.6, 42.3, 28.6, 16.2

$\text{MS (ESI, m/z)}$  306 ( $\text{M}+\text{Na}$ ) $^+$

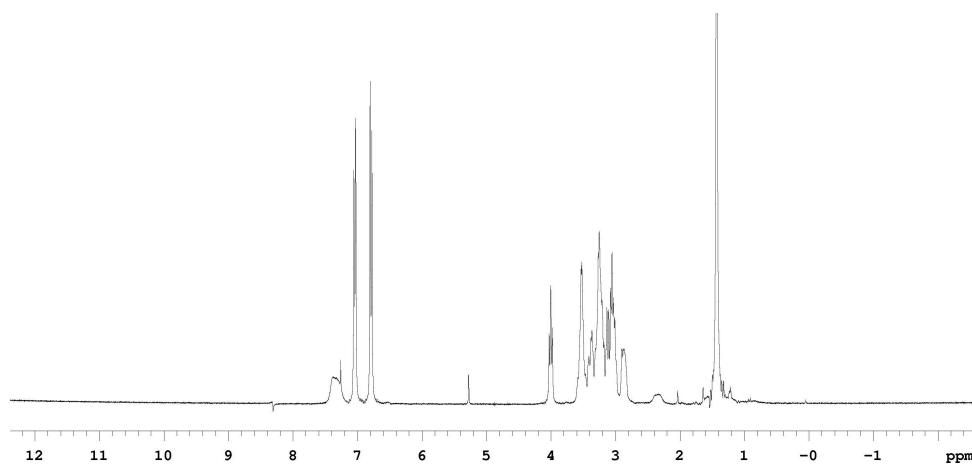
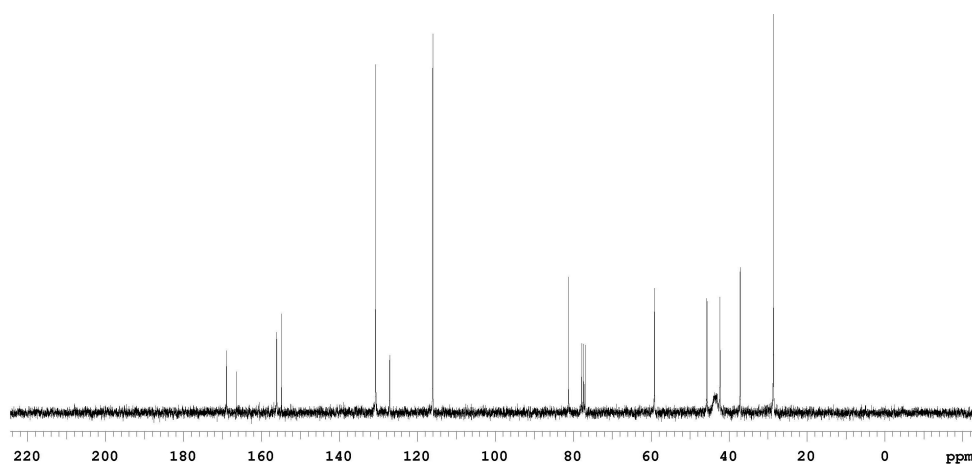
 $^1\text{H NMR}$  of 73d $^{13}\text{C NMR}$  of 73d

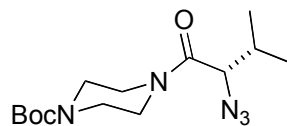
**73e****Data for Compound 73e**

**<sup>1</sup>H NMR (CDCl<sub>3</sub>)** δ 7.04 (d, 2H, J = 8.4 Hz), 6.80 (d, 2H, J = 8.4 Hz), 4.00 (t, 1H, J = 7.5 Hz), 3.53-2.87 (m, 10H), 1.43 (s, 9H)

**<sup>13</sup>C NMR (CDCl<sub>3</sub>)** δ 169.0, 156.1, 145.8, 130.6, 127.0, 116.0, 81.1, 59.1, 45.6, 43.4, 42.3, 37.1, 28.6

**MS (ESI, m/z)** 376 (M+H)<sup>+</sup>

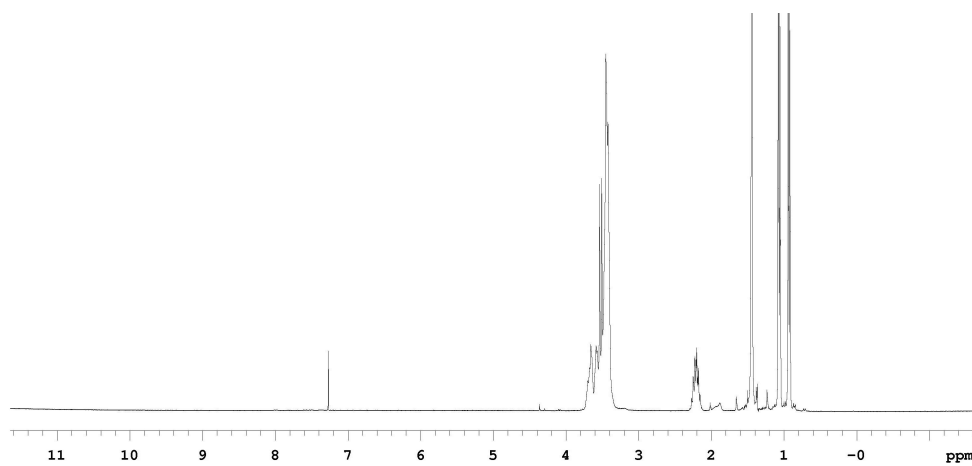
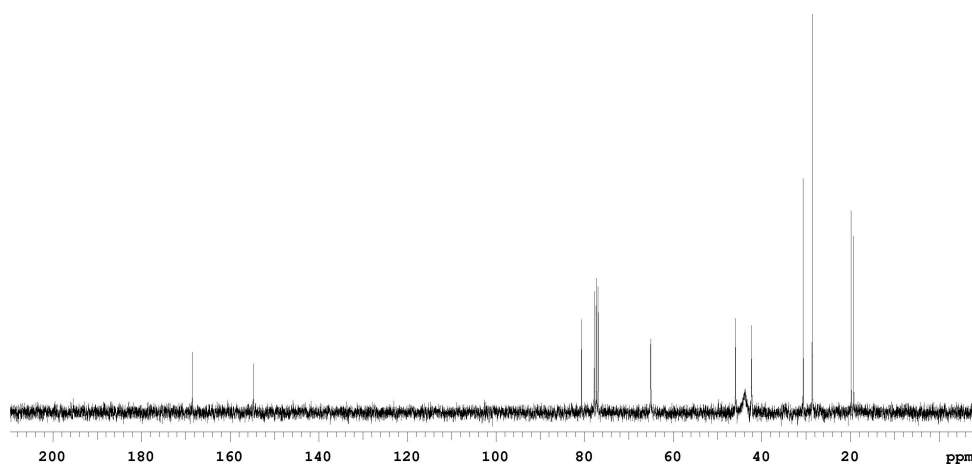
**<sup>1</sup>H NMR of 73e****<sup>13</sup>C NMR of 73e**

**73f****Data for Compound 73f**

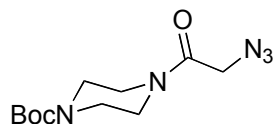
$^1\text{H NMR}$  ( $\text{CDCl}_3$ )  $\delta$  3.68-3.44 (m, 9H), 2.24 (m, 1H), 1.47 (s, 9H), 1.08 (d, 3H,  $J = 6.6$  Hz), 0.94 (d, 3H,  $J = 6.6$  Hz)

$^{13}\text{C NMR}$  ( $\text{CDCl}_3$ )  $\delta$  168.8, 154.7, 80.7, 65.0, 45.9, 43.8, 42.3, 30.6, 28.6, 19.8, 19.2

$\text{MS}$  (ESI,  $m/z$ ) 312 ( $\text{M}+\text{H}$ ) $^+$

 **$^1\text{H NMR}$  of 73f** **$^{13}\text{C NMR}$  of 73f**



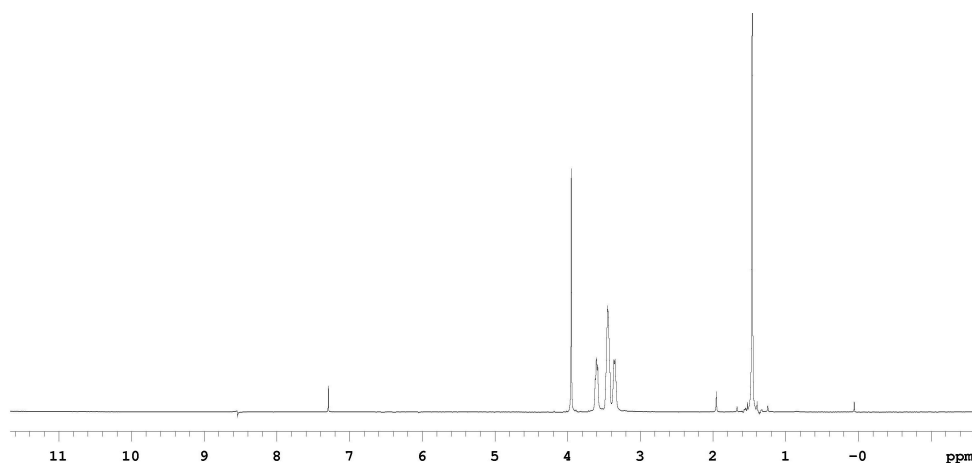
**73g**

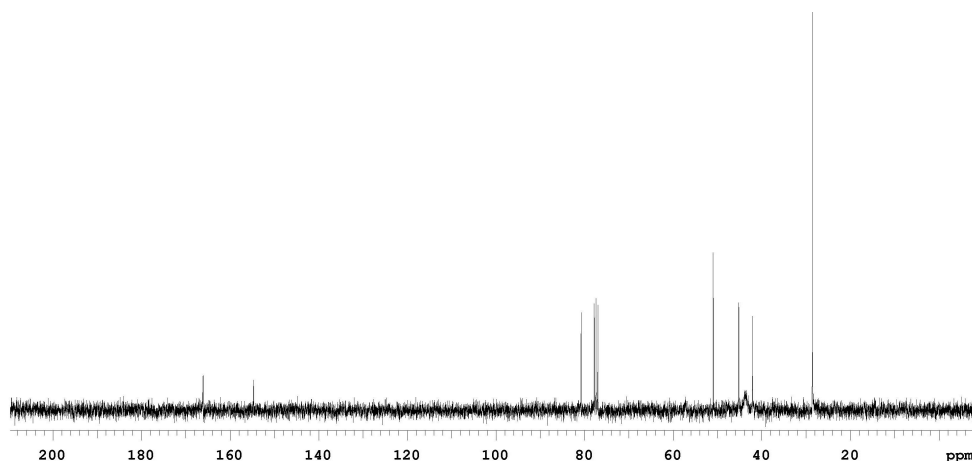
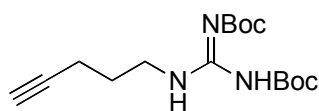
**Preparation of Compound 73g.** Boc-piperazine (3.00 mmol, 0.56 g) was dissolved in 10 ml 5% Na<sub>2</sub>CO<sub>3</sub> and 10 ml of CH<sub>2</sub>Cl<sub>2</sub> was added. The solution was cooled in ice water bath and bromoacetyl bromide (3.30 mmol, 0.43 ml) was added. The resulting mixture was stirred at 0 °C for 40 min and warmed to 25 °C and stirred for another 2 h. The reaction mixture was separated and the organic layer was washed with water, 5% HCl, water and brine. The CH<sub>2</sub>Cl<sub>2</sub> solution was dried with Na<sub>2</sub>SO<sub>4</sub>, concentrated to dryness and recrystallized to afford Boc-piperazine acetyl bromide (0.91g, 99%) as a white solid. The above intermediate (2.9 mmol, 0.91 g) was dissolved in 15 ml of CH<sub>3</sub>CN and NaN<sub>3</sub> (8.0 mmol, 0.52 g) was added. The resulting suspension was stirred and heated to reflux 14 h. The product was isolated with extraction and recrystallized (EtOAc and hexanes) to afford **73g** (0.76 g, 95%) as a white solid.

<sup>1</sup>H NMR (CDCl<sub>3</sub>) δ 3.95 (s, 2H), 3.62-3.35 (m, 8H), 1.46 (s, 9H)

<sup>13</sup>C NMR (CDCl<sub>3</sub>) δ 166.1, 154.6, 80.8, 50.9, 45.2, 43.8, 42.1, 28.6

MS (ESI, m/z) 292 (M+Na)<sup>+</sup>

**<sup>1</sup>H NMR of 73g**

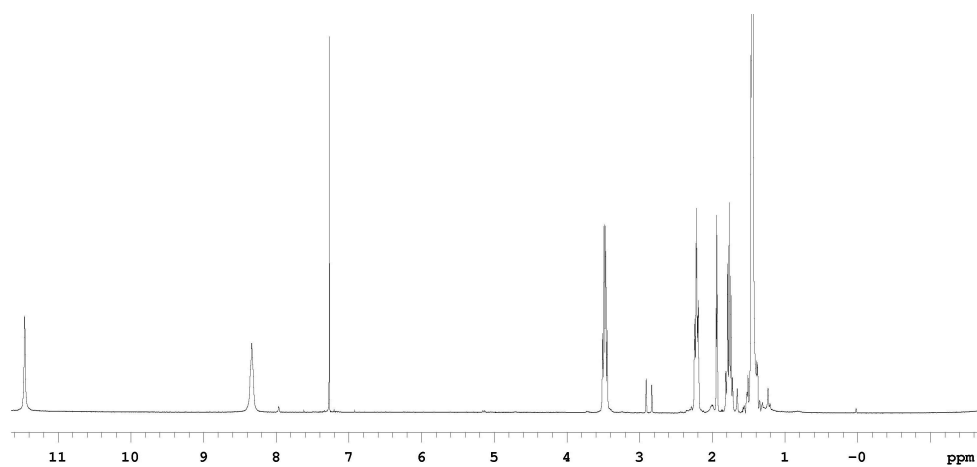
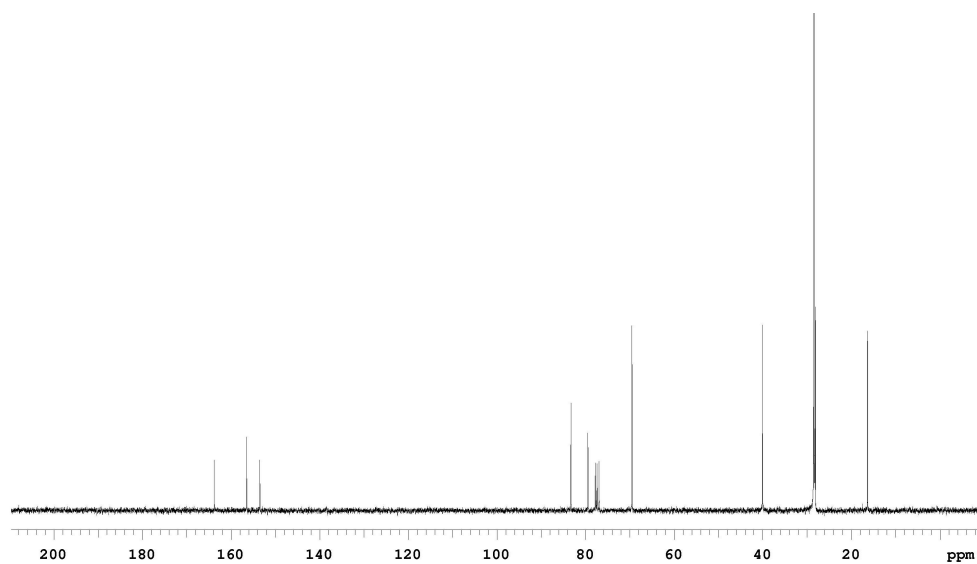
 $^{13}\text{C}$  NMR of **79g****79**

**Procedure for Preparation of Compound 79.** Boc protected 4-pentynyl amine (10.00 mmol, 1.83 g) was dissolved in a mixture of ethyl acetate and methanol (50 ml, v:v = 10:1) and the solution was cooled to 0 °C. Acetyl chloride (5ml) was added to the above solution slowly and the resulting mixture was stirred at 0 °C for 2 h and warmed to room temperature and kept for 4 h. The solvent was removed and the residue was redissolved in 10 ml of dry THF. *tert*-Butyl (1H-pyrazol-1-yl)methylenedicarbamate (10.00 mmol, 1.20 g) was added and followed with 1.0 ml of *N,N*-diisopropylethylamine. The resulting suspension was stirred at 25 °C for 48 h and the solvent was removed. Flash chromatography afforded **79** (2.0 g, 62%) as a white solid.

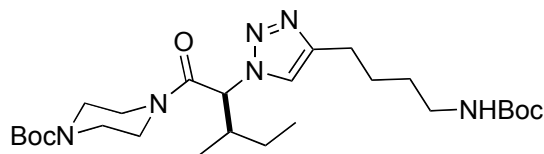
$^1\text{H}$  NMR (CDCl<sub>3</sub>)  $\delta$  11.50 (s, 1H), 8.39 (s, 1H), 3.60 (m, 2H), 2.27 (m, 2H), 1.97 (t, 1H,  $J = 2.4$  Hz), 1.81 (m, 2H), 1.49 (s, 18H)

$^{13}\text{C}$  NMR (CDCl<sub>3</sub>)  $\delta$  163.8, 156.5, 153.5, 100.2, 83.4, 79.6, 69.5, 40.1, 28.6, 28.3, 28.1, 16.3

MS (ESI,  $m/z$ ) 326 (M+H)<sup>+</sup>

 $^1\text{H}$  NMR of 79 $^{13}\text{C}$  NMR of 79

### General Procedure for Preparation of Triazole Compound 74a-o



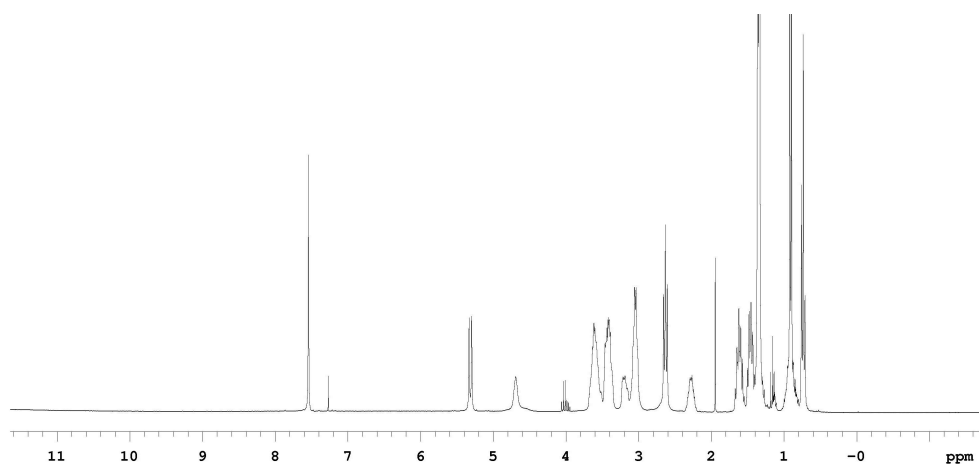
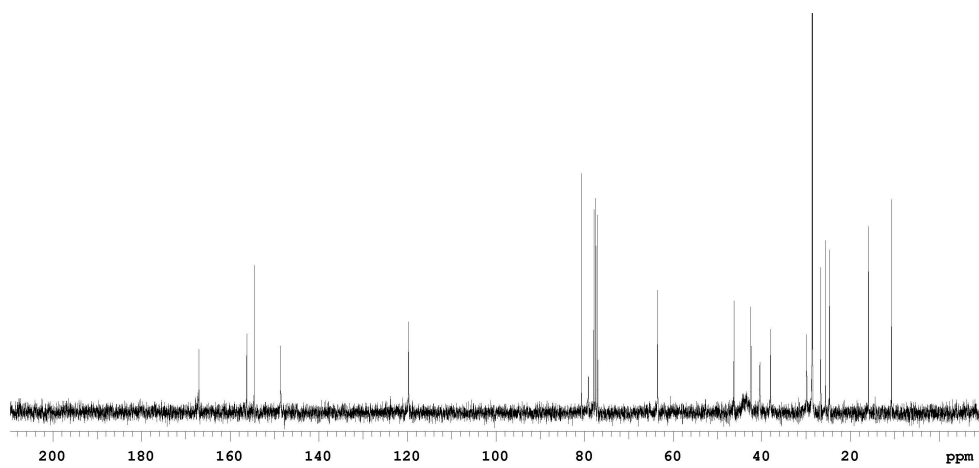
**74a**

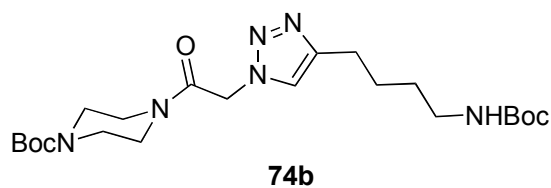
To the 20 ml dry THF solution of **74a** (3.0 mmol, 0.98 g) was added Boc protected hexynyl amine (3.0 mmol, 0.59 g) followed with DIEA (6.0 mmol, 1.0 ml) and CuI (3.0 mmol, 0.57 g). The resulting mixture was stirred at room temperature under nitrogen for 4 h and the solvent was removed. Dichloromethane (40 ml) was added to the above residue and extracted with 20 ml of NH<sub>4</sub>Cl/NH<sub>4</sub>OH (9:1). The organic layer was separated and the aqueous layer was extracted with CH<sub>2</sub>Cl<sub>2</sub> (2 X 20 ml). The organic layers were combined and washed with brine, 5 % HCl and brine and dried with Na<sub>2</sub>SO<sub>4</sub>. Flash chromatography (2 % MeOH in CH<sub>2</sub>Cl<sub>2</sub>) afforded compound **5a** (1.21 g, 78 %) as a white solid.

<sup>1</sup>H NMR (CDCl<sub>3</sub>) δ 5.42 (d, 1H, J = 10.5 Hz), 5.28 (s, 1H), 4.56 (s, 2H), 3.67-3.29 (m, 12H), 2.36 (m, 1H), 1.04 (s, 18H), 1.02-0.78 (m, 8H)

<sup>13</sup>C NMR (CDCl<sub>3</sub>) δ 166.9, 156.2, 154.6, 145.5, 121.7, 80.8, 79.5, 70.0, 64.7, 63.5, 46.3, 43.8, 42.5, 40.5, 38.2, 28.6, 28.5, 24.7, 15.9, 10.6

MS (ESI, m/z) 531 (M+Li)<sup>+</sup>

 $^1\text{H}$  NMR of 74a $^{13}\text{C}$  NMR of 74a

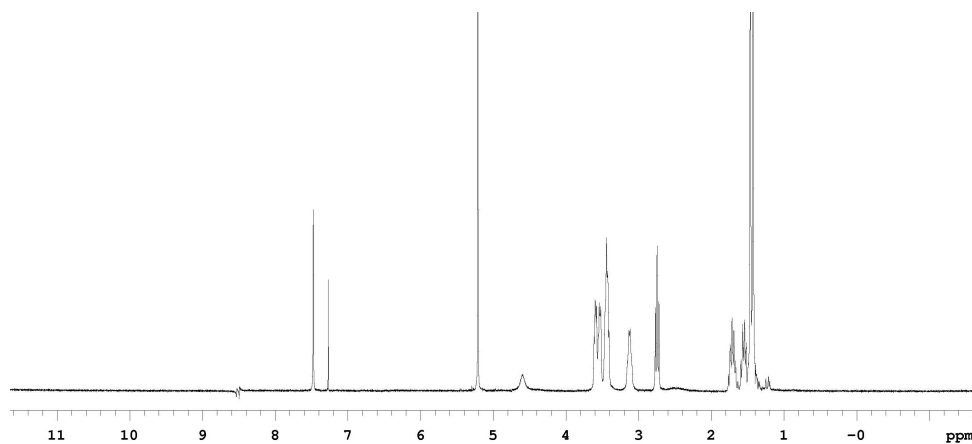


Compound **74b** was prepared from compound **4g** and Boc protected hexynyl amine. Flash chromatography (5 % MeOH in CH<sub>2</sub>Cl<sub>2</sub>) afforded **5b** (1.80 g, 79%) as a white solid.

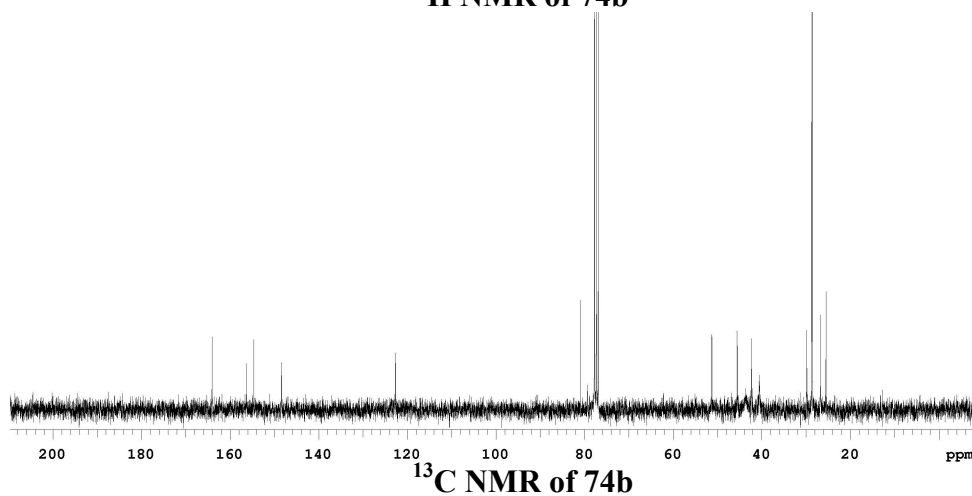
<sup>1</sup>H NMR (CDCl<sub>3</sub>) δ 7.48 (s, 1H), 5.21 (s, 2H), 4.60 (s, 1H), 3.61-3.52 (m, 8H), 3.12 (m, 2H), 2.75 (t, 2H, J = 7.5 Hz), 1.71 (m, 2H), 1.55 (m, 2H), 1.52 (s, 9H), 1.43 (s, 9H)

<sup>13</sup>C NMR (CDCl<sub>3</sub>) δ 164.0, 156.2, 154.6, 148.4, 122.7, 80.9, 79.3, 51.2, 45.3, 44.0, 42.4, 40.5, 29.8, 28.7, 28.6, 26.7, 25.5

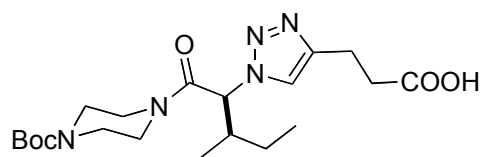
MS (ESI, m/z) 467 (M+H)<sup>+</sup>



<sup>1</sup>H NMR of **74b**



<sup>13</sup>C NMR of **74b**

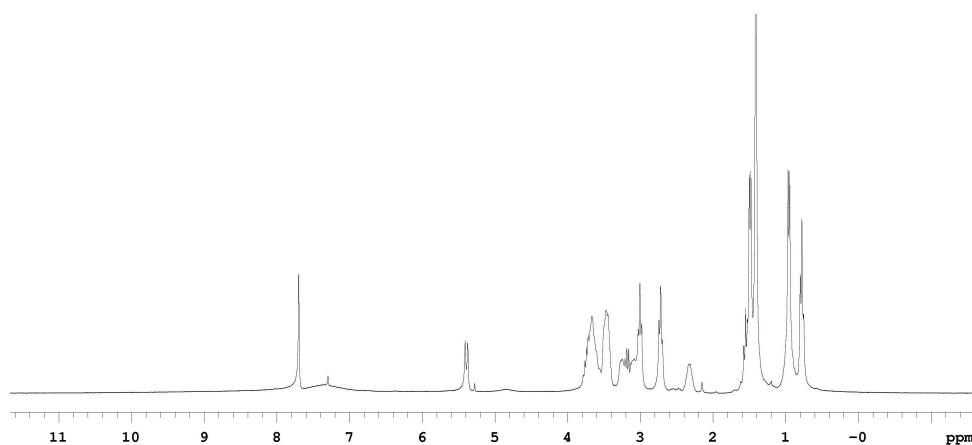
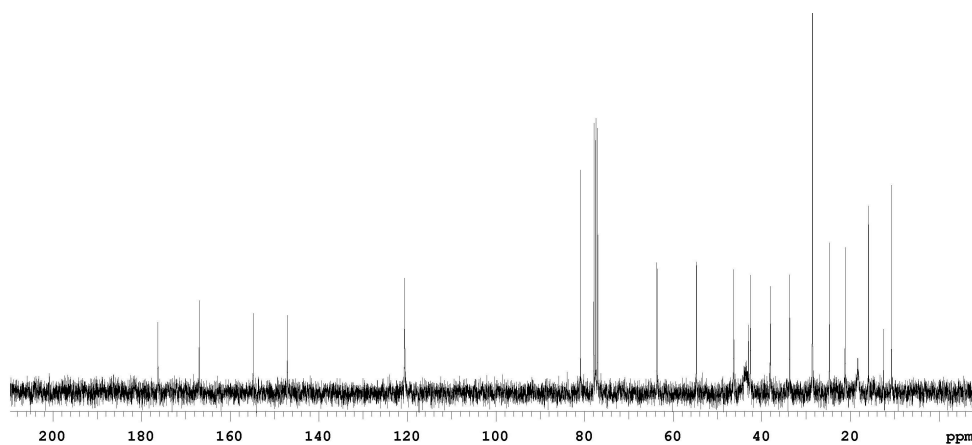
**74c**

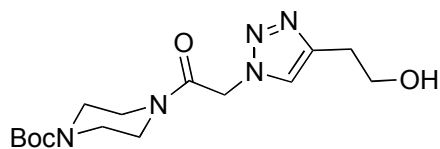
Compound **74c** was prepared from compound **73a** and 4-pentynoic acid. Flash Chromatography (5 % MeOH in CH<sub>2</sub>Cl<sub>2</sub>) afforded **74c** (1.04 g, 80%) as a yellow solid.

<sup>1</sup>H NMR (CDCl<sub>3</sub>) δ 8.75 (b, 1H), 7.71 (s, 1H), 5.40 (d, 1H, J = 10.5 Hz), 3.67-3.04 (m, 8H), 3.02 (t, 2H, J = 7.2 Hz), 2.74 (t, 2H, 7.2 Hz), 1.23 (s, 9H), 0.97-0.76 (m, 8H)

<sup>13</sup>C NMR (CDCl<sub>3</sub>) δ 176.4, 167.0, 154.8, 147.0, 120.6, 80.9, 63.6, 46.3, 43.9, 42.5, 38.1, 33.6, 28.5, 24.7, 21.1, 15.9, 10.7

MS (ESI, m/z) 422 (M-H)<sup>+</sup>

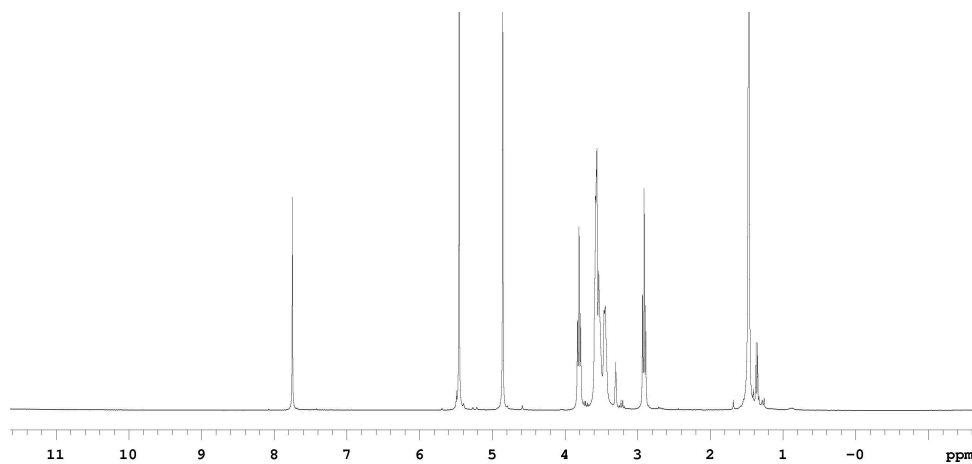
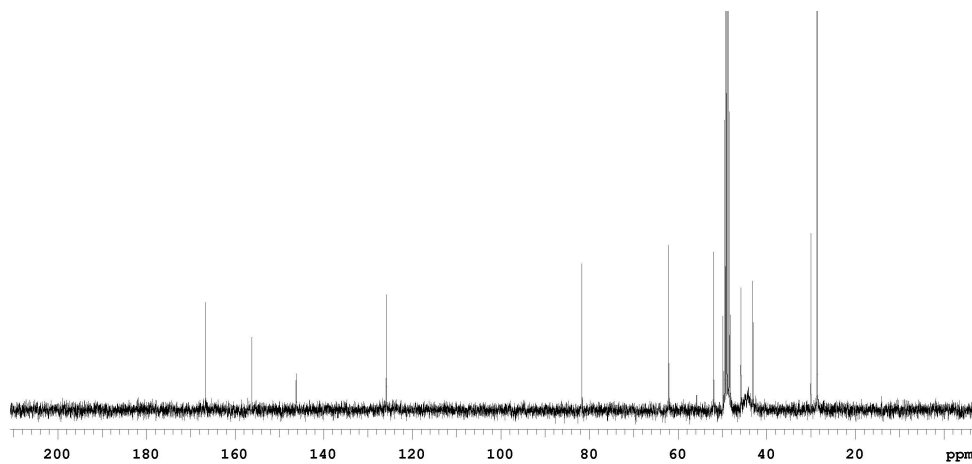
<sup>1</sup>H NMR of **74c**<sup>13</sup>C NMR of **74c**

**74d**

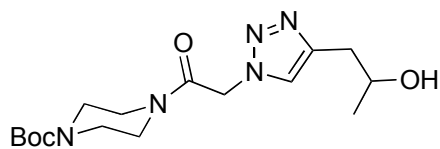
Compound **74d** was prepared from **73g** and 3-butynol. Flash chromatography (5 % MeOH in CH<sub>2</sub>Cl<sub>2</sub>) afforded **74d** (1.60 g, 94%) as a white solid.

<sup>1</sup>H NMR (CD<sub>3</sub>OD) δ 7.75 (b, 1H), 5.45 (s, 2H), 3.82 (t, 2H, J = 6.3 Hz), 3.60-3.52 (m, 8H), 2.91 (t, 2H, J = 6.3 Hz), 1.47 (s, 9H)

<sup>13</sup>C NMR (CDCl<sub>3</sub>) δ 164.1, 154.6, 146.2, 123.7, 80.9, 61.7, 51.1, 45.4, 44.0, 42.4, 31.2, 28.6; MS (ESI, m/z) 340 (M+H)<sup>+</sup>

**<sup>1</sup>H NMR of 74d****<sup>13</sup>C NMR of 74d**



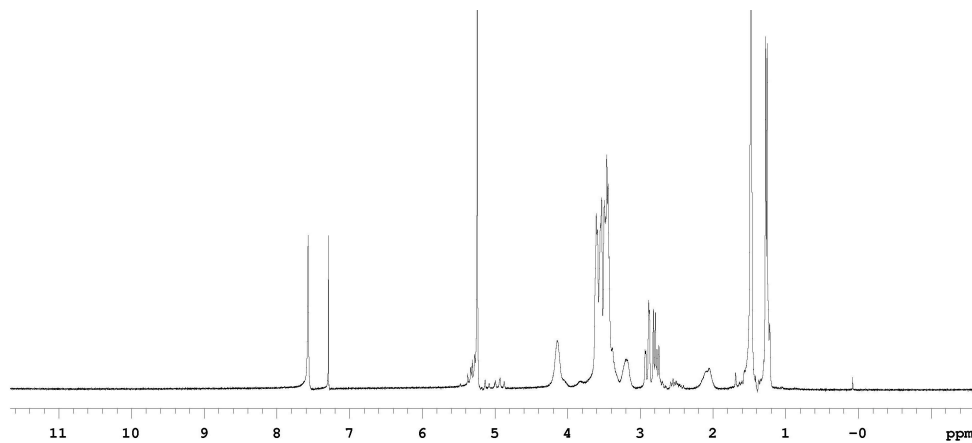
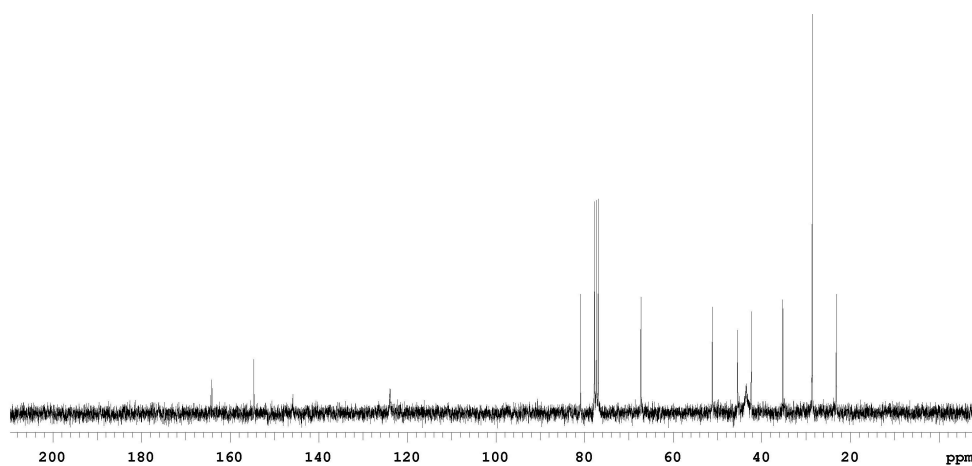
**74e**

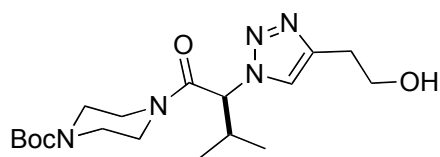
Compound **74e** was prepared from **73g** and 4-pentyn-2-ol. Flash chromatography (3 % MeOH in CH<sub>2</sub>Cl<sub>2</sub>) afforded **74e** (2.20 g, 96%) as a white solid.

**<sup>1</sup>H NMR (CD<sub>3</sub>OD)** δ 7.74 (s, 1H), 5.49 (s, 2H), 4.00 (m, 1H), 3.60-3.54 (m, 8H), 2.81 (d, 2H, J = 6.3 Hz), 1.47 (s, 9H), 1.20 (d, 3H, J = 6.3 Hz)

**<sup>13</sup>C NMR (CDCl<sub>3</sub>)** δ 164.1, 154.6, 145.8, 123.9, 80.9, 67.3, 51.1, 45.4, 44.0, 42.4, 35.2, 28.6, 23.2

**MS (ESI, m/z)** 360 (M+Li)<sup>+</sup>

**<sup>1</sup>H NMR of 74e****<sup>13</sup>C NMR of 74e**

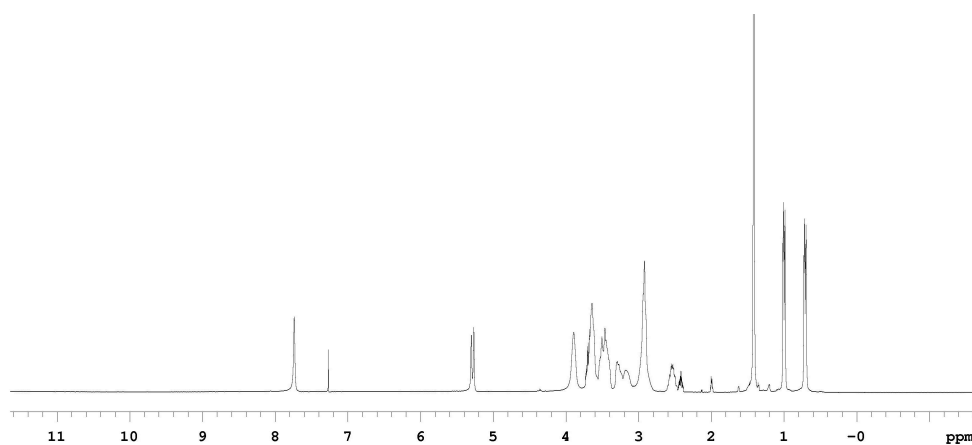
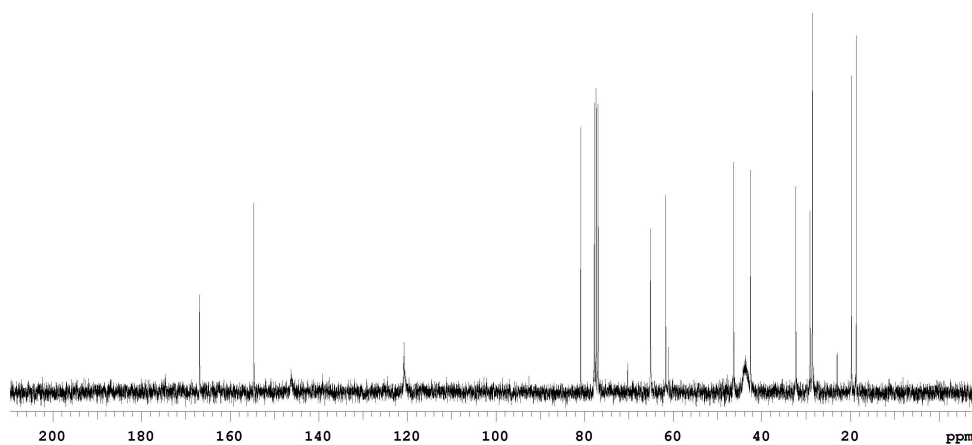
**74f**

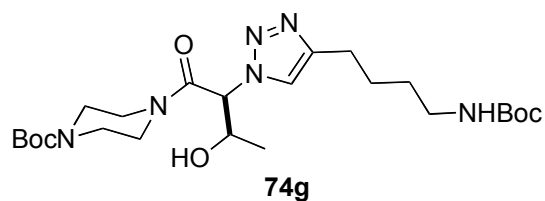
Compound **74f** was prepared from **73f** and 4-butyne-1-ol. Flash chromatography (3 % MeOH in CH<sub>2</sub>Cl<sub>2</sub>) afforded **74f** (1.03 g, 80%) as a white solid.

<sup>1</sup>H NMR (CDCl<sub>3</sub>) δ 7.74 (s, 1H), 5.28 (d, 1H, 7.5 Hz), 3.89 (s, 2H), 3.72-3.17 (m, 8H), 2.94 (m, 4H), 2.55 (m, 1H), 1.42 (s, 9H), 0.99 (m, 3H), 0.74 (m, 3H)

<sup>13</sup>C NMR (CDCl<sub>3</sub>) δ 166.9, 154.6, 146.2, 120.7, 80.8, 65.1, 61.0, 46.3, 44.2, 43.6, 42.5, 32.2, 28.6, 19.7, 18.6

MS (ESI, m/z) 382 (M+H)<sup>+</sup>

**<sup>1</sup>H NMR of 74f****<sup>13</sup>C NMR of 74f**

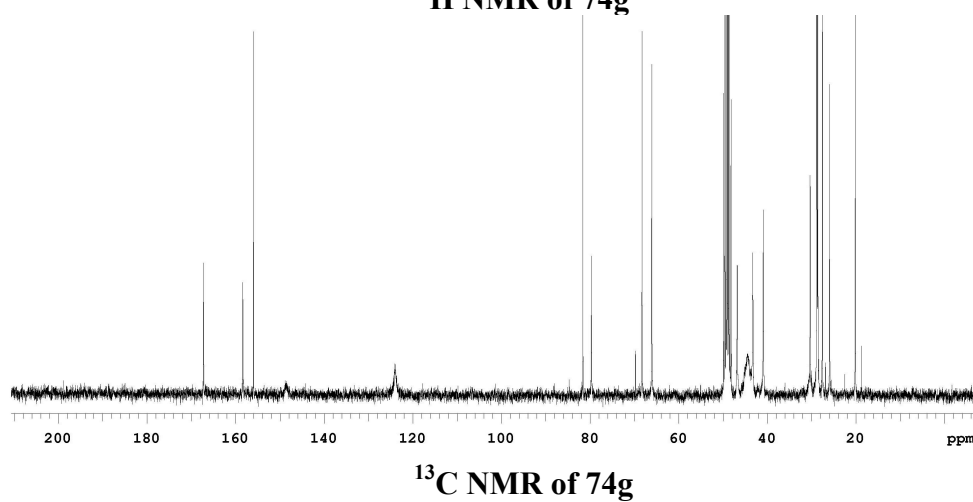
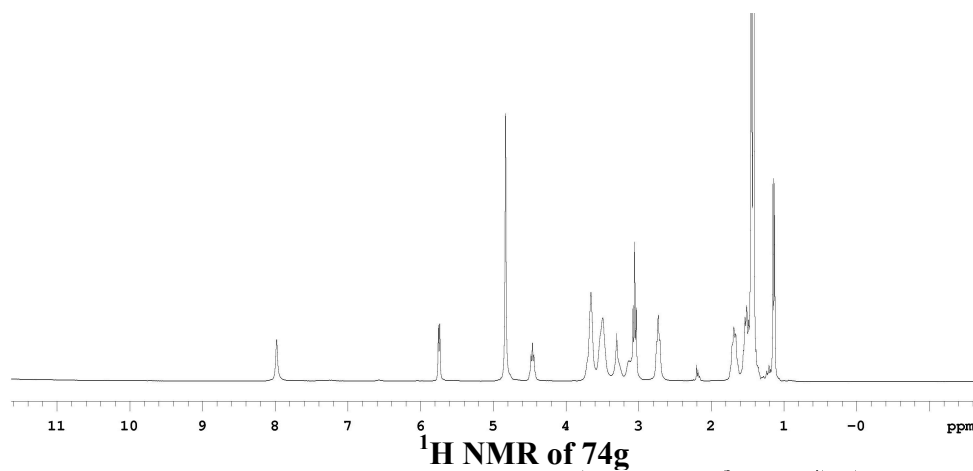


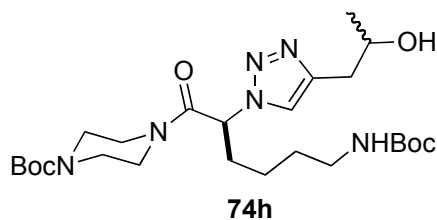
Compound **74g** was prepared from **73c** and Boc protected hexynyl amine. Flash chromatography (3 % MeOH in CH<sub>2</sub>Cl<sub>2</sub>) afforded **74g** (1.14 g, 71%) as a white solid.

<sup>1</sup>H NMR (CD<sub>3</sub>OD) δ 7.98 (s, 1H), 5.74 (d, 1H, J = 5.7 Hz), 4.83 (s, 2H), 4.46 (m, 1H), 3.66-3.12 (m, 8H), 3.05 (t, 2H, J = 6.6 Hz), 2.73 (m, 2H), 1.67 (m, 2H), 1.54 (m, 2H), 1.48 (s, 9H), 1.44 (s, 9H), 1.13 (d, 3H, J = 6.3 Hz)

<sup>13</sup>C NMR (CD<sub>3</sub>OD) δ 167.2, 158.3, 156.0, 148.3, 124.0, 81.6, 79.7, 68.3, 66.1, 46.8, 44.0, 43.3, 40.9, 30.3, 28.8, 28.6, 27.6, 25.9, 20.1

MS (ESI, m/z) 511 (M+H)<sup>+</sup>



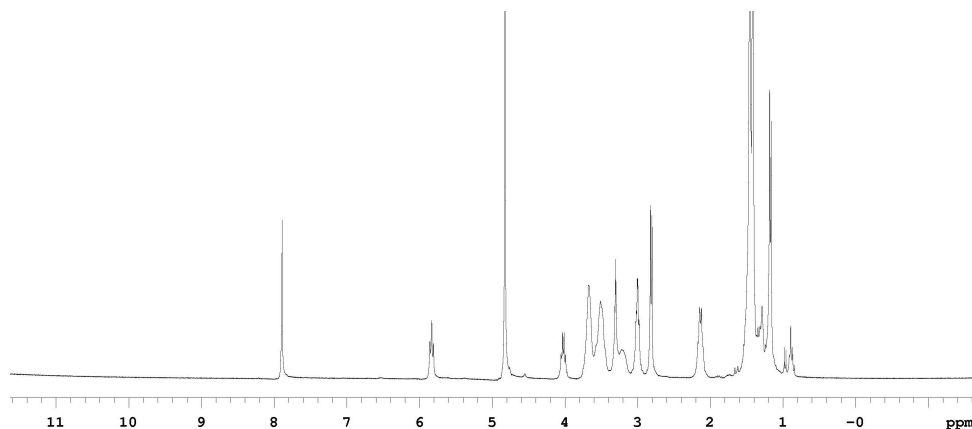


Compound **74h** was prepared from **73c** and *tert*-Boc protected hexynyl amine. Flash Chromatography (3 % MeOH in CH<sub>2</sub>Cl<sub>2</sub>) afforded **74h** (1.28 g, 92%) as a white solid.

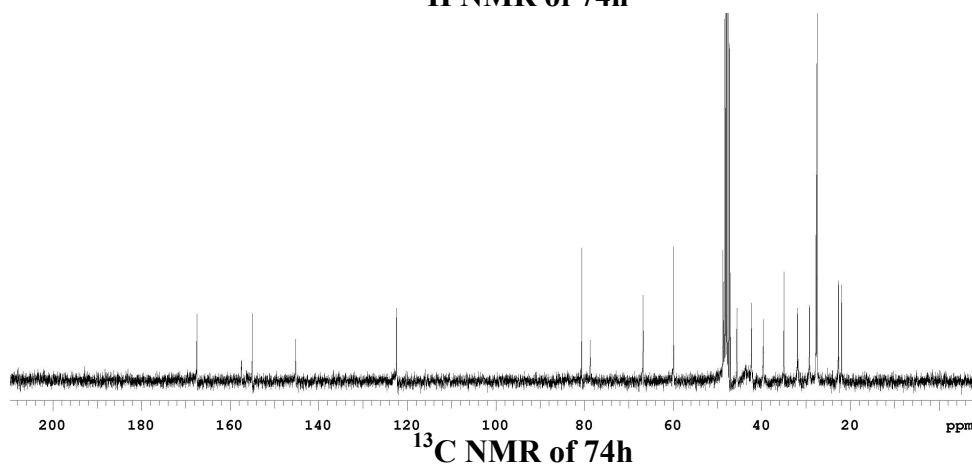
**<sup>1</sup>H NMR (CD<sub>3</sub>OD)** δ 7.93 (s, 1H), 5.88 (t, 1H, J = 7.2 Hz), 4.05 (m, 1H), 3.71-3.05 (m, 8H), 2.86 (m, 2H), 2.84 (d, 2H, J = 6.3 Hz), 2.14 (m, 2H), 1.39 (m, 11H), 1.27 (m, 11H), 1.20 (d, 3H, J = 6.3 Hz)

**<sup>13</sup>C NMR (CD<sub>3</sub>OD)** δ 167.5, 157.4, 155.0, 145.2, 122.4, 80.6, 78.7, 66.8, 59.9, 45.6, 44.0, 42.3, 39.6, 35.0, 31.9, 29.2, 27.7, 27.5, 22.7, 21.9

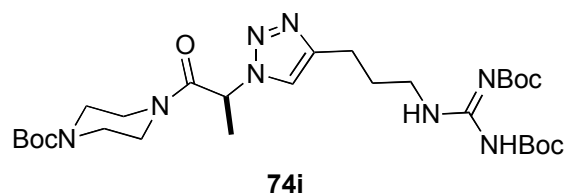
**MS (ESI, m/z)** 531 (M+Li)<sup>+</sup>



**<sup>1</sup>H NMR of 74h**



**<sup>13</sup>C NMR of 74h**

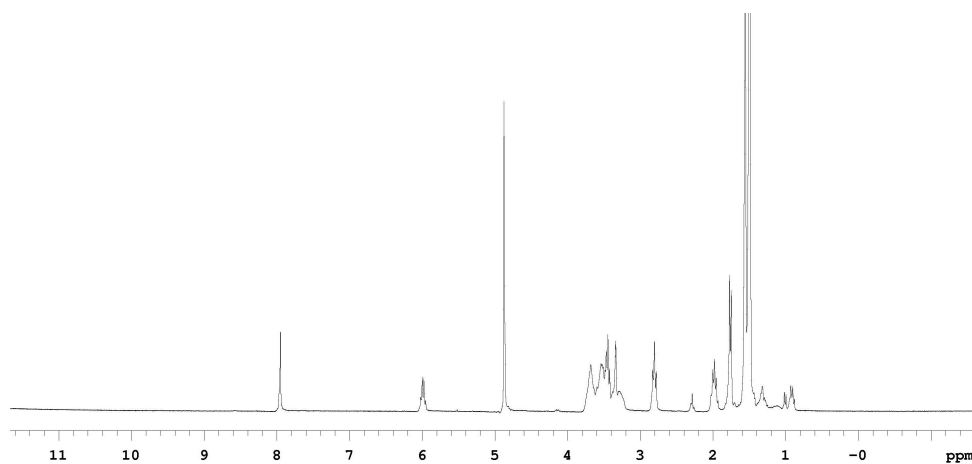


Compound **74i** was prepared from **73d** and **79**. Flash chromatography (60 % EtOAc in hexanes) afforded **74i** (1.13 g, 77%) as a white solid.

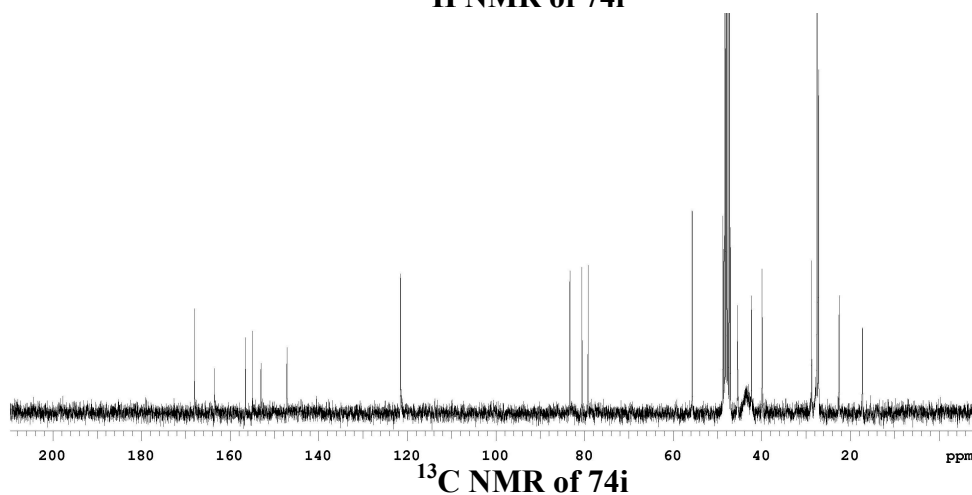
$^1\text{H NMR}$  ( $\text{CD}_3\text{OD}$ )  $\delta$  7.95 (s, 1H), 6.00 (q, 1H,  $J = 6.6$  Hz), 3.68-3.34 (m, 10H), 2.83 (t, 2H,  $J = 7.5$  Hz), 1.80 (m, 2H), 1.76 (d, 3H,  $J = 6.6$  Hz), 1.74 (s, 9H), 1.54 (s, 9H)

$^{13}\text{C NMR}$  ( $\text{CD}_3\text{OD}$ )  $\delta$  168.0, 163.5, 156.5, 155.0, 153.0, 147.2, 121.5, 83.3, 80.6, 79.2, 55.7, 45.4, 44.0, 42.3, 40.0, 28.7, 27.4, 27.1, 22.5, 17.2

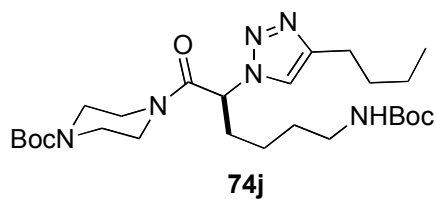
$\text{MS}$  (ESI,  $m/z$ ) 609 ( $\text{M}+\text{H}$ ) $^+$



$^1\text{H NMR}$  of **74i**



$^{13}\text{C NMR}$  of **74i**

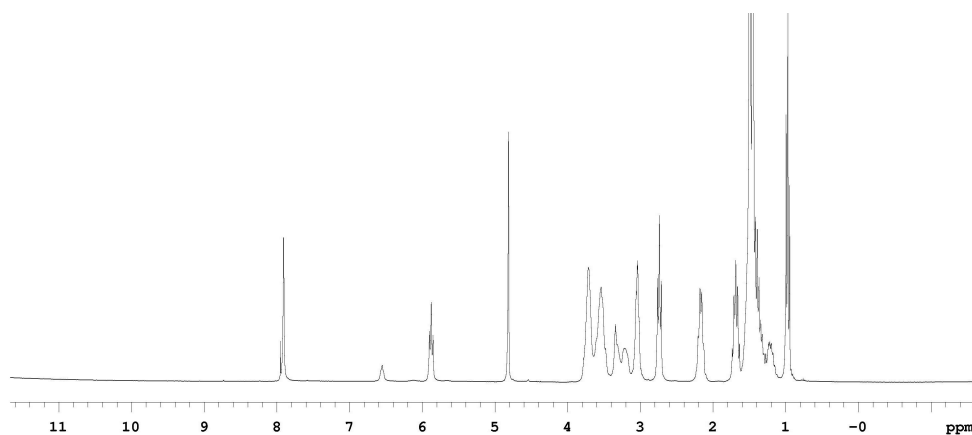


Compound **74j** was prepared from **73b** and n-hexyne. Flash chromatography (40 % EtOAc in hexanes) afforded **74j** (1.89 g, 94%) as a white foam like solid.

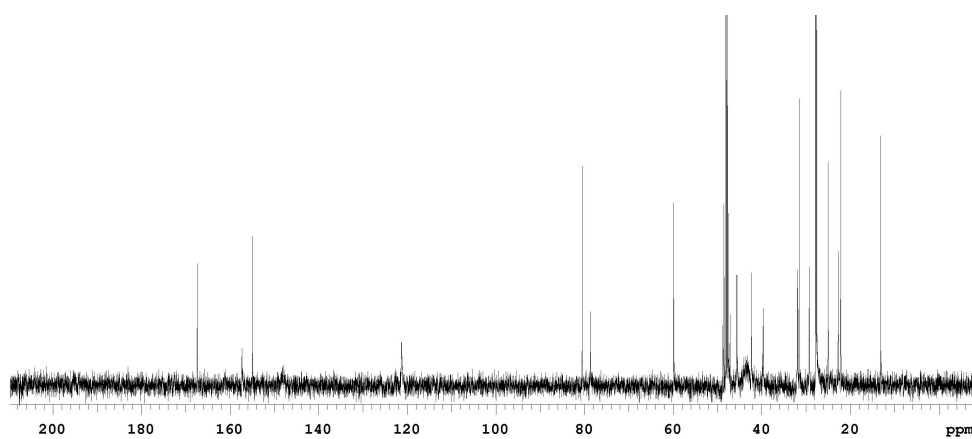
$^1\text{H NMR}$  ( $\text{CD}_3\text{OD}$ )  $\delta$  7.91 (s, 1H), 5.87 (t, 1H,  $J = 7.2$  Hz), 3.72-3.33 (m, 8H), 3.04 (t, 2H,  $J = 7.5$  Hz), 2.74 (t, 2H,  $J = 7.2$  Hz), 2.18 (m, 2H), 1.69 (2H)

$^{13}\text{C NMR}$  ( $\text{CD}_3\text{OD}$ )  $\delta$  167.4, 157.3, 154.9, 121.3, 80.5, 78.6, 59.9, 47.1, 45.6, 44.0, 42.3, 39.7, 31.9, 31.6, 29.3, 27.8, 27.6, 25.0, 22.7, 22.1, 13.1

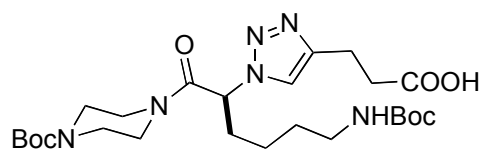
$\text{MS (ESI, } m/z) 523 (M+H)^+$



$^1\text{H NMR}$  of **74j**



$^{13}\text{C NMR}$  of **74j**

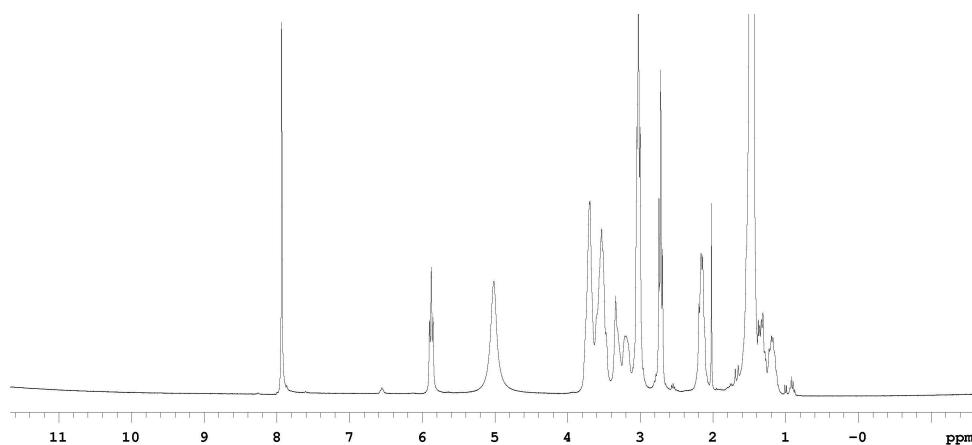
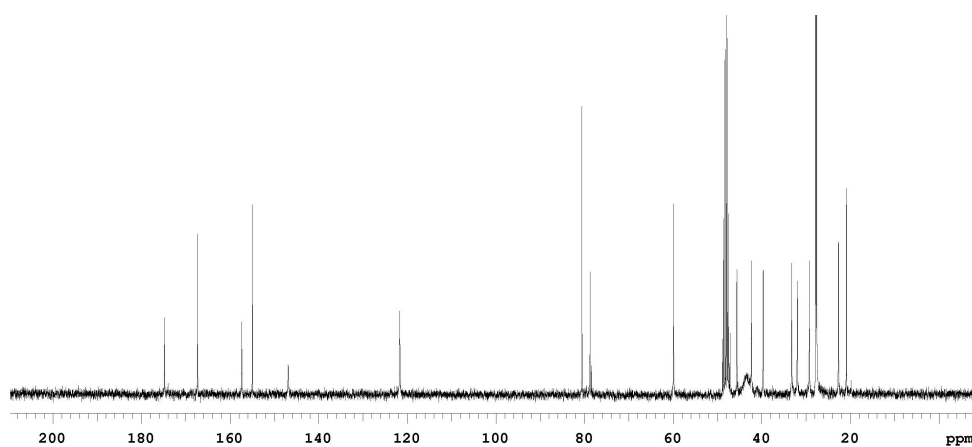
**74k**

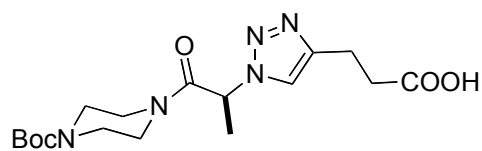
Compound **74k** was prepared from **73b** and 4-pentynoic acid. Flash chromatography (5 % MeOH in CH<sub>2</sub>Cl<sub>2</sub>) afforded **74k** (1.60 g, 87%) as yellow foam like solid.

<sup>1</sup>H NMR (CD<sub>3</sub>OD) δ 7.91 (s, 1H), 5.87 (t, 1H, J = 7.2 Hz), 3.72-3.33 (m, 8H), 3.04 (t, 2H, J = 7.5 Hz), 2.74 (t, 2H, J = 7.2 Hz), 2.18 (m, 2H), 1.69 (2 Hz)

<sup>13</sup>C NMR (CD<sub>3</sub>OD) δ 167.4, 157.3, 154.9, 121.3, 80.5, 78.6, 59.9, 47.1, 45.6, 44.0, 42.3, 39.7, 31.9, 31.6, 29.3, 27.8, 27.6, 25.0, 22.7, 22.1, 13.1

MS (ESI, m/z) 537 (M-H)<sup>+</sup>

<sup>1</sup>H NMR of **74k**<sup>13</sup>C NMR of **74k**

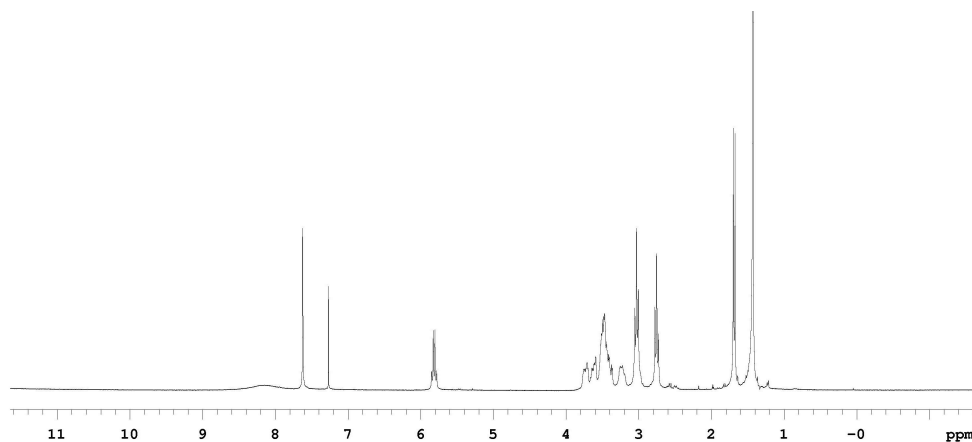
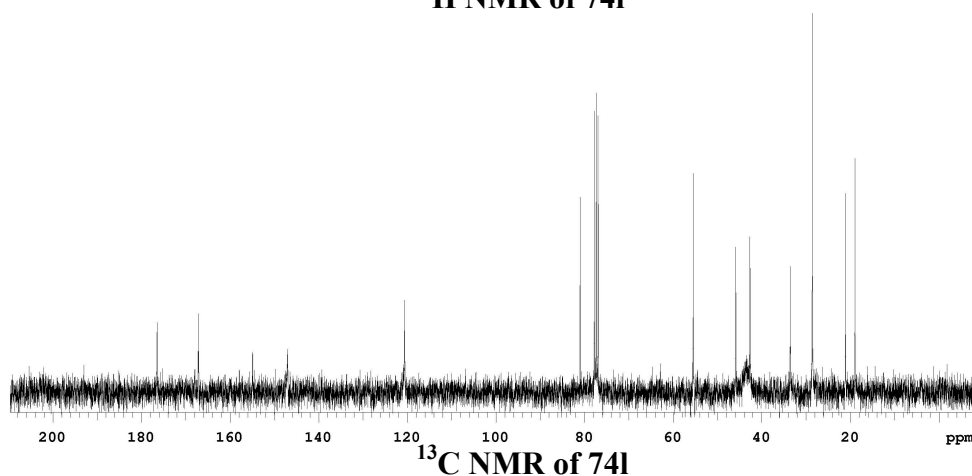
**74I**

Compound **74I** was prepared from **73d** and 4-pentynoic acid. Flash chromatography (5 % MeOH in CH<sub>2</sub>Cl<sub>2</sub>) afforded **74I** (0.80 g, 87%) as yellow foam like solid.

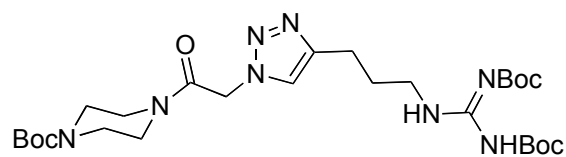
**<sup>1</sup>H NMR (CDCl<sub>3</sub>)** δ 7.62 (b, 1H), 7.27 (s, 1H), 5.81 (q, 1H, J = 7.2 Hz), 3.75-3.20 (m, 8H), 3.03 (t, 2H, J = 7.2 Hz), 2.75 (t, 2H, J = 7.2 Hz), 1.68 (d, 3H, J = 7.2 Hz), 1.43 (s, 9H)

**<sup>13</sup>C NMR (CDCl<sub>3</sub>)** δ 176.4, 167.1, 154.9, 146.9, 120.6, 80.9, 55.4, 45.8, 43.9, 42.6, 33.5, 28.6, 21.1, 18.9

**MS (ESI, m/z)** 380 (M-H)<sup>+</sup>

**<sup>1</sup>H NMR of 74I****<sup>13</sup>C NMR of 74I**



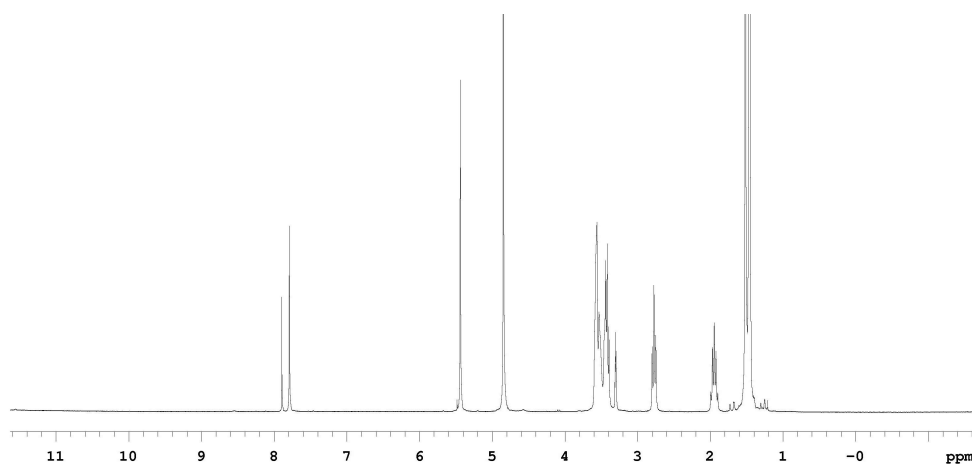
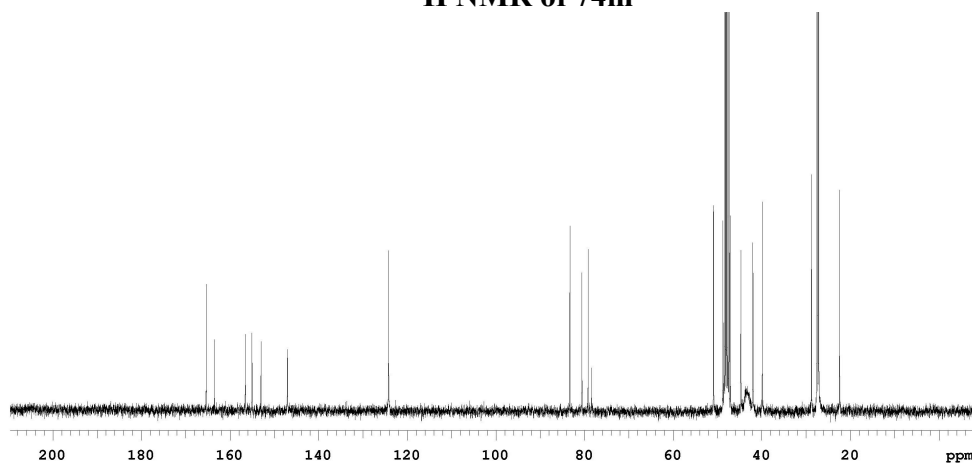
**74m**

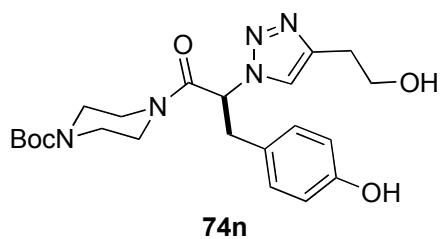
Compound **74m** was prepared from **73g** and **79**. Flash chromatography (60 % EtOAc in hexanes) afforded **5m** (1.9 g, 86%) as a white solid.

$^1\text{H NMR}$  ( $\text{CD}_3\text{OD}$ )  $\delta$  7.89 (s, 1H), 7.79 (s, 1H), 5.44 (s, 2H), 3.56-3.30 (m, 10H), 2.77 (t, 2H,  $J = 7.5$  Hz), 1.94 (m, 2H), 1.52 (s, 9H), 1.46 (s, 18H)

$^{13}\text{C NMR}$  ( $\text{CD}_3\text{OD}$ )  $\delta$  165.3, 163.4, 156.5, 155.0, 153.0, 147.0, 124.2, 83.3, 80.6, 79.2, 50.9, 44.7, 43.5, 42.0, 39.8, 28.8, 27.5, 27.1, 22.4

$\text{MS}$  (ESI,  $m/z$ ) 595 ( $\text{M}+\text{H}$ ) $^+$

 $^1\text{H NMR}$  of **74m** $^{13}\text{C NMR}$  of **74m**

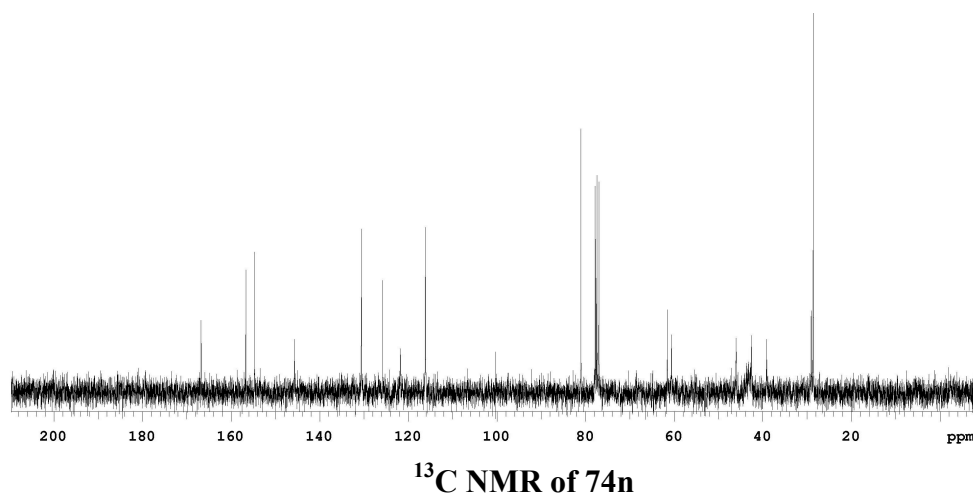
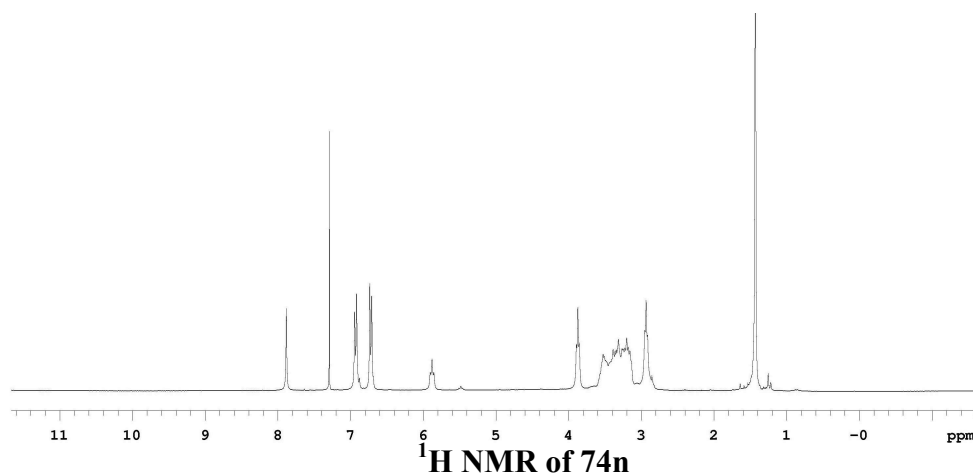


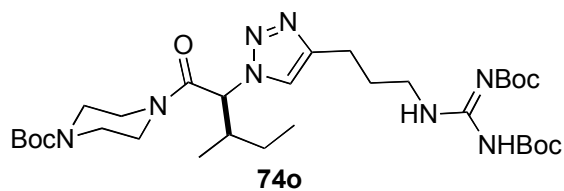
Compound **74n** was prepared from **73e** and 4-butynol. Flash chromatography (40 % EtOAc in hexanes) afforded **74n** (0.30 g, 89%) as a white solid.

$^1\text{H NMR}$  ( $\text{CDCl}_3$ )  $\delta$  7.88 (s, 1H), 6.92 (d, 2H,  $J = 8.4$  Hz), 6.72 (d, 2H,  $J = 8.4$  Hz), 5.88 (t, 1H,  $J = 7.8$  Hz), 3.87 (t, 2H,  $J = 6.0$  Hz), 3.52-3.16 (m, 9H), 2.93 (m, 3H), 1.43 (s, 9H)

$^{13}\text{C NMR}$  ( $\text{CDCl}_3$ )  $\delta$  166.8, 156.6, 154.7, 145.7, 130.6, 125.8, 121.8, 116.1, 81.0, 61.5, 60.6, 46.0, 43.8, 42.5, 39.1, 28.6

$\text{MS (ESI, } m/z)$  446 ( $\text{M}+\text{H}$ ) $^+$



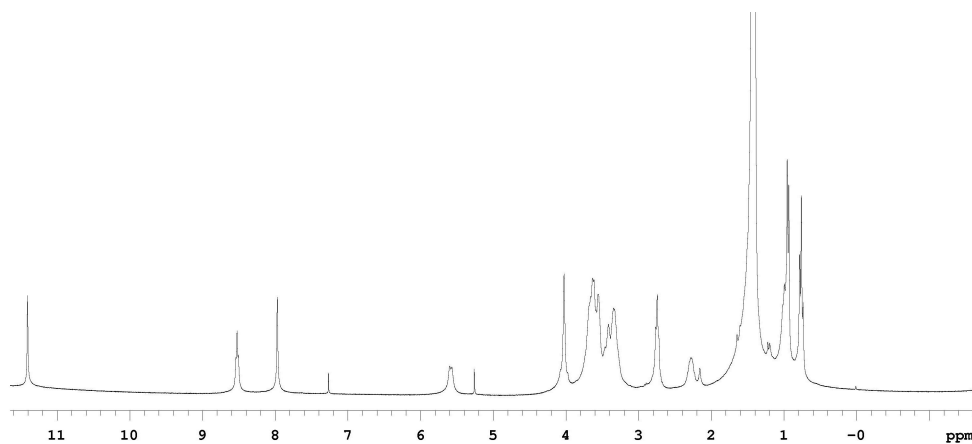


Compound **74o** was prepared from **73a** and **79**. Flash chromatography (40 % EtOAc in hexanes) afforded **74o** (2.00 g, 96%) as a white solid.

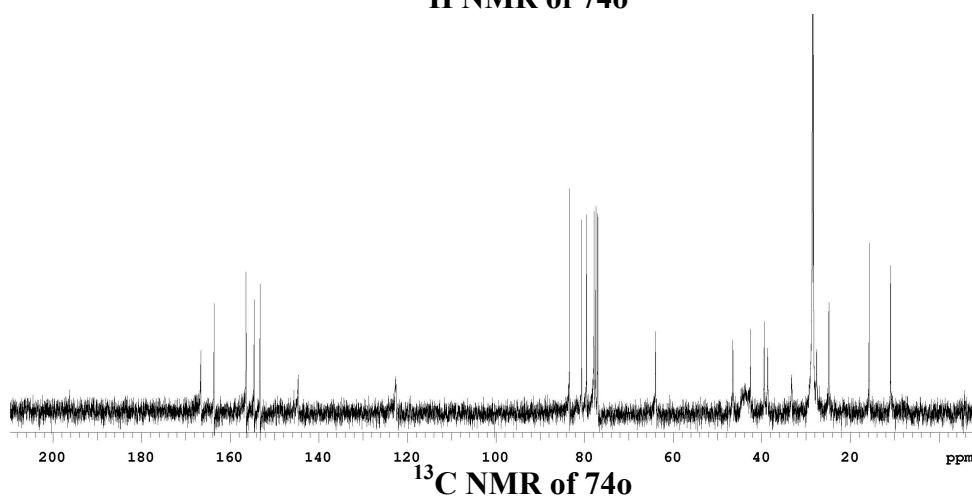
**<sup>1</sup>H NMR (CDCl<sub>3</sub>)** δ 11.44 (s, 1H), 8.36 (s, 1H), 7.62 (s, 1H), 5.33 (d, 1H, J = 9.9 Hz), 3.61-3.11 (m, 10H), 2.71 (m, 2H), 2.32 (s, 1H), 1.93 (m, 2H), 1.43 (s, 18H), 1.32 (s, 9H), 0.94(m, 5H), 0.74 (m, 3H)

**<sup>13</sup>C NMR (CDCl<sub>3</sub>)** δ 166.9, 163.7, 156.4, 154.5, 153.4, 147.6, 119.8, 83.2, 80.5, 79.3, 63.4, 53.7, 46.2, 43.8, 42.4, 40.4, 37.9, 28.8, 28.4, 28.2, 24.6, 23.3, 15.9, 10.6

**MS (ESI, m/z)** 651 (M+H)<sup>+</sup>



**<sup>1</sup>H NMR of 74o**



**<sup>13</sup>C NMR of 74o**

**General Procedure for Preparation of Fluorescent Labeled Monomers.** Boc-protected monomeric compounds **74a-o** (1.0 eq.) were treated with 30% TFA in CH<sub>2</sub>Cl<sub>2</sub>, stirred in sealed glass vials for 4h and solvent was removed. The resulting residue was dissolved in THF (0.1 M) and DTAF (1.0 equiv.) and K<sub>2</sub>CO<sub>3</sub> (4.0 eq.) were added. The suspension was stirred for 2 h and solvent was removed. The crude product **76a-o** was used for the next step without further purification. Analytical HPLC and MALDI MS were used to check the purities of these crude samples.

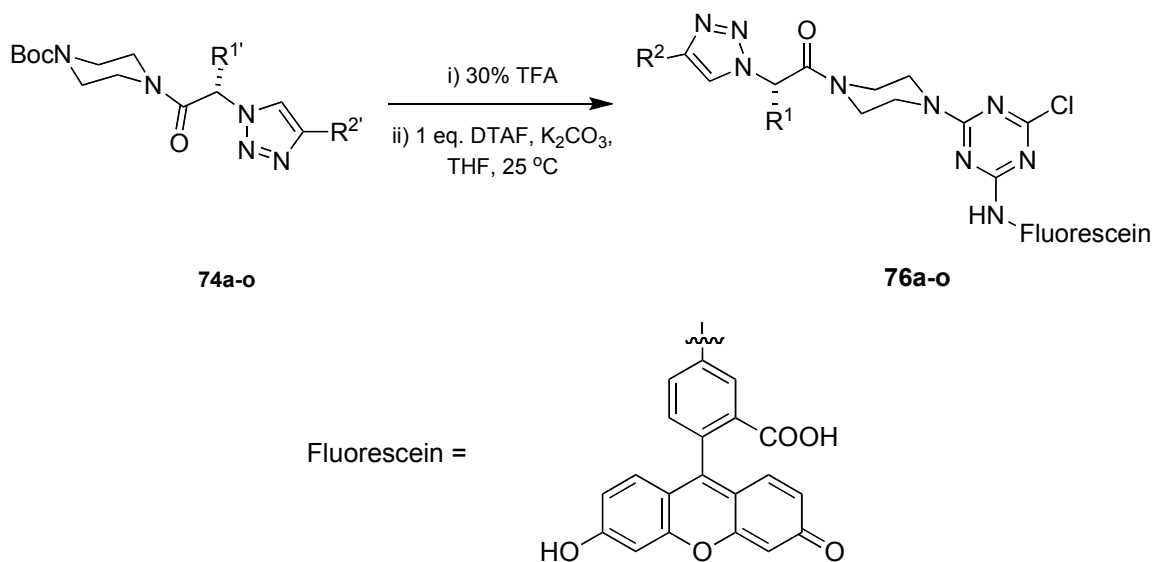


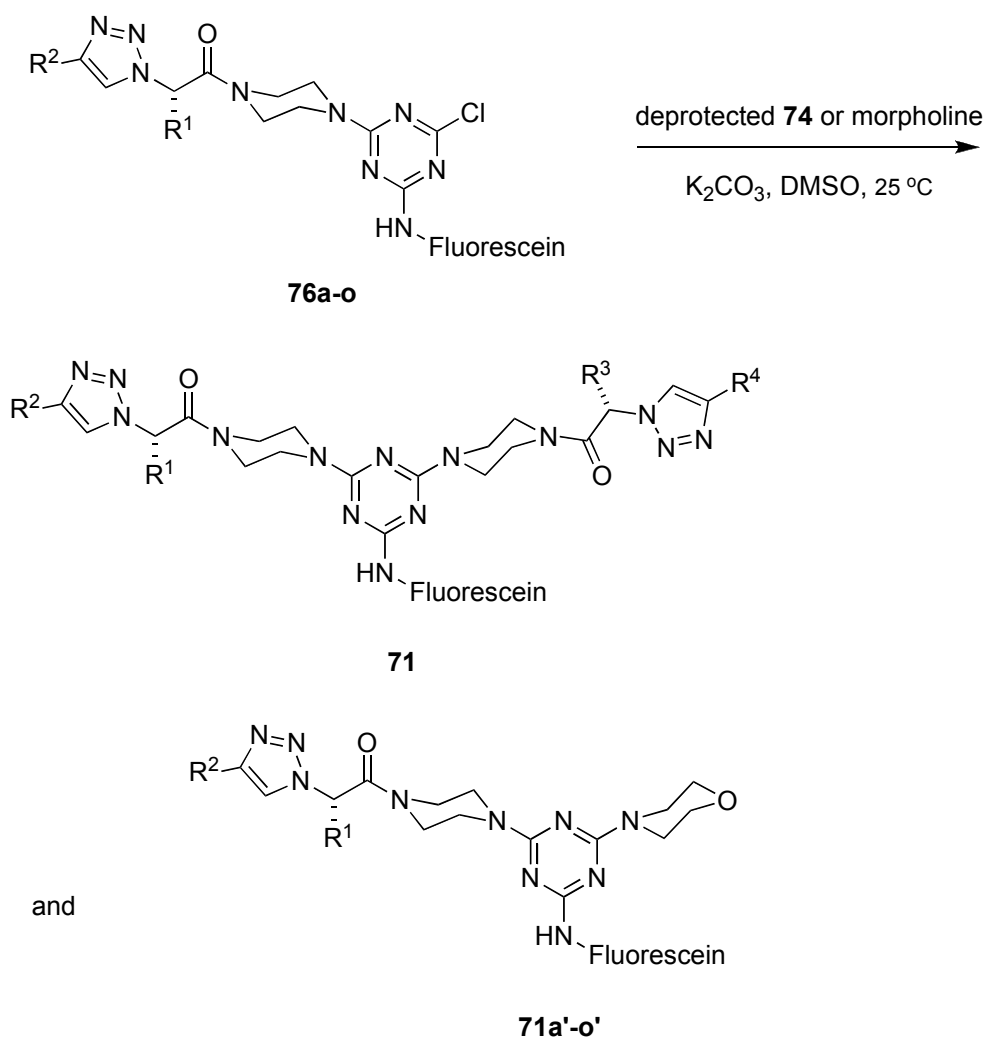
**Table B1.** Characterization of crude compounds **76a-o**.

Comp'd <b>76</b>	MALDI-MS		HPLC Purity (%)	
	Calc'd	Found	UV	Sedex
<b>a</b>	781	781	94	92
<b>b</b>	725	725	100	100
<b>c</b>	782	782	91	98
<b>d</b>	698	698	91	92
<b>e</b>	712	712	95	100
<b>f</b>	740	740	92	95
<b>g</b>	769	769	92	95
<b>h</b>	783	783	87	92
<b>i</b>	767	767	100	100
<b>j</b>	781	781	91	100
<b>k</b>	797	797	94	100
<b>l</b>	740	740	100	100
<b>m</b>	753	753	93	100
<b>n</b>	804	804	88	100
<b>o</b>	809	809	100	100

**Preparation of Fluorescent Labeled Dimers 71 and Monomers 71a'-o'.**

Dimerization was carried out in 2 ml glass vials. The monomeric compounds **74a-o** were treated with 30% TFA/CH<sub>2</sub>Cl<sub>2</sub> for 4 h. Stock solutions of **76** (0.03 M) and deprotected **74** (0.03 M) or morpholine (0.33 M) in DMSO were prepared. One stock solution of **76** (0.5 ml) and one of deprotected **74** (0.5 ml) or morpholine (0.5 ml) were added to a glass vial and followed with solid K<sub>2</sub>CO<sub>3</sub> (*ca* 20 mg). The reaction vial was sealed and sonicated for 15 min. The reaction mixture was agitated at 25 °C for 48 h then the DMSO was lyophilized. Aqueous HCl solution (5%, *ca* 0.5 ml) was added to the above solid residue and sonicated for 3 min. Most of the compounds were precipitated in the acidic aqueous solution and they were transferred to a 15 mL centrifuge tube and centrifuged for 15 min and the aqueous solution was carefully removed with a glass pipette. The solid products were dried under vacuum 14 h to give the final products **71**. Some of the compounds with monovalent units like **g**, **h** and **k** are

highly water-soluble. The aqueous solution of these compounds were lyophilized and redissolved in 0.5 ml MeOH. The inorganic salts were precipitated out and removed. The MeOH solution was then concentrated to give compounds **71**. All crude products were analyzed by analytical HPLC (5-95% B in 30 min) and MALDI-MS.



**Data for 71o'**

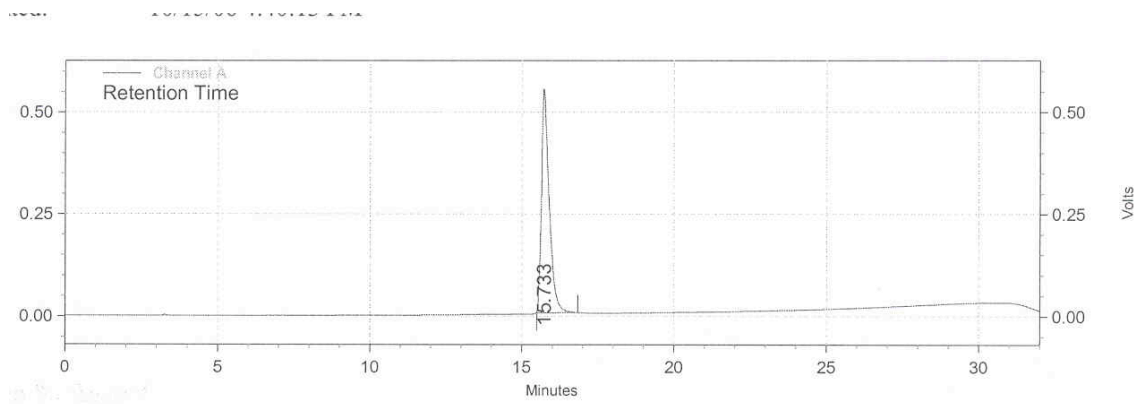
**<sup>1</sup>H NMR (500 MHz, DMSO-d<sub>6</sub>)** δ 9.72 (s, 1H), 8.39 (s, 1H), 8.03 (d, 1H, J = 6.0 Hz), 7.99 (s, 1H), 7.66 (t, 1H, 6.0 Hz), 7.15 (d, 1H, J = 8.5 Hz), 6.67 (d, 2H, J = 2.0 Hz), 6.62 (d, 2H, J = 8.5 Hz), 6.56 (dd, 2H, J = 8.5 Hz, 2.0 Hz), 5.69 (d, 1H, J = 9.0 Hz), 3.99-3.60 (m, 16H), 3.15 (m, 2H), 2.65 (t, 2H, J = 7.5 Hz), 2.30 (m, 1H), 1.80 (m, 2H), 0.95 (m, 5H), 0.77 (t, 3H, J = 7.5 Hz)

**<sup>13</sup>C NMR (500 MHz, DMSO-d<sub>6</sub>)** δ 168.9, 166.3, 164.4, 163.9, 159.5, 157.7, 156.9, 156.8, 151.9, 146.2, 145.0, 142.0, 129.1, 126.8, 124.0, 121.1, 113.3, 112.6, 109.9, 102.2, 66.0, 62.9, 45.2, 43.4, 43.1, 42.9, 41.6, 37.8, 28.2, 24.1, 22.1, 15.0, 10.5

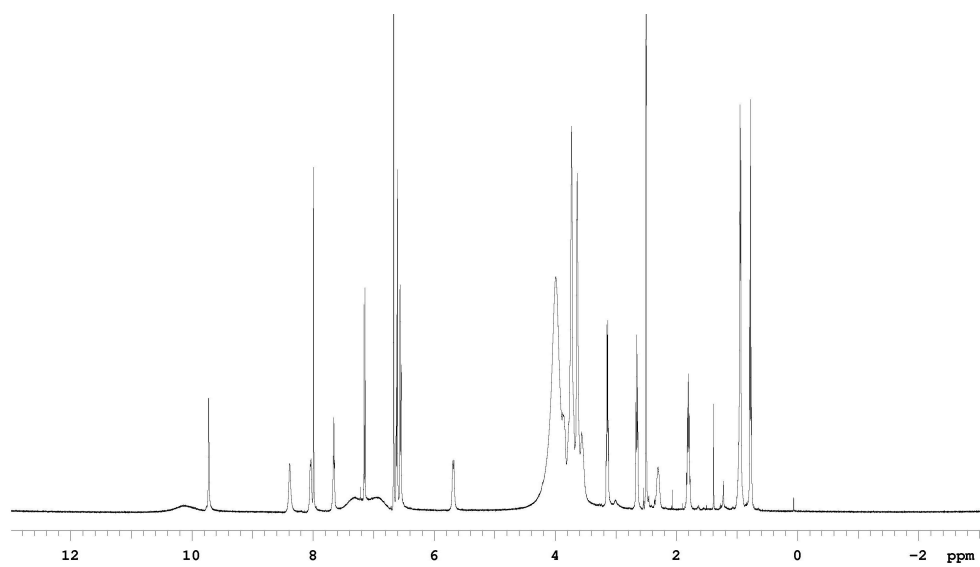
**MS (MALDI, m/z)** 860 (M+H)<sup>+</sup>

**Analytical HPLC (UV)** purity 100%, retention time = 16.73 min

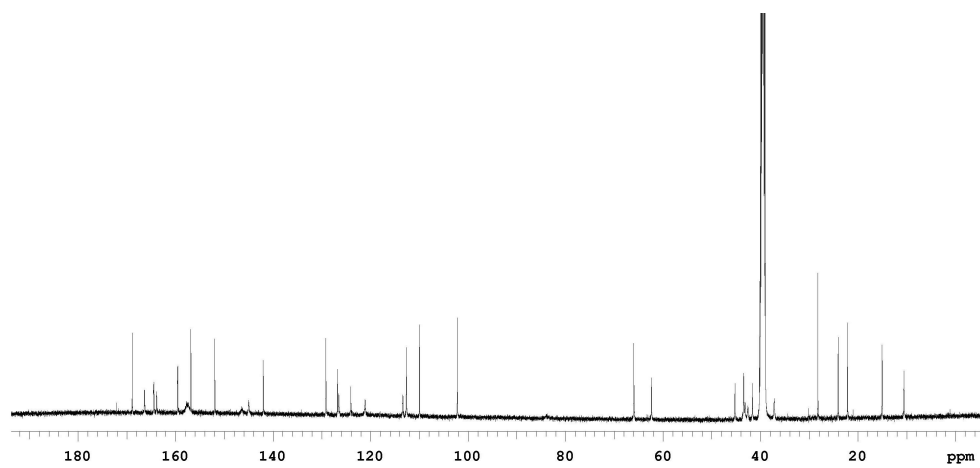
**Analytical HPLC (Sedex)** purity 100%, retention time = 16.78 min



**UV HPLC of Compound 71o'**

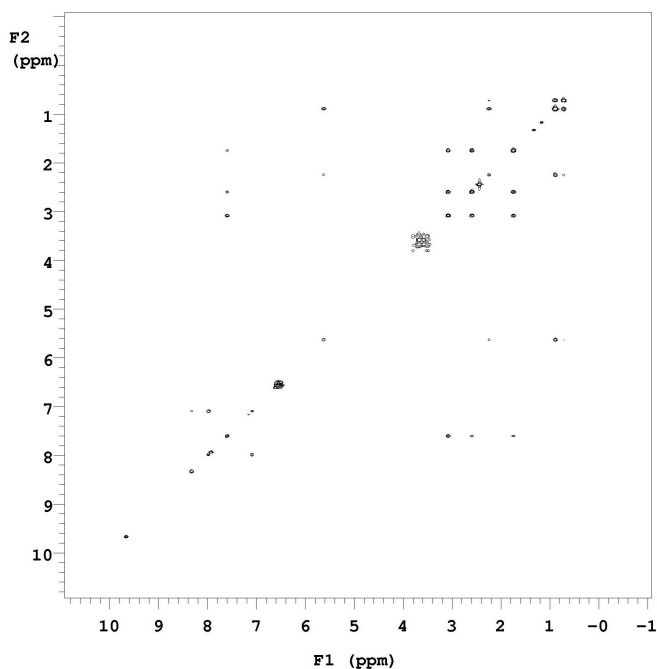


$^1\text{H}$  NMR of Compound 71o'



$^{13}\text{C}$  NMR of Compound 71o'





**TOCSY of Compound 71o'**

**Data for 71gi**

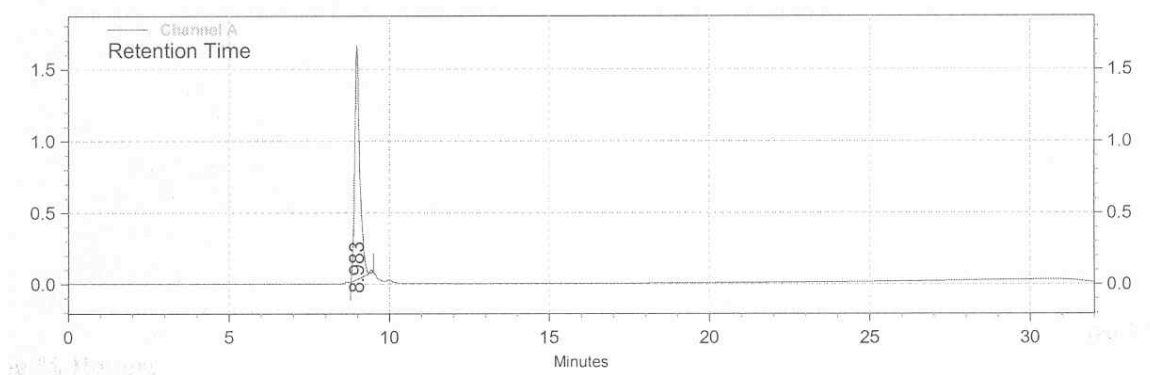
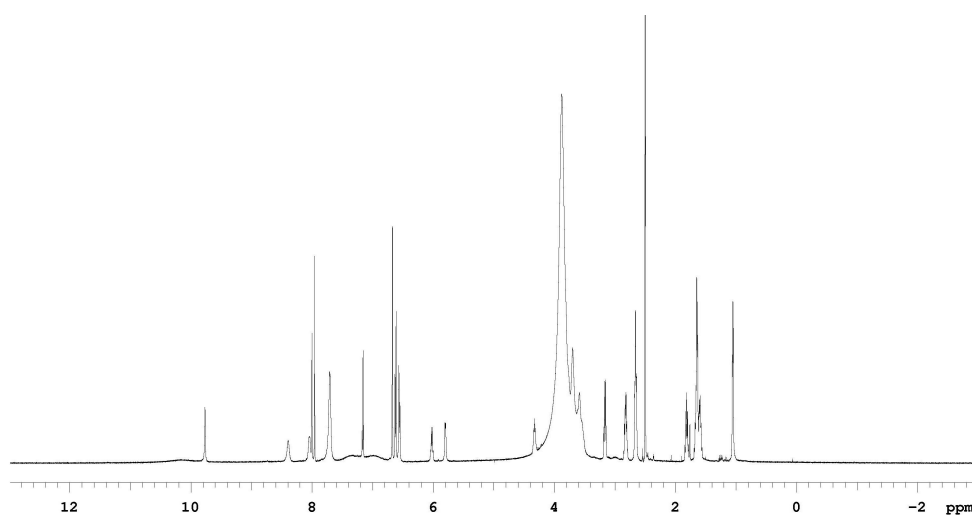
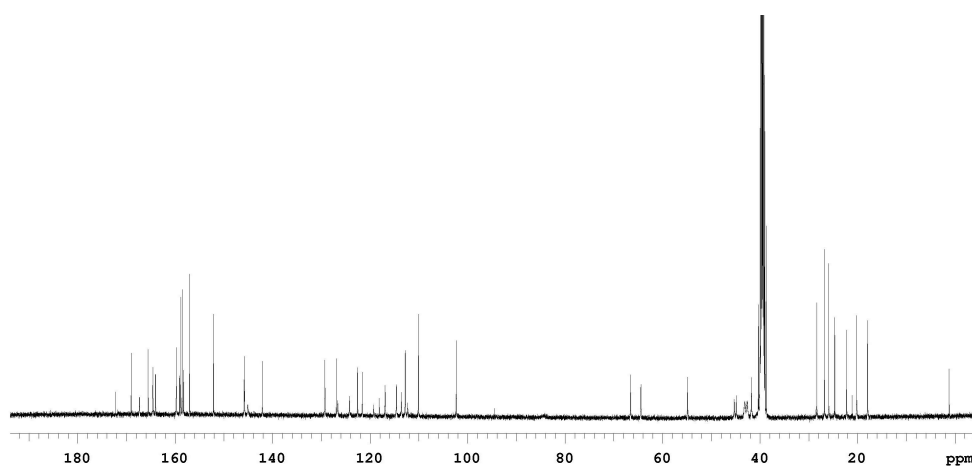
**$^1\text{H}$  NMR (500 MHz, DMSO- $d_6$ )**  $\delta$  9.77 (s, 1H), 8.39 (s, 1H), 8.04 (d, 1H,  $J = 2.0$  Hz), 8.00 (s, 1H), 7.95 (s, 1H), 7.71 (m, 4H), 7.17 (d, 1H,  $J = 8.5$  Hz), 6.67 (d, 2H,  $J = 2.5$  Hz), 6.63 (d, 2H,  $J = 8.5$  Hz), 6.56 (dd, 2H,  $J = 8.5$  Hz, 2.5 Hz), 6.03 (q, 1H,  $J = 7.0$  Hz), 5.80 (d, 1H,  $J = 5.0$  Hz), 4.33 (t, 1H,  $J = 6.0$  Hz), 3.90-3.60 (m, 16H), 3.17 (t, 2H,  $J = 6.5$  Hz), 2.81 (t, 2H,  $J = 6.5$  Hz), 2.65 (m, 4H), 1.80 (m, 2H), 1.64 (m, 5H), 1.61 (m, 2H), 1.05 (d, 3H,  $J = 6.0$  Hz)

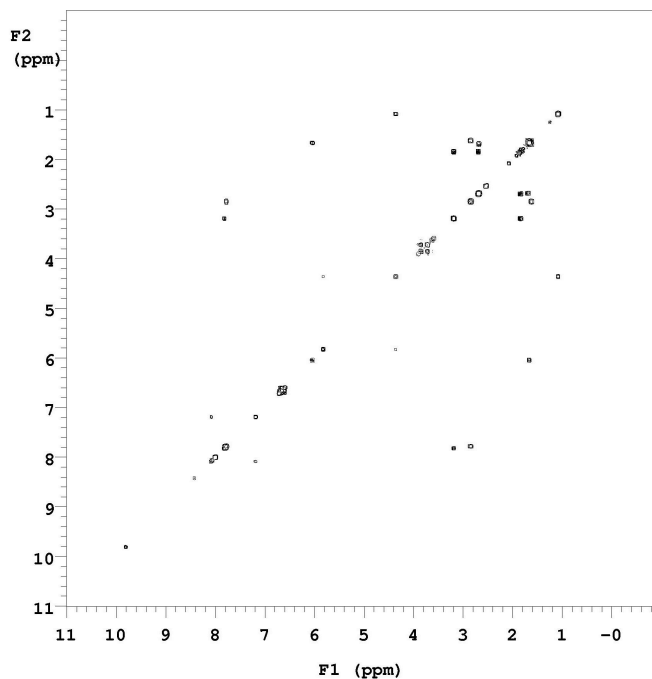
**$^{13}\text{C}$  NMR (500 MHz, DMSO- $d_6$ )**  $\delta$  169.0, 167.3, 165.5, 164.5, 164.0, 159.7, 158.7 (q,  $J = 150$  Hz, from  $\text{CF}_3\text{COO}^-$ ), 157.0, 152.1, 145.9, 145.8, 145.1, 142.1, 129.3, 126.9, 126.6, 124.2, 122.6, 121.6, 119.2, 116.9, 114.6, 113.6, 112.8, 110.1, 102.3, 66.5, 64.4, 54.8, 45.3, 44.9, 43.1, 42.6, 41.7, 28.3, 26.8, 25.9, 24.6, 22.2, 20.2, 17.9

**MS (MALDI,  $m/z$ )** 1041 ( $\text{M}+\text{H}$ )<sup>+</sup>

**Analytical HPLC (UV)** purity 98%, retention time = 8.98 min

**Analytical HPLC (Sedex)** purity 100%, retention time = 9.02 min

**UV HPLC of Compound 71gi** **$^1\text{H}$  NMR of Compound 71gi** **$^{13}\text{C}$  NMR of Compound 71gi**



**COSY of Compound 71gi**

**Data for 71gm**

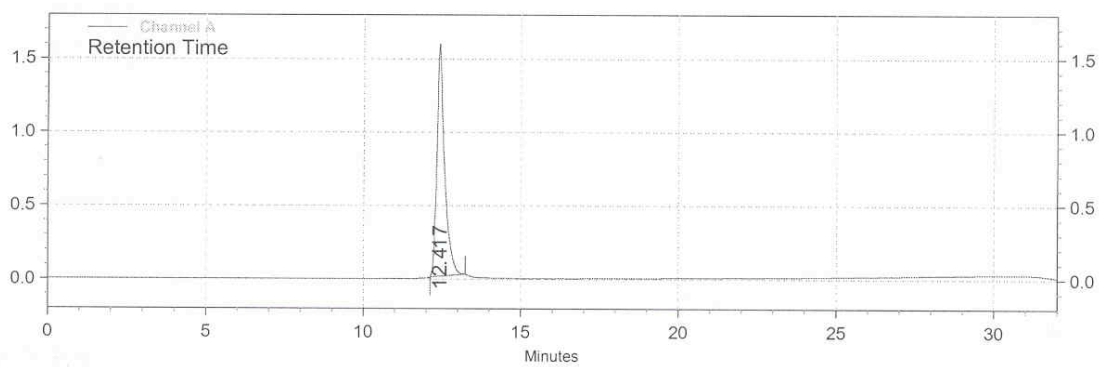
**<sup>1</sup>H NMR (500 MHz, DMSO-*d*<sub>6</sub>)** δ 9.77 (s, 1H), 8.41 (s, 1H), 8.05 (d, 2H, *J* = 2.0 Hz), 7.96 (s, 1H), 7.80 (s, 1H), 7.71 (bs, 2H), 7.17 (d, 1H, *J* = 8.5 Hz), 6.66 (d, 2H, *J* = 2.5 Hz), 6.63 (d, 2H, *J* = 8.5 Hz), 6.56 (dd, 2H, *J* = 8.5 Hz, 2.5 Hz), 5.81 (d, 1H, *J* = 6.0 Hz), 5.48 (s, 2H), 4.33 (m, 1H), 4.04-3.57 (m, 16H), 3.18 (dd, 2H, *J* = 6.0 Hz, 7.0 Hz), 2.83 (t, 2H, *J* = 7.0 Hz), 2.67 (m, 4H), 1.82 (m, 2H), 1.67 (m, 2H), 1.62 (m, 2H), 1.06 (d, 3H, *J* = 6.0 Hz)

**<sup>13</sup>C NMR (500 MHz, DMSO-*d*<sub>6</sub>)** δ 169.0, 165.5, 164.7, 164.5, 164.0, 159.7, 158.7 (q, *J* = 150 Hz, from CF<sub>3</sub>COO<sup>-</sup>), 157.0, 152.1, 145.8, 145.7, 145.1, 142.1, 129.3, 126.9, 126.7, 124.2, 123.9, 122.6, 119.2, 117.0, 114.7, 113.6, 112.8, 110.1, 102.3, 66.5, 64.4, 50.7, 45.3, 44.1, 42.7, 41.7, 41.4, 28.4, 26.7, 25.9, 24.6, 22.1, 20.2

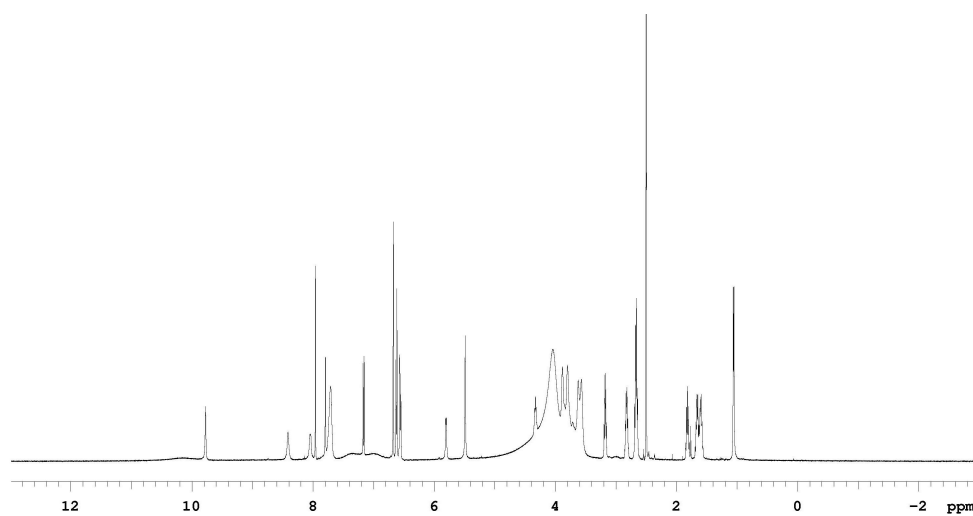
**MS (MALDI, *m/z*)** 1027 (M+H)<sup>+</sup>

**Analytical HPLC (UV) purity 100%, retention time = 12.42 min**

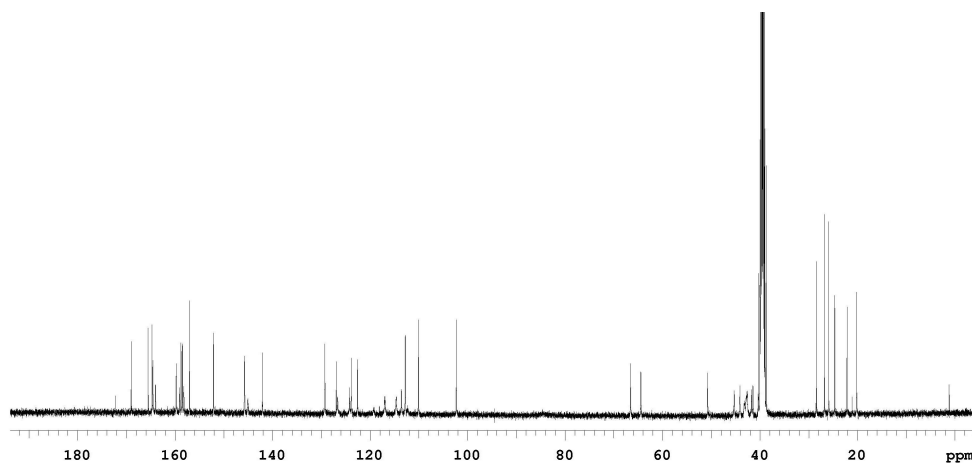
**Analytical HPLC (Sedex) purity 100%, retention time = 12.47 min**



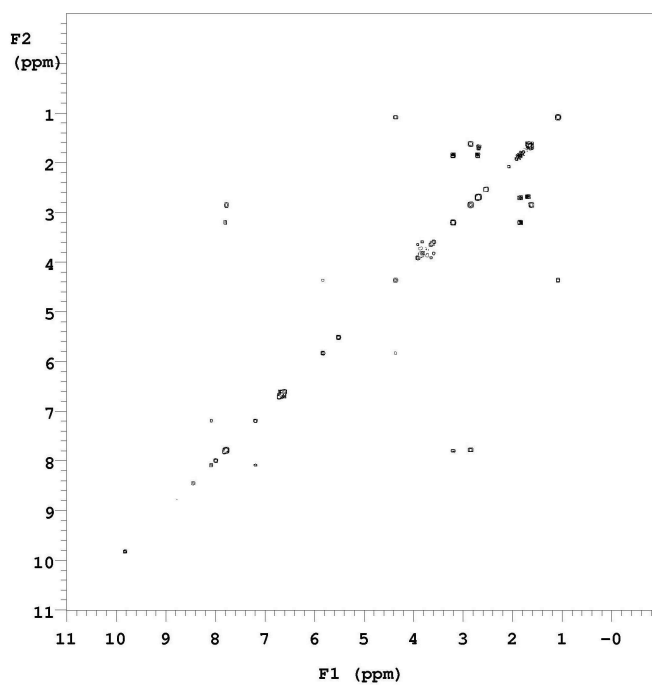
**UV HPLC for Compound 71gm**



**<sup>1</sup>H NMR of Compound 71gm**



$^{13}\text{C}$  NMR of Compound 71gm



COSY of Compound 71gm

**Data for 71gn**

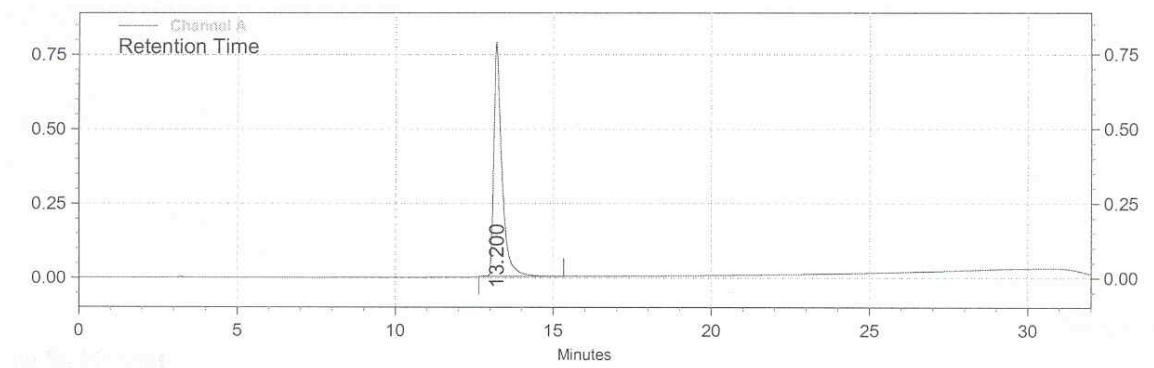
**$^1\text{H}$  NMR (500 MHz, DMSO- $d_6$ )**  $\delta$  9.75 (s, 1H), 8.37 (s, 1H), 8.02 (m, 3H), 7.96 (s, 1H), 7.68 (bs, 2H), 7.17 (d, 1H,  $J = 9.0$  Hz), 7.03 (d, 2H,  $J = 8.5$  Hz), 6.67 (d, 2H,  $J = 2.0$  Hz), 6.63 (m, 3H), 6.55 (d, 2H,  $J = 8.5$  Hz), 6.06 (m, 1H), 5.79 (d, 1H,  $J = 6.0$  Hz), 4.33 (m, 1H), 3.90-3.60 (m, 18H), 3.31 (m, 1H), 3.21 (m, 1H), 2.82 (dd, 2H,  $J = 6.5$  Hz, 6.0 Hz), 2.75 (t, 2H,  $J = 7.0$  Hz), 2.66 (t, 2H,  $J = 7.0$  Hz), 1.65 (m, 2H), 1.61 (m, 2H), 1.06 (d, 3H,  $J = 6.0$  Hz)

**$^{13}\text{C}$  NMR (500 MHz, DMSO- $d_6$ )**  $\delta$  169.0, 166.3, 165.5, 164.5, 164.4, 163.9, 159.8, 158.7 (q,  $J = 150$  Hz, from  $\text{CF}_3\text{COO}^-$ ), 156.4, 152.2, 145.8, 145.0, 142.1, 130.5, 129.3, 126.9, 126.6, 125.8, 124.3, 122.6, 122.2, 119.2, 116.7, 115.2, 114.6, 113.7, 112.9, 110.2, 102.3, 66.6, 64.5, 60.5, 59.8, 45.3, 45.1, 43.2, 42.8, 41.8, 37.3, 29.3, 26.8, 25.9, 24.6, 20.2

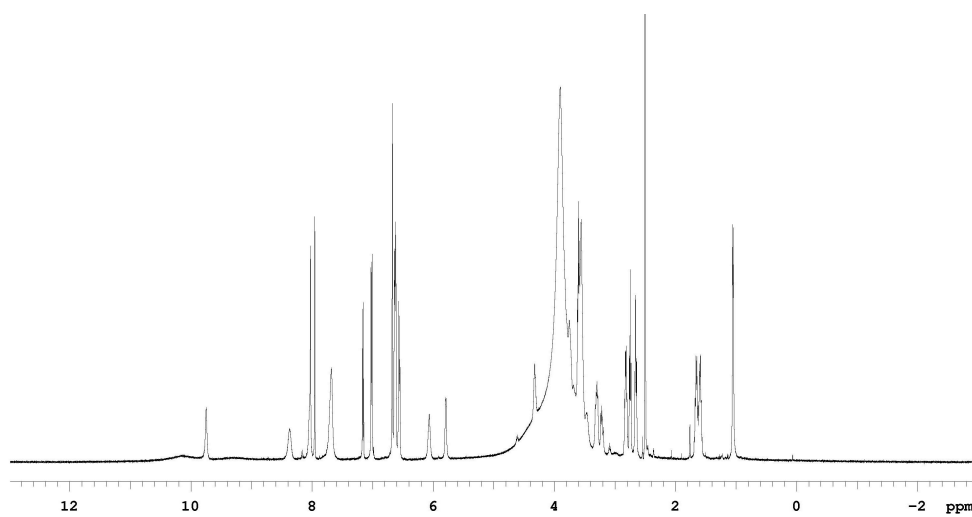
**MS (MALDI,  $m/z$ )** 1078 ( $\text{M}+\text{H}$ ) $^+$

**Analytical HPLC (UV)** purity 100%, retention time = 13.20 min

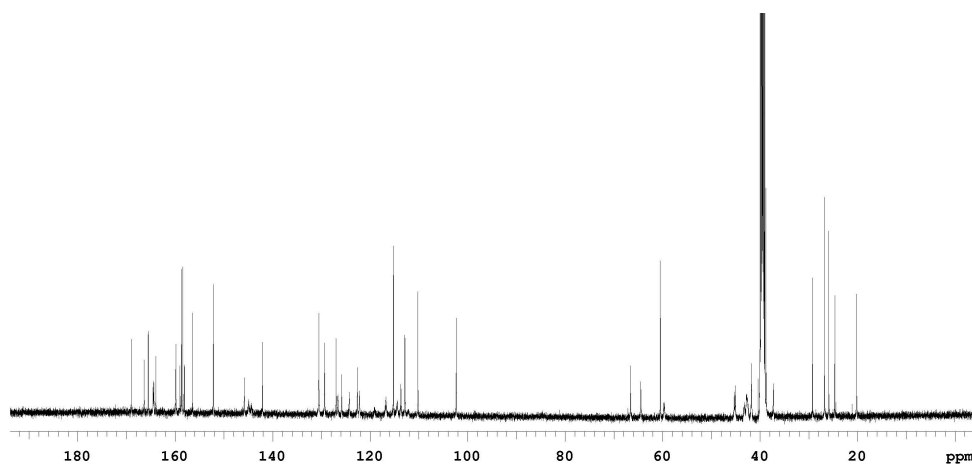
**Analytical HPLC (Sedex)** purity 100%, retention time = 13.24 min



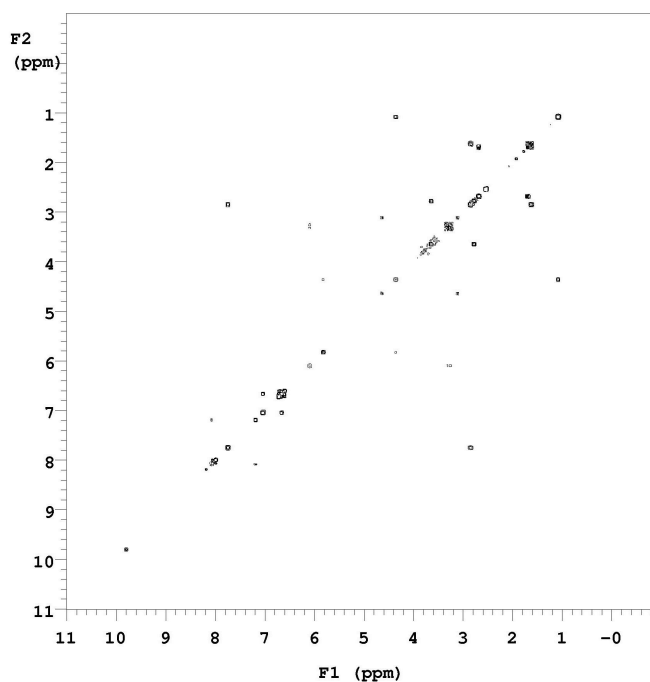
**UV HPLC of Compound 71gn**



$^1\text{H}$  NMR of Compound 71gn



$^{13}\text{C}$  NMR of Compound 71gn



**COSY of Compound 71gn**

**Data for 71gj**

**$^1\text{H}$  NMR (500 MHz, DMSO- $d_6$ )**  $\delta$  9.76 (s, 1H), 8.39 (s, 1H), 8.03 (m, 1H), 7.96 (s, 1H), 7.95 (s, 1H), 7.72 (bs, 2H), 7.17 (d, 1H,  $J = 8.5$  Hz), 5.86 (m, 1H), 5.81 (d, 1H,  $J = 5.0$  Hz), 4.32 (m, 1H), 3.90-3.50 (m, 16H), 2.82 (dd, 2H,  $J = 13.0$  Hz, 6.5 Hz), 2.75 (m, 2H), 2.66 (t, 2H,  $J = 7.5$  Hz), 2.63 (t, 2H,  $J = 7.5$  Hz), 2.05 (m, 2H), 1.68 (m, 2H), 1.57 (m, 6H), 1.30 (m, 4H), 1.06 (d, 3H,  $J = 6.0$  Hz), 0.87 (t, 3H,  $J = 7.0$  Hz)

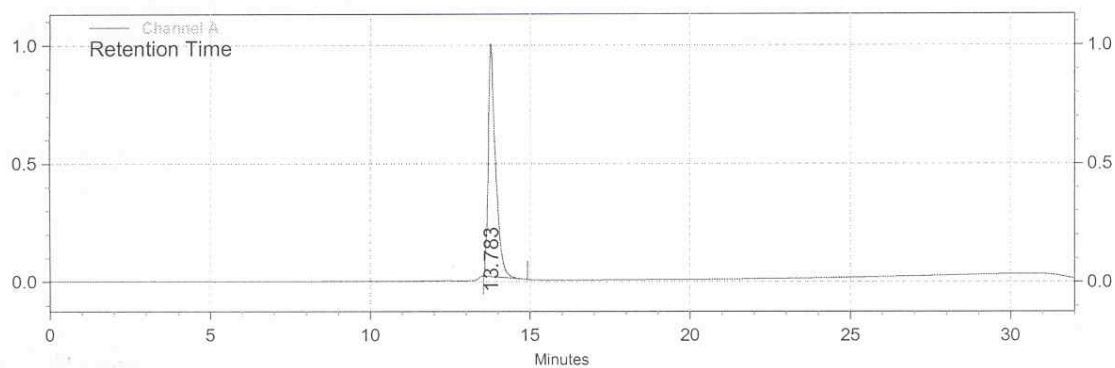
**$^{13}\text{C}$  NMR (500 MHz, DMSO- $d_6$ )**  $\delta$  169.0, 166.4, 165.5, 164.6, 164.1, 159.7, 158.7 (q,  $J = 150$  Hz, from  $\text{CF}_3\text{COO}^-$ ), 152.0, 147.1, 145.8, 145.2, 142.1, 129.2, 126.9, 126.6, 124.1, 122.5, 121.2, 119.8, 117.2, 114.9, 113.5, 112.7, 110.0, 102.3, 66.5, 64.4, 58.7, 45.2, 44.9, 43.1, 42.6, 41.8, 38.7, 31.4, 31.1, 26.7, 26.6, 25.9, 24.8, 24.6, 22.2, 21.7, 20.1, 13.7

**MS (MALDI,  $m/z$ )** 1055 ( $\text{M}+\text{H}$ ) $^+$

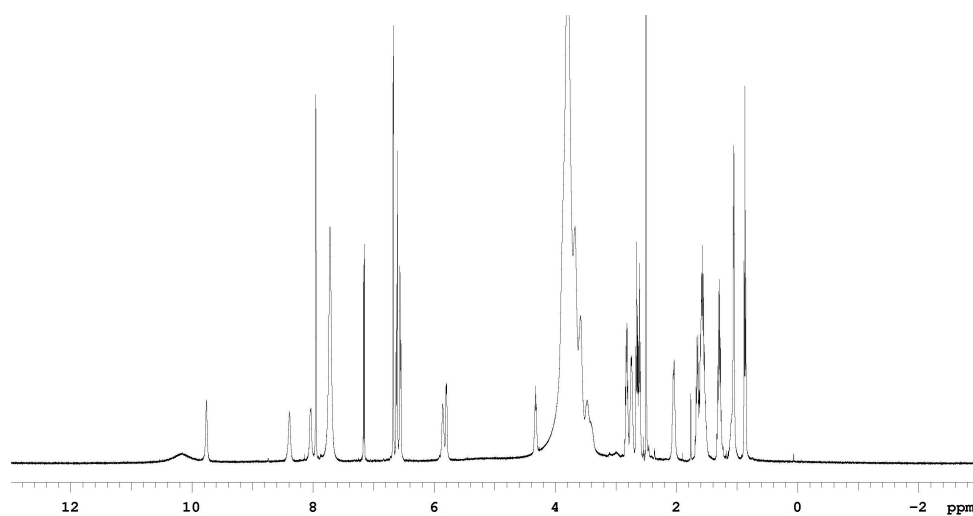
**Analytical HPLC (UV)** purity 100%, retention time = 13.78 min

**Analytical HPLC (Sedex)** purity 100%, retention time = 13.93 min

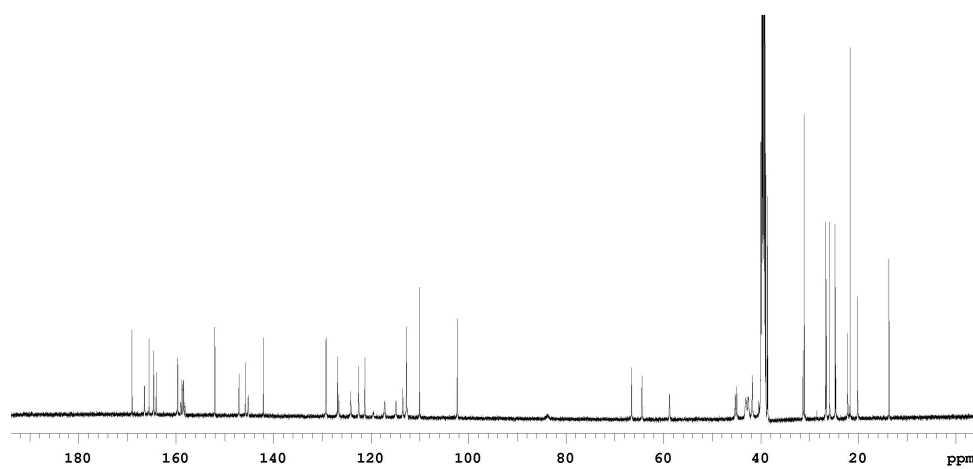




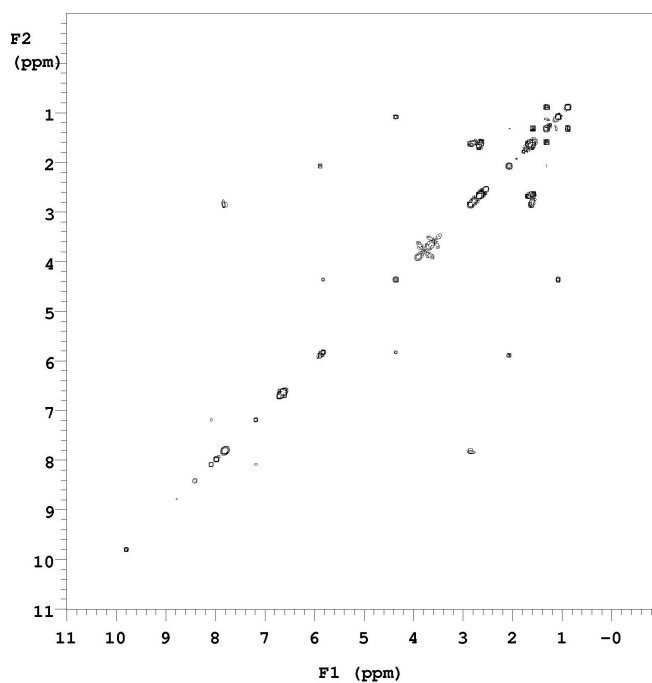
**UV HPLC of Compound 71gj**



**$^1\text{H}$  NMR of Compound 71gj**



**$^{13}\text{C}$  NMR of Compound 71gj**



**COSY of Compound 71gj**

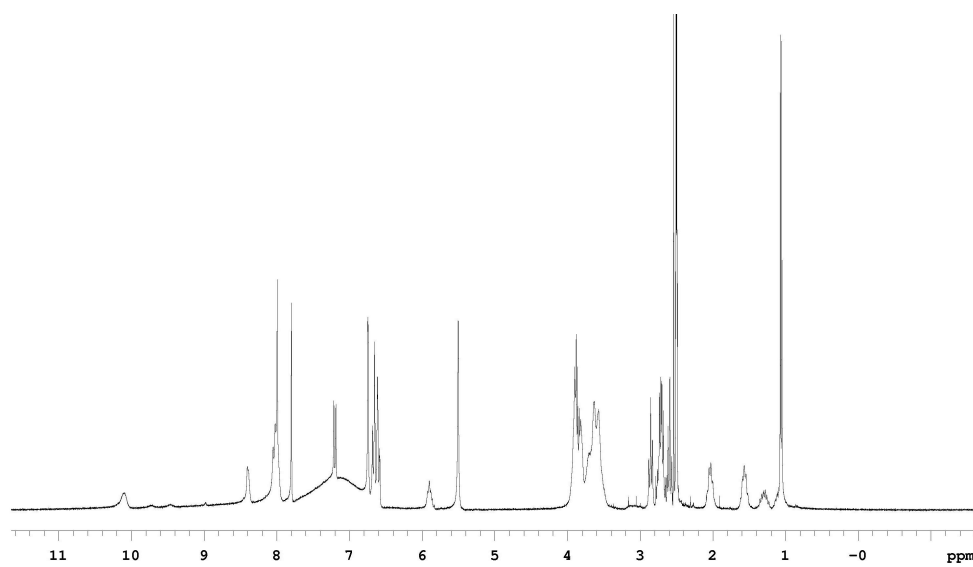
**Data for 71ek**

**$^1\text{H}$  NMR (300 MHz, DMSO- $d_6$ )**  $\delta$  10.10 (s, 1H), 8.40 (s, 1H), 8.05 (m, 2H), 8.02 (s, 2H), 7.80 (s, 1H), 7.20 (d, 1H,  $J = 8.4$  Hz), 6.74 (d, 2H,  $J = 1.8$  Hz), 6.66 (d, 2H,  $J = 8.4$  Hz), 6.59 (dd, 2H,  $J = 8.4$  Hz, 1.8 Hz), 5.90 (m, 1H), 5.5 (s, 2H), 3.90-3.60 (m, 14H), 2.86 (t, 2H,  $J = 7.5$  Hz), 2.70 (m, 2H), 2.59 (t, 2H,  $J = 7.5$  Hz), 2.03 (m, 2H), 1.57 (m, 2H), 1.30 (m, 1H), 1.06 (d, 3H,  $J = 8.4$  Hz)

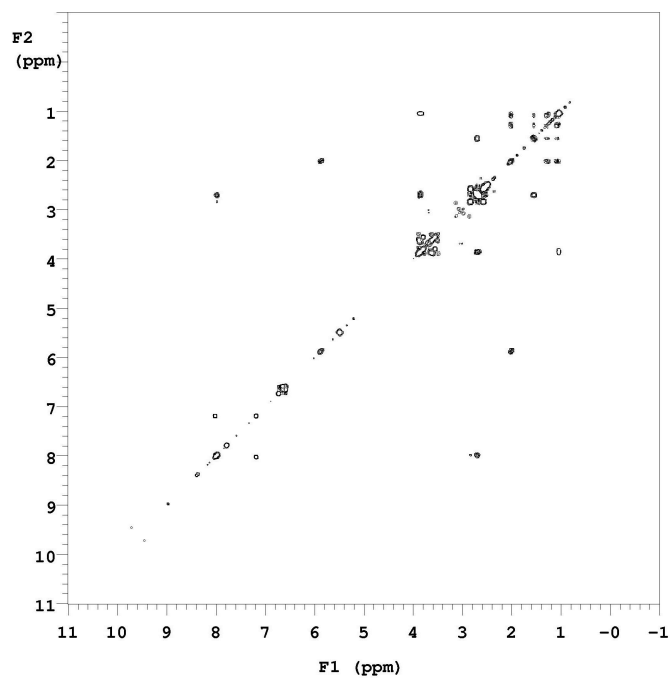
**MS (MALDI,  $m/z$ )** 1015 ( $M+H$ ) $^+$

**Analytical HPLC (UV)** purity 100%, retention time = 10.78 min

**Analytical HPLC (Sedex)** purity 100%, retention time = 10.93 min



$^1\text{H}$  NMR of 71ek



COSY NMR of 71ek

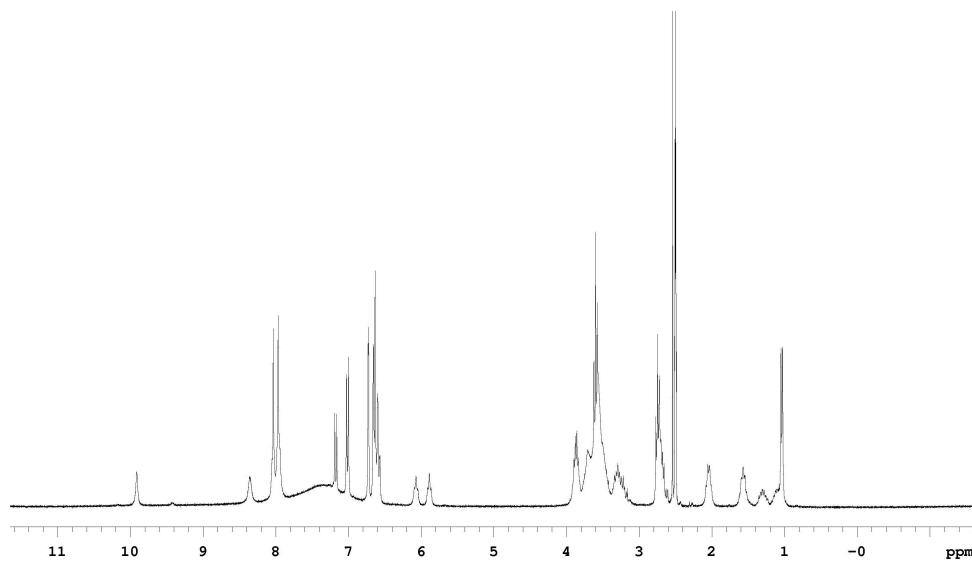
**Data for 71hn**

**<sup>1</sup>H NMR (300 MHz, DMSO-d<sub>6</sub>)** δ 9.91 (s, 1H), 8.36 (s, 1H), 8.03 (s, 2H), 7.91 (s, 2H), 7.18 (d, 1H, J = 8.4 Hz), 7.01 (d, 2H, J = 8.7 Hz), 6.73 (d, 2H, J = 2.1 Hz), 6.64 (d, 4H, J = 8.7), 6.61 (dd, 2H, J = 8.4 Hz, 2.1 Hz), 6.07 (t, 1H, J = 6.0 Hz), 5.89 (t, 1H, J = 6.0 Hz), 3.80-3.58 (m, 19H), 3.27 (m, 2H), 2.68 (m, 4H), 2.06 (m, 2H), 1.54 (m, 2H), 1.33 (m, 1H), 1.04 (m, 1H), 1.03 (d, 3H, J = 6.3 Hz)

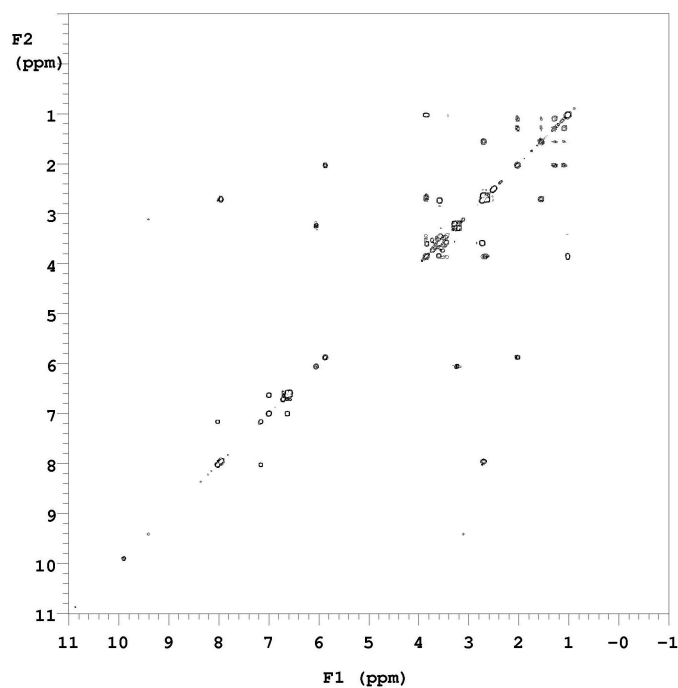
**MS (MALDI, m/z)** 1093 (M+H)<sup>+</sup>

**Analytical HPLC (UV)** purity 92%, retention time = 9.82 min

**Analytical HPLC (Sedex)** purity 100%, retention time = 9.97 min



**<sup>1</sup>H NMR of 71hn**



**COSY NMR of 71hn**

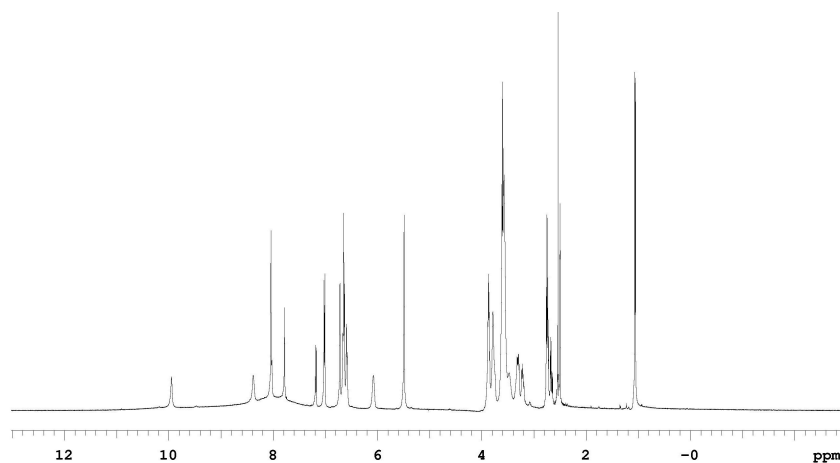
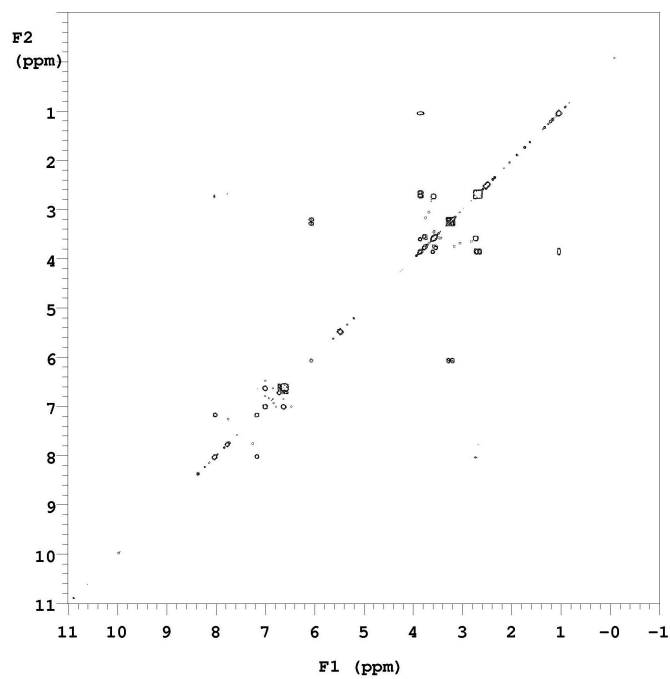
**Data for 71en**

**$^1\text{H}$  NMR (300 MHz, DMSO- $d_6$ )**  $\delta$  9.95 (s, 1H), 8.38 (s, 1H), 8.04 (s, 2H), 8.02 (s, 1H), 7.74 (s, 1H), 7.18 (d, 1H,  $J = 8.4$  Hz), 7.02 (d, 2H,  $J = 8.7$  Hz), 6.71 (d, 2H,  $J = 2.1$  Hz), 6.56 (d, 4H,  $J = 8.7$  Hz), 6.58 (dd, 2H,  $J = 8.4$  Hz, 2.1 Hz), 6.07 (t, 1H,  $J = 6.0$  Hz), 5.49 (s, 2H), 3.90-3.58 (m, 19H), 3.28 (m, 2H), 2.75 (m, 3H), 2.64 (dd, 1H,  $J = 14.4$  Hz, 6.3 Hz), 1.06 (d, 3H,  $J = 6.3$  Hz)

**MS (MALDI,  $m/z$ )** 1021 ( $M+H$ )<sup>+</sup>

**Analytical HPLC (UV)** purity 100%, retention time = 12.24 min

**Analytical HPLC (Sedex)** purity 100%, retention time = 9.40 min

 **$^1\text{H}$  NMR of 71en****COSY NMR of 71en**

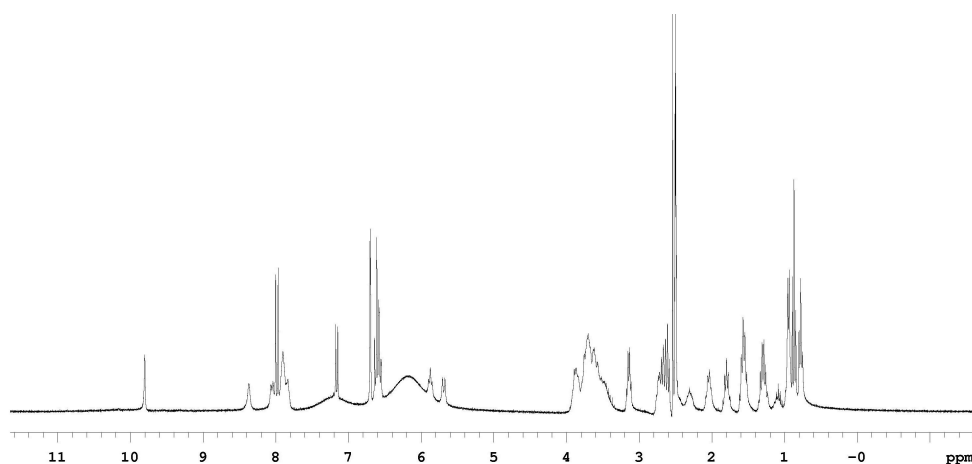
**Data for 71jo**

**<sup>1</sup>H NMR (300 MHz, DMSO-d<sub>6</sub>)** δ 9.80 (s, 1H), 8.37 (s, 1H), 8.06 (d, 1H, J = 8.4 Hz), 8.04 (s, 1H), 8.00 (s, 1H), 7.90 (b, 2H), 7.16 (d, 1H, J = 8.4 Hz), 6.70 (d, 2H, J = 2.1 Hz), 6.65 (d, 2H, J = 8.7 Hz), 6.55 (dd, 2H, J = 8.7 Hz, 2.1 Hz), 5.99 (t, 1H, J = 7.2 Hz), 5.68 (d, 1H, J = 9.6 Hz), 3.89-3.39 (m, 16H), 3.15 (m, 2H), 2.67 (m, 4H), 2.31 (m, 1H), 2.05 (m, 2H), 1.78 (m, 2H), 1.57 (m, 4H), 1.31 (m, 2H), 1.09 (m, 1H), 0.96 (m, 5H), 0.85 (t, 3H, J = 7.2 Hz), 0.78 (t, 3H, J = 7.2 Hz)

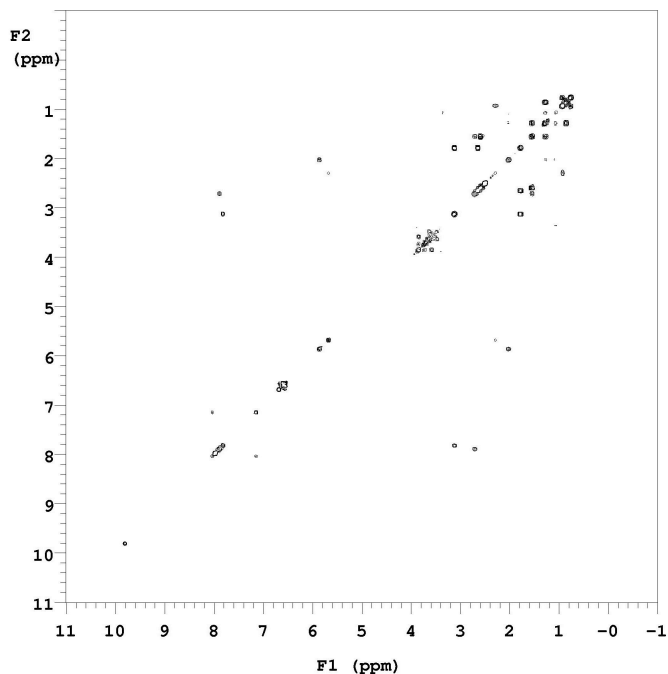
**MS (MALDI, m/z)** 1096 (M+H)<sup>+</sup>

**Analytical HPLC (UV)** purity 100%, retention time = 13.83 min

**Analytical HPLC (Sedex)** purity 98%, retention time = 13.98 min



**<sup>1</sup>H NMR of 71jo**



**COSY NMR of 71jo**

**Data for 71ab**

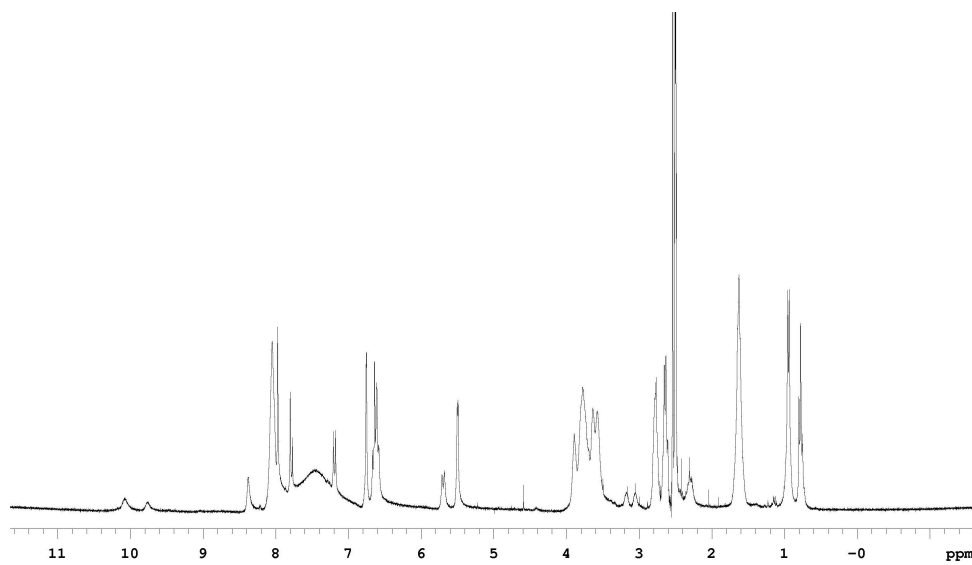
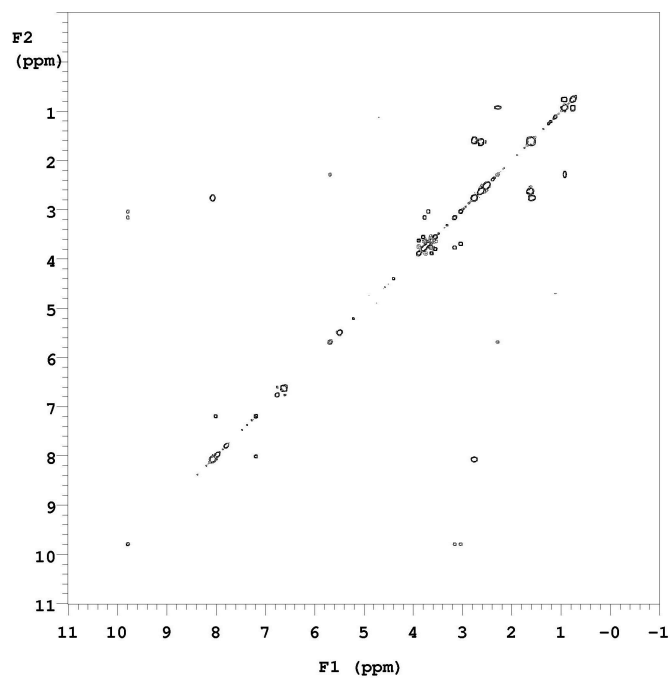
**$^1\text{H}$  NMR (300 MHz, DMSO- $d_6$ )**  $\delta$  8.38 (s, 1H), 8.05 (s, 4H), 7.97 (s, 1H), 7.80 (s, 1H), 7.18 (d, 1H,  $J = 8.4$  Hz), 6.75 (s, 2H), 6.65 (d, 2H,  $J = 8.7$  Hz), 6.59 (d, 2H,  $J = 8.7$  Hz), 5.68 (d, 1H,  $J = 7.2$  Hz), 5.50 (s, 2H), 3.89-3.49 (m, 16H), 2.70 (m, 4H), 2.60 (m, 4H), 2.31 (m, 1H), 1.63 (m, 8H), 0.94 (m, 5H), 0.78 (t, 3H,  $J = 7.2$  Hz)

**MS (MALDI,  $m/z$ )** 1012 ( $M+H$ ) $^+$

**Analytical HPLC (UV)** purity 86%, retention time = 9.85 min

**Analytical HPLC (Sedex)** purity 100%, retention time = 10.01 min



 **$^1\text{H}$  NMR of 71ab****COSY NMR of 71ab**

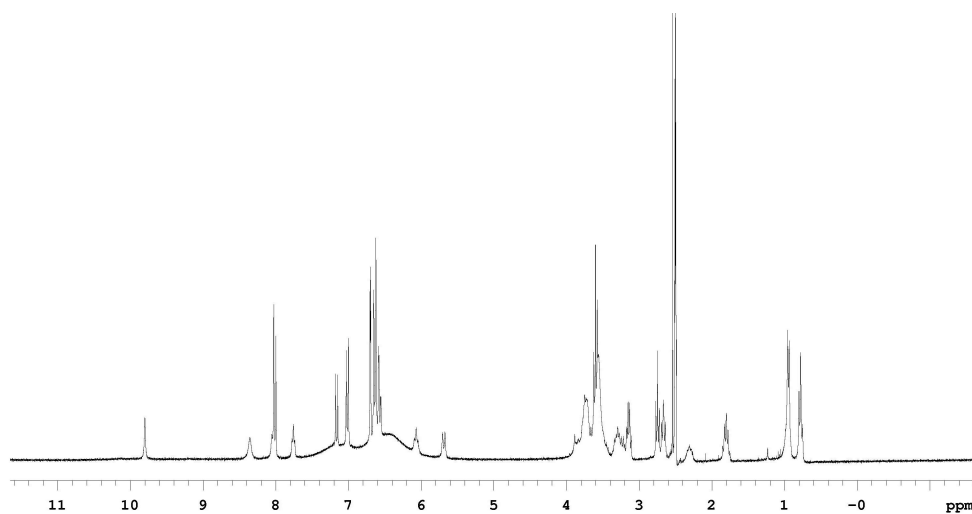
**Data for 71no**

**<sup>1</sup>H NMR (300 MHz, DMSO-d<sub>6</sub>)** δ 9.80 (s, 1H), 9.36 (s, 1H), 8.05 (s, 1H), 8.03 (s, 1H), 8.00 (s, 1H), 7.76 (t, 1H, J = 7.2 Hz), 7.15 (d, 1H, J = 8.4 Hz), 7.01 (d, 2H, J = 8.7 Hz), 6.70 (d, 2H, J = 2.1 Hz), 6.22 (d, 4H, J = 8.7 Hz), 6.56 (dd, 2H, J = 8.7 Hz, 2.1 Hz), 6.07 (t, 1H, J = 7.2 Hz), 5.68 (d, 1H, J = 7.2 Hz), 3.89-3.58 (m, 18 Hz), 3.28 (m, 2H), 3.15 (m, 2H), 2.75 (t, 2H, J = 6.9 Hz), 2.67 (t, 2H, J = 7.2 Hz), 2.31 (m, 1H), 1.80 (m, 2H), 0.94 (m, 5H), 0.78 (t, 3H, J = 7.2 Hz)

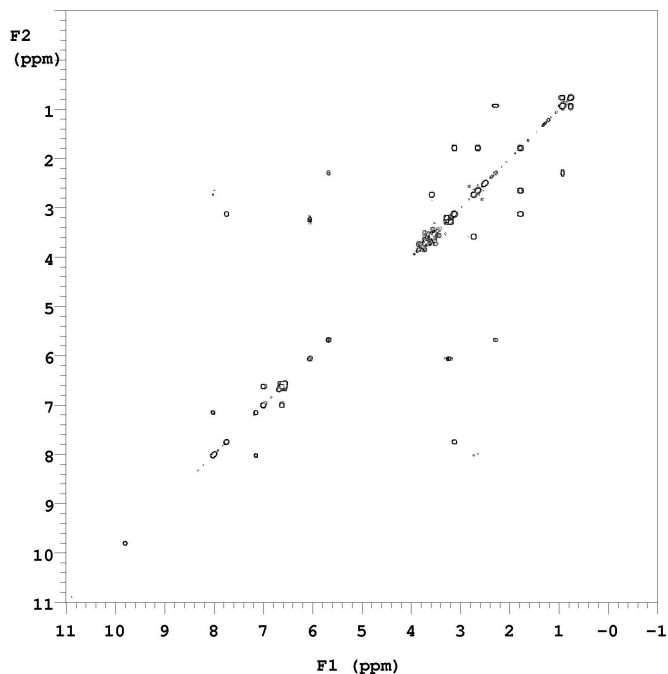
**MS (MALDI, m/z)** 1119 (M+H)<sup>+</sup>

**Analytical HPLC (UV)** purity 100%, retention time = 12.72 min

**Analytical HPLC (Sedex)** purity 100%, retention time = 12.87 min



**<sup>1</sup>H NMR of 71no**



**COSY NMR of 71no**

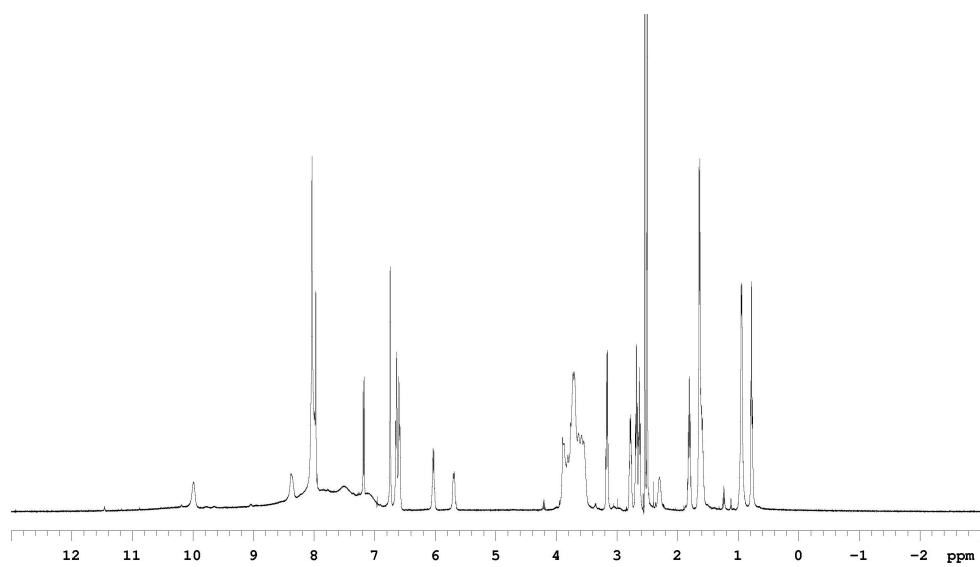
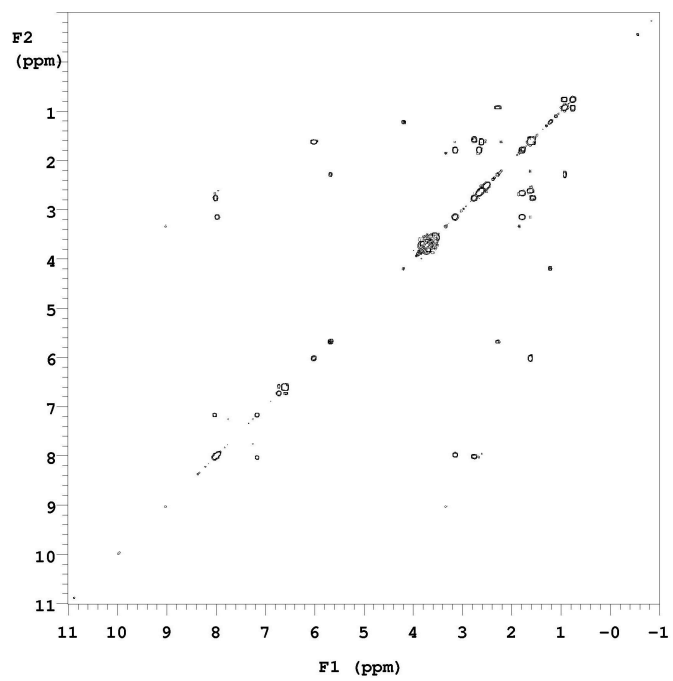
**Data for 71ai**

**$^1\text{H}$  NMR (500 MHz, DMSO- $d_6$ )**  $\delta$  9.99 (s, 1H), 8.38 (s, 1H), 7.99 (m, 5H), 7.17 (d, 1H,  $J = 8.5$  Hz), 6.74 (s, 2H), 6.64 (d, 2H,  $J = 8.5$  Hz), 6.59 (d, 2H,  $J = 8.5$  Hz), 6.02 (q, 1H,  $J = 6.5$  Hz), 5.69 (d, 1H,  $J = 9.0$  Hz), 3.89-3.55 (m, 16 Hz), 3.17 (, 2H), 2.78 (m, 2H), 2.68 (t, 2H,  $J = 7.5$  Hz), 2.63 (t, 2H,  $J = 7.5$  Hz), 2.40 (m, 1H), 1.82 (m, 2H), 1.64 (m, 4H), 0.94 (m, 5H), 0.78 (t, 3H,  $J = 7.5$  Hz)

**MS (MALDI,  $m/z$ )** 1054 ( $M+H$ ) $^+$

**Analytical HPLC (UV)** purity 93%, retention time = 10.77 min

**Analytical HPLC (Sedex)** purity 91%, retention time = 10.92 min

 **$^1\text{H}$  NMR of 71ai****COSY NMR of 71ai**

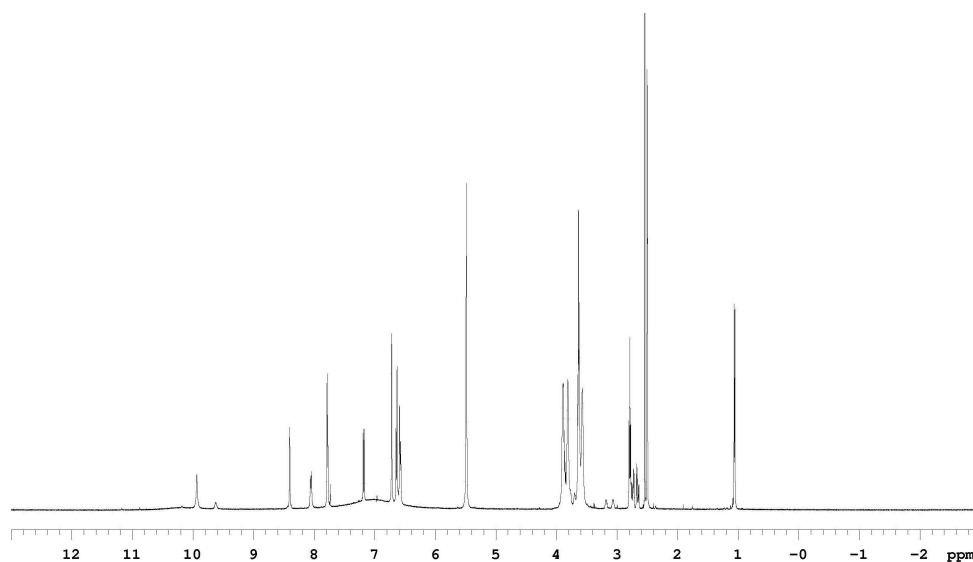
**Data for 71de**

**<sup>1</sup>H NMR (500 MHz, DMSO-d<sub>6</sub>)** δ 9.94 (s, 1H), 8.40 (s, 1H), 8.05 (d, 1H, J = 8.5 Hz), 7.79 (s, 1H), 7.77 (s, 1H), 7.17 (d, 1H, J = 8.5 Hz), 6.72 (s, 2H), 6.64 (d, 2H, J = 8.5 Hz), 6.58 (d, 2H, J = 8.5 Hz), 5.48 (s, 4H), 3.90-3.57 (m, 18H), 2.79 (t, 2H, J = 7.0 Hz), 2.74 (dd, 1H, J = 14.5 Hz, 6.5 Hz), 2.65 (dd, 1H, J = 14.5 Hz, 6.0 Hz), 1.05 (d, 3H, J = 6.0 Hz)

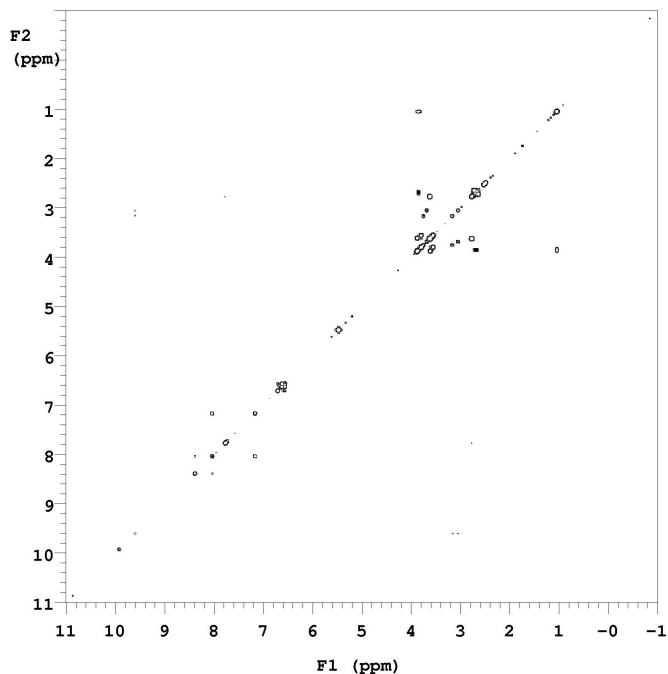
**MS (MALDI, m/z)** 916 (M+H)<sup>+</sup>

**Analytical HPLC (UV)** purity 100%, retention time = 9.77 min

**Analytical HPLC (Sedex)** purity 100%, retention time = 9.92 min



**<sup>1</sup>H NMR of 71de**



**COSY NMR of 71de**

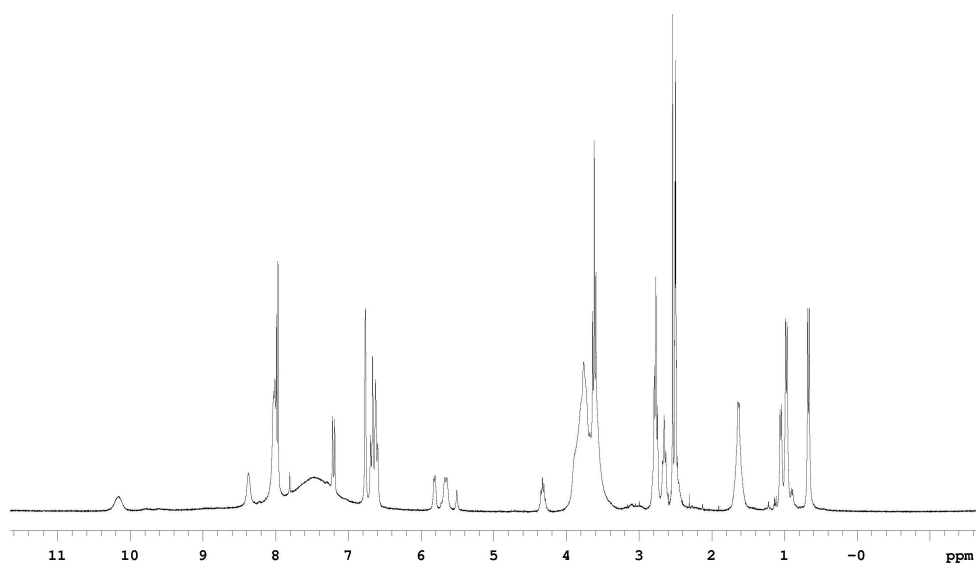
**Data for 71fg**

**$^1\text{H}$  NMR (300 MHz, DMSO- $d_6$ )**  $\delta$  10.21 (s, 1H), 8.38 (s, 1H), 8.02 (b, 2H), 7.99 (s, 1H), 7.97 (s, 1H), 7.20 (d, 1H,  $J = 8.4$  Hz), 6.76 (s, 2H), 6.68 (d, 2H,  $J = 8.4$  Hz), 6.61 (d, 2H,  $J = 8.4$  Hz), 5.81 (d, 1H,  $J = 6.0$  Hz), 5.65 (d, 1H,  $J = 9.0$  Hz), 4.33 (m, 1H), 3.76-3.59 (m, 18H), 2.77 (t, 4H,  $J = 6.9$  Hz), 2.66 (t, 2H,  $J = 6.6$  Hz), 1.63 (m, 4H), 1.05 (d, 3H,  $J = 6.0$  Hz), 0.97 (d, 3H,  $J = 6.0$  Hz), 0.66 (d, 3H,  $J = 6.0$  Hz)

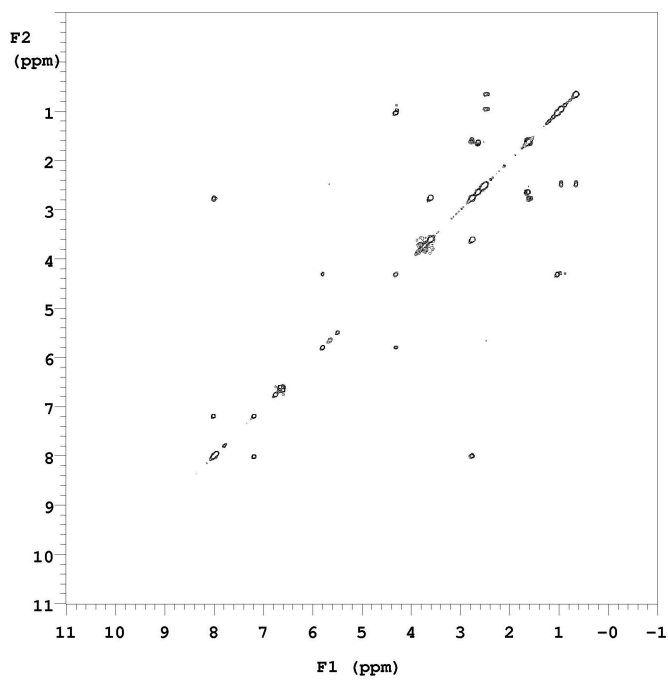
**MS (MALDI,  $m/z$ )** 1015 ( $M+H$ )<sup>+</sup>

**Analytical HPLC (UV)** purity 96%, retention time = 10.12 min

**Analytical HPLC (Sedex)** purity 100%, retention time = 10.37min



$^1\text{H}$  NMR of 71fg



COSY NMR of 71fg

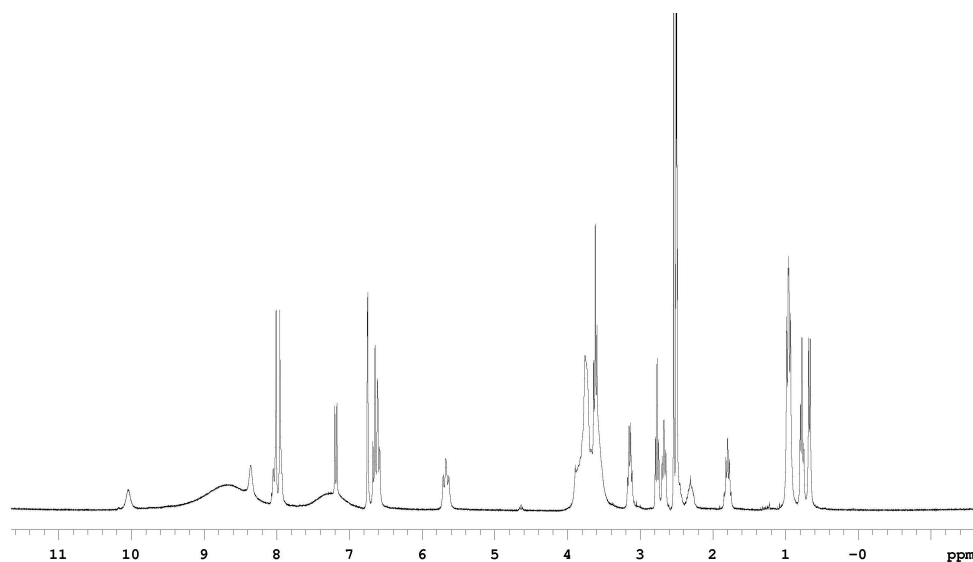
**Data for 71fo**

**<sup>1</sup>H NMR (300 MHz, DMSO-d<sub>6</sub>)** δ 10.04 (s, 1H), 8.69 (s, 1H), 8.07 (s, 1H), 8.04 (s, 1H), 8.01 (s, 1H), 7.96 (s, 1H), 7.18 (d, 1H, J = 8.4 Hz), 6.75 (s, 2H), 6.65 (d, 2H, J = 8.4 Hz), 6.59 (d, 2H, J = 8.4 Hz), 5.68 (m, 2H), 3.89-3.59 (m, 18H), 3.14 (m, 2H), 2.78 (t, 2H, J = 6.9 Hz), 2.67 (t, 2H, J = 7.5 Hz), 2.31 (m, 1H), 1.79 (m, 2H), 0.96 (m, 7H), 0.78 (t, 3H, J = 7.2 Hz), 0.67 (d, 3H, J = 6.6 Hz)

**MS (MALDI, m/z)** 1055 (M+H)<sup>+</sup>

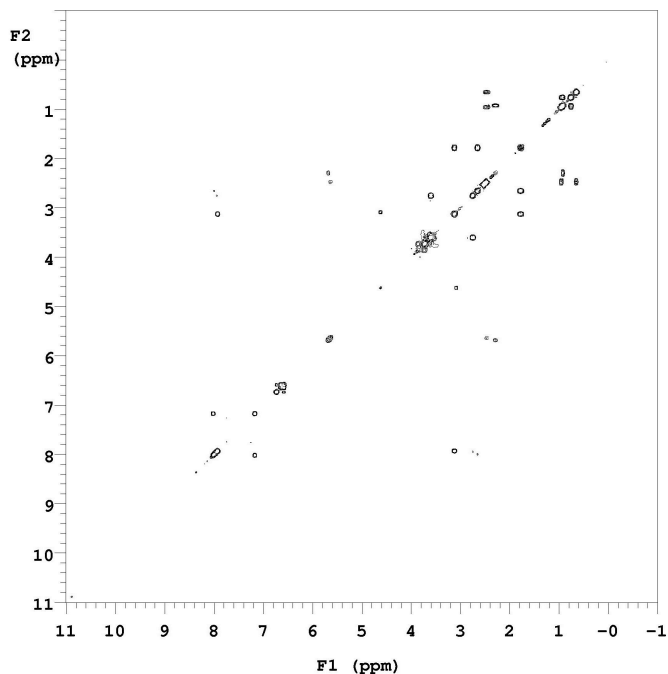
**Analytical HPLC (UV)** purity 100%, retention time = 11.35 min

**Analytical HPLC (Sedex)** purity 100%, retention time = 11.50 min



**<sup>1</sup>H NMR of 71fo**





**COSY NMR of 71fo**

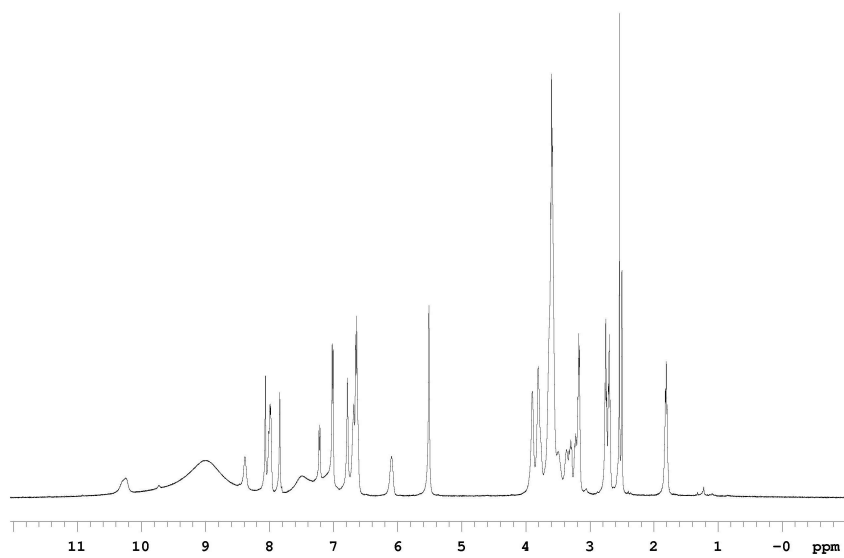
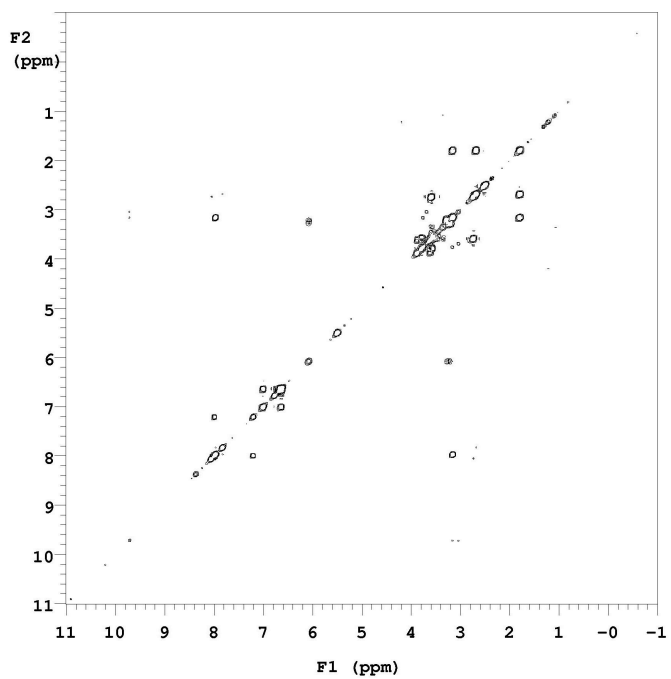
**Data for 71mn**

**$^1\text{H}$  NMR (500 MHz, DMSO- $d_6$ )**  $\delta$  10.24 (s, 1H), 8.38 (s, 1H), 8.06 (s, 1H), 8.01 (m, 2H), 7.84 (s, 1H), 7.21 (d, 1H,  $J = 8.5$  Hz), 7.01 (d, 2H,  $J = 8.5$  Hz), 6.78 (s, 2H), 6.66 (m, 4H), 6.09 (s, 1H), 5.51 (s, 2H), 3.90-3.49 (m, 18H), 3.36 (m, 2H), 3.19 (m, 2H), 2.75 (t, 2H,  $J = 6.5$  Hz), 2.70 (t, 2H,  $J = 7.0$  Hz), 1.81 (m, 2H)

**MS (MALDI,  $m/z$ )** 1063 ( $M+H$ )<sup>+</sup>

**Analytical HPLC (UV)** purity 100%, retention time = 12.82 min

**Analytical HPLC (Sedex)** purity 100%, retention time = 12.97 min

 **$^1\text{H}$  NMR of 71mn****COSY NMR of 71mn**

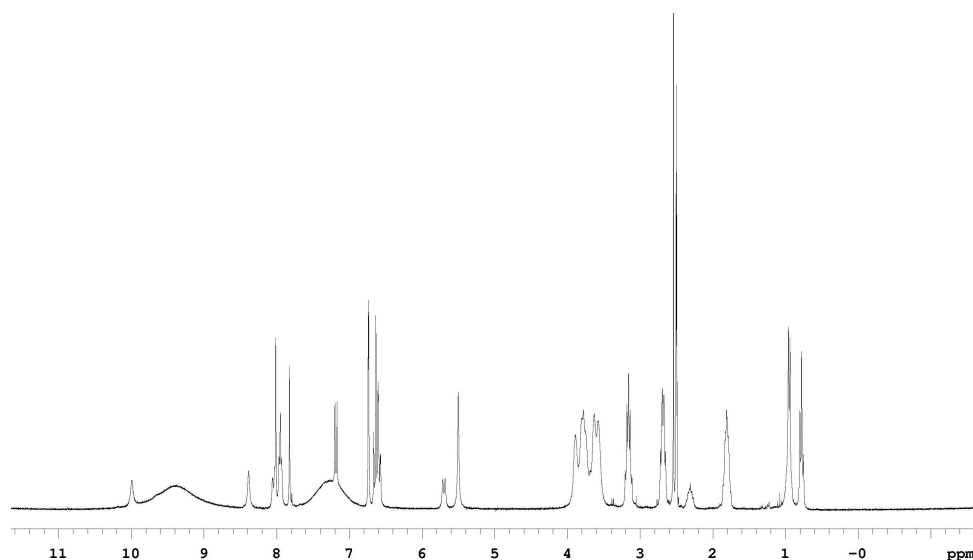
**Data for 71mo**

**<sup>1</sup>H NMR (300 MHz, DMSO-d<sub>6</sub>)** δ 9.99 (s, 1H), 8.39 (s, 1H), 8.05 (d, 1H, J = 8.4 Hz), 8.01 (s, 1H), 7.95 (t, 2H, J = 5.7 Hz), 7.82 (s, 1H), 7.18 (d, 1H, J = 8.4 Hz), 6.74 (d, 2H, J = 2.1 Hz), 6.34 (d, 2H, J = 8.4 Hz), 6.58 (dd, 2H, J = 8.4 Hz, 2.1 Hz), 5.70 (d, 1H, J = 9.0 Hz), 5.50 (s, 2H), 3.89-3.58 (m, 16H), 3.16 (m, 4H), 2.67 (m, 2H), 2.31 (m, 1H), 1.81 (m, 4H), 0.94 (m, 5H), 0.78 (t, 3H, J = 7.2 Hz)

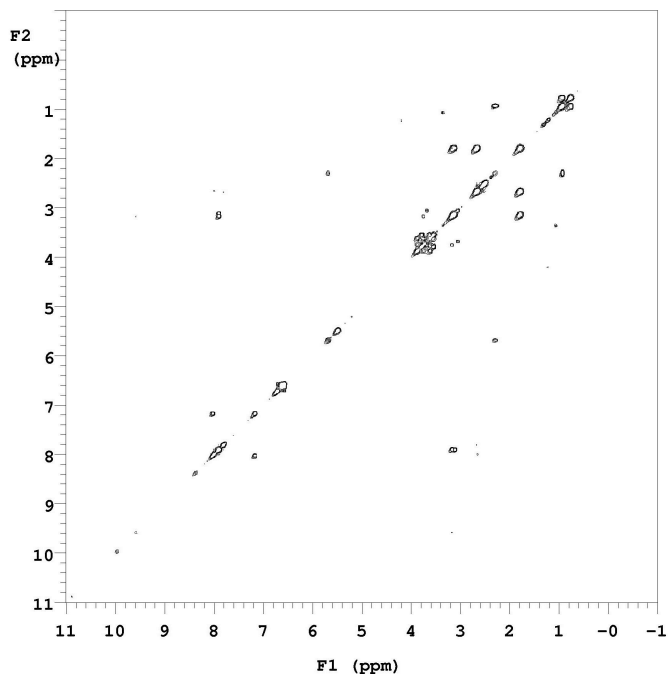
**MS (MALDI, m/z)** 1068 (M+H)<sup>+</sup>

**Analytical HPLC (UV)** purity 100%, retention time = 13.45 min

**Analytical HPLC (Sedex)** purity 100%, retention time = 13.60 min



**<sup>1</sup>H NMR of 71mo**



**COSY NMR of 71mo**

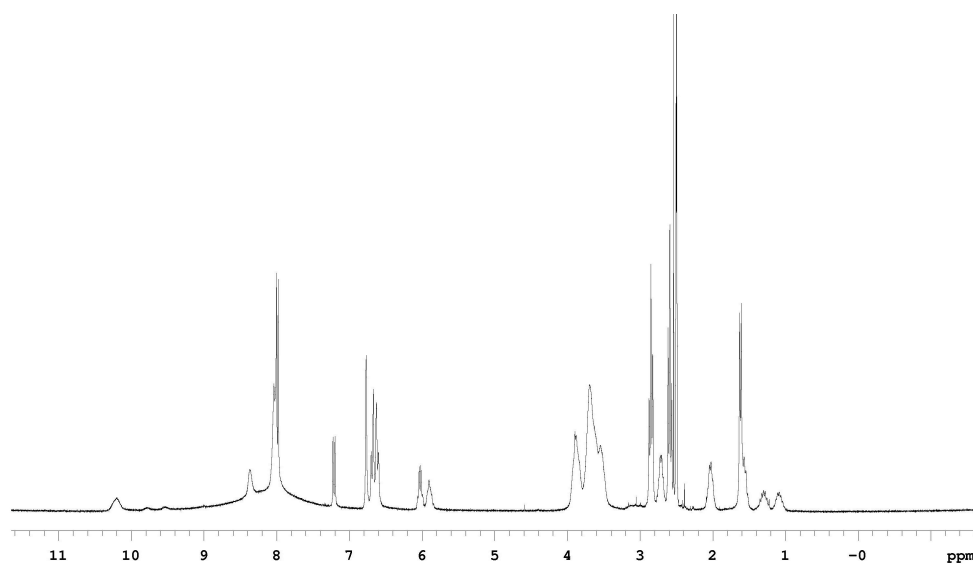
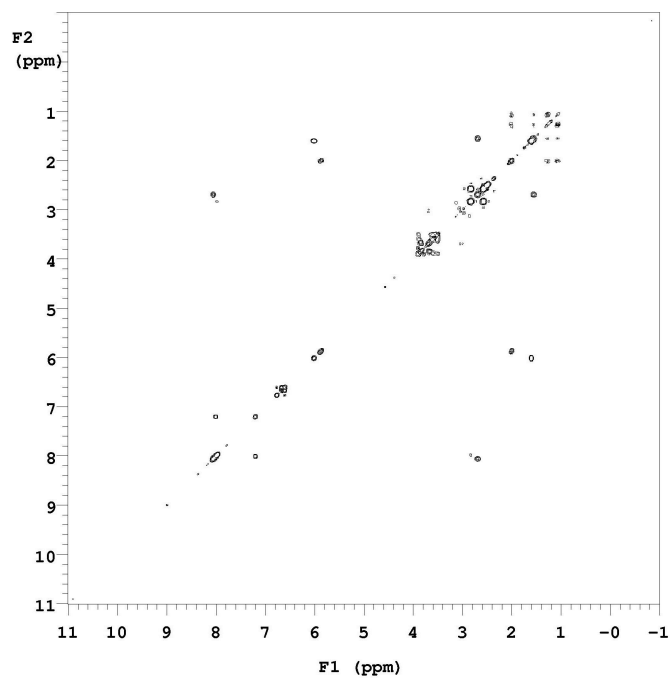
**Data for 71kl**

**$^1\text{H}$  NMR (300 MHz, DMSO- $d_6$ )**  $\delta$  10.40 (s, 1H), 8.37 (s, 1H), 8.04 (s, 2H), 8.00 (s, 1H), 7.98 (s, 1H), 7.19 (d, 1H,  $J=8.4$  Hz), 6.77 (s, 2H), 6.68 (d, 2H,  $J=8.7$  Hz), 6.10 (d, 2H,  $J=8.7$  Hz), 6.02 (q, 1H,  $J=7.2$  Hz), 5.91 (t, 1H,  $J=7.2$  Hz), 3.90-3.54 (m, 16H), 3.05 (t, 4H,  $J=7.2$  Hz), 2.71 (m, 2H), 2.59 (t, 2H,  $J=7.2$  Hz), 2.04 (m, 2H), 1.62 (d, 3H,  $J=7.2$  Hz), 1.58 (m, 2H), 1.31 (m, 1H), 1.06 (m, 1H)

**MS (MALDI,  $m/z$ )** 1043 ( $M+H$ )<sup>+</sup>

**Analytical HPLC (UV)** purity 100%, retention time = 9.15 min

**Analytical HPLC (Sedex)** purity 100%, retention time = 9.30 min

 **$^1\text{H}$  NMR of 71kl****COSY NMR of 71kl**

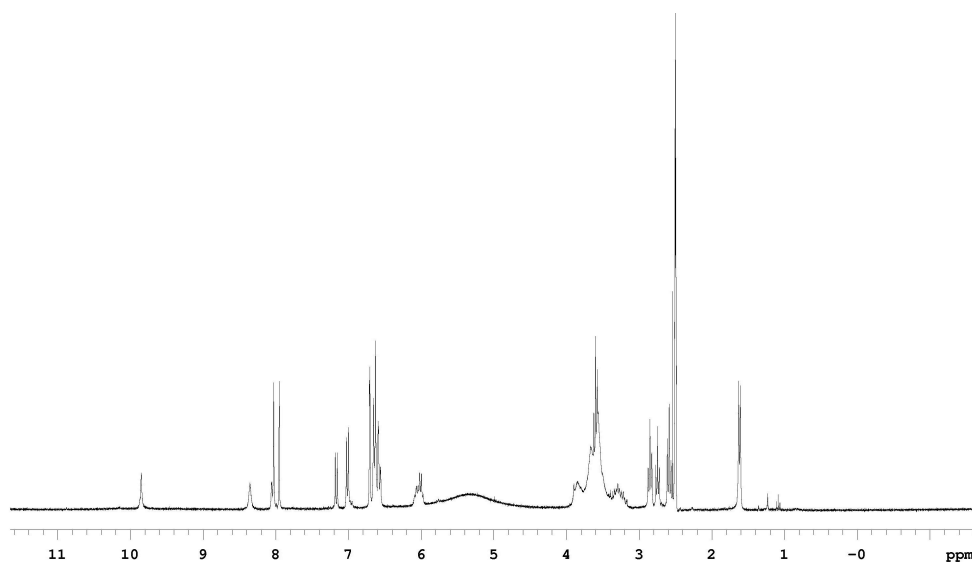
**Data for 71ln**

**<sup>1</sup>H NMR (300 MHz, DMSO-d<sub>6</sub>)** δ 9.85 (s, 1H), 8.35 (s, 1H), 8.05 (s, 1H), 8.03 (s, 1H), 7.95 (s, 1H), 7.17 (d, 1H, J = 8.4 Hz), 7.01 (d, 2H, J = 8.4 Hz), 6.71 (d, 2H, J = 2.1 Hz), 6.63 (d, 2H, J = 8.4 Hz), 6.57 (dd, 2H, J = 8.4 Hz, 2.1 Hz), 6.02 (m, 2H), 3.90-3.58 (m, 18H), 3.32 (m, 2H), 2.85 (t, 2H, J = 7.2 Hz), 2.75 (t, 2H, J = 7.2 Hz), 2.54 (t, 2H, J = 7.5 Hz), 1.61 (d, 3H, J = 7.2 Hz)

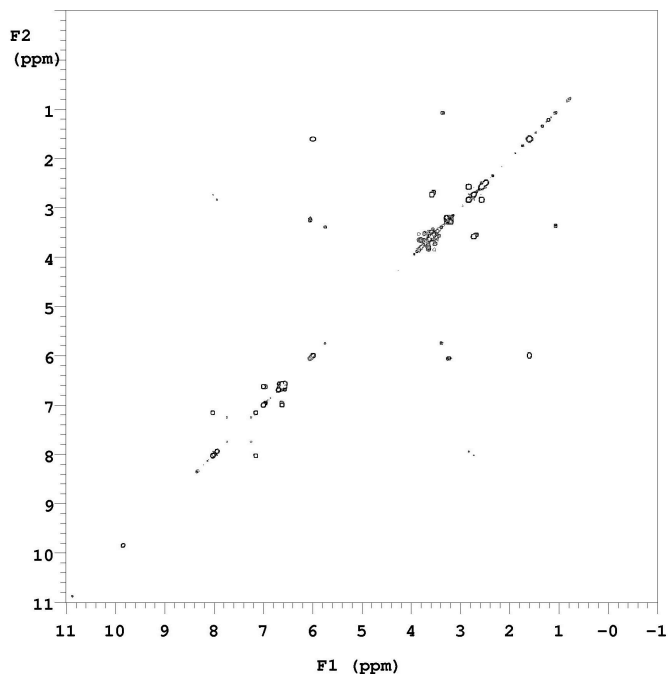
**MS (MALDI, m/z)** 1050 (M+H)<sup>+</sup>

**Analytical HPLC (UV)** purity 100%, retention time = 10.02 min

**Analytical HPLC (Sedex)** purity 100%, retention time = 10.17 min



**<sup>1</sup>H NMR of 71ln**



**COSY NMR of 71ln**

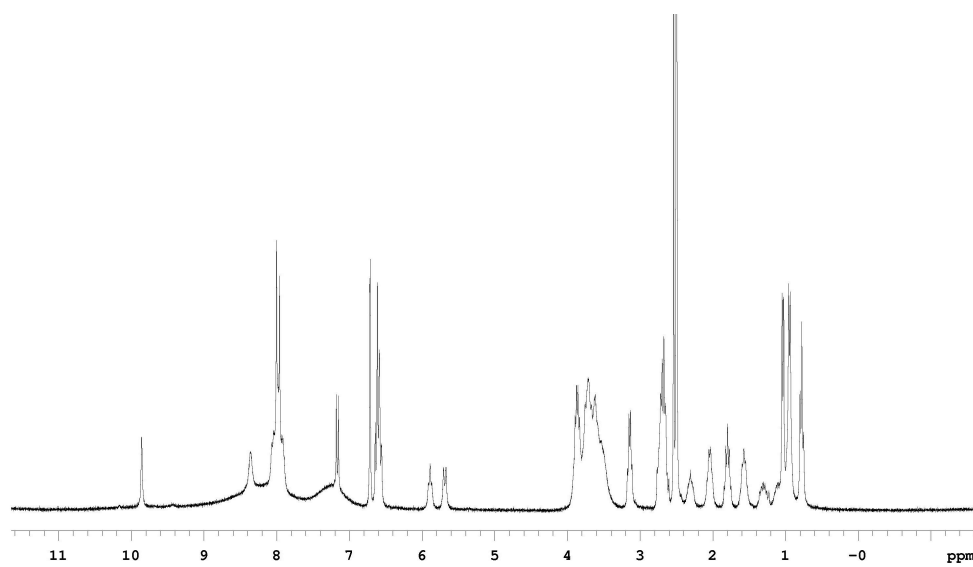
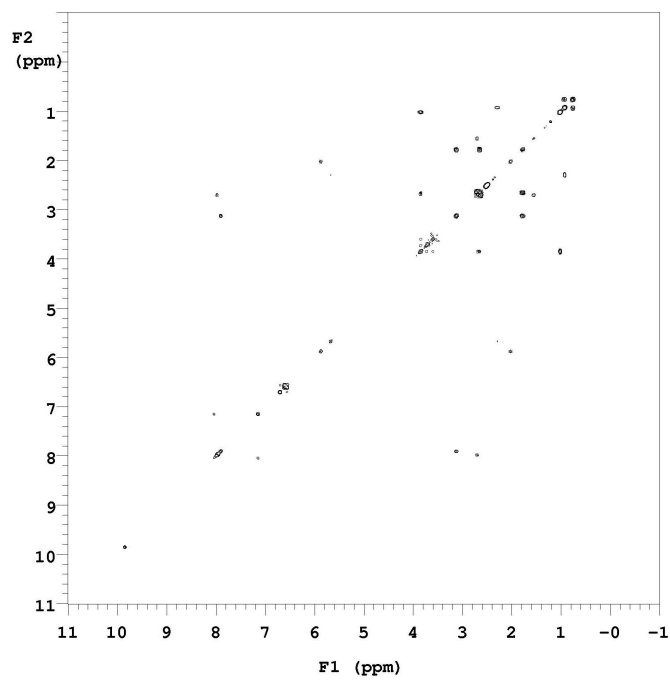
**Data for 71ho**

$^1\text{H}$  NMR (300 MHz, DMSO- $d_6$ )  $\delta$  9.95 (s, 1H), 8.36 (s, 1H), 8.00 (m, 5H), 7.16 (d, 1H,  $J = 8.4$  Hz), 6.71 (s, 2H), 6.62 (d, 2H,  $J = 8.4$  Hz), 6.57 (d, 2H,  $J = 8.4$  Hz), 5.89 (t, 1H,  $J = 7.2$  Hz), 5.68 (d, 1H,  $J = 10.5$  Hz), 3.95-3.61 (m, 17H), 3.15 (m, 2H), 2.69 (m, 6H), 2.31 (m, 1H), 2.05 (m, 2H), 1.79 (m, 2H), 1.57 (m, 2H), 1.31 (m, 1H), 1.00 (m, 1H), 1.04 (d, 3H,  $J = 6.0$  Hz), 0.94 (m, 5H), 0.78 (t, 3H,  $J = 7.2$  Hz)

**MS (MALDI,  $m/z$ )** 1098 ( $M+H$ ) $^+$

**Analytical HPLC (UV)** purity 96%, retention time = 10.25 min

**Analytical HPLC (Sedex)** purity 100%, retention time = 10.40 min

 **$^1\text{H}$  NMR of 71ho****COSY NMR of 71ho**



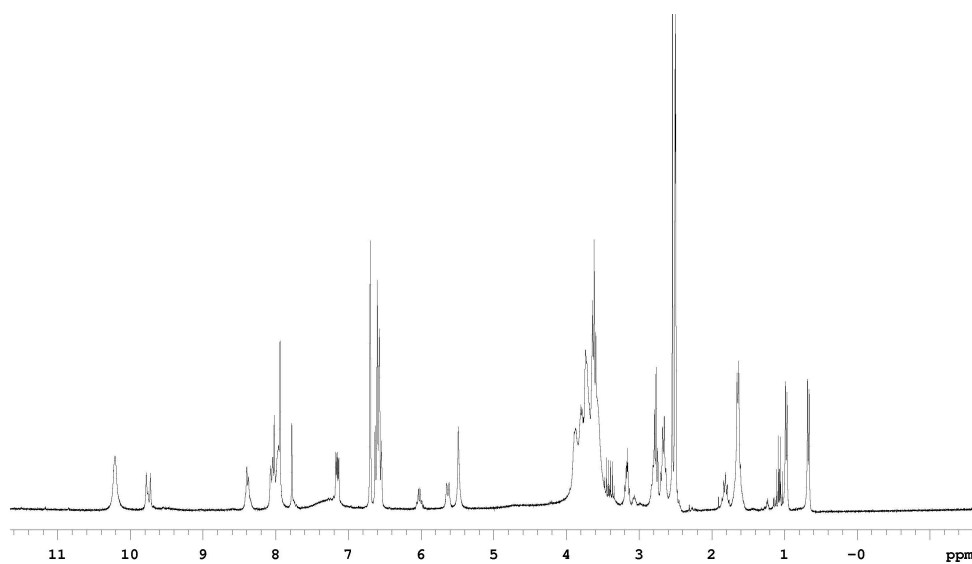
**Data for 71bi**

**$^1\text{H}$  NMR (300 MHz, DMSO- $d_6$ )**  $\delta$  9.88 (s, 1H), 8.39 (s, 1H), 8.06 (m, 6H), 7.79 (s, 1H), 6.71 (d, 2H,  $J = 2.1$  Hz), 6.63 (d, 2H,  $J = 8.4$  Hz), 6.56 (dd, 2H,  $J = 8.4$  Hz, 2.1 Hz), 5.89 (t, 1H,  $J = 7.2$  Hz), 5.49 (s, 2H), 3.89-3.50 (m, 16H), 2.81 (m, 2H), 2.73 (m, 2H), 2.64 (m, 4H), 2.06 (m, 2H), 1.61 (m, 8H), 1.31 (m, 3H), 1.13 (m, 1H), 0.87 (t, 3H,  $J = 7.2$  Hz)

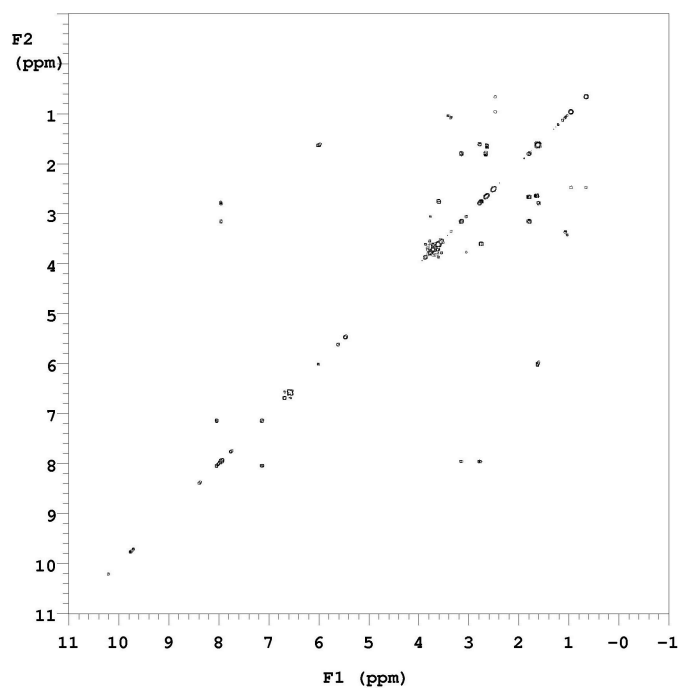
**MS (MALDI,  $m/z$ )** 998 ( $\text{M}+\text{H}$ ) $^+$

**Analytical HPLC (UV)** purity 100%, retention time = 9.02 min

**Analytical HPLC (Sedex)** purity 100%, retention time = 9.17 min



**$^1\text{H}$  NMR of 71bi**



**COSY NMR of 71bi**

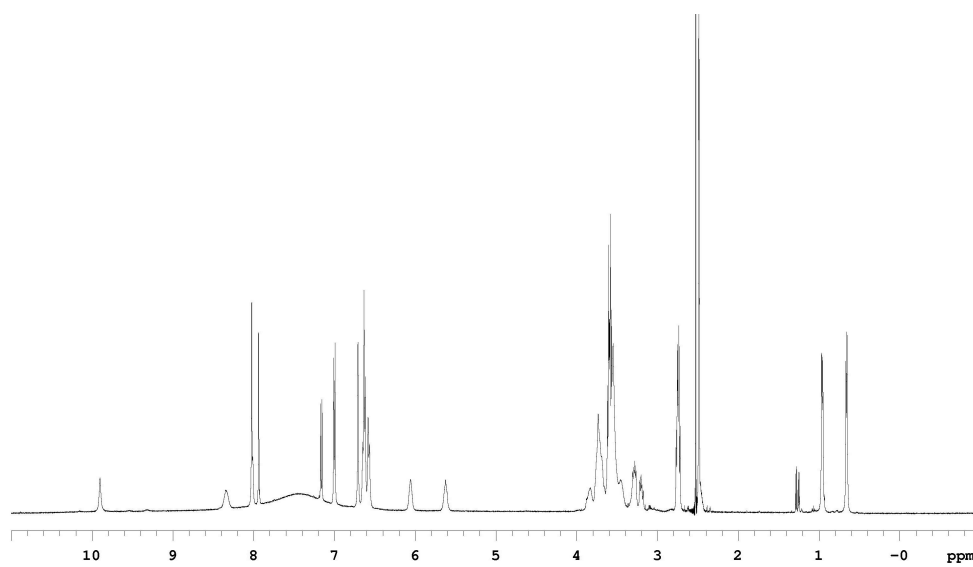
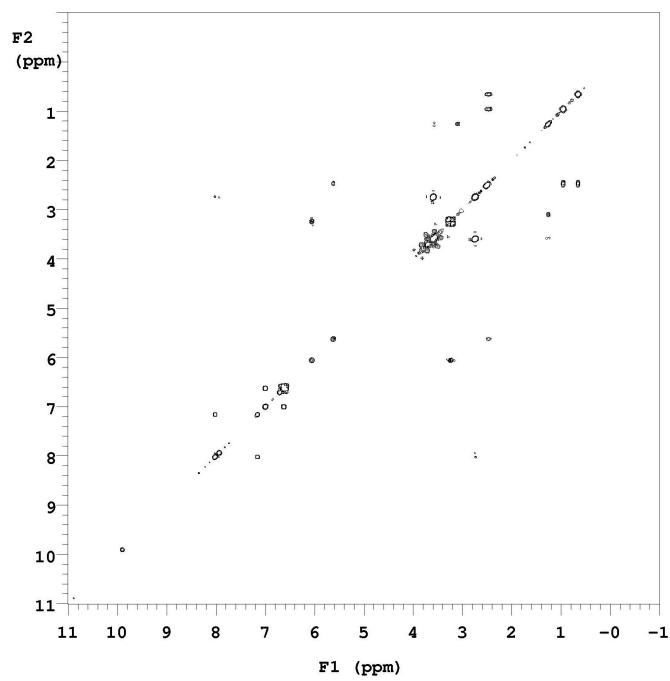
**Data for 71fn**

$^1\text{H}$  NMR (300 MHz, DMSO- $d_6$ )  $\delta$  9.95 (s, 1H), 8.36 (s, 1H), 8.07 (s, 1H), 8.04 (s, 1H), 7.96 (s, 1H), 7.31 (d, 1H,  $J = 8.4$  Hz), 7.02 (d, 2H,  $J = 8.4$  Hz), 6.62 (d, 2H,  $J = 2.1$  Hz), 6.64 (d, 4H,  $J = 8.4$  Hz), 6.60 (dd, 2H,  $J = 8.4$  Hz, 2.1 Hz), 6.07 (t, 1H,  $J = 7.2$  Hz), 5.63 (d, 1H,  $J = 9.0$  Hz), 3.89-3.44 (m, 18H), 3.30 (m, 2H), 2.77 (m, 2H), 1.28 (m, 1H), 0.94 (d, 3H,  $J = 7.2$  Hz), 0.78 (d, 3H,  $J = 7.2$  Hz)

**MS (MALDI,  $m/z$ )** 1050 ( $\text{M}+\text{H}$ ) $^+$

**Analytical HPLC (UV)** purity 100%, retention time = 10.37 min

**Analytical HPLC (Sedex)** purity 100%, retention time = 10.52 min

 **$^1\text{H}$  NMR of 71fn****COSY NMR of 71fn**

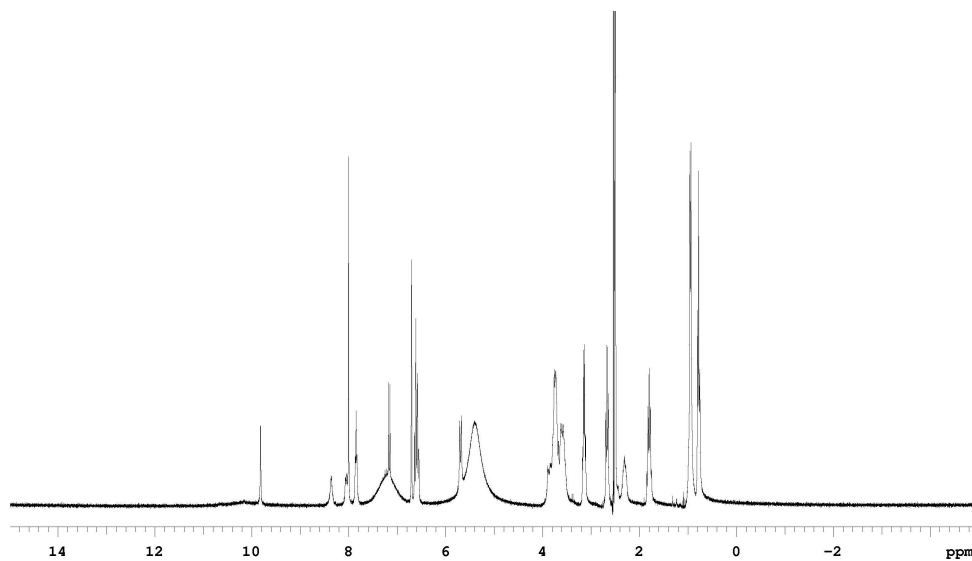
**Data for 7100**

**<sup>1</sup>H NMR (300 MHz, DMSO-d<sub>6</sub>)** δ 9.82 (s, 1H), 8.36 (s, 1H), 8.06 (d, 1H, J = 8.4 Hz), 8.04 (s, 2H), 7.85 (t, 2H, J = 8.1 Hz), 7.23 (d, 1H, J = 8.4 Hz), 6.70 (d, 2H, J = 2.1 Hz), 6.63 (d, 2H, J = 8.4 Hz), 6.56 (dd, 2H, J = 8.4 Hz, 2.1 Hz), 5.67 (d, 2H, J = 10.2 Hz), 3.89-3.58 (m, 16 Hz), 3.15 (m, 4H), 2.67 (m, 4H), 2.30 (m, 2H), 1.80 (m, 4H), 0.95 (m, 10H), 0.78 (t, 6H, J = 7.2 Hz)

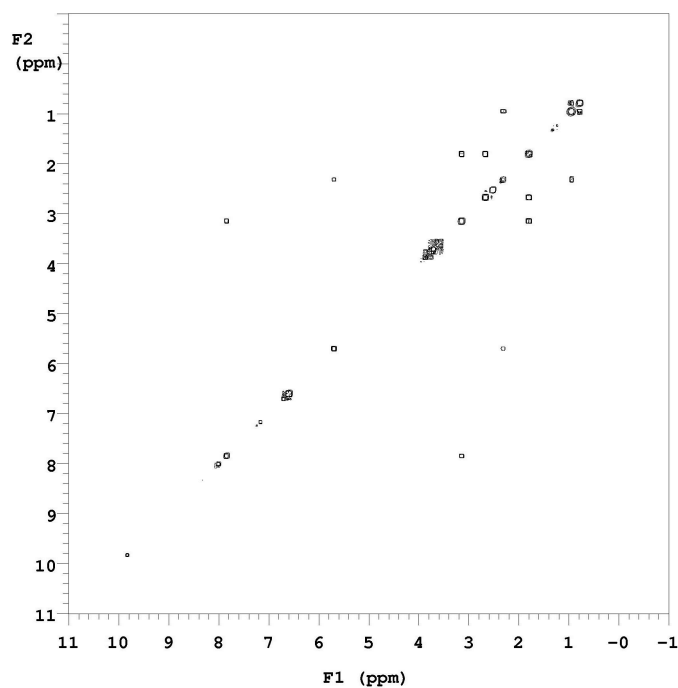
**MS (MALDI, m/z)** 1124 (M+H)<sup>+</sup>

**Analytical HPLC (UV)** purity 100%, retention time = 9.75 min

**Analytical HPLC (Sedex)** purity 100%, retention time = 9.90 min



**<sup>1</sup>H NMR of 7100**



**COSY NMR of 7100**

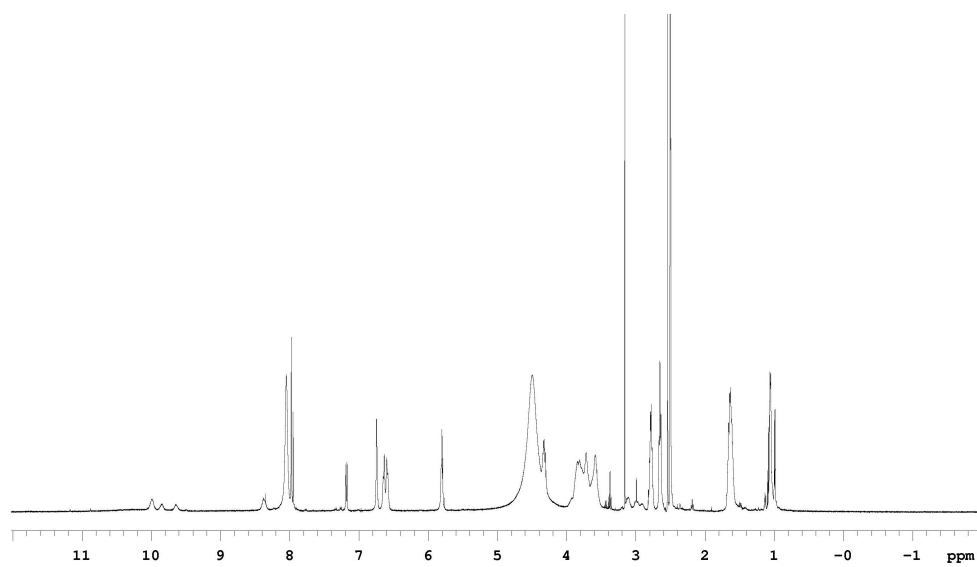
**Data for 71gg**

**$^1\text{H}$  NMR (500 MHz, DMSO- $d_6$ )**  $\delta$  9.99 (s, 1H), 8.38 (s, 1H), 8.05 (s, 6H), 7.98 (s, 2H), 7.17 (d, 1H,  $J = 8.5$  Hz), 6.74 (s, 2H), 6.65 (d, 2H,  $J = 8.5$  Hz), 6.60 (d, 2H,  $J = 8.5$  Hz), 5.79 (d, 2H,  $J = 10.0$  Hz), 4.31 (m, 2H), 3.84-3.56 (m, 16H), 2.76 (m, 4H), 2.54 (m, 4H), 1.65 (m, 8H), 1.07 (d, 6H,  $J = 7.5$  Hz)

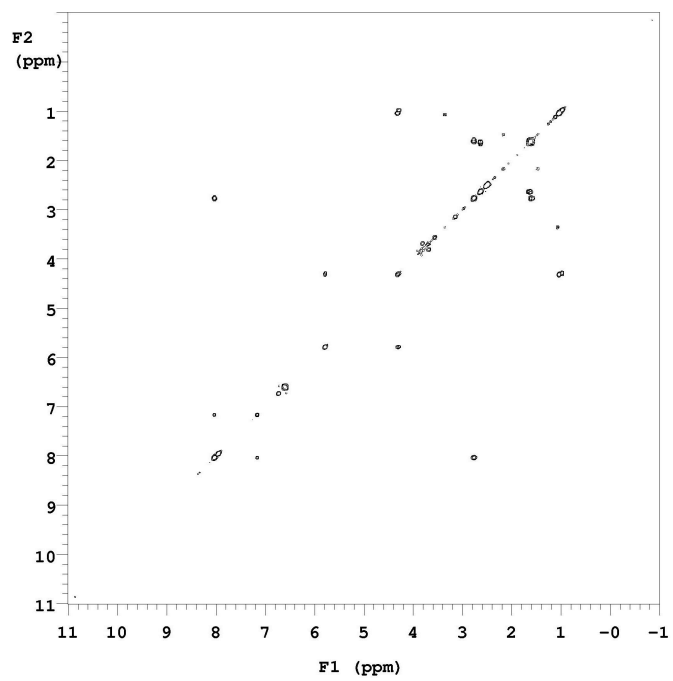
**MS (MALDI,  $m/z$ )** 1044 ( $M+H$ ) $^+$

**Analytical HPLC (UV)** purity 86%, retention time = 8.78 min

**Analytical HPLC (Sedex)** purity 100%, retention time = 8.93 min



**$^1\text{H}$  NMR of 71gg**



**COSY NMR of 71gg**

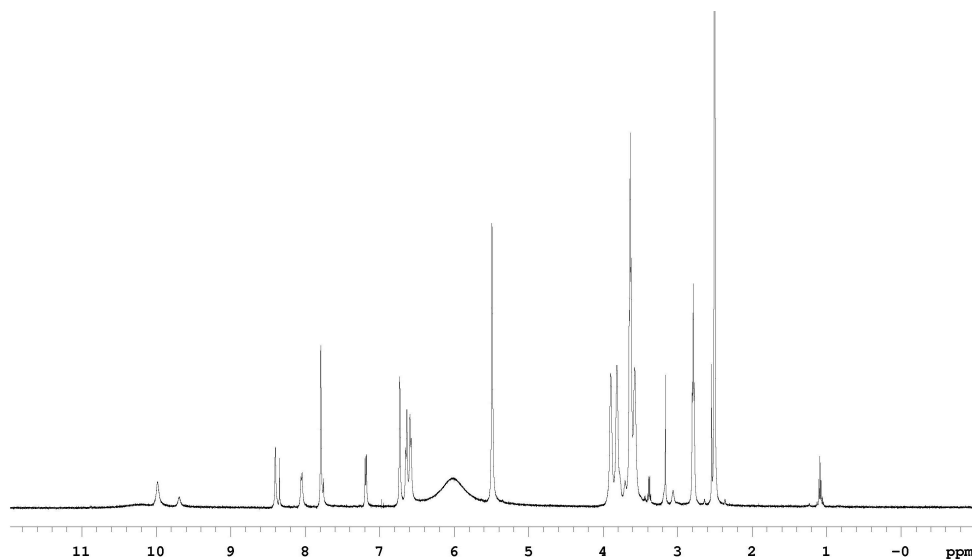
**Data for 71dd**

**<sup>1</sup>H NMR (500 MHz, DMSO-d<sub>6</sub>)** δ 9.98 (s, 1H), 8.40 (s, 1H), 8.05 (d, 1H, J = 7.0 Hz), 7.79 (s, 2H), 7.18 (d, 1H, J = 8.5 Hz), 6.73 (s, 2H), 6.64 (d, 2H, J = 8.5 Hz), 6.58 (d, 2H, J = 8.5 Hz), 5.49 (s, 4H), 3.90 (m, 20H), 2.79 (t, 4H, J = 7.0 Hz)

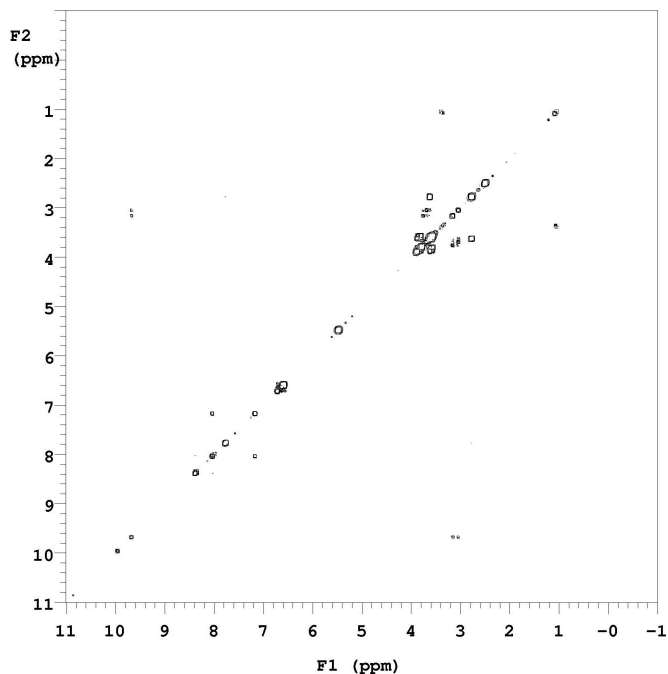
**MS (MALDI, m/z)** 902 (M+H)<sup>+</sup>

**Analytical HPLC (UV)** purity 92%, retention time = 10.07 min

**Analytical HPLC (Sedex)** purity 100%, retention time = 10.22 min



**<sup>1</sup>H NMR of 71dd**



**COSY NMR of 71dd**

**Data for 71n'**

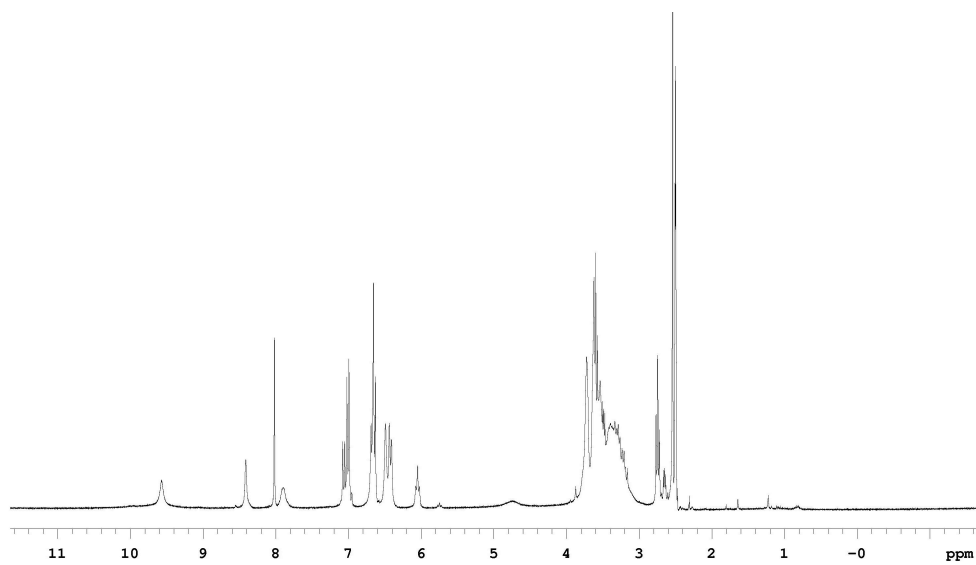
**$^1\text{H}$  NMR (300 MHz, DMSO- $d_6$ )**  $\delta$  9.57 (s, 1H), 8.41 (s, 1H), 8.02 (s, 1H), 7.90 (s, 1H), 7.06 (d, 1H,  $J = 8.4$  Hz), 7.01 (d, 2H,  $J = 8.4$  Hz), 6.56 (m, 4H), 6.49 (s, 2H), 6.42 (d, 2H,  $J = 8.4$  Hz), 6.05 (t, 1H,  $J = 7.5$  Hz), 3.87-3.47 (m, 18H), 3.29 (m, 2H), 2.74 (t, 2H,  $J = 6.9$  Hz)

**MS (MALDI,  $m/z$ )** 1114 ( $M+H$ ) $^+$

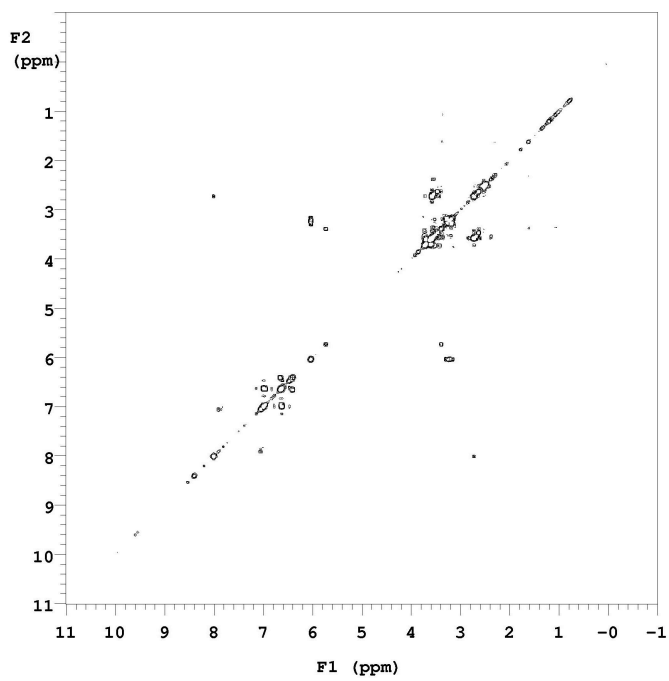
**Analytical HPLC (UV)** purity 100%, retention time = 10.57 min

**Analytical HPLC (Sedex)** purity 100%, retention time = 10.72 min





**$^1\text{H}$  NMR of 71n'**



**COSY NMR of 71n'**

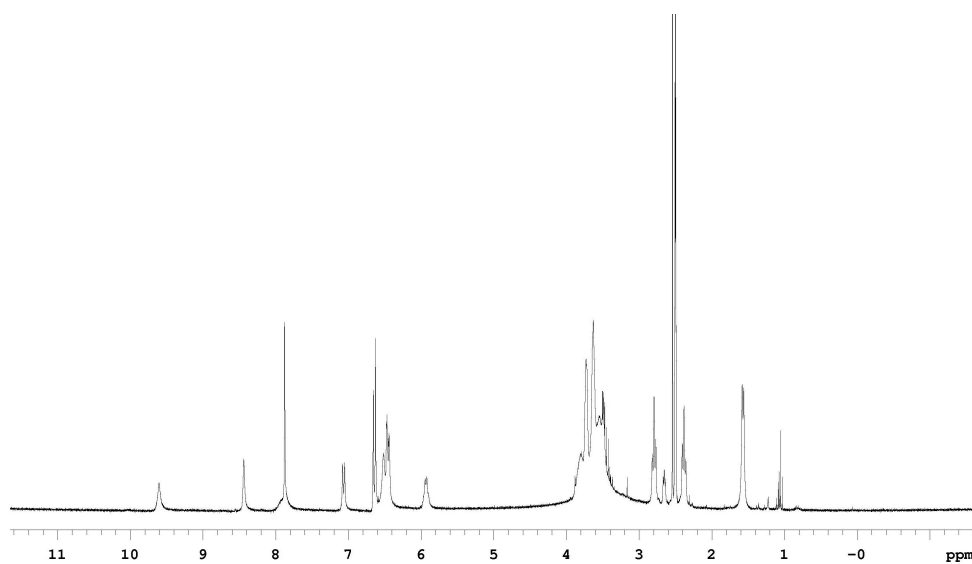
**Data for 711'**

**<sup>1</sup>H NMR (300 MHz, DMSO-d<sub>6</sub>)** δ 9.61 (s, 1H), 8.44 (s, 1H), 7.88 (s, 1H), 7.06 (d, 1H, J = 8.4 Hz), 6.63 (d, 2H, J = 8.4 Hz), 6.52 (s, 2H), 6.47 (d, 2H, J = 8.4 Hz), 5.94 (q, 1H, J = 6.0 Hz), 3.88-3.67 (m, 16 Hz), 2.79 (t, 2H, J = 7.2 Hz), 2.38 (t, 2H, J = 7.2 Hz), 1.57 (d, 3H, J = 6.0 Hz)

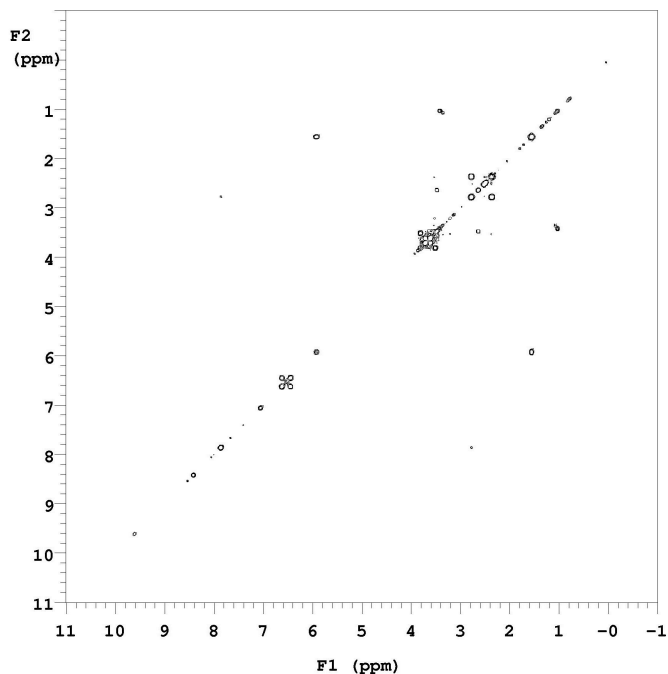
**MS (MALDI, m/z)** 986 (M+H)<sup>+</sup>

**Analytical HPLC (UV)** purity 100%, retention time = 10.75 min

**Analytical HPLC (Sedex)** purity 100%, retention time = 10.90 min



**<sup>1</sup>H NMR of 711'**



**COSY NMR of 711'**

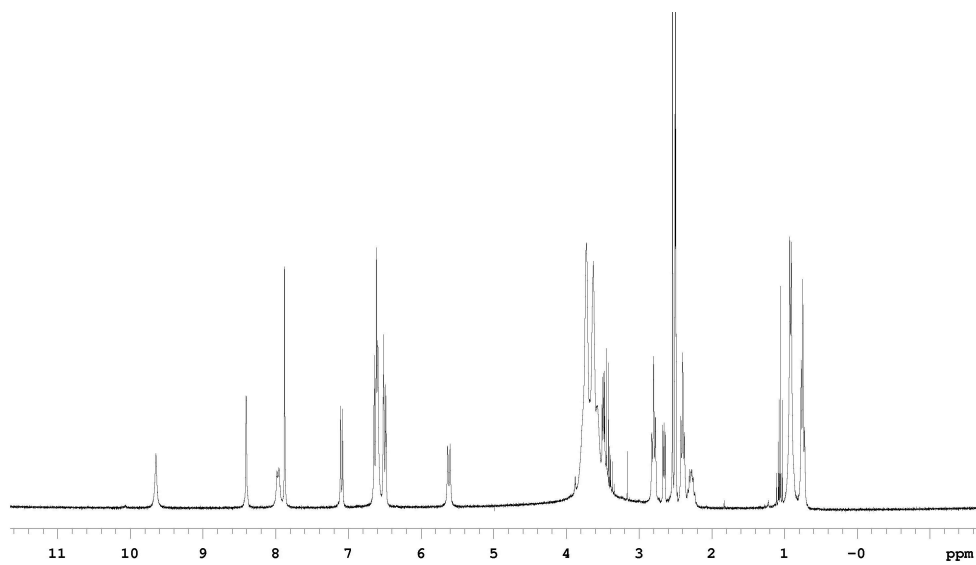
**Data for 71c'**

**$^1\text{H}$  NMR (300 MHz, DMSO- $d_6$ )**  $\delta$  9.65 (s, 1H), 8.41 (s, 1H), 7.96 (d, 1H,  $J = 8.4$  Hz), 7.88 (s, 1H), 7.09 (d, 1H,  $J = 8.4$  Hz), 6.63 (d, 2H,  $J = 8.4$  Hz), 6.60 (s, 2H), 6.48 (d, 2H,  $J = 8.4$  Hz), 5.60 (d, 1H,  $J = 10.2$  Hz), 3.87-3.42 (m, 16 Hz), 2.80 (t, 2H,  $J = 7.2$  Hz), 2.40 (t, 2H,  $J = 7.2$  Hz), 2.75 (m, 1H), 0.94 (m, 5H), 0.75 (t, 3H,  $J = 7.2$  Hz)

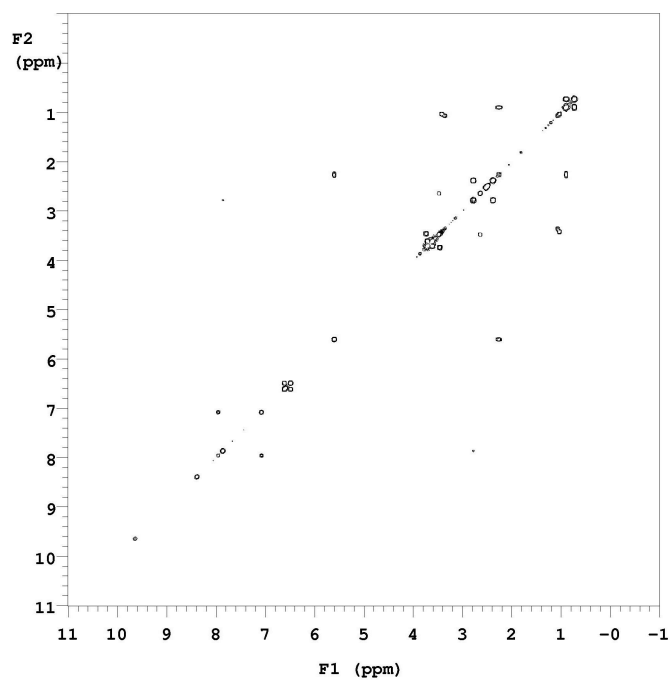
**MS (MALDI,  $m/z$ )** 1070 ( $M+H$ )<sup>+</sup>

**Analytical HPLC (UV)** purity 100%, retention time = 10.58 min

**Analytical HPLC (Sedex)** purity 100%, retention time = 10.73 min



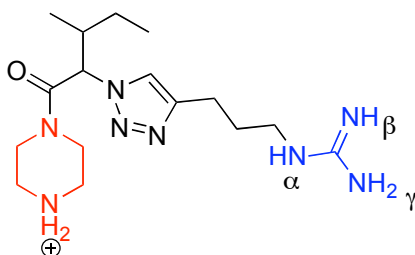
$^1\text{H}$  NMR of 71c'



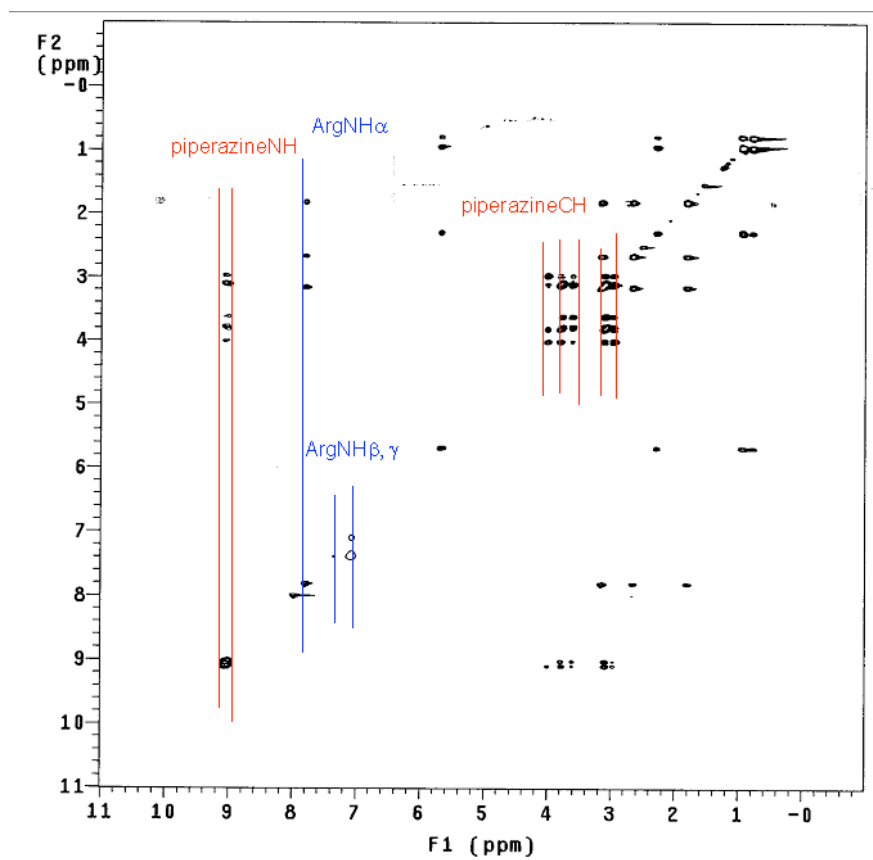
COSY NMR of 71c'

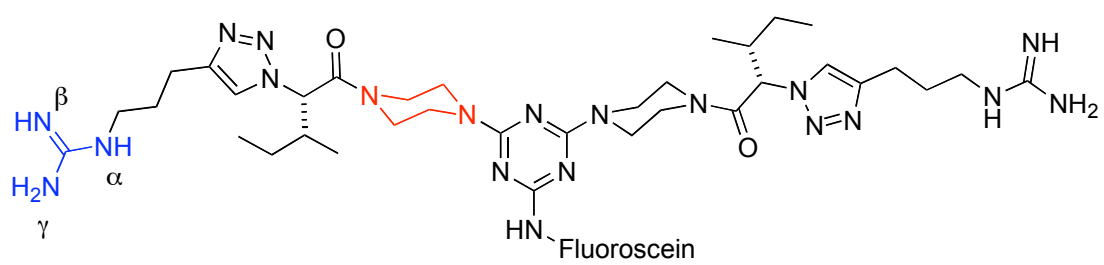
## Further Coupling Selectivity Evidence

TOCSY Spectra of **71gg**, **71oo** and their monomeric fragments **70g**, **70o** are analyzed to indicate that monochloro- and dichloro- triazine derivatives couple to the amine of piperazine linker residue selectively over other active sites in the deprotected monomeric fragments. Compared to the spectra of **70g** and **70o**, the piperazine NH is absent and the chemical shifts of piperazine ring have changed in that of **71gg** and **71oo**.

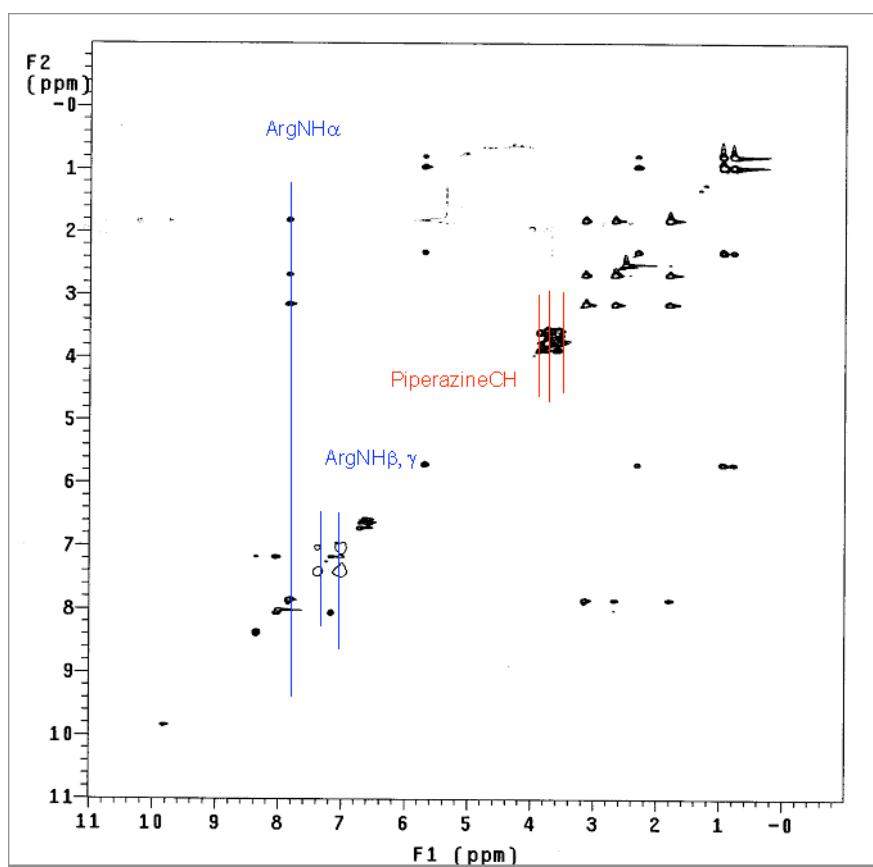


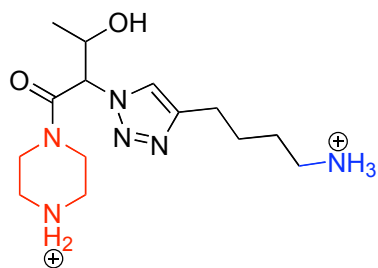
**70o**



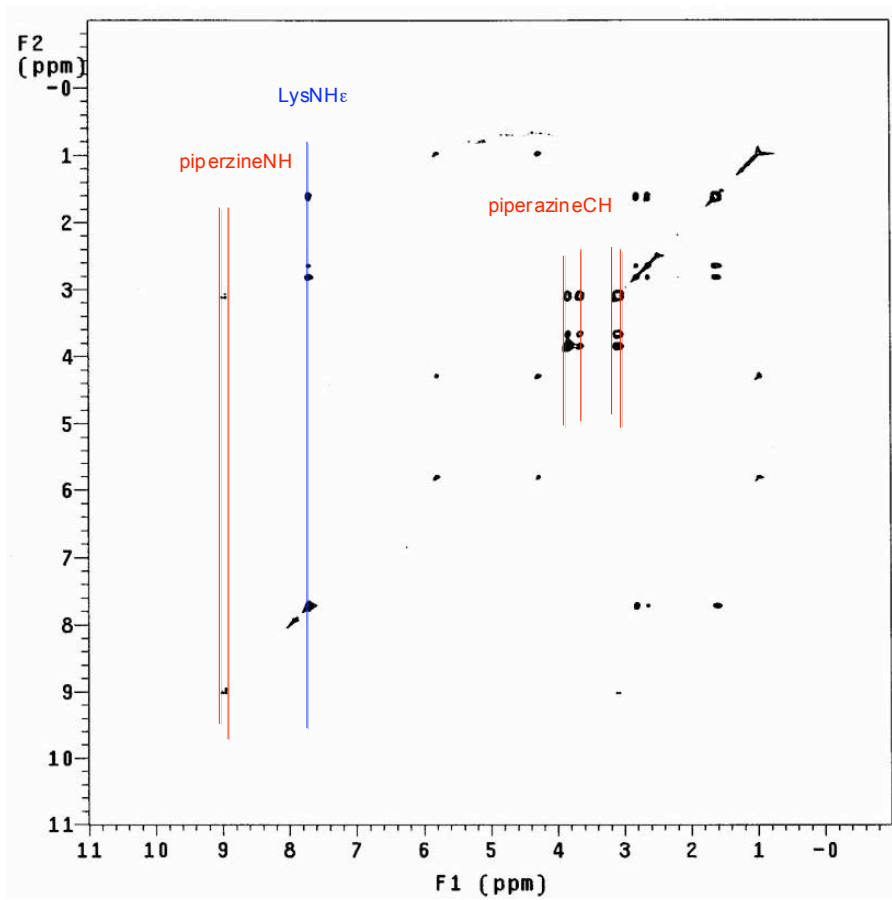


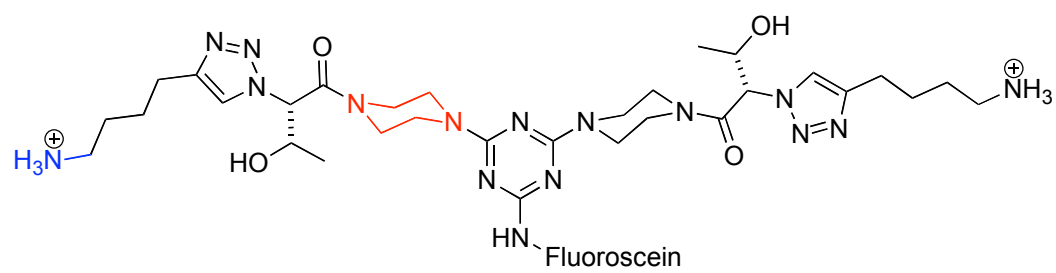
7100



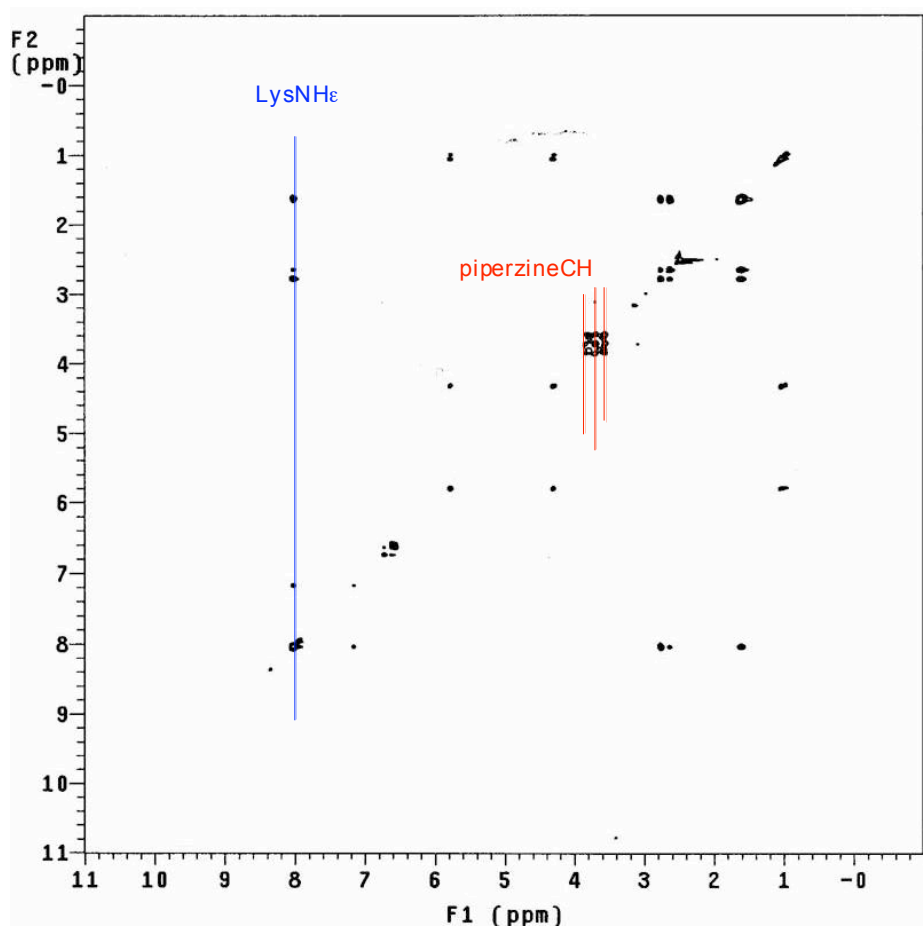


70g





71gg

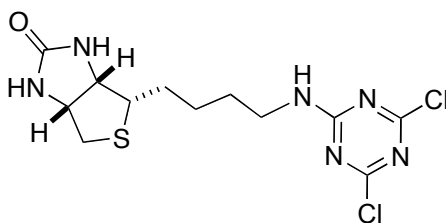




### General Procedure for Preparation of Biotin Labeled Bivalent Compounds **72** and Monovalent Compounds **72a'-o'**

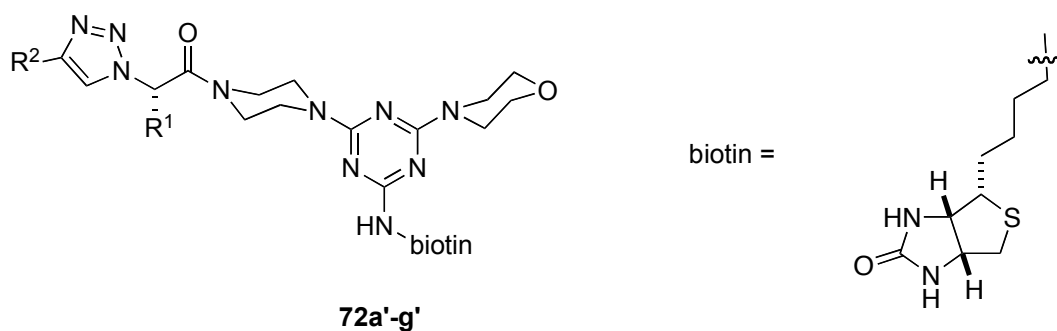
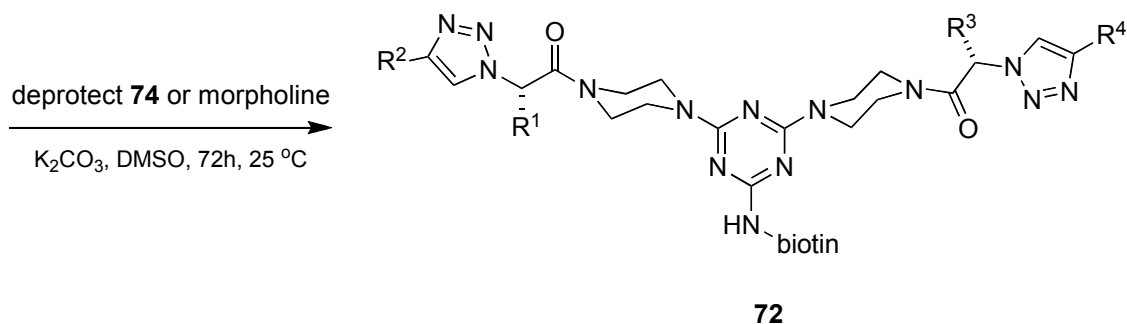
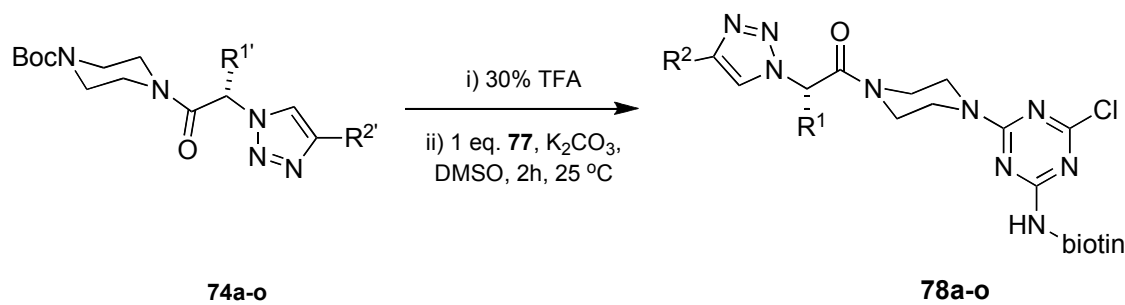
Boc-protected monomeric compounds **74a-o** (1.0 eq.) were treated with 30% TFA in  $\text{CH}_2\text{Cl}_2$ , stirred in sealed glass vials for 4h and solvent was removed. The resulting residue was dissolved in DMSO (0.05 M) and DTAF (1.0 equiv.) and  $\text{K}_2\text{CO}_3$  (4.0 eq.) were added. The suspension was stirred for 2 h. The crude product **78a-o** was used for the next step without further purification. Analytical HPLC and MALDI MS were used to check the purities of these crude samples.

Dimerization was carried out in 2 ml glass vials. The monomeric compounds **74a-o** were treated with 30% TFA/ $\text{CH}_2\text{Cl}_2$  for 4 h. Stock solutions of **78** (0.05 M) and deprotected **74** (0.05 M) or morpholine (0.05 M) in DMSO were prepared. One stock solution of **7** (0.5 ml) and one of deprotected **74** (0.5 ml) or morpholine (0.5 ml) were added to a glass vial and followed with solid  $\text{K}_2\text{CO}_3$  (*ca* 20 mg). The reaction vial was sealed and sonicated for 15 min. The reaction mixture was agitated at 25 °C for 48 h then the DMSO was lyophilized. Aqueous HCl solution (5%, *ca* 0.5 ml) was added to the above solid residue and sonicated for 3 min. The aqueous solution of these compounds were lyophilized and redissolved in 0.5 ml MeOH. The inorganic salts were precipitated out and removed. The MeOH solution was then concentrated to give compounds **73**. All crude products were analyzed by analytical HPLC (5-95% B in 30 min) and MALDI-MS.



77

**Preparation of Biotin Labeled Linker 77.** To the ice-water bath cooled  $\text{CHCl}_3$  solution (5 ml) of cyanuric chloride (0.52 mmol, 0.10 g) was added norbiotin amine hydrochloride salt (0.4 mmol, 0.10 g) and *N,N*-diisopropyl ethyl amine (1.00 mmol, 0.17 ml). The resulting mixture was stirred at 0 °C for 2 h. The white solid precipitate was filtered, washed with cooled  $\text{CHCl}_3$  (5 ml),  $\text{H}_2\text{O}$  (5 ml), and dried under vacuum for 14 h to give compound **77** (0.10 g, 71 %).



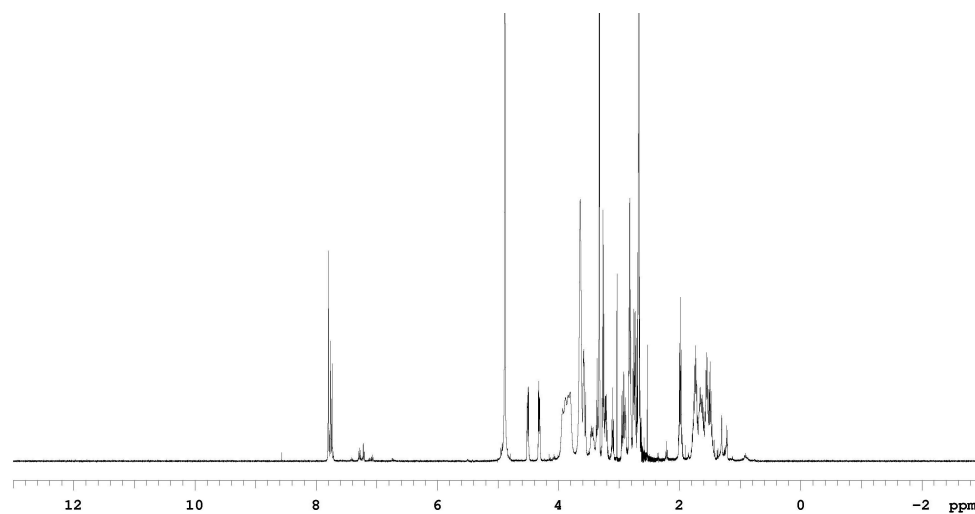
**Data for Biotin Labeled Bivalent Compounds 72****72bm**

**<sup>1</sup>H NMR (500 MHz, CD<sub>3</sub>OD)** δ 7.77 (s, 1H), 7.72 (s, 1H), 4.48 (dd, 1H, J = 7.5 Hz, 4.5 Hz), 4.29 (dd, 1H, J = 7.5 Hz, 4.0 Hz), 3.98-3.52 (m, 18H), 3.06 (t, 2H, J = 7.0 Hz), 3.00 (m, 1H), 2.88 (m, 2H), 2.81 (m, 2H), 1.75 (m, 2H), 1.68 (m, 3H), 1.62 (m, 2H), 1.52 (m, 2H), 1.46 (m, 2H)

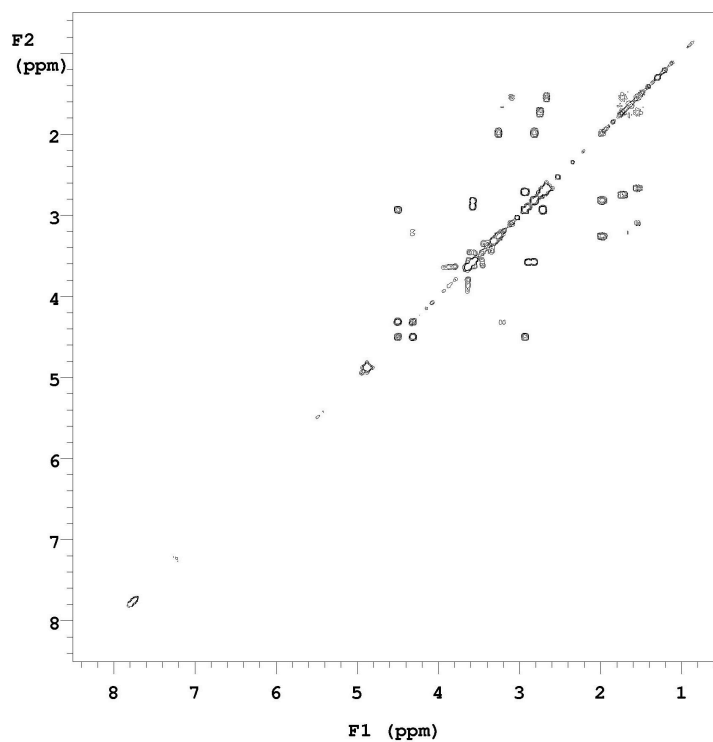
**MS (MALDI, m/z)** 852 (M+H)<sup>+</sup>

**Analytical HPLC (UV)** purity 100%, retention time = 8.65 min

**Analytical HPLC (Sedex)** purity 100%, retention time = 8.80 min



**<sup>1</sup>H NMR of 72bm**



**gCOSY NMR of 72bm**

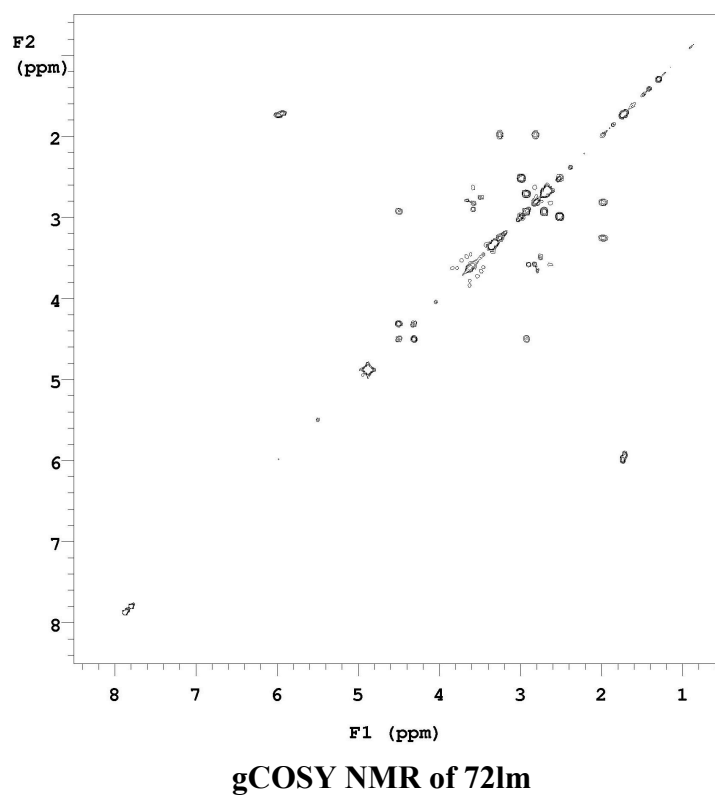
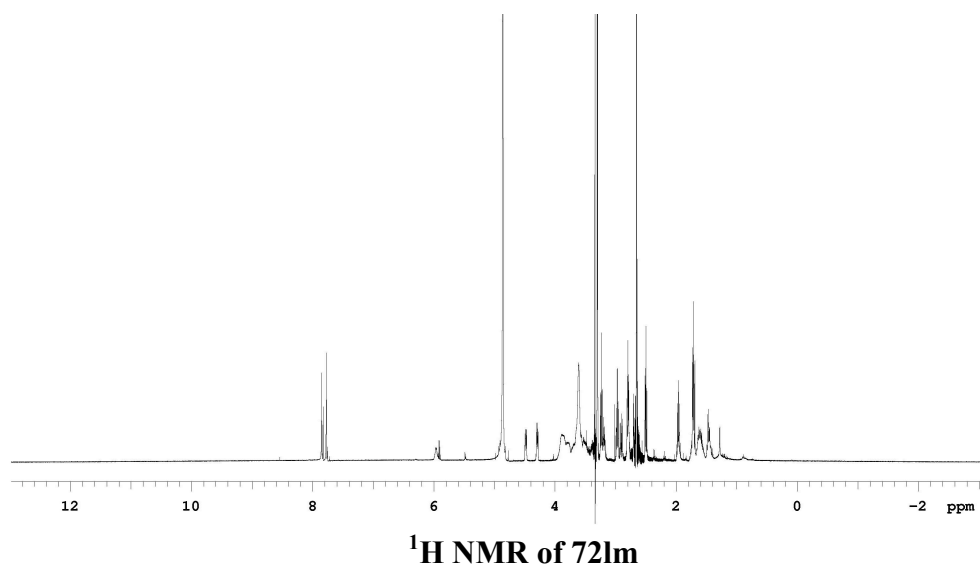
**72lm**

**$^1\text{H}$  NMR (500 MHz,  $\text{CD}_3\text{OD}$ )**  $\delta$  7.83 (s, 1H), 7.76 (s, 1H), 5.96 (s, 2H), 5.92 (q, 1H,  $J = 7.0$  Hz), 4.48 (dd, 1H,  $J = 7.5$  Hz, 4.5 Hz), 4.29 (dd, 1H,  $J = 7.5$  Hz, 4.5 Hz), 3.89-3.51 (m, 16H), 3.33 (t, 2H,  $J = 7.0$  Hz), 3.28 (m, 1H), 3.19 (t, 2H,  $J = 7.0$  Hz), 3.17 (m, 1H), 2.98 (m, 2H), 2.70 (t, 2H,  $J = 7.5$  Hz), 1.96 (m, 2H), 1.69 (d, 3H,  $J = 7.0$  Hz), 1.58 (m, 2H), 1.46 (m, 2H)

**MS (MALDI,  $m/z$ )** 867 ( $\text{M}+\text{H}$ )<sup>+</sup>

**Analytical HPLC (UV)** purity 94%, retention time = 9.27 min

**Analytical HPLC (Sedex)** purity 100%, retention time = 9.41 min



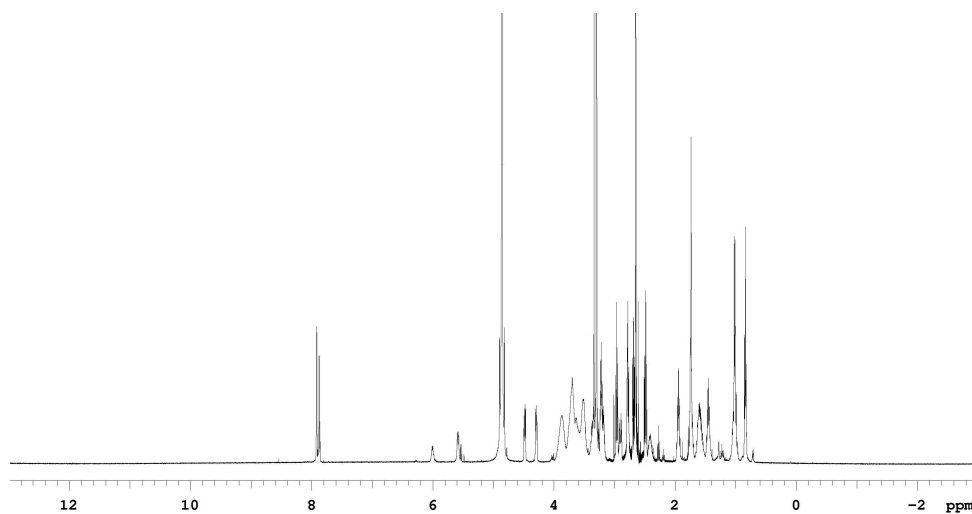
**72ci**

**<sup>1</sup>H NMR (500 MHz, CD<sub>3</sub>OD)** δ 7.91 (s, 1H), 7.89 (s, 1H), 6.01 (q, 1H, J = 7.0 Hz), 5.59 (d, 1H, J = 9.5 Hz), 4.48 (dd, 1H, J = 7.5 Hz, 5.0 Hz), 4.29 (dd, 1H, J = 7.5 Hz, 4.5 Hz), 3.87-3.35 (m, 16H), 3.19 (m, 2H), 3.17 (m, 1H), 2.92 (t, 2H, J = 7.0 Hz), 2.89 (m, 1H), 2.79 (t, 2H, J = 7.5 Hz), 2.65 (t, 2H, J = 7.0 Hz), 2.48 (m, 2H), 1.95 (m, 2H), 1.72 (d, 3H, J = 7.0 Hz), 1.71 (m, 2H), 1.57 (m, 2H), 1.03 (m, 5H), 0.82 (m, 3H)

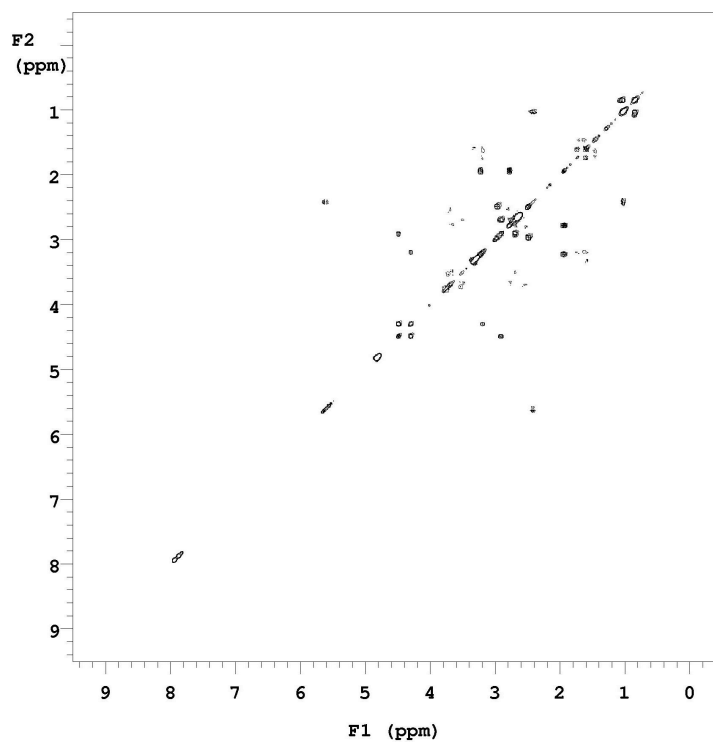
**MS (MALDI, m/z)** 923 (M+H)<sup>+</sup>

**Analytical HPLC (UV)** purity 96%, retention time = 10.58 min

**Analytical HPLC (Sedex)** purity 97%, retention time = 10.73 min



**<sup>1</sup>H NMR of 72ci**



**gCOSY NMR of 72ci**

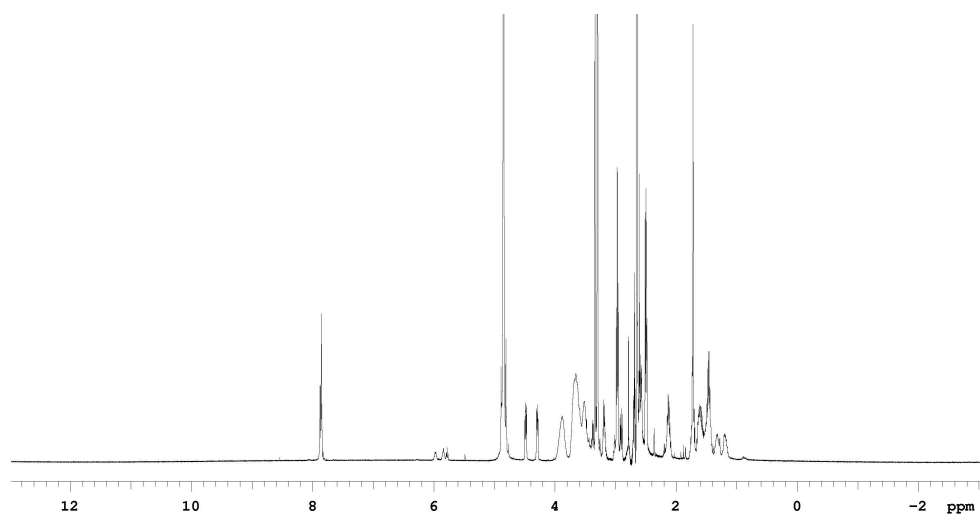
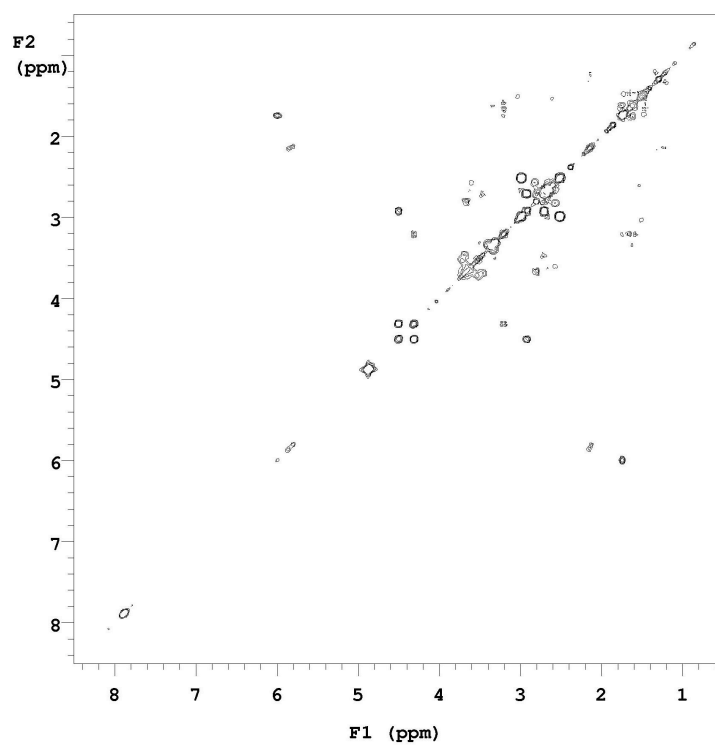
**72kl**

**$^1\text{H}$  NMR (500 MHz,  $\text{CD}_3\text{OD}$ )**  $\delta$  7.87 (s, 1H), 7.85 (s, 1H), 5.96 (q, 1H,  $J = 7.5$  Hz), 5.79 (t, 1H,  $J = 7.5$  Hz), 4.48 (dd, 1H,  $J = 7.5$  Hz, 5.0 Hz), 4.28 (dd, 1H,  $J = 7.5$  Hz, 4.0 Hz), 3.88-3.46 (m, 16H), 2.98 (m, 1H), 2.78 (t, 4H,  $J = 7.5$  Hz), 2.69 (m, 1H), 2.64 (m, 2H), 2.61 (m, 2H), 2.58 (t, 4H,  $J = 7.5$  Hz), 2.14 (m, 2H), 1.75 (d, 3H,  $J = 7.5$  Hz), 1.62 (m, 2H), 1.54 (m, 4H), 1.33 (m, 1H), 1.02 (m, 1H)

**MS (MALDI,  $m/z$ )** 911 ( $\text{M}+\text{H}$ )<sup>+</sup>

**Analytical HPLC (UV)** purity 92%, retention time = 9.18 min

**Analytical HPLC (Sedex)** purity 92%, retention time = 9.35 min

 **$^1\text{H}$  NMR of 72kl****gCOSY NMR of 72kl**



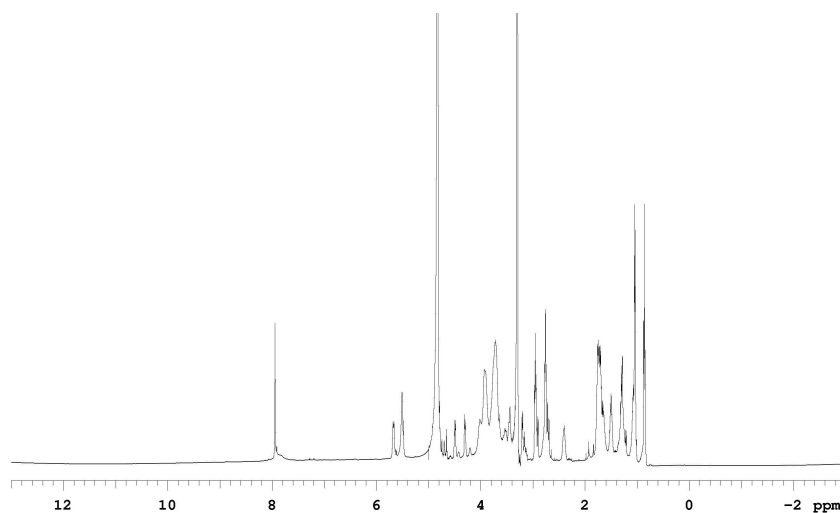
**72ae**

**<sup>1</sup>H NMR (500 MHz, CD<sub>3</sub>OD)** δ 7.94 (s, 2H), 5.68 (d, 1H, J = 10.0 Hz), 5.66 (s, 2H), 4.49 (dd, 1H, J = 7.5 Hz, 5.0 Hz), 4.29 (dd, 1H, J = 7.5 Hz, 5.0 Hz), 3.87-3.38 (m, 16H), 3.19 (m, 2H), 2.90 (m, 2H), 2.68 (m, 3H), 2.39 (m, 2H), 1.73 (m, 1H), 1.65 (m, 7H), 1.51 (m, 2H), 1.07 (m, 5H), 0.84 (m, 3H)

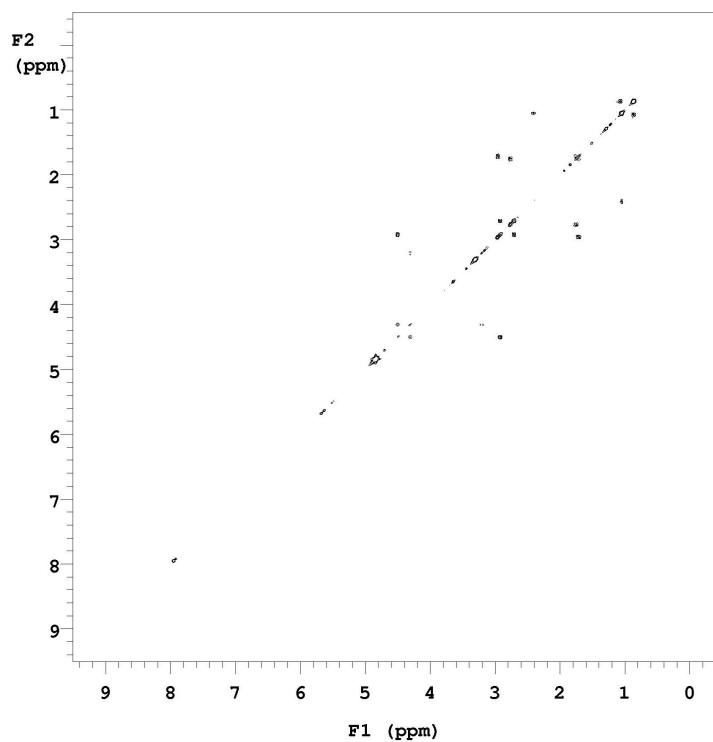
**MS (MALDI, m/z)** 867 (M+H)<sup>+</sup>

**Analytical HPLC (UV)** purity 100%, retention time = 8.93 min

**Analytical HPLC (Sedex)** purity 100%, retention time = 9.08 min



**<sup>1</sup>H NMR of 72ae**



**gCOSY NMR of 72ae**

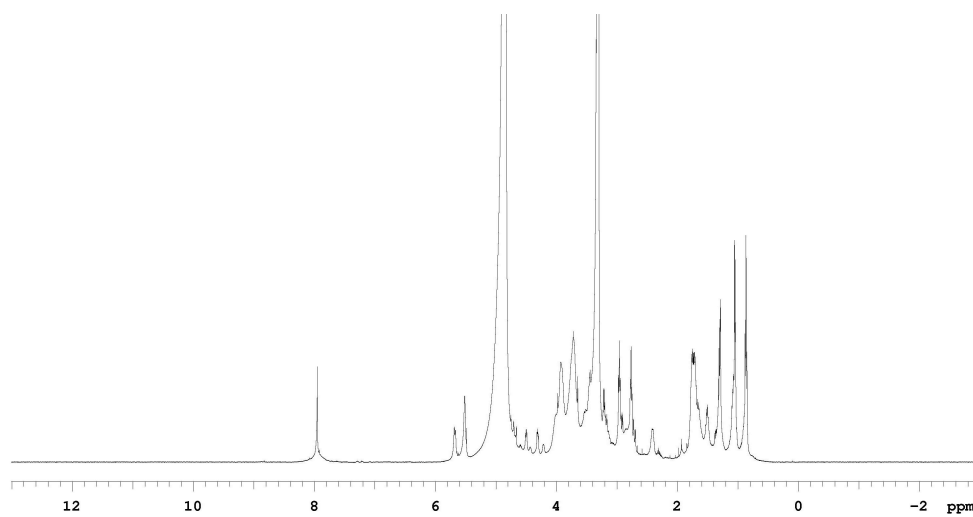
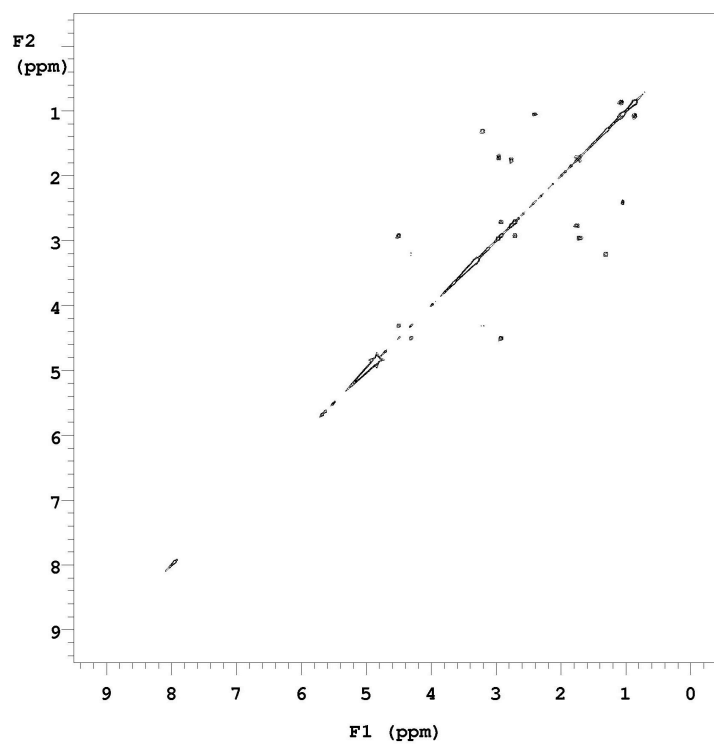
**72ad**

**$^1\text{H}$  NMR (500 MHz,  $\text{CD}_3\text{OD}$ )**  $\delta$  7.95 (s, 2H), 5.69 (d, 1H,  $J = 10.0$  Hz), 5.51 (s, 2H), 4.48 (dd, 1H,  $J = 7.5$  Hz, 5.0 Hz), 4.30 (dd, 1H,  $J = 7.5$  Hz, 5.0 Hz), 3.98-3.38 (m, 16H), 3.19 (m, 2H), 2.95 (t, 2H,  $J = 8.0$  Hz), 2.90 (t, 2H,  $J = 8.0$  Hz), 2.69 (m, 2H), 1.75 (m, 7H), 1.52 (m, 2H), 1.37 (m, 4H), 1.09 (m, 5H), 0.84 (m, 3H)

**MS (MALDI,  $m/z$ )** 853 ( $\text{M}+\text{H}$ )<sup>+</sup>

**Analytical HPLC (UV)** purity 100%, retention time = 10.95 min

**Analytical HPLC (Sedex)** purity 100%, retention time = 11.11 min

 **$^1\text{H}$  NMR of 72ad****gCOSY NMR of 72ad**

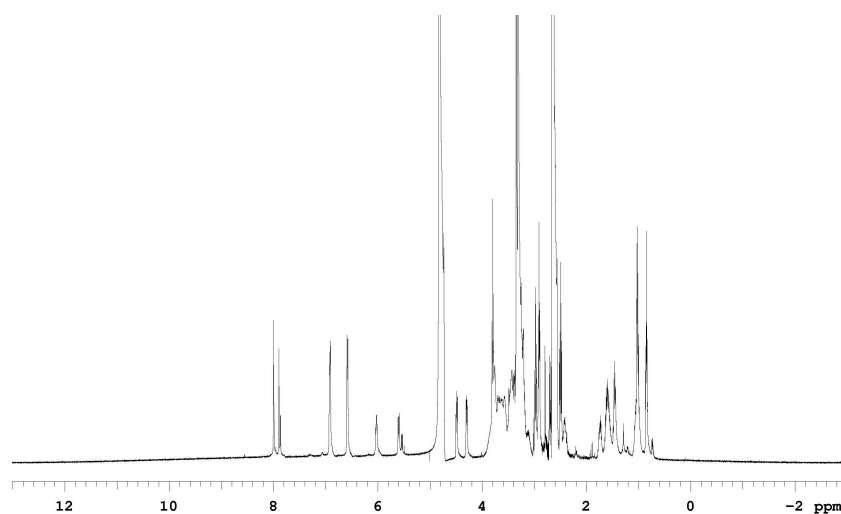
**72cn**

**$^1\text{H}$  NMR (500 MHz,  $\text{CD}_3\text{OD}$ )**  $\delta$  7.99 (s, 1H), 7.89 (s, 1H), 6.92 (d, 2H,  $J = 8.0$  Hz), 6.59 (d, 2H,  $J = 8.0$  Hz), 6.02 (t, 1H,  $J = 7.0$  Hz), 5.61 (d, 1H,  $J = 10.0$  Hz), 4.48 (dd, 1H,  $J = 7.5$  Hz, 5.0 Hz), 4.30 (dd, 1H,  $J = 7.5$  Hz, 5.0 Hz), 3.79 (t, 2H,  $J = 7.0$  Hz), 3.75-3.38 (m, 18H), 3.01 (t, 2H,  $J = 7.0$  Hz), 2.95 (t, 2H,  $J = 8.0$  Hz), 2.92 (m, 1H), 2.56 (t, 2H,  $J = 8.0$  Hz), 2.42 (m, 2H), 1.73 (m, 1H), 1.60 (m, 2H), 1.55 (m, 2H), 1.28 (m, 5H), 0.87 (m, 3H)

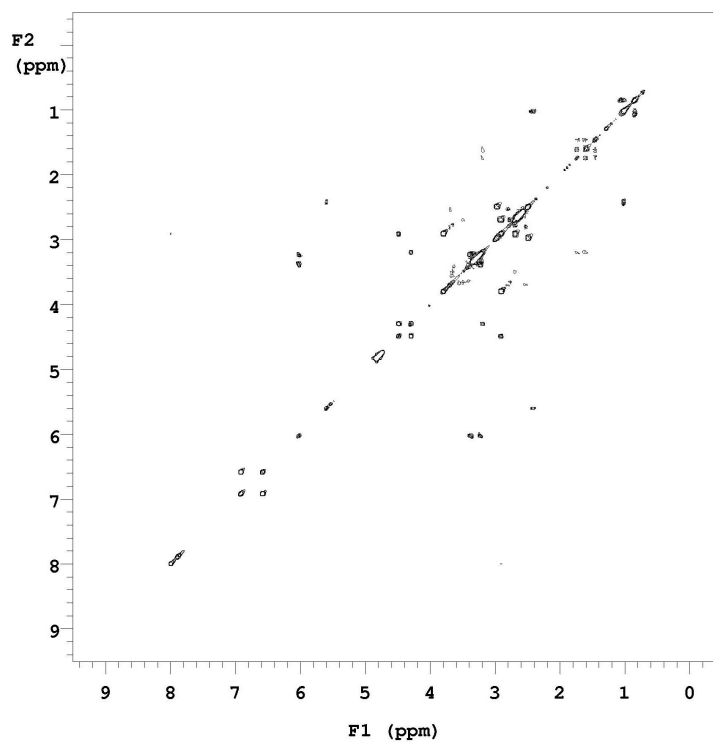
**MS (MALDI,  $m/z$ )** 960 ( $\text{M}+\text{H}$ )<sup>+</sup>

**Analytical HPLC (UV)** purity 93%, retention time = 11.38 min

**Analytical HPLC (Sedex)** purity 90%, retention time = 11.55 min



**$^1\text{H}$  NMR of 72cn**



**gCOSY NMR of 72cn**

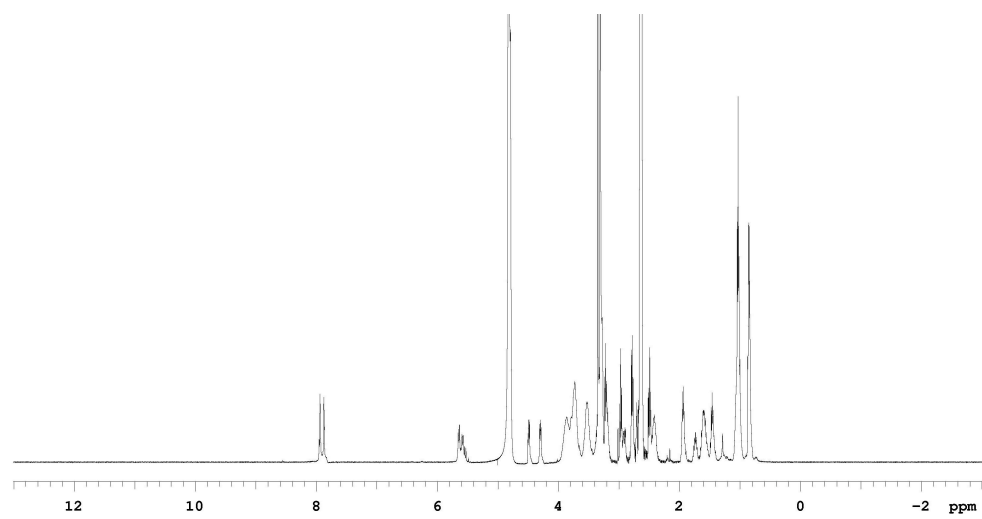
**72co**

**$^1\text{H}$  NMR (500 MHz,  $\text{CD}_3\text{OD}$ )**  $\delta$  7.93 (s, 1H), 7.87 (s, 1H), 5.64 (d, 1H,  $J = 10.0$  Hz), 5.56 (d, 1H,  $J = 9.5$  Hz), 4.48 (dd, 1H,  $J = 7.5$  Hz, 5.0 Hz), 4.30 (dd, 1H,  $J = 7.5$  Hz, 5.0 Hz), 3.75-3.38 (m, 16H), 3.23 (t, 2H,  $J = 7.0$  Hz), 2.97 (t, 2H,  $J = 8.0$  Hz), 2.89 (m, 1H), 2.78 (t, 2H,  $J = 8.0$  Hz), 2.49 (m, 2H), 2.44 (m, 2H), 1.93 (m, 2H), 1.72 (m, 1H), 1.58 (m, 2H), 1.45 (m, 2H), 1.08 (m, 10H), 0.86 (m, 6H)

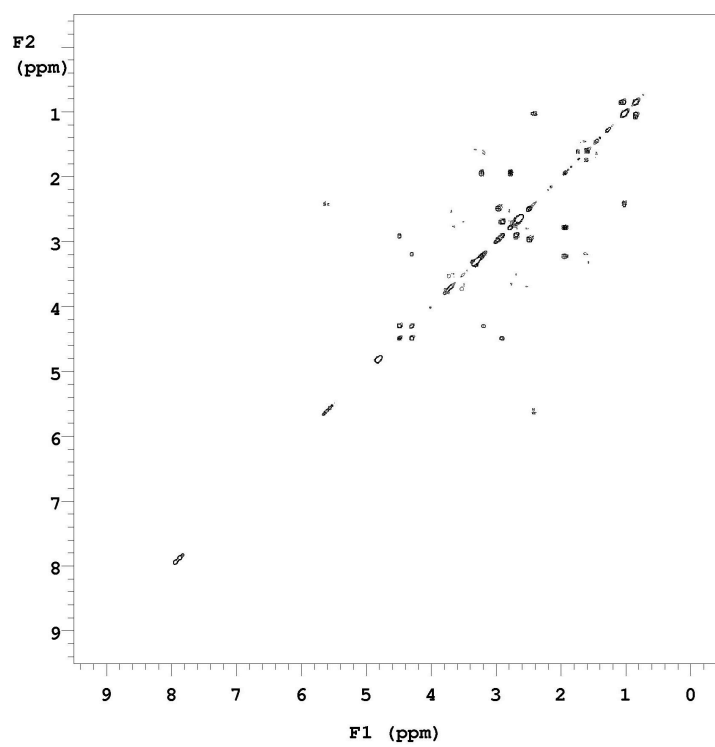
**MS (MALDI,  $m/z$ )** 965 ( $\text{M}+\text{H}$ )<sup>+</sup>

**Analytical HPLC (UV)** purity 93%, retention time = 10.80 min

**Analytical HPLC (Sedex)** purity 100%, retention time = 10.95 min



$^1\text{H}$  NMR of 72co



gCOSY NMR of 72co

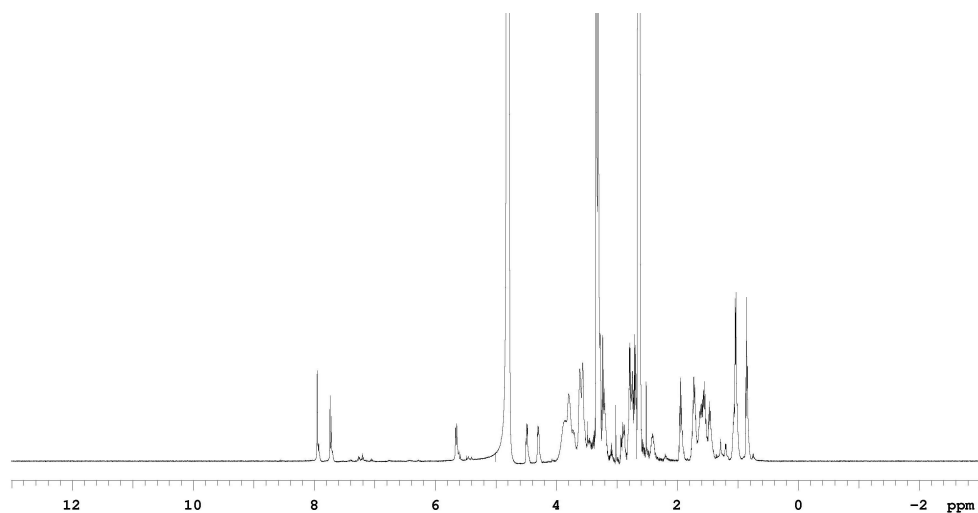
**72bo**

**<sup>1</sup>H NMR (500 MHz, CD<sub>3</sub>OD)** δ 7.95 (s, 1H), 7.74 (s, 1H), 5.67 (d, 1H, J = 10.0 Hz), 4.82 (s, 2H), 4.48 (dd, 1H, J = 7.5 Hz, 5.0 Hz), 4.30 (dd, 1H, J = 7.5 Hz, 5.0 Hz), 3.78-3.38 (m, 16H), 3.20 (t, 2H, J = 7.0 Hz), 2.78 (m, 1H), 2.74 (t, 2H, J = 8.0 Hz), 2.71 (m, 2H), 2.69 (m, 2H), 2.42 (m, 2H), 1.93 (m, 2H), 1.72 (m, 2H), 1.63 (m, 1H), 1.60 (m, 4H), 1.50 (m, 2H), 1.05 (m, 5H), 0.87 (m, 3H)

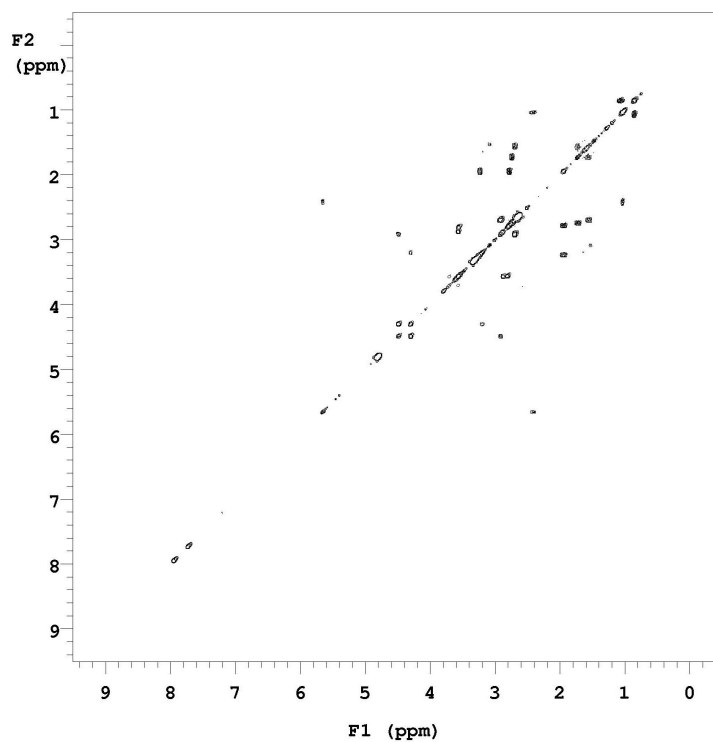
**MS (MALDI, m/z)** 908 (M+H)<sup>+</sup>

**Analytical HPLC (UV)** purity 100%, retention time = 10.03 min

**Analytical HPLC (Sedex)** purity 100%, retention time = 10.19 min



**<sup>1</sup>H NMR of 72bo**



**gCOSY NMR of 72bo**

**72jm**

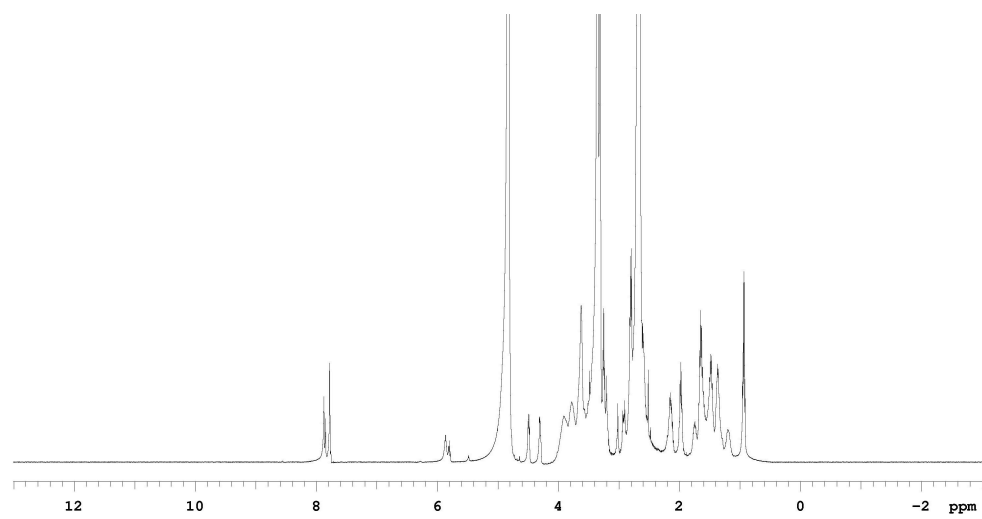
**$^1\text{H}$  NMR (500 MHz,  $\text{CD}_3\text{OD}$ )**  $\delta$  7.97 (s, 1H), 7.84 (s, 1H), 5.86 (t, 1H,  $J = 7.5$  Hz), 4.82 (s, 2H), 4.48 (dd, 1H,  $J = 7.5$  Hz, 5.0 Hz), 4.30 (dd, 1H,  $J = 7.5$  Hz, 4.0 Hz), 3.75-3.38 (m, 16H), 3.20 (t, 2H,  $J = 7.0$  Hz), 2.93 (m, 1H), 2.82 (m, 1H), 2.70 (t, 2H,  $J = 8.0$  Hz), 2.61 (t, 2H,  $J = 8.0$  Hz), 2.14 (m, 2H), 1.89 (m, 2H), 1.73 (m, 1H), 1.66 (m, 4H), 1.58 (m, 2H), 1.46 (m, 2H), 1.35 (m, 2H), 0.93 (t, 3H,  $J = 7.0$  Hz)

**MS (MALDI,  $m/z$ )** 908 ( $\text{M}+\text{H}$ )<sup>+</sup>

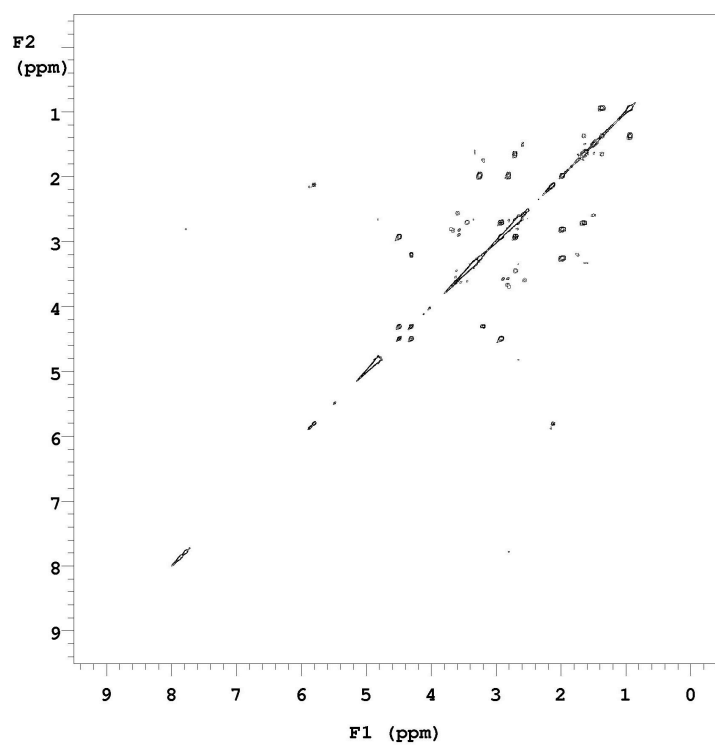
**Analytical HPLC (UV)** purity 94%, retention time = 10.11 min

**Analytical HPLC (Sedex)** purity 100%, retention time = 10.27 min





$^1\text{H}$  NMR of 72jm



gCOSY NMR of 72jm

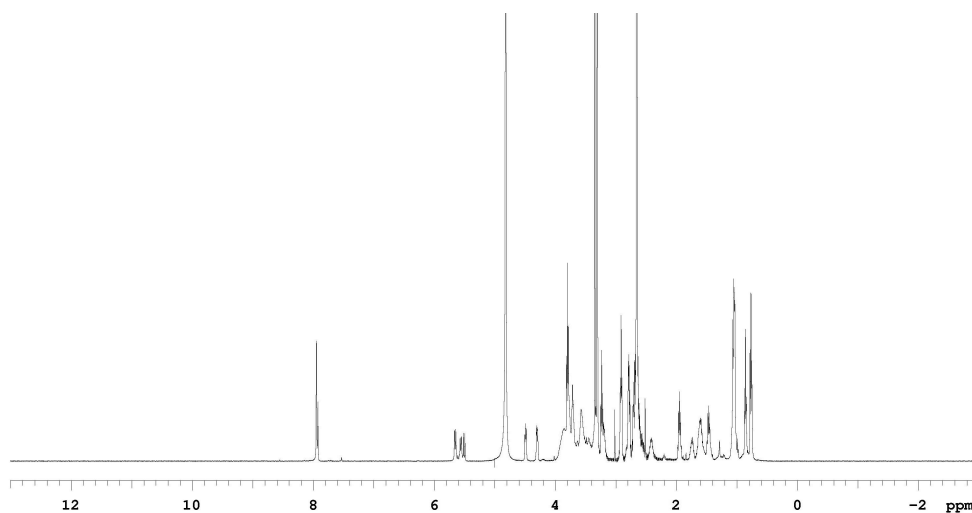
**72fo**

**<sup>1</sup>H NMR (500 MHz, CD<sub>3</sub>OD)** δ 7.94 (s, 1H), 7.91 (s, 1H), 5.64 (d, 1H, J = 10.0 Hz), 5.56 (d, 1H, J = 9.5 Hz), 4.48 (dd, 1H, J = 7.5 Hz, 5.0 Hz), 4.30 (dd, 1H, J = 7.5 Hz, 4.0 Hz), 3.75-3.38 (m, 18H), 3.24 (t, 2H, J = 7.0 Hz), 3.22 (m, 1H), 2.92 (t, 2H, J = 8.0 Hz), 2.78 (m, 3H), 2.56 (m, 1H), 2.40 (m, 2H), 1.92 (m, 1H), 1.61 (m, 2H), 1.56 (m, 2H), 1.06 (m, 6H), 1.08 (m, 5H), 0.84 (m, 3H)

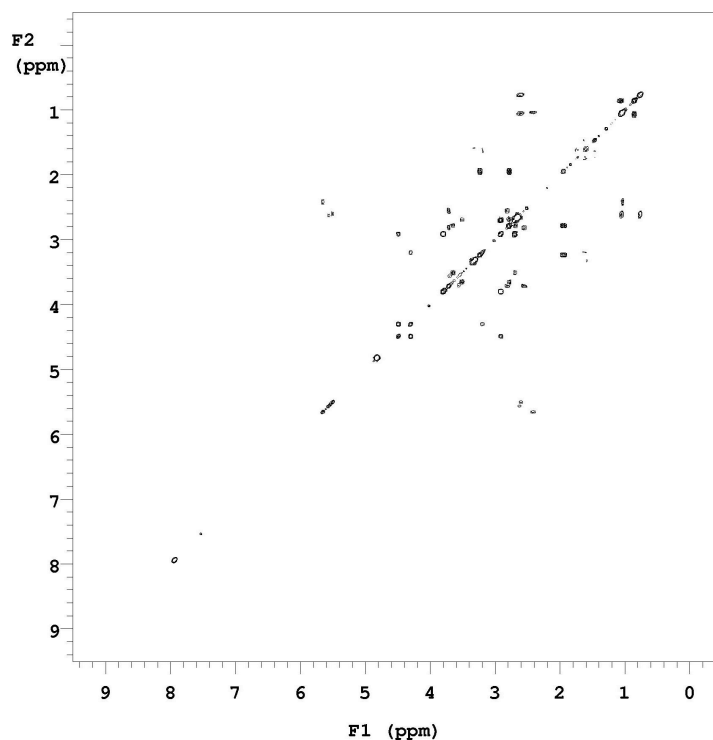
**MS (MALDI, m/z)** 923 (M+H)<sup>+</sup>

**Analytical HPLC (UV)** purity 100%, retention time = 11.12 min

**Analytical HPLC (Sedex)** purity 94%, retention time = 11.27 min



**<sup>1</sup>H NMR of 72fo**



**gCOSY NMR of 72fo**

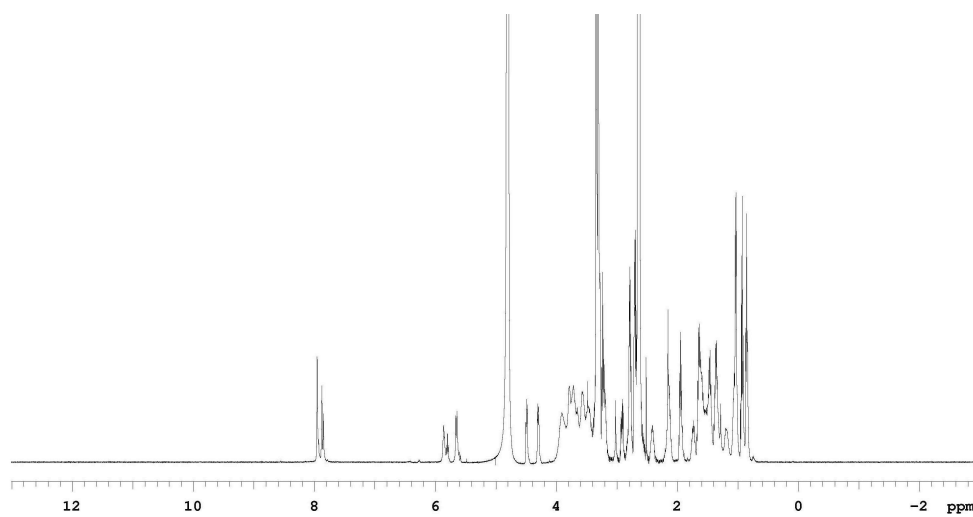
### **72jo**

**<sup>1</sup>H NMR (500 MHz, CD<sub>3</sub>OD)**  $\delta$  7.95 (s, 1H), 7.87 (s, 1H), 5.86 (t, 1H, J = 7.5 Hz), 5.66 (d, 1H, J = 10.0 Hz), 4.48 (dd, 1H, J = 7.5 Hz, 5.0 Hz), 4.30 (dd, 1H, J = 7.5 Hz, 4.5 Hz), 3.91-3.38 (m, 16H), 3.02 (t, 2H, J = 7.0 Hz), 3.02 (m, 1H), 2.75 (m, 1H), 2.66 (t, 2H, J = 8.0 Hz), 2.59 (t, 2H, J = 8.0 Hz), 2.11 (m, 1H), 1.75 (m, 2H), 1.65 (m, 2H), 1.58 (m, 1H), 1.53 (m, 4H), 1.39 (m, 2H), 1.34 (m, 2H), 1.20 (m, 1H), 1.06 (t, 3H, J = 7.0 Hz), 1.03 (m, 5H), 0.86 (m, 3H)

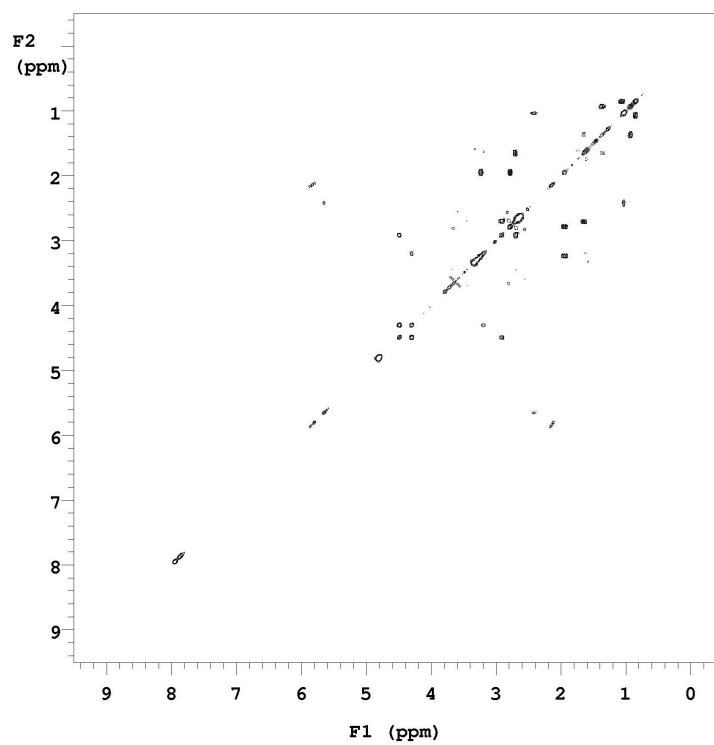
**MS (MALDI, m/z)** 964 (M+H)<sup>+</sup>

**Analytical HPLC (UV)** purity 100%, retention time = 11.25 min

**Analytical HPLC (Sedex)** purity 100%, retention time = 11.39 min



$^1\text{H}$  NMR of 72jo



gCOSY NMR of 72jo

**72dn**

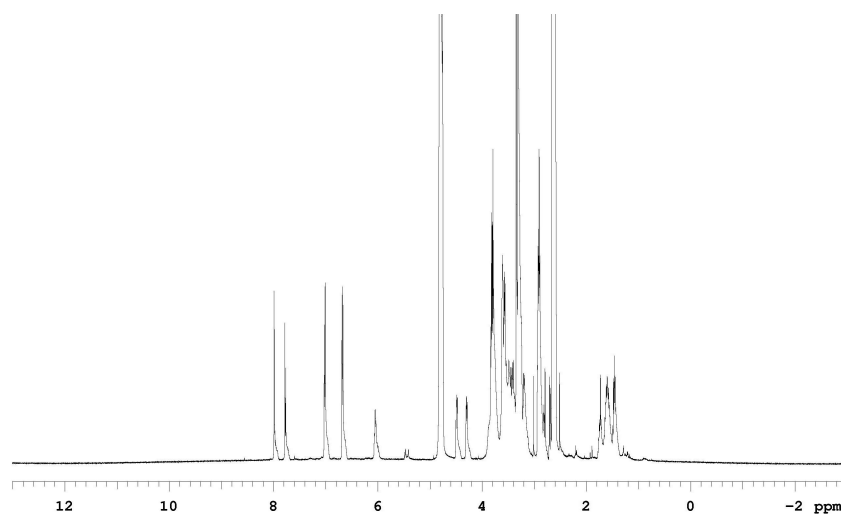
**<sup>1</sup>H NMR (500 MHz, CD<sub>3</sub>OD)** δ 7.99 (s, 1H), 7.78 (s, 1H), 7.02 (d, 2H, J = 8.5 Hz), 6.86 (d, 2H, J = 8.5 Hz), 6.05 (m, 2H), 4.48 (dd, 1H, J = 7.5 Hz, 5.0 Hz), 4.30 (dd, 1H, J = 7.5 Hz, 5.0 Hz), 3.89 (m, 4H), 3.75-3.38 (m, 16H), 3.36 (m, 2H), 3.21 (m, 2H), 2.92 (m, 4H),

1.72 (m, 1H), 1.60 (m, 2H), 1.45 (m, 2H)

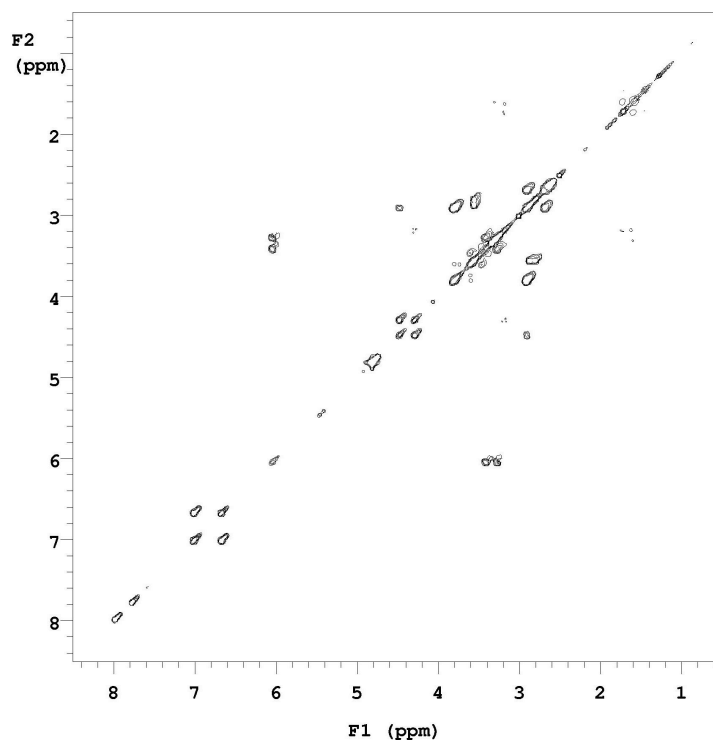
**MS (MALDI, m/z)** 876 (M+H)<sup>+</sup>

**Analytical HPLC (UV)** purity 92%, retention time = 9.62 min

**Analytical HPLC (Sedex)** purity 100%, retention time = 9.77 min



**<sup>1</sup>H NMR of 72dn**



**gCOSY NMR of 72dn**

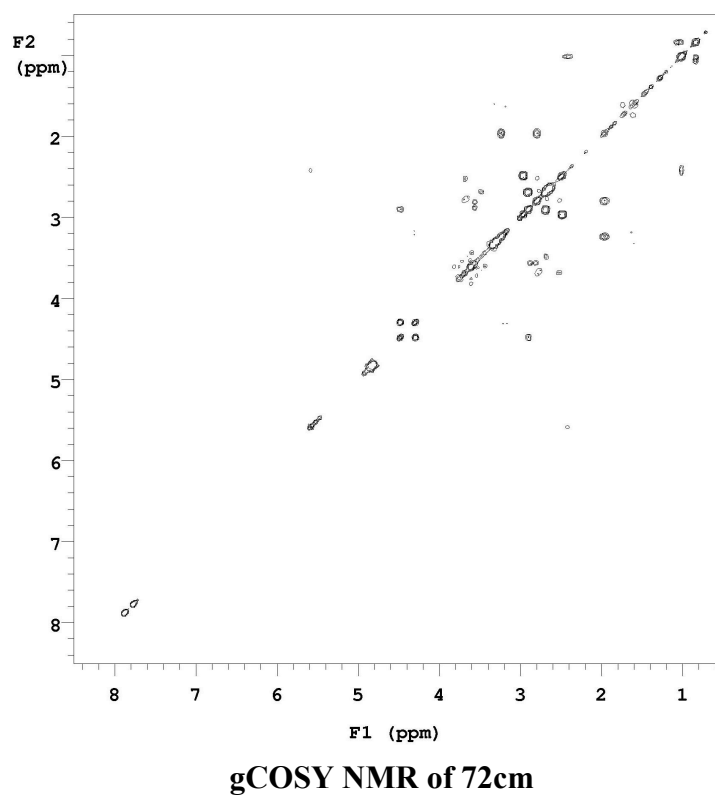
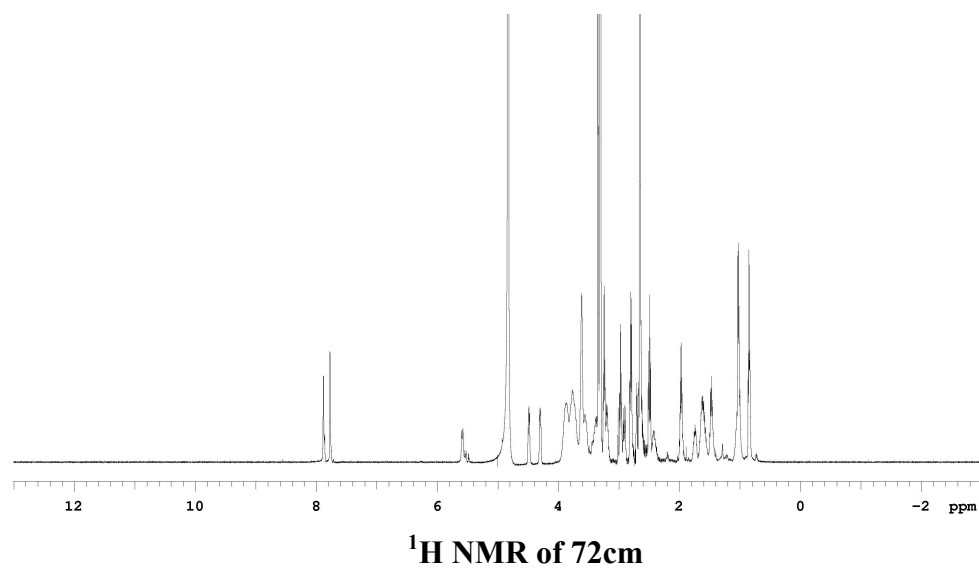
**72cm**

**$^1\text{H}$  NMR (500 MHz,  $\text{CD}_3\text{OD}$ )**  $\delta$  7.88 (s, 1H), 7.77 (s, 1H), 5.59 (d, 1H,  $J = 10.0$  Hz), 4.82 (s, 2H), 4.48 (dd, 1H,  $J = 7.5$  Hz, 5.0 Hz), 4.30 (dd, 1H,  $J = 7.5$  Hz, 5.0 Hz), 3.87-3.38 (m, 16H), 3.20 (t, 2H,  $J = 7.0$  Hz), 3.18 (m, 1H), 2.96 (t, 2H,  $J = 7.5$  Hz), 2.90 (m, 1H), 2.82 (t, 2H,  $J = 7.0$  Hz), 2.59 (t, 2H,  $J = 8.0$  Hz), 2.49 (m, 1H), 2.41 (m, 2H), 1.73 (m, 1H), 1.61 (m, 2H), 1.49 (m, 2H), 1.08 (m, 5H), 0.86 (m, 3H)

**MS (MALDI,  $m/z$ )** 909 ( $\text{M}+\text{H}$ )<sup>+</sup>

**Analytical HPLC (UV)** purity 96%, retention time = 10.67 min

**Analytical HPLC (Sedex)** purity 95%, retention time = 10.83 min



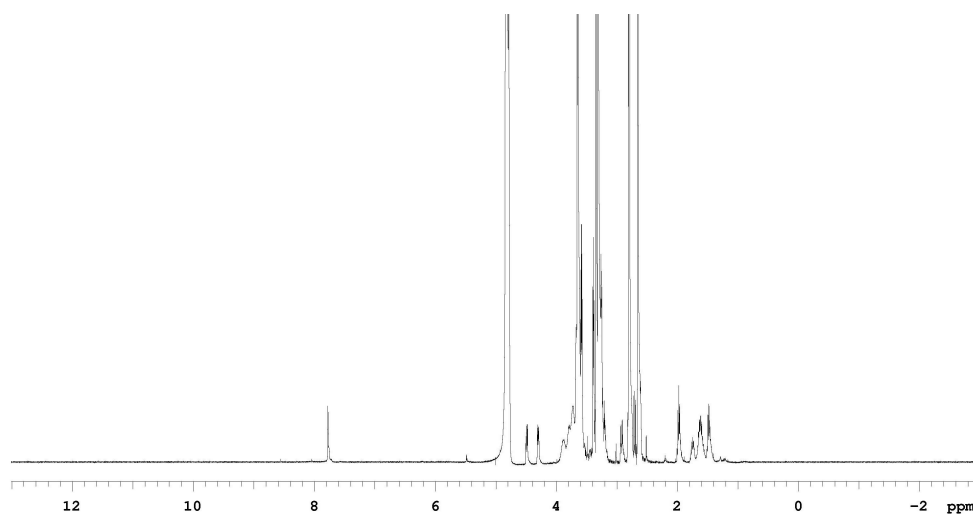
**72m'**

**$^1\text{H}$  NMR (500 MHz,  $\text{CD}_3\text{OD}$ )**  $\delta$  7.77 (s, 1H), 4.84 (s, 2H), 4.49 (dd, 1H,  $J = 7.5$  Hz, 5.0 Hz), 4.30 (dd, 1H,  $J = 7.5$  Hz, 5.0 Hz), 3.89-3.68 (m, 16H), 3.64 (t, 2H,  $J = 7.0$  Hz), 3.44 (t, 2H,  $J = 7.0$  Hz), 3.29 (m, 2H), 2.93 (m, 1H), 1.97 (m, 2H), 1.72 (m, 1H), 1.62 (m, 2H), 1.48 (m, 2H)

**MS (MALDI,  $m/z$ )** 672 ( $\text{M}+\text{H}$ )<sup>+</sup>

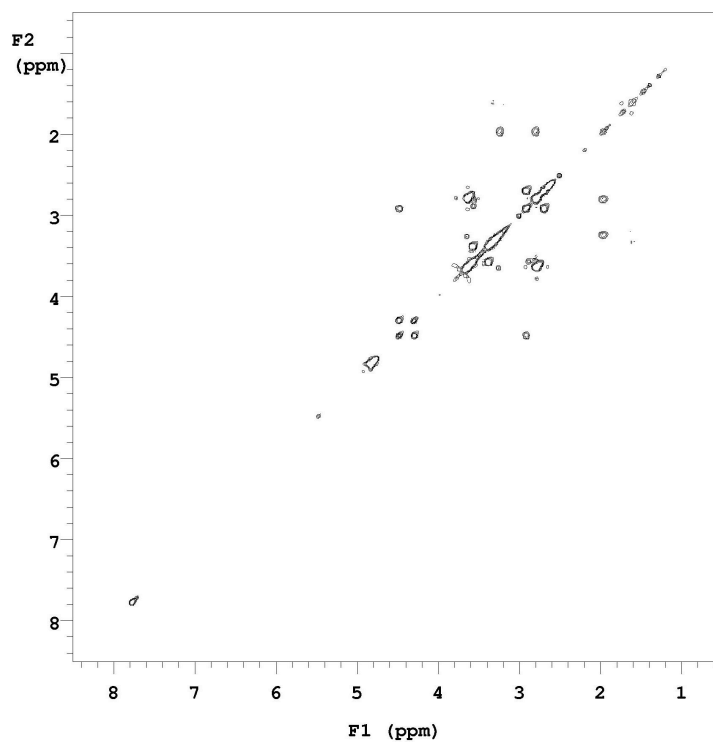
**Analytical HPLC (UV)** purity 100%, retention time = 10.38 min

**Analytical HPLC (Sedex)** purity 100%, retention time = 10.54 min



**$^1\text{H}$  NMR of 72m'**





**gCOSY NMR of 72m'**

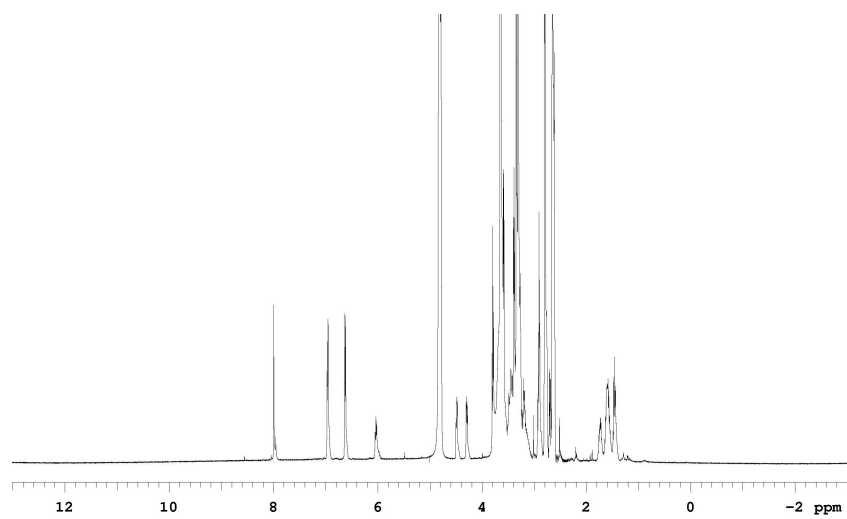
**72n'**

**$^1\text{H}$  NMR (500 MHz,  $\text{CD}_3\text{OD}$ )**  $\delta$  7.99 (s, 1H), 6.97 (d, 2H,  $J = 8.0$  Hz), 6.63 (d, 2H,  $J = 8.0$  Hz), 6.03 (t, 1H,  $J = 7.5$  Hz), 4.48 (dd, 1H,  $J = 7.5$  Hz, 5.0 Hz), 4.30 (dd, 1H,  $J = 7.5$  Hz, 4.0 Hz), 3.80-3.38 (m, 18H), 3.37 (t, 2H,  $J = 7.0$  Hz), 3.28 (m, 2H), 3.20 (t, 2H,  $J = 7.0$  Hz), 2.92 (m, 1H), 1.73 (m, 1H), 1.59 (m, 2H), 1.46 (m, 2H)

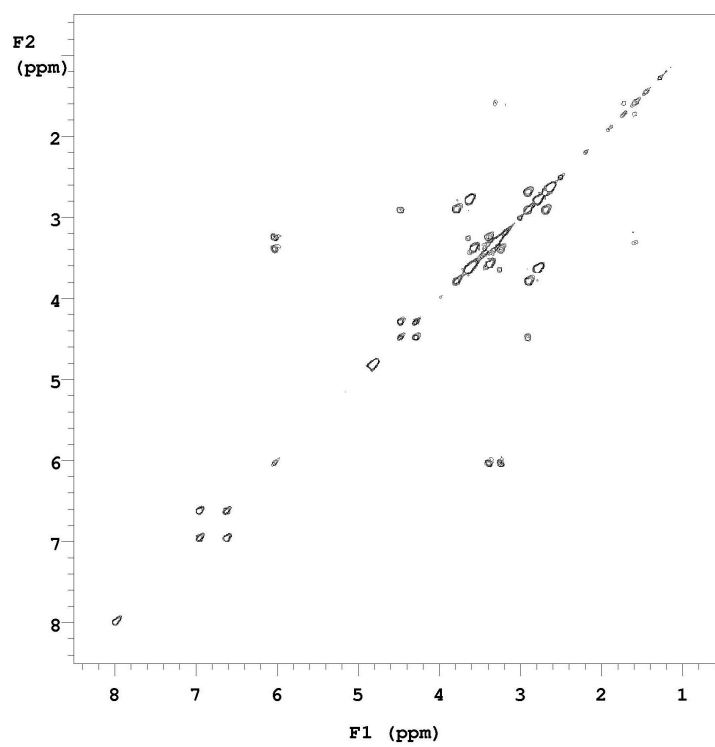
**MS (MALDI,  $m/z$ )** 723 ( $\text{M}+\text{H}$ )<sup>+</sup>

**Analytical HPLC (UV)** purity 100%, retention time = 10.30 min

**Analytical HPLC (Sedex)** purity 100%, retention time = 10.47 min



$^1\text{H}$  NMR of 72n'



gCOSY NMR of 72n'

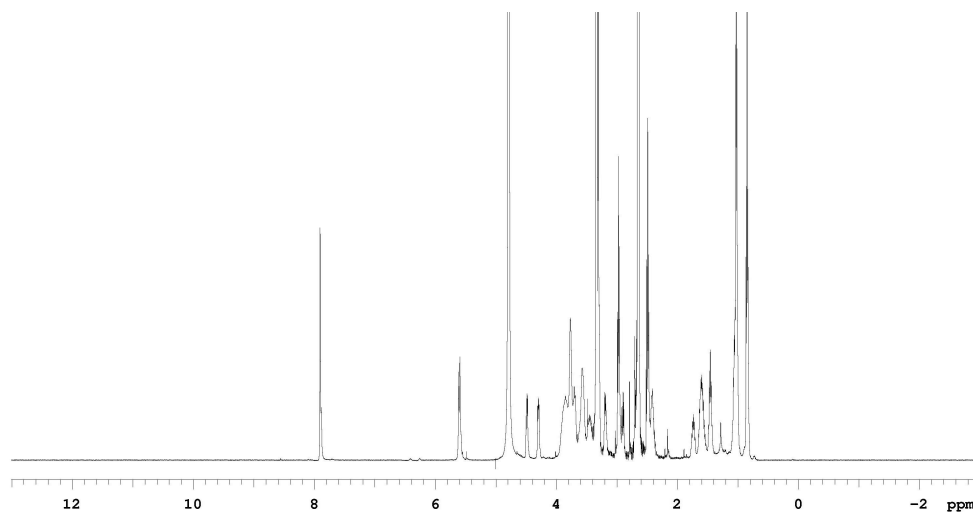
**72cc**

**$^1\text{H}$  NMR (500 MHz,  $\text{CD}_3\text{OD}$ )**  $\delta$  7.90 (s, 2H), 5.61 (d, 2H,  $J = 10.0$  Hz), 4.49 (dd, 1H,  $J = 7.5$  Hz, 5.0 Hz), 4.29 (dd, 1H,  $J = 7.5$  Hz, 5.0 Hz), 3.85-3.38 (m, 16H), 3.19 (m, 2H), 2.95 (t, 4H,  $J = 8.0$  Hz), 2.90 (m, 1H), 2.68 (t, 4H,  $J = 8.0$  Hz), 2.39 (m, 2H), 1.75 (m, 1H), 1.61 (m, 2H), 1.47 (m, 2H), 1.09 (m, 10H), 0.84 (m, 6H)

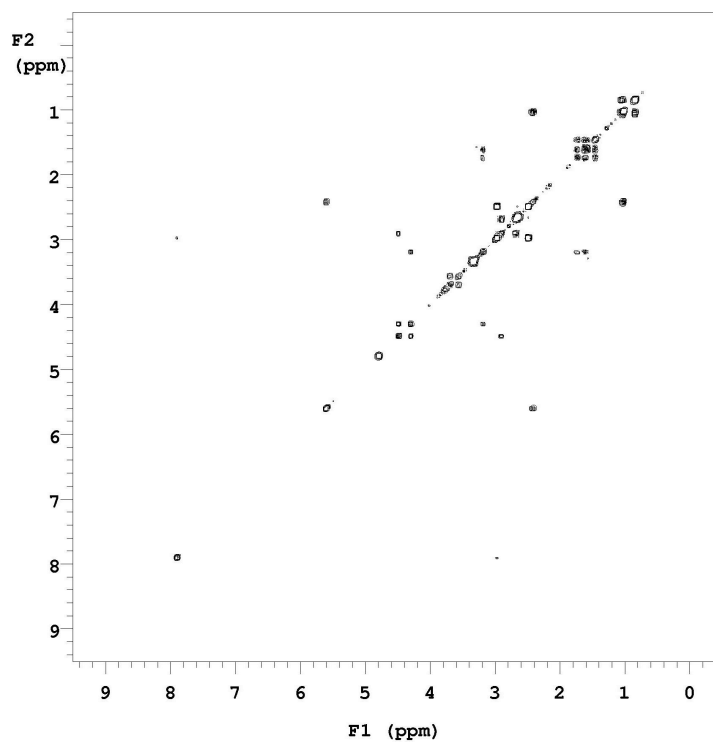
**MS (MALDI,  $m/z$ )** 938 ( $\text{M}+\text{H}$ )<sup>+</sup>

**Analytical HPLC (UV)** purity 100%, retention time = 12.28 min

**Analytical HPLC (Sedex)** purity 87%, retention time = 12.41 min



**$^1\text{H}$  NMR of 72cc**



**gCOSY NMR of 72c**

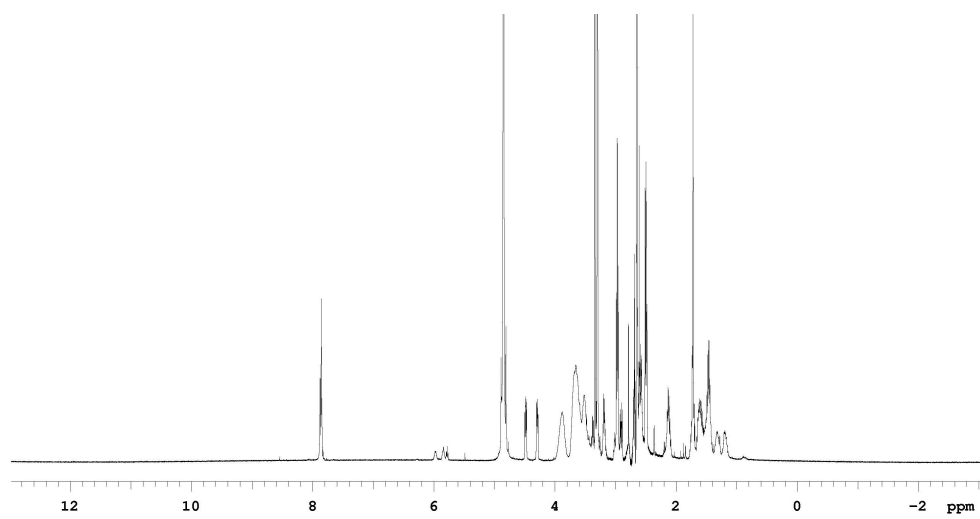
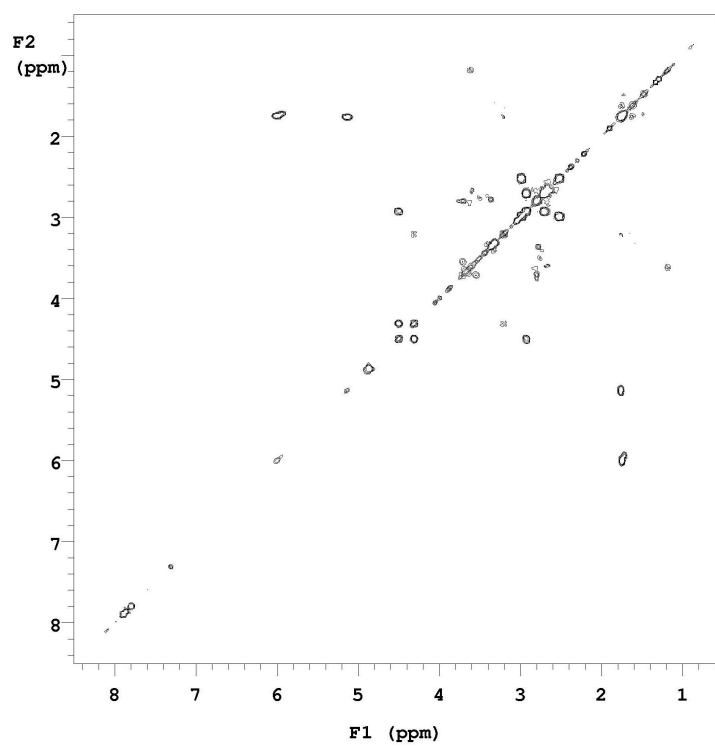
## **72II**

**<sup>1</sup>H NMR (500 MHz, CD<sub>3</sub>OD)** δ 7.89 (s, 1H), 7.79 (s, 1H), 6.01 (s, 1H), 5.14 (q, 2H, J = 7.5 Hz), 4.51 (dd, 1H, J = 7.5 Hz, 5.0 Hz), 4.31 (dd, 1H, J = 7.5 Hz, 4.0 Hz), 3.89-3.76 (m, 16 H), 3.22 (m, 1H), 3.05 (m, 1H), 2.98 (m, 4H), 2.95 (m, 1H), 2.92 (m, 2H), 2.53 (m, 4H), 1.76 (d, 6H, J = 7.5 Hz), 1.62 (m, 2H), 1.54 (m, 2H)

**MS (MALDI, m/z)** 854 (M+H)<sup>+</sup>

**Analytical HPLC (UV)** purity 91%, retention time = 9.65 min

**Analytical HPLC (Sedex)** purity 89%, retention time = 9.79 min

 **$^1\text{H}$  NMR of 72II****gCOSY NMR of 72II**

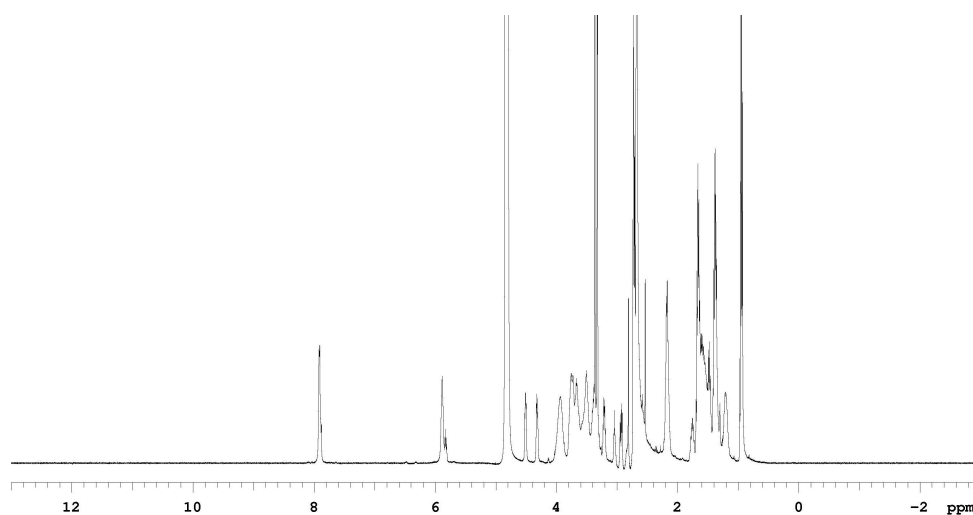
**72jj**

**$^1\text{H}$  NMR (500 MHz,  $\text{CD}_3\text{OD}$ )**  $\delta$  7.88 (s, 2H), 5.86 (m, 2H), 4.48 (dd, 1H,  $J = 7.5$  Hz, 5.0 Hz), 4.29 (dd, 1H,  $J = 7.5$  Hz, 4.0 Hz), 3.98-3.32 (m, 16H), 3.20 (m, 1H), 2.92 (m, 1H), 2.79 (m, 2H), 2.15 (m, 4H), 1.64 (m, 4H), 1.59 (m, 2H), 1.53 (m, 2H), 1.38 (m, 4H), 1.95 (t, 6H,  $J = 7.5$  Hz)

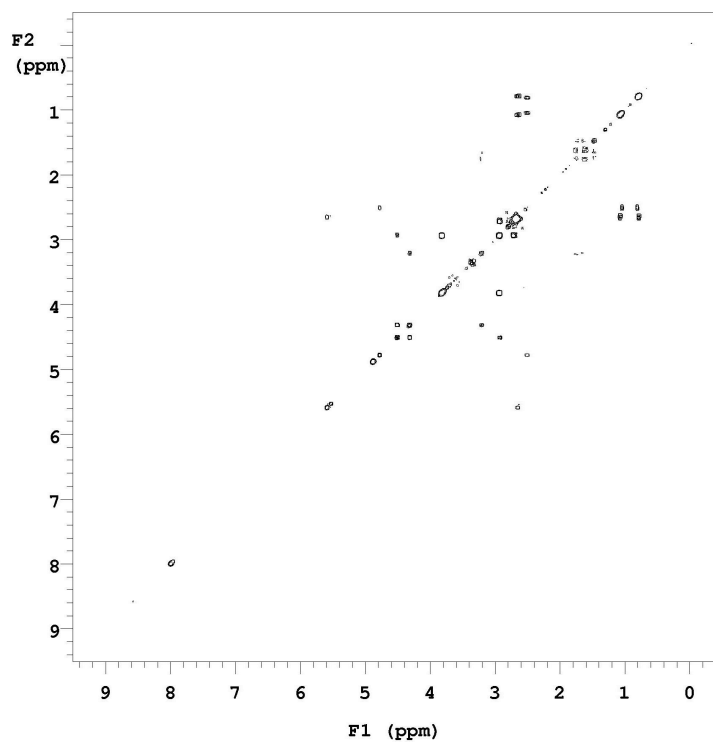
**MS (MALDI,  $m/z$ )** 936 ( $\text{M}+\text{H}$ )<sup>+</sup>

**Analytical HPLC (UV)** purity 90%, retention time = 11.10 min

**Analytical HPLC (Sedex)** purity 92%, retention time = 11.25 min



**$^1\text{H}$  NMR of 72jj**



**gCOSY NMR of 72jj**

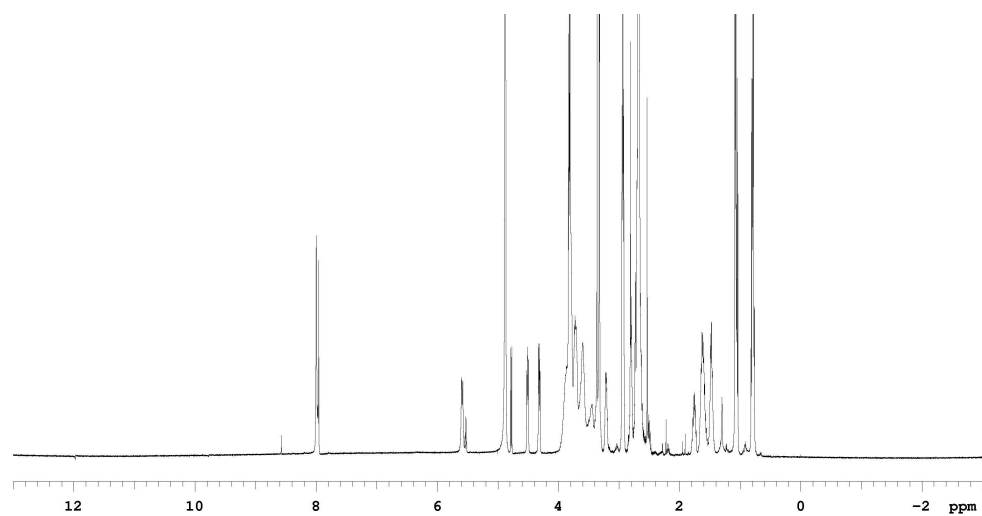
**72ff**

**<sup>1</sup>H NMR (500 MHz, CD<sub>3</sub>OD)** δ 8.00 (s, 1H), 7.96 (s, 1H), 5.60 (d, 2H, J = 4.5 Hz), 4.51 (dd, 1H, J = 7.5 Hz, 5.5 Hz), 4.31 (dd, 1H, J = 8.0 Hz, 4.5 Hz), 3.98-3.36 (m, 18H), 3.20 (m, 1H), 2.95 (t, 4H, J = 7.0 Hz), 2.72 (m, 2H), 2.54 (m, 1H), 1.63 (m, 2H), 1.47 (m, 2H), 1.08 (d, 3H, J = 7.0 Hz), 1.07 (d, 3H, J = 7.0 Hz), 0.79 (d, 3H, J = 7.0 Hz), 0.76 (d, 3H, J = 7.0 Hz)

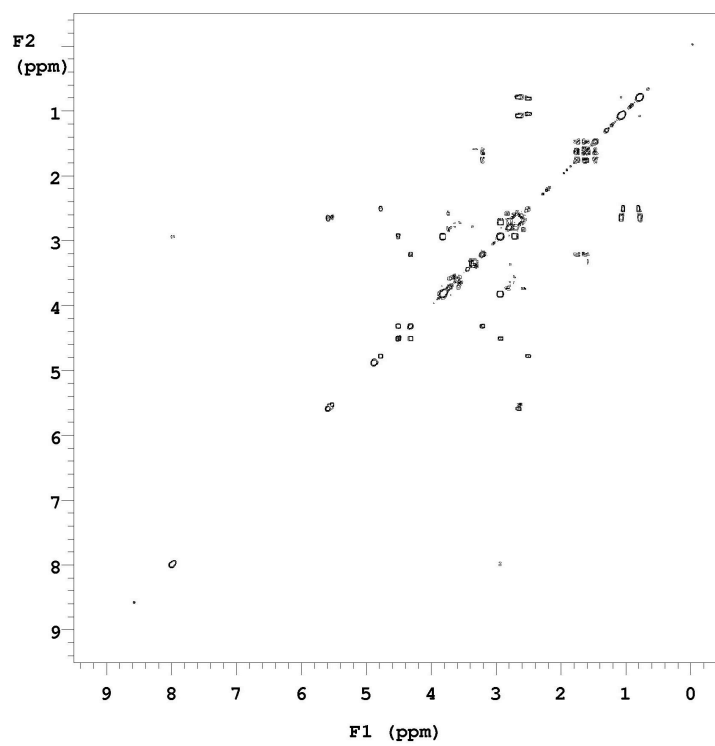
**MS (MALDI, m/z)** 854 (M+H)<sup>+</sup>

**Analytical HPLC (UV)** purity 100%, retention time = 10.78 min

**Analytical HPLC (Sedex)** purity 99%, retention time = 10.93 min



$^1\text{H}$  NMR of 72ff



gCOSY NMR of 72ff



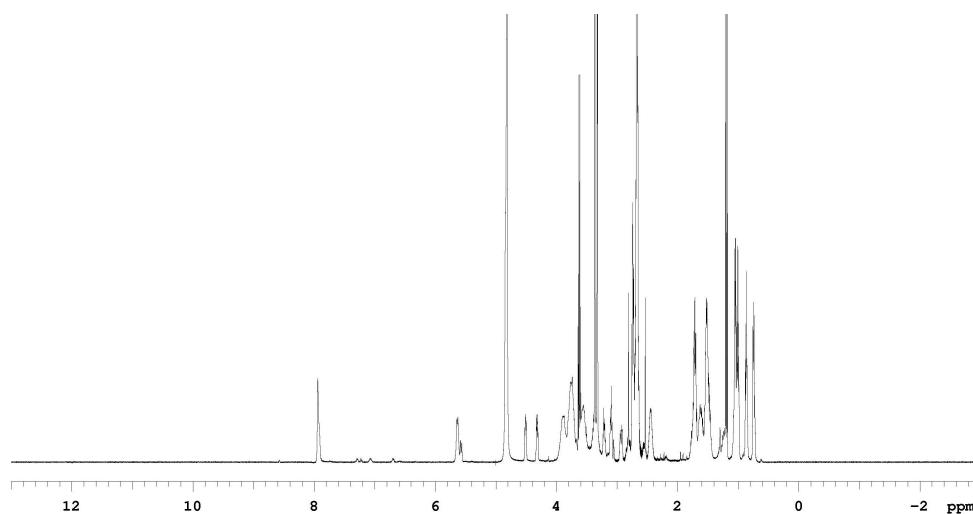
**72aa**

**<sup>1</sup>H NMR (500 MHz, CD<sub>3</sub>OD)** δ 7.92 (s, 2H), 5.60 (d, 1H, J = 9.0 Hz), 5.54 (d, 1H, J = 9.0 Hz), 4.48 (dd, 1H, J = 7.5 Hz, 5.5 Hz), 4.29 (dd, 1H, J = 7.5 Hz, 4.0 Hz), 3.86-3.38 (m, 20H), 3.18 (m, 1H), 3.07 (m, 2H), 2.89 (m, 1H), 2.73 (m, 4H), 2.43 (m, 2H), 1.73 (m, 4H), 1.56 (m, 2H), 1.45 (m, 6H), 1.81 (m, 6H), 1.05 (m, 6H), 0.96 (m, 4H)

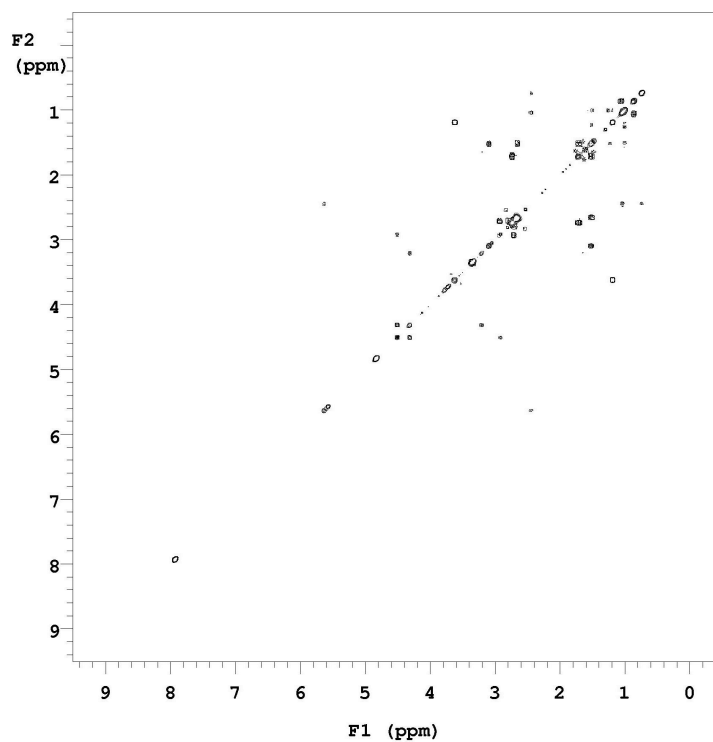
**MS (MALDI, m/z)** 936 (M+H)<sup>+</sup>

**Analytical HPLC (UV)** purity 93%, retention time = 10.88 min

**Analytical HPLC (Sedex)** purity 100%, retention time = 11.95 min



**<sup>1</sup>H NMR of 72aa**



**gCOSY NMR of 72aa**

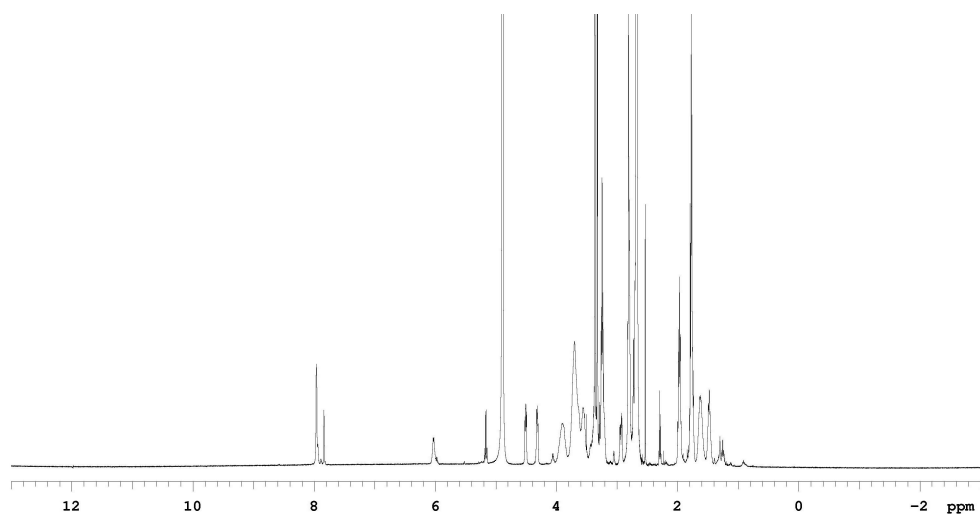
**72ii**

**$^1\text{H}$  NMR (500 MHz,  $\text{CD}_3\text{OD}$ )**  $\delta$  7.94 (s, 1H), 7.82 (s, 1H), 6.01 (q, 1H,  $J = 7.5$  Hz), 5.15 (q, 1H,  $J = 7.5$  Hz), 4.48 (dd, 1H,  $J = 7.5$  Hz, 5.0 Hz), 4.29 (q, 1H,  $J = 7.5$  Hz, 4.5 Hz), 3.87-3.43 (m, 16H), 3.29 (t, 4H,  $J = 7.5$  Hz), 3.23 (m, 1H), 3.19 (t, 4H,  $J = 7.0$  Hz), 2.62 (m, 4H), 1.95 (d, 6H,  $J = 7.5$  Hz), 1.74 (m, 2H), 1.48 (m, 2H)

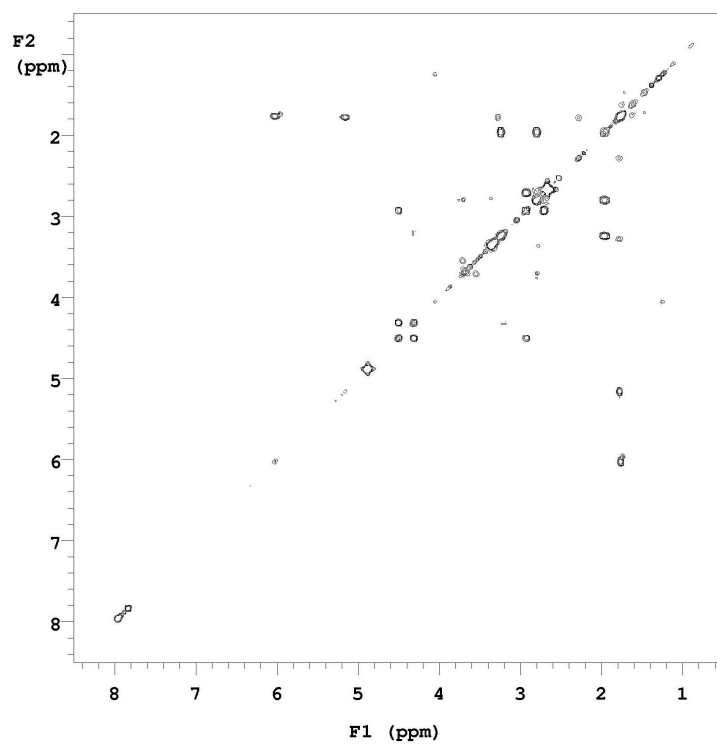
**MS (MALDI,  $m/z$ )** 908 ( $\text{M}+\text{H}$ )<sup>+</sup>

**Analytical HPLC (UV)** purity 91%, retention time = 9.10 min

**Analytical HPLC (Sedex)** purity 95%, retention time = 9.24 min



$^1\text{H}$  NMR of 72ii



gCOSY NMR of 72ii

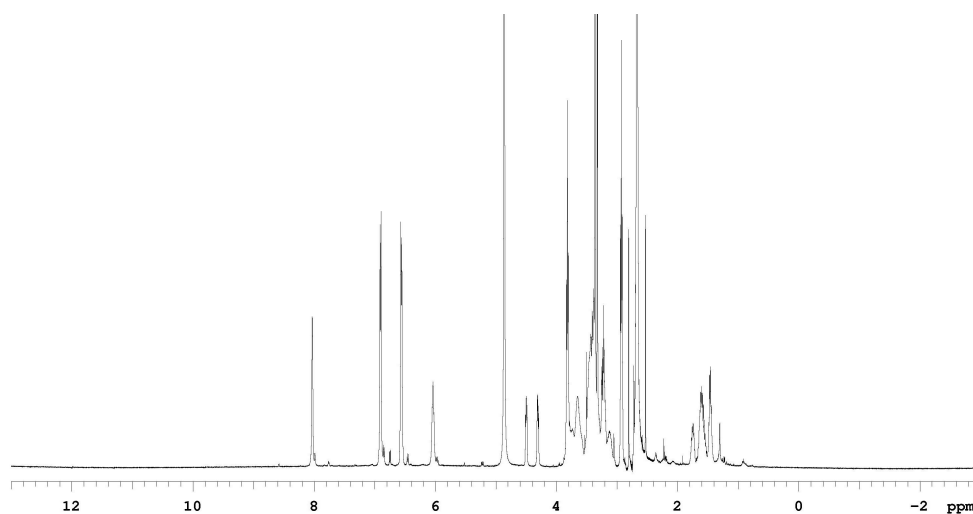
**72nn**

**$^1\text{H}$  NMR (500 MHz,  $\text{CD}_3\text{OD}$ )**  $\delta$  8.08 (s, 2H), 6.91 (d, 4H,  $J = 8.0$  Hz), 6.56 (d, 4H,  $J = 8.0$  Hz), 6.04 (t, 2H,  $J = 7.5$  Hz), 4.95 (dd, 1H,  $J = 7.5$  Hz, 5.0 Hz), 4.30 (dd, 1H,  $J = 7.5$  Hz, 4.5 Hz), 3.80 (t, 4H,  $J = 6.5$  Hz), 3.74-3.34 (m, 16H), 3.32 (m, 4H), 3.19 (t, 4H,  $J = 6.5$  Hz), 3.15 (m, 2H), 2.80 (m, 2H), 1.76 (m, 1H), 1.67 (m, 2H), 1.48 (m, 2H)

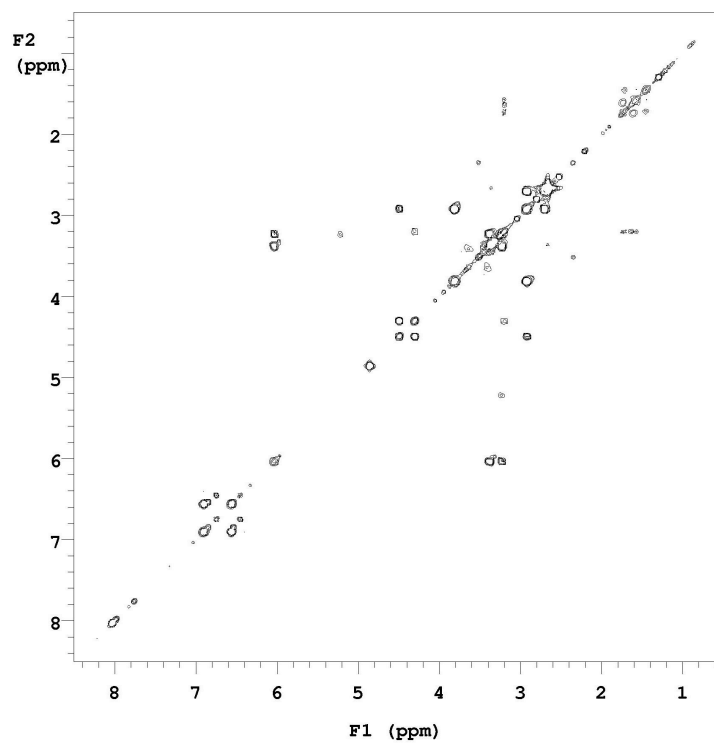
**MS (MALDI,  $m/z$ )** 982 ( $\text{M}+\text{H}$ )<sup>+</sup>

**Analytical HPLC (UV)** purity 96%, retention time = 10.28 min

**Analytical HPLC (Sedex)** purity 96%, retention time = 10.42 min

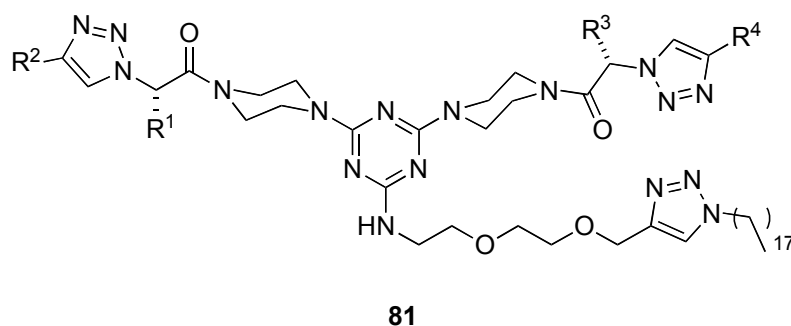
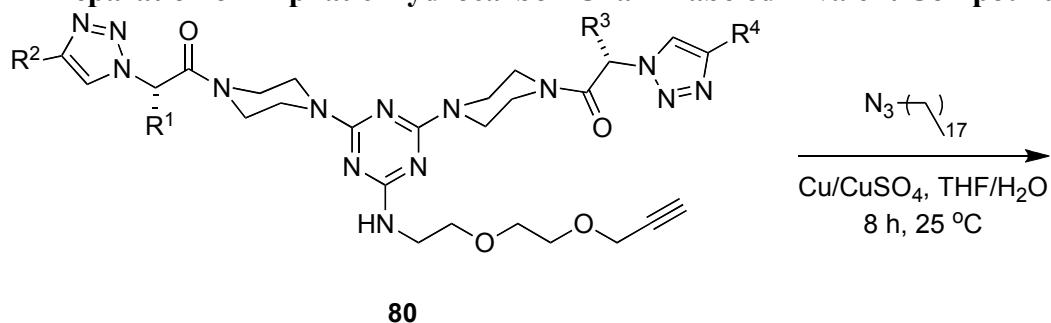


**$^1\text{H}$  NMR of 72nn**



**gCOSY NMR of 72nn**

### Preparation of Aliphatic Hydrocarbon Chain Labeled Bivalent Compounds **81**



Alkyne labeled Compounds **80** were prepared by another member in our group.

Compounds **80** (ca 10.0 mg) were dissolved in 1.0 ml THF/H<sub>2</sub>O (v:v = 1:1) and CuSO<sub>4</sub> solution (1.0 M, 10 μl) was added to the above solution and followed by Cu powder (1.0 mg). The azidooctadecane in THF solution (0.1 mmol, 0.2 ml) was then added and the resulting suspension was stirred at 25 °C for 24 h and filtered through a glass pipette filled with silica gel with 30 % methanol in CH<sub>2</sub>Cl<sub>2</sub> as eluent. The solution was dried and concentrated to give compounds **81**.

Compounds **81** were originally analyzed by HPLC with CH<sub>3</sub>CN/H<sub>2</sub>O as eluents but the compounds couldn't pass through the column. The eluents later used were: solvent A (20% H<sub>2</sub>O, 5% THF and 75% MeOH with 0.1% TFA) and solvent B (20% H<sub>2</sub>O, 5% MeOH and 75% THF with 0.1% TFA). Analytical HPLC analyses were carried out on 25 x 0.46 cm C-18 column using gradient conditions (5 – 95% B) for 30 minutes. However, the peaks of the HPLC spectra were still broad. The HPLC data of compounds **81** was not obtained at this stage.

### **Luciferase Assay for Compounds 81 on cancer cell lines**

Luciferase assay was performed on the hydrocarbon chain labeled compounds **81** by Professor Nancy Templeton's group at Rice University. The purpose of this experiment is to scan compounds that increase the transfection efficiency of Dr. Templeton's patented complexes for specific cell lines. Using a luciferase assay, compounds that result in a significant increase of light emitted relative to transfection of complexes without compound coating will be identified.

The compounds were first dissolved in water at 50 °C with sonication and then coated on the liposomes at different concentrations [3, 1.6, 0.3, -1 log (pg compound/ug DNA)] by mixing and incubation overnight. The transfection efficiency of each compound at different concentration was measured using luciferase assay. Of the 108 compounds that have been screened (the other 27 compounds contain large chunky or overly gelatinous material and they were not tested), the following showed significant increase (about 1.5 to 3 fold) post-transfection of the lung cancer (Figure B2) and breast cancer cell lines (Figure B3).

a.

Concentration	3		1.6		0.3		-1	
	norm	error	norm	error	norm	error	norm	error
<b>81ae</b>	1.66	0.73	2.49	0.71	0.42	0.25	0.69	0.17
<b>81ag</b>	2.68	1.21	1.46	0.12	1.35	0.41	1.94	0.77
<b>81bg</b>	0.80	0.21	0.46	0.05	0.94	0.30	2.07	0.36
<b>81dm</b>	2.06	0.51	0.83	0.09	1.12	0.55	0.80	0.32
<b>81en</b>	1.04	0.55	1.16	0.46	2.96	0.25	0.67	0.31
<b>81ij</b>	0.82	0.14	0.56	0.32	0.54	0.21	1.76	0.74

\* the concentration is measured by log (pg compound/ug DNA)

b.

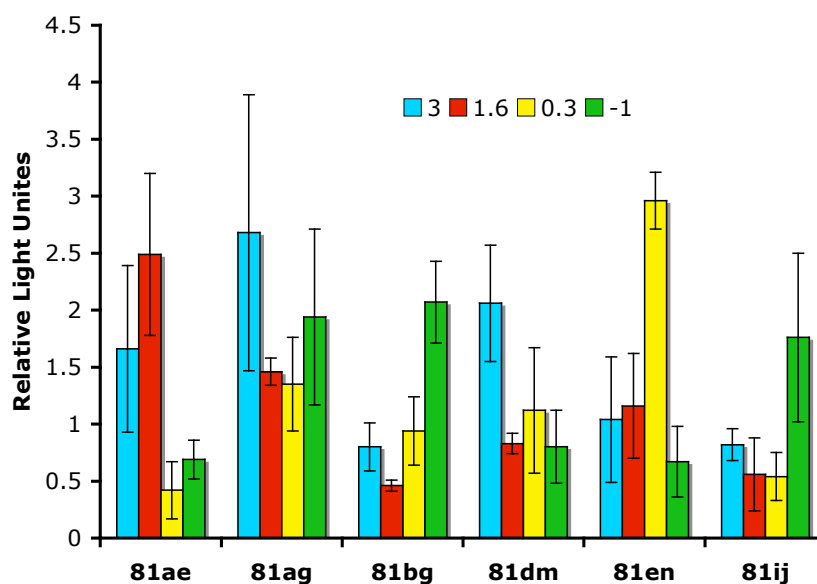


**Figure B 2.** (a) Data of the positive “hits” from lung cancer cell lines and (b) the corresponding graph presentation..



a.

Concentration	3		1.6		0.3		-1	
	norm	error	norm	error	norm	error	norm	error
<b>81m'</b>	2.40	0.01	1.05	0.15	1.03	0.24	0.90	0.04
<b>81mn</b>	2.15	0.21	0.80	0.12	0.94	0.26	0.84	0.12
<b>81mk</b>	1.88	0.45	0.83	0.07	0.85	0.23	0.67	0.22
<b>81bj</b>	1.81	0.03	2.25	0.69	0.90	0.17	1.02	0.27
<b>81ab</b>	2.31	0.46	1.54	0.39	0.60	0.11	0.97	0.28
<b>81bd</b>	3.03	0.36	1.43	0.29	0.86	0.04	0.89	0.39

\* the concentration is measured by log (pg compound/ug DNA)

b.

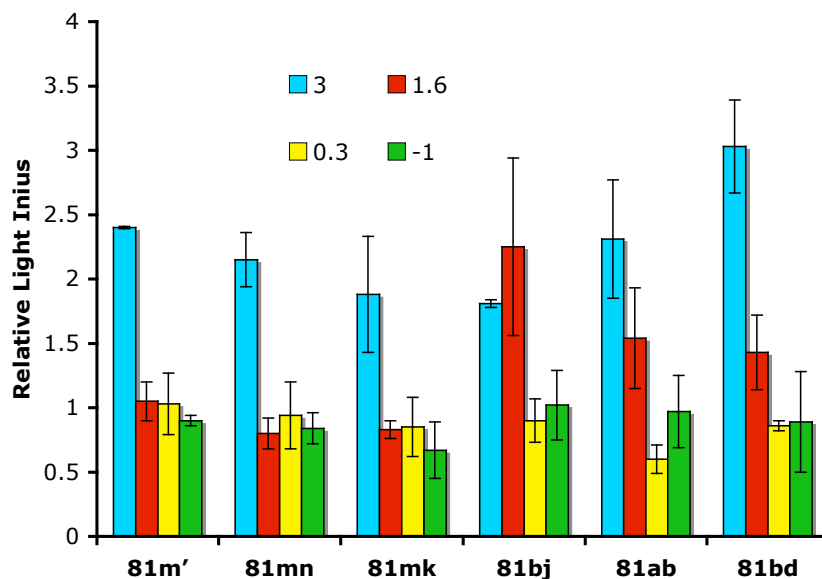


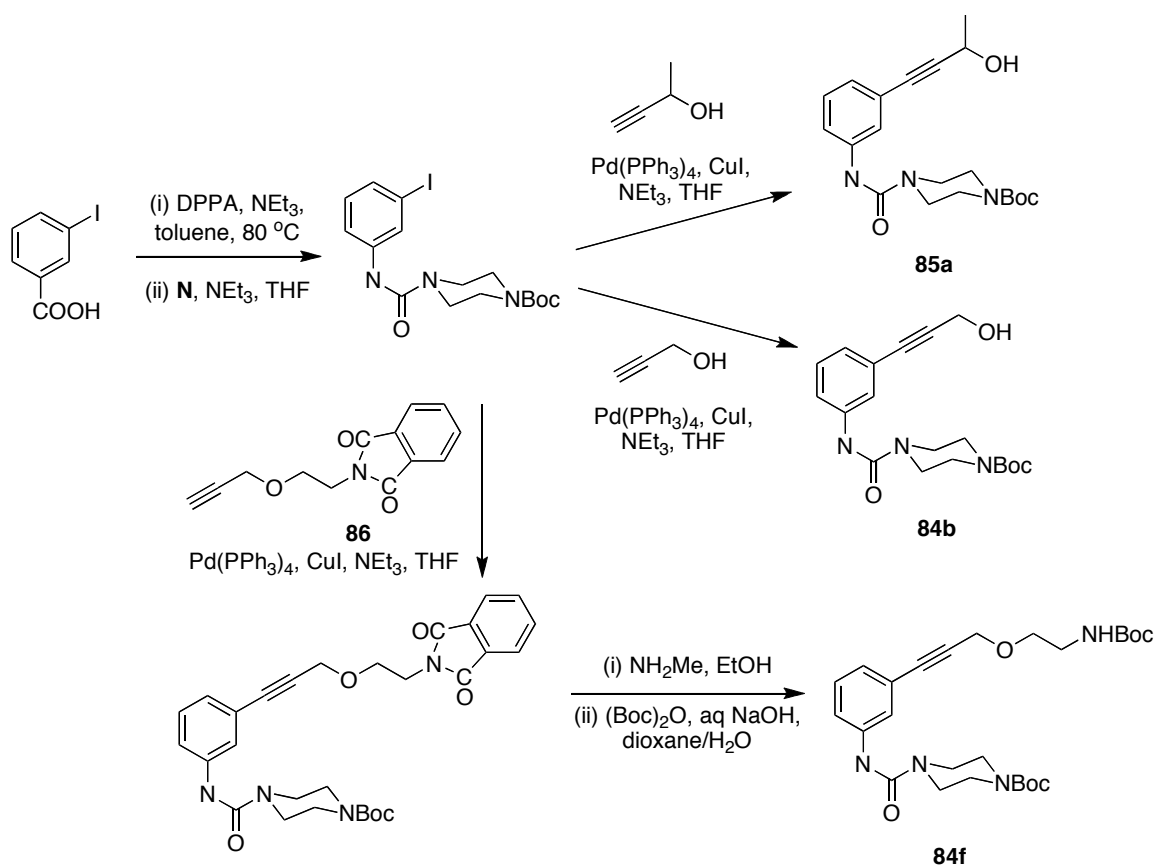
**Figure B 3.** (a) Data of the positive “hits” from lung cancer cell lines and (b) the corresponding graph presentation..

## APPENDIX C

### EXPERIMENTAL ON CHAPTER IV

**General Methods.** All chemicals were obtained from commercial suppliers and used without further purification. Analytical HPLC analyses were carried out on 25 x 0.46 cm C-18 column using gradient conditions (5 – 95% B) for 30 minutes. The eluents used were: solvent A (H<sub>2</sub>O with 0.1% TFA) and solvent B (CH<sub>3</sub>CN with 0.1% TFA). The flow rate used was 1.0 ml/min. Flash chromatography was performed using silica gel (230-600 mesh). NMR spectra were recorded at 500 MHz if otherwise indicated. NMR chemical shifts were expressed in ppm relative to internal solvent peaks, and coupling constants were measured in Hz. Through bond connectivities were elucidated by COSY spectra, which were recorded with 256  $t_1$  increments and 8 scans per  $t_1$  increments.

**General Procedure for Preparation of Compounds 84a, 84b and 84f.** The preparation of compounds **84a**, **84b** and **84f** was accomplished as shown in Scheme C1. The short linker **N** was attached to the scaffold 3-iodobenzoic acid by the activation of the acid group with diphenylphosphoryl azide (DPPA) followed by the addition of **N**. Sonogashira coupling of the resulting intermediate with corresponding alkynes afforded target molecules with good yields.



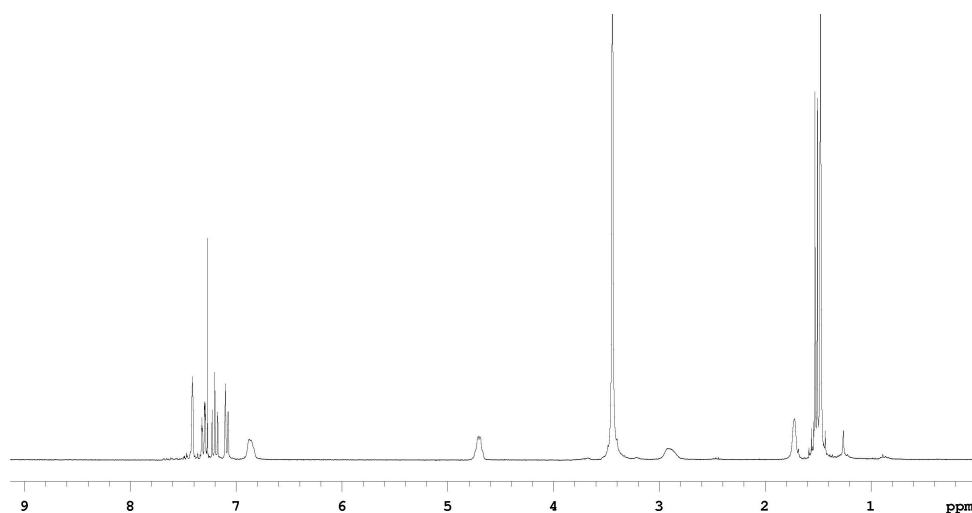
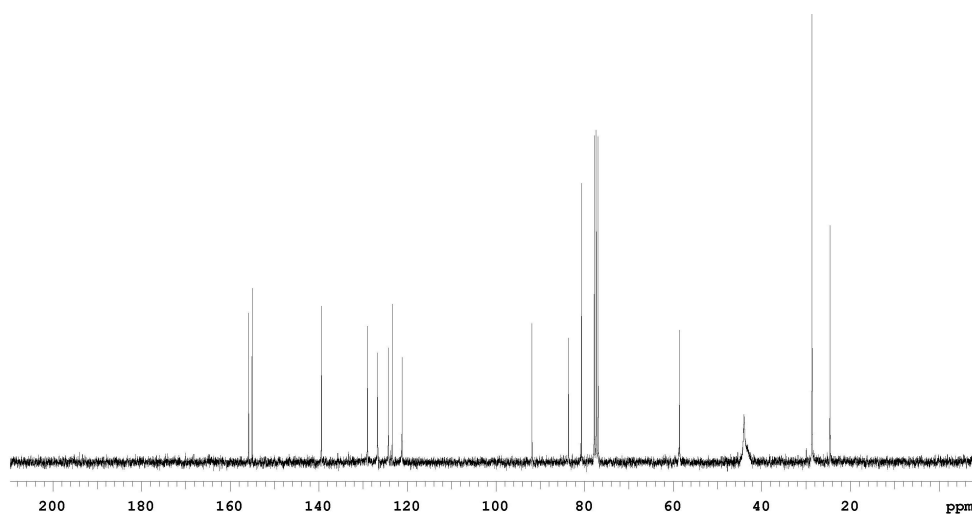
**Scheme C1.** Preparation of compounds **84a**, **84b** and **84f**.

**Data for Compound 84a**

**$^1\text{H}$  NMR (300 MHz,  $\text{CDCl}_3$ )**  $\delta$  7.41 (s, 1H), 7.32 (d, 1H,  $J = 4.5$  Hz), 7.20 (t, 1H,  $J = 4.5$  Hz), 7.10 (d, 1H,  $J = 4.5$  Hz), 6.87 (bs, 1H), 4.71 (q, 1H,  $J = 3.9$  Hz), 3.44 (m, 8H), 1.72 (s, 1H), 1.53 (d, 3H,  $J = 3.9$  Hz), 1.48 (s, 9H)

**$^{13}\text{C}$  NMR (300 MHz,  $\text{CDCl}_3$ )**  $\delta$  155.8, 155.0, 139.4, 129.0, 126.7, 124.2, 123.4, 121.2, 91.8, 83.6, 80.7, 58.6, 28.6, 24.6

**MS (ESI,  $m/z$ )** 373 ( $\text{M}+\text{H}$ )<sup>+</sup>

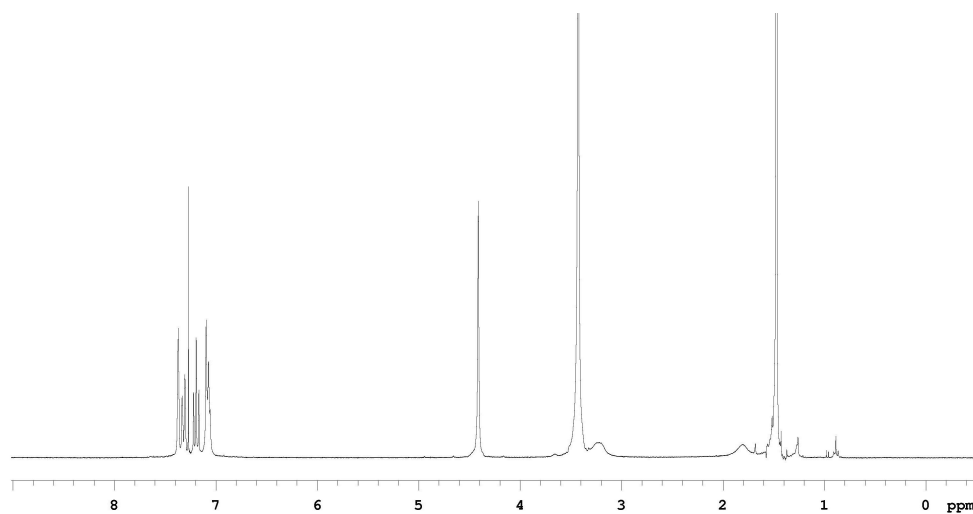
 **$^1\text{H}$  NMR of 84a** **$^{13}\text{C}$  NMR of 84a**

**Data for Compound 84b**

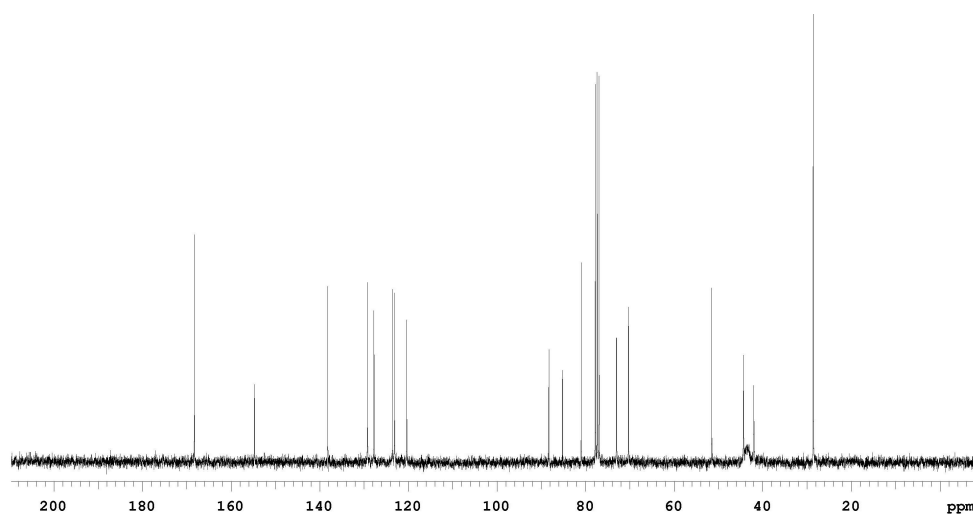
**$^1\text{H}$  NMR (300 MHz,  $\text{CDCl}_3$ )**  $\delta$  7.37 (s, 1H), 7.31 (d, 1H,  $J = 7.8$  Hz), 7.19 (t, 1H,  $J = 7.8$  Hz), 7.07 (d, 1H,  $J = 7.8$  Hz), 4.41 (s, 2H), 3.43 (m, 8H), 1.47 (s, 9H)

**$^{13}\text{C}$  NMR (300 MHz,  $\text{CDCl}_3$ )**  $\delta$  155.6, 155.1, 139.4, 129.0, 126.7, 124.3, 123.3, 121.3, 88.2, 85.1, 80.7, 15.3, 28.6

**MS (ESI,  $m/z$ )** 359 ( $\text{M}+\text{H}$ )<sup>+</sup>



**$^1\text{H}$  NMR of 84b**



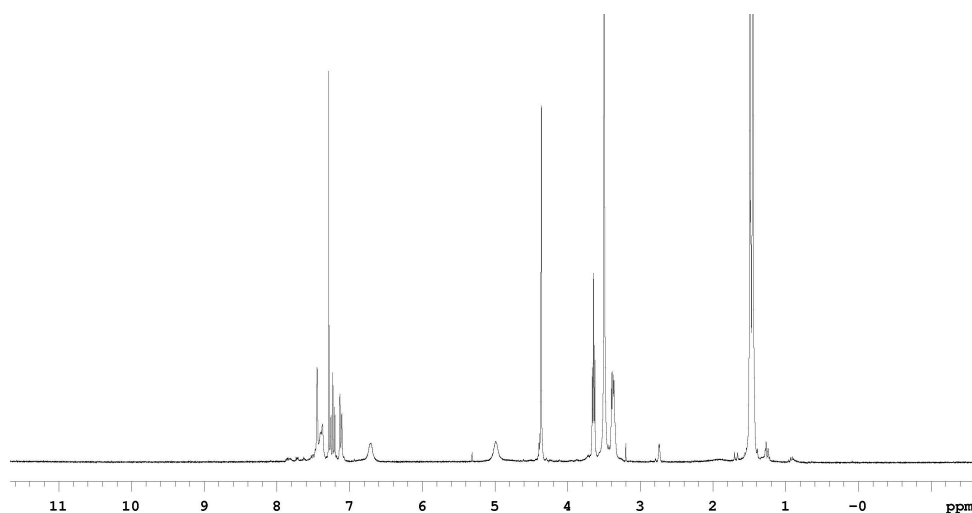
**$^{13}\text{C}$  NMR of 84b**

**Data for Compound 84f**

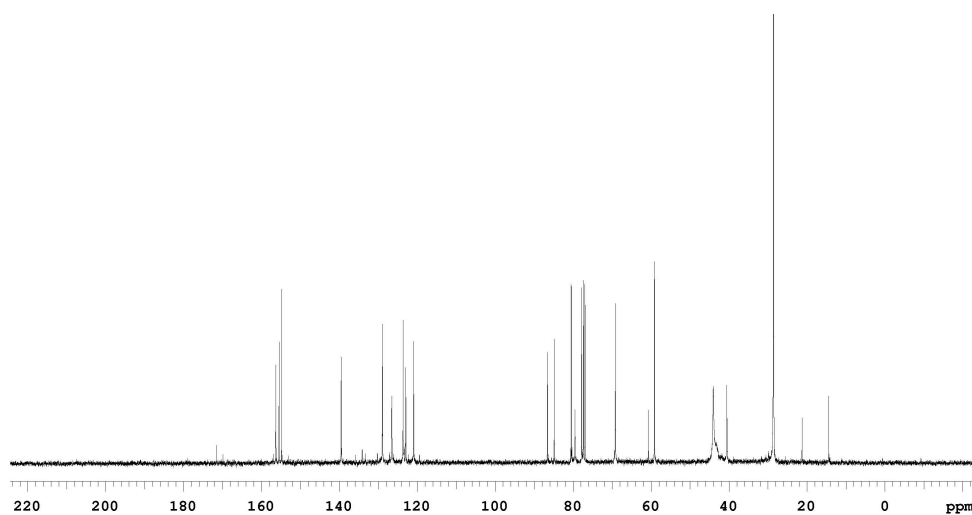
**$^1\text{H}$  NMR (300 MHz,  $\text{CDCl}_3$ )**  $\delta$  7.45 (s, 1H), 7.39 (d, 1H,  $J = 7.5$  Hz), 7.27 (t, 1H,  $J = 7.5$  Hz), 7.12 (d, 1H,  $J = 7.5$  Hz), 6.71 (bs, 1H), 4.98 (bs, 1H), 4.35 (s, 2H), 3.63 (t, 2H,  $J = 5.4$  Hz), 3.48 (m, 8H), 3.36 (t, 2H,  $J = 5.4$  Hz), 1.48 (s, 9H), 1.47 (s, 9H)

**$^{13}\text{C}$  NMR (300 MHz,  $\text{CDCl}_3$ )**  $\delta$  156.3, 155.5, 154.8, 139.5, 128.9, 126.5, 123.6, 122.9, 120.9, 86.6, 84.8, 80.5, 79.5, 69.2, 60.6, 59.1, 44.0, 40.5, 28.6

**MS (ESI,  $m/z$ )** 502 ( $\text{M}+\text{H}$ )<sup>+</sup>



**$^1\text{H}$  NMR of 84f**



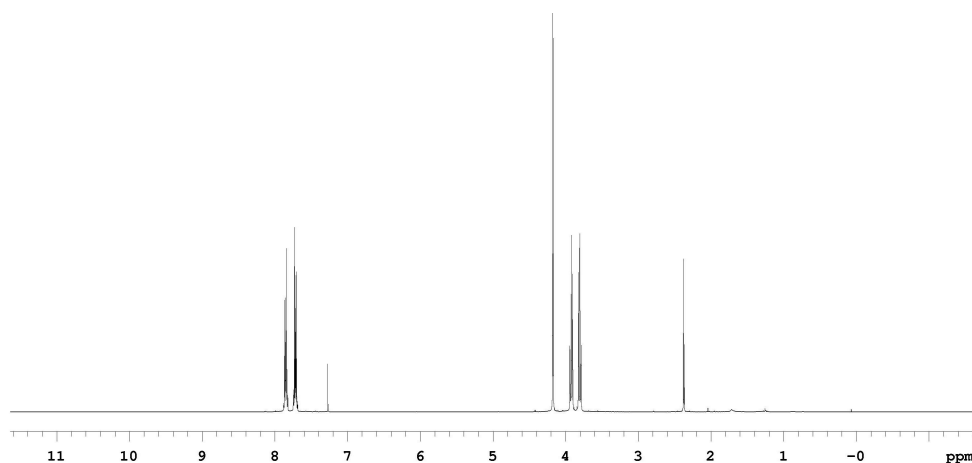
**$^{13}\text{C}$  NMR of 84f**

**Procedure for Preparation of Compound 86.** To a solution of *N*-(2-Hydroxyethyl) phthalimide (0.38 g, 2.0 mmol) in 10 ml dry THF was added 0.1 g of NaH (60% w.t. in mineral oil) and the resulting suspension was stirred at 25 °C for 15 min. Tetra-nbutylidide (0.15 g, 0.4 mmol) in 10 ml THF was added to the above suspension followed by propargyl bromide (0.45 ml, 4.0 mmol). The reaction mixture was heated to reflux for 8 h, cooled to 25 °C and concentrated. The residue was extracted with ethyl acetate and brine and the organic layer was concentrated and purified by flash chromatography (25% ethyl acetate in hexanes). Compound **86** was isolated as a white solid with the yield of 52%.

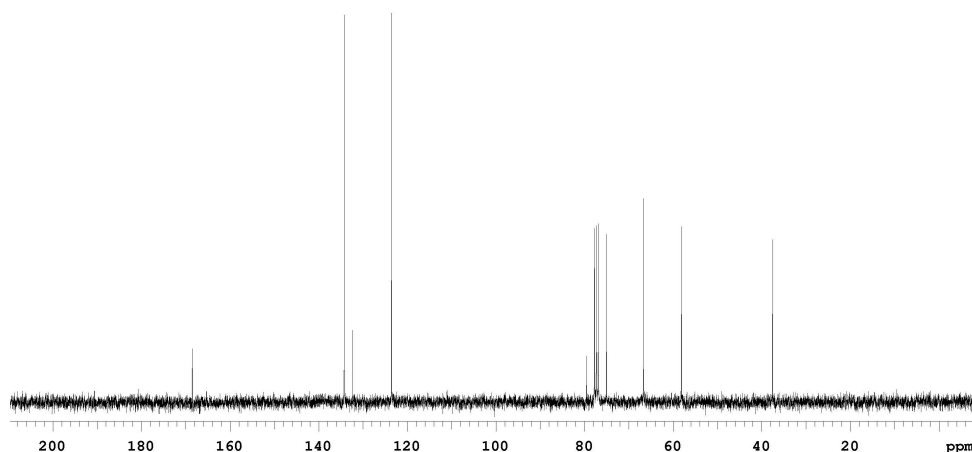
**<sup>1</sup>H NMR (300 MHz, CDCl<sub>3</sub>)** δ 7.85 (dd, 2H, J = 5.4 Hz, 2.1 Hz), 7.71 (dd, 2H, J = 5.4 Hz, 2.4 Hz), 4.17 (d, 2H, J = 2.4 Hz), 3.90 (t, 2H, J = 4.8 Hz), 3.82 (t, 2H, J = 4.8 Hz), 2.38 (t, 1H, J = 2.4 Hz)

**<sup>13</sup>C NMR (300 MHz, CDCl<sub>3</sub>)** δ 168.5, 134.2, 132.4, 132.6, 79.5, 75.1, 66.6, 58.1, 37.5

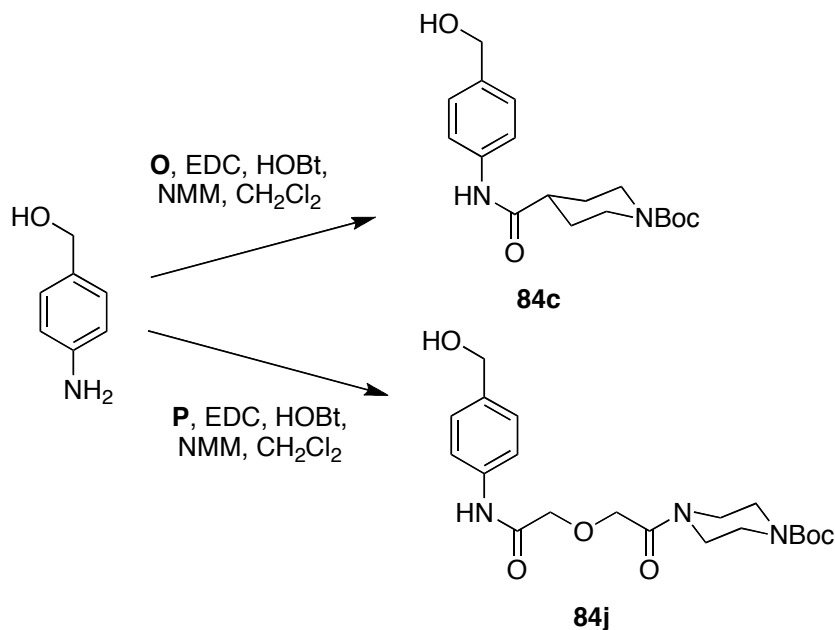
**MS (ESI, m/z)** 230 (M+H)<sup>+</sup>



**<sup>1</sup>H NMR of 86**

 $^{13}\text{C}$  NMR of **86**

**General Procedure for Preparation of Compounds **84c** and **84j**.** Synthesis of **84c** and **84j** is very straightforward. Short and long linkers were attached to the 4-aminobenzoyl alcohol directly by EDC coupling reaction (Scheme C2). The benzoyl alcohol is a mimic of serine side chain and the proton on the score structure is mimicking glycine side chain. The alkyne is used in this case is for the synthetic convenience.



**Scheme C2.** Preparation of compounds **84c** and **84j**.

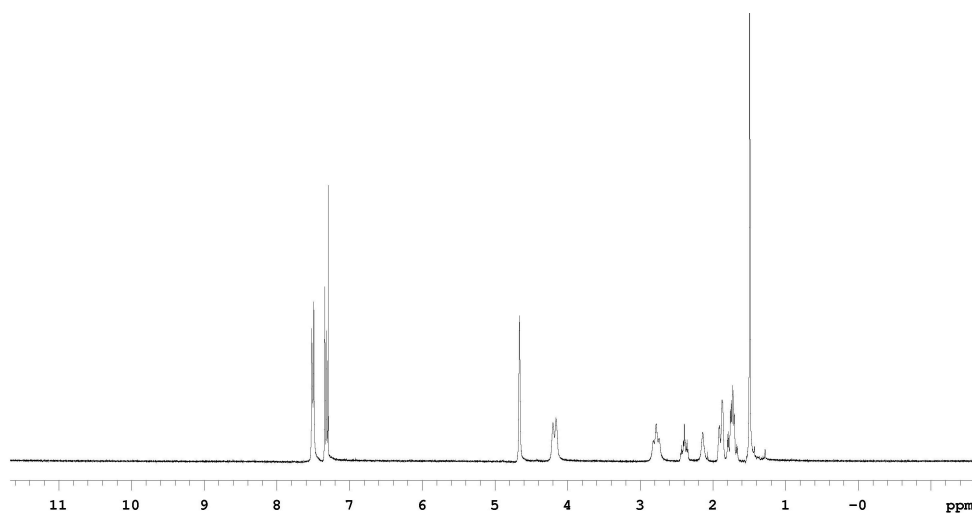


**Data for 84c**

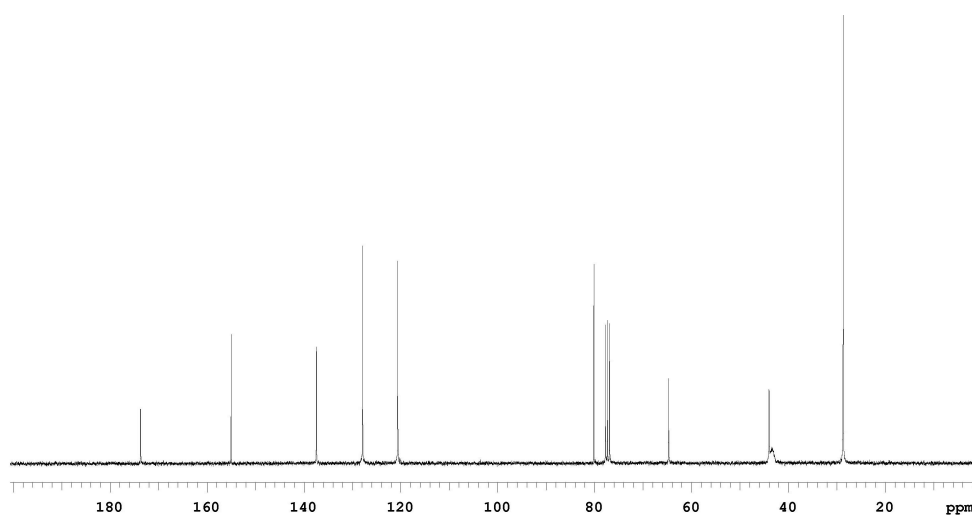
**$^1\text{H}$  NMR (300 MHz,  $\text{CDCl}_3$ )**  $\delta$  7.50 (d, 2H,  $J = 8.4$  Hz), 7.32 (d, 2H,  $J = 8.4$  Hz), 4.66 (s, 2H), 4.20 (d, 2H,  $J = 13.2$  Hz), 2.78 (t, 2H,  $J = 13.2$  Hz), 2.93 (m, 1H), 2.14 (s, 1H), 1.91 (m, 2H), 1.75 (m, 2H), 1.49 (s, 9H)

**$^{13}\text{C}$  NMR (300 MHz,  $\text{CDCl}_3$ )**  $\delta$  173.3, 155.0, 137.42, 137.37, 127.9, 120.6, 80.1, 64.7, 44.0, 28.7

**MS (ESI,  $m/z$ )** 335 ( $\text{M}+\text{H}$ )<sup>+</sup>



**$^1\text{H}$  NMR of 84c**



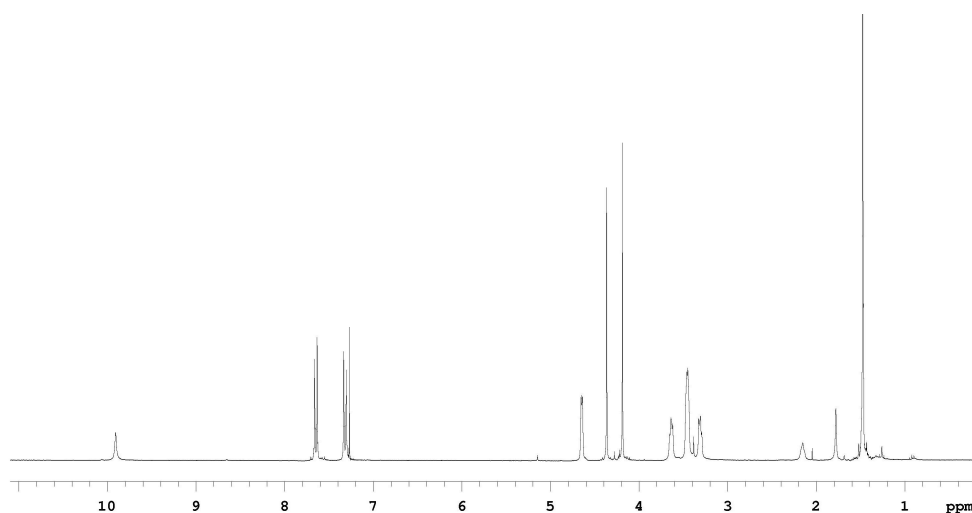
**$^{13}\text{C}$  NMR of 84c**

**Data for 84j**

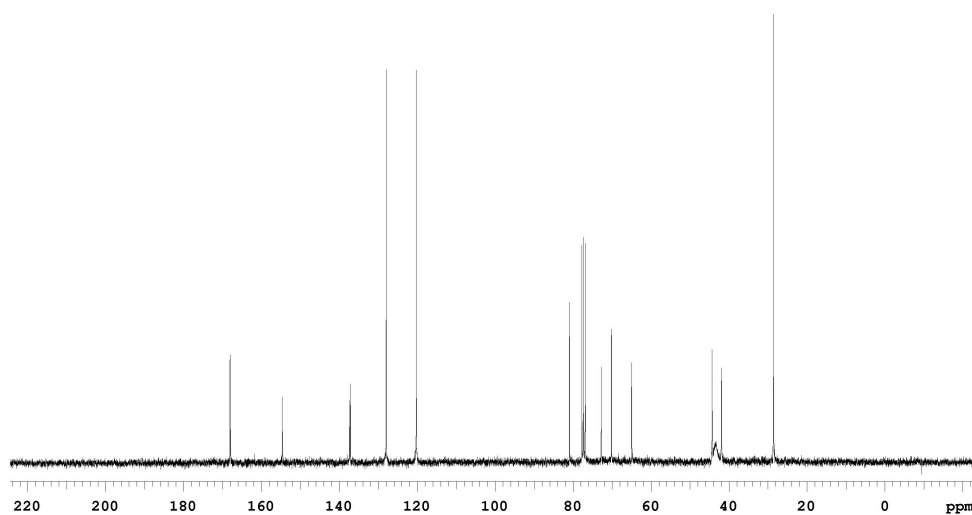
**$^1\text{H}$  NMR (300 MHz,  $\text{CDCl}_3$ )**  $\delta$  9.91 (s, 1H), 7.65 (d, 2H,  $J = 8.4$  Hz), 7.32 (d, 2H,  $J = 8.4$  Hz), 4.44 (d, 2H,  $J = 3.6$  Hz), 4.37 (s, 2H), 4.19 (s, 2H), 3.45-3.29 (m, 8H), 2.16 (t, 1H,  $J = 3.6$  Hz), 1.47 (s, 9H)

**$^{13}\text{C}$  NMR (300 MHz,  $\text{CDCl}_3$ )**  $\delta$  168.1, 167.9, 154.7, 137.4, 137.2, 128.0, 120.2, 80.9, 72.8, 70.2, 64.9, 44.3, 41.9, 28.6

**MS (ESI,  $m/z$ )** 430 ( $\text{M}+\text{Na}$ ) $^+$

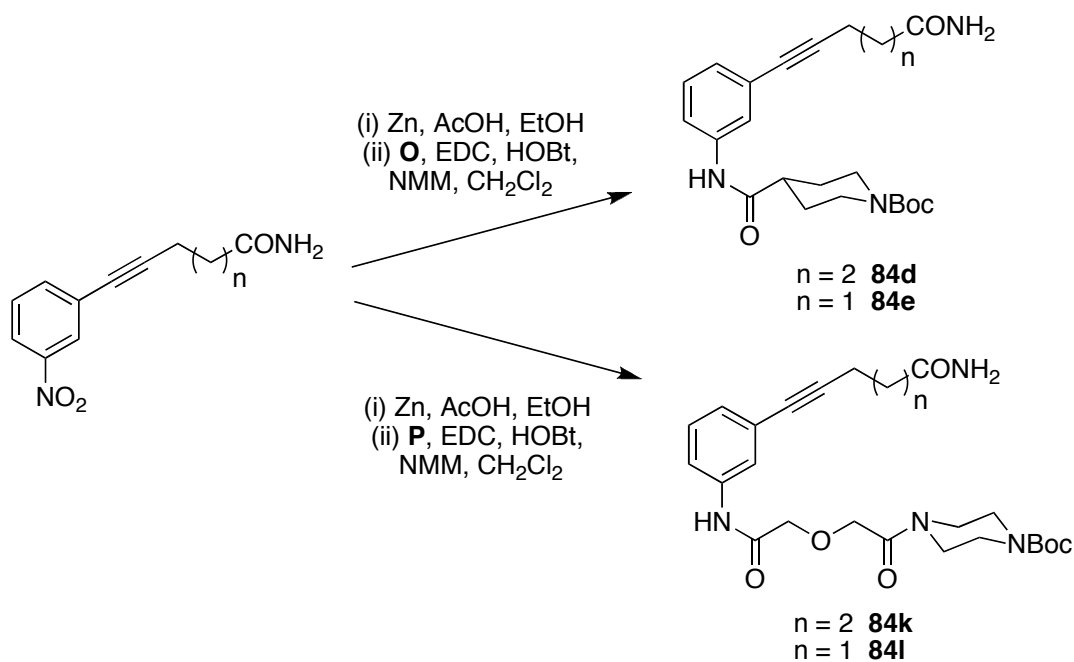


**$^1\text{H}$  NMR of 84j**



**$^{13}\text{C}$  NMR of 84j**

Sonogashira coupling of 3-iodonitrobenzene with carboxylic acid functionalized alkynes afforded acid intermediates that were converted to amides by the oxalyl chloride activation and ammonia addition. The nitro groups of the resulting amides were reduced by zinc dust and the short or long linker was attached to give compounds **84d**, **84e**, **84k** and **84l** (Scheme C3).



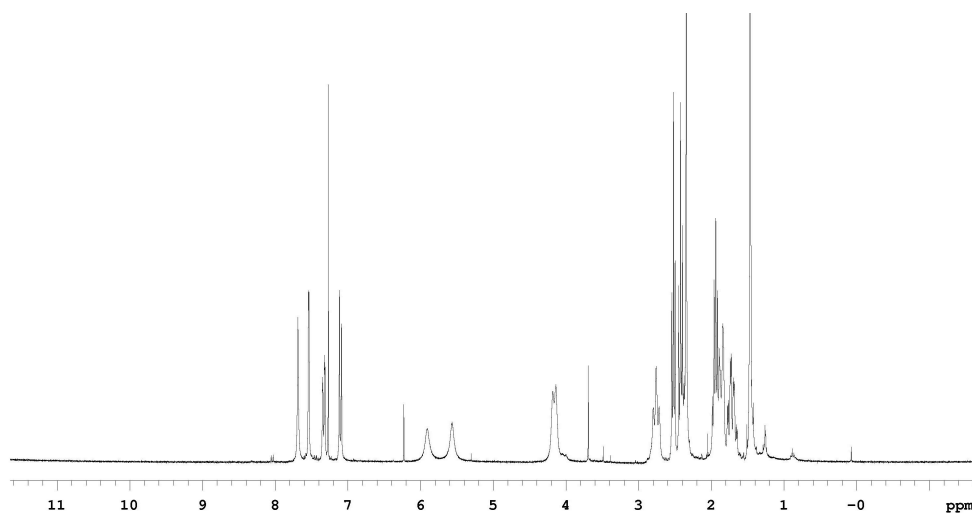
**Scheme C3.** Preparation of compounds **84d**, **84e**, **84k** and **84l**.

**Data for 84d**

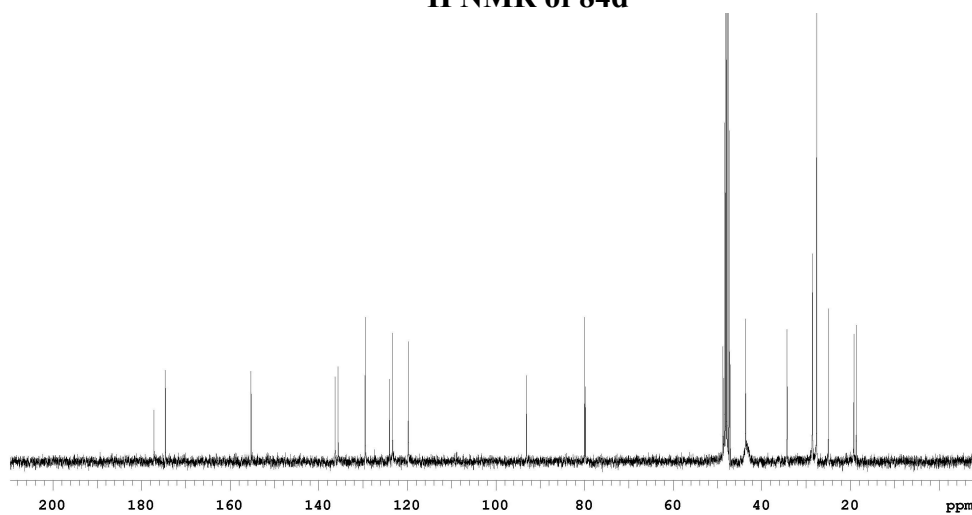
**$^1\text{H}$  NMR (300 MHz,  $\text{CDCl}_3$ )**  $\delta$  7.69 (s, 1H), 7.54 (d, 1H,  $J = 2.1$  Hz), 7.32 (dd, 1H,  $J = 8.4$  Hz, 2.1 Hz), 7.10 (d, 1H,  $J = 8.4$  Hz), 5.90 (s, 1H), 5.57 (s, 1H), 4.18 (d, 2H,  $J = 12.0$  Hz), 2.76 (t, 2H,  $J = 12.0$  Hz), 2.52 (t, 2H,  $J = 6.6$  Hz), 2.42 (t, 2H,  $J = 6.6$  Hz), 2.34 (m, 4H), 1.96 (m, 2H), 1.84 (m, 2H), 1.68 (m, 2H), 1.46 (s, 9H)

**$^{13}\text{C}$  NMR (300 MHz,  $\text{CD}_3\text{OD}$ )**  $\delta$  177.2, 174.6, 155.2, 136.3, 135.6, 129.5, 124.0, 123.3, 119.8, 93.1, 80.0, 79.7, 43.6, 34.3, 28.5, 27.6, 24.9, 19.2, 18.6

**MS (ESI,  $m/z$ )** 400 ( $\text{M}+\text{H}$ )<sup>+</sup>



**$^1\text{H}$  NMR of 84d**



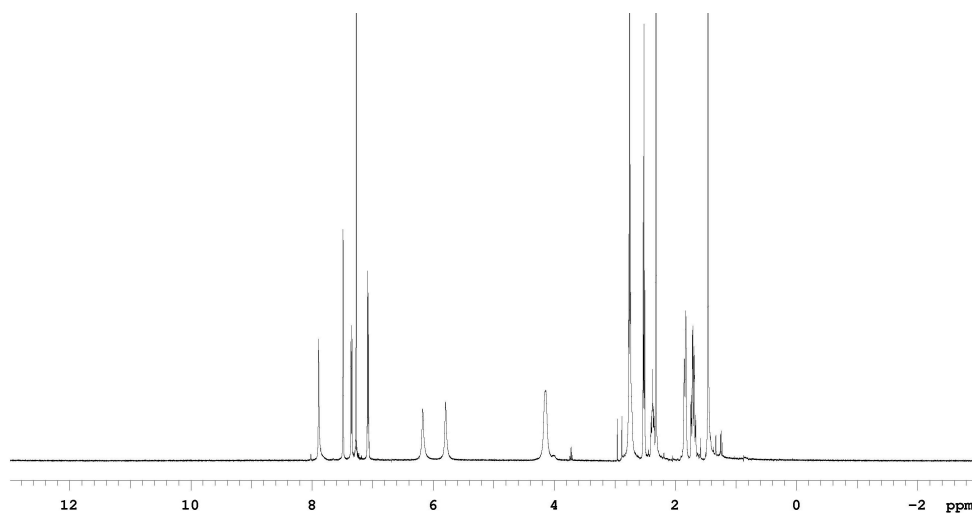
**$^{13}\text{C}$  NMR of 84d**

**Data for 84e**

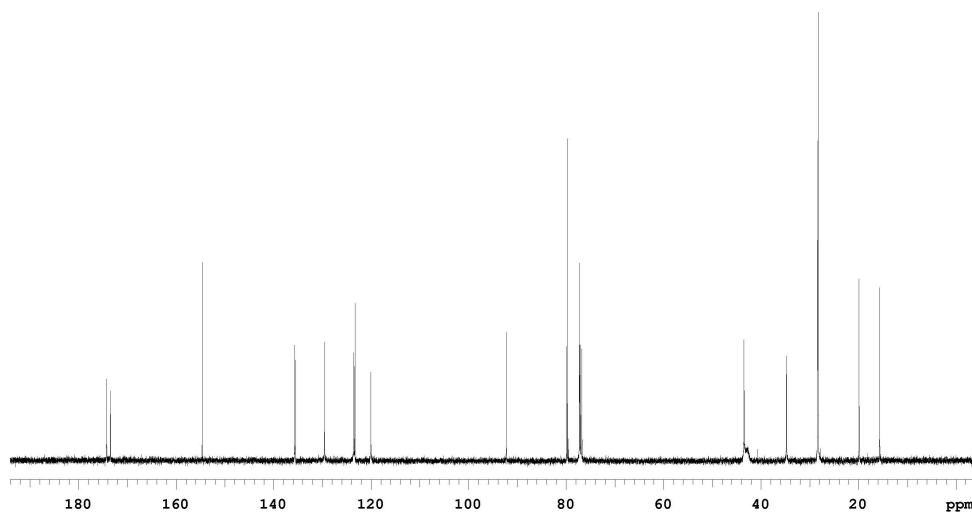
**$^1\text{H}$  NMR (500 MHz,  $\text{CDCl}_3$ )**  $\delta$  7.89 (s, 1H), 7.49 (d, 1H,  $J = 2.0$  Hz), 7.36 (dd, 1H,  $J = 8.0$  Hz, 2.0 Hz), 7.08 (d, 1H,  $J = 8.0$  Hz), 6.17 (s, 1H), 5.79 (s, 1H), 4.14 (m, 2H), 2.75 (t, 4H,  $J = 7.0$  Hz), 2.51 (t, 2H,  $J = 7.0$  Hz), 2.38 (m, 1H), 2.32 (s, 3H), 1.83 (m, 2H), 1.71 (m, 2H), 1.46 (s, 9H)

**$^{13}\text{C}$  NMR (500 MHz,  $\text{CDCl}_3$ )**  $\delta$  174.3, 173.5, 154.6, 135.7, 135.6, 129.6, 123.5, 123.3, 120.0, 92.3, 79.8, 79.6, 43.5, 34.8, 28.4, 28.3, 19.9, 15.7

**MS (ESI,  $m/z$ )** 414 ( $\text{M}+\text{H}$ )<sup>+</sup>



**$^1\text{H}$  NMR of 84e**



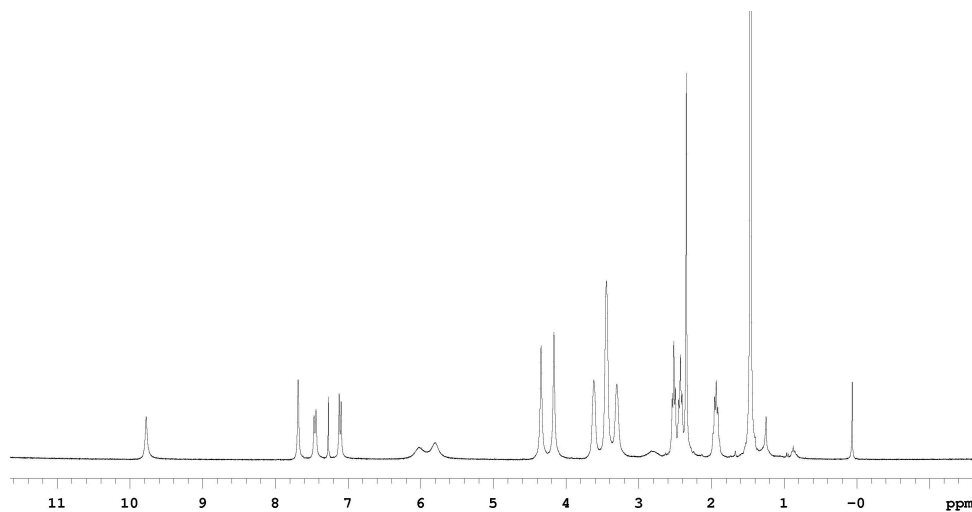
**$^{13}\text{C}$  NMR of 84e**

**Data for 84k**

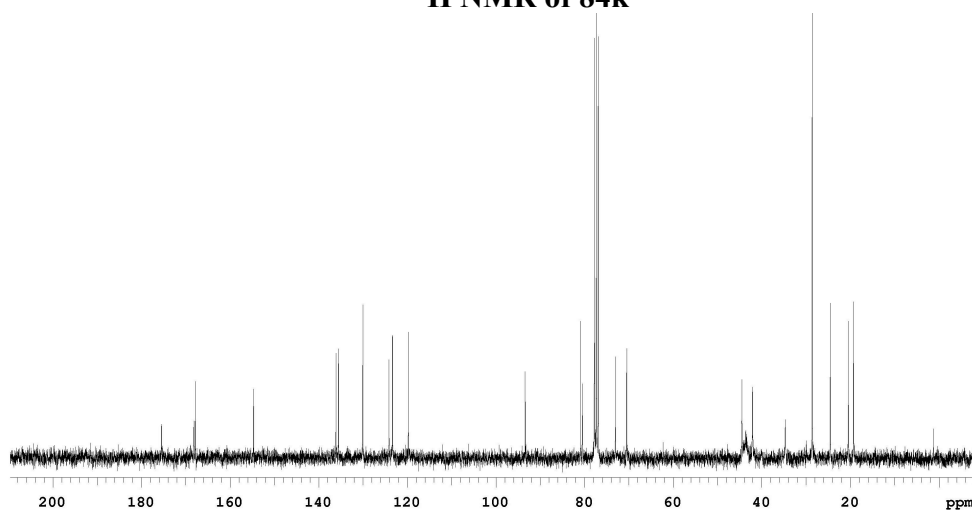
**<sup>1</sup>H NMR (300 MHz, CDCl<sub>3</sub>)** δ 9.77 (s, 1H), 7.69 (s, 1H), 7.46 (d, 1H, J = 7.5 Hz), 7.10 (d, 1H, J = 7.5 Hz), 6.02 (s, 1H), 5.80 (s, 1H), 4.34 (s, 2H), 4.16 (s, 2H), 3.62-3.42 (m, 8H), 2.54 (t, 2H, J = 6.6 Hz), 2.43 (t, 2H, J = 6.6 Hz), 2.40 (s, 3H), 1.93 (m, 2H), 1.46 (s, 9H)

**<sup>13</sup>C NMR (300 MHz, CDCl<sub>3</sub>)** δ 175.4, 167.8, 154.7, 136.1, 135.5, 130.0, 124.1, 123.3, 119.7, 93.4, 80.9, 80.5, 73.0, 70.4, 44.4, 42.0, 34.7, 28.6, 24.5, 20.4, 19.2

**MS (ESI, m/z)** 473 (M+H)<sup>+</sup>



**<sup>1</sup>H NMR of 84k**



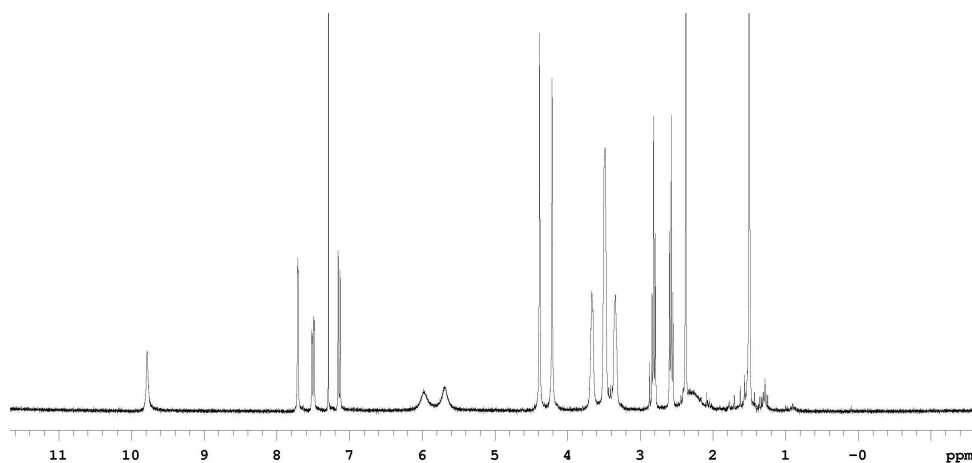
**<sup>13</sup>C NMR of 84k**

**Data for 84l**

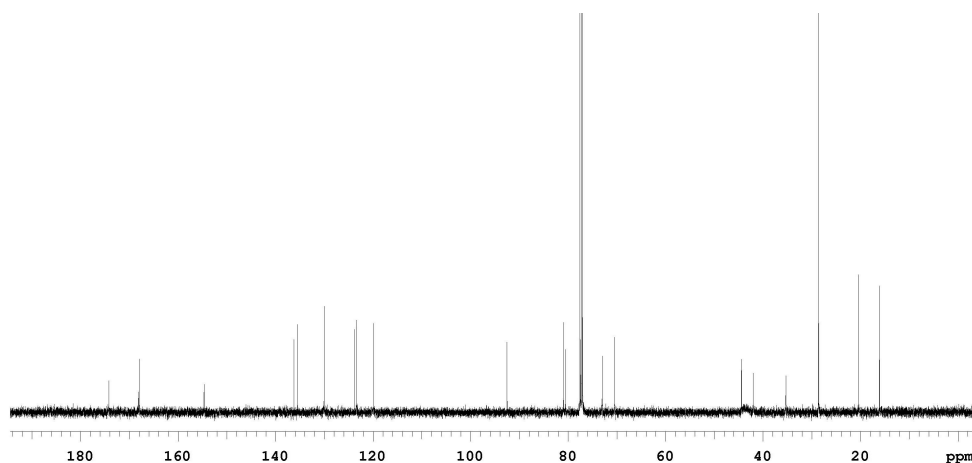
**$^1\text{H}$  NMR (300 MHz,  $\text{CDCl}_3$ )**  $\delta$  9.78 (s, 1H), 7.71 (d, 1H,  $J = 1.8$  Hz), 7.51 (dd, 1H,  $J = 8.1$  Hz, 1.8 Hz), 7.16 (d, 1H,  $J = 8.1$  Hz), 5.80 (s, 1H), 5.69 (s, 1H), 4.38 (s, 2H), 4.21 (s, 2H), 3.67-3.34 (m, 8H), 2.81 (t, 2H,  $J = 7.2$  Hz), 2.57 (t, 2H,  $J = 7.2$  Hz), 2.37 (t, 3H), 1.50 (s, 9H)

**$^{13}\text{C}$  NMR (300 MHz,  $\text{CDCl}_3$ )**  $\delta$  174.2, 167.8, 154.6, 136.2, 135.5, 130.0, 123.7, 123.3, 119.9, 92.5, 80.9, 80.5, 73.0, 70.4, 44.4, 42.0, 35.3, 28.6, 20.4, 16.1

**MS (ESI,  $m/z$ )** 487 ( $\text{M}+\text{H}$ )<sup>+</sup>

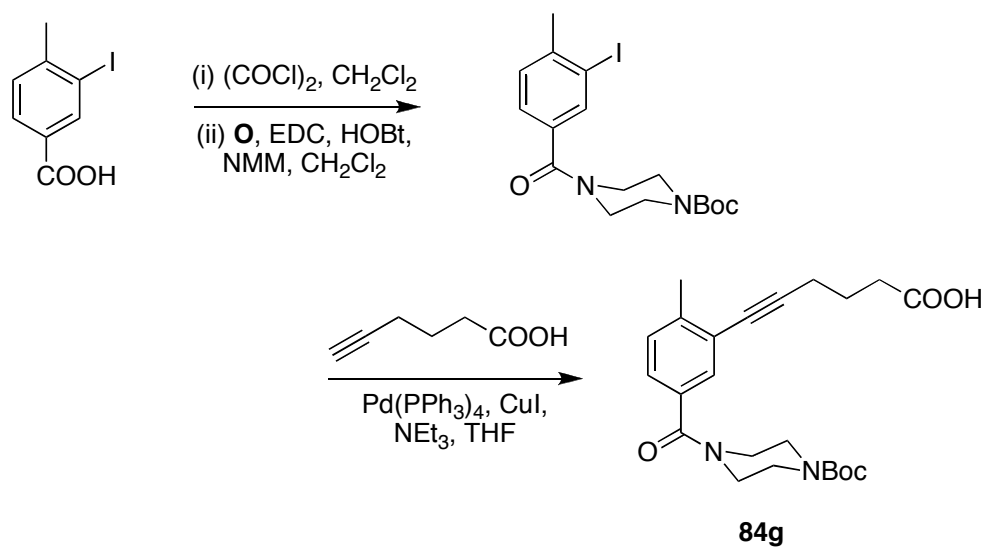


**$^1\text{H}$  NMR of 84l**



**$^{13}\text{C}$  NMR of 84l**

Compound **84g** was prepared from 3-iodo-4-methylbenzoic acid. Amide bond coupling followed with Sonogashira reaction with 5-hexynoic acid afforded **84g** (Scheme C4).



**Scheme C4.** Preparation of compound **84g**.

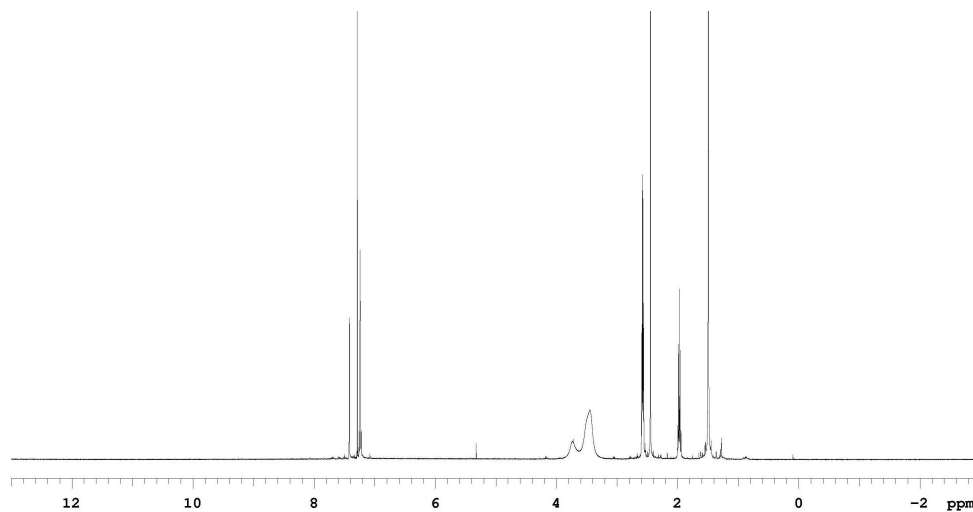


**Data for 84g**

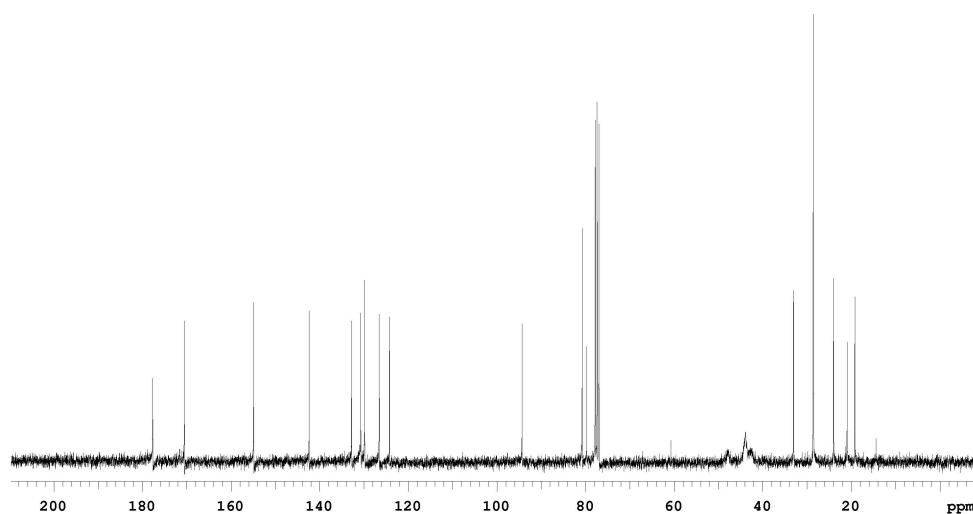
**<sup>1</sup>H NMR (500 MHz, CDCl<sub>3</sub>)** δ 7.40 (s, 1H), 7.22 (m, 2H), 3.80-3.43 (m, 8H), 2.56 (m, 4H), 2.43 (s, 3H), 1.95 (m, 2H), 1.47 (s, 9H)

**<sup>13</sup>C NMR (300 MHz, CDCl<sub>3</sub>)** δ 177.7, 170.5, 154.9, 142.3, 132.7, 130.7, 129.8, 126.5, 124.2, 94.3, 80.7, 79.7, 48.2, 43.9, 33.0, 28.6, 24.0, 20.9, 19.1

**MS (ESI, m/z)** 415 (M+H)<sup>+</sup>

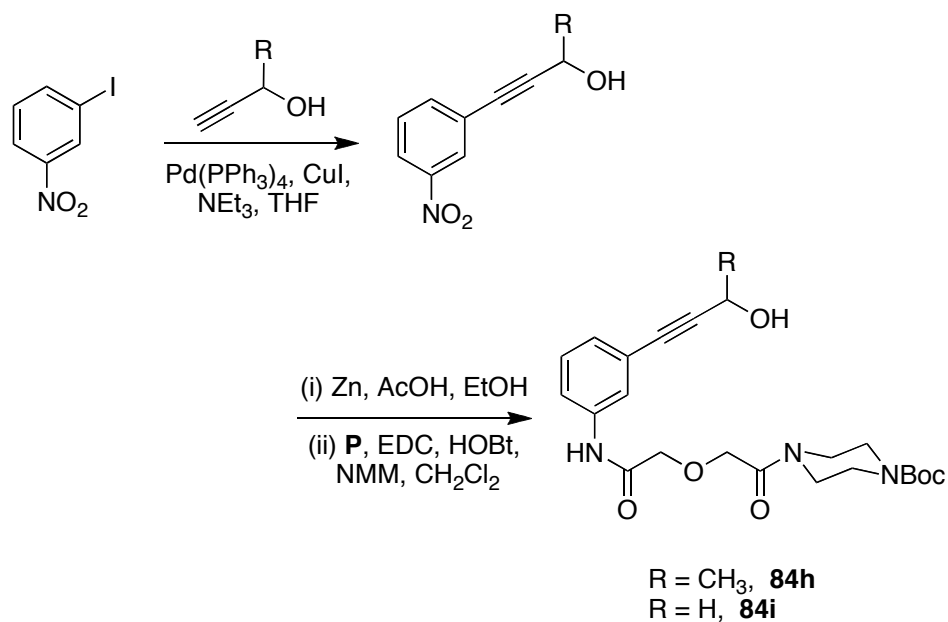


**<sup>13</sup>C NMR of 84g**



**<sup>13</sup>C NMR of 84g**

Compound **84h** and **84i** were prepared from 3-iodonitrobenzene in parallel (Scheme C5). Sonogashira coupling with corresponding alkynes gave the phenyl acetylene intermediate which was reduced with zinc dust and the short linker was attached by coupling reactions.



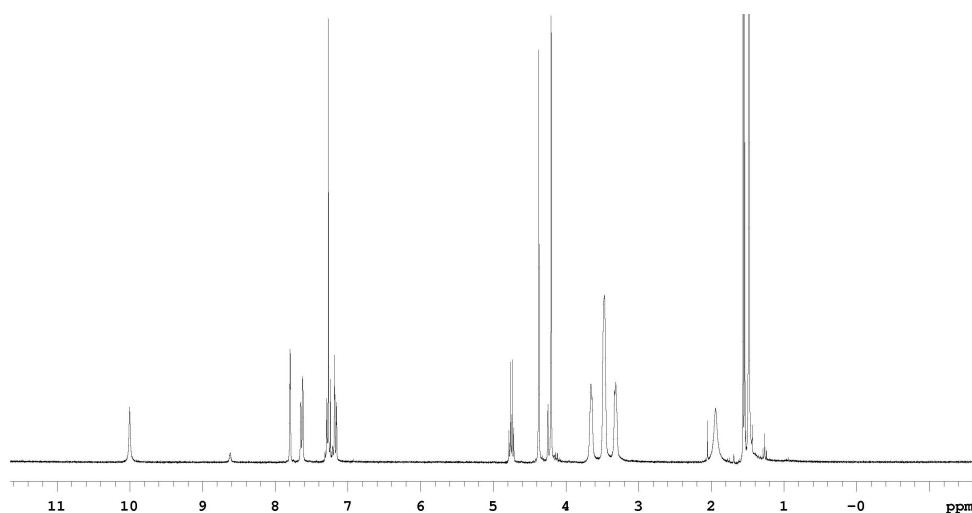
**Scheme C5.** Preparation of compound **84h** and **84i**.

**Data for 84h**

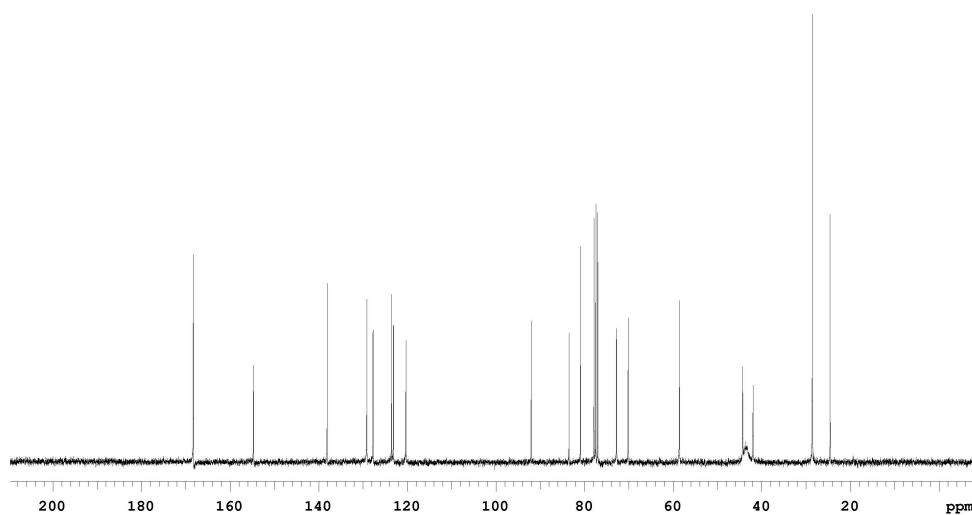
**$^1\text{H}$  NMR (300 MHz,  $\text{CDCl}_3$ )**  $\delta$  10.00 (s, 1H), 7.79 (d, 1H,  $J = 1.8$  Hz), 7.64 (dd, 1H,  $J = 7.8$  Hz, 1.8 Hz), 7.27 (m, 1H), 7.15 (dd, 1H,  $J = 6.6$  Hz, 1.2 Hz), 4.76 (q, 1H,  $J = 6.6$  Hz), 4.37 (s, 2H), 4.20 (s, 2H), 3.65-3.31 (m, 8H), 1.55 (d, 3H,  $J = 6.6$  Hz), 1.48 (s, 9H)

**$^{13}\text{C}$  NMR (300 MHz,  $\text{CDCl}_3$ )**  $\delta$  168.3, 168.2, 154.7, 138.1, 129.1, 127.7, 123.6, 123.1, 120.3, 92.0, 83.5, 80.9, 72.7, 70.1, 58.6, 44.3, 41.9, 28.6, 24.5

**MS (ESI,  $m/z$ )** 446 ( $\text{M}+\text{H}$ ) $^+$



**$^1\text{H}$  NMR of 84h**



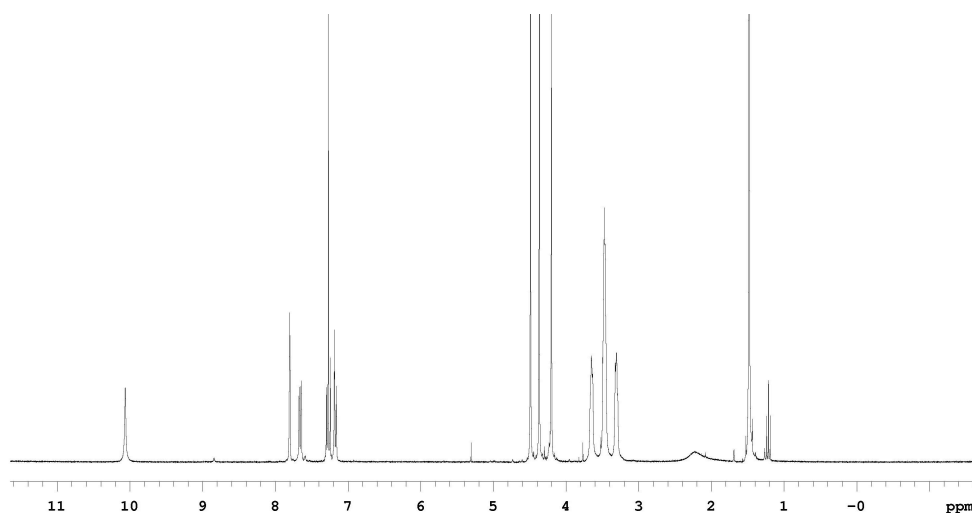
**$^{13}\text{C}$  NMR of 84h**

**Data for 84i**

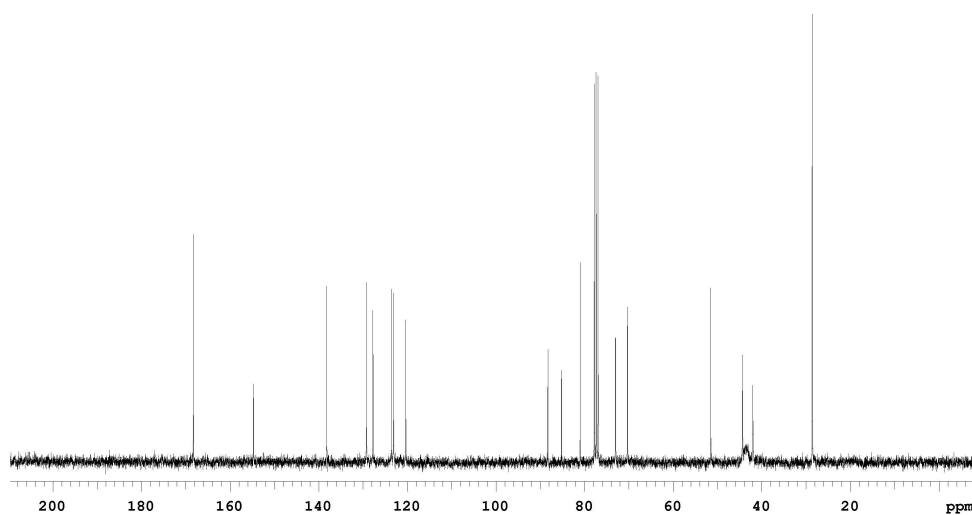
**<sup>1</sup>H NMR (300 MHz, CDCl<sub>3</sub>)** δ 10.06 (s, 1H), 7.80 (d, 1H, J = 1.8 Hz), 7.66 (dd, 1H, J = 7.8 Hz, 1.8 Hz), 7.27 (m, 1H), 7.15 (dd, 1H, J = 6.6 Hz, 1.5 Hz), 4.49 (s, 2H), 4.37 (s, 2H), 4.20 (s, 2H), 3.65-3.30 (m, 8H), 1.48 (s, 9H)

**<sup>13</sup>C NMR (300 MHz, CDCl<sub>3</sub>)** δ 168.2, 154.7, 138.1, 129.2, 127.7, 123.5, 123.1, 120.3, 88.2, 85.1, 81.0, 73.0, 70.3, 51.5, 44.3, 42.0, 28.6

**MS (ESI, m/z)** 432 (M+H)<sup>+</sup>

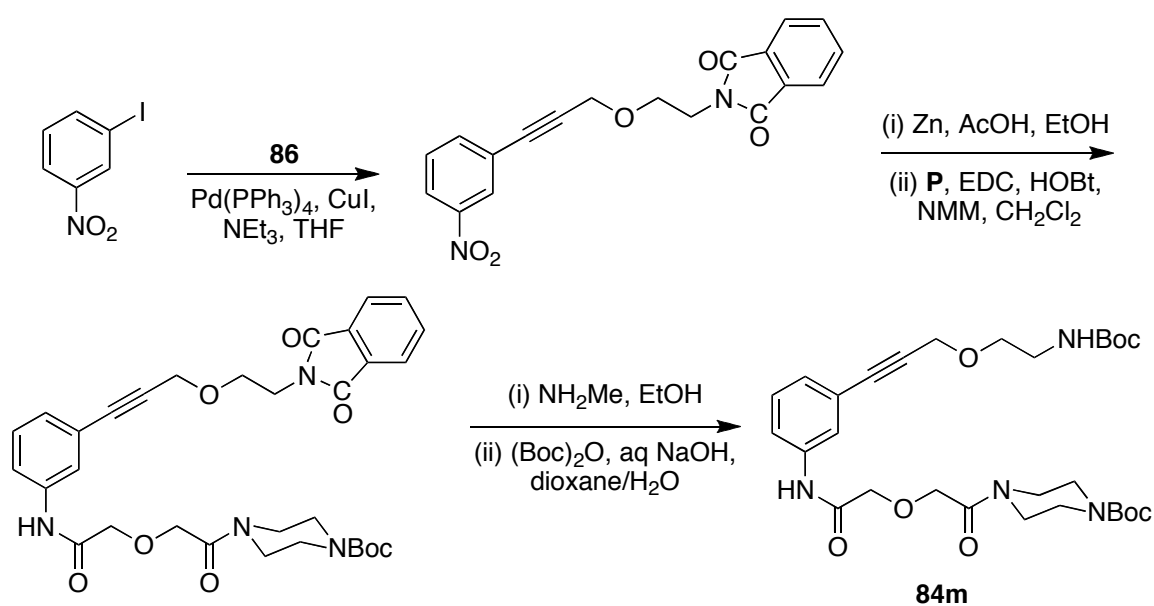


**<sup>1</sup>H NMR of 84i**



**<sup>13</sup>C NMR of 84i**

As shown in Scheme C6, Sonogashira coupling of 3-iodonitrobenzene with alkyne **86** gave the phthalimide protected intermediate, which was reduced with zinc and linker **P** was attached. The following deprotection of phthalimide group with methylamine and the re-protection with Boc anhydride afforded **84m** in good yield.



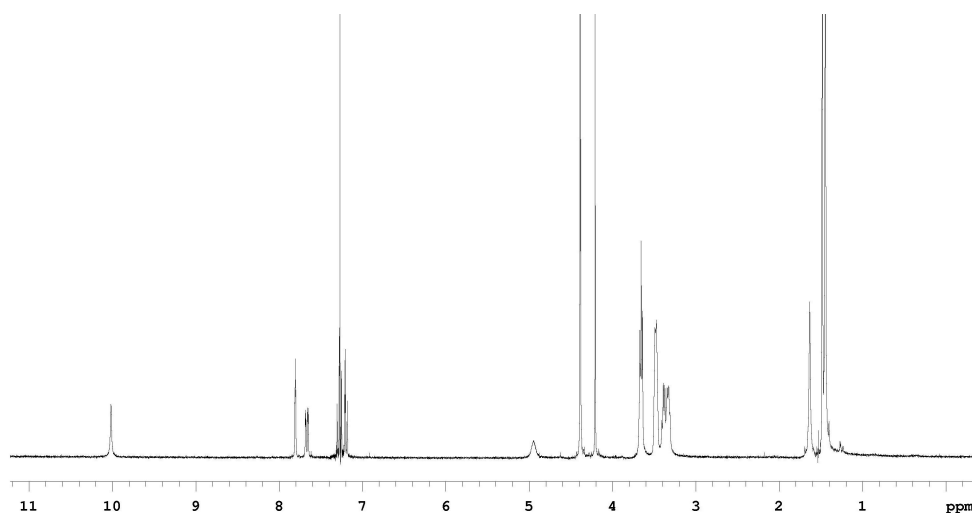
**Scheme C6.** Preparation of compound **84m**.

**Data for 84m**

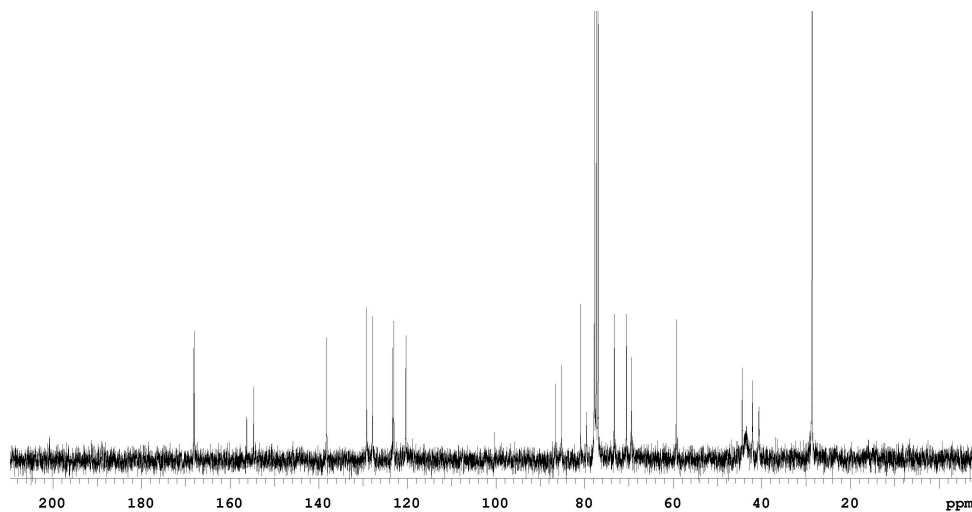
**<sup>1</sup>H NMR (300 MHz, CDCl<sub>3</sub>)** δ 10.02 (s, 1H), 7.80 (s, 1H), 7.65 (d, 1H, J = 8.4 Hz), 7.28 (t, 1H, J = 8.4 Hz), 7.18 (d, 1H, J = 8.4 Hz), 4.38 (s, 4H), 4.20 (s, 2H), 3.65 (t, 4H, J = 8.4 Hz), 3.66-3.12 (m, 8H), 1.48 (s, 9H), 1.44 (s, 9H)

**<sup>13</sup>C NMR (300 MHz, CDCl<sub>3</sub>)** δ 168.2, 168.0, 156.2, 154.6, 138.1, 129.1, 127.8, 123.3, 123.0, 120.3, 86.5, 85.1, 80.9, 79.5, 73.3, 70.5, 69.4, 59.3, 44.4, 42.0, 40.6, 28.6, 28.5

**MS (ESI, m/z)** 575 (M+H)<sup>+</sup>

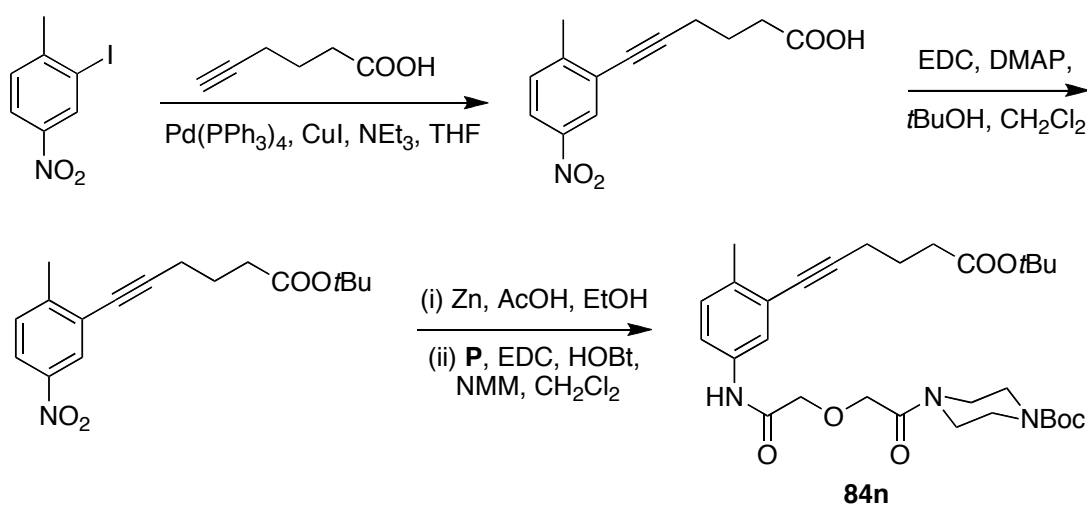


**<sup>1</sup>H NMR of 84m**



**<sup>13</sup>C NMR of 84m**

Preparation of compound **84n** started from the commercially available 3-iodo-4-methyl-nitrobenzene (Scheme C7). Sonogashira coupling with 5-hexynoic acid gave the acid intermediate which was protected with *t*-butyl group. The resulting nitro compound was reduced and long linker was attached to produce compound **84n**.



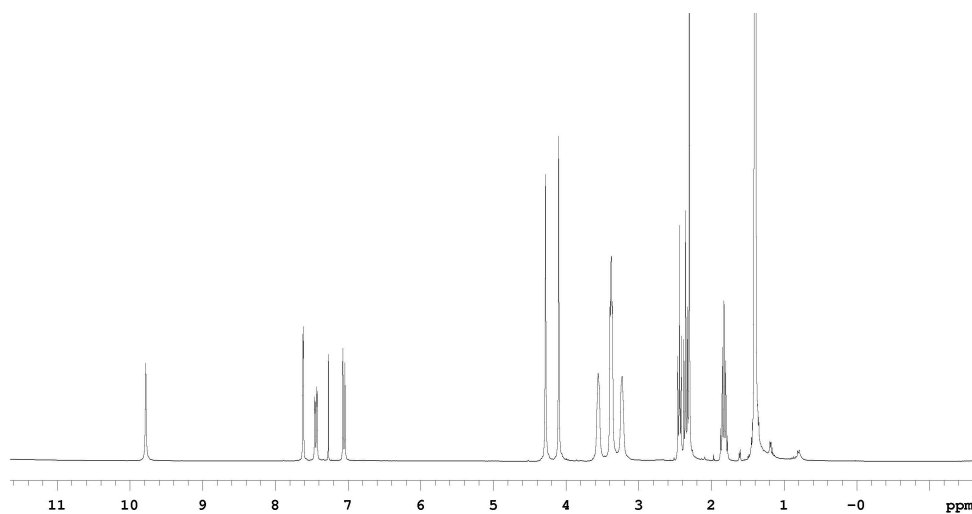
**Scheme C7.** Preparation of compound **84n**.

**Data for 84n**

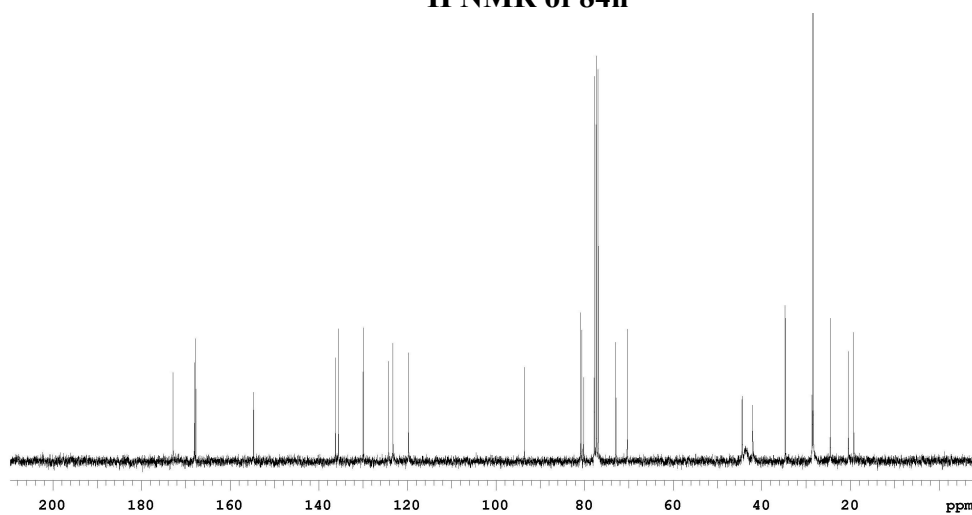
**$^1\text{H}$  NMR (300 MHz,  $\text{CDCl}_3$ )**  $\delta$  9.68 (s, 1H), 7.65 (d, 1H,  $J = 2.1$  Hz), 7.52 (dd, 1H,  $J = 6.9$  Hz, 2.1 Hz), 7.14 (d, 1H,  $J = 6.9$  Hz), 4.37 (s, 2H), 4.19 (s, 2H), 3.65-3.32 (m, 8H), 2.50 (t, 2H,  $J = 6.9$  Hz), 2.42 (t, 2H,  $J = 7.5$  Hz), 2.37 (s, 3H), 1.89 (m, 2H), 1.48 (s, 9H), 1.46 (s, 9H)

**$^{13}\text{C}$  NMR (300 MHz,  $\text{CDCl}_3$ )**  $\delta$  172.9, 168.0, 167.7, 154.6, 136.2, 135.5, 129.9, 124.2, 123.2, 119.7, 93.5, 80.9, 80.6, 80.1, 72.9, 70.3, 44.4, 42.0, 34.7, 28.6, 28.4, 24.5, 20.4, 19.2

**MS (ESI,  $m/z$ )** 457 ( $\text{M}+\text{H}$ )<sup>+</sup>



**$^1\text{H}$  NMR of 84n**

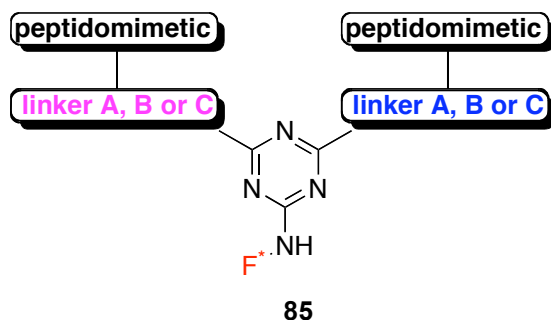


**$^{13}\text{C}$  NMR of 84n**



**General Procedure for preparation of Dimers 85.** Boc-protected monomeric compounds **84a-n** (1.0 eq.) were treated with 30% TFA in CH<sub>2</sub>Cl<sub>2</sub>, stirred in sealed glass vials for 4h and solvent was removed. The resulting residue was dissolved in THF (0.1 M) and DTAF (1.0 equiv.) and K<sub>2</sub>CO<sub>3</sub> (4.0 eq.) were added. The suspension was stirred for 2 h and solvent was removed. The crude product was used for the next step without further purification. Analytical HPLC was used to check the crude purity at this stage and 95% is the cutoff of the satisfactory purity.

Dimerization was carried out in 2 ml glass vials. Stock solutions of the above crude material (0.03 M) and deprotected **84** (0.03 M) in DMSO were prepared. One stock solution of the crude material (0.5 ml) and one of deprotected **84** (0.5 ml) were added to a glass vial and followed with solid K<sub>2</sub>CO<sub>3</sub> (*ca* 20 mg). The reaction vial was sealed and sonicated for 15 min. The reaction mixture was agitated at room temperature for 48 h and DMSO was lyophilized. Aqueous HCl solution (1%, *ca* 0.5 ml) was added to the above solid residue and the suspension was transferred to a 5ml centrifuge tube and centrifuged for 15 min and the aqueous solution was carefully decanted. The solid products were dried under vacuum overnight to give the final products **85**. All crude products were analyzed by analytical HPLC (5-95% B in 30 min) and MALDI-MS.



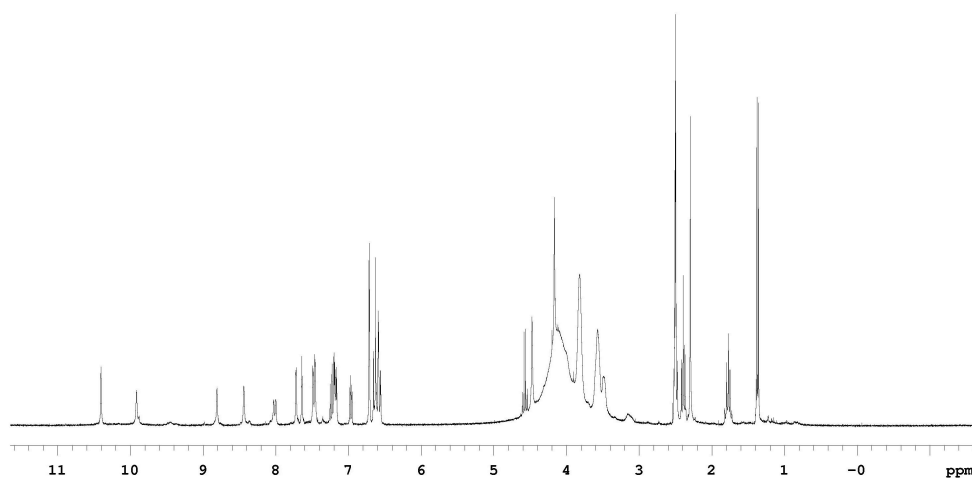
### **85an**

<sup>1</sup>H NMR (300 MHz, DMSO-d<sub>6</sub>) δ 10.40 (s, 1H), 9.92 (s, 1H), 8.81 (s, 1H), 8.44 (s, 1H), 8.01 (d, 1H, J = 8.4 Hz), 7.21 (d, 1H, J = 1.8 Hz), 7.64 (t, 1H, J = 1.8 Hz), 7.47 (dd, 2H, J = 8.4 Hz, 1.8 Hz), 7.18 (m, 3H), 6.92 (d, 1H, J = 8.4 Hz), 6.71 (d, 2H, J = 2.4 Hz), 6.63

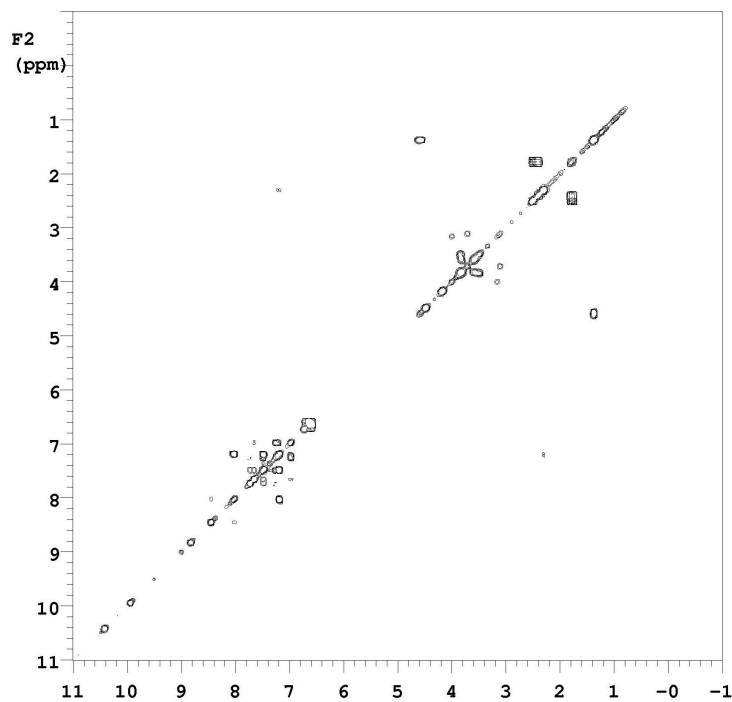
(d, 2H, J = 9.0 Hz), 6.57 (dd, 2H, J = 9.0 Hz, 2.4 Hz), 4.58 (q, 1H, J = 6.6 Hz), 4.19-3.48 (m, 22H), 2.39 (t, 2H, J = 7.8 Hz), 2.29 (s, 3H), 1.77 (m, 2H), 1.36 (d, 3H, J = 6.6 Hz)

**LRMS (MALDI)** calc'd for  $[M+H]^+$  1097, found 1097

**Analytical HPLC** purity = 94%, retention time = 19.6 min



**$^1\text{H}$  NMR of 85an**



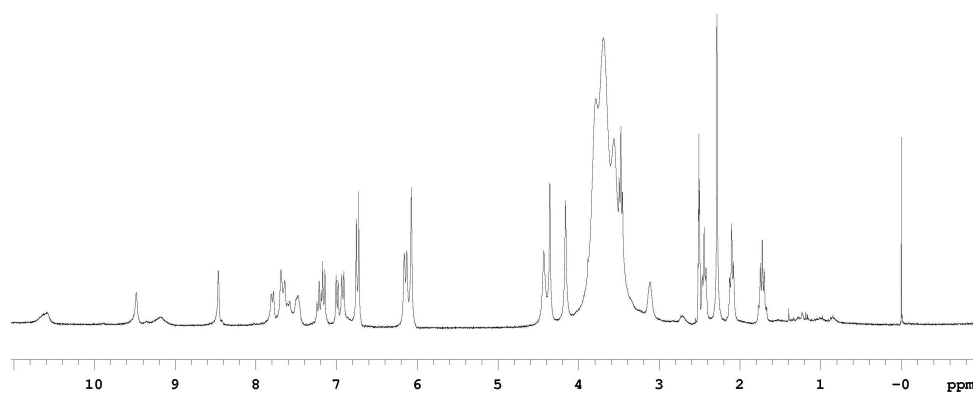
**COSY NMR of 85an**

**85fn**

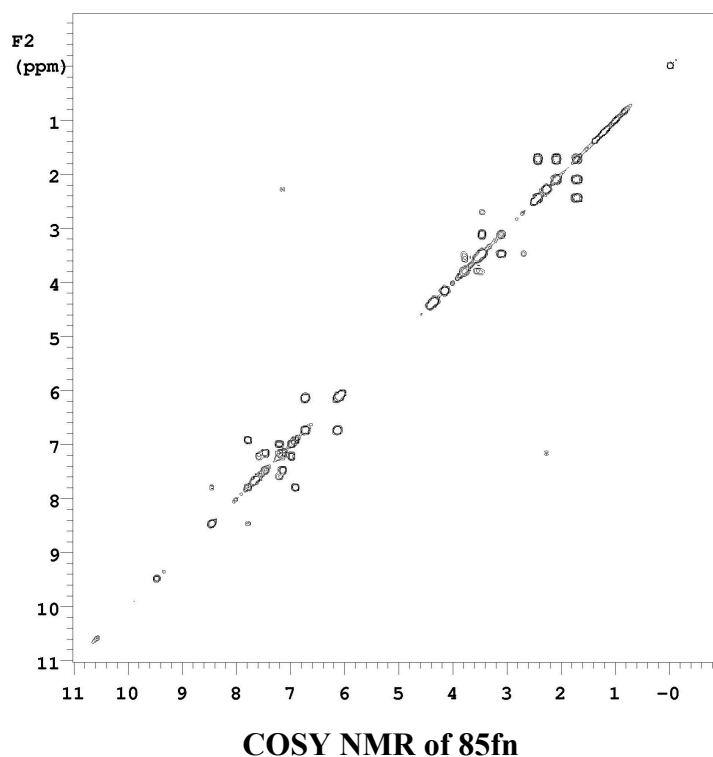
**<sup>1</sup>H NMR (300 MHz, DMSO-d<sub>6</sub>)** δ 10.71 (s, 1H), 9.46 (s, 1H), 9.15 (s, 1H), 8.45 (s, 1H), 7.79 (d, 1H, J = 8.4 Hz), 7.67 (m, 2H), 7.46 (m, 2H), 7.20 (t, 1H, J = 8.1 Hz), 7.15 (d, 1H, J = 8.1 Hz), 6.97 (d, 1H, J = 8.4 Hz), 6.90 (d, 2H, J = 8.4 Hz), 6.71 (d, 2H, J = 9.6 Hz), 6.14 (d, 2H, J = 9.6 Hz), 6.05 (s, 2H), 4.41 (s, 1H), 4.34 (s, 2H), 4.14 (s, 2H), 3.76-3.44 (m, 22H), 2.43 (t, 2H, J = 7.2 Hz), 2.27 (s, 3H), 2.08 (t, 2H, J = 7.2 Hz), 1.70 (m, 2H),

**LRMS (MALDI)** calc'd for [M+H]<sup>+</sup> 1067, found 1067

**Analytical HPLC** purity = 90%, retention time = 17.5 min



**<sup>1</sup>H NMR of 85fn**

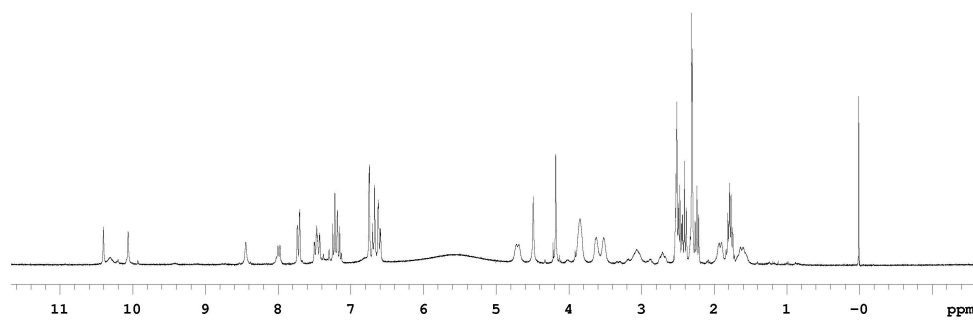


### 85dn

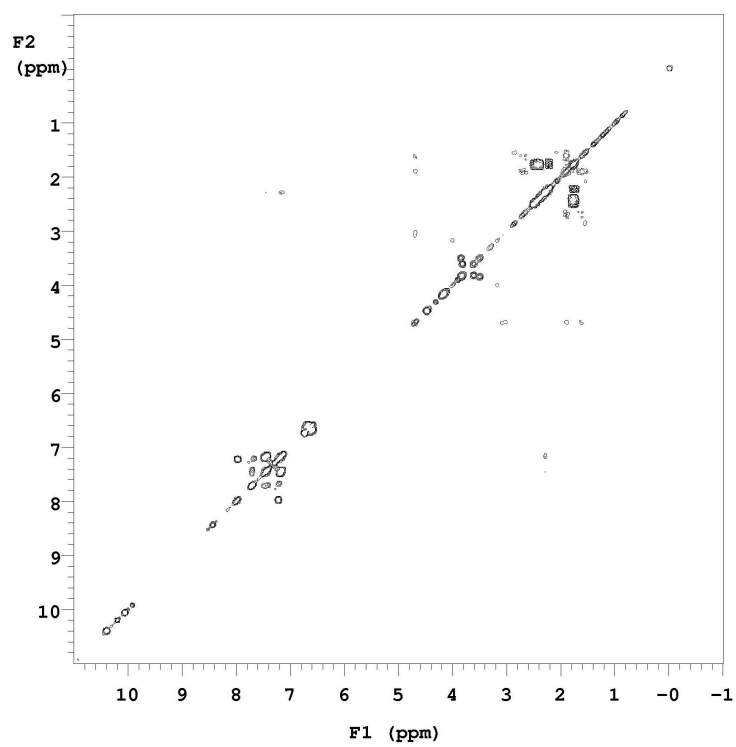
**<sup>1</sup>H NMR (300 MHz, DMSO-d<sub>6</sub>)** δ 10.40 (s, 1H), 10.07 (s, 1H), 8.44 (s, 1H), 7.98 (d, 1H, J = 7.8 Hz), 7.71 (d, 2H, J = 7.2 Hz), 7.46 (m, 2H), 7.24 (m, 4H), 6.75 (d, 2H, J = 2.1 Hz), 6.62 (d, 2H, J = 8.4 Hz), 6.59 (dd, 2H, J = 8.4 Hz, 2.1 Hz), 4.72 (d, 2H, J = 10.2 Hz), 4.49 (s, 2H), 4.18 (s, 2H), 3.92-3.48 (m, 16H), 3.06 (m, 2H), 2.72 (t, 2H, J = 7.2 Hz), 2.45 (t, 2H, J = 7.2 Hz), 2.41 (t, 2H, J = 7.5 Hz), 2.39 (s, 6H), 2.24 (t, 2H, J = 7.5 Hz), 1.93 (d, 2H, J = 10.2 Hz), 1.77 (m, 4H), 1.64 (m, 2H)

**LRMS (MALDI)** calc'd for [M+H]<sup>+</sup> 1151, found 1151

**Analytical HPLC** purity = 95%, retention time = 19.1 min



**<sup>1</sup>H NMR of 85dn**



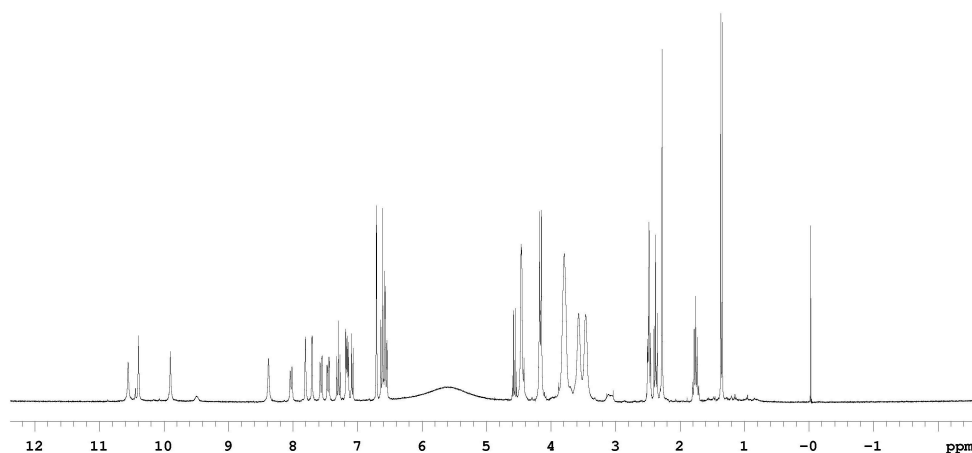
**COSY NMR of 85dn (300 MHz)**

**85hn**

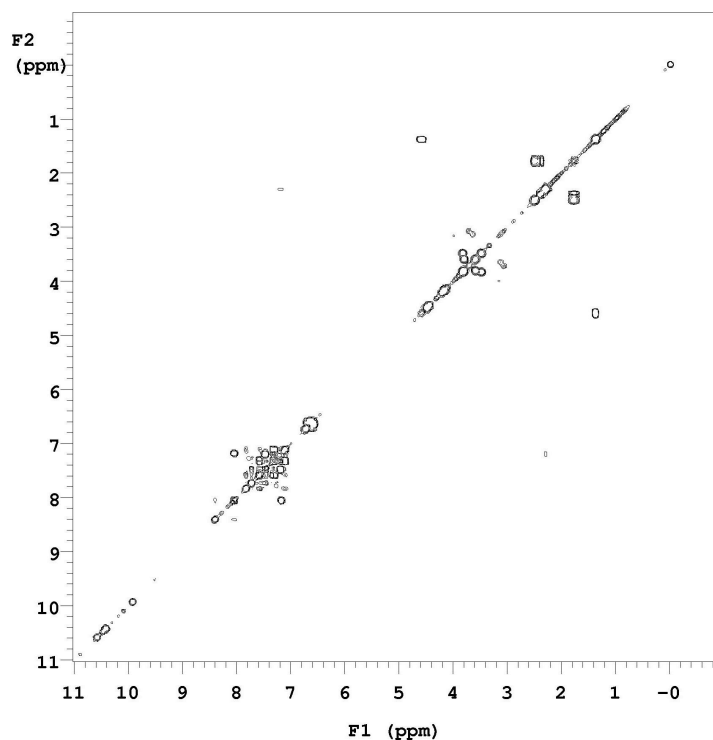
**$^1\text{H}$  NMR (300 MHz, DMSO- $d_6$ )**  $\delta$  10.58 (s, 1H), 10.42 (s, 1H), 9.93 (s, 1H), 8.41 (s, 1H), 8.05 (d, 1H,  $J = 8.4$  Hz), 7.84 (s, 1H), 7.73 (d, 1H,  $J = 1.8$  Hz), 7.60 (d, 1H,  $J = 6.3$  Hz), 7.48 (dd, 1H,  $J = 8.4$  Hz, 2.1 Hz), 7.32 (t, 1H,  $J = 8.4$  Hz), 7.10 (m, 2H), 7.09 (d, 1H,  $J = 8.1$  Hz), 6.73 (d, 2H,  $J = 2.4$  Hz), 6.64 (d, 2H,  $J = 9.0$  Hz), 6.57 (dd, 2H,  $J = 9.0$  Hz, 2.4 Hz), 4.58 (q, 1H,  $J = 6.6$  Hz), 4.49 (s, 2H), 4.48 (s, 2H), 4.21 (s, 2H), 4.18 (s, 2H), 3.82-3.48 (m, 16H), 2.43 (t, 2H,  $J = 7.8$  Hz), 2.31 (s, 3H), 1.77 (m, 2H), 1.39 (d, 3H,  $J = 6.6$  Hz)

**LRMS (MALDI)** calc'd for  $[\text{M}+\text{H}]^+$  1068, found 1069

**Analytical HPLC** purity = 90%, retention time = 18.7 min



**$^1\text{H}$  NMR of 85hn**



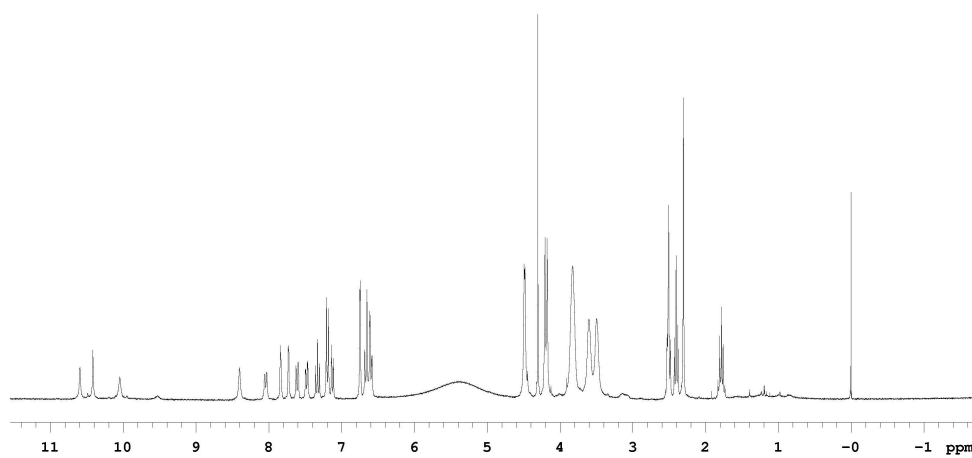
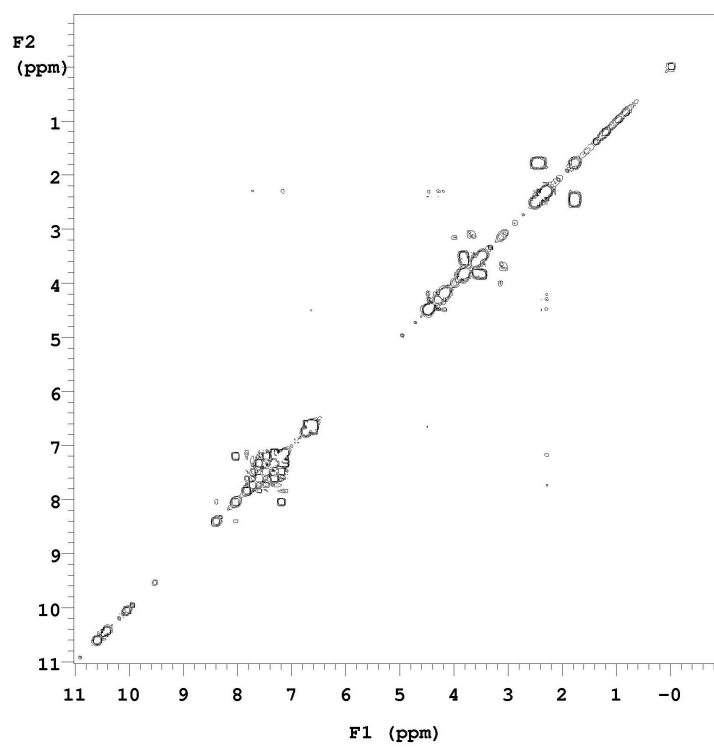
**COSY NMR of 85hn**

### 85in

**$^1\text{H}$  NMR (300 MHz, DMSO- $d_6$ )**  $\delta$  10.58 (s, 1H), 10.42 (s, 1H), 10.05 (s, 1H), 8.40 (s, 1H), 8.04 (d, 1H,  $J = 7.2$  Hz), 7.84 (s, 1H), 7.73 (d, 1H,  $J = 1.8$  Hz), 7.60 (d, 1H,  $J = 9.3$  Hz), 7.48 (dd, 1H,  $J = 8.4$  Hz, 1.8 Hz), 7.33 (t, 1H,  $J = 8.4$  Hz), 7.20 (d, 2H), 7.12 (d, 1H,  $J = 7.8$  Hz), 6.73 (d, 2H,  $J = 2.4$  Hz), 6.67 (d, 2H,  $J = 9.0$  Hz), 6.57 (dd, 2H,  $J = 9.0$  Hz, 2.4 Hz), 4.49 (s, 2H), 4.48 (s, 2H), 4.30 (s, 2H), 4.21 (s, 2H), 4.17 (s, 2H), 3.91-3.49 (m, 16H), 2.43 (t, 2H,  $J = 7.2$  Hz), 2.30 (s, 3H), 1.77 (m, 2H)

**LRMS (MALDI)** calc'd for  $[\text{M}+\text{H}]^+$  1155, found 1155

**Analytical HPLC** purity = 95%, retention time = 17.9 min

**<sup>1</sup>H NMR of 85in****COSY NMR of 58in**

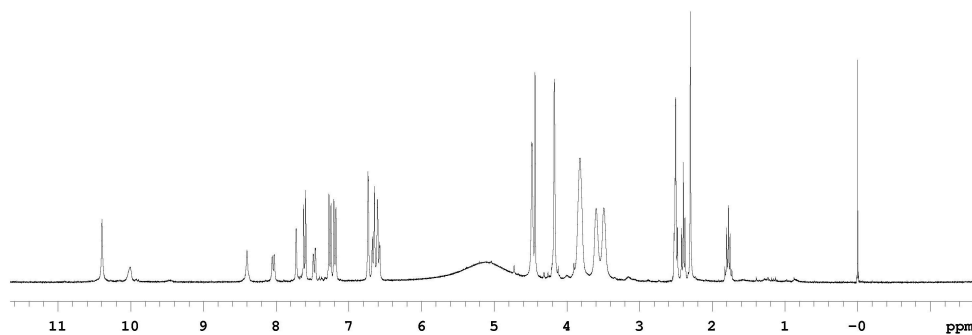


**85jn**

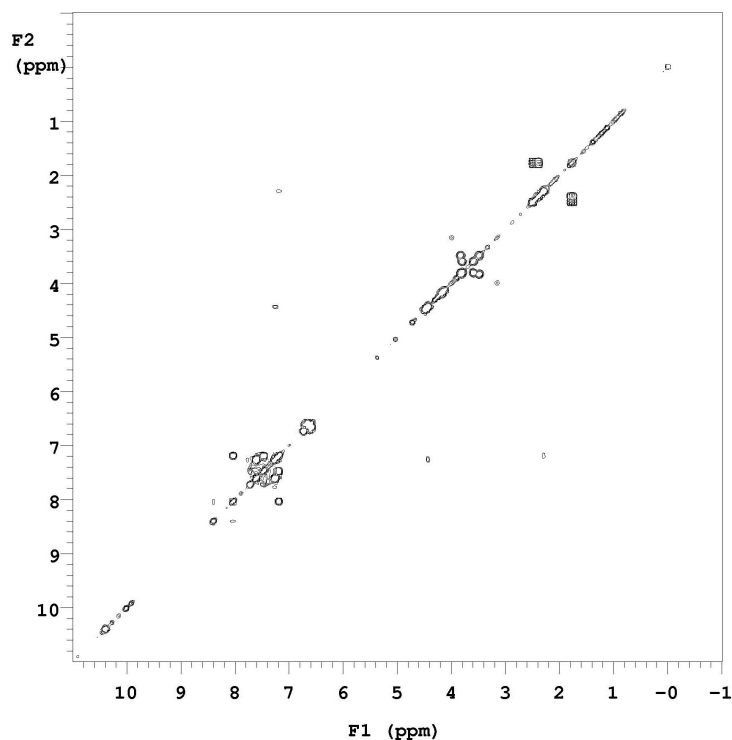
**<sup>1</sup>H NMR (300 MHz, DMSO-d<sub>6</sub>)** δ 10.35 (s, 1H), 10.01 (s, 1H), 8.41(s, 1H), 8.03 (d, 1H), 8.05 (d, 1H, J = 8.4 Hz), 7.72 (s, 1H), 7.65 (d, 2H, J = 8.4 Hz), 7.49 (d, 1H, J = 10.2 Hz), 7.27 (d, 2H, J = 8.4 Hz), 7.20 (d, 2H, J = 8.4 Hz), 6.73 (d, 2H, J = 1.8 Hz), 6.65 (d, 2H, J = 9.0 Hz), 6.58 (dd, 2H, J = 9.0 Hz, 1.8 Hz), 4.48 (s, 2H), 4.47 (s, 2H), 4.44 (s, 2H), 4.18 (s, 4H), 3.90-3.40 (m, 16H), 2.43 (t, 2H, J = 7.2 Hz), 2.37 (s, 3H), 1.77 (m, 2H),

**LRMS (MALDI)** calc'd for [M+H]<sup>+</sup> 1131, found 1131

**Analytical HPLC** purity = 98%, retention time = 18.2 min



**<sup>1</sup>H NMR of 85jn**



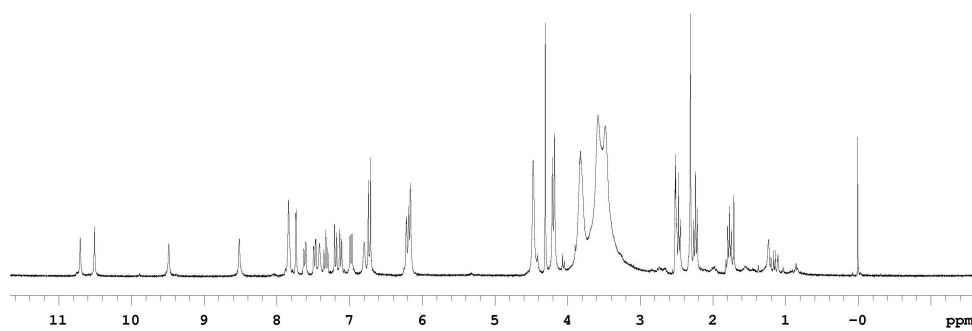
**COSY NMR of 85jn (300 MHz)**

**85ik**

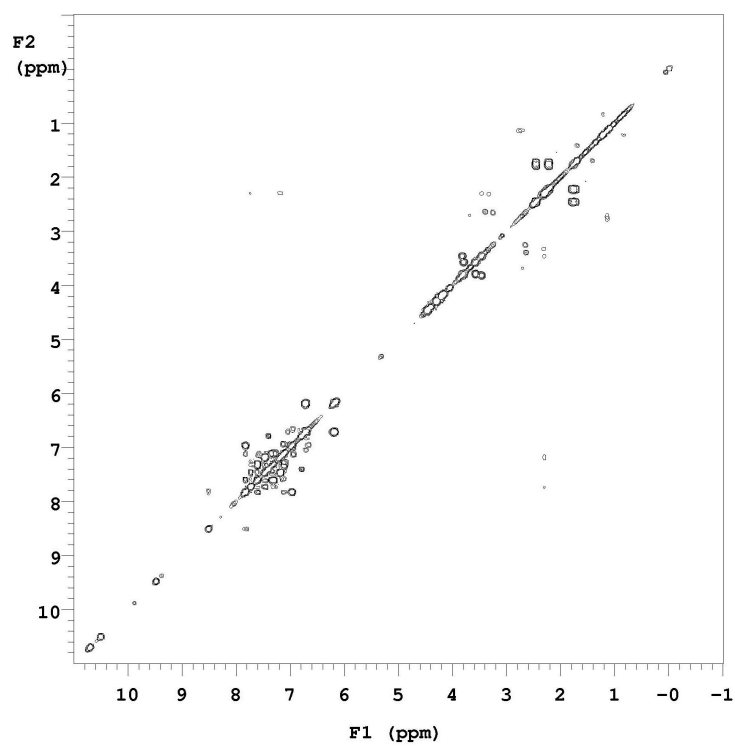
**$^1\text{H}$  NMR (300 MHz, DMSO- $d_6$ )**  $\delta$  10.70 (s, 1H), 10.51 (s, 1H), 9.49 (s, 1H), 8.51 (s, 1H), 7.84 (s, 2H), 7.74 (d, 1H,  $J = 1.8$  Hz), 7.61 (d, 1H,  $J = 8.1$  Hz), 7.46 (dd, 1H,  $J = 8.4$  Hz, 2.1 Hz), 7.41 (s, 1H), 7.33 (t, 1H,  $J = 8.1$  Hz), 7.18 (d, 1H,  $J = 8.4$  Hz), 7.11 (d, 1H,  $J = 7.8$  Hz), 6.98 (d, 2H,  $J = 8.4$  Hz), 6.79 (s, 1H), 6.73 (d, 2H,  $J = 9.0$  Hz), 6.22 (s, 2H), 6.17 (d, 2H,  $J = 9.0$  Hz), 4.47 (s, 4H), 4.31 (s, 2H), 4.21 (s, 2H), 4.18 (s, 2H), 3.89-3.48 (m, 16H), 2.47 (t, 2H,  $J = 7.2$  Hz), 2.31 (s, 3H), 2.24 (t, 2H,  $J = 7.2$  Hz), 1.74 (m, 2H)

**LRMS (MALDI)** calc'd for  $[\text{M}+\text{H}]^+$  1054, found 1054

**Analytical HPLC** purity = 89%, retention time = 17.7 min



**$^1\text{H}$  NMR of 85ik**



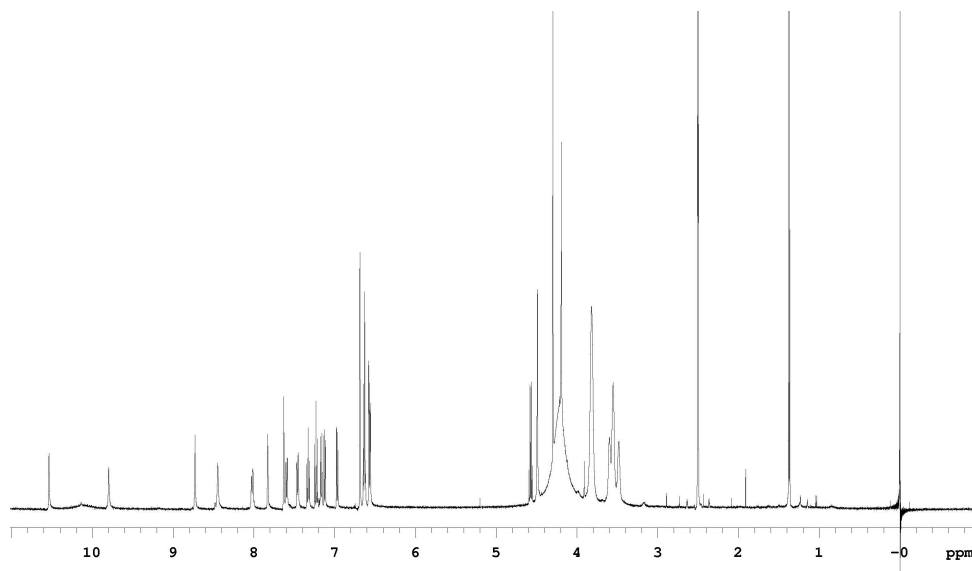
**COSY NMR of 85ik (300 MHz)**

**85ai**

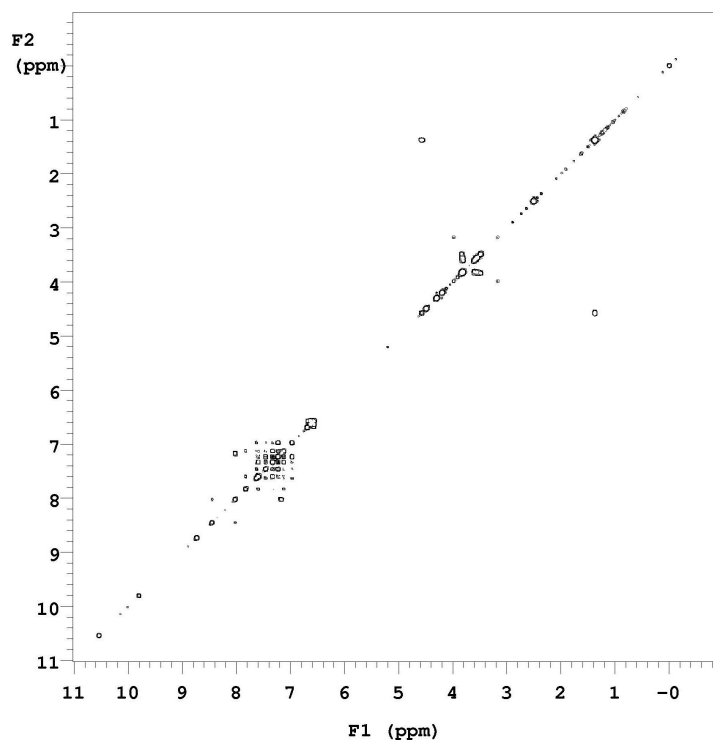
**<sup>1</sup>H NMR (500 MHz, DMSO-d<sub>6</sub>)** δ 10.58 (s, 1H), 9.78 (s, 1H), 8.73 (s, 1H), 8.45 (s, 1H), 8.01 (d, 1H, J = 7.5 Hz), 7.83 (s, 1H), 7.63 (s, 1H), 7.59 (d, 1H, J = 7.0 Hz), 7.45 (d, 1H, J = 8.5 Hz), 7.33 (t, 1H, J = 7.5 Hz), 7.23 (t, 1H, J = 7.5 Hz), 7.16 (d, 1H, J = 8.0 Hz), 7.12 (d, 1H, J = 7.5 Hz), 6.96 (d, 1H, J = 7.5 Hz), 6.68 (d, 2H, J = 2.0 Hz), 6.62 (d, 2H, J = 9.0 Hz), 6.58 (dd, 2H, J = 9.0 Hz, 2.0 Hz), 4.56 (q, 1H, J = 6.5 Hz), 4.48 (s, 2H), 4.30 (s, 2H), 4.19 (s, 2H), 3.82-3.48 (m, 16H), 1.37 (d, 3H, J = 6.5 Hz)

**LRMS (MALDI)** calc'd for [M+H]<sup>+</sup> 1027, found 1027

**Analytical HPLC** purity = 99%, retention time = 18.9 min



**<sup>1</sup>H NMR of 85ai**



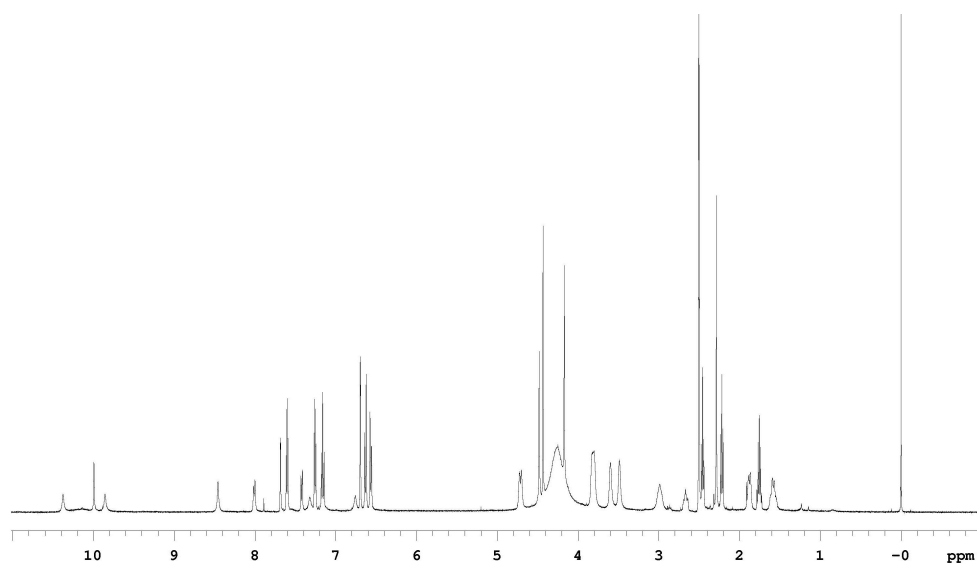
**COSY NMR of 85ai**

### 85dj

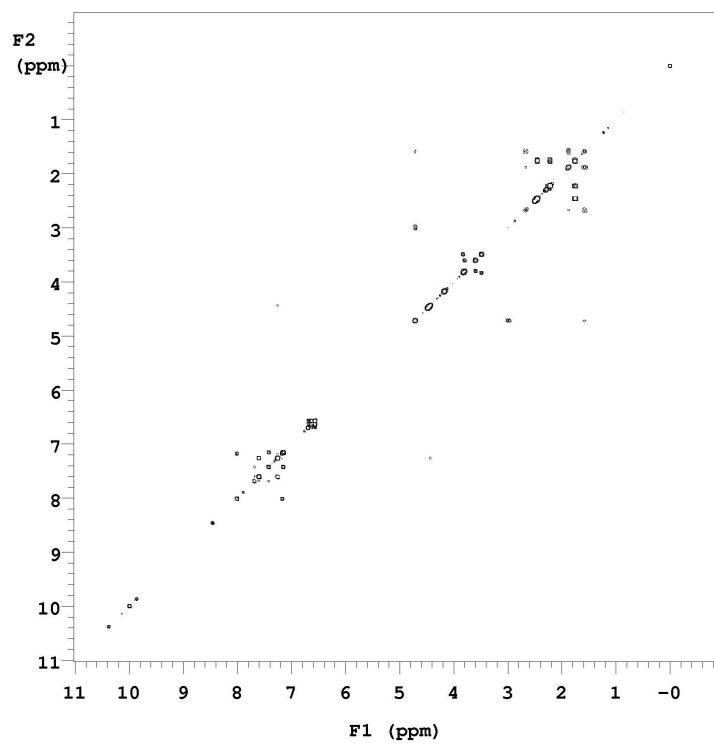
**$^1\text{H}$  NMR (500 MHz, DMSO- $d_6$ )**  $\delta$  10.48 (s, 1H), 9.98 (s, 1H), 9.83 (s, 1H), 8.46 (s, 1H), 8.01 (d, 1H,  $J = 8.0$  Hz), 7.68 (d, 1H,  $J = 2.0$  Hz), 7.60 (d, 2H,  $J = 8.5$  Hz), 7.42 (dd, 1H,  $J = 8.5$  Hz, 2.0 Hz), 7.32 (s, 1H), 7.25 (d, 2H,  $J = 8.5$  Hz), 7.16 (t, 2H,  $J = 8.5$  Hz), 6.76 (s, 1H), 6.69 (d, 2H,  $J = 2.0$  Hz), 6.63 (d, 2H,  $J = 9.0$  Hz), 6.58 (dd, 2H,  $J = 9.0$  Hz, 2.4 Hz), 4.71 (d, 2H,  $J = 7.0$  Hz), 4.48 (s, 2H), 4.43 (s, 2H), 4.17 (s, 2H), 3.80-3.49 (m, 8H), 2.99 (m, 2H), 2.67 (m, 1H), 2.46 (t, 2H,  $J = 7.5$  Hz), 2.32 (s, 3H), 2.22 (t, 2H,  $J = 7.5$  Hz), 1.89 (d, 2H,  $J = 10.0$  Hz), 1.76 (m, 2H), 1.58 (m, 2H)

**LRMS (MALDI)** calc'd for  $[\text{M}+\text{H}]^+$  1057, found 1057

**Analytical HPLC** purity = 99%, retention time = 18.5 min



**<sup>1</sup>H NMR of 85dj**



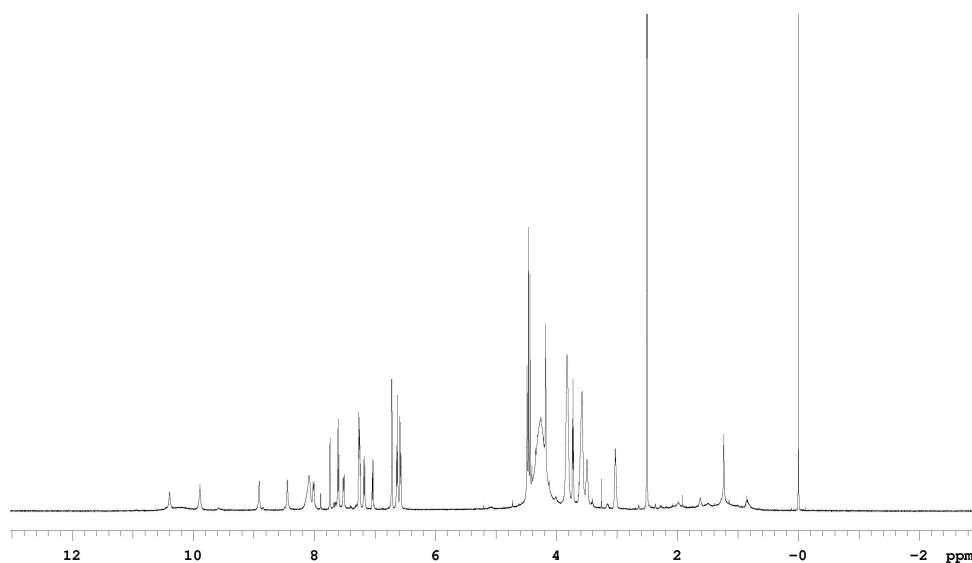
**COSY NMR of 85dj**

**85fj**

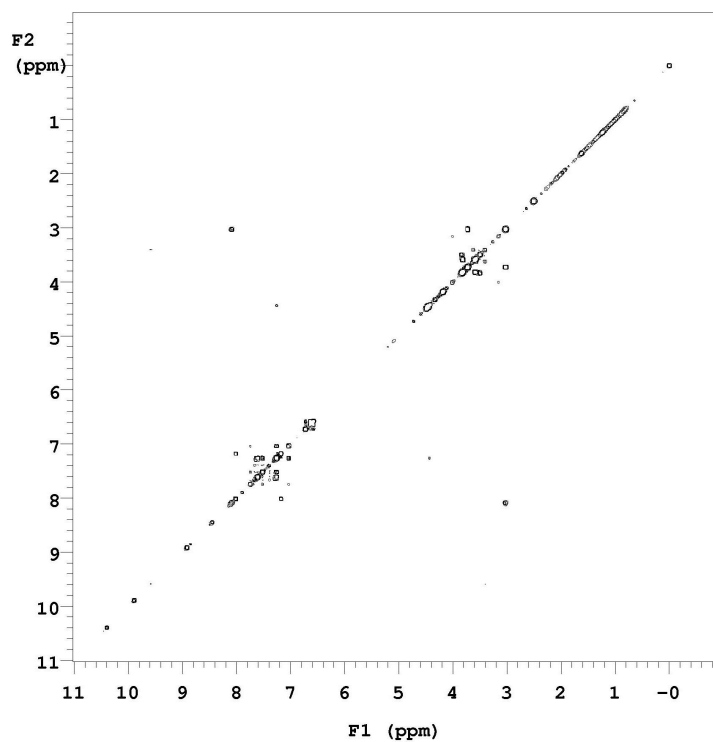
**<sup>1</sup>H NMR (500 MHz, DMSO-d<sub>6</sub>)** δ 10.39 (s, 1H), 9.89 (s, 1H), 9.83 (s, 1H), 8.91 (s, 1H), 8.45 (s, 1H), 8.08 (s, 2H), 8.01 (d, 1H, J = 8.0 Hz), 7.74 (s, 1H), 7.60 (d, 2H, J = 8.5 Hz), 7.51 (s, 1H, J = 8.0 Hz), 7.28 (m, 3H), 7.22 (d, 1H, J = 9.0 Hz), 7.03 (d, 1H, J = 9.0 Hz), 6.72 (d, 2H, J = 2.4 Hz), 6.59 (d, 2H, J = 9.0 Hz), 6.56 (dd, 2H, J = 9.0 Hz, 2.4 Hz), 4.51 (s, 2H), 4.48 (s, 2H), 4.46 (s, 2H), 3.82-3.49 (m, 20H), 3.03 (m, 2H)

**LRMS (MALDI)** calc'd for [M+H]<sup>+</sup> 1033, found 1033

**Analytical HPLC** purity = 90%, retention time = 17.8 min



**<sup>1</sup>H NMR of 85fj**



**COSY NMR of 85fj**

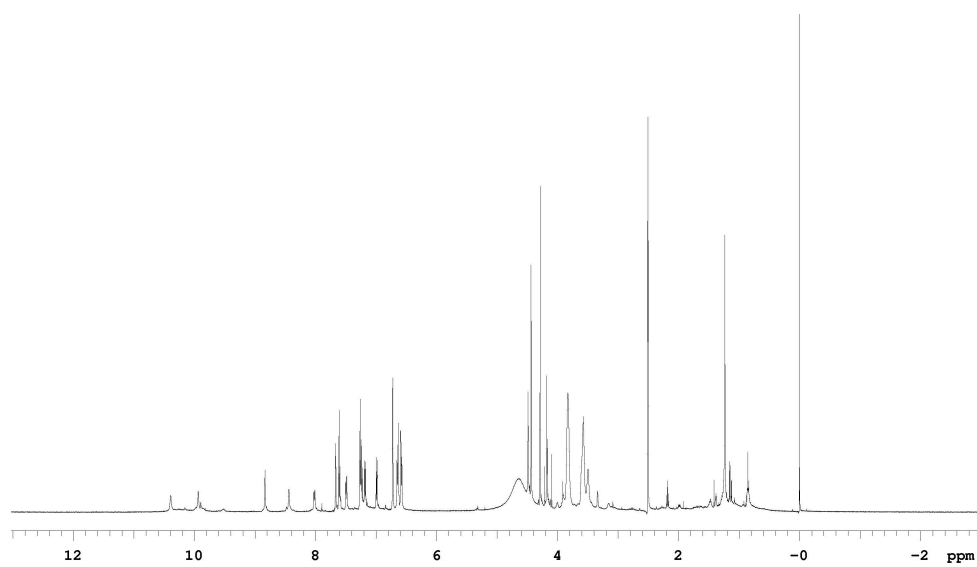
### **85bj**

**$^1\text{H}$  NMR (500 MHz, DMSO- $d_6$ )**  $\delta$  10.50 (s, 1H), 9.94 (s, 1H), 8.83 (s, 1H), 8.44 (s, 1H), 8.01 (d, 1H,  $J = 8.5$  Hz), 7.66 (d, 1H,  $J = 1.5$  Hz), 7.60 (d, 2H,  $J = 9.0$  Hz), 7.49 (d, 1H,  $J = 9.0$  Hz), 7.24 (m, 3H), 7.19 (d, 1H,  $J = 8.5$  Hz), 6.98 (d, 1H,  $J = 7.5$  Hz), 6.72 (d, 2H,  $J = 2.0$  Hz), 6.58 (d, 2H,  $J = 9.0$  Hz), 6.57 (dd, 2H,  $J = 9.0$  Hz, 2.4 Hz), 4.49 (s, 2H), 4.44 (s, 2H), 4.29 (s, 2H), 4.17 (s, 2H), 3.83-3.57 (m, 16H)

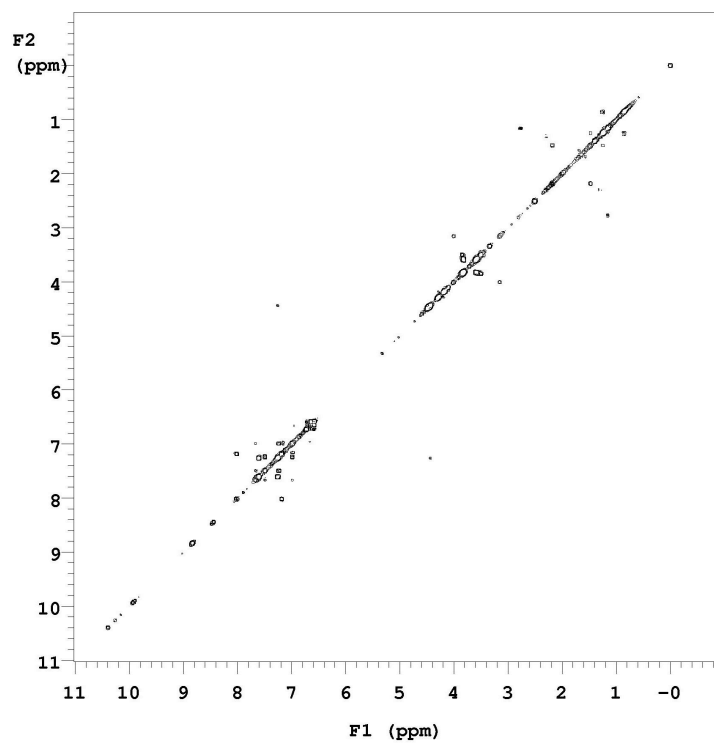
**LRMS (MALDI)** calc'd for  $[\text{M}+\text{H}]^+$  989, found 989

**Analytical HPLC** purity = 88%, retention time = 18.8 min





$^1\text{H}$  NMR of 85bj



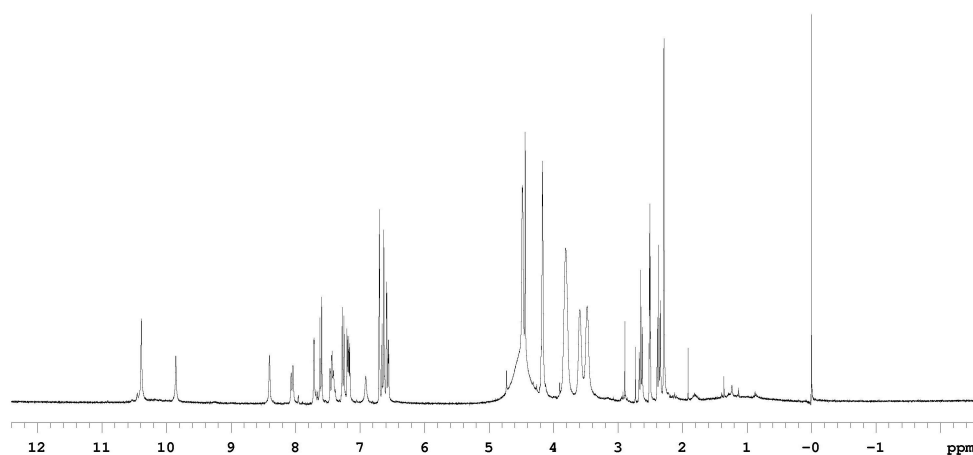
COSY NMR of 85bj

**85jl**

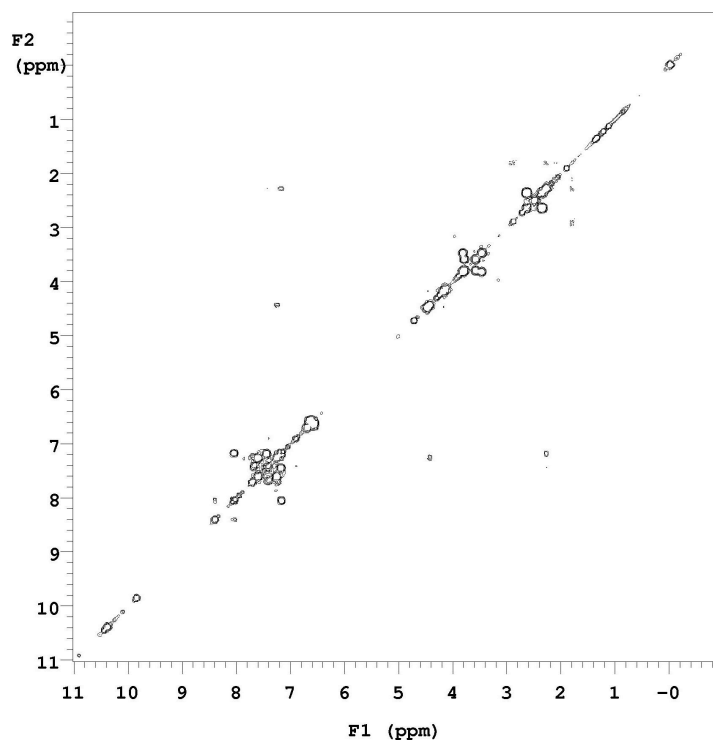
**<sup>1</sup>H NMR (300 MHz, DMSO-d<sub>6</sub>)** δ 10.39 (s, 1H), 9.85 (s, 1H), 8.40 (s, 1H), 8.06 (d, 1H, J = 8.4 Hz), 7.71 (d, 1H, J = 1.8 Hz), 7.60 (d, 2H, J = 9.0 Hz), 7.43 (m, 3H), 7.25 (d, 2H, J = 8.4 Hz), 7.18 (d, 1H, J = 4.2 Hz), 7.16 (d, 1H, J = 4.2 Hz), 6.91 (s, 1H), 6.70 (d, 2H, J = 2.4 Hz), 6.60 (d, 2H, J = 9.0 Hz), 6.56 (dd, 2H, J = 9.0 Hz, 2.4 Hz), 4.49 (s, 2H), 4.48 (s, 2H), 4.44 (s, 2H), 4.19 (s, 2H), 4.17 (s, 2H), 3.81-3.48 (m, 16H), 2.65 (t, 2H, J = 7.5 Hz), 2.37 (t, 3H, J = 7.5 Hz), 2.29 (s, 3H)

**LRMS (MALDI)** calc'd for [M+H]<sup>+</sup> 1116, found 1116

**Analytical HPLC** purity = 85%, retention time = 18.7 min



**<sup>1</sup>H NMR of 85jl**



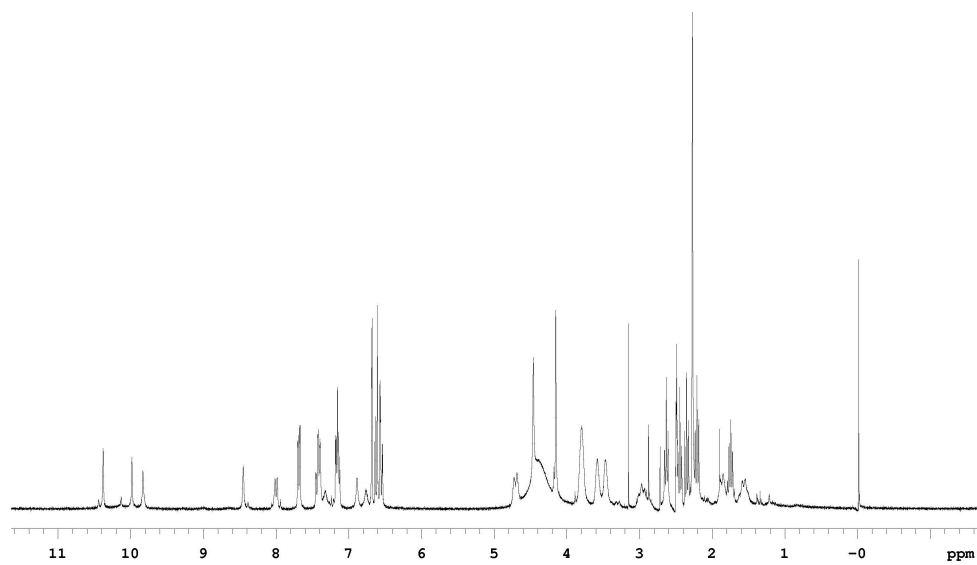
**COSY NMR of 85jl**

### 85dl

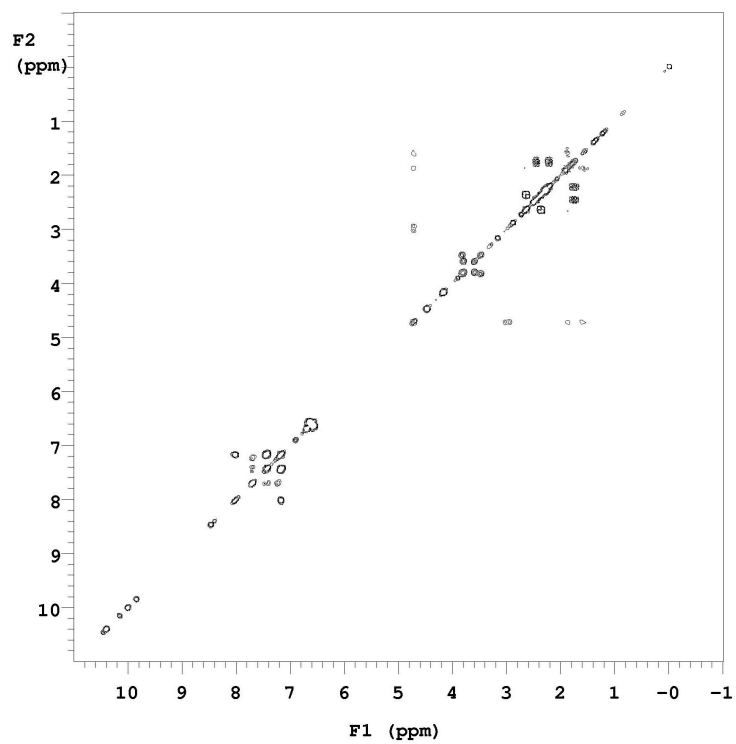
**$^1\text{H}$  NMR (300 MHz, DMSO- $d_6$ )**  $\delta$  10.87 (s, 1H), 9.98 (s, 1H), 9.83 (s, 1H), 8.45 (s, 1H), 7.99 (d, 1H,  $J = 8.4$  Hz), 7.68 (dd, 1H,  $J = 8.4$  Hz, 1.8 Hz), 7.39 (m, 4H), 7.17 (m, 4H), 6.68 (d, 2H,  $J = 2.4$  Hz), 6.61 (d, 2H,  $J = 9.0$  Hz), 6.58 (dd, 2H,  $J = 9.0$  Hz, 2.4 Hz), 4.69 (d, 2H,  $J = 12.0$  Hz), 4.46 (s, 2H), 4.18 (s, 2H), 3.79-3.48 (m, 8H), 2.93 (m, 3H), 2.51 (t, 2H,  $J = 7.5$  Hz), 2.48 (t, 3H,  $J = 7.5$  Hz), 2.38 (t, 2H,  $J = 7.5$  Hz), 2.36 (s, 6H), 2.23 (t, 2H,  $J = 7.5$  Hz), 1.84 (m, 2H), 1.72 (m, 2H) 1.58 (m, 2H)

**LRMS (MALDI)** calc'd for  $[\text{M}+\text{H}]^+$  1136, found 1136

**Analytical HPLC** purity = 85%, retention time = 18.5 min



$^1\text{H}$  NMR of 85dl



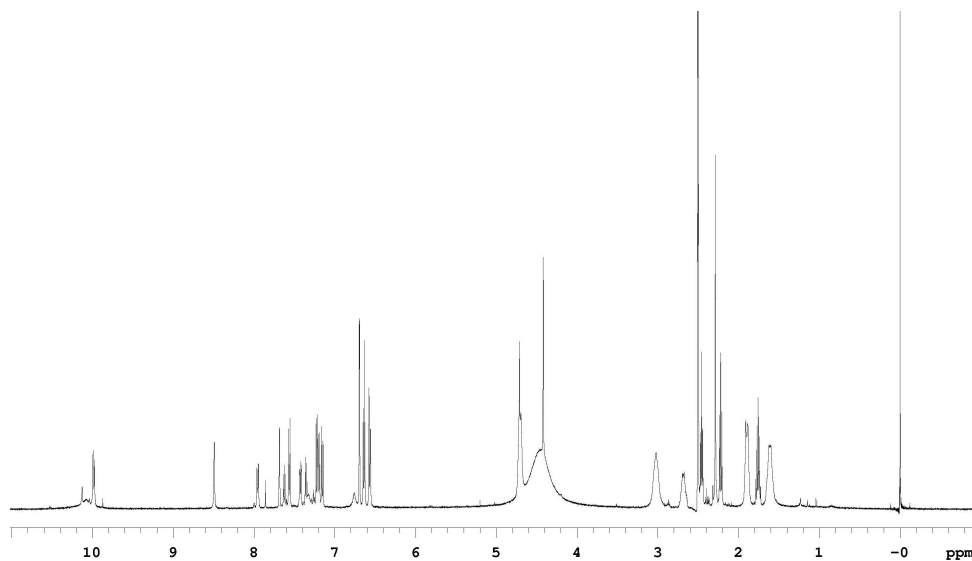
COSY NMR of 85dl (300 MHz)

**85cd**

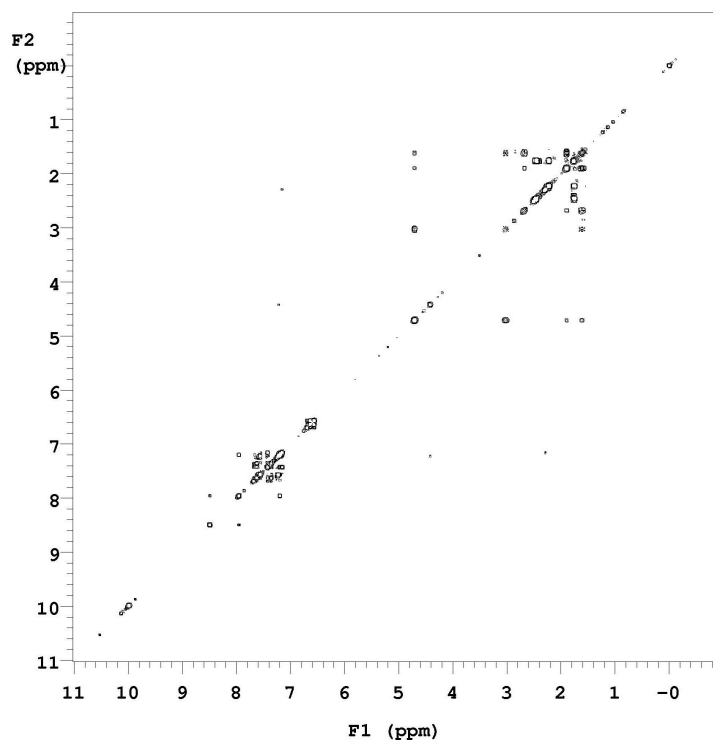
**<sup>1</sup>H NMR (500 MHz, DMSO-d<sub>6</sub>)** δ 9.99 (s, 1H), 9.97 (s, 1H), 9.49 (s, 1H), 7.96 (dd, 1H, J = 8.5 Hz, 2.0 Hz), 7.68 (d, 1H, J = 2.0 Hz), 7.63 (d, 1H, J = 8.5 Hz), 7.56 (d, 1H, J = 8.5 Hz), 7.41 (dd, 1H, J = 8.5 Hz, 2.0 Hz), 7.35 (d, 1H, J = 8.5 Hz), 7.21 (d, 1H, J = 8.5 Hz), 7.19 (d, 1H, J = 8.5 Hz), 7.15 (d, 1H, J = 8.5 Hz), 6.69 (d, 2H, J = 2.0 Hz), 6.63 (d, 2H, J = 9.0 Hz), 6.56 (dd, 2H, J = 9.0 Hz, 2.0 Hz), 4.59 (m, 4H), 4.42 (s, 2H), 3.02 (m, 4H), 2.69 (m, 2H), 2.46 (t, 2H, J = 7.0 Hz), 2.29 (s, 3H), 2.22 (t, 2H, J = 7.0 Hz), 1.91 (m, 4H), 1.75 (m, 2H), 1.62 (m, 4H)

**LRMS (MALDI)** calc'd for [M+H]<sup>+</sup> 970, found 970

**Analytical HPLC** purity = 99%, retention time = 17.8 min



**<sup>1</sup>H NMR of 85cd**



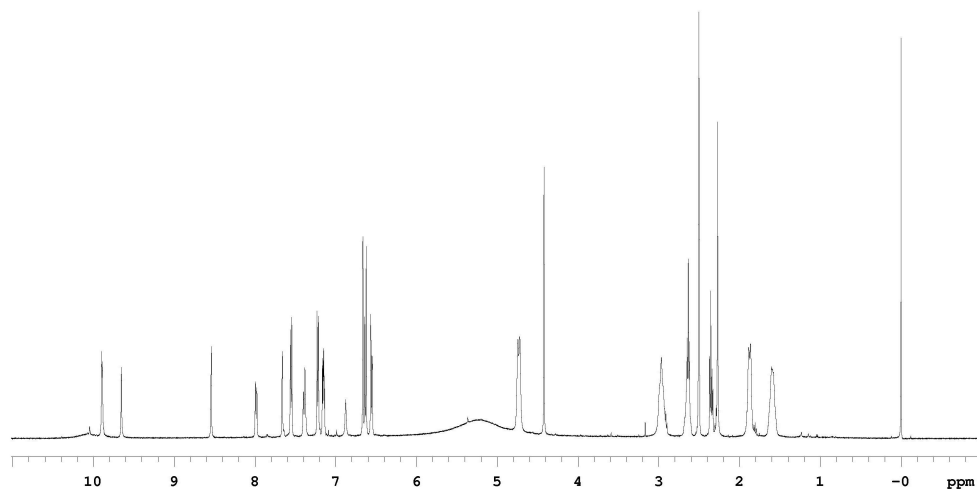
**COSY NMR of 85cd**

**85ce**

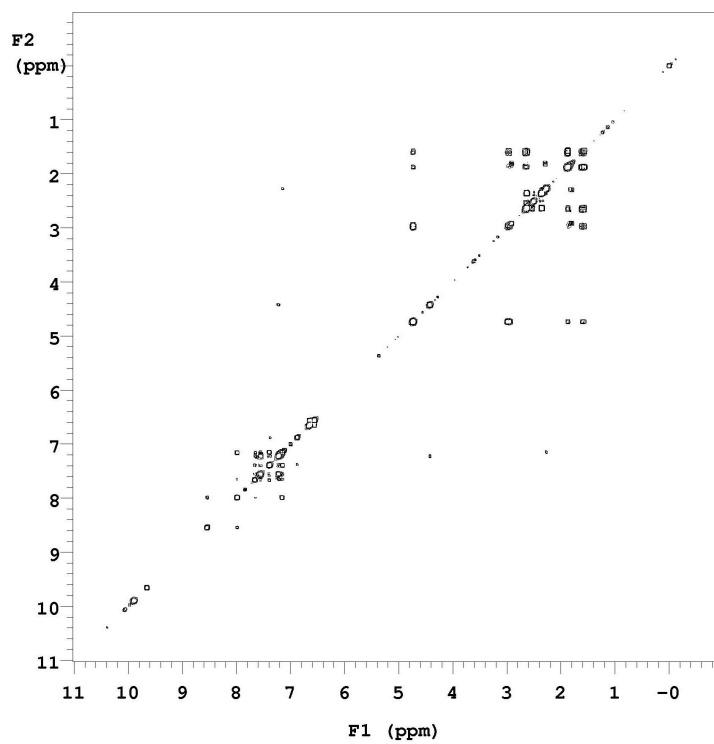
**<sup>1</sup>H NMR (500 MHz, DMSO-d<sub>6</sub>)** δ 9.90 (s, 1H), 9.88 (s, 1H), 9.65 (s, 1H), 8.54 (s, 1H), 7.98 (d, 1H, J = 8.5 Hz), 7.66 (s, 1H), 7.54 (d, 2H, J = 8.5 Hz), 7.40 (s, 1H), 7.38 (s, 1H), 7.22 (d, 2H, J = 8.5 Hz), 7.15 (m, 2H), 6.88 (s, 1H), 6.66 (d, 2H, J = 2.0 Hz), 6.64 (d, 2H, J = 9.0 Hz), 6.56 (dd, 2H, J = 9.0 Hz, 2.0 Hz), 4.74 (d, 4H, J = 11.5 Hz), 4.42 (s, 2H), 2.97 (m, 4H), 2.63 (m, 4H), 2.34 (t, 2H, J = 7.5 Hz), 2.29 (s, 3H), 1.89 (m, 4H), 1.60 (m, 2H)

**LRMS (MALDI)** calc'd for [M+H]<sup>+</sup> 956, found 956

**Analytical HPLC** purity = 94%, retention time = 17.4 min



**$^1\text{H}$  NMR of 85ce**



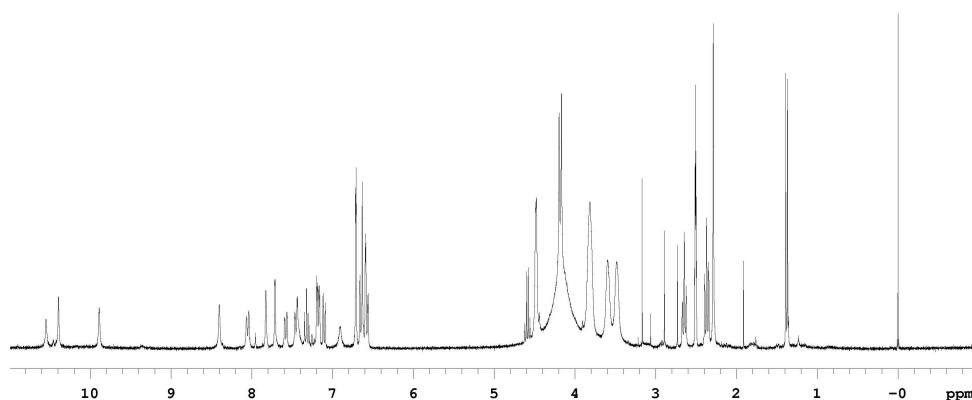
**COSY NMR of 85ce**

**85hl**

**<sup>1</sup>H NMR (300 MHz, DMSO-d<sub>6</sub>)** δ 10.55 (s, 1H), 10.39 (s, 1H), 9.89 (s, 1H), 8.40 (s, 1H), 8.04 (d, 1H, J = 9.0 Hz), 7.83 (s, 1H), 7.71 (d, 1H, J = 1.8 Hz), 7.59 (d, 1H, J = 8.4 Hz), 7.46 (9dd, 2H, J = 8.4 Hz, 1.8 Hz), 7.32 (t, 1H, J = 7.8 Hz), 7.17 (dd, 2H, J = 8.4 Hz, 3.0 Hz), 7.10 (d, 1H, J = 7.8 Hz), 6.91 (s, 1H), 6.72 (d, 2H, J = 2.4 Hz), 6.64 (d, 2H, J = 9.0 Hz), 6.58 (dd, 2H, J = 9.0 Hz, 2.4 Hz), 4.58 (q, 1H, J = 6.6 Hz), 4.48 (s, 2H), 4.46 (s, 2H), 4.19 (s, 2H), 4.18 (s, 2H), 3.81-3.48 (m, 16H), 2.67 (t, 2H, J = 7.5 Hz), 2.37 (t, 2H, J = 7.5 Hz), 2.29 (s, 3H), 1.39 (d, 3H, J = 6.6 Hz)

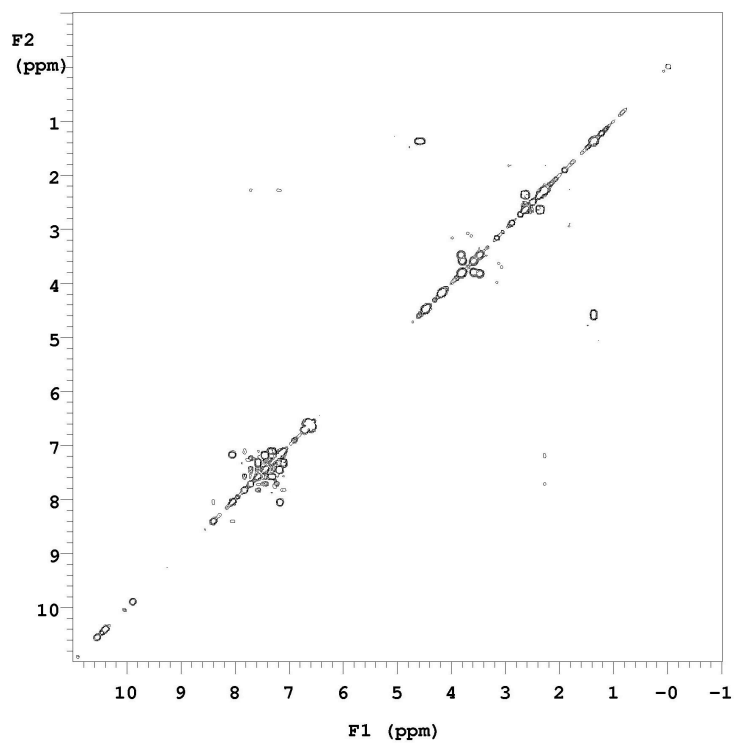
**LRMS (MALDI)** calc'd for [M+H]<sup>+</sup> 1154, found 1154

**Analytical HPLC** purity = 89%, retention time = 18.2 min



**<sup>1</sup>H NMR of 85hl**



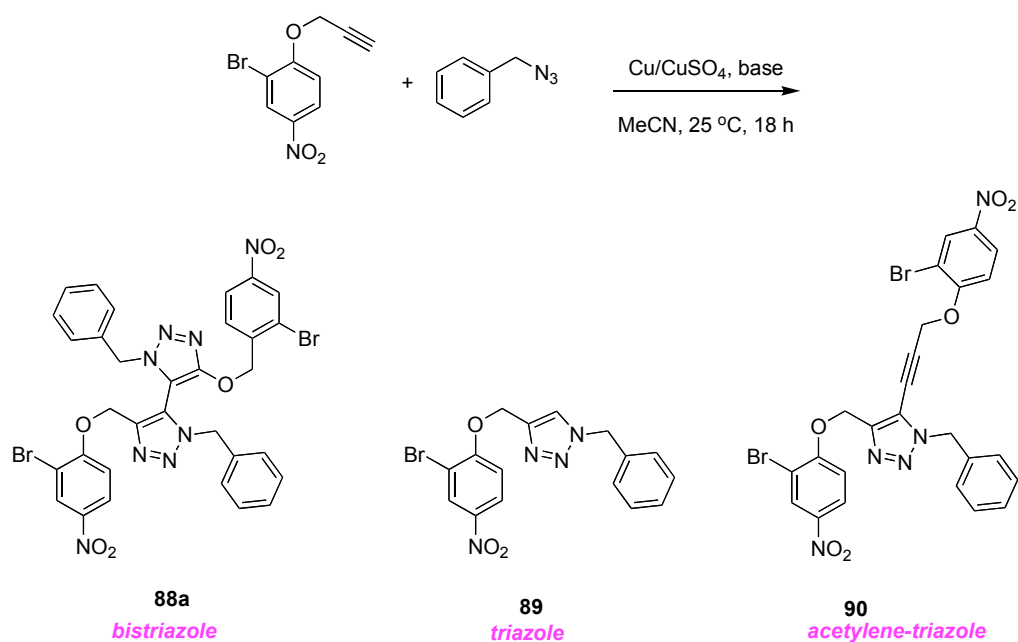


**COSY NMR of 85hl (300 MHz)**

## APPENDIX D

## EXPERIMENTAL ON CHAPTER V

**General Methods.** All chemicals were obtained from commercial suppliers and used without further purification. Analytical HPLC analyses were carried out on 25 x 0.46 cm C-18 column using gradient conditions (50 – 95% B). The eluents used were: solvent A (H<sub>2</sub>O with 0.1% TFA) and solvent B (CH<sub>3</sub>CN with 0.1% TFA). The flow rate used was 1.0 ml/min. NMR spectra were recorded at 500 MHz if otherwise indicated. NMR chemical shifts were expressed in ppm relative to internal solvent peaks, and coupling constants were measured in Hz.

**Optimization of Bistriazole Formation.**

**a. Base Screening.** The alkyne (1.0 mmol, 1.0 equiv) was added to a mixture of azide (1.0 equiv) in acetonitrile (1.5 ml) and base solution (1.5 ml). Copper sulfate (1.0 M, 0.1 ml) was added to the above suspension followed by copper powder (64.0 mg, 1.0 equiv). The resulting suspension was stirred at 25 °C for 18 h and 10  $\mu$ l of the solution was taken and dissolved in 1.0 ml of methanol. Analytical HPLC (sedex) data with different bases is shown in Table D1.

**Table D1.** Product distribution with different bases.

entry	base	concentration (mol/l)	product distribution		
			<b>88a</b> (%)	<b>89</b> (%)	<b>90</b> (%)
1	NaHCO <sub>3</sub>	0.2	0	100	0
2	NaHCO <sub>3</sub>	1.5	12	88	0
3	K <sub>2</sub> CO <sub>3</sub>	0.5	92	3	4
4	K <sub>2</sub> CO <sub>3</sub>	1.0	95	2	3
5	K <sub>2</sub> CO <sub>3</sub>	1.5	95	2	3
6	K <sub>2</sub> CO <sub>3</sub>	2.0	93	3	4
7	K <sub>2</sub> CO <sub>3</sub>	3.0	86	5	7
8	K <sub>2</sub> CO <sub>3</sub>	4.0	84	2	13
9	K <sub>2</sub> CO <sub>3</sub>	5.0	60	11	28
10	Li <sub>2</sub> CO <sub>3</sub>	Sat.	42	58	0
11	Na <sub>2</sub> CO <sub>3</sub>	2.0	95	3	2
12	Cs <sub>2</sub> CO <sub>3</sub>	4.0	85	1	13
13	(NH <sub>4</sub> ) <sub>2</sub> CO <sub>3</sub>	2.0	0	100	0
14	LiOH	1.5	33	57	10
15	KOH	5.0	50	0	50
16	K <sub>3</sub> PO <sub>4</sub>	4.0	56	38	6

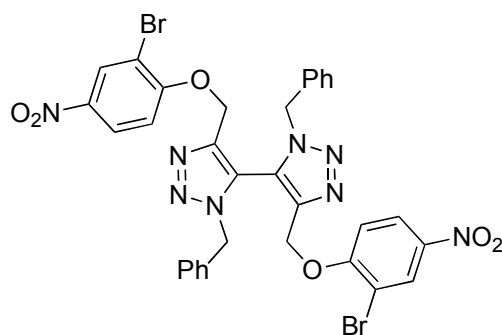
**b. Atmosphere Effect.** The alkyne (1.0 mmol, 1.0 equiv) was added to a mixture of azide (1.0 equiv) in acetonitrile (1.5 ml) and base solution or water (1.5 ml). Copper sulfate (1.0 M, 0.1 ml) was added to the above suspension followed by copper powder (64.0 mg, 0.1 equiv). The resulting suspension was stirred at 25 °C for 18 h and 10  $\mu$ l of the solution was taken and dissolved in 1.0 ml of methanol. Analytical HPLC (sedex) data is showed in Table S2.

**Table D2.** Product distribution under different atmosphere.

entry	base	atmosphere	product distribution		
			<b>88a</b>	<b>89</b>	<b>90</b>
1	1.5 M K <sub>2</sub> CO <sub>3</sub>	air	95	2	3
2	1.5 M K <sub>2</sub> CO <sub>3</sub>	N <sub>2</sub>	17	82	1
3	no base	air	3	97	0
4	no base	N <sub>2</sub>	0	100	0
5*	no base	O <sub>2</sub>	0	100	0

\* Large amount of starting material was left and only small amount of **89** was formed

**General Preparation For Syntheses of Compound 88a-k.** The alkyne (1.0 mmol, 1.0 equiv) was added to a mixture of azide (1.0 equiv) in acetonitrile (1.5 ml) and aqueous Na<sub>2</sub>CO<sub>3</sub> solution (2.0 M, 1.5 ml). Copper sulfate (1.0 M, 0.1 ml) was added to the above suspension followed by copper powder (64.0 mg, 1.0 equiv). The resulting suspension was stirred at 25 °C for 18 h and passed through a pad of Celite. The filtrate was extracted with ethyl acetate and brine and the organic layer was dried and concentrated. Flash chromatography afforded the bistriazole product **88a-k**.



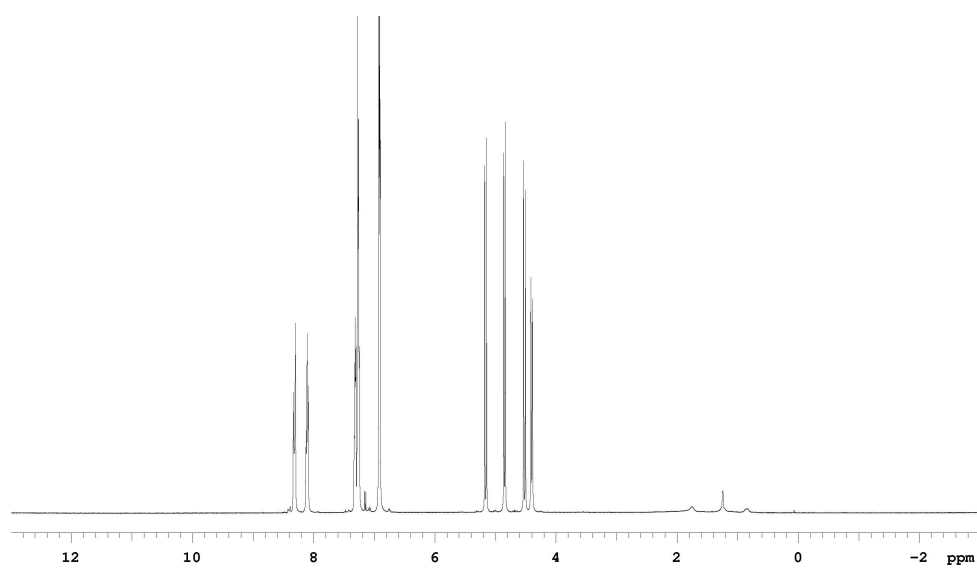
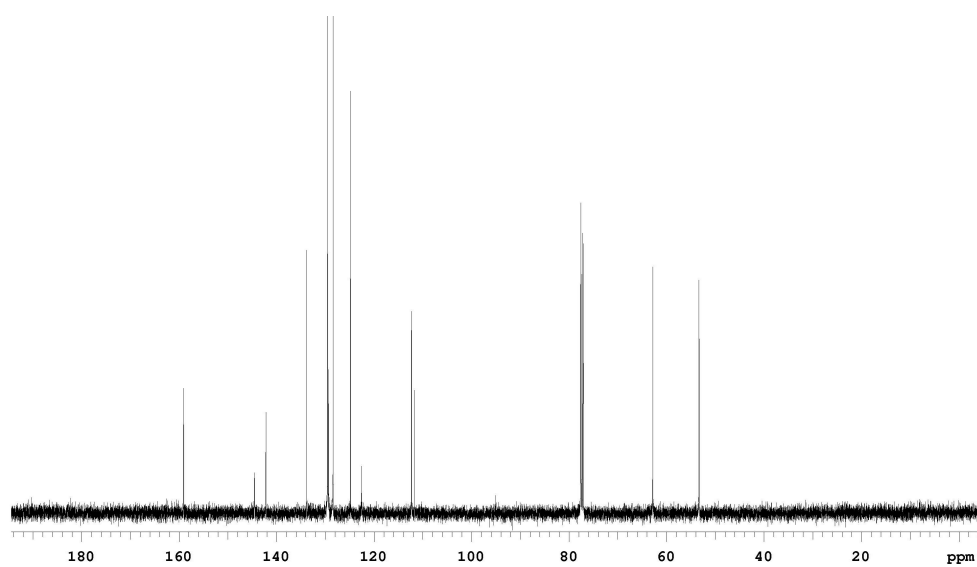
**88a**

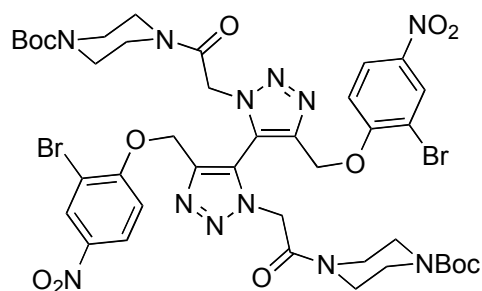
Bistriazole **88a** was prepared from benzyl azide and 2-bromo-4-nitro-1-(prop-2-ynyloxy)benzene. Flash chromatography (hexane/EtOAc = 3:2) afforded **88a** as a white solid (0.35 g, 87 %).

<sup>1</sup>H NMR (CDCl<sub>3</sub>) δ 8.32 (m, 2H), 8.11 (m, 2H), 7.32 (m, 2H), 7.26 (m, 4H), 6.92 (m, 6H), 5.16 (d, 2H, J = 15.0 Hz), 4.85 (d, 2H, J = 12.0 Hz), 4.52 (d, 2H, J = 15.0 Hz), 4.40 (d, 2H, J = 12.0 Hz)

<sup>13</sup>C NMR (CDCl<sub>3</sub>) δ 159.1, 144.5, 142.2, 133.8, 129.5, 129.33, 129.28, 128.4, 124.9, 122.5, 112.3, 111.7, 62.8, 53.3

MS (ESI, m/z): (M+H)<sup>+</sup> calcd for C<sub>32</sub>H<sub>25</sub>Br<sub>2</sub>N<sub>8</sub>O<sub>6</sub> 777.0243, found 777.2166

 **$^1\text{H}$  NMR of 88a** **$^{13}\text{C}$  NMR of 88a**

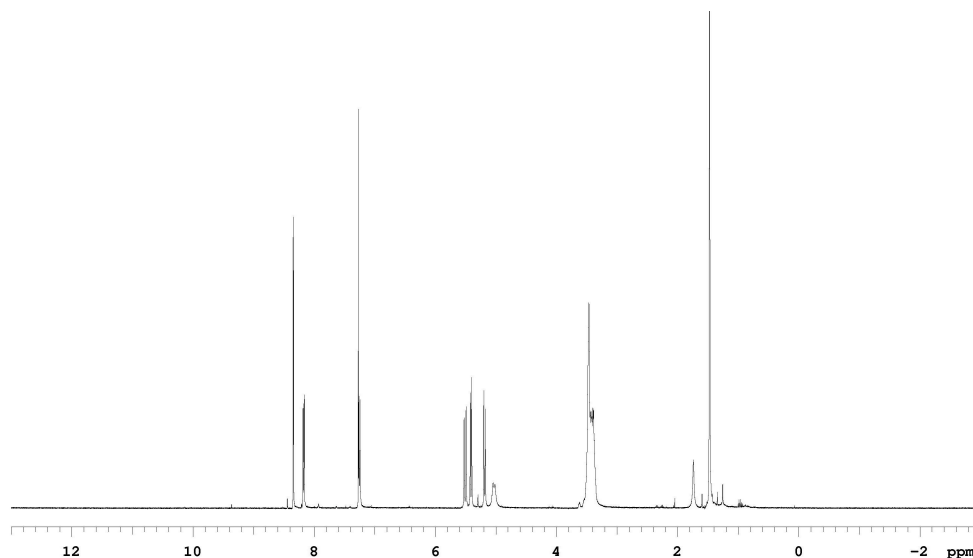
**88b**

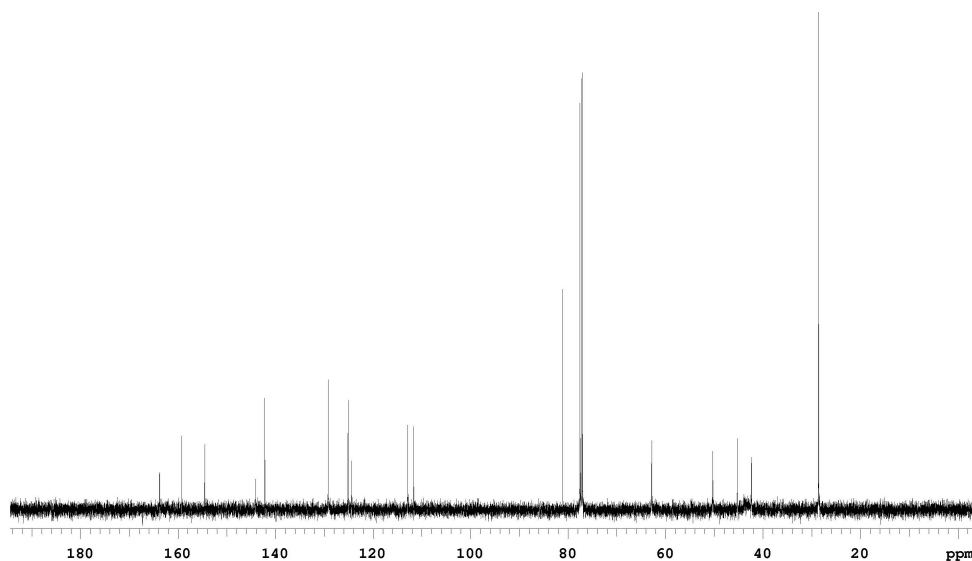
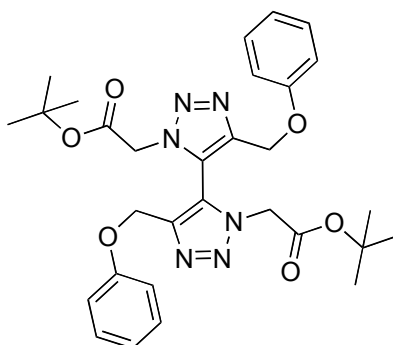
Bistriazole **88b** was prepared from tert-butyl 4-(2-azidoacetyl)piperazine-1-carboxylate and 2-bromo-4-nitro-1-(prop-2-ynyloxy)benzene. Flash chromatography (hexane/EtOAc = 3:2) afforded **88b** as a white solid (0.37 g, 72 %).

$^1\text{H NMR}$  ( $\text{CDCl}_3$ )  $\delta$  8.34 (d, 2H,  $J = 3.0$  Hz), 7.25 (d, 2H,  $J = 9.5$  Hz), 5.51 (d, 2H,  $J = 15.0$  Hz), 5.41 (d, 2H,  $J = 12.0$  Hz), 5.19 (d, 2H,  $J = 12.0$  Hz), 5.03 (d, 2H,  $J = 15.0$  Hz), 3.46-3.39 (m, 16H), 1.47 (s, 18H)

$^{13}\text{C NMR}$  ( $\text{CDCl}_3$ )  $\delta$  163.8, 159.3, 154.5, 144.2, 142.2, 129.2, 125.1, 124.5, 112.9, 111.6, 81.0, 62.8, 50.3, 45.3, 42.4, 28.6

**MS (MALDI,  $m/z$ ):** ( $M+\text{Na}$ ) $^+$  calcd for  $\text{C}_{40}\text{H}_{48}\text{Br}_2\text{N}_{12}\text{NaO}_{12}$  1071.1759, found 1070.8820

 $^1\text{H NMR}$  of **88b**

 $^{13}\text{C}$  NMR of **88b****88c**

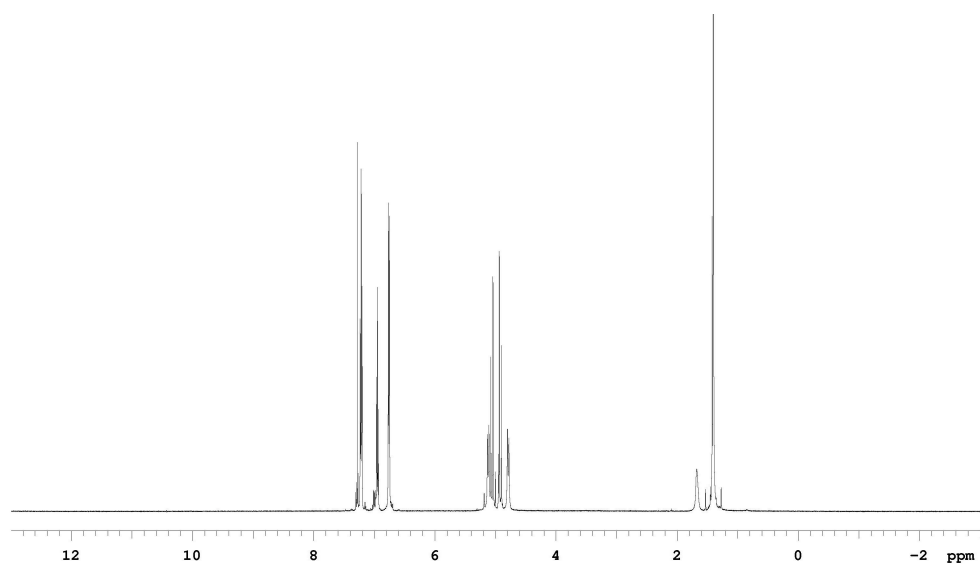
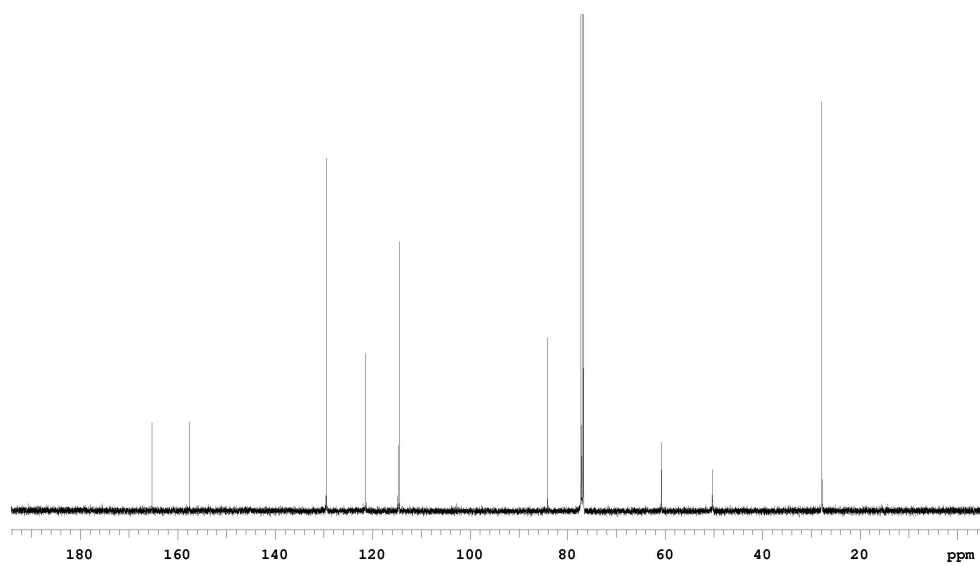
Bistriazole **88c** was prepared from tert-butyl 2-azidoacetate and (prop-2-ynyloxy)benzene. Flash chromatography (hexane/EtOAc = 9:1) afforded **88c** as a clear oil (0.13 g, 47 %).

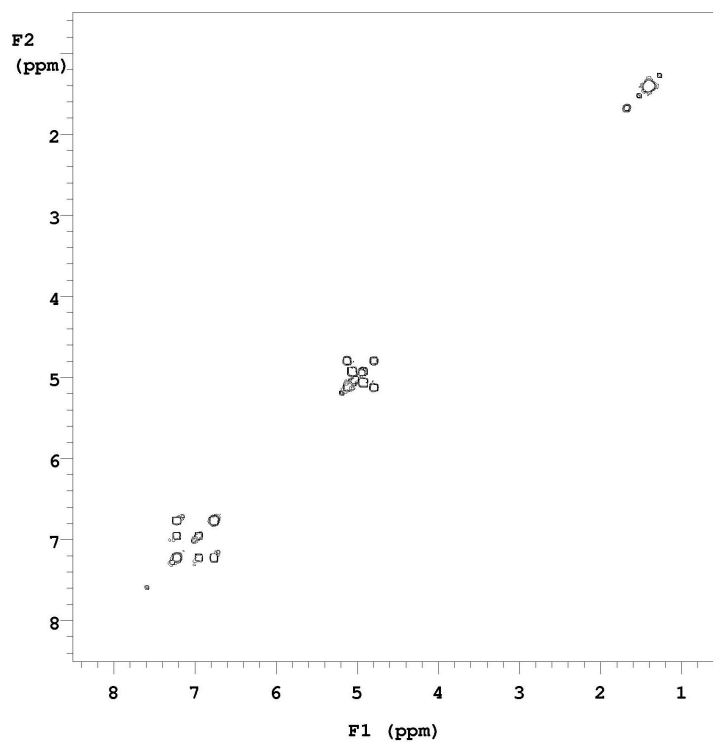
$^1\text{H}$  NMR ( $\text{CDCl}_3$ )  $\delta$  7.22 (t, 4H,  $J = 8.0$  Hz), 6.94 (t, 2H,  $J = 7.5$  Hz), 6.75 (d, 4H,  $J = 8.0$  Hz), 5.12 (d, 2H,  $J = 12.0$  Hz), 5.05 (d, 2H,  $J = 17.5$  Hz), 4.92 (d, 2H,  $J = 17.5$  Hz), 4.78 (d, 2H,  $J = 12.0$  Hz), 1.40 (s, 18H)

$^{13}\text{C}$  NMR ( $\text{CDCl}_3$ )  $\delta$  165.3, 157.5, 129.5, 121.5, 114.6, 84.1, 60.8, 50.3, 27.8 (two C not observed as distinct peaks)

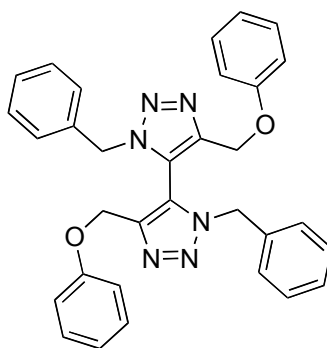
MS (ESI,  $m/z$ ): ( $\text{M}+\text{H}$ ) $^+$  calcd for  $\text{C}_{30}\text{H}_{37}\text{N}_6\text{O}_6$  577.2775, found 577.2754



 $^1\text{H}$  NMR of 88c $^{13}\text{C}$  NMR of 88c



**gCOSY of 88c**



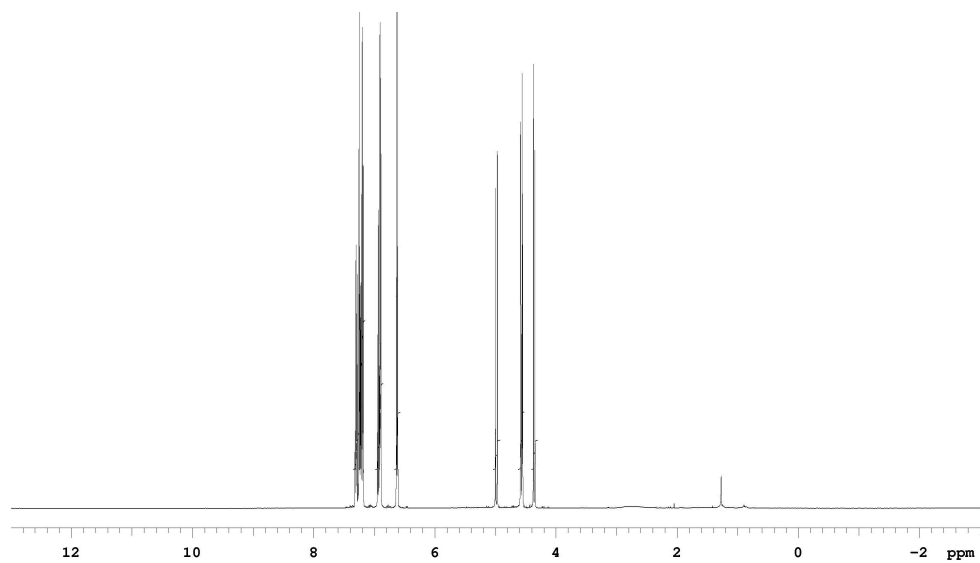
**88d**

Bistriazole **88d** was prepared from benzyl azide and phenyl propargyl ether. Flash chromatography (hexane/EtOAc = 9:1) afforded **88d** as a white solid (0.18 g, 69 %).

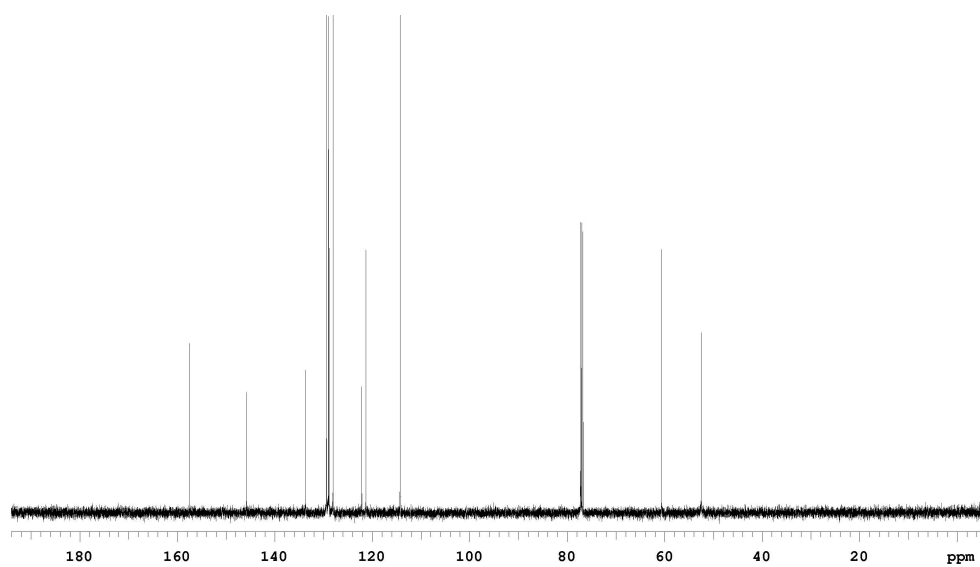
$^1\text{H NMR}$  ( $\text{CDCl}_3$ )  $\delta$  7.32-7.18 (m, 10H), 6.95-6.70 (m, 6H), 6.64-6.62 (m, 4H), 4.98 (d, 2H,  $J = 14.5$  Hz), 4.58-4.55 (m, 4H), 4.35 (d, 2H,  $J = 12.5$  Hz)

$^{13}\text{C}$  NMR ( $\text{CDCl}_3$ )  $\delta$  157.4, 145.8, 133.7, 129.4, 129.0, 128.8, 128.0, 122.1, 121.3, 114.3, 60.7, 52.5

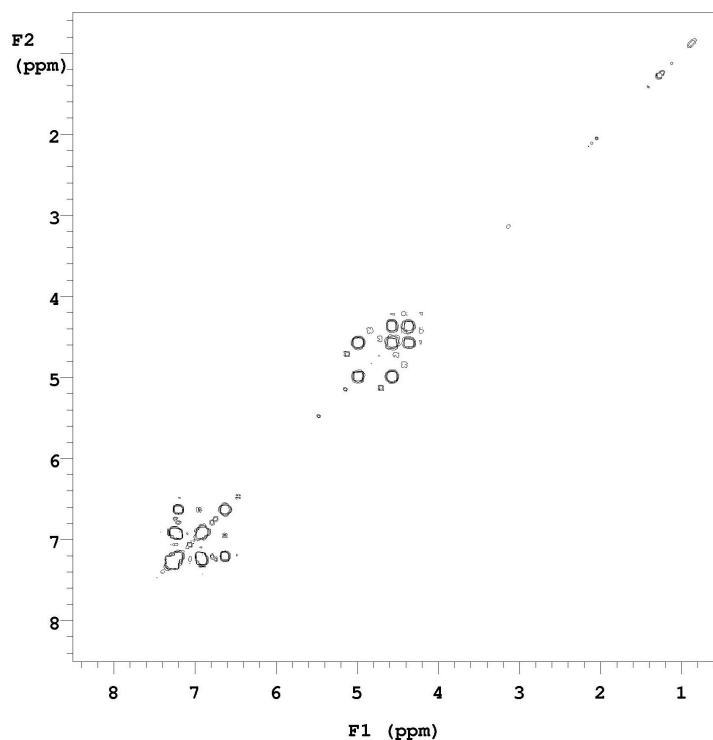
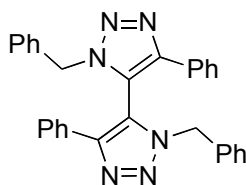
MS (ESI,  $m/z$ ):  $(\text{M}+\text{H})^+$  calcd for  $\text{C}_{32}\text{H}_{29}\text{N}_6\text{O}_2$  529.2352, found 529.2317.



$^1\text{H}$  NMR of 88d



$^{13}\text{C}$  NMR of 88d

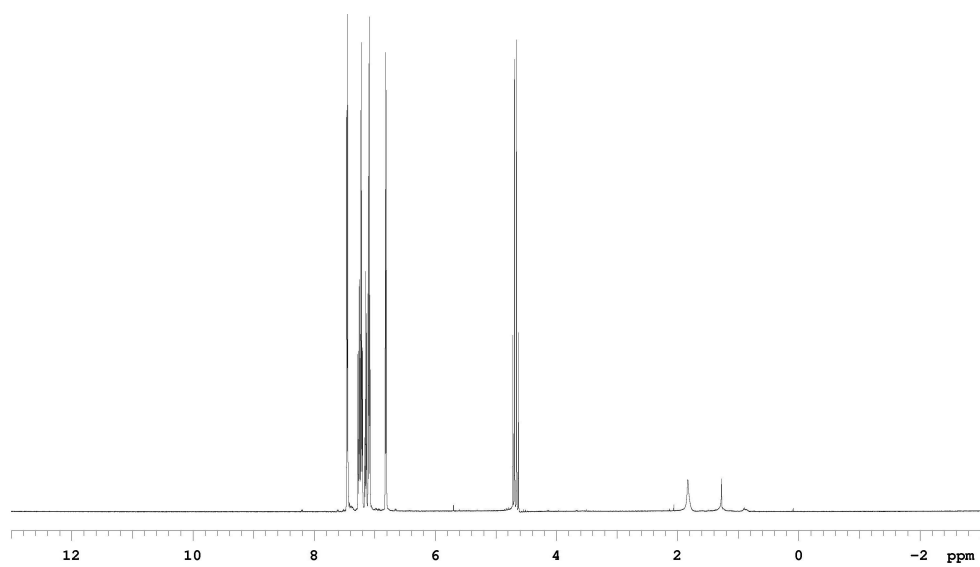
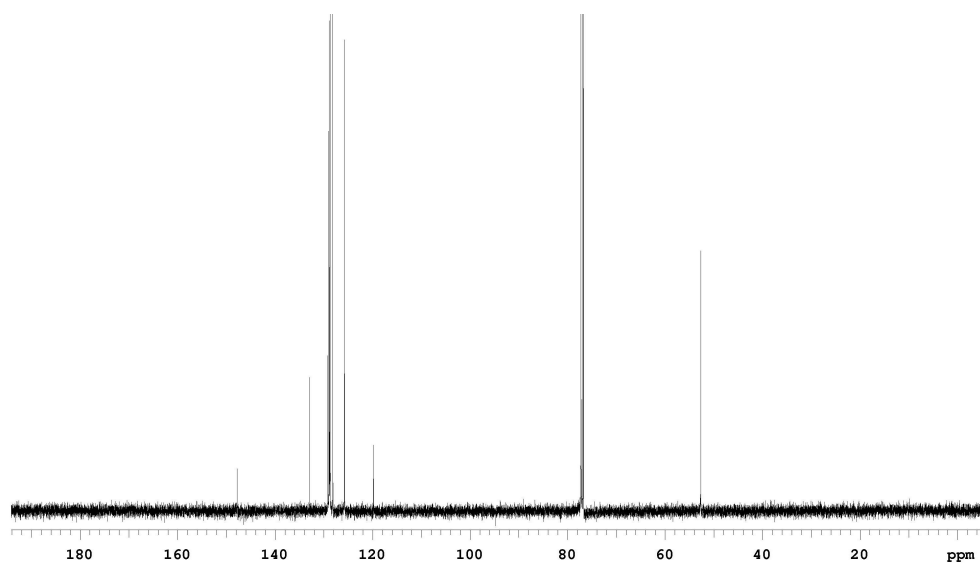
gCOSY of **88d****88e**

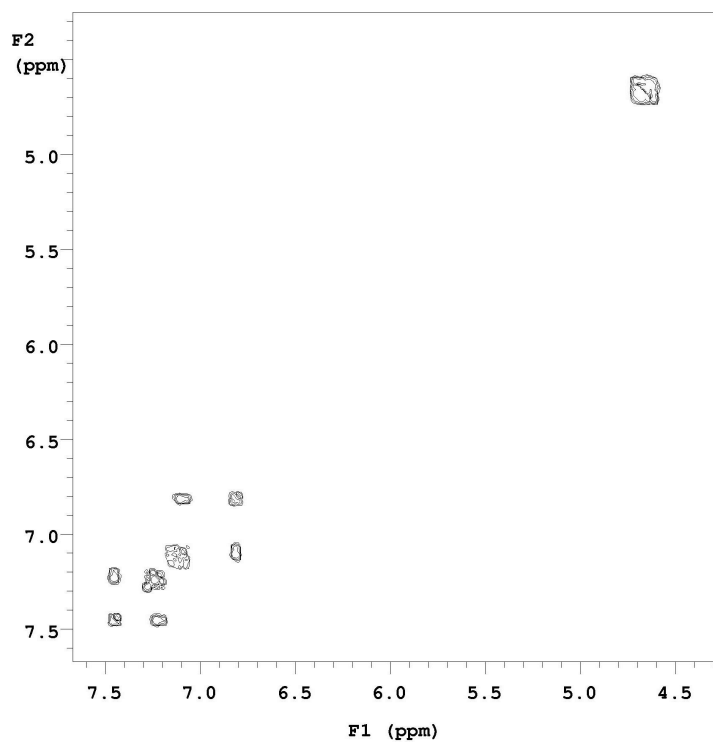
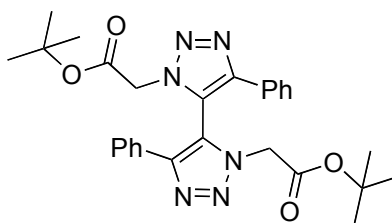
Bistriazole **88e** was prepared from benzyl azide and phenyl acetylene. Flash chromatography (hexane/EtOAc = 4:1) afforded **88e** as a white solid (0.08 g, 37 %).

$^1\text{H NMR}$  ( $\text{CDCl}_3$ )  $\delta$  7.45 (m, 4H), 7.28-7.20 (m, 6H), 7.14 (m, 2H), 7.09 (m, 4H), 6.81 (d, 4H,  $J = 8.0$  Hz), 4.70 (d, 2H,  $J = 14.5$  Hz), 4.64 (d, 2H,  $J = 14.5$  Hz)

$^{13}\text{C NMR}$  ( $\text{CDCl}_3$ )  $\delta$  147.8, 132.9, 129.2, 128.9, 128.8, 128.74, 128.68, 128.1, 125.8, 119.8, 52.6

$\text{MS (ESI, m/z)}$ :  $(\text{M}+\text{H})^+$  calcd for  $\text{C}_{30}\text{H}_{25}\text{N}_6$  469.2141, found 469.1979

 **$^1\text{H}$  NMR of 88e** **$^{13}\text{C}$  NMR of 88e**

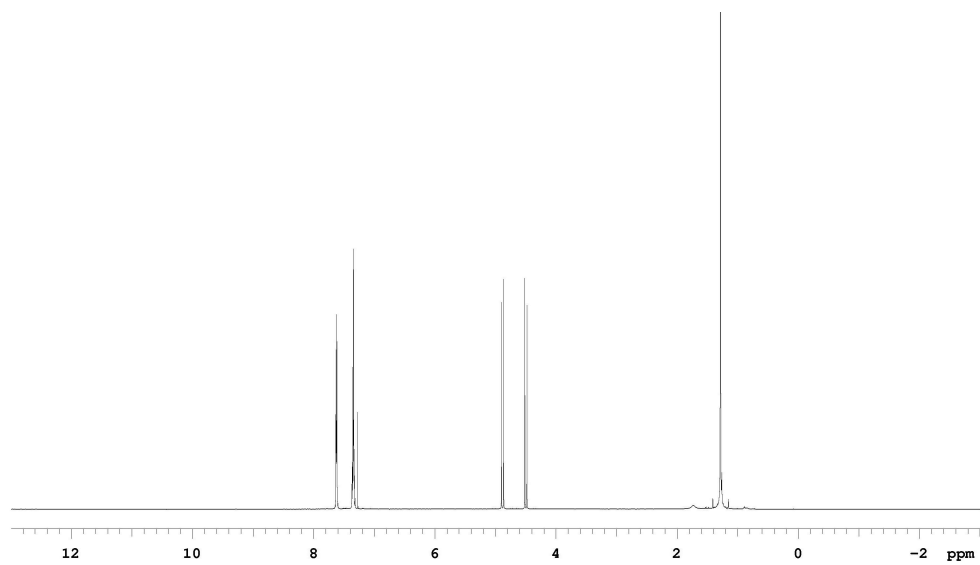
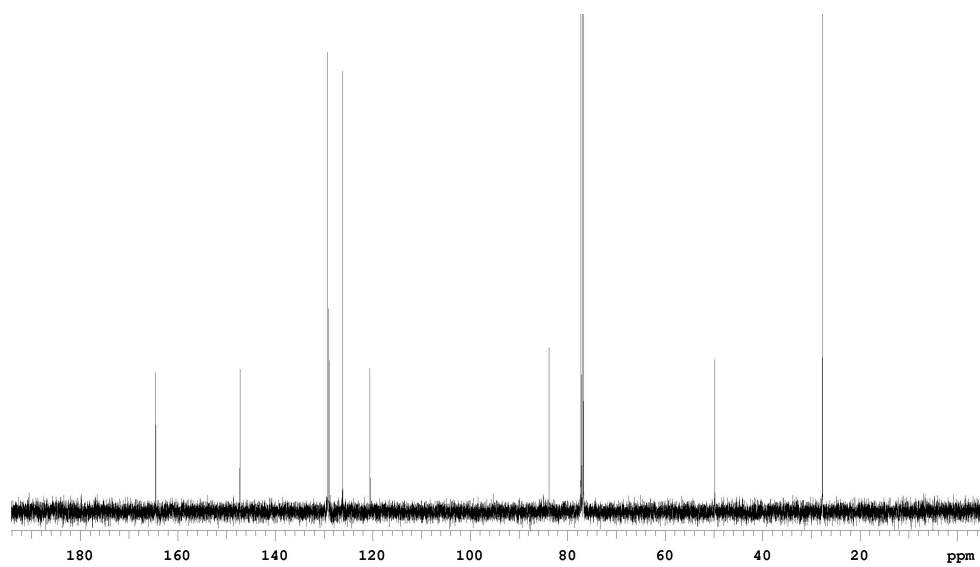
gCOSY of **88e****88f**

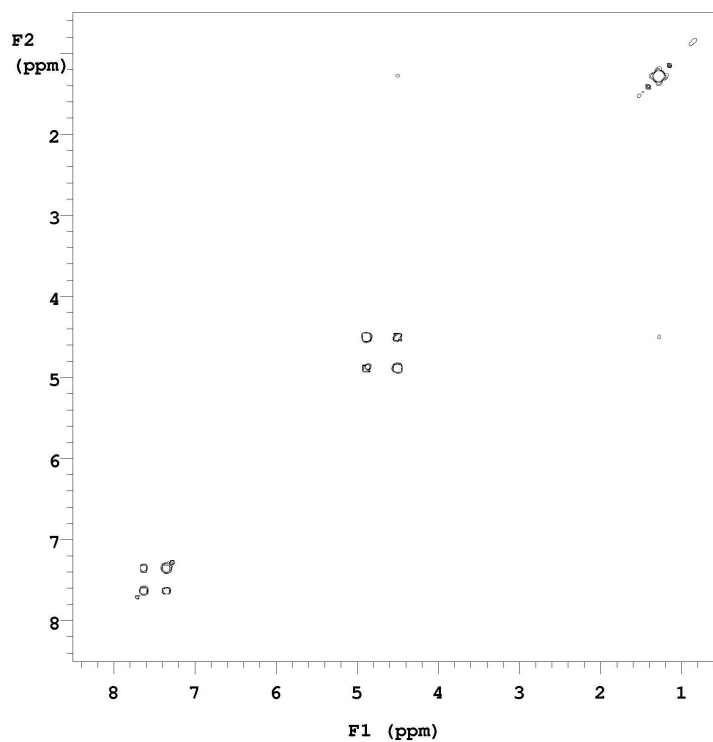
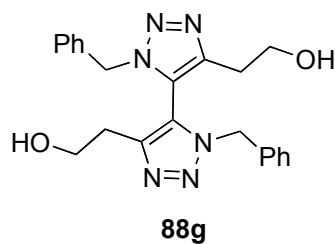
Bistriazole **88f** was prepared from tert-butyl 2-azidoacetate and phenyl acetylene. Flash chromatography (hexane/EtOAc = 9:1) afforded **88f** as a clear oil (0.06 g, 23 %).

$^1\text{H NMR}$  ( $\text{CDCl}_3$ )  $\delta$  7.63-7.61 (m, 4H), 7.37-7.33 (m, 6H), 4.87 (d, 2H,  $J = 18.0$  Hz), 4.50 (d, 2H,  $J = 18.0$  Hz), 1.28 (s, 18H)

$^{13}\text{C NMR}$  ( $\text{CDCl}_3$ )  $\delta$  164.5, 147.2, 129.2, 129.1, 128.8, 126.1, 120.5, 83.8, 49.8, 27.7;

$\text{MS}$  (ESI,  $m/z$ ):  $(\text{M}+\text{H})^+$  calcd for  $\text{C}_{28}\text{H}_{33}\text{N}_6\text{O}_4$  517.2563, found 517.2067

 $^1\text{H}$  NMR of 88f $^{13}\text{C}$  NMR of 88f

gCOSY of **88f**

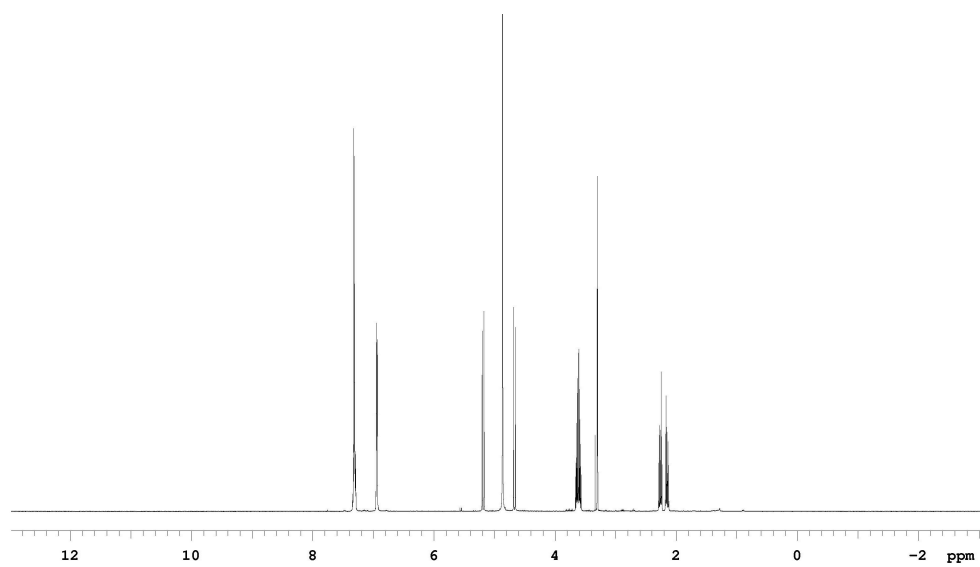
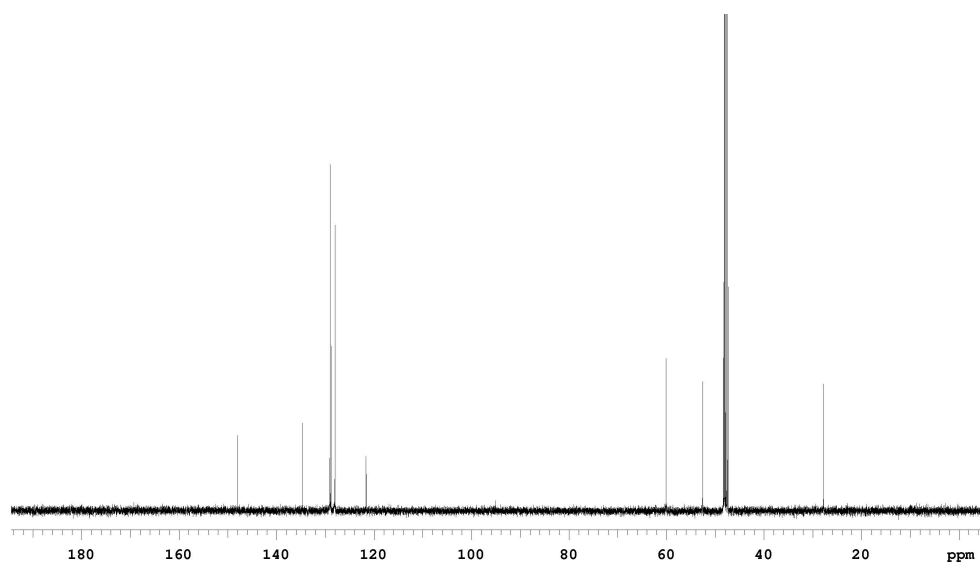
Bistriazole **88g** was prepared from benzyl azide and 1-butynol. Flash chromatography ( $\text{CH}_2\text{Cl}_2/\text{MeOH} = 19:1$ ) afforded **88g** as a white solid (0.08 g, 34 %).

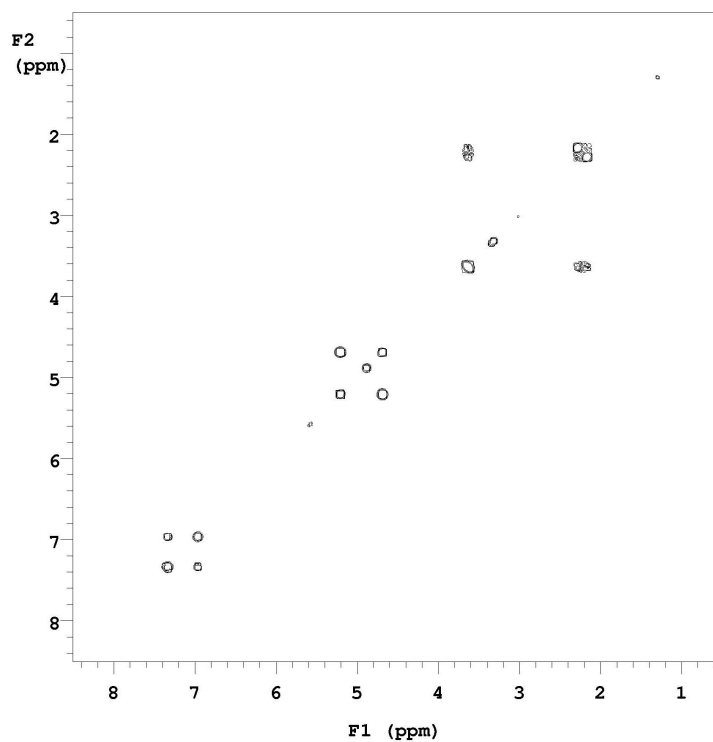
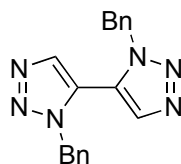
$^1\text{H NMR}$  ( $\text{CD}_3\text{OD}$ )  $\delta$  7.50 (s, 2H), 7.35-7.29 (m, 6H), 6.96-6.92 (m, 4H), 5.18 (d, 2H,  $J = 15.0$  Hz), 4.87 (d, 2H,  $J = 15.0$  Hz), 3.62 (m, 4H), 2.28 (t, 1H,  $J = 6.5$  Hz), 2.25 (t, 1H,  $J = 6.5$  Hz), 2.17 (t, 1H,  $J = 6.5$  Hz), 2.14 (t, 1H,  $J = 6.5$  Hz)

$^{13}\text{C NMR}$  ( $\text{CDCl}_3$ )  $\delta$  148.0, 134.6, 129.0, 128.8, 128.0, 121.6, 60.1, 52.5, 27.8

$\text{MS}$  (APCI,  $m/z$ ) 405 ( $\text{M}+\text{H}$ ) $^+$



 **$^1\text{H}$  NMR of 88g** **$^{13}\text{C}$  NMR of 88g**

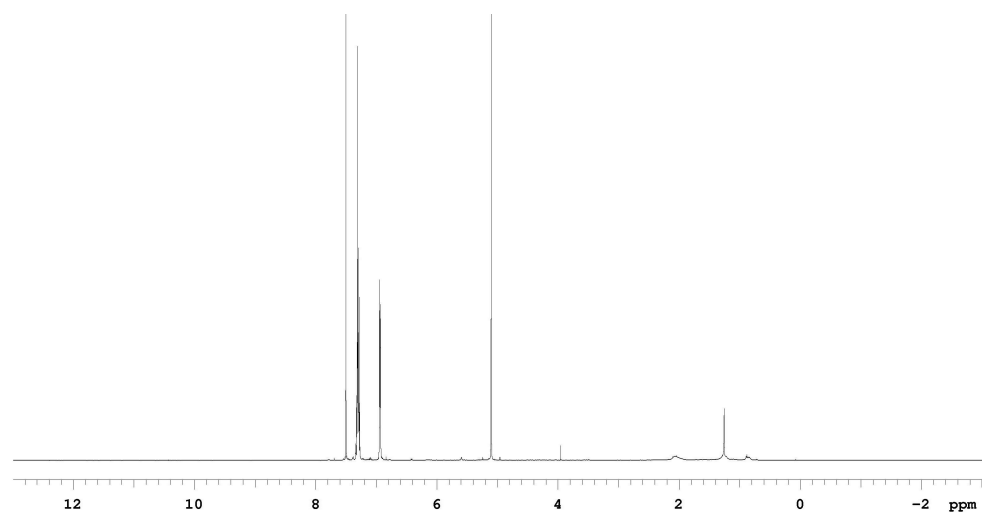
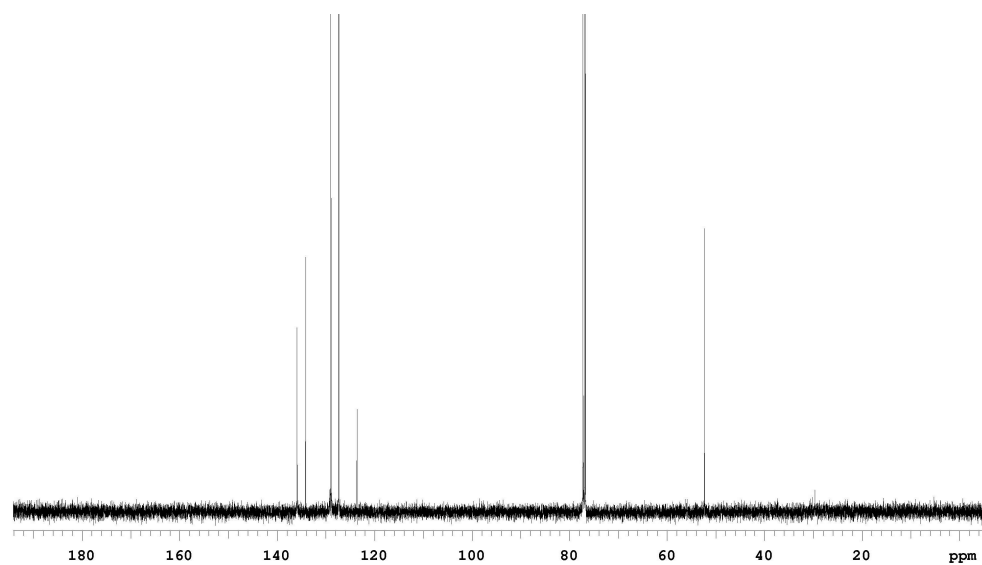
gCOSY of **88g****88h**

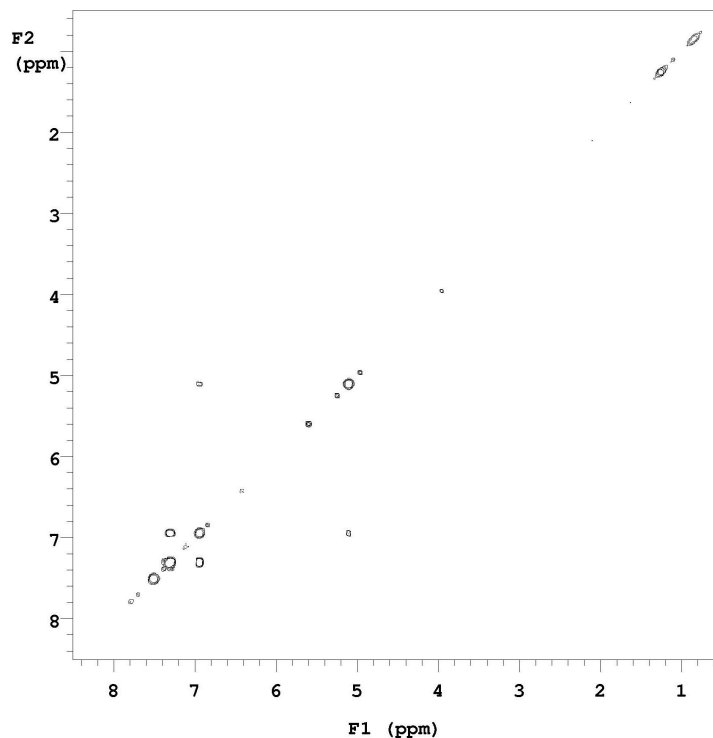
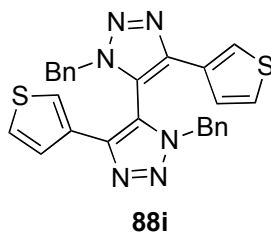
Bistriazole **88h** was prepared from benzyl azide and trimethylsilyl-acetylene. Flash chromatography (hexane/EtOAc = 4:1) afforded **88h** as a white solid (0.06 g, 25 %).

$^1\text{H NMR}$  ( $\text{CDCl}_3$ )  $\delta$  7.50 (s, 2H), 7.31-7.29 (m, 6H), 6.93 (m, 4H), 5.10 (s, 4H)

$^{13}\text{C NMR}$  ( $\text{CDCl}_3$ )  $\delta$  135.9, 134.1, 129.1, 128.8, 127.3, 123.6, 52.3

$\text{MS}$  (APCI,  $m/z$ ):  $(\text{M}+\text{H})^+$  calcd for  $\text{C}_{18}\text{H}_{17}\text{N}_6$  317.1515, found 317.1200

 **$^1\text{H}$  NMR of 88h** **$^{13}\text{C}$  NMR of 88h**

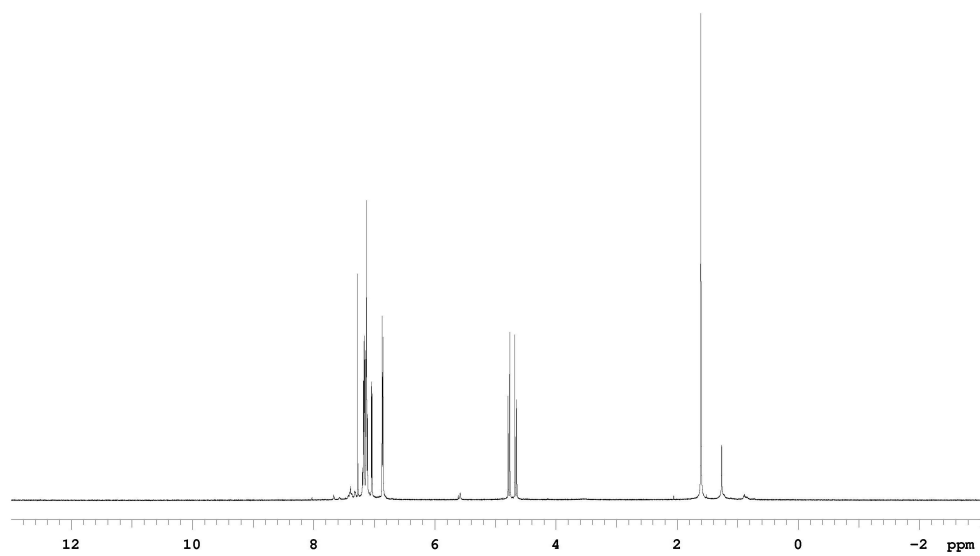
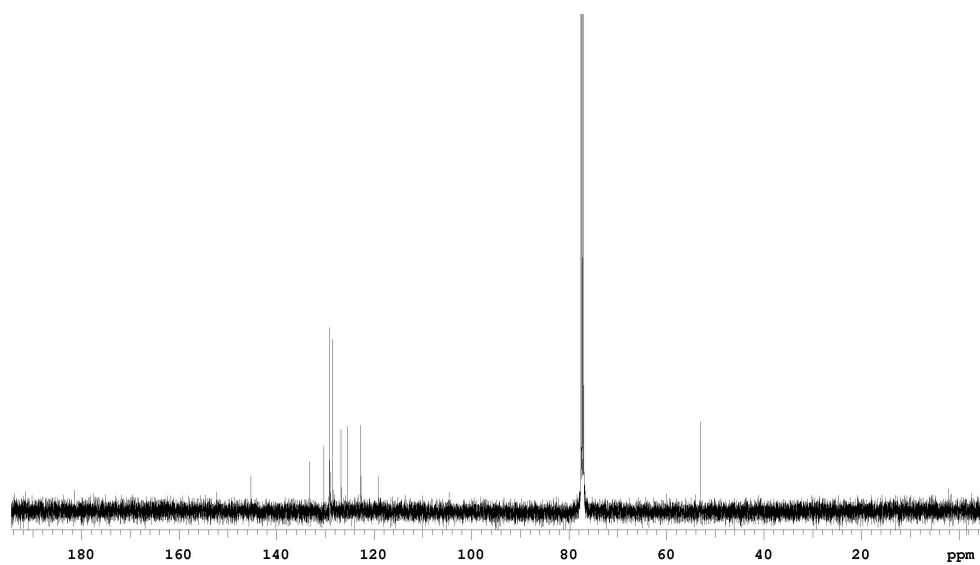
gCOSY of **88h**

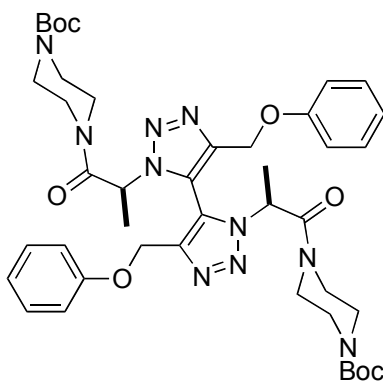
Bistriazole **88i** was prepared from benzyl azide and trimethyl(thiophen-3-ylethynyl)silane. Flash chromatography (hexane/EtOAc = 9:1) afforded **88i** as a white solid (0.09 g, 38 %).

$^1\text{H NMR}$  ( $\text{CDCl}_3$ )  $\delta$  7.19-7.11 (m, 10H), 7.04 (m, 2H), 6.86 (m, 4H), 4.78 (d, 2H,  $J = 15.0$  Hz), 4.65 (d, 2H,  $J = 15.0$  Hz)

$^{13}\text{C NMR}$  ( $\text{CDCl}_3$ )  $\delta$  145.2, 133.2, 130.3, 129.10, 129.05, 128.5, 126.8, 125.5, 122.7, 119.2, 53.1

$\text{MS (ESI, m/z)}$ :  $(\text{M}+\text{H})^+$  calcd for  $\text{C}_{26}\text{H}_{21}\text{N}_6\text{S}_2$  481.1269, found 481.1297

 $^1\text{H}$  NMR of 88i $^{13}\text{C}$  NMR of 88i

**88j**

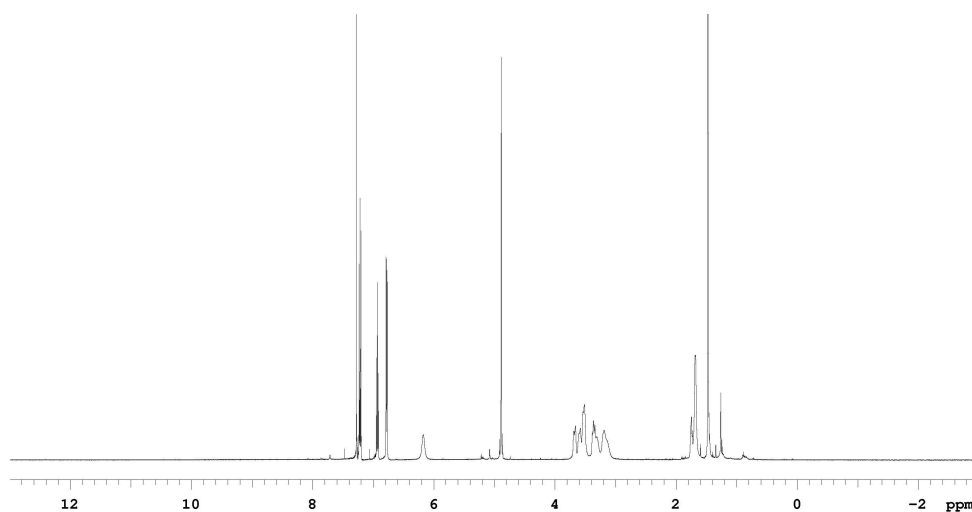
With the same condition that prepared the above compounds, (*S*)-*tert*-butyl 4-(2-azidopropanoyl)piperazine-1-carboxylate (1.0 mmol) and phenyl propargyl ether (1.0 mmol) gave two diastereomers in a ratio of 3:2 as measured by HPLC analysis of the crude product mixture.

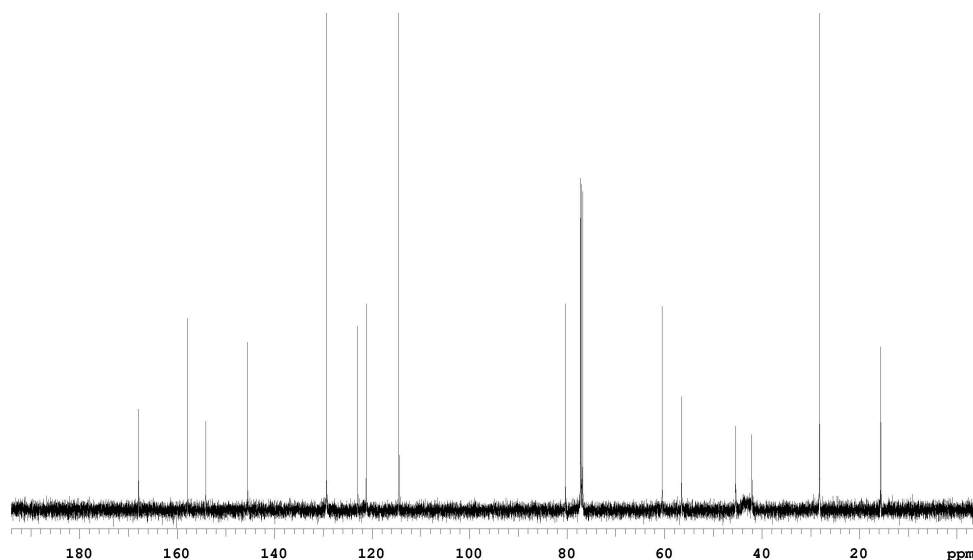
Flash chromatography (hexane/EtOAc = 1:1) afforded bis-triazole **88j** (major diastereomer) as a colorless oil (0.18 g, 42%).  $[\alpha]_D^{25} = +41.1$  ( $c = 1.0$ ,  $\text{CH}_2\text{Cl}_2$ ).

$^1\text{H NMR}$  ( $\text{CDCl}_3$ )  $\delta$  7.17 (m, 4H), 6.90 (m, 2H), 6.74 (d, 4H,  $J = 8.0$  Hz), 6.16 (bs, 2H), 4.85 (s, 4H), 3.66-3.10 (m, 16H), 1.65 (d, 6H,  $J = 5.5$  Hz), 1.44 (s, 18H)

$^{13}\text{C NMR}$  ( $\text{CDCl}_3$ )  $\delta$  167.8, 157.8, 154.1, 145.5, 129.3, 122.9, 121.2, 114.5, 80.4, 60.5, 56.4, 45.4, 42.1, 28.2, 15.6

**MS (ESI,  $m/z$ ):** ( $M+H$ ) $^+$  calcd for  $\text{C}_{42}\text{H}_{57}\text{N}_{10}\text{O}_8$  829.4361, found 829.4454

 $^1\text{H NMR}$  of **88j**



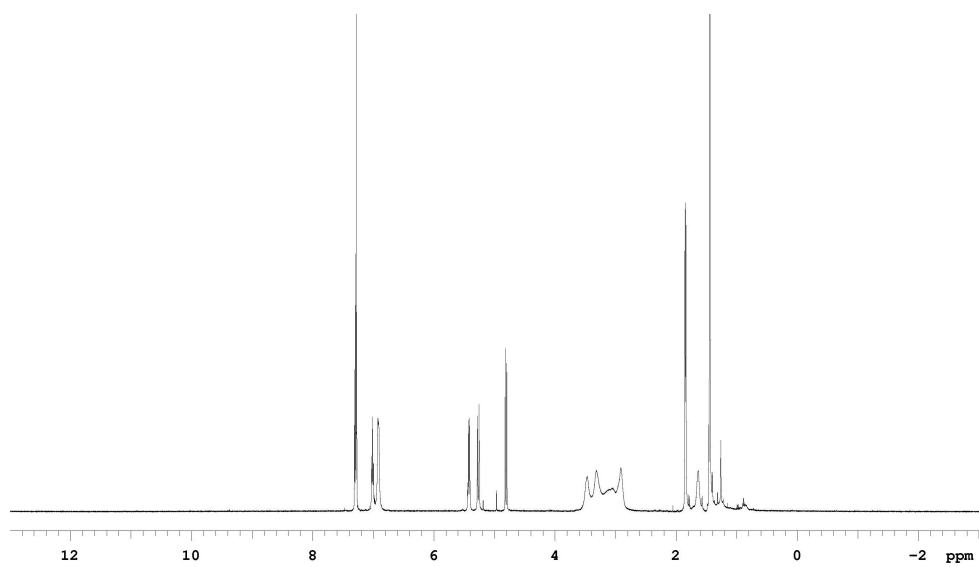
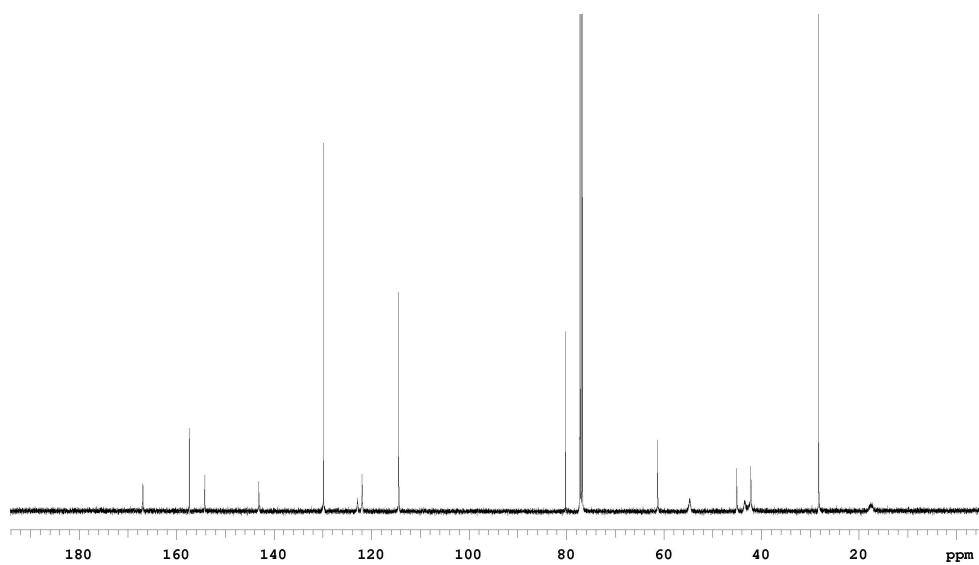
**$^{13}\text{C}$  NMR of **88j****

Flash chromatography (hexane/EtOAc = 1:1) afforded bistriazole **88j'** (minor diastereomer) as a colorless oil (0.06 g, 14%).  $[\alpha]_{\text{D}}^{25} = +76.6$  (c = 1.0,  $\text{CH}_2\text{Cl}_2$ ).

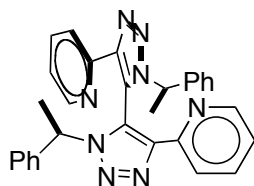
$^1\text{H}$  NMR ( $\text{CDCl}_3$ )  $\delta$  7.30 (m, 4H), 7.01 (m, 2H), 6.92 (m, 4H), 5.41 (q, 2H,  $J = 7.0$  Hz), 5.26 (d, 2H,  $J = 13.0$  Hz), 4.80 (d, 2H,  $J = 13.0$  Hz), 3.47-2.91 (m, 16H), 1.84 (d, 6H,  $J = 7.0$  Hz), 1.45 (s, 18H)

$^{13}\text{C}$  NMR ( $\text{CDCl}_3$ )  $\delta$  166.9, 157.8, 154.1, 143.5, 129.3, 122.9, 121.2, 114.5, 80.4, 60.5, 54.4, 45.4, 42.1, 28.2, 15.6

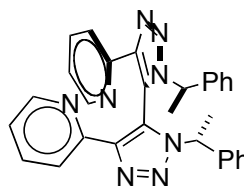
MS (ESI,  $m/z$ ): ( $\text{M}+\text{Na}$ ) $^+$  calcd for  $\text{C}_{42}\text{H}_{56}\text{N}_{10}\text{NaO}_8$  851.4180, found 851.4316

 $^1\text{H}$  NMR of 88j' $^{13}\text{C}$  NMR of 88j'





**88k**  
(major diastereomer  
*R,S,R*)



**88k'**  
(minor diastereomer  
*R,R,R*)

Bistriazoles **88k** and **88k'** were prepared from 2-ethynylpyridine (1.0 mmol) and (R)-(1-azidoethyl)benzene (1.0 mmol).

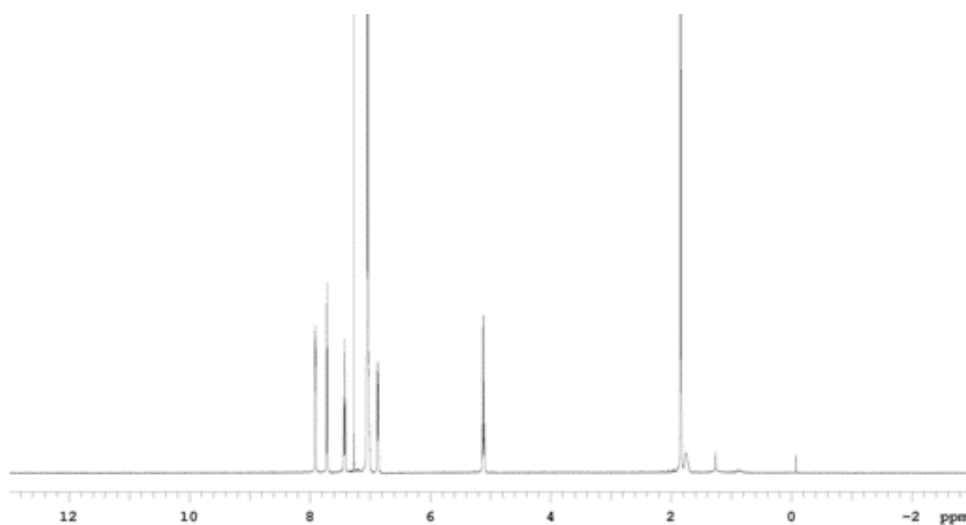
Diastereomeric ratio of **88k** to **88k'** is 2:1 from the  $^1\text{H}$  NMR of the crude material.

Bistriazole **88k** was isolated by column chromatography (40 % ethyl acetate in hexanes) in 8 % yield.

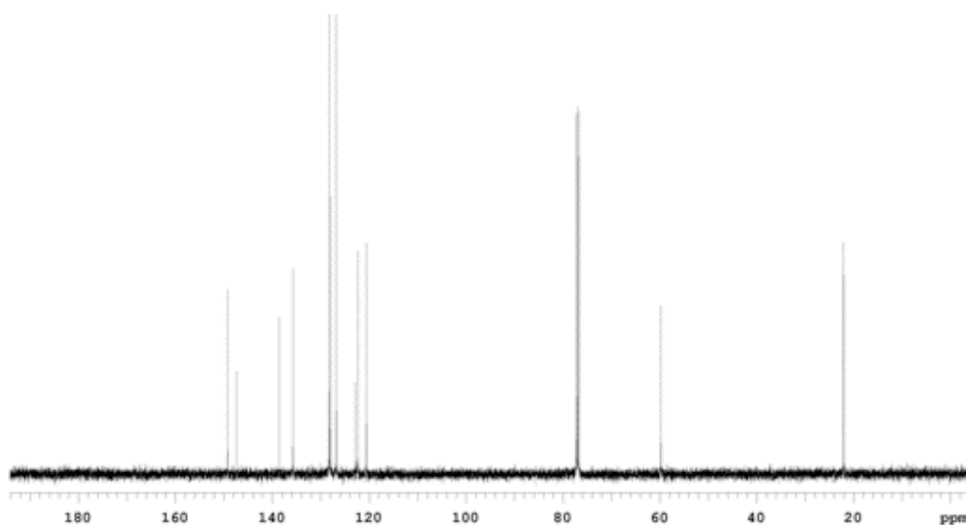
$^1\text{H}$  NMR ( $\text{CDCl}_3$ )  $\delta$  8.38 (d, 2H,  $J = 4.5$  Hz), 8.30 (d, 2H,  $J = 8.0$  Hz), 7.76 (m, 2H), 7.16 (m, 2H), 7.01 (m, 2H), 6.89 (m, 4H), 6.90 (m, 4H), 6.83 (m, 4H), 5.18 (q, 2H,  $J = 7.0$  Hz), 1.83 (d, 6H,  $J = 7.0$  Hz)

$^{13}\text{C}$  NMR ( $\text{CDCl}_3$ )  $\delta$  150.2, 149.4, 145.3, 139.5, 136.6, 128.5, 127.7, 125.9, 123.2, 122.9, 121.2, 59.4, 23.2

MS (ESI,  $m/z$ ): ( $\text{M}+\text{H}$ ) $^+$  calcd for  $\text{C}_{30}\text{H}_{27}\text{N}_8$  499.24, found 499.13



**<sup>1</sup>H NMR of 88k**



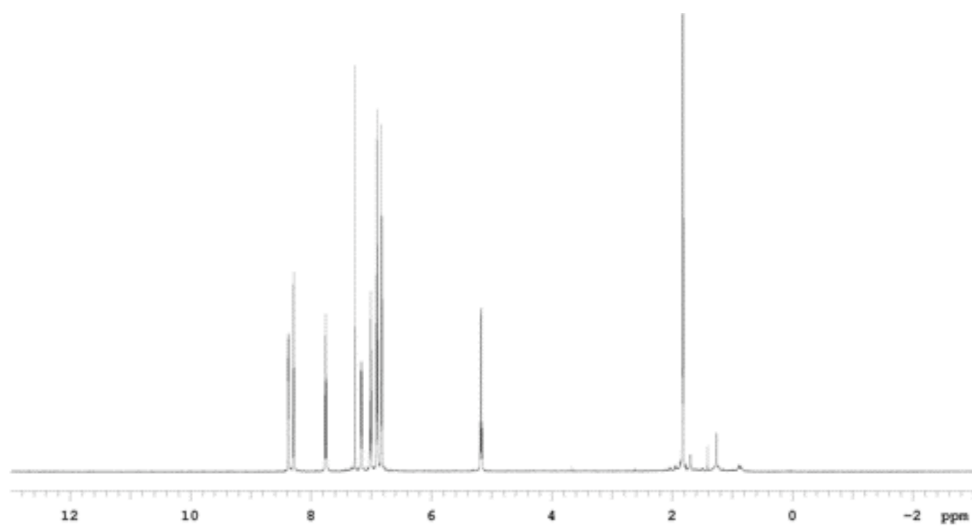
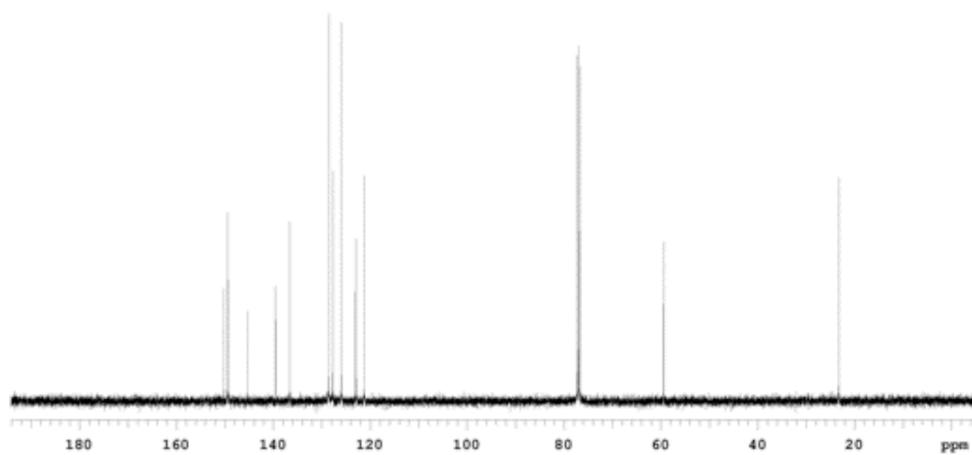
**<sup>13</sup>C NMR of 88k**

Bistriazole **88k'** was isolated by column chromatography (40 % ethyl acetate in hexanes) in 16 % yield.

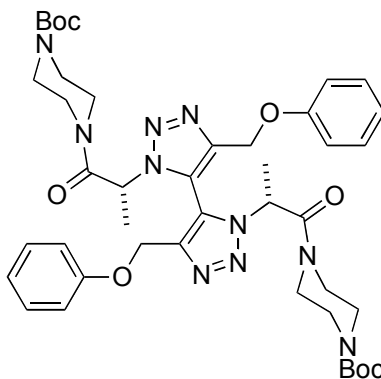
**<sup>1</sup>H NMR (CDCl<sub>3</sub>)**  $\delta$  7.91 (m, 2H), 7.73 (d, 2H,  $J = 7.5$  Hz), 7.42 (m, 2H), 7.04 (m, 10 H), 6.87 (m, 2H), 5.12 (q, 2H,  $J = 7.0$  Hz), 1.85 (d, 7.0 Hz)

**<sup>13</sup>C NMR (CDCl<sub>3</sub>)**  $\delta$  149.22, 149.19, 147.4, 138.5, 135.7, 128.3, 128.0, 126.8, 122.8, 122.3, 120.6, 59.8, 22.1

**MS (ESI,  $m/z$ ):** (M+H)<sup>+</sup> calcd for C<sub>30</sub>H<sub>27</sub>N<sub>8</sub> 499.24, found 499.14

 $^1\text{H}$  NMR of 88k' $^{13}\text{C}$  NMR of 88k'

Bistriazoles **881** were prepared from (*R*)-*tert*-butyl 4-(2-azidopropanoyl)piperazine-1-carboxylate (1.0 mmol) and phenyl propargyl ether (1.0 mmol). The ratio of the major and minor diastereomers was 3:2 as measured by HPLC analysis of the crude product mixture.

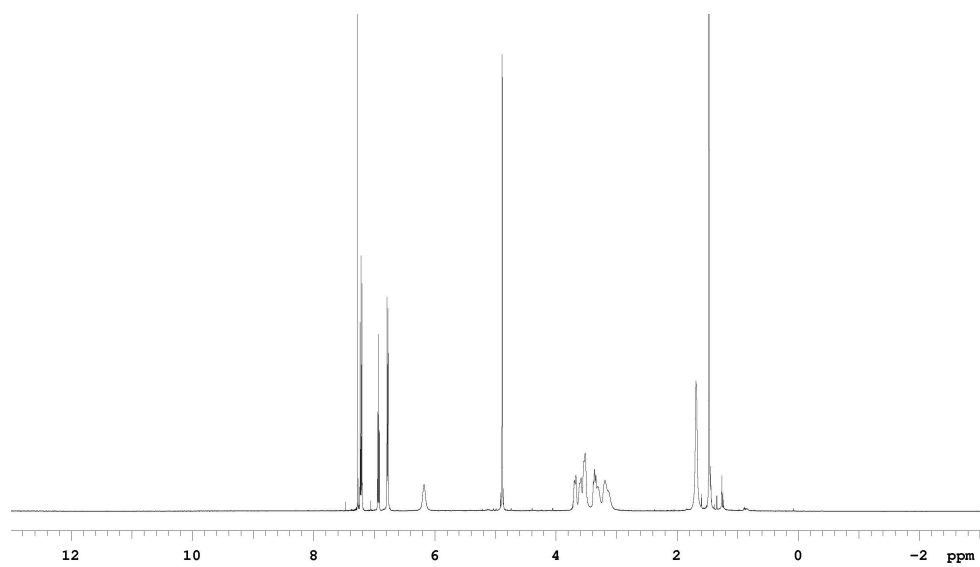
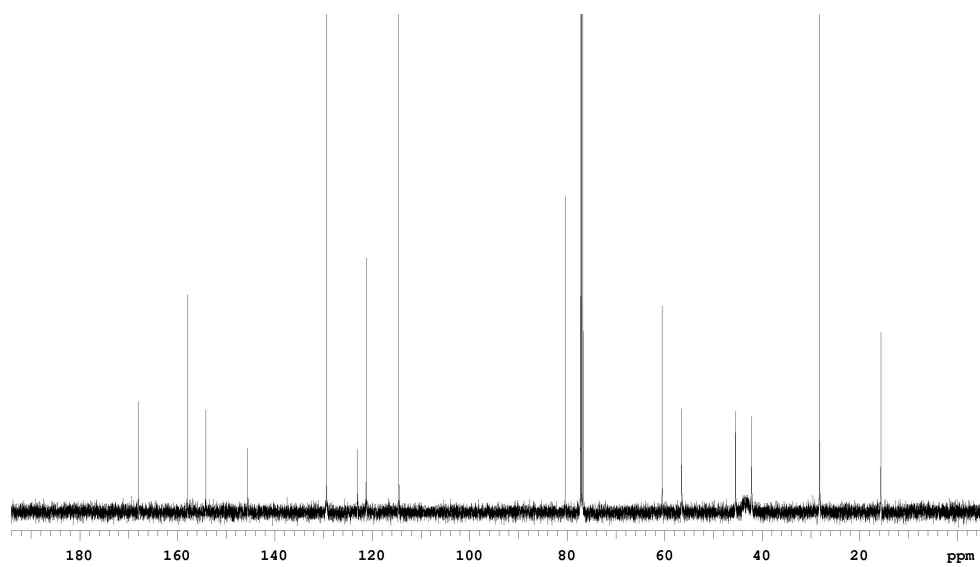
**881**

Flash chromatography (hexane/EtOAc = 1:1) afforded bistriazole **881** (major diastereomer) as a colorless oil (0.22 g, 54%).  $[\alpha]_D^{25} = -43.7$  (c = 1.0, CH<sub>2</sub>Cl<sub>2</sub>).

<sup>1</sup>H NMR (CDCl<sub>3</sub>) δ 7.18 (m, 4H), 6.90 (t, 2H, J = 7.0 Hz), 6.75 (d, 4H, J = 8.0 Hz), 6.16 (bs, 2H), 4.86 (s, 4H), 3.67-3.11 (m, 16H), 1.65 (d, 6H, J = 6.0 Hz), 1.45 (s, 18H)

<sup>13</sup>C NMR (CDCl<sub>3</sub>) δ 167.9, 157.8, 154.1, 145.5, 129.4, 123.0, 121.2, 114.5, 80.4, 60.5, 56.4, 45.4, 42.1, 28.2, 15.6

MS (ESI, m/z): (M+H)<sup>+</sup> calcd for C<sub>42</sub>H<sub>57</sub>N<sub>10</sub>O<sub>8</sub> 829.4361, found 829.4391

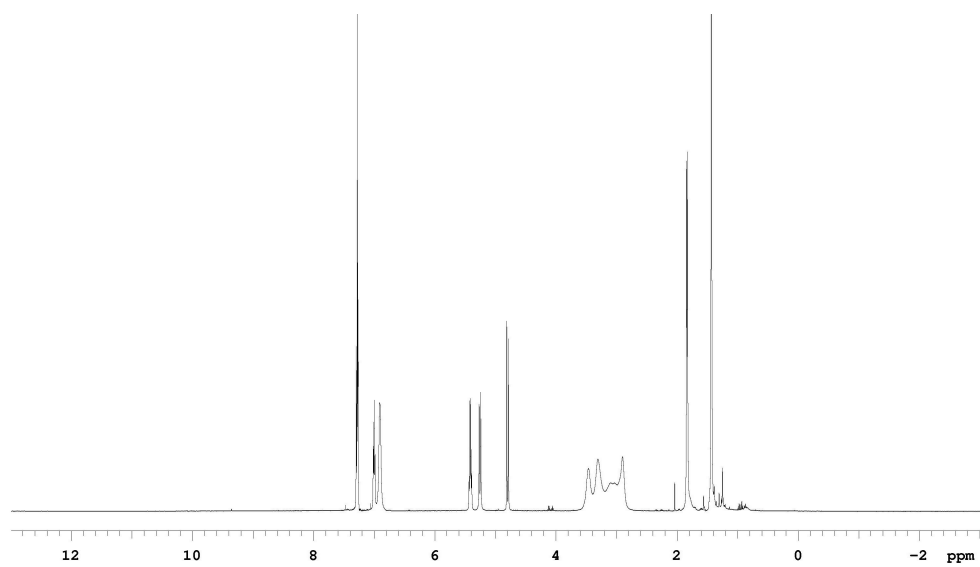
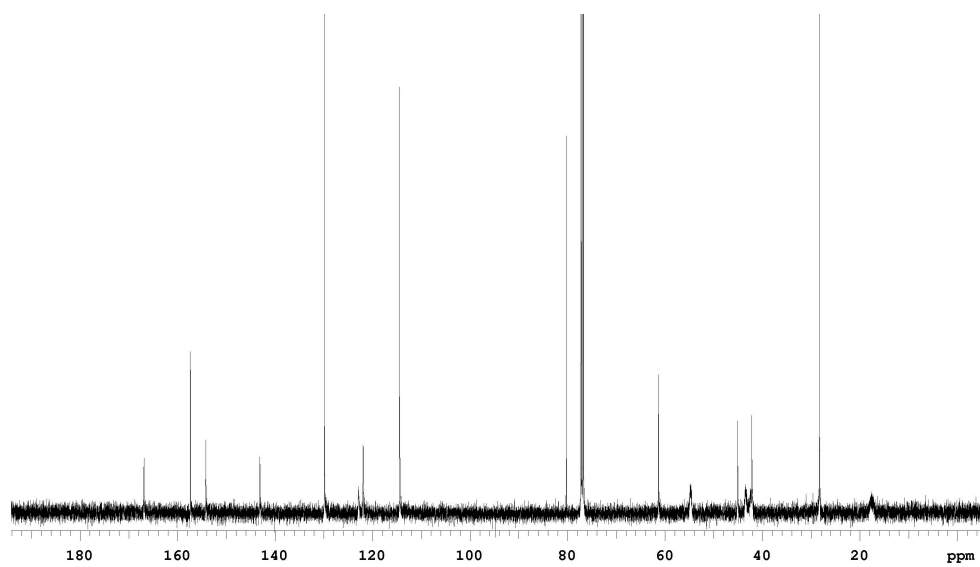
 **$^1\text{H}$  NMR of 881** **$^{13}\text{C}$  NMR of 881**

Flash chromatography (hexane/EtOAc = 1:1) afforded bistriazole **881'** (minor diastereomer) as a colorless oil (0.10 g, 24%).  $[\alpha]_D^{25} = -74.4$  (c = 0.3, CH<sub>2</sub>Cl<sub>2</sub>).

**<sup>1</sup>H NMR (CDCl<sub>3</sub>)** δ 7.28 (m, 4H), 7.00 (t, 2H, J = 7.0 Hz), 6.91 (m, 4H), 5.41 (q, 2H, J = 7.0 Hz), 5.25 (d, 2H, J = 13.0 Hz), 4.82 (d, 2H, J = 13.0 Hz), 3.46-2.90 (m, 16H), 1.83 (d, 6H, J = 7.0 Hz), 1.43 (s, 18H)

**<sup>13</sup>C NMR (CDCl<sub>3</sub>)** δ 166.9, 157.4, 154.2, 143.1, 129.9, 122.9, 121.9, 114.4, 80.2, 61.3, 54.8, 45.1, 42.2, 28.3, 16.6

**MS (ESI, m/z):** (M+Na)<sup>+</sup> calcd for C<sub>42</sub>H<sub>56</sub>N<sub>10</sub>NaO<sub>8</sub> 851.4180, found 851.4269

 $^1\text{H}$  NMR of 881' $^{13}\text{C}$  NMR of 881'

**Variable Temperature NMR Experiments for Compounds 88e and 88g.** To study the rotation barrier around the C-C bond that connects the two triazole rings, the variable temperature NMR experiments were conducted on compounds **17e** and **17g** in DMSO-d<sub>6</sub> at the concentration of 5mg/ml. The chemical shift difference between the H<sub>a</sub> and H<sub>b</sub> was calculated and plotted in Figure D1.

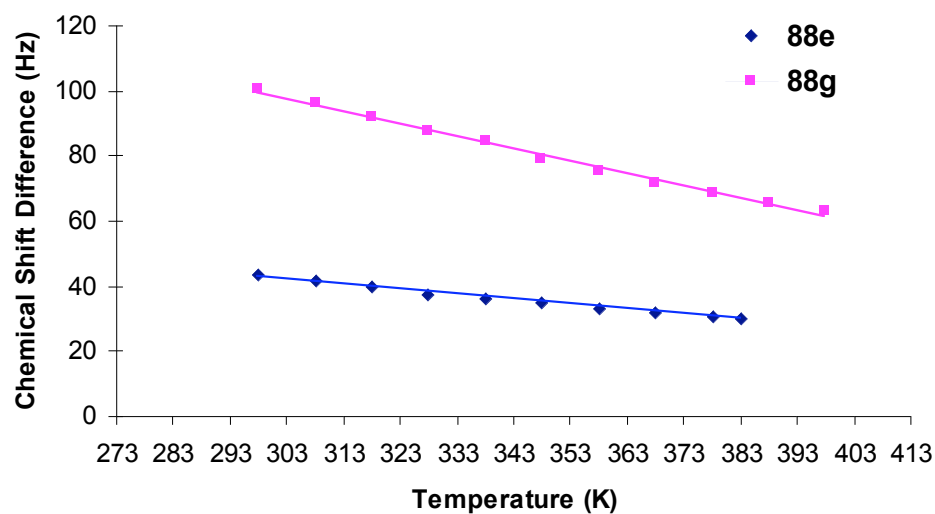
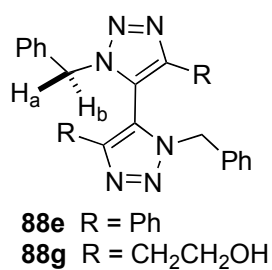


**Figure D1.** Chemical shift difference between H<sub>a</sub> and H<sub>b</sub>.



**CD Experiment for Compounds 88j and 88l.** The CD spectra were recorded at 25 °C. For these experiments diastereomers were dissolved in 5:1 methanol/water (v:v) (c = 0.2 mg/ml, 0.1 cm path length).

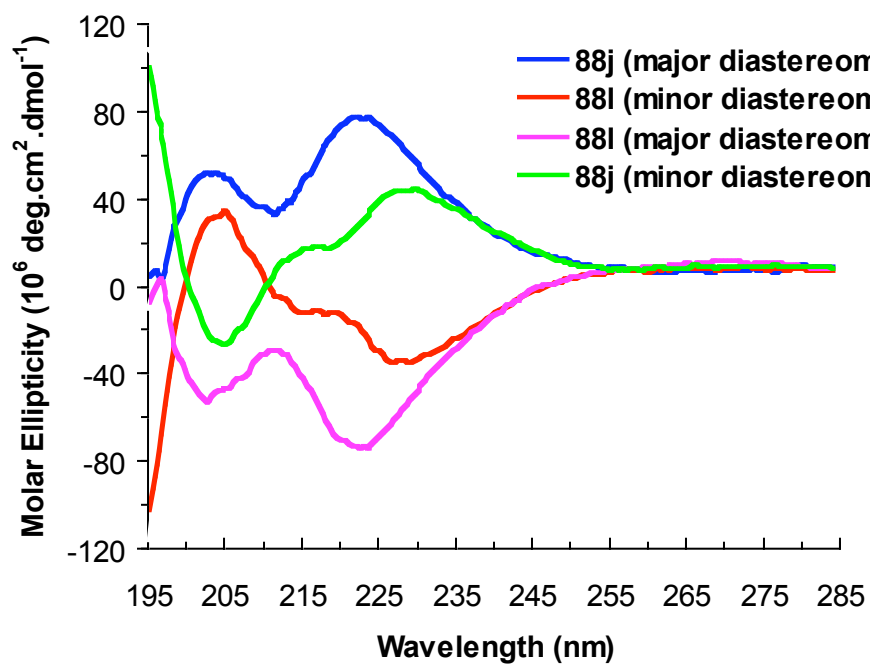


**Figure D2.** CD spectra of compounds **88j** and **88l** in 5:1 methanol/water at 0.2 mg/ml.

**VITA**

Name: Yu Li Angell

Permanent Address: Pinyun #3, Yiling Street  
YiChang, Hubei, China

Education: 2001-present Ph.D. Chemistry  
Texas A&M University  
College Station, TX 77843  
Advisor: Dr. Kevin Burgess

1996-2001 B. S. Chemistry  
Wuhan University  
Wuhan  
China  
Advisor: Dr. Lingzhi Meng

1999-2000 Exchange Student  
Osaka University  
Osaka  
Japan  
Advisor: Dr. Takashi Norisuye